Asymptotic Hodge Theory and String Theory

An application to the swampland program

PhD thesis, Utrecht University, June 2022
The cover is designed with the help of 赵一然, and Mercedes Benjaminse from ProefschriftMaken, based on the picture purchased from iStock.
This thesis is printed by ProefschriftMaken on 100% recycled paper.

Asymptotic Hodge Theory and String Theory

An application to the swampland program

Asymptotische Hodge-Theorie en Snaartheorie

Een toepassing in het moeraslandprogramma

(met een samenvatting in het Nederlands)

Proefschrift

ter verkrijging van de graad van doctor aan de Universiteit Utrecht
op gezag van de rector magnificus, prof. dr. H.R.B.M. Kummeling,
ingevolge het besluit van het college voor promoties in het openbaar
te verdedigen op vrijdag 17 juni 2022 des ochtends te 10.15 uur

door

Chongchuo Li

geboren op 28 januari 1993
te Tianjin, China

Promotor:
Prof. dr. T.W. Grimm

Copromotor:
Dr. U. Gürsoy

To 赵一然

Publications

This thesis is based on the following publications:

- T. W. Grimm, C. Li and E. Palti, *Infinite Distance Networks in Field Space and Charge Orbits*, JHEP **03** (2019), 016, [arXiv:1811.02571].
- T. W. Grimm, C. Li and I. Valenzuela, *Asymptotic Flux Compactifications and the Swampland*, JHEP **06** (2020), 009, [erratum: JHEP **01** (2021), 007], [arXiv:1910.09549].
- T. W. Grimm and C. Li, *Universal axion backreaction in flux compactifications*, JHEP **06** (2021), 067, [arXiv:2012.08272].

An upcoming work with T. W. Grimm and S. Lanza, in which we investigate the implications of tame geometry on the swampland distance conjecture, will be mentioned briefly in the Introduction.

Contents

1 Introduction **1**

1.1 String theory, Swampland, and Hodge theory 1
1.2 String compactification 4
1.2.1 5D gravity on cylinder $\longrightarrow$ 4D gravity + Maxwell 4
1.2.2 Compactification of string theory on Calabi-Yau spaces . . 7
1.2.3 Type IIB String Theory on Calabi-Yau threefolds 8
1.2.4 F-theory on Calabi-Yau fourfolds 14
1.3 Swampland conjectures 19
1.3.1 Distance conjecture 20
1.3.2 de Sitter conjecture 23
1.4 Asymptotic Hodge Theory 24
1.4.1 The cohomology of a smooth Calabi-Yau threefold 25
1.4.2 Variation of Hodge structure on elliptic curves 28
1.4.3 Degeneration of Hodge structures on elliptic curves 30
1.4.4 Using asymptotic Hodge theory in string theory 33
1.A Convention 38
1.B Details of 5D compactifications 40
1.C An example of the $\mathcal{N} = 2$ symplectic formalism 42
1.D Technicalities about mixed Hodge structures 43
1.D.1 Mixed Hodge structure and Deligne splitting 43
1.D.2 The limiting mixed Hodge structure 47

2 Infinite Distance Networks in Field Space and Charge Orbits **49**

2.1 Introduction 49
2.2 Monodromy and Orbit Theorems in Calabi-Yau Moduli Spaces . . 55
2.2.1 Complex Structure Moduli Spaces and Monodromy 55
2.2.2 Approximating the periods: Nilpotent orbits 59
2.2.3 Characterizing Singularities in Calabi-Yau Threefolds . . . 62
2.2.4 Commuting $\mathfrak{sl}(2)$s and the Sl(2)-orbit 67
2.2.5 Growth of the Hodge norm 71

2.3 Classifying Singularities in Calabi-Yau Moduli Spaces 76
2.3.1 A Classification of Calabi-Yau Threefold Singularities . . . 76
2.3.2 A Classification of allowed Singularity Enhancements . . . 79
2.3.3 On the Classification of Infinite Distance Points 83
2.3.4 The Large Complex Structure and Large Volume Point . . 85
2.4 Charge orbits and the Swampland Distance Conjecture 90
2.4.1 Single parameter charge orbits 91
2.4.2 Defining the general charge orbit 95
2.4.3 Masslessness of the charge orbit 99
2.4.4 The two-divisor analysis 102
2.4.5 The general multi-divisor analysis 113
2.4.6 A two parameter example: mirror of $\mathbb{P}^{(1,1,1,6,9)}[18]$ 117
2.4.7 Discussion on properties of the charge orbit 121
2.5 Conclusions 123
2.A Monodromy filtrations and mixed Hodge structures 126
2.B Construction of the SL(2)-splitting 127
2.C General procedure to construct the commuting $\mathfrak{sl}(2)$s 129
2.D An example: commuting $\mathfrak{sl}(2)$s in the mirror of $\mathbb{P}^{(1,1,1,6,9)}[18]$ . . . 131
2.D.1 Introduction to the example 131
2.D.2 The commuting $\mathfrak{sl}(2)$-pair associated to $\mathrm{III}_0 \to \mathrm{IV}_2$ 133
2.D.3 The commuting $\mathfrak{sl}(2)$-pair associated to $\mathrm{IV}_1 \to \mathrm{IV}_2$ 142
2.E Deriving the polarised relations 147

3 Asymptotic Flux Compactifications and the Swampland 151
3.1 Introduction 151
3.2 Flux compactifications on Calabi-Yau fourfolds 155
3.2.1 Four-form flux and the scalar potential 156
3.2.2 Relation to flux vacua in Type IIB and Type IIA orientifolds 159
3.3 Asymptotic flux potential 162
3.3.1 Asymptotic limits in Calabi-Yau fourfolds 162
3.3.2 Asymptotic split of the flux space 164
3.3.3 The asymptotic behavior of the Hodge norm 166
3.3.4 Self-dual fluxes in the strict asymptotic regime 170
3.3.5 Unbounded asymptotically massless fluxes 172
3.4 Supergravity embedding and three-forms 174
3.4.1 Asymptotic limits and the $\mathcal{N} = 1$ supergravity data 174
3.4.2 Relation to Minkowski three-form gauge fields 177

3.5 General two-moduli limits . . . 180
3.5.1 Asymptotic flux splitting and scalar potential . . . 180
3.5.2 Classification of two-moduli limits and enhancements therein 182
3.5.3 Main example: enhancement from type II singularity . . . 186
3.6 Asymptotic structure of flux vacua . . . 190
3.6.1 Flux ansatz and parametric control . . . 192
3.6.2 Minimization conditions . . . 195
3.6.3 Parametrically controlled vacua for the main example . . . 197
3.6.4 No-go results for de Sitter at parametric control . . . 201
3.6.5 Candidates for AdS minima at parametric control . . . 205
3.7 Asymptotic structure of flux vacua: axion dependence . . . 208
3.7.1 Axion stabilization . . . 208
3.7.2 Backreaction in axion monodromy inflation . . . 212
3.8 Conclusions . . . 219
3.A Brief summary of the underlying mathematical machinery . . . 222
3.B Norms associated with some special Hodge structures . . . 224

4 Universal Axion Backreaction in Flux Compactifications 231
4.1 Introduction and discussion . . . 231
4.2 F-theory on Calabi-Yau fourfolds with G_4-flux . . . 236
4.2.1 Scalar potential and its complex structure dependence . . . 236
4.2.2 Scalar potential and the Hodge filtration . . . 238
4.3 Complex structure axions and asymptotic Hodge theory . . . 240
4.3.1 Axions at the boundary of moduli space . . . 240
4.3.2 The boundary $\mathfrak{sl}(2)$-structures associated to a degeneration 243
4.3.3 Asymptotic form of periods and the scalar potential . . . 245
4.4 Axion backreaction on the saxion vacuum . . . 249
4.4.1 A brief review of representations of the $\mathfrak{sl}(2)$-algebra . . . 251
4.4.2 A brief review of the Puiseux expansion . . . 252
4.4.3 Determining the backreacted saxion vacuum . . . 255
4.4.4 Bad cases and their elimination . . . 261
4.A More detailed properties of the commuting $\mathfrak{sl}(2)$-triples . . . 266
4.A.1 The map $e(s)e^{\phi^i N_i}e(s)^{-1}$ . . . 269
4.A.2 The map $e(s)e^{\Gamma(z)}e(s)^{-1}$ in the limit . . . 271
4.A.3 The filtration $e(s)F_0$ in the limit . . . 273

Summary 275

Samenvatting **277**

Acknowledgements **279**

About the author **281**

Bibliography **283**

1 Introduction

1.1 String theory, Swampland, and Hodge theory

Two major achievements of the twentieth century physics are quantum mechanics and general relativity. Quantum mechanics governs the physics at ultra-short scales, an example of which would be the interaction of electrons and nucleus inside an atom. General relativity dictates the physics of extreme gravity fields, an example of which would be the gravitation field around an astronomical object with a very large mass. With such two theories at hand, a natural question arises: can one combine quantum mechanics and general relativity together so as to cook up a quantum theory of gravity? Besides theoretical curiosity, direct motivation of such a question is abundant. For example, the start of everything is the Big Bang, an instant after which the entire universe is concentrated within a very tiny space while experiencing extreme gravitational effects. If we want to study the physics of the early universe, we must employ a theory of quantum gravity. A more contemporary example comes from the physics of black holes. A black hole is also a tiny object that concentrates a large amount of mass, to the extent that even light rays cannot escape the gravitation field of the black hole. With the direct observation of the black hole [1], understanding their physics becomes a realistic problem transcending theoretical interest. Hence a quantum theory of gravity is desirable.

Unfortunately, naïvely combining the computations of quantum mechanics and general relativity presents immediate trouble — the two theory are simply not compatible with each other. In technical words, the resulting theory is non-renormalisable. While a non-renormalisable effective field theory is by itself not a problem, in quantum gravity, which is considered to be a fundamental theory, non-renormalisability poses serious obstacles.

So something must be changed. There are at least two ways to modify the current theory to describe quantum gravity. On the one hand, one can abandon the hypothesis that the fundamental objects in a unifying theory of nature should be zero-dimensional points. This is the approach of string theory. Equipped with the hypothesis that the fundamental building blocks are one-dimensional strings

and the frameworks of quantum mechanics and general relativity, string theory is shown to be a consistent theory of quantum gravity. On the other hand, one can just abandon perusing an all-encompassing microscopic theory, but rather pragmatically work only with low-energy effective theories. The question then becomes: what type of effective theory is compatible with the mysterious quantum gravity at ultra high energy scale? This is the central question of the swampland program.

String theory is the most promising candidate for quantum gravity. Its tiny conceptual shift, that is replacing the point particles by strings, has a huge implication on the physics: It is now a quantum theory that is consistent with Einstein gravity. Two elementary features of string theory are:

1. It has just one external parameter, which is the string tension, i.e. energy of the string per unit length.

2. It is only consistent in 10-dimensional spacetime.

Feature 1 is nice, compared to the standard model, which has 19 external parameters, such as the electron mass. On the other hand, Feature 2 is not nice, compared with our four-dimensional real world. How to link the 10-dimensional string universe to the four-dimensional physical universe?

The answer dates back to the ancient proposal of Kaluza and Klein [2, 3]. Suppose that the spacetime is now five-dimensional and is a direct product of our four-dimensional universe and a one-dimensional "internal" circle. This amounts to saying that, locally, we can parametrise the spacetime by coordinates of the form $(\mathbf{x}_4, \theta)$, where $\mathbf{x}_4 = (t, x, y, z)$ is the local coordinate on our four-dimensional universe, and θ is the local coordinate on the internal circle. Kaluza and Klein propose that by making the size of the internal circle extremely tiny, human beings cannot detect the internal circle at all. Thus the dimensionality of the universe being four is realised as an "illusion" in the Kaluza-Klein theory. Moreover, if we just turn on Einstein gravity with the five-dimensional metric as the basic degree of freedom on the five-dimensional spacetime, then from the four-dimensional point of view, one gets a four-dimensional Einstein gravity theory, plus the theory of Maxwell. An important feature is that the four-dimensional physics, such as the gauge and gravitational coupling constants, are controlled by the geometry of the circle. In this way, Kaluza-Klein unifies the gravity and the electromagnetic interactions by dimensional reduction.

In string theory, the mechanism of making contact with four-dimensional physics is exactly the same. One focuses on those 10-dimensional string solutions that are locally a direct product of our four-dimensional universe and a intricately chosen

six-dimensional internal space. Reducing the 10-dimensional physics to the four-dimensional spacetime, assuming that the six-dimensional internal space is tiny, one is able to get four-dimensional worlds. Moreover, the four-dimensional physics is related to the six-dimensional compactification geometry, and by tweaking the geometry, we can engineer a plethora of four-dimensional physics, possibly including the very world we live in. The set of all four-dimensional worlds acquired this way is called the *string landscape*. The existence of the string landscape prompts the following question: Does our universe belong to the string landscape? Phrased differently: Can string theory describe real-world physics?

We would like to pause the discussion on string theory for a moment, and consider the other possibility for quantum gravity, namely just focusing on the observable sector of the energy spectrum. In this direction, one is satisfied if one can construct effective quantum field theories that describes the observed universe; such effective theories should have a cut-off scale higher than the energy scale at which we can make the observation. It should be a quantum field theory because we do know that the Standard Model, a quantum field theory, has already been agreeing with experiments extremely well.

Such approaches are called bottom-up. In a bottom-up construction, one typically starts by imposing a set of symmetry constraints, and then writes down the most general theory that satisfies the symmetry constraints. Next, one checks if the resulting theory satisfies other important self-consistency constraints, such as being gauge anomaly-free. Obviously, the theories one gets from a bottom-up approach are far from unique; there is an immense number of effective field theories that satisfy all such constraints, all of which contains Einstein gravity. This leads to another natural question: Do all the consistent-looking effective theories one gets from the bottom-up approach live in the string landscape?

Clearly, the answer is negative [4]. There are indeed consistent-looking effective theories that do lot live in the string landscape. Those consistent-looking effective field theories that do not belong to the Landscape form a set called the *swampland*.

The swampland program aims to acquire a set of criteria about whether an effective field theory is consistent with quantum gravity at very high energy. The criteria on the market are mostly conjectural, because we do not have an undebatable quantum gravity theory yet. However, we do have string theory, which is the most promising candidate for quantum gravity. Moreover, one can try to argue in an indirect way, resorting to semi-classical black hole arguments, for quantum gravity. Hence, all the criteria are called *swampland conjectures* at this moment, and they are mostly proposed using string theory and semi-classical black hole

arguments.

A swampland conjecture is most powerful if it is at least proven in the framework of string theory. But verifying the conjectures in string theory can be highly non-trivial, as our understanding of string theory is yet to be completed. Our contribution in this thesis is to bridge mathematics and string theory. We import the asymptotic Hodge theory from mathematics into string theory, following the seminal work [5]. This interplay between mathematics and physics turns out to be extremely powerful in the study of swampland conjectures.

Let us finish this section by mentioning an exciting recent development that connects the Hodge conjecture [6], a well-known "millennium prize problem", with the long-standing problem of the finiteness of string flux vacua [7–10]. It is perhaps surprising that the mathematical techniques used in showing (arguably) the strongest evidence about the Hodge conjecture in [11] and [12] can be used to show the finiteness of string flux vacua in [13, 14].

1.2 String compactification

In this section, we review the idea of string compactification, which is the foundation of all the researches in string phenomenology and the relevant mathematics.

1.2.1 5D gravity on cylinder $\longrightarrow$ 4D gravity + Maxwell

The idea of compactifying a higher dimensional theory down to a lower one dates back to the ancient works in 1920's by Kaluza [2] and Klein [3]. In this section, we briefly go through compactification in a simplified setting, where a five-dimensional gravity theory reduces to a four-dimensional theory mixing gravity and electromagnetism, once one of the five-dimensional space is taken to be a circle. The result is not unexpected if one adopts a principal bundle viewpoint of gauge theories: The compactified spacetime $\mathbb{R}^{3,1} \times S^1$ is exactly a trivial principal $U(1)$-bundle[1] over the four-dimensional $\mathbb{R}^{3,1}$, and should be related to the $U(1)$ gauge theory, the electromagnetism.

To set up notation, we denote the coordinates on $\mathbb{R}^{3,1} \times S^1$ by (x^μ, θ), where $x^\mu \in \mathbb{R}^{3,1}$ is the coordinate in the four-dimensional Minkowski spacetime, and θ labels the wrapped fifth direction. We identify $\theta \sim \theta + 2\pi$, and denote the radius of the circle by $r \geq 0$.

[1] Recall that S^1 is isomorphic to $U(1)$ as Lie groups.

Before diving into the complicated, non-linear gravity theory, let us first consider an even simpler model of a five-dimensional real massless scalar field $\hat{\phi}$ living on the five-dimensional Minkowski spacetime with a non-dynamical metric $ds_5^2 = \eta_{\mu\nu}dx^\mu dx^\nu + r^2 d\theta^2$, where r is a constant. The 5D action reads

$$\begin{aligned}\hat{S}[\hat{\phi}] &= -\frac{1}{2}\int_{\mathbb{R}^{3,1}\times S^1} d\hat{\phi}(x,\theta)\wedge *d\hat{\phi}(x,\theta) \\ &= -\frac{r}{2}\int_{\mathbb{R}^{3,1}\times S^1} d^4x\, d\theta \left\{\partial_\mu\hat{\phi}\partial^\mu\hat{\phi} + \frac{1}{r^2}(\partial_\theta\hat{\phi})^2\right\} . \end{aligned} \tag{1.2.1}$$

Since the field $\hat{\phi}$ is periodic in its fifth-direction, it can be re-expressed in terms of the Fourier basis

$$\hat{\phi}(x,y) = \sum_{n\in\mathbb{Z}} \phi_n(x) e^{\mathbf{i}n\theta} , \tag{1.2.2}$$

and the reality condition translates to the fact that $\phi_{-n} = \bar{\phi}_n$. Plugging (1.2.2) into (1.2.1), we have arrived at the 4D action

$$S[\phi_n] = -\pi r \sum_n \int_{\mathbb{R}^{3,1}} d\phi_n \wedge *d\bar{\phi}_n + \frac{n^2}{r^2}\phi_n\bar{\phi}_n * 1 . \tag{1.2.3}$$

Here are a few remarks about this expression. By compactifying the fifth dimension, a five-dimensional massless scalar field becomes a tower of four-dimensional scalar fields. The scalar fields in this tower are called *Kaluza-Klein modes* and are labelled by a natural number n. Moreover, the scalar field with $n = 0$ stays massless, while those scalar fields with $n > 0$ are complex, massive with mass n^2/r^2. If we postulate that the fifth dimension is not observable, meaning that we impose a cut-off scale $0 < \Lambda < 1/r$, then the fields with $n > 0$ are integrated out in the low energy effective field theory, while the field with $n = 0$ is always included in the effective theory. This is a general feature of compactification, and in the following we will only include the zero-mass field in the four-dimensional effective theory.

Having seen the appearance of Kaluza-Klein modes in a simple setting, let us now make the gravity dynamical. Let the five-dimensional metric be

$$(\hat{g}_{MN}) = \begin{pmatrix} g_{\mu\nu} + r^2 A_\mu A_\nu & r^2 A_\mu \\ r^2 A_\nu & r^2 \end{pmatrix} , \tag{1.2.4}$$

which is the most general metric[2] on $\mathbb{R}^{3,1}\times S^1$. For simplicity, we are sloppy about the (mass) dimensions of the various fields and this will be fixed near the end of

[2]The particular form of this Ansatz is chosen to make sure that the inverse of the metric takes a simple form.

this section. Note that from now on, every component in the metric is already truncated down to the zero-mass component, so all fields entering $\hat{g}_{MN}$ does not depend on θ. The 5D action is given by

$$\hat{S}[\hat{g}_{MN}] = \frac{1}{2\kappa_5^2}\int_{\mathbb{R}^{3,1}\times S^1} \hat{R} * 1\,, \tag{1.2.5}$$

where $*1 = \sqrt{-\hat{g}}\, d^4x d\theta$ is the volume form and κ_5 is the 5D gravitation interaction strength.

After a straightforward computation (see Appendix 1.B), we get the 4D action in string frame, where the Ricci scalar is multiplied by the scalar field r

$$S[g_{\mu\nu}, A_\mu, r] = \frac{2\pi}{2\kappa_5^2}\int_{\mathbb{R}^{3,1}} rR * 1 - \frac{r^3}{2} F \wedge *F\,, \tag{1.2.6}$$

where $F = dA$ is the four-dimensional gauge field strength.

Perhaps it is now the time to be careful about the dimensions. We denote the ground state radius of the circle by R_0, so the the fifth dimension θ is replaced by $R_0\theta$, which has mass dimension -1. Moreover, we keep the scalar field r dimensionless, and this scalar field is sometimes called the *breathing mode*, representing the small dynamical deviation of the circle from its radius R_0. Next, we replace A_μ by $\kappa_4 A_\mu$, where κ_4 is the 4D gravitational interaction strength that is related to κ_5 by (1.2.8), such that A_μ has the correct mass dimension one. After these rescalings, the action looks like

$$S[g_{\mu\nu}, A_\mu, r] = \frac{1}{2\kappa_4^2}\int_{\mathbb{R}^{3,1}} rR * 1 - \frac{\kappa_4^2 r^3}{2} F \wedge *F\,, \tag{1.2.7}$$

where we have identified

$$\frac{1}{2\kappa_4^2} = \frac{2\pi R_0}{2\kappa_5^2}\,. \tag{1.2.8}$$

The final step is to perform a Weyl rescaling, replacing $g_{\mu\nu}$ by $r g_{\mu\nu}$, so that the r in front of R is eliminated, and we arrive at the action written in Einstein frame. Moreover, the Weyl rescaling generates a kinetic term for the breathing mode r

$$S[g_{\mu\nu}, A_\mu, r] = \int_{\mathbb{R}^{3,1}} \frac{1}{2\kappa_4^2} R * 1 - \frac{3}{2\kappa_4^2 r^2} dr \wedge *dr - \frac{r^3}{2} F \wedge *F\,. \tag{1.2.9}$$

Hence, by dimensional reduction, we get a 4D theory that includes gravity, scalar, $U(1)$ gauge fields, and their interactions.

In summary, we have seen that starting from a higher dimensional gravitational action, and assuming that the spacetime is (locally) a direct product, one is able

to generate an interacting theory containing gravity, scalar and gauge fields. Because of the dynamics of gravity, the internal geometry oscillates around its stable configuration. This drives us to consider a family of internal geometry instead of a single one. The parameters controlling the internal geometry become massless scalar fields in the four-dimensional theory and are called *moduli fields*. Viewed differently, these moduli fields are mappings from the four-dimensional spacetime to the moduli space of the internal geometry. In Figure 1.1, we illustrate these ideas in the context of circle compactification.

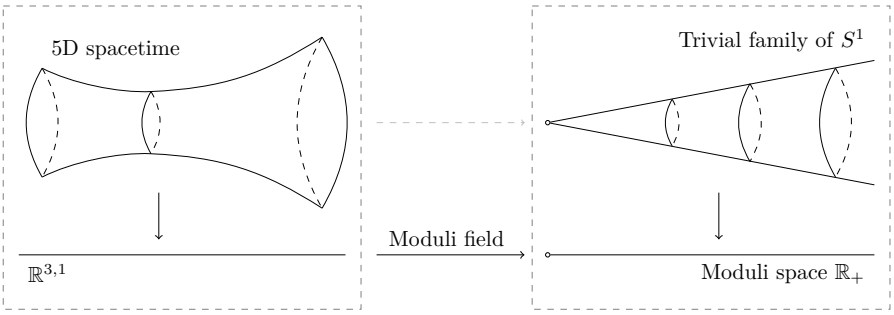

Figure 1.1: Left panel: The five-dimensional spacetime is a family of circles fibred over the four-dimensional $\mathbb{R}^{3,1}$. Right panel: A trivial family of regular S^1 fibred over the moduli space consisting the radius $r > 0$ of S^1. The moduli field $r(x^\mu)$ from the four-dimensional spacetime to the moduli space of S^1 remembers the radii of the internal circles. In mathematics this moduli field is called a moduli map. Note that one can compactify the moduli space into $\mathbb{R}_{\geq 0}$ by adding a degenerate circle with $r = 0$ at the tip of the cone in the right panel. This intuition is used later in the study of asymptotic Hodge theory.

1.2.2 Compactification of string theory on Calabi-Yau spaces

In this section, we introduce the compactification settings that we will investigate in the remainder of the thesis. As we will see shortly, such settings are valuable for phenomenology, since they deliver four-dimensional theories that preserve only a fraction of the 10-dimensional supersymmetry. The microscopic theory under consideration is of course various string theories, and the more general M-theory that unifies all string theories via dualities. More precisely, we will be particularly interested in type II strings, and the closely related F-theory. For the compactification manifold, we choose Calabi-Yau threefolds and Calabi-Yau fourfolds.

Putting our microscopic string theories on such Calabi-Yau spaces will induce four-dimensional supergravity theories in the low-energy, which are severely constrained and amenable for exact analysis since many useful physical quantities are protected by supersymmetry. In Table 1.1, we show the correspondence among the microscopic theories, the compactification manifolds, and the lower-dimensional effective field theories that are discussed in this thesis.

Critical dimensions	Microscopic theory	Compactification manifold	Macroscopic supergravity	Lower dimensions
10	Type II	CY3	$\mathcal{N}=2$	4
		CY3 orientifold	$\mathcal{N}=1$	
11	M-theory	CY4	$\mathcal{N}=2$	3
12	F-theory	Elliptic CY4	$\mathcal{N}=1$	4

Table 1.1: A table relating the the microscopic theories, the spacetime dimensions at which they are consistent, the compactification manifolds, and the lower-dimensional effective field theories that are considered in this thesis. In order to get four-dimensional $\mathcal{N}=1$ theories from F-theory, the Calabi-Yau fourfold must be elliptically fibred.

In the following, we go deeper into the compactification scenario in Table 1.1. We will describe the structure of the four-dimensional effective supergravities, the geometric quantities of the Calabi-Yau spaces, and the relation between the effective physics and the geometric quantities.

1.2.3 Type IIB String Theory on Calabi-Yau threefolds

Two different type II string theories, namely IIA and IIB, exist in 10-dimensions. The IIA theory is non-chiral, and IIB is chiral. The low energy EFT of type II theories compactified on Calabi-Yau threefolds are four-dimensional $\mathcal{N}=2$ ungauged supergravities which includes an amount of massless moduli scalar fields. An orientifold projection further truncates the theory down to $\mathcal{N}=1$ and can support fluxes to stabilise the moduli and induce gauged supergravity. In this section, we discuss the vector sector of type IIB theory compactified on Calabi-Yau threefolds. We will not discuss the orientifold compactification in this section, and we recommend the interested reader to consult [15–17]. For simplicity we work in units where the gravitational interaction constant $\kappa_4 = 1$.

$\mathcal{N} = 2$ supergravity in four-dimensions

We list here the basic ingredients of four-dimensional $\mathcal{N} = 2$ supergravity and refer the reader to the textbooks [18, 19] for detailed discussion. There are three types of supergravity multiplets in $D = 4$, $\mathcal{N} = 2$ supergravity: the gravity, vector, and hypermultiplets[3]. Our focus will be on the vector multiplets. The bosonic fields in each vector multiplet include a massless vector field A_μ and a complex scalar field z. Besides the vector multiplet, there is also the gravity multiplet, whose bosonic fields are the metric $g_{\mu\nu}$ and a vector A^0_μ named the graviphoton. Fixing $n_{\rm V}$, the number of vector multiplets in the theory, the bosonic action of four-dimensional ungauged $\mathcal{N} = 2$ supergravity looks like

$$S = \int_{\mathbb{R}^{3,1}} \frac{1}{2} R * 1 - g_{i\bar{\jmath}} dz^i \wedge * d\bar{z}^{\bar{\jmath}} + \frac{1}{2} \operatorname{Im} \mathcal{N}_{IJ} F^I \wedge * F^J - \frac{1}{2} \operatorname{Re} \mathcal{N}_{IJ} F^I \wedge F^J \,, \quad (1.2.10)$$

where z^i with $i = 1, \ldots, n_{\rm V}$ runs over the scalars in the vector multiplets, and F^I with $I = 0, \ldots, n_{\rm V}$ runs over the vectors in the vector multiplets, together with the graviphoton. There are in fact many different conventions on the form of the $\mathcal{N} = 2$ action. Here we follow the convention in [18], and we refer to [18, Appendix C] for a nice comparison between different conventions. We have also adopted convention so that F^0 corresponds to the field strength of the graviphoton. The $\mathcal{N} = 2$ supersymmetry poses constraints on the kinetic matrices $g_{i\bar{\jmath}}$ and $\mathcal{N}_{IJ}$ via *(projective) special Kähler geometry* [20–23]. The special geometry encodes the symplectic invariance, a generalisation of the electro-magnetic duality, that is present in $\mathcal{N} = 2$ supergravity. It works as follows. To specify an $\mathcal{N} = 2$ theory with scalar fields z^i in the vector multiplets, one needs to provide a $2(n_{\rm V} + 1)$-dimensional symplectic vector $v(z)$ consisting of holomorphic functions of z^i

$$v(z) = \begin{pmatrix} Z^I(z) \\ \mathcal{F}_I(z) \end{pmatrix} \,, \quad (1.2.11)$$

subjected to a constraint that will be introduced later. Two such vectors $v = (Z^I, \mathcal{F}_I)^{\mathsf{T}}$ and $\tilde{v} = (\tilde{Z}^I, \tilde{\mathcal{F}}_I)^{\mathsf{T}}$ can be multiplied using the symplectic pairing

$$Q(v, \tilde{v}) = Z^I \tilde{\mathcal{F}}_I - \tilde{Z}^I \mathcal{F}_I \,, \quad (1.2.12)$$

and we can change the basis while preserving the symplectic pairing, so the symplectic vector $v(z)$ carries an $\mathrm{Sp}(2(n_{\rm V} + 1), \mathbb{R})$-action.

[3] These are the on-shell multiplets. Including the off-shell multiplets, one can dualise a real scalar in a vector multiplet into a two-form, resulting in a vector-tensor multiplet, or do the same to a real scalar in a hypermultiplet, yielding a linear multiplet.

In order to describe the constraint on $v(z)$, we need to define more gadgets. The real-valued Kähler potential $K(z,\bar{z})$ is defined to be

$$e^{-K} = -\mathbf{i}Q(v,\bar{v})\,, \tag{1.2.13}$$

and the Kähler covariant derivative $\mathcal{D}_i v$ is given by

$$\mathcal{D}_i v = \partial_i v + (\partial_i K)v\,. \tag{1.2.14}$$

Then special geometry constraint on the symplectic vector $v(z)$ is given by

$$Q(\mathcal{D}_i v, \mathcal{D}_j v) = 0\,. \tag{1.2.15}$$

Fixing the data $v(z)$ subject to the constraint (1.2.15), the kinetic matrices $g_{i\bar{\jmath}}$ and $\mathcal{N}_{IJ}$ in the $\mathcal{N}=2$ action (1.2.10) can be determined as follows. For the scalars, one has

$$g_{i\bar{\jmath}} = \partial_i\partial_{\bar{\jmath}}K = \mathbf{i}e^K Q(\mathcal{D}_i v, \mathcal{D}_{\bar{\jmath}}\bar{v})\,, \tag{1.2.16}$$

and the gauge kinetic term is given by the $(n_{\mathrm{V}}+1)\times(n_{\mathrm{V}}+1)$ matrix

$$\mathcal{N}_{IJ} = (\mathcal{F}_I, \mathcal{D}_{\bar{\imath}}\overline{\mathcal{F}}_I)(Z^J, \mathcal{D}_{\bar{\imath}}\overline{Z}^J)^{-1}\,, \tag{1.2.17}$$

whose imaginary part is negative definite.

It is often useful to organise the above data into a single holomorphic function $\mathcal{F}(Z)$ called the *prepotential*. This is not always doable, but it is shown [21] that every four-dimensional $\mathcal{N}=2$ supergravity can be rotated into a duality frame by a symplectic transformation where a prepotential exists. We refer the reader to the textbooks [18, 19] for detailed discussion on this issue. The prepotential $\mathcal{F}(Z)$ is homogeneous of degree two in the variable $Z^I(z)$, and one has

$$\mathcal{F}_I = \frac{\partial\mathcal{F}}{\partial Z^I}\,, \tag{1.2.18}$$

so that $v(z) = (Z^I(z), \mathcal{F}_I(z))^{\mathsf{T}}$ defines the symplectic vector. Moreover, the gauge kinetic function can be rewritten, in the presence of a prepotential, as

$$\mathcal{N}_{IJ} = \overline{\mathcal{F}}_{IJ} + 2\mathbf{i}\frac{\operatorname{Im}\mathcal{F}_{IN}Z^N \operatorname{Im}\mathcal{F}_{JK}Z^K}{Z^L \operatorname{Im}\mathcal{F}_{LM}Z^M}\,, \tag{1.2.19}$$

where we understood $\mathcal{F}_{IJ} = \frac{\partial^2\mathcal{F}}{\partial Z^I\partial Z^J}$ and $\operatorname{Im}\mathcal{F}_{IJ} = \frac{1}{2}(-\mathbf{i}\mathcal{F}_{IJ} + \mathbf{i}\overline{\mathcal{F}}_{IJ})$ for clarity.

For the convenience of the reader, we present a toy example illustrating the construction of $\mathcal{N}=2$ actions from the choice of a symplectic vector in Appendix 1.C.

Calabi-Yau threefolds and four-dimensional physics

Here we review the basic properties of Calabi-Yau threefolds. For detailed discussion, see [24–31]. A Calabi-Yau threefold Y_3 is a compact Kähler manifold of (complex) dimension three with a (holomorphically) trivial canonical bundle $\omega_{Y_3} \cong \mathcal{O}_{Y_3}$. The definition is equivalent to that there exists a unique up to rescaling $(3,0)$-form Ω. As a Kähler manifold, Y_3 has a basic holomorphic invariant[4] called the Hodge diamond, which records the dimensions of the Dolbeault cohomology $h^{p,q} = \dim_{\mathbb{C}} H^{p,q}(Y_3)$. The Hodge numbers are constrained by inherent symmetries $h^{p,q} = h^{q,p} = h^{n-p,n-q}$, where n is the dimension of the Kähler manifold. Almost all Hodge numbers are fixed by the Calabi-Yau condition or the inherent symmetries of the Hodge diamond, and the only free ones are $h^{1,1}$ and $h^{2,1}$. The Hodge diamond of a Calabi-Yau threefold is shown in Figure 1.2.

$$
\begin{array}{ccccccc}
 & & & h^{3,3} & & & \\
 & & h^{3,2} & & h^{2,3} & & \\
 & h^{3,1} & & h^{2,2} & & h^{1,3} & \\
h^{3,0} & & h^{2,1} & & h^{1,2} & & h^{0,3} \\
 & h^{2,0} & & h^{1,1} & & h^{0,2} & \\
 & & h^{1,0} & & h^{0,1} & & \\
 & & & h^{0,0} & & &
\end{array}
\quad = \quad
\begin{array}{ccccccc}
 & & & 1 & & & \\
 & & 0 & & 0 & & \\
 & 0 & & h^{1,1} & & 0 & \\
1 & & h^{2,1} & & h^{2,1} & & 1 \\
 & 0 & & h^{1,1} & & 0 & \\
 & & 0 & & 0 & & \\
 & & & 1 & & &
\end{array}
$$

Figure 1.2: Hodge diamond of a Calabi-Yau threefold. The only two free parameters are $h^{1,1}$ controlling the (complexified) Kähler deformation, and $h^{2,1}$ controlling the complex structure deformation.

Fixing a Calabi-Yau threefold Y_3, one can slightly deform its metric, while preserving the Calabi-Yau condition. Since in gravity the metric itself is dynamic, this means that one has to consider a family of Calabi-Yau threefolds that are small deformations of Y_3, instead of a single Y_3. This resembles the family of circles in the circle compactification in Section 1.2.1. It turns out that there are two types of deformations of Y_3, namely the complex structure deformation and the (complexified) Kähler structure deformation. And the moduli space of Y_3 splits into a

[4] In general, the Hodge diamond is neither a diffeomorphic nor homeomorphic invariant; there exists pairs of Kähler manifolds sharing the same Hodge diamond but are not diffeomorphic or homeomorphic to each other. However, certain linear combinations of Hodge numbers can be diffeomorphic or homeomorphic invariants. See [32] for a complete discussion on this problem.

direct product of the complex and Kähler structure moduli spaces.

$$\mathcal{M} = \mathcal{M}_{\rm cs} \times \mathcal{M}_{\rm ks}\,. \tag{1.2.20}$$

This thesis focuses on the complex structure deformation, which gives the scalar fields in the vector multiplet of the four-dimensional $\mathcal{N} = 2$ supergravity. The complex structure moduli space $\mathcal{M}_{\rm cs}$ of a Calabi-Yau threefold Y_3 is a (projective) special Kähler manifold of dimension $h^{2,1}$ [22, 33]. To specify the special Kähler structure, we need to give the data of a symplectic vector and the symplectic pairing. The symplectic vector can be constructed from the so-called period vector, which tracks how the complex structure of Y_3 deforms by looking at the Hodge structure on the middle cohomology $H^3(Y_3, \mathbb{C})$ of Y_3. Hodge structures are the central object of this thesis and more detail on Hodge structures will be reviewed in section 1.4. For the present discussion, it suffices to recall that there is (p, q)-form decomposition of the middle cohomology

$$H^3(Y_3, \mathbb{C}) = H^{3,0} \oplus H^{2,1} \oplus H^{1,2} \oplus H^{0,3}\,, \tag{1.2.21}$$

satisfying

$$H^{p,q} = \overline{H}^{q,p}\,. \tag{1.2.22}$$

The decomposition defines a pure Hodge structure of weight three. Note that the notion of complex conjugation is closely tied with the choice of a complex structure on Y_3; changing the complex structure will change the conjugation of a (p, q)-form, which implies that the deformation of complex structure on Y_3 can be effectively tracked by the variation of Hodge structure on $H^3(Y_3, \mathbb{C})$. In practice, the variation of Hodge structure is tracked by the *period vector*, which works as follows. Firstly, to record the effect of the deformation of complex structure, we need to choose a basis of $H^3(Y_3, \mathbb{C})$ that is invariant under the change of complex structure. A commonly used basis is a symplectic basis generating the integral cohomology[5], so we choose an integral three-form basis[6] $\{\alpha_I, \beta^J\}$ with $I, J = 0, \ldots, h^{2,1}$ that generates the integral cohomology $H^3(Y_3, \mathbb{Z}) = \mathbb{Z}\langle\alpha_I, \beta^J\rangle$ and satisfies that

$$Q(\alpha_I, \alpha_J) = Q(\beta^I, \beta^J) = 0\,, \qquad Q(\alpha_I, \beta^J) = \delta_I^J\,, \tag{1.2.23}$$

[5]We do not consider the torsion part of the integral cohomology, hence all $H^*(Y, \mathbb{Z})$ in this paper is understood as $H^*(Y, \mathbb{Z})/\texttt{Tors}$. It is also possible to choose integral basis other than the symplectic ones, and this is done in the Appendix 2.D in order to adapt the homological mirror symmetry computation. For more information, see [34–38].

[6]This basis is sometimes defined to be the Poincaré dual of integral cohomology three-cycles. Technically, this is defining a flat Gauss-Manin connection by requiring that the flat frames are α_I, β^J.

where $Q(\alpha,\beta)=\int_{Y_3}\alpha\wedge\beta$ is the intersection product on the cohomology. Special geometry on the complex structure moduli space tells us that to track the change of the complex structure on a Calabi-Yau threefold Y_3, it suffices to track the change of the $(3,0)$-form Ω. Expanding the Ω in terms of the symplectic basis $\left\{\alpha_I,\beta^J\right\}$, we get the *period vector* $\Pi(z)=(Z^I,\mathcal{F}_I)^{\mathsf{T}}$, where z is a local coordinate in the complex structure moduli space[7]:

$$\Omega(z)=Z^I\alpha_I-\mathcal{F}_I\beta^I\,. \tag{1.2.24}$$

And the period vector Π is the symplectic vector defining the $\mathcal{N}=2$ effective theory. Now we see a good example relating the geometry of the compactification manifold to four-dimensional effective physics. For example, the complex structure moduli fields can be realised as the *special coordinates* of $\mathcal{M}_{\rm cs}$,

$$z^i=\frac{Z^i}{Z^0}\,,\qquad i=1,\ldots,h^{2,1}\,, \tag{1.2.25}$$

and using the general construction of $\mathcal{N}=2$ theories, we see that the Kähler potential of the scalar part of the theory that corresponds to the complex structure deformation of Y_3 is given by

$$e^{-K}=\mathbf{i}Q(\Pi,\overline{\Pi})=\mathbf{i}\int_{Y_3}\Omega\wedge\overline{\Omega}=\int_{Y_3}\Omega\wedge*\overline{\Omega}\,, \tag{1.2.26}$$

where the first equality is the $\mathcal{N}=2$ construction, the second equality follows from identifying the symplectic vector in $\mathcal{N}=2$ as the period vector of Y_3 which is basis-independent, and the third equality follows from the complex geometry of Y_3. Note that the expression for the Kähler potential depends on the complex structure moduli z^i, because a change of the complex structure results in a change of the complex conjugation $\overline{\Omega}$. The form of rightmost integral in (1.2.26) appears recurrently in geometry and we call it the *Hodge norm* of Ω. More precisely, for any two cohomology classes α,β on Y_3, we define their *Hodge inner product* as

$$h(\alpha,\beta)=\int_{Y_3}\alpha\wedge*\overline{\beta}\,, \tag{1.2.27}$$

and then the Hodge norm of a class α is denoted by

$$\|\alpha\|^2=h(\alpha,\alpha)\,. \tag{1.2.28}$$

[7]The minus sign in front of $\mathcal{F}_I$ is due to the convention of picking $\left\{Q(-,\alpha_I),Q(-,\beta^I)\right\}$ as a basis in the vector space dual of $H^3(Y_3,\mathbb{C})$, i.e., $Z^I=Q(\Omega,\beta^I),\mathcal{F}_I=Q(\Omega,\alpha_I)$. This is possible due to the non-degeneracy of Q. Another possible choice is to directly use the canonical dual basis of α_I,β^I, eliminating the minus sign. The latter is the convention used in Chapter 2.

So we see that the Kähler potential can be written simply as

$$e^{-K} = \|\Omega\|_z^2 \,, \tag{1.2.29}$$

where we use the subscript z to stress the dependency on the complex structure moduli. Note that the $(3,0)$-form must be consistently normalised; the freedom of a rescaling of Ω results in a Kähler transformation on the Kähler potential. The Hodge norm and Hodge inner product appears frequently in the four-dimensional physics coming from string compactification, and this enables the study of four-dimensional physics by Hodge theory on the compactification manifold in this thesis.

As a side remark, with the Kähler potential K defined, special Kähler geometry on the complex structure moduli space of Calabi-Yau threefolds implies that the entire $H^{2,1}$ space can be generated by taking Kähler covariant derivatives of Ω, namely

$$H^{2,1} = \mathbb{C}\langle \mathcal{D}_i \Omega \rangle \,, \tag{1.2.30}$$

where we define the Kähler covariant derivative[8] $\mathcal{D}_i\Omega = \partial_i\Omega + (\partial_i K)\Omega$ as in the $\mathcal{N}=2$ theory, and $i = 1, \ldots, h^{2,1}$ runs over the complex structure moduli z^i.

Besides the complex structure deformation, there is of course Kähler deformation in type IIB compactification, together with their counterparts in type IIA theory. We refer the more detailed discussion on these topics to standard literatures, for example [24, 25, 39]. This finishes our brief discussion on the Calabi-Yau threefold compactification of type II string theories.

1.2.4 F-theory on Calabi-Yau fourfolds

Compactifying type II string theory on Calabi-Yau threefolds result in $\mathcal{N}=2$ supergravity in four dimensions. It would be nice to reduce the amount of supersymmetry to make contact with real world, while retaining computational control of the theory. It turns out that this can be achieved by orientifolding the Calabi-Yau threefold, which projects out half of the physical degrees of freedom, resulting in an $\mathcal{N}=1$ supergravity. The type IIB Calabi-Yau orientifold construction can be nicely embedded in the so-called F-theory framework, which will be the physical setting of Chapter 3 and 4. In the following, we briefly introduce F-theory,

[8] We are being sloppy here. The true definition is that $\mathcal{D}_i\Omega = \nabla_i\Omega + (\partial_i K)\Omega$, where ∇_i is the Gauss-Manin connection in the i-th coordinate direction. Since our choice of three-form basis α_I, β^J are flat with respect to the Gauss-Manin connection, the covariant derivative on Ω becomes a normal derivative on the coefficients, i.e. the period vector.

review basics of $\mathcal{N} = 1$ supergravity in four-dimensions, set up basic notation of Calabi-Yau fourfolds, and link the $\mathcal{N} = 1$ physics to the geometry.

A brief introduction to F-theory

F-theory [40–43] is a strong coupling incarnation of type IIB string theory. One motivation is that when D7-branes are present in the 10-dimensional type IIB spacetime, the string coupling has to become strong in some region of the 10-dimensional spacetime. The problem of D7-branes cannot be ignored, because even if one starts with a type IIB setting without D7-brane, S-duality can transform the D7-brane-free theory into a theory with D7-branes. Thus, a generalised picture that includes the strong and weak coupling type IIB theory is desired. F-theory solves the problem by assuming a 12-dimensional quantum theory, which upon compactifying on a torus results in a 10-dimensional type IIB string theory with varying axio-dilaton, thus probing the full type IIB theory.

There are multiple ways to characterise F-theory and we will adopt the practical way of defining F-theory via M-theory and dualities. The definition goes as follows. Starting with M-theory and compactify it on a torus, topologically of the form $T^2 = S^1_{\mathrm{T}} \times S^1_{\mathrm{M}}$, one obtains type IIA theory compactified on the circle S^1_{T}, whose string coupling is given by (see, e.g., [25, Chapter 8])

$$g_{\mathrm{IIA}} = \frac{R_{\mathrm{M}}}{l_{\mathrm{s}}}\,, \tag{1.2.31}$$

where R_{M} is the radius of the circle S^1_{M} and l_{s} is the string length (inverse of the string tension). By taking R_{M} to be very small, a weakly coupled type IIA theory compactified on the remaining circle S^1_{T} pops out. Next, applying T-duality along the circle S^1_{T} results in type IIB theory compactified on a circle of radius (see, e.g., [25, Chapter 6])

$$R_{\mathrm{IIB}} = \frac{l_{\mathrm{s}}^2}{R_{\mathrm{T}}}\,. \tag{1.2.32}$$

Thus, by making R_{T} also small, the 10-dimensional type IIB theory is restored. The complex structure modulus of the M-theory torus T^2 exactly corresponds to the type IIB axio-dilaton. In this way, F-theory defined via M-theory is a generalisation of type IIB string theory with varying axio-dilaton. The process is shown in Figure 1.3.

Having related the 12-dimensional F-theory to 10-dimensional type IIB theory, the next step is to work for a four-dimensional spacetime. This can also be done with Calabi-Yau compactifications, but with four-folds instead of three-folds. Putting the 11-dimensional M-theory on a Calabi-Yau fourfold results in a

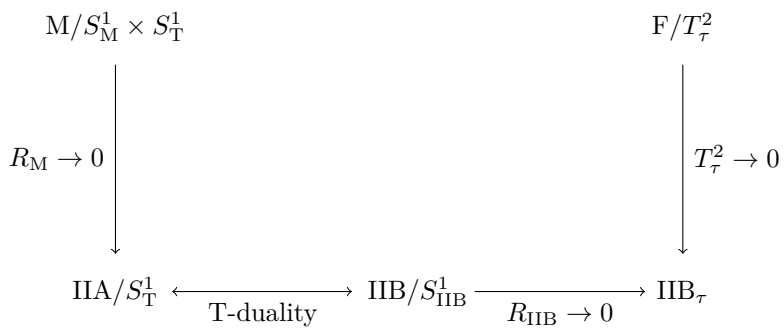

Figure 1.3: Defining F-theory via M-theory. The torus T^2_τ remembers the complex structure τ of $S^1_{\rm M} \times S^1_{\rm T}$, which corresponds to type IIB axio-dilaton τ. Under T-duality, one relates $R_{\rm IIB} = 1/R_{\rm T}$. The Kähler modulus $R_{\rm M}R_{\rm T}$ of T^2_τ is sent to zero in the F-theory limit.

three-dimensional $\mathcal{N} = 2$ supergravity. If we require the Calabi-Yau fourfold to be an elliptic fibration, then the three-dimensional $\mathcal{N} = 2$ supergravity can be lifted to a four-dimensional $\mathcal{N} = 1$ supergravity. We call the latter theory as coming from F-theory compactified on elliptic-fibred Calabi-Yau fourfolds.

We stress here that the above definition of F-theory via M-theory, and the compactification of F-theory on elliptic-fibred Calabi-Yau fourfolds are just heuristic. In practice, there are subtleties that need to be taken into account. We refer the interested reader to [44, 45] for more detailed discussion. The relation between F-theory and type IIB and type IIA orientifold vacua is discussed in Section 3.2.2.

$\mathcal{N} = 1$ supergravity in four-dimensions

Four-dimensional $\mathcal{N} = 1$ supergravity is structurally simpler but less constrained than its $\mathcal{N} = 2$ counterpart. The $\mathcal{N} = 1$ multiplets are the gravity multiplet, chiral multiplets, and vector multiplets. Our focus will be on the chiral multiplets, each of which contains a complex scalar field as the bosonic field. Complete treatment of $\mathcal{N} = 1$ supergravity can be found in [19, 46].

To define an $\mathcal{N} = 1$ theory with $n_{\rm C}$ chiral multiplets containing scalar fields z^i, one needs to provide the following data

- A *Kähler potential* $K(z, \bar{z})$, which is a real smooth strictly plurisubharmonic function[9] ;

[9] In the context of Kähler geometry, this is saying that the Hessian $(\partial_i \partial_{\bar{\jmath}} K)$ is positive semi-definite.

- A *superpotential* $W(z)$, which is a holomorphic function .

With the above data, the action of a four-dimensional $\mathcal{N}=1$ supergravity with $n_{\rm C}$ chiral multiplets takes the following form

$$S=\int_{\mathbb{R}^{3,1}}\frac{1}{2}R*1-g_{i\bar{j}}dz^i\wedge *d\bar{z}^{\bar{j}}-V\,, \tag{1.2.33}$$

where $i=1,\ldots,n_{\rm C}$ and the kinetic matrix $g_{i\bar{j}}$ is given by

$$g_{i\bar{j}}=\partial_i\partial_{\bar{j}}K\,, \tag{1.2.34}$$

while the scalar potential V is given by

$$V=e^K(g^{i\bar{j}}\mathcal{D}_iW\overline{\mathcal{D}}_{\bar{j}}\overline{W}-3W\overline{W})\,, \tag{1.2.35}$$

where the Kähler covariant derivative is defined as

$$\mathcal{D}_iW=\partial_iW+(\partial_iK)W\,. \tag{1.2.36}$$

Calabi-Yau fourfolds and the four-dimensional physics

A Calabi-Yau fourfold Y_4 is a four-dimensional Kähler space with trivial canonical bundle. It has three free Hodge numbers $h^{1,1},h^{2,1}$, and $h^{3,1}$. Similar to Calabi-Yau threefolds, $h^{1,1}$ parametrises the (complexified) Kähler moduli deformation, while $h^{3,1}$ corresponds to the complex structure deformation. A subtlety here is the three-form number $h^{2,1}$. This part is not understood as well as the other two Hodge numbers. In this work we will not touch this Hodge number, and its physical significance is discussed in [47, 48]. The Hodge diamond of a Calabi-Yau fourfold is shown in Figure 1.4. We will again focus on the middle cohomology $H^4(Y_4,\mathbb{C})$ and consider the complex structure deformation of Y_4. Like Calabi-Yau threefolds, the complex structure moduli space of Y_4 is a Kähler manifold. Unlike Calabi-Yau threefolds, the complex structure moduli space of Y_4 is not special Kähler. This will make a general analysis of Calabi-Yau fourfold compactifications more complicated. Detailed discussion can be found in [34, 49, 50]. Fortunately, for our purpose, considering a part of $H^4(Y_4,\mathbb{C})$ that mimics the middle cohomology of Calabi-Yau threefolds is enough. This is a subspace of $H^4(Y_4,\mathbb{C})$ that is called the *primitive, horizontal* subspace.

As usual, we denote the local coordinate on the complex structure moduli space of Y_4 by z^i, and the unique $(4,0)$-form on Y_4 by Ω. Then the Kähler potential K of the complex structure moduli space is given by

$$e^{-K}=\int_{Y_4}\Omega\wedge *\overline{\Omega}\,, \tag{1.2.37}$$

$$
\begin{array}{ccccccccc}
 & & & h^{4,4} & & & & & \\
 & & h^{4,3} & & h^{3,4} & & & & \\
 & h^{4,2} & & h^{3,3} & & h^{2,4} & & & \\
h^{4,1} & & h^{3,2} & & h^{2,3} & & h^{1,4} & & \\
h^{4,0} & & h^{3,1} & & h^{2,2} & & h^{1,3} & & h^{0,4} \\
 & h^{3,0} & & h^{2,1} & & h^{1,2} & & h^{0,3} & \\
 & & h^{2,0} & & h^{1,1} & & h^{0,2} & & \\
 & & & h^{1,0} & & h^{0,1} & & & \\
 & & & & h^{0,0} & & & &
\end{array}
\quad = \quad
\begin{array}{ccccccccc}
 & & & 1 & & & & & \\
 & & 0 & & 0 & & & & \\
 & 0 & & h^{1,1} & & 0 & & & \\
0 & & h^{2,1} & & h^{2,1} & & 0 & & \\
1 & & h^{3,1} & & h^{2,2} & & h^{3,1} & & 1 \\
 & 0 & & h^{2,1} & & h^{2,1} & & 0 & \\
 & & 0 & & h^{1,1} & & 0 & & \\
 & & & 0 & & 0 & & & \\
 & & & & 1 & & & &
\end{array}
$$

Figure 1.4: The Hodge diamond of a Calabi-Yau fourfold. The free parameters are $h^{1,1}$ parametrising the (complexified) Kähler deformation, $h^{3,1}$ parametrising the complex structure deformation, and a special sector $h^{2,1}$. The $h^{2,2}$ is fixed by $h^{2,2} = 2(22 + 2h^{1,1} + 2h^{3,1} - h^{2,1})$. See [49].

which is again the Hodge norm of Ω. Define similarly $\mathcal{D}_i\Omega = \partial_i\Omega + (\partial_i K)\Omega$, then the horizontal part of $H^4(Y_4, \mathbb{C})$ is generated by iterated action of $\mathcal{D}_i$ on Ω. In particular, the $H^{3,1}$ space automatically horizontal, as in Calabi-Yau threefolds,

$$H^{3,1} = \mathbb{C}\langle \mathcal{D}_i\Omega \rangle \,. \tag{1.2.38}$$

By conjugation, the subspaces $H^{1,3}$ and $H^{0,4}$ are also horizontal. Thus, the horizontal condition only affects $H^{2,2}$, and we denote the horizontal part of $H^{2,2}$ by $H^{2,2}_{\mathrm{h}}$.

To define the primitive part, we need the Kähler class ω of Y_4. Then the primitive middle cohomology consists of those classes that are annihilated by wedging with ω. Similar to the horizontal classes, all subspaces except for $H^{2,2}$ are primitive because of the structure of the Hodge diamond of a Calabi-Yau fourfold, and we denote the primitive part of $H^{2,2}$ by

$$H^{2,2}_{\mathrm{p}} = \left\{ \alpha \in H^{2,2} | \omega \wedge \alpha = 0 \right\} \,. \tag{1.2.39}$$

To relate the Calabi-Yau fourfold geometry to the $\mathcal{N} = 1$ data, we first stress that in order to have a valid four-dimensional $\mathcal{N} = 1$ theory, the Calabi-Yau fourfold has to be elliptically fibred. Then the complex structure moduli fields z^i belong to the $\mathcal{N} = 1$ chiral multiplets, whose kinetic matrix $g_{i\bar{\jmath}}$ is derived from the Kähler potential (1.2.37). Without further modification of the theory, the scalar fields z^i

are massless. One way to generate masses for the complex structure moduli is to turn on the G_4-flux, which originates from the 11D supergravity three-form field in M-theory, and is a cohomology class in the primitive horizontal middle cohomology $H^4_{\rm ph}(Y_4, \mathbb{Z})$. This will generate a superpotential W given by [51]

$$W(z) = Q(\Omega, G_4)\,, \tag{1.2.40}$$

where $Q(\alpha, \beta) = \int_{Y_4} \alpha \wedge \beta$ is the intersection form on Y_4. The scalar potential can then be derived from the superpotential. It can be neatly written in terms of the geometric quantities as

$$V(z) = c\left(\int_{Y_4} G_4 \wedge *G_4 - \int_{Y_4} G_4 \wedge G_4\right)\,, \tag{1.2.41}$$

where c is a function that does not depend on the complex structure moduli of Y_4. The scalar potential V in fact works both for $D = 3$, $\mathcal{N} = 2$ M-theory and $D = 4$, $\mathcal{N} = 1$ F-theory compactifications, and the difference lies in the coefficient function c. For example, in the context of F-theory compactified on an elliptically fibred Calabi-Yau fourfold, the coefficient is $c = \mathcal{V}_{\rm b}^{-2}$, where $\mathcal{V}_{\rm b}$ is the volume of the base. More discussion on this coefficient can be found in Section 3.2.1.

Note that the scalar potential (1.2.41) can be further rewritten as

$$V(z) = c\|G_4 - *G_4\|_z^2\,. \tag{1.2.42}$$

So this enables the study of $V(z)$ by asymptotic Hodge theory. In some sense the scalar potential generated by a G_4-flux measures the deviation of G_4 from being self-dual. This picture is adopted in Chapter 3.

1.3 Swampland conjectures

In this section, we introduce the swampland distance conjecture and the de Sitter conjecture that are studied in this thesis. As discussed earlier in the introduction, the swampland program refines the bottom-up approach of quantum gravity theory. It aims to distinguish those effective field theories that can be obtained by string compactification from the apparently consistent (anomaly-free) quantum field theories. The exact criteria are still unclear, because of the absence of a complete picture of quantum gravity. So the criteria are called swampland *conjectures*, and they are mostly inspired by string theory, and semi-classical arguments about black holes. One of the best understood swampland conjectures is the swampland

distance conjecture, together with its generalisations, which, roughly speaking, postulates the emergence of a tower of massless states that invalidates an effective field theory consistent with quantum gravity in some corners of the moduli space. The tower of states appearing in the distance conjecture also appears to be useful for other swampland conjectures, hence the distance conjecture is central in the zoo of swampland conjectures. Detailed review of the Swampland Program can be found in [52–56].

1.3.1 Distance conjecture

Now we would like to discuss the swampland distance conjecture [57] in more detail. The assumption is that the effective theory admits a UV completion into quantum gravity, and includes, besides the spacetime metric $g_{\mu\nu}$, real scalar fields ϕ^i valued in a field space $\mathcal{M}$, which carries a field space metric $G_{ij}(\phi)$ depending on the scalar fields. The field space metric defines the kinetic term of the scalar fields. In four dimensions, the action looks like

$$S = \frac{1}{\kappa_4^2}\int_{\mathbb{R}^{3,1}} \frac{1}{2}R * 1 - G_{ij} d\phi^i \wedge *d\phi^j + \cdots , \tag{1.3.1}$$

where "$\cdots$" denotes other couplings that can also depend on the scalar fields ϕ^i. The field space metric can be used to measure the traverse distance of a field configuration. The distance conjecture asserts:

- There exists a boundary point ϕ_{b} that is at infinite distance away from any other point ϕ in $\mathcal{M}$.
- Upon approaching the boundary point ϕ_{b}, the effective theory breaks down because an infinite tower of light states descends from the ultraviolet. Their masses are exponentially suppressed with respect to the minimal *geodesic distance* traversed by the scalar field ϕ.

One can be more precise about the statements in the swampland distance conjecture. The field space $\mathcal{M}$ is a Riemannian manifold with metric G_{ij} hence it is a metric space; its topology is generated by the minimal geodesic distance. So the first bullet of the distance conjecture implies that the field space $\mathcal{M}$ cannot be compact[10]. Mathematically speaking, the field space can be compactified $\mathcal{M} \hookrightarrow \overline{\mathcal{M}}$, where the compactified field space $\overline{\mathcal{M}}$ augments the original $\mathcal{M}$ by the boundary

[10] Note that this part is often presented as a conjecture independent from the distance conjecture.

points $\phi_{\rm b}$. Thus, the setting is perfectly in line with the moduli problem in geometry: The moduli spaces one encounters in geometry, such as the moduli spaces of Calabi-Yau manifolds, are rarely compact. When studying the geometry by deforming the regular spaces, one always runs into degenerate versions of the regular space, and these degenerate spaces populate the boundary of the original moduli space. By adding the boundary points, one obtains a compactified moduli space. Here in the swampland distance conjecture, the bulk of the moduli space consists of consistent-looking effective field theories, and the boundary corresponds to possible breakdown of the effective field theories when coupled with quantum gravity.

Next, we turn to the second bullet point in the distance conjecture by giving a more concrete statement. Denote the minimal geodesic distance[11] between ϕ and ϕ_0 by $d(\phi, \phi_0)$. Then the setting in the distance conjecture is that one considers a trajectory ϕ in the field space, starting from a point ϕ_0, and aiming towards an infinite boundary point $\phi_{\rm b}$. In this process, an infinite tower of states become increasingly light, whose mass follows the relation

$$M(\phi) = M(\phi_0) e^{-\gamma d(\phi, \phi_0)} \,, \tag{1.3.2}$$

with γ a constant not depending on the parameter of the path. We would like to stress that although the path ϕ is assumed to be general, the distance that enters into the mass of the tower is required to be the minimal geodesic distance $d(\phi, \phi_0)$. The physical setting is displayed in Figure 1.5.

There are still ambiguities in the distance conjecture and we would like to point out two of them here. One questions is about the onset of the exponentially light states: As we travel in the field space towards an infinite distance boundary point, when does the light tower start to show the exponential scaling in their masses? Put differently, this question is related to whether an infinite distance traverse in the field space is really needed in order to see the exponentially light tower. This is addressed in the refined distance conjecture [58], which says that the exponentially light tower is already important when the field displacement is transplanckian. We will discuss an important phenomenological consequence of the refined distance conjecture in the next paragraph. Another question regarding the distance conjecture is that: Suppose along one path towards the infinite distance point, one finds an exponentially light tower of states, is it the correct tower along

[11] Note that multiple geodesics with different lengths connecting any two points in a Riemannian manifold is possible. A Riemannian manifold in which every two points are connected by a unique geodesic is called a *uniquely geodesic space*. In general, it is non-trivial to determine if a Riemannian manifold is uniquely geodesic.

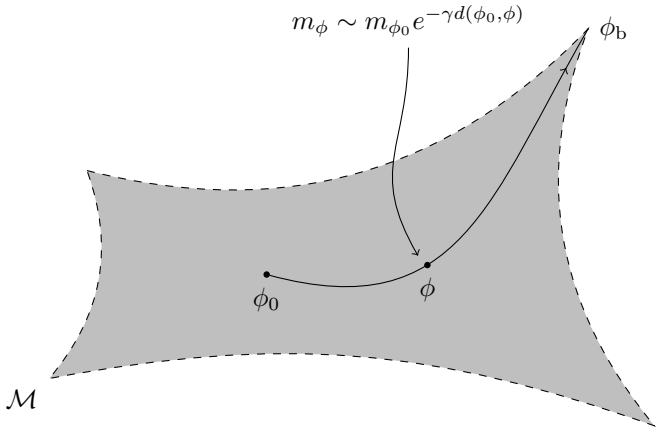

Figure 1.5: The physical setting of swampland distance conjecture. The field space $\mathcal{M}$ has an infinite distance boundary point $\phi_{\rm b}$. Starting from ϕ_0 and travelling towards $\phi_{\rm b}$, an infinite tower of exponentially light states descends from the ultraviolet. Note that $d(\phi_0, \phi)$ is the minimal geodesic distance.

other paths? This question will be addressed in a forthcoming work [59] utilising the tamed geometry framework that is successfully used to establish the finiteness of flux vacua [14]. This question can also be tied with the classification of the origin of possible light towers in the limit, which prompts the emergent string conjecture [60]. The emergent string conjecture states that, under string dualities, the light tower in the infinite distance limit is either the tower of states living on a tensionless string, or a light Kaluza-Klein tower inducing a decompactification. For a review on the emergent string conjecture, see [61].

The refined distance conjecture has a direct impact on the inflation cosmology. There exists many large-field inflation models trying to explain the inflation of our universe using a scalar field that has a transplanckian displacement in the field space. According to the refined distance conjecture, such operations are not compatible with the effective field theory one started with; passing certain stage in the field space, the effective field theory compatible with quantum gravity will inevitably break down due to the light tower of states. An example of large-field inflation model is the family of axion monodromy inflation models and we will use asymptotic Hodge theory to study the break down of such models when the field excursion is large in Section 3.7 and Chapter 4.

1.3.2 de Sitter conjecture

The de Sitter conjecture is a swampland conjecture that will be addressed in Chapter 3. The basic idea is that while constructing anti de Sitter and Minkowski vacua is easy in string theory, it is extremely hard to obtain an undebatable de Sitter solution that is capable of describing our observed universe. This phenomenon motivates the authors of [62] to propose a conjecture on the shape of all scalar potentials that can appear in string theory, which forbids the existence of any semi-stable vacua with positive cosmological constant, i.e. de Sitter vacua. Soon after the original de Sitter conjecture was proposed, the authors of [63] completed the proposal to exclude some counter-examples to the original conjecture. We now review the statement of the de Sitter conjecture in [63], and relate it with the previously discussed swampland distance conjecture.

The setting of the de Sitter conjecture is similar to the distance conjecture. The assumption is that the four-dimensional effective action admits a UV completion into quantum gravity, and is of the form

$$S = \frac{1}{\kappa_4^2}\int_{\mathbb{R}^{3,1}} \frac{1}{2}R * 1 - G_{ij} d\phi^i \wedge *d\phi^j - V(\phi) + \cdots , \tag{1.3.3}$$

where we have included a potential $V(\phi)$ for the scalar fields ϕ^i. As usual, a vacuum of the theory is realised by a minimum of the scalar potential, which is identified as the cosmological constant of the vacuum. The vacuum under consideration can be global or local. The first case is dubbed as stable, while the latter is called meta-stable. The de Sitter conjecture states that the scalar potential must satisfy either

$$\|\nabla V\| \geq \frac{c}{M_{\mathrm{p}}} V , \tag{1.3.4}$$

or

$$\min(\mathrm{Hess}\, V) \leq -\frac{c'}{M_{\mathrm{p}}^2} V , \tag{1.3.5}$$

where $\|\nabla V\|$ is computed with respect to the field space metric G_{ij} and $\min(\mathrm{Hess}\, V)$ is a shorthand for the minimal eigenvalue of the Hessian[12] of V. The constant c is conjectured to be $\mathcal{O}(1)$. The original de Sitter conjecture [62] only asserts property (1.3.4) on the scalar potential.

[12]The Hessian is defined as the matrix of the second covariant derivatives of V; in the coordinate basis, we have $\mathrm{Hess}\, V = (\nabla_i \nabla_j V)$, where the covariant derivatives are defined on the scalar field space $\mathcal{M}$ carrying the field space metric G_{ij}.

An immediate consequence of the first condition in the de Sitter conjecture is that there is no possible scalar potential that realises de Sitter minima, as such vacua violate the inequality (1.3.4).

The de Sitter conjecture is related to the distance conjecture, when we work around infinite distance singularities in the field space. The idea is that the infinite tower of light states will contribute to the total entropy of the de Sitter vacuum of the effective field theory. But a result from Bousso [64] bounds the total entropy by the Gibbons-Hawking entropy of the de Sitter event horizon, which depends on the cosmological constant of the vacuum. The interplay of these two statements implies a runaway behaviour of the scalar potential $V(\phi)$ along certain direction that is pushed towards the limit, and the runaway behaviour is consistent with the de Sitter conjecture. For more detailed discussion, see the original paper [63] and the review [54].

In closing this section, we would like to point out a recent proposal of an underlying principle of the swampland conjectures. This proposal is called the tameness conjecture [65] and it has attracted substantial interest in the community. One motivation of the tameness conjecture is the observation that in all string vacua constructed so far, the four-dimensional physical couplings, scalar potentials, etc., are clearly not arbitrary functions. On the other hand, a similar observation also exists in the Hodge theory community on the mathematical side. Recently, the paper [12] made an important progress by realising this picture, showing that the period mappings in Hodge theory are not arbitrary holomorphic functions, but must be some well-behaved "tamed" functions. This mathematical work inspired the authors of [14] to use the tamed geometry, as a replacement to the asymptotic Hodge theory, to show the finiteness of flux vacua, and finally resulting in the tameness conjecture. Compared to the asymptotic Hodge theory which is quite complicated and works over the complex numbers, the tamed geometry is considerably much simpler, and works well even in real geometries. It is expected that the tamed geometry will bring fruitful insights into the Swampland Program in the future.

1.4 Asymptotic Hodge Theory

In this section, we discuss informally the motivation behind asymptotic Hodge theory. Our viewpoint will be geometrical, mainly focusing on studying possible algebraic structures on the middle cohomology of a family of degenerating Calabi-Yau spaces. We use two example geometries to illustrate the various constructions

in asymptotic Hodge theory. They are Calabi-Yau one-folds, a.k.a torus, and Calabi-Yau threefolds.

1.4.1 The cohomology of a smooth Calabi-Yau threefold

Let us first review the well-known structure on the cohomology of a Calabi-Yau threefold. The conclusion actually holds for any compact Kähler manifold, but we choose Calabi-Yau threefolds because they are complicated enough for physicists to play with and carry cohomology with many degrees, while at the same time simple enough, to the extent that many of their cohomologies are vanishing, so that it is fairly easy to illustrate some classical aspects of Hodge theory with them. Complete discussion on this topic can be found in [66–70] and [71, Chapter 1].

Let Y be a smooth Calabi-Yau threefold, which is a smooth Kähler manifold of complex dimension $n = 3$, whose canonical bundle is holomorphically trivial.

From the theory of complex manifolds, the Calabi-Yau Y has cohomologies with degrees k varying from zero to six. At each degree, there is a Hodge decomposition

$$H^k(Y,\mathbb{C}) = H^{k,0}(Y) \oplus H^{k-1,1}(Y) \oplus \cdots \oplus H^{0,k}(Y)\,, \tag{1.4.1}$$

satisfying

$$H^{p,q}(Y) = \overline{H}^{q,p}(Y)\,. \tag{1.4.2}$$

When there is no danger of confusion, we will often omit the argument Y in $H^{p,q}(Y)$ and write $H^{p,q}$ for simplicity. In the space $H^{p,q}$ lives those cohomology classes that can be locally represented by complex differential forms with $p\ dz$'s and $q\ d\bar{z}$'s. We say that $H^k(Y,\mathbb{C})$ carries a *Hodge structure of weight k*. For simplicity, we will also write $H^k_{\mathbb{C}}$ for $H^k(Y,\mathbb{C})$. Similar notations apply to the integral, rational, and real cohomologies.

It is natural to work with the total cohomology of the Calabi-Yau Y, which is the sum of cohomologies of all degrees $H^*(Y,\mathbb{C}) = \bigoplus_k H^k(Y,\mathbb{C})$. The total cohomology is a complex vector space, and there is a nice way to pictorially work with it. We depict the $H^*_{\mathbb{C}} = \bigoplus_{p,q} H^{p,q}$ resembling the Hodge diamond with a rotation, but this time we focus on the vector subspaces $H^{p,q}$ instead of the numerical dimensions $h^{p,q}$. We fill in different $H^{p,q}$ with dots that can be understood as basis elements of $H^{p,q}$, and later on when we discuss special operators acting on $H^*_{\mathbb{C}}$ we can directly specify the operators using arrows on the diagram. Such a diagram is also called *Hodge diamond* and it will be clear from context which version of Hodge diamond is under discussion. A Calabi-Yau threefold with $h^{1,1} = 1$ and $h^{2,1} = 2$ has a Hodge diamond of the form shown in Figure 1.6.

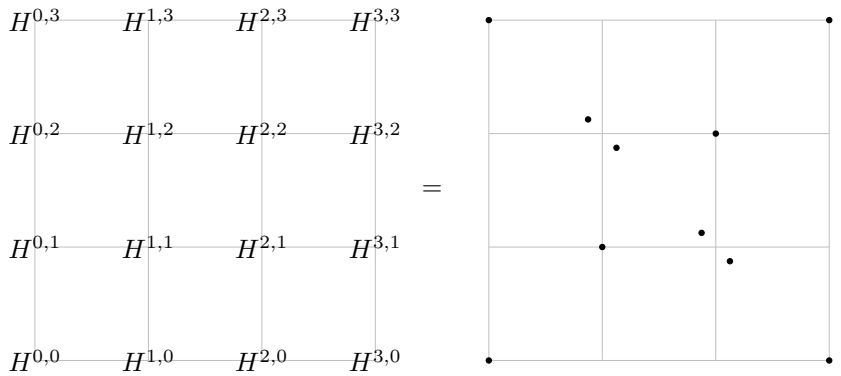

Figure 1.6: The Hodge diamond of a Calabi-Yau threefold with $h^{1,1} = 1$ and $h^{2,1} = 2$. Every dot in the diagram represents a suitably chosen basis vector of the corresponding subspace $H^{p,q}$.

Since the cohomology at each degree carries a Hodge structure of that degree, an immediate question arises: Does $H^*_{\mathbb{C}}$ carry any Hodge structure? If so, what is the weight of that Hodge structure?

To answer this question, one might be able to cook up some Hodge structure with some definite weight in some *ad hoc* way for some very special Kähler manifolds. However, it turns out that a more natural and useful thing to do is to extend the notion of a Hodge structure of a fixed weight, by allowing a Hodge structure with a *mix* of different weights. Such generalised Hodge structures are called *mixed Hodge structures*, and a mixed Hodge structure consisting of a single weight, such as those living on $H^k_{\mathbb{C}}$, is called a *pure Hodge structure*. So, a prototypical example of a mixed structure is exactly the total cohomology $H^*_{\mathbb{C}}$ of a Calabi-Yau threefold, which is a mix of pure Hodge structures of degree k varying from zero to six. Moreover, it satisfies a nice property that $H^{p,q} = \overline{H}^{q,p}$ for all p, q. Any mixed Hodge structure that resembles the mixed Hodge structure on $H^*_{\mathbb{C}}$ is called $\mathbb{R}$-split, and such a mixed Hodge structure can be understood as a direct sum[13] of pure Hodge structures. Note that we have not touched the precise definition of a mixed Hodge structure, and it will be addressed in Appendix 1.D.1.

Now we would like to introduce an example of the most important concept in asymptotic Hodge theory applied to string theory: The mixed Hodge structure,

[13] More precisely, we are talking about direct sums in the category of mixed Hodge structures. So a direct sum of the underlying vector space does not suffice to be a direct sum of mixed Hodge structures, which has to be compatible with the various filtrations.

which is the total cohomology $H^*_{\mathbb{C}}$ under discussion, is actually compatible with a representation of the Lie algebra $\mathfrak{sl}(2)$. Recall that the Lie algebra $\mathfrak{sl}(2)$ is generated by three operators: the lowering operator N, the rising operator N^+, and the neutral operator Y. They satisfy the following commutation relations

$$[Y, N] = -2N\,, \quad [Y, N^+] = 2N^+\,, \quad [N^+, N] = Y\,. \tag{1.4.3}$$

To make $H^*_{\mathbb{C}}$ into an $\mathfrak{sl}(2)$-representation, we need to specify how the operators representing N, N^+, and Y act on $H^*_{\mathbb{C}}$.

The rising operator is immediate. Define the *Lefschetz operator* L by wedging with the Kähler class ω

$$L\alpha = \omega \wedge \alpha\,, \qquad \text{for} \quad \alpha \in H^*_{\mathbb{C}}\,. \tag{1.4.4}$$

Note that the point of using another notation L instead of using ω is to emphasise that the Lefschetz operator is defined at the level of cohomology, instead of forms. Then we identify the rising operator with the Lefschetz operator $N^+ = L$.

To find the lowering operator, we need the Hodge inner product h, define on $H^*_{\mathbb{C}}$ by

$$h(\alpha, \beta) = \int_Y \alpha \wedge *\overline{\beta}\,, \qquad \text{for} \quad \alpha, \beta \in H^*_{\mathbb{C}}\,. \tag{1.4.5}$$

And we define the adjoint Lefschetz operator Λ as the hermitian conjugate of the Lefschetz L with respect to h, i.e.,

$$h(\Lambda\alpha, \beta) = h(\alpha, L\beta)\,, \qquad \text{for all} \quad \alpha, \beta \in H^*_{\mathbb{C}}\,. \tag{1.4.6}$$

A straightforward computation, using $*^2 = (-1)^{\frac{k(k-1)}{2}}$ on $H^k_{\mathbb{C}}$, leads to

$$\Lambda = *^{-1} \circ L \circ *\,. \tag{1.4.7}$$

The lowering operator is then given by the adjoint Lefschetz operator, $N = \Lambda$.

Finally, computing $[L, \Lambda]$ yields the neutral operator Y, given by

$$Y\alpha = (k - n)\alpha\,, \qquad \text{for} \quad \alpha \in H^k_{\mathbb{C}}\,, \tag{1.4.8}$$

satisfying $[L, \Lambda] = Y$. For Calabi-Yau threefolds we have $n = 3$. It can be further checked that (1.4.3) is satisfied [66–69, 72].

Interestingly, the $\mathfrak{sl}(2)$-action on $H^*_{\mathbb{C}}$ plays well with the mixed Hodge structure on $H^*_{\mathbb{C}}$. One has

$$L : H^{p,q} \to H^{p+1,q+1}\,, \qquad \text{and} \qquad \Lambda : H^{p,q} \to H^{p-1,q-1}\,, \tag{1.4.9}$$

and Y stabilises $H^{p,q}$ with the scalar multiplication of $p+q-n$.

It is instructive to picture the entire mixed Hodge structure with its $\mathfrak{sl}(2)$-action in the Hodge diamond of a Calabi-Yau threefold with $h^{1,1}=1$ and $h^{2,1}=2$ shown in Figure 1.7.

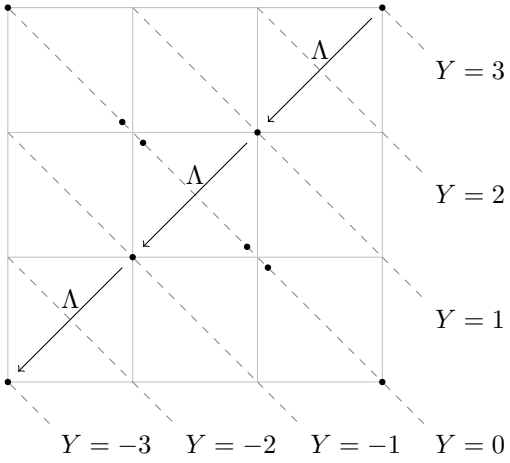

Figure 1.7: The total cohomology $H^*(Y,\mathbb{C})$ of a Calabi-Yau threefold with $h^{1,1}=1$ and $h^{2,1}=2$. The $\mathfrak{sl}(2)$-actions of Y and Λ are shown. The operator L acts exactly in the opposite direction of Λ. Note that Λ kills the entire H^3.

We have now seen that the total cohomology of a smooth Calabi-Yau threefold carries an $\mathbb{R}$-split mixed Hodge structure. In string theory, we would also like to consider Calabi-Yau's varying in a family, with different complex and Kähler structures. In Hodge theory, this amounts to a variation of Hodge structure.

1.4.2 Variation of Hodge structure on elliptic curves

Let us illustrate the basic concepts in variation of Hodge structures using the elliptic curve as an example. The concrete example that we will consider will be the Legendre family of an elliptic curve. We follow the approach in [73, Chapter 1]. The defining equation of an elliptic curve E_λ is given by

$$y^2 = x(x-1)(x-\lambda)\,, \quad \lambda \in \mathbb{P}^1\,. \tag{1.4.10}$$

Although for every $\lambda \neq 0, 1$, the resulting manifolds are all diffeomorphic as a two-dimensional torus, they are not isomorphic as complex manifolds[14], i.e., they can have different complex structures.

It is convenient to assemble the family of all elliptic curves together, so that we obtain a fibration $\mathsf{E} \to \mathbb{P}^1$, with the fibre over $\lambda \in \mathbb{P}^1$ the elliptic curve E_λ. We pick any $\lambda \neq 0, 1$, and take a disc Δ centred around λ that does not include 0 or 1. Thus we get a local picture of a smooth family of elliptic curves. The picture we should have in mind is given in Figure 1.8.

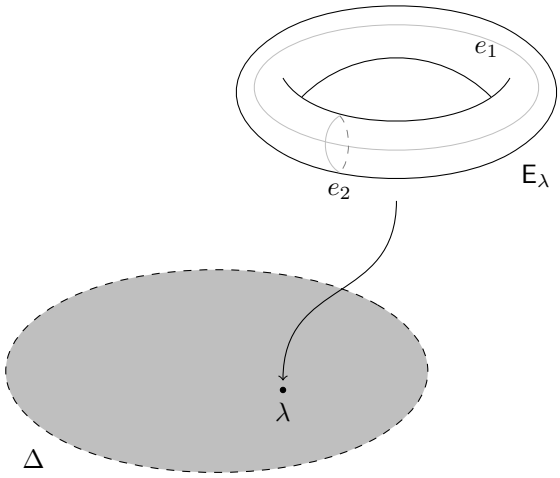

Figure 1.8: A local picture of a smooth family of elliptic curves. The open disk Δ does not contain 0 or 1. Over each $\lambda \in \Delta$ there is a smooth elliptic curve E_λ. The chosen real homology cycles e_1 and e_2 are the Poincaré dual of the cohomology basis e^1 and e^2.

We will be interested in the deformation of the Hodge structure on the middle cohomology $H^1(\mathsf{E}_\lambda, \mathbb{C})$ as we change λ. In order to do this, we use the period vector as we did in Calabi-Yau threefolds in Section 1.2.3. It is defined as follows. Suppose at a fixed λ, we have chosen an integral basis e^1, e^2 of the cohomology $H^1(\mathsf{E}_\lambda, \mathbb{Z})$ that is unaffected by the deformation of complex structures. We also

[14]For example, a holomorphic function on E_λ might not be holomorphic any more on $\mathsf{E}_{\lambda'}$ with $\lambda' \neq \lambda$.

choose a complex basis $\omega, \overline{\omega}$ of the complex cohomology, satisfying

$$H^{1,0} = \mathbb{C}\omega\,, \quad H^{0,1} = \overline{H}^{1,0} = \mathbb{C}\overline{\omega}\,. \tag{1.4.11}$$

Then the complex basis ω can be expanded into the integral basis as follows

$$\omega = \Pi_1 e^1 + \Pi_2 e^2 = (e^1, e^2)\mathbf{\Pi}\,, \tag{1.4.12}$$

where the complex vector of coefficients $\mathbf{\Pi} = (\Pi_1, \Pi_2)^{\mathrm{T}}$ is called the period vector, and is a function on the parameter λ. Now let us change λ. To record and compare the change of ω, we can either keep the period vector constant and let the integral basis e^1, e^2 vary, or keep the integral basis constant and let the period vector be a function of λ. It turns out that the latter approach is more useful, and we will adopt this convention throughout the thesis. Namely, locally, we fix an integral basis e^1, e^2 and describe the variation of Hodge structure by making the period vector $\mathbf{\Pi}(\lambda)$ a function of λ. In this way, the period vector can be shown to satisfy the *Picard-Fuchs differential equation*, which in the elliptic curve example has the following form [73, Equation 1.11]

$$\lambda(\lambda - 1)\mathbf{\Pi}'' + (2\lambda - 1)\mathbf{\Pi}' + \frac{1}{4}\mathbf{\Pi} = 0 \tag{1.4.13}$$

By solving the Picard-Fuchs equations, we get the period vector describing the variation of Hodge structure. Note that we have omitted the discussion about the boundary condition in the Picard-Fuchs equation, without which one cannot fix a solution. The boundary condition is usually supplied by looking into the degenerate manifold, say at $\lambda = 0, 1$. Since this is not the focus of this thesis, we refer to [74] for a practical discussion in the context of mirror symmetry.

Now we have discussed how to track the variation of Hodge structure along a smooth local family of elliptic curves. The next step would be to globalise the discussion, glueing the period vectors along the overlapping discs. But one immediately runs into a problem: The elliptic curve ceases to be a smooth manifold at $\lambda = 0, 1$. So we need a way to describe the behaviour of the Hodge structures as the manifold degenerates, and preferably in differential geometric language. This is achieved by the theory of degenerating variation of Hodge structures.

1.4.3 Degeneration of Hodge structures on elliptic curves

In this section, we enter the core topic of this thesis, namely how to manage the Hodge structure in a degenerating family. We continue following [73, Chapter 1].

To be concrete, let us first be clear with the setup and the goal. We focus on a neighbourhood of the singular elliptic curve E_0 with $\lambda = 0$, and work locally in a punctured disc Δ^* centering at $\lambda = 0$, which does not contain the other singularity $\lambda = 1$. On the whole punctured disc Δ^*, the family is still smooth. The singular fibre E_0 exactly fills in the hole of the punctured disc, and it is called the *central fibre*. We would like to describe the Hodge structure on $H^1(\mathsf{E}_\lambda, \mathbb{C})$ as $\lambda \to 0$.

It turns out that the Hodge structure on $H^1(\mathsf{E}_\lambda, \mathbb{C})$ is closely related to the structure of $H^1(\mathsf{E}_0, \mathbb{C})$, where the latter needs to be properly defined in the framework of algebraic geometry in order to allow the direct study of singular spaces. We will not go into algebraic geometry, but, instead, describe the result heuristically, so that one can see how mixed Hodge structure emerges. Topologically, the central fibre E_0 is a "pinched torus", a curve with a node. We display its shape in Figure 1.9.

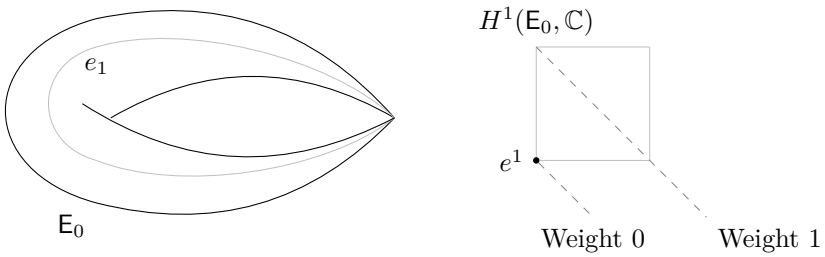

Figure 1.9: The topology of the central fibre E_0. On the left picture, we see that only one of the homology cycle e_1 survives. On the right picture, the middle cohomology is a mixed Hodge structure with weight zero and weight one pieces. The weight one part happens to be zero for the pinched elliptic curve, and the weight one piece is provided by e^1.

From Figure 1.9, we immediately see that the Hodge structure on $H^1(\mathsf{E}_0, \mathbb{C})$ cannot be a pure weight one Hodge structure, because there is only one one-cycle surviving. In order to get a pure Hodge structure of weight one, i.e. $H^1(\mathsf{E}_0, \mathbb{C}) = H^{1,0} \oplus \overline{H}^{1,0}$, by (a suitable version of) Poincaré duality, the number of one-cycles has to be even.

It turns out that the middle cohomology $H^1(\mathsf{E}_0, \mathbb{C})$ in this case carries a mixed Hodge structure consisting of weight zero and weight one parts. It happens that the weight one part is vanishing, and the dual of the single one cycle concentrates in the weight zero sector. It is regarded as a mixed Hodge structure, instead of a

pure weight zero structure, because this fits in the more general pattern in the degeneration of algebraic curves. If we start from a curve of higher genus and shrink one of its one-cycle to zero, then the middle cohomology will have both weight one and weight zero parts. The weight one part consists of those one-cycles away from the vanishing cycle, and the weight zero part is still populated by the cycles that intersects with the vanishing cycle. The Hodge diamond of $H^1(\mathsf{E}_0, \mathbb{C})$ is also shown in 1.9. The reader can temporarily use the intuition in Figure 1.6 to understand this Hodge diamond, except that the diamond provides a decomposition of the middle cohomology $H^1(\mathsf{E}_0, \mathbb{C})$, instead of the total cohomology. Actually, the Hodge diamond of a mixed Hodge structure is depicting its Deligne splitting, which is discussed in Appendix 1.D.1.

So this is the middle cohomology of a singular algebraic curve. In fact, modern mathematics and physics tell us that it is unnatural to just study one singular object on its own. For example, in circle compactification, the dynamics of gravity could drive the compactification space to jump between singular circle ($r = 0$) and a normal circle ($r > 0$). Hence, it is more natural to assemble the singular space together with its nearby regular spaces into a family and study them as a whole. Thus, it would be nice to relate the mixed Hodge structure on $H^1(\mathsf{E}_0, \mathbb{C})$ with some structure on $H^1(\mathsf{E}_\lambda, \mathbb{C})$ when λ is close to 0. This is indeed the case, and the result is that $H^1(\mathsf{E}_\lambda, \mathbb{C})$ also carries a mixed Hodge structure, called the *limiting mixed Hodge structure*.

Note that for $\lambda \neq 0$, the middle cohomology $H^1(\mathsf{E}_\lambda, \mathbb{C})$ is two-dimensional. So the limiting mixed Hodge structure on $H^1(\mathsf{E}_\lambda, \mathbb{C})$ cannot be exactly the same as the mixed Hodge structure on $H^1(\mathsf{E}_0, \mathbb{C})$. In fact, the limiting mixed Hodge structure on $H^1(\mathsf{E}_\lambda, \mathbb{C})$ can be interpreted as a combination of two mixed Hodge structures, one of them comes from the singular variety E_0, and the other comes from the open variety that is $\mathbb{P}^1$ with two points deleted. See [73, Chapter 1] for a complete discussion. This geometric picture is shown in Figure 1.10.

The proper way to construct the limiting mixed Hodge structure needs the monodromy data of the family E_λ. Namely, if we go around the singularity $\lambda = 0$ in the local patch Δ^*, then the differential forms e^1, e^2 will enjoy a monodromy. The asymptotic Hodge theory [75, 76] then produce the limiting mixed Hodge structure on $H^1(\mathsf{E}_\lambda, \mathbb{C})$ by using this monodromy operator. The theory also further modifies the limiting mixed Hodge structure into something as simple as the mixed Hodge structure on the total cohomology that is discussed in Section 1.4.1, and make the modified mixed Hodge structure on $H^1(\mathsf{E}_\lambda, \mathbb{C})$ compatible with an $\mathfrak{sl}(2)$-algebra that is constructed out of the monodromy. Thus asymptotic Hodge theory simpli-

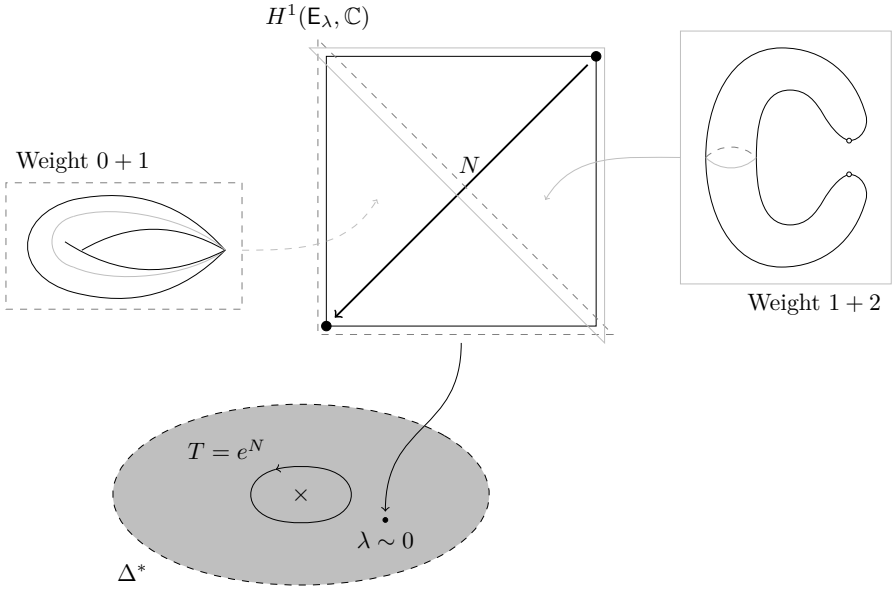

Figure 1.10: The limiting mixed Hodge structure on $H^1(\mathsf{E}_\lambda, \mathbb{C})$ with $\lambda \sim 0$ is a combination of two mixed Hodge structures. The monodromy operator acts on the integral basis e^1 and e^2 of $H^1(\mathsf{E}_\lambda, \mathbb{C})$, and its logarithm N is in analogy to the Λ operator in Figure 1.7. The weight zero and one part of the limiting mixed Hodge structure encircled by thin dashed triangle comes from surviving cycle the degenerate torus, and the weight one and two part encircled by the thin solid triangle comes from the surviving cycle in the two-punctured sphere. Note that after filling the two punctures in the punctured sphere, and identifying these two puncture locations in the filled sphere, we get topologically the pinched torus E_0. The filled sphere, remembering the two puncture locations, is called a normalisation of the pinched torus. See [73, Chapter 1] for a precise discussion about this picture.

fies the study of degenerations in a family, which is desired in the verification of swampland conjectures. More discussion on this will be in the next sections.

1.4.4 Using asymptotic Hodge theory in string theory

In this section, we briefly discuss the important results in asymptotic Hodge theory that are applied to the study of swampland conjectures in this thesis. Detailed mathematical discussion on this topic can be found in [77–80] and [71, Chapter 7].

For physical applications, see [5, 13, 14, 53, 81–93]. The idea is very simple: many interesting physical quantities, such as the mass of a physical state, or the scalar potential of the effective four-dimensional physics, can be expressed into the Hodge norm or Hodge inner product of certain cohomology classes on the Calabi-Yau manifolds. Asymptotic Hodge theory exactly provides the tools to study these norms and inner products, by interpreting the cohomology as a mixed Hodge structure compatible with a representation of commuting $\mathfrak{sl}(2)$-triples. One can then get useful estimates of these physical quantities as the Calabi-Yau degenerates, hence check some of the swampland conjectures in the context of Calabi-Yau compactification.

Singularity in the period and monodromy

First we need to specify the geometric setting. We work with a (complex) N-dimensional moduli space with singularities. Focusing on one singular locus, we choose local coordinates z_i on the moduli space, such that the singular locus is at $z_1 = \cdots = z_n = 0$. In other words, we work in a local neighbourhood of the singularity of the form

$$(\Delta^*)^n \times \Delta^{N-n}\,, \tag{1.4.14}$$

where $\Delta^* = \{0 < |z| < 1\}$ is the punctured disk, and $\Delta = \{|z| < 1\}$ is the unit disk. To simplify the discussion, we will now assume $n = N$. The point is that all the data computed by asymptotic Hodge theory focuses on the degenerating part, i.e. the part depending on $(\Delta^*)^n$. And if $n < N$, then these data will depend on the coordinates on Δ^{N-n} real-analytically. We refer to [76, Remarks (4.65) Part (ii)] for a through discussion.

Around a singularity, we denote the period mapping by $\Phi(z)$. We understand it as an abstract holomorphic mapping

$$\Phi : \text{Moduli space} \longrightarrow \text{Space of Hodge filtrations}\,, \tag{1.4.15}$$

so it assigns to each point z the corresponding Hodge filtration $\Phi^p(z)$ on the middle cohomology of the Calabi-Yau. A special case is the period vector in Calabi-Yau threefolds, which is understood as $\Phi^3(z)$. Because of the special geometry on Calabi-Yau threefold moduli spaces, we can generate lower flags by taking derivatives. Note that the target of this map remembers the Hodge filtrations, instead of the Hodge decomposition. This is because in this way the map Φ is holomorphic. It is impossible to get a non-trivial holomorphic period map if the target remembers the Hodge decomposition.

The point $z = 0$ corresponds to the singular Calabi-Yau threefold, so the holomorphic period mapping develops monodromy around $z = 0$. Analytic continuation

around $z_i = 0$ defines a monodromy operator T_i for every $i = 1, \ldots, n$

$$\Phi(z_1, \ldots, e^{2\pi \mathbf{i}} z_i, \ldots, z_n) = T_i \Phi(z)\,. \tag{1.4.16}$$

It is often useful to not work with the coordinates z_i, where the period mapping is multi-valued because of monodromy. To make this simpler, we work with the universal covering of $(\Delta^*)^n$, which is the n-dimensional upper half plane $\mathfrak{H}^n = \{t_i = x_i + \mathbf{i} y_i | y_i > 0\}$. The covering map is given by

$$\begin{aligned} p : \mathfrak{H}^n &\to (\Delta^*)^n \\ (t_i) &\mapsto (e^{2\pi \mathbf{i} t_i} = z_i)\,. \end{aligned} \tag{1.4.17}$$

The singularity at $z_i = 0$ is now located at $t_i \to \mathbf{i}\infty$ on the upper half plane. The period map $\Phi(z)$ lifts to a period mapping on the upper half plane $\Phi(t)$. We distinguish these two mapping by their arguments, and without further clarification, a period mapping Φ always refers to the lifted one. The monodromy property of the lifted period mapping is characterised by

$$\Phi(t_1, \ldots, t_i + 1, \ldots, t_n) = T_i \Phi(t)\,. \tag{1.4.18}$$

Lastly, the monodromy operators T_i coming from geometry is always *quasi-unipotent*, meaning that there are positive integers m, n such that

$$(T_i^m - \mathbb{1})^n = 0\,. \tag{1.4.19}$$

It can be shown that by a base-change, i.e. twisting the base coordinates $z \mapsto z^k$ for some k, the exponent m can always be set to $m = 1$, and the monodromy is then unipotent of order n. We assume such a modification is always done. And we denote the logarithm of the monodromy operators T_i by N_i

$$N_i = \log T_i\,. \tag{1.4.20}$$

Because of (1.4.19) with $m = 1$, the operators N_i are all nilpotent of order n

$$N_i^n = 0\,, \quad \text{for all} \quad i\,. \tag{1.4.21}$$

Nilpotent orbits and limiting mixed Hodge structures

The period map $\Phi(t)$ can be very complicated near the singularity $t \to \mathbf{i}\infty$. The *nilpotent orbit theorem* provides a powerful yet simple approximation of Φ near the singularity. The theorem produces an important quantity called the *limiting Hodge filtration* $F_{\lim}$, which is given by

$$F_{\lim} = \lim_{t \to \mathbf{i}\infty} e^{-\sum_j t_j N_j} \Phi(t)\,, \tag{1.4.22}$$

where N_j is the logarithm of the monodromy operator T_i. It is important to remark that the limiting Hodge filtration $F_{\lim}$ is not a pure Hodge filtration, i.e. if we define $H^{p,q}_{\lim} = F^p_{\lim} \cap \overline{F}^q_{\lim}$, then the cohomology does *not* split into a direct sum of $H^{p,q}_{\lim}$. In fact, the limiting Hodge filtration defines a mixed Hodge structure on the cohomology. We will come back to this point later.

The nilpotent orbit theorem states that the nilpotent orbit

$$\Psi(t) = e^{\sum_j t_j N_j} F_{\lim} \tag{1.4.23}$$

approximates the original period mapping $\Phi(t)$ very well, as $t \to \mathbf{i}\infty$. Since $F_{\lim}$ is not a pure Hodge filtration in general, while $\Phi(t)$ is a pure Hodge filtration, the theorem also implies that for $\operatorname{Im} t_i$ large enough, $\Psi(t)$ is again a pure Hodge filtration. In fact, for any reasonable distance function d measuring the distance between two Hodge filtrations, there is an estimate

$$d(\Phi(t), \Psi(t)) \leq K \sum_{j=1}^{n} (\operatorname{Im} t_j)^\beta e^{-2\pi \operatorname{Im} t_j} , \tag{1.4.24}$$

where K and β are positive real numbers. For a complete discussion on the nilpotent orbit theorem, see [76, Section 1].

The most important data one gets out of the nilpotent orbit theorem is that there is a *limiting mixed Hodge structure* $(F_{\lim}, N_1, \ldots, N_n)$ constructed out of the limiting Hodge filtration and the logarithm of the monodromy matrices. The precise definition of the limiting mixed Hodge structure will be presented in Appendix 1.D.2.

The growth of Hodge norm and inner product

The most important theorem in asymptotic Hodge theory is the $\mathfrak{sl}(2)$-*orbit theorem* [75, 76]. For our brief introduction to its application in string theory, it suffices to know that this theorem equips the middle cohomology of Calabi-Yau manifolds with an $\mathbb{R}$-split mixed Hodge structure that mimics the mixed Hodge structure on the total cohomology of a Kähler manifold, and it also provides a set of commuting $\mathfrak{sl}(2)$-triples acting on the middle cohomology, whose action plays well with the $\mathbb{R}$-split mixed Hodge structure.

Let us discuss in the context of Calabi-Yau threefolds for concreteness. Let Y_3 be a Calabi-Yau threefold, and we study its middle cohomology H^3. The $\mathfrak{sl}(2)$-orbit theorem tells us that the middle cohomology H^3 carries an $\mathbb{R}$-split $\mathfrak{sl}(2)$-*mixed Hodge structure*, whose Deligne splitting is

$$H^3 = \bigoplus_{0 \leq p,q \leq 3} I^{p,q} , \tag{1.4.25}$$

such that $I^{p,q} = \overline{I}^{q,p}$ and the direct sum of subspaces with $p+q=k$ gives a pure Hodge structure of weight $k = 0, \ldots, 6$. Moreover, the $\mathfrak{sl}(2)$-orbit theorem states that there are n copies of $\mathfrak{sl}(2)$-triples

$$(N_i, Y_i, N_i^+)\,, \quad i = 1, \ldots, n\,, \tag{1.4.26}$$

that are mutually commuting and act on the middle cohomology H^3. These operators play well with the $\mathfrak{sl}(2)$-mixed Hodge structure. Compared with the situation in the total cohomology in Section 1.4.1, the neutral operator Y_i is like the Y-operator, which determines the subspaces with pure weights; here Y_i diagonalise on H^3, and the eigenvalue runs over $l = -3, -2, \ldots, +3$, while the eigenspace of Y_i with eigenvalue l is a pure Hodge structure of $l+3$,

$$\bigoplus_{p+q=l+3} I^{p,q} \text{ is the eigenspace of } Y_3 \text{ with eigenvalue } l+3\,.$$

The N_i operators are like the dual Lefschetz operator Λ, which moves the weight down by two,

$$N_i(I^{p,q}) \subset I^{p-1,q-1}\,, \tag{1.4.27}$$

while the N_i^+ operators are like the Lefschetz operator L, which moves the weights up by two,

$$N_i^+(I^{p,q}) \subset I^{p+1,q+1}\,. \tag{1.4.28}$$

So the middle cohomology H^3 becomes an $\mathfrak{sl}(2)^n$-representation. We can relate the commuting $\mathfrak{sl}(2)$-operators to useful geometric operators that appear in Calabi-Yau geometry, and use the link between geometry and the effective four-dimensional physics to study the swampland conjectures. Among the connections, let us mention here the most prototypical one, that is the estimate of the Hodge norm in the limit. For a differential three-form α living in H^3, we would like to know the growth behaviour of

$$\|\alpha\|_t^2 = \int_Y \alpha \wedge *\overline{\alpha}\,, \tag{1.4.29}$$

as the moduli $t_i \to \mathbf{i}\infty$ are pushed towards the limit. Since the particular expression of this norm depends on the geometry, we have to resort to answering some general questions, such as whether the norm is vanishing, tending towards a constant, or blowing up in the limit? Such questions can be answered precisely by the $\mathfrak{sl}(2)$-orbit theorem. The way to do it is simple, once one has the data of the $\mathfrak{sl}(2)$-mixed

Hodge structure, and the commuting $\mathfrak{sl}(2)$-triples. Namely, we decompose the differential form α into the eigenspace of the Y_i-operators,

$$\alpha = \sum_{l_1,\ldots,l_n} \alpha_{l_1,\ldots,l_n} \,, \tag{1.4.30}$$

where

$$Y_i \alpha_{l_1,\ldots,l_n} = l_i \alpha_{l_1,\ldots,l_n} \,. \tag{1.4.31}$$

And the Hodge norm estimate [75, 76] tells us that

$$\|\alpha_{l_1,\ldots,l_n}\|_t^2 \sim \left(\frac{y_1}{y_2}\right)^{l_1} \left(\frac{y_2}{y_3}\right)^{l_2} \cdots \left(\frac{y_{n-1}}{y_n}\right)^{l_{n-1}} y_n^{l_n} \,, \tag{1.4.32}$$

in the limit $t^i \to \mathbf{i}\infty$, where the $f \sim g$ symbol means that f and g are bounded by a constant multiple of each other. Moreover, every eigenspace of Y_i with different labels $(l_1, \ldots, l_n)$ are orthogonal under this estimate, so taking a linear combination of everything does the job. An example would be an $\alpha_{l_1,\ldots,l_n}$ with all $l_i < 0$, so that its Hodge norm is vanishing in the limit.

The subspaces $I^{p,q}$, and the $\mathfrak{sl}(2)$-triples N, Y, N^+ are constructed out of the limiting mixed Hodge structure $(F_{\lim}, N_1, \ldots, N_n)$. The precise construction is non-trivial, and is briefly reviewed in the Appendices in Chapter 2. For a nice physical review, see [92, Section 3].

Appendices

1.A Convention

In this appendix we list some conventions adopted in this chapter. We write $\mathbb{R}^{3,1}$ to denote the four-dimensional Minkowski spacetime with signature $(-,+,+,+)$. We use extensively the language of differential forms, because of its succinctness and compatibility with the geometric picture. But practical computation often requires working with local coordinates. On a (pseudo-)Riemannian manifold of (real) dimension n with metric g, in a local patch U, we write a p-form $A \in \Omega_M^p(U)$ as

$$A = \frac{1}{p!} A_{\mu_1\cdots\mu_p} dx^{\mu_1} \wedge \cdots \wedge dx^{\mu_p} \,, \tag{1.A.1}$$

and the Hodge dual $*A \in \Omega_M^{n-p}(U)$ is defined to be the unique $(n-p)$-form satisfying

$$A \wedge *A = \frac{1}{p!} A_{\mu_1\cdots\mu_p} A^{\mu_1\cdots\mu_p} \sqrt{|\det g|} dx^1 \wedge \cdots \wedge dx^n \,. \tag{1.A.2}$$

In particular,

$$*1 = \sqrt{|\det g|}dx^1 \wedge \cdots \wedge dx^n \tag{1.A.3}$$

gives the volume form.

Next we list our conventions adopted in regards with the curvatures. The Levi-Civita connection coefficients are

$$\Gamma^\mu_{\nu\rho} = \frac{1}{2}g^{\mu\lambda}(\partial_\nu g_{\rho\lambda} + \partial_\rho g_{\lambda\mu} - \partial_\lambda g_{\nu\rho})\,. \tag{1.A.4}$$

In the moving frame formalism, choosing the natural coordinate basis $dx^\mu \in \Omega^1_M(U)$ of one-forms and let $\omega^\mu_\nu \in \Omega^1_M(U)$ be the associated connection matrix, then

$$\omega^\mu_\nu = \Gamma^\mu_{\nu\rho}dx^\rho\,. \tag{1.A.5}$$

The Riemann curvature tensor is given by

$$R^\mu{}_{\nu\rho\sigma} = \partial_\rho\Gamma^\mu_{\sigma\nu} - \partial_\sigma\Gamma^\mu_{\rho\nu} + \Gamma^\mu_{\rho\lambda}\Gamma^\lambda_{\sigma\nu} - \Gamma^\mu_{\sigma\lambda}\Gamma^\lambda_{\rho\nu}\,, \tag{1.A.6}$$

which corresponds to the curvature matrix $\Omega^\mu_\nu \in \Omega^2_M(U)$

$$\Omega^\mu_\nu = d\omega^\mu_\nu - \omega^\lambda_\nu \wedge \omega^\mu_\lambda = -\frac{1}{2}R^\mu{}_{\nu\rho\sigma}dx^\rho \wedge dx^\sigma\,. \tag{1.A.7}$$

Note the extra minus sign at right-most part of this expression. Note also that, although we write down local expressions of the connection and curvature forms, they are actually defined on the whole manifold M.

The Ricci curvature tensor and Ricci scalar curvature are then defined by successively tracing out indices in the Riemann curvature tensor

$$R_{\mu\nu} = R^\lambda{}_{\mu\lambda\nu}\,, \qquad \text{and} \qquad R = g^{\mu\nu}R_{\mu\nu}\,. \tag{1.A.8}$$

Finally, in n-dimensional spacetime, the gravitational interaction strength κ_n and Planck mass $M_{\mathrm{P},n}$ are related by

$$\frac{1}{\kappa_n^2} = M_{\mathrm{P},n}^{n-2}\,. \tag{1.A.9}$$

A nice comparison of all different conventions can be found in [19, Appendix A] and [18, Appendix C].

1.B Details of 5D compactifications

In this appendix we present some details of the Kaluza-Klein circle compactification discussed in Section 1.2.1. The computation is most simply done with Cartan's moving frame method/tetrad method. For review, see [94, 95]. For its particular application to Kaluza-Klein compactification, [96, 97] are some original sources. In this appendix, we present the necessary steps in the computation. For physicists familiar with the tetrad formalism, the method presented here differs from the traditional tetrad formalism in that we do not use orthonormal basis along all directions. In other words, the tetrad formalism is only applied to the extra dimension.

Let us repeat the metric (1.2.4) here for convenience. Everything with a $\hat{}$, such as $d\hat{s}^2$, denotes a quantity in the 5D cylinder spacetime. The infinitesimal line element is given by

$$d\hat{s}^2 = \hat{g}_{MN}dx^M dx^N = g_{\mu\nu}dx^\mu dx^\nu + 2r^2(x)A_\mu(x)dx^\mu d\theta + r^2(x)d\theta^2 \,. \tag{1.B.1}$$

The cross-term among the dx^μ and $d\theta$ is particularly unpleasant. The first step in the calculation is to change basis in the tangent space such that the cross-term goes away. Our choice of basis e^A $(A = \mu, 4)$ is

$$e^\mu \coloneqq dx^\mu \,, \qquad e^4 \coloneqq r(x)(d\theta + A_\mu(x)dx^\mu) \,. \tag{1.B.2}$$

So the metric becomes

$$d\hat{s}^2 = \hat{g}_{AB}e^A e^B = g_{\mu\nu}dx^\mu dx^\nu + (e^4)^2 \,. \tag{1.B.3}$$

Next, we need to find out the Levi-Civita connection matrix $\hat{\omega}^A_B$ under the e^A basis. This is done by solving the Cartan structure equations

$$\begin{aligned} de^A &= -\hat{\omega}^A_B \wedge e^B \,, \\ d\hat{g}_{AB} &= \hat{\omega}_{AB} + \hat{\omega}_{BA} \,, \end{aligned} \tag{1.B.4}$$

where we have lowered the index

$$\hat{\omega}_{AB} \coloneqq \hat{\omega}^C_A g_{CB} \,. \tag{1.B.5}$$

Please pay attention to the position of the contracted indices. The first equation means that the connection is torsion-free, and the second means that the connection is compatible with the metric.

Using the metric (1.B.3) and the choice of e^A in (1.B.2), we solve for the connection matrix $\hat{\omega}$. It is given by

$$\begin{aligned}
\hat{\omega}^4_\mu &= \frac{1}{2} r F_{\mu\nu} dx^\nu + \frac{\partial_\mu r}{r} e^4 \,, \\
\hat{\omega}^\mu_4 &= -\frac{1}{2} r F^\mu{}_\nu \, dx^\nu - \frac{\partial^\mu r}{r} e^4 \,, \\
\hat{\omega}^\mu_\nu &= \omega^\mu_\nu - \frac{1}{2} F^\mu{}_\nu \, e^4 \,,
\end{aligned} \tag{1.B.6}$$

where $F_{\mu\nu} = \partial_\mu A_\nu - \partial_\nu A_\mu$ as usual, and ω^μ_ν is the connection matrix of the 4D Levi-Civita connection associated with the metric $g_{\mu\nu}$, so

$$\omega^\mu_\nu = \Gamma^\mu_{\nu\rho} dx^\rho \,. \tag{1.B.7}$$

The next step is to compute the anti-symmetric curvature matrix $\hat{\Omega}_{AB}$, which is defined as

$$\hat{\Omega}_{AB} = d\hat{\omega}_{AB} + \hat{\omega}^C_A \wedge \hat{\omega}_{BC} \,. \tag{1.B.8}$$

Please pay attention to the location of the summed indices. Using the expression for the connection matrix (1.B.6), it is straightforward to compute

$$\begin{aligned}
\hat{\Omega}_{\mu\nu} = \;& \Omega_{\mu\nu} + \frac{r^2}{4}(F_{\mu\nu}F_{\rho\sigma} + F_{\mu\rho}F_{\nu\sigma}) dx^\rho \wedge dx^\sigma \\
& + \frac{1}{2}(r\nabla_\rho F_{\mu\nu} + 2F_{\mu\nu}\partial_\rho r - \partial_\mu r F_{\nu\rho} + \partial_\nu r F_{\mu\rho}) dx^\rho \wedge e^4 \,, \\
\hat{\Omega}_{\mu 4} = \;& \frac{1}{2}(\partial_\rho r F_{\mu\sigma} + r\partial_\rho F_{\mu\sigma} + \partial_\mu r F_{\rho\sigma} - r\Gamma^\lambda_{\mu\rho} F_{\lambda\sigma}) dx^\rho \wedge dx^\sigma \\
& + \left(\frac{1}{r}\nabla_\mu \partial_\rho r - \frac{r^2}{4} F^\lambda{}_\mu \, F_{\lambda\rho} \right) dx^\rho \wedge e^4 \,,
\end{aligned} \tag{1.B.9}$$

where ∇ is the 4D Levi-Civita connection. The curvature matrix is related to the Riemannian curvature tensor, expressed under the e^A basis, as follows.

$$\hat{\Omega}_{AB} = -\frac{1}{2} \hat{R}_{ABCD} e^C \wedge c^D \,, \tag{1.B.10}$$

so that (after antisymmetrisation on the indices C and D) the curvature tensor[15] is given by

$$\begin{aligned}
\hat{R}_{\mu\nu\rho\sigma} &= R_{\mu\nu\rho\sigma} - \frac{1}{2} r^2 F_{\mu\nu} F_{\rho\sigma} - \frac{r^2}{4}(F_{\mu\rho}F_{\nu\sigma} - F_{\mu\sigma}F_{\nu\rho}) \,, \\
\hat{R}_{\mu\nu\rho 4} &= -\frac{r}{2}\nabla_\rho F_{\mu\nu} - \partial_\rho r F_{\mu\nu} + \frac{1}{2}\partial_\mu r F_{\nu\rho} - \frac{1}{2}\partial_\nu r F_{\mu\rho} \,, \\
\hat{R}_{\mu 4\rho 4} &= -\frac{1}{r}\nabla_\mu \partial_\rho r + \frac{1}{4} r^2 F^\lambda{}_\mu \, F_{\lambda\rho} \,.
\end{aligned} \tag{1.B.11}$$

[15] To really check that the resulting curvature tensor satisfies the usual symmetries, the Bianchi identity $\partial_\mu F_{\nu\rho} + \partial_\nu F_{\rho\mu} + \partial_\rho F_{\mu\nu} = 0$ should be used.

Contract twice to get the Ricci scalar $\hat{R}$ and we have finally arrived at

$$\hat{R} = R - \frac{2}{r}\nabla_\mu \nabla^\mu r - \frac{r^2}{4} F_{\mu\nu}F^{\mu\nu}\,, \tag{1.B.12}$$

where we have used $\partial_\mu r = \nabla_\mu r$ since r is a scalar field. Note that the second term contributes a total (covariant) derivative under the action integral, so it is not present in the 4D action (1.2.7) since the spacetime $\mathbb{R}^{1,4}$ is boundary-less.

For the Weyl rescaling, we record the relevant formula below. If $g_{\mu\nu} = e^{2\Omega(x)}\tilde{g}_{\mu\nu}$ in D-dimensions, then their Ricci scalars are related by

$$R = e^{-2\Omega}(\tilde{R} - 2(D-1)\tilde{\nabla}^2\Omega - (D-1)(D-2)\partial_\mu\Omega\partial^\mu\Omega)\,, \tag{1.B.13}$$

while their Laplacian operators are related by $\nabla^2 = e^{-2\Omega}\tilde{\nabla}^2$.

1.C An example of the $\mathcal{N} = 2$ symplectic formalism

We would like to present a toy example to exemplify the general discussion about $\mathcal{N} = 2, D = 4$ supergravity in Section 1.2.3. This example is taken from [19, Exercise 20.18]. There is $n_{\mathrm{V}} = 1$ vector multiplet with the complex scalar denoted $z = x + \mathbf{i}y$ with x, y real scalar fields, so the symplectic vector $v(z) = (Z^0, Z^1, \mathcal{F}_0, \mathcal{F}_1)^{\mathsf{T}}$ consists of four components. The theory is defined by a prepotential

$$\mathcal{F}(Z) = -\mathbf{i}Z^0 Z^1\,, \tag{1.C.1}$$

and we choose the so-called *special coordinates*, which means selecting $Z^0 = 1$, and $Z^1 = -\mathbf{i}z$ is a constant multiple of the scalar z. Then the symplectic vector is given by

$$v(z) = (Z^0, Z^1, \mathcal{F}_0, \mathcal{F}_1)^{\mathsf{T}} = (1, -\mathbf{i}z, -z, -\mathbf{i})^{\mathsf{T}}\,, \tag{1.C.2}$$

where $\mathcal{F}_I = \frac{\partial \mathcal{F}}{\partial Z^I}$. Computing the Kähler potential, we get

$$K(z,\bar{z}) = -\mathbf{i}\log\Big(Z^I\overline{\mathcal{F}}_I - \overline{Z^I}\mathcal{F}_I\Big) = -\log 2(z-\bar{z})\,, \tag{1.C.3}$$

so that the kinetic matrix for the scalar z is

$$g_{z\bar{z}} = \partial_z\partial_{\bar{z}}K = -\frac{1}{(z-\bar{z})^2} = \frac{1}{4y^2} > 0\,. \tag{1.C.4}$$

To compute the gauge kinetic matrix $\mathcal{N}_{IJ}$, we first list the relevant matrices

$$\begin{aligned}(\mathcal{F}_I, \mathcal{D}_{\bar{\imath}}\overline{\mathcal{F}}_I) &= \begin{pmatrix}\mathcal{F}_0 & \mathcal{D}_{\bar{z}}\overline{\mathcal{F}}_0\\ \mathcal{F}_1 & \mathcal{D}_{\bar{z}}\overline{\mathcal{F}}_1\end{pmatrix} = \begin{pmatrix}-z & -\frac{z}{z-\bar{z}}\\ -\mathbf{i} & \frac{\mathbf{i}}{z-\bar{z}}\end{pmatrix}\,,\\ (Z^J, \mathcal{D}_{\bar{\imath}}\overline{Z}^J) &= \begin{pmatrix}Z^0 & \mathcal{D}_{\bar{z}}\overline{Z}^0\\ Z^1 & \mathcal{D}_{\bar{z}}\overline{Z}^1\end{pmatrix} = \begin{pmatrix}1 & \frac{1}{z-\bar{z}}\\ -\mathbf{i}z & \frac{\mathbf{i}z}{z-\bar{z}}\end{pmatrix}\,.\end{aligned} \tag{1.C.5}$$

And note that $\det\big(Z^J, \mathcal{D}_{\bar{i}}\overline{Z}^J\big) = \frac{2\mathbf{i}z}{z-\bar{z}} \neq 0$ as long as $z \neq 0$ so it is invertible with

$$(Z^J, \mathcal{D}_{\bar{i}}\overline{Z}^J)^{-1} = \begin{pmatrix} \frac{1}{2} & \frac{\mathbf{i}}{2z} \\ \frac{z-\bar{z}}{2} & -\frac{\mathbf{i}(z-\bar{z})}{2z} \end{pmatrix} . \tag{1.C.6}$$

Then

$$(\mathcal{N}_{IJ}) = (\mathcal{F}_I, \mathcal{D}_{\bar{i}}\overline{\mathcal{F}}_I)(Z^J, \mathcal{D}_{\bar{i}}\overline{Z}^J)^{-1} = \begin{pmatrix} -z & 0 \\ 0 & 1/z \end{pmatrix} . \tag{1.C.7}$$

Finally, the bosonic action for this theory is given by

$$\begin{aligned} S = \int_{\mathbb{R}^{3,1}} & \frac{1}{2}R * 1 - \frac{1}{4y^2}dx \wedge *dx - \frac{1}{4y^2}dy \wedge *dy \\ & + \frac{y}{2}F^0 \wedge *F^0 + \frac{x}{2}F^0 \wedge F^0 \\ & + \frac{y}{2(x^2+y^2)}F^1 \wedge *F^1 - \frac{x}{2(x^2+y^2)}F^1 \wedge F^1 . \end{aligned} \tag{1.C.8}$$

Note that, had one been presented directly with the above action, it would be hard to observe that it is the bosonic part of a theory with extended supersymmetry. This demonstrates the effectiveness of the symplectic formalism.

1.D Technicalities about mixed Hodge structures

In this appendix, we list several elementary definitions related to mixed Hodge structures. If the reader is really interested in using asymptotic Hodge theory, we strongly recommend learning it from mathematical literatures. Nice review articles include [77, 79, 80, 98–104]. The books [71, 78, 105] can be useful to consult. If the reader is addicted to the linear algebraic yoga about filtrations, the papers [106–110] are definitely worth reading. Finally, the original papers on asymptotic Hodge theory are [75, 76], and the general estimate of the Hodge norm is independently developed, without using the multi-variable $\mathfrak{sl}(2)$-orbit theorem, in [107].

1.D.1 Mixed Hodge structure and Deligne splitting

We would now state the definition of a mixed Hodge structure. Fixing a rational vector space $V_{\mathbb{Q}}$, and its complexification $V_{\mathbb{C}} = V_{\mathbb{Q}} \otimes \mathbb{C}$, a *mixed Hodge structure* $(V_{\mathbb{Q}}, V_{\mathbb{C}}, W, F)$ consists of the following data

1. A finite increasing *weight filtration* W on the rational vector space $V_{\mathbb{Q}}$

$$0 \subset \cdots \subset W_{-1} \subset W_0 \subset W_1 \subset \cdots \subset V_{\mathbb{Q}} , \tag{1.D.1}$$

2. A finite decreasing *Hodge filtration* F on the complex vector space $V_{\mathbb{C}}$

$$0 \subset \cdots \subset F^1 \subset F^0 \subset F^{-1} \subset \cdots \subset V_{\mathbb{C}}\,, \tag{1.D.2}$$

where an increasing filtration being finite means that $W_k = 0$ for sufficiently small k and $W_k = V_{\mathbb{Q}}$ for sufficiently large k. Similar notion holds for finite decreasing filtrations. These data satisfy the condition that, over each graded piece

$$\mathrm{Gr}_k^W \coloneqq \frac{W_k}{W_{k-1}}\,, \tag{1.D.3}$$

the induced filtrations

$$F^p\mathrm{Gr}_k^W \coloneqq \frac{F^p \cap W_k}{F^p \cap W_{k-1}}\,, \tag{1.D.4}$$

defines a weight k Hodge structure on Gr_k^W, i.e. it satisfies the *k-opposed* condition

$$F^p\mathrm{Gr}_k^W \oplus \overline{F^{k+1-p}\mathrm{Gr}_k^W} \cong \mathrm{Gr}_k^W\,, \qquad \text{for all } p\,. \tag{1.D.5}$$

We would like to point out that, in order to support pure Hodge structures on the graded pieces Gr_k^W, it is necessary to have the increasing filtration W_k defined over a vector space that is fixed by the complex conjugation, which is the rational vector space $V_{\mathbb{Q}}$.

It is also possible to replace the rational vector space $V_{\mathbb{Q}}$ by a real vector space $V_{\mathbb{R}}$, or a lattice ($\mathbb{Z}$-module) $V_{\mathbb{Z}}$ and the definition goes in parallel with our definition. In our physical application, we usually have V as cohomologies. So it would be useful to think $V_{\mathbb{Z}}, V_{\mathbb{Q}}, V_{\mathbb{R}}, V_{\mathbb{C}}$ as the (free part of the) integral, rational, real, and complex cohomologies of a Kähler manifold.

Following [99, Section 2], it is instructive to list some common ranges of indices on the filtrations that appear in mixed Hodge structures. Let X be a quasi-projective variety and let $V = H^n(X)$ be the degree n-cohomology , then one has the Hodge filtration

$$0 = F^{n+1} \subset F^n \subset \cdots \subset F^1 \subset F^0 = V_{\mathbb{C}}\,. \tag{1.D.6}$$

Moreover, it is shown by Deligne [106,111] and Schmid [75] (See [79, Section 9] for historical remarks) that the weight filtration on $H^n(X)$ takes the following form:

- If X if smooth and projective, for example if X is a torus, or a smooth compact Calabi-Yau manifold, then

$$0 = W_{n-1} \subset W_n = H^n(X)\,, \tag{1.D.7}$$

so that $H^n(X)$ carries a pure Hodge structure of weight n. This is the familiar story.

- If X is projective, but not necessarily smooth, for example if X is a pinched torus, or a compact degenerate Calabi-Yau manifold where some cycles shrink to zero, then
$$0 = W_{-1} \subset W_0 \subset \cdots \subset W_n = H^n(X)\,. \tag{1.D.8}$$
- If X is smooth, but not necessarily projective, for example if X is a punctured torus, or an open Calabi-Yau manifold, then
$$0 = W_{n-1} \subset W_n \subset \cdots \subset W_{2n} = H^n(X)\,. \tag{1.D.9}$$
- If, instead of a single space, we have a family X_t of Kähler manifolds labelled by t, where for $t \neq 0$ the X_t is smooth and compact, while $t = 0$ corresponds to a singular fibre X_0. The limiting mixed Hodge structure on $H^n(X_t)$ with $t \sim 0$ will carry a weight filtration that is a combination of the above types
$$0 = W_{-1} \subset W_0 \subset \cdots \subset W_{2n} = H^n(X_t)\,. \tag{1.D.10}$$
This is in fact given by the monodromy weight filtration that will be discussed later.

It would be useful to have an analogy to the Hodge decomposition for a mixed Hodge structure, so that one can work directly with a direct sum decomposition of $V_{\mathbb{C}}$, instead of a filtration. Such a decomposition would look like $V_{\mathbb{C}} = \bigoplus H^{p,q}$, and satisfy the following property
$$W_k = \bigoplus_{p+q=k} H^{p,q}\,, \qquad \text{and} \qquad F^p = \bigoplus_{r\geq p} H^{r,s}\,, \tag{1.D.11}$$
where in the second equation, the omitted index s is implicitly summed over its possible range. In fact, there exists many such splittings, and any such splitting satisfies
$$H^{p,q} = \overline{H^{q,p}} \mod \bigoplus_{r+s\leq p+q-1} H^{r,s}\,, \tag{1.D.12}$$
which generalises the usual property that conjugation exchanges $H^{p,q}$ and $H^{q,p}$ for pure Hodge structures. The above two problems, the non-uniqueness and the complex conjugation issue, can be both cured by the so called Deligne splitting [112], [76, Theorem (2.13)], which for clarity is often denoted by $V_{\mathbb{C}} = \bigoplus I^{p,q}$. It is the unique splitting of a mixed Hodge structure $(V_{\mathbb{Q}}, V_{\mathbb{C}}, W, F)$ that satisfies the properties in (1.D.11) which we reproduce for clarity
$$W_k = \bigoplus_{p+q=k} I^{p,q}\,, \qquad \text{and} \qquad F^p = \bigoplus_{r\geq p} I^{r,s}\,, \tag{1.D.13}$$

together with an upgraded conjugation property

$$I^{p,q} = \overline{I^{q,p}} \mod \bigoplus_{r<p,s<q} I^{r,s}\,, \tag{1.D.14}$$

where the expression means that any vector in $I^{p,q}$ can be written as the conjugation of a vector in $I^{q,p}$, plus some corrections living in the big direct sum. The Deligne splitting can be explicitly constructed out of the W and F filtrations by the following formula [76, Equation (2.12)]

$$I^{p,q} = F^p \cap W_{p+q} \cap (\overline{F}^q \cap W_{p+q} + \overline{F}^{q-1} \cap W_{p+q-2} + \overline{F}^{q-2} \cap W_{p+q-3} + \cdots)\,. \tag{1.D.15}$$

Please be careful about every symbol in the above equation when applying it. Note the jump in the levels in the weight filtration between the first term and the remaining terms in the bracket. We also stress that the subspaces in the bracket are summed, instead of directly summed, because there might be non-zero overlaps between different summands. Moreover, we would like to warn the reader that, in general, the intersection of vector spaces does *not* distribute over the summation, so for U, V, W vector spaces,

$$U \cap (V + W) \neq (U \cap V) + (U \cap W)\,! \tag{1.D.16}$$

If the Deligne splitting of a mixed Hodge structure (W, F) satisfies

$$I^{p,q} = \overline{I^{q,p}}\,, \tag{1.D.17}$$

then the mixed Hodge structure is called $\mathbb{R}$-*split*. Such mixed Hodge structures are particularly pleasant to study, because it can be just understood as a direct sum of a series of pure Hodge structures of different weights, like the mixed Hodge structure on the total cohomology on a Calabi-Yau threefold discussed in section 1.4.1.

Not all mixed Hodge structures is $\mathbb{R}$-split, but for any mixed Hodge structure (W, F), Deligne [112], [76, Proposition (2.20)] constructs an operator δ such that the modified mixed Hodge structure $(W, e^{\mathbf{i}\delta} F)$ is $\mathbb{R}$-split.

The works by Schmid [75] and Cattani-Kaplan-Schmid [76] start from the limiting mixed Hodge structures coming from a degenerating variation of Hodge structure, apply the Deligne δ-construction to make it $\mathbb{R}$-split, and construct another $\mathbb{R}$-split mixed Hodge structure called the $\mathfrak{sl}(2)$-splitting. It is this $\mathfrak{sl}(2)$-splitting that enables one to regard the middle cohomology as a representation of a set of commuting $\mathfrak{sl}(2)$-algebras. There is a simple algebraic way to classify all possible $\mathbb{R}$-split limiting mixed Hodge structures on the cohomology $H^n(X)$ [113, 114] and the degeneration patterns among them. This classification will be reviewed and used in Chapter 2 and 3.

1.D.2 The limiting mixed Hodge structure

We work in the context of 1.4.4 and let $V = H^n(X_t)$ be the cohomology of the non-singular Calabi-Yau manifold nearby the singular fibre. The initial data for the definition of a limiting mixed Hodge structure is the limiting Hodge filtration $F_{\lim}$ defined in Section 1.4.4. Namely, define

$$F_{\lim} = \lim_{t \to \mathbf{i}\infty} e^{-\sum_j t_j N_j} \Phi(t)\,, \tag{1.D.18}$$

where Φ is the lifted period mapping, and N_j are the log-monodromy operators. We assume that a base transformation is already made so that the monodromy operators are unipotent. The $F_{\lim}$ will be the decreasing Hodge F-filtration in the defining data of a limiting mixed Hodge structure. The next step is to define the increasing weight W-filtration.

The construction of the W-filtration is purely algebraic. Note that the operators N_j are actually nilpotent with

$$N_j^n = 0\,, \qquad \text{for all } j\,, \tag{1.D.19}$$

because of the unipotency (1.4.19) with $m = 1$ of the monodromy operators. Then the W-filtration is constructed by a theorem of Jacobson–Morosov. The theorem works as follows. Starting with any nilpotent operator N, satisfying $N^n = 0$, acting on a vector space V, there is a unique increasing Jacobson–Morosov filtration $W(N)$ centred at zero

$$0 = W(N)_{-n-1} \subset W(N)_{-n} \subset \cdots \subset W(N)_n = V\,, \tag{1.D.20}$$

such that

$$N(W(N)_k) \subset W(N)_{k-2}\,, \quad \text{and} \quad N^k : \mathrm{Gr}^W_k \xrightarrow{\sim} \mathrm{Gr}^W_{-k}\,, \tag{1.D.21}$$

for all k, where the latter map is an isomorphism. Recall that $\mathrm{Gr}^W_k = \frac{W_k}{W_{k-1}}$.

Coming back to the asymptotic Hodge theory setting, we have a series of nilpotent operators $N_1, \ldots, N_n$ acting on the cohomology $V = H^n(X_t)$, and it is shown in [115] that any positive linear combination $a_1N_1 + \cdots a_nN_n$ with $a_1, \ldots, a_n > 0$ is nilpotent of order n, and that the filtration $W(a_1N_1 + \cdots + a_nN_n)$ does not depend on the choice of $a_1, \ldots, a_n$. So we define the *monodromy weight filtration* associated to $N_1, \ldots, N_n$ by $W(N_1, \ldots, N_n)[-n]$, where

$$W(N_1, \ldots, N_n)[-n]_k \coloneqq W(a_1N_1 + \cdots + a_nN_n)_{k-n}\,, \tag{1.D.22}$$

for all k. The monodromy weight filtration is a shift of the Jacobson – Morosov filtration by minus the weight of the cohomology n, and its non-trivial indices runs over $k = 0, \ldots, 2n$, realising the previous discussion around equation (1.D.10). When the data $N_1, \ldots, N_n$ is clear from the context, we will also write $W^{(n)}$ for the long expression $W(N_1, \ldots, N_n)[-n]$. Concrete expressions for $W^{(n)}$ in Calabi-Yau three-folds can be found in equation (2.2.38).

A fundamental result in asymptotic Hodge theory [75, 76] then says that the filtrations $(F_{\lim}, W(N_1, \ldots, N_n)[-n])$ defines a limiting mixed Hodge structure on the cohomology $V = H^n(X_t)$.

2 Infinite Distance Networks in Field Space and Charge Orbits

This chapter is based on: T. W. Grimm, C. Li and E. Palti, *Infinite Distance Networks in Field Space and Charge Orbits*, JHEP **03** (2019), 016, [arXiv:1811.02571].

In this chapter, we study the swampland distance conjecture for the complex structure moduli space of Calabi-Yau manifolds. In this context, we uncover significant structure within the proposal by showing that there is a rich spectrum of different infinite distance loci that can be classified by certain topological data derived from an associated discrete symmetry. We show how this data also determines the rules for how the different infinite distance loci can intersect and form an infinite distance network. We study the properties of the intersections in detail and, in particular, propose an identification of the infinite tower of states near such intersections in terms of what we term charge orbits. These orbits have the property that they are not completely local, but depend on data within a finite patch around the intersection, thereby forming an initial step towards understanding global aspects of the distance conjecture in field spaces. Our results follow from a deep mathematical structure captured by the so-called orbit theorems, which gives a handle on singularities in the moduli space through mixed Hodge structures, and is related to a local notion of mirror symmetry thereby allowing us to apply it also to the large volume setting. These theorems are general and apply far beyond Calabi-Yau moduli spaces, leading us to propose that similarly the infinite distance structures we uncover are also more general.

2.1 Introduction

The Swampland Distance Conjecture (SDC), states that infinite distances in moduli space lead to an infinite tower of states becoming massless exponentially fast in the proper field distance [57]. As reviewed in Section 1.3.1, if we consider two points in field space P and Q, with a geodesic proper distance between them of

$d(P,Q)$, then upon approaching the point P there should exist an infinite tower of states with characteristic mass scale m such that

$$m(P) \sim m(Q)\, e^{-\gamma d(P,Q)} \text{ as } d(P,Q) \to \infty \,. \tag{2.1.1}$$

Here γ is some positive constant which depends on the choice of P and Q but which is not specified in generality.

The conjecture, as stated in (2.1.1) is rather coarse. It does not say anything about properties of the tower of states beyond their mass, and in particular, about what is the overall structure of different infinite distances in the field space. In order to build up intuition about these questions, and evidence for the conjecture, it is useful to study large rich classes of field spaces in string theory. In [5] such a systematic study was initiated for the complex structure moduli space of Calabi-Yau manifolds in compactifications of type IIB string theory to four dimensions. We will retain this setting in this chapter.[1] The conjecture was shown to hold for a large class of infinite distances without referring to any specific example. The reason such a general approach is possible is because infinite distance loci in moduli space have some very general properties. In particular, they have a discrete set of data associated to monodromies when circling them, and this data determined the local form of the moduli space as well as the spectrum of charged states. In this chapter we will build on these ideas and uncover more of the structure contained in this discrete data. In terms of the distance conjecture, this structure will 'resolve' the infinite distance divergence into a fine classification of different types of infinite distances, and begin to shed light on how such infinite distance types can intersect and form a complex network of infinite distance loci. It will also determine how the towers of states can arise and be inter-related within such a network.

First, we recall the local aspect of the data. The results of [5] showed that infinite distance loci are singular loci in the moduli space and have an associated discrete monodromy transformation, denoted by T. This transformation determines the local geometry of the moduli space. It also picks out an infinite tower of states where it acts as the transformation moving one step up the tower. This general picture is illustrated in figure 2.1. The presence of such a universal structure allowed for a very general analysis and so to proofs of very general results. It was also proposed that the infinite distance is itself induced by integrating out the tower of states. In this sense, it is quite natural that the same object T controls both the tower of states and the infinite distance behaviour.

[1] See [116,117] for a general analysis of weak gauge coupling limits in compactifications of F-theory to six-dimensions.

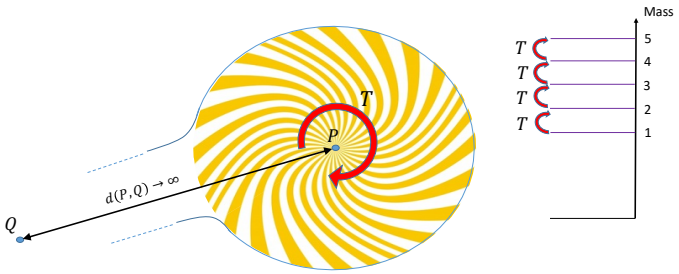

Figure 2.1: Figure illustrating the relation between the distance conjecture and monodromy. The point P is at infinite distance and the monodromy about it is denoted by T. The monodromy determines the local singular geometry of the moduli space, which leads to the exponential behaviour of the mass of the tower of states. The monodromy also acts on the spectrum of states picking out a specific infinite set of states.

So far we have only considered a single point P at infinite distance. But the moduli space is a high-dimensional space, and P actually belongs to a continuous set of points which together form an infinite distance locus. This full locus can be characterised by discrete data related to T. The locus can also intersect other similar infinite distance loci. Together, all these loci form a network of infinite distances. This structure is perhaps best illustrated with an example. In figure 2.2 we present an example field space, the complex structure moduli space of a particular Calabi-Yau manifold. Each locus of infinite distance in the moduli space is denoted by a solid line, and the full structure of the network is manifest. The loci in figure 2.2 are labelled by a type, which (for Calabi-Yau threefolds) can be I, II, III, or IV. Type I loci are at finite distance in moduli space. Type II, III or IV loci are at infinite distance and the increasing type denotes a sense of increasingly strongly divergent distances. In [5] a generic point P on one of the infinite distance loci was assigned a type inherited from the locus type.[2] This was done away from the intersection points and is in this sense a purely local analysis.

In this chapter we will begin to explore the global structure of the infinite distance network. The first thing we will introduce is a more refined classification of the

[2]The notation in [5] is that types I, II, III, IV are labelled by $d = 0, 1, 2, 3$ respectively.

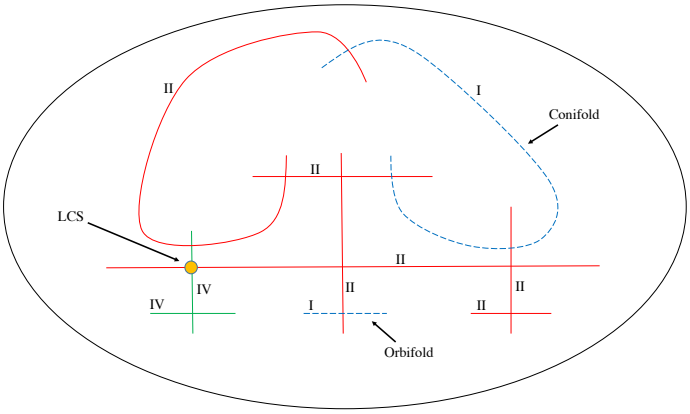

Figure 2.2: Figure showing an example field space with multiple infinite distance loci. The example is the (resolved) complex structure moduli space of the (mirror of the) two parameter Calabi-Yau $\mathbb{P}^{1,1,2,2,2}[8]$ as studied in [118]. Each infinite distance locus is denoted by a solid line and assigned a type labelled by II, III, or IV. We also show special finite distance loci with dashed lines, and these are associated to type I. Some well-known loci are labelled explicitly, the finite distance conifold and orbifold loci, and the infinite distance large complex-structure point.

infinite distance loci which takes into account important additional data. The type will now be supplemented by a numerical sub-index, so for example, will take the form II_2. This more refined type can then change, or enhance, at points where the loci intersect. In figure 2.3 we give a different example of an infinite distance network where we now focus in on the intersection structure in a particular region. We see that the loci are assigned a more refined data type and also each intersection locus has an associated type which may differ from the generic point on the locus. We will explain what the more refined data captures, and how it can be calculated from the monodromy T.

The next step will be to understand the distance conjecture when approaching the intersection points themselves. The whole notion of the nature of the infinite distance is vastly more complicated at the intersection points. In particular, the finiteness of the distance itself, as well as the masses of states, become path dependent questions. So whether a state becomes massless or not at the intersection loci depends on how one approaches them. We will show how to incorporate this path dependence into the formalism.

The refined discrete data not only gives the properties of the infinite distance loci

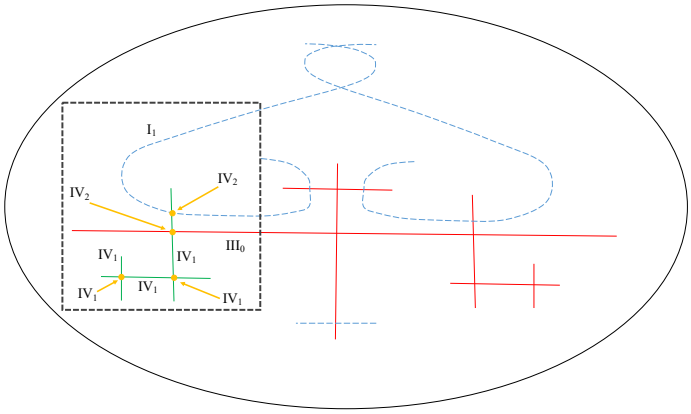

Figure 2.3: Figure showing an example intersecting network for the (mirror of the) Calabi-Yau $\mathbb{P}^{1,1,1,6,9}[18]$ as studied in [119]. In this case we focus in one a particular region of the network, within the box, and show the more refined data for each locus including the sub-index. At the points of intersections the type of a locus can be modified. We show the types associated to each intersection point in the focused region.

but also the rules for which types of infinite distance loci can intersect each other and what are the possible types to which they could enhance on the intersection points. We therefore find rules for what type of infinite distance networks could be built. These intersection rules have deep mathematics behind them, as initially developed in [76] and studied recently in [113]. The rules can be expressed in terms of which types of infinite distance loci can enhance to which types over certain sub-loci corresponding to intersections. Expressed this way the intersection, or enhancement, rules for two example classes of networks are shown in figure 2.4. The example network in figure 2.3 falls into the type $h^{2,1} = 2$. One can then readily check that the enhancement of the locus types at the intersections indeed follows the general rules.

In [5] the tower of states was identified as generated by an infinite action of the monodromy matrix T on some BPS state charge. In this chapter we will introduce a more general notion of such a tower that is associated to the monodromy action, which we term a *charge orbit*. A crucial aspect of the charge orbit is that it will not be associated to a point on an infinite distance locus, but to a patch, which means that it can capture the structure of intersections. This will therefore form a first step towards connecting the towers of the different infinite distance loci into a network. A non-trivial result which we will be able to prove already is that if the

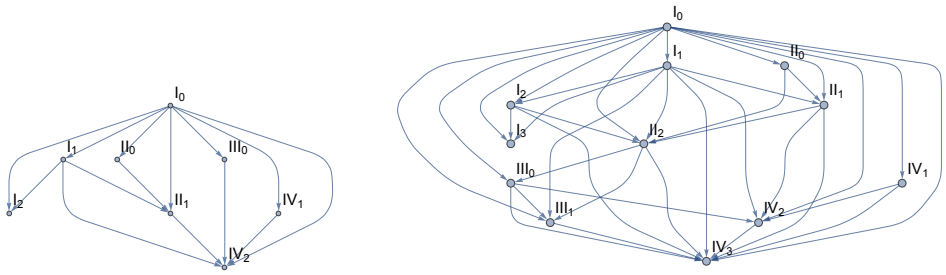

$h^{2,1} = 2$ $h^{2,1} = 3$

Figure 2.4: Graphs of allowed type enhancements for field spaces with $h^{2,1}$ complex fields. In terms of Calabi-Yau geometries, $h^{2,1}$ is the associated Hodge number. An arrow denotes that a starting type of locus may enhance over a sub-locus, corresponding to an intersection, to the end type. Note that the enhancement relations are not transitive. For example, in the $h^{2,1} = 2$ case, there is a chain of $\mathrm{II}_0 \to \mathrm{II}_1 \to \mathrm{IV}_2$ enhancements, but there is no direct enhancement from II_0 to IV_2.

type of the infinite distance increases at the intersection, then there is an infinite charge orbit of states which become massless approaching the locus even away from the intersection point itself. We call this an inheritance of a charge orbit by a locus from its intersection point. It is important to note, however, that in [5] the monodromy induced tower was shown to be populated by BPS states, while in this chapter we will identify the charge orbit but will be unable to prove that it is populated by BPS states. Nonetheless, we propose that it indeed captures the tower of states of the distance conjecture, while leaving a proof in terms of BPS states for future work.

The chapter is structured as follows. In section 2.2 we introduce the formalism and underlying theorems which we will use in the chapter. In section 2.3 we show how the data of the type of infinite distance locus can be used to form a complete classification of such loci, and how this type can be extracted from the discrete monodromy. In section 2.4 we utilise these results to define the charge orbits at intersections of infinite distance loci. We summarise our results, and discuss extensions and interpretations of them in section 2.5. In the appendix we present a detailed analysis of some example intersection loci as well as collect some of the more technical formalism.

2.2 Monodromy and Orbit Theorems in Calabi-Yau Moduli Spaces

In this section we introduce, and develop in a way adapted to our needs, the crucial mathematical theorems and structures associated to so-called orbits. As briefly discussed in Section 1.4, the central elements are the nilpotent orbit theorem, the Sl(2)-Orbit theorem and the growth theorems. The theorems lead to a detailed and powerful description of the moduli space locally around any singular loci. In particular, we will utilise their multi-variable versions which will allow for a description of a patch of moduli space that can include intersections of infinite distance loci.

2.2.1 Complex Structure Moduli Spaces and Monodromy

The focus of this chapter lies on a particular sector of Type II string compactifications on Calabi-Yau threefolds and we will develop the concepts reviewed in Section 1.2.3 further. More precisely, we will investigate the geometry of the field space spanned by the scalars in the $\mathcal{N} = 2$ vector multiplets arising in these compactifications. These scalars correspond to complex structure deformations of the Calabi-Yau threefold in Type IIB string theory and complexified Kähler structure deformations in Type IIA. Since these two compactifications are deeply linked via mirror symmetry, it will often suffice to address only one of the two sides. In particular, it is important to recall that the complex structure side captures the more general perspective and hence will be the focus for the first part of our exposition. Later on, we will address aspects of the Kähler structure side by discussing large volume compactifications.

To begin with, let us denote the complex structure moduli space by $\mathcal{M}_{\rm cs}$ and introduce the Weil-Petersson metric $g_{\rm WP}$ that arises in the Type IIB string theory comactification. The space $\mathcal{M}_{\rm cs}$ has complex dimension $h^{2,1}$, where $h^{p,q} = \dim_{\mathbb{C}}(H^{p,q}(Y_3))$ are the Hodge numbers of the Calabi-Yau threefold Y_3. In a local patch we can thus introduce complex coordinates z^I, $I = 1, \ldots, h^{2,1}$, which are called the complex structure moduli. The metric $g_{\rm WP}$ on $\mathcal{M}_{\rm cs}$ is special Kähler and determined by the complex structure variations of the holomorphic $(3,0)$-form Ω on Y_3 [20, 21, 120]. Its components $g_{I\bar{J}} = \partial_{z^I}\partial_{\bar{z}^J} K$ can locally be obtained from the Kähler potential

$$K(z,\bar{z}) = -\log\left[\mathbf{i}\int_{Y_3}\Omega\wedge\bar{\Omega}\right] \equiv -\log\left[\mathbf{i}\,\bar{\Pi}^{\mathcal{I}}\eta_{\mathcal{I}\mathcal{J}}\Pi^{\mathcal{J}}\right]\,. \tag{2.2.1}$$

In the second equality we have expanded Ω into a real integral basis $\gamma_{\mathcal{I}}$, $\mathcal{I} = 1, \ldots, 2h^{2,1}+2$ spanning $H^3(Y_3, \mathbb{Z})$. More precisely, we introduced

$$\Omega = \Pi^{\mathcal{I}} \gamma_{\mathcal{I}} \ , \qquad \eta_{\mathcal{I}\mathcal{J}} = -\int_{Y_3} \gamma_{\mathcal{I}} \wedge \gamma_{\mathcal{J}} \ . \tag{2.2.2}$$

In order to simplify notation we will introduce bold-faced letters to denote coefficient vectors in the three-form basis $\gamma_{\mathcal{I}}$, i.e.

$$\mathbf{\Pi} \equiv \left(\Pi^1, \ldots, \Pi^{2h^{2,1}+2}\right)^{\mathrm{T}} \ . \tag{2.2.3}$$

The complex coefficients $\Pi^{\mathcal{I}}$ can be shown to be holomorphic function and are called the *periods* of Ω. Let us stress that z^I, $\Pi^{\mathcal{I}}$, and $\gamma_{\mathcal{I}}$ are adapted to the considered patch in $\mathcal{M}_{\mathrm{cs}}$ and can very non-trivially change when moving to different patches in $\mathcal{M}_{\mathrm{cs}}$.[3]

It is important to discuss the possible transformations preserving the above structure. To begin with, we note that $\eta = (\eta_{\mathcal{I}\mathcal{J}})$ is an anti-symmetric matrix. It defines an anti-symmetric bilinear form

$$S(v, w) \equiv S(\mathbf{v}, \mathbf{w}) = \mathbf{v}^{\mathrm{T}} \, \eta \, \mathbf{w} \equiv -\int_{Y_3} v \wedge w \ , \tag{2.2.4}$$

where v, w are three-forms in $H^3(Y_3, \mathbb{C})$ and $\mathbf{v}$, $\mathbf{w}$ are their coefficient vectors in the integral basis $\gamma_{\mathcal{I}}$. We will use the notations $S(v, w)$ and $S(\mathbf{v}, \mathbf{w})$ interchangeably. One shows that the group preserving η is the real symplectic group $\mathrm{Sp}(2h^{2,1}+2, \mathbb{R})$ acting as

$$M^{\mathrm{T}} \eta M = \eta \ , \quad M \in \mathrm{Sp}(2h^{2,1}+2, \mathbb{R}) \ . \tag{2.2.5}$$

The action of this group thus corresponds to actions on the basis that preserve $S(\mathbf{v}, \mathbf{w}) = S(M\mathbf{v}, M\mathbf{w})$. Crucially, we stress that they do not correspond to a symmetry of the effective theory, but rather to a choice of frame in which to consider the fields. The true symmetry of the effective theory is encoded by the so-called *monodromy group* $\Gamma \subset \mathrm{Sp}(2h^{2,1}+2)$, which we will discuss next.

A crucial fact about the complex structure moduli space $\mathcal{M}_{\mathrm{cs}}$ is that it is neither smooth nor compact. It generally admits points at which the Calabi-Yau manifold becomes singular. These form the so-called discriminant locus. Clearly, it is non-trivial to show general results about these discriminant loci and we first

[3] Furthermore, there is the freedom to rescale the whole vector $\mathbf{\Pi}$ with a holomorphic function $f(z)$, which corresponds to a Kähler transformation of (2.2.1). While one should keep this freedom in mind, we will not mention it again.

summarize some of the main abstract results. Later on we will give a more detailed classification of what actually can happen at this locus. Firstly, we note that the moduli space of smooth Calabi-Yau threefolds is quasi-projective [121], which roughly implies that as long as one removes a divisor Δ_s corresponding to singular Calabi-Yau manifolds it can be embedded into a projective space. The discriminant locus Δ_s can have a very non-trivial structure, since it will generically consist of many intersecting components. Crucially the singularities of the Calabi-Yau manifolds can get worse when moving along Δ_s. A cartoon picture of this is shown in figure 2.5 and we already gave a more realistic description of an actually occurring moduli space in the introduction, see figures 2.2 and 2.3. It was

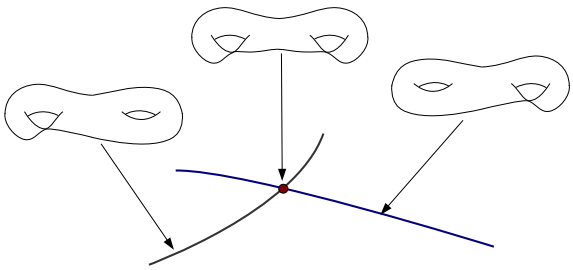

Figure 2.5: Two normally intersecting divisors of the discriminant locus Δ. The singularity of the Calabi-Yau threefold, here depicted as genus-two Riemann surface, worsens at the intersection.

also shown [121, 122] that one can resolve Δ_s to $\Delta = \cup_k \Delta_k$ such that it consists of divisors Δ_k that intersect normally. This result is crucial to justify the local model that we employ to describe the individual patches of the moduli space. Hence, in the following we will always work with the desingularized discriminant locus Δ. It will also be convenient to introduce a shorthand notation for the intersection of l divisors we define

$$\Delta_{k_1 \ldots k_l} = \Delta_{k_1} \cap \ldots \cap \Delta_{k_l} \ . \tag{2.2.6}$$

Another important aspect of the above description of $\mathcal{M}_{\rm cs}$ is the fact that $\mathbf{\Pi}$ can be understood as being multi-valued and experience monodromies along paths encircling the divisor components Δ_k of Δ. To make this more precise, let us introduce local coordinates z^I, such that the divisor Δ_k is given by $z^k = 0$ for some $k \in \{1, \ldots, h^{2,1}\}$. The intersection of divisors Δ_k and Δ_l can be parametrized if one introduces several vanishing local coordinates $z^k = z^l = 0$. We encircle Δ_k

by sending $z^k \to e^{2\pi \mathbf{i}} z^k$. In general the periods will non-trivially transform with a matrix T_k. When defining the monodromy, especially when writing T_k as a matrix, there is a choice between whether the T_k is defined to act on the homology 3-cycles or the cohomology 3-forms. Our convention in this chapter is to let the monodromy act on the integral basis of the 3-forms. Explicitly, with a multi-valued integral basis of 3-forms chosen to be $\{\gamma_{\mathcal{I}}\}$, the monodromy operator T_k induced by the loop $z^k \to e^{2\pi \mathbf{i}} z^k$ is defined by

$$\gamma_{\mathcal{I}}(\ldots, e^{2\pi \mathbf{i}} z^k, \ldots) = \gamma_{\mathcal{J}}(\ldots, z^k, \ldots)\,(T_k)^{\mathcal{J}}_{\mathcal{I}}\ , \text{ for all } \mathcal{I}. \tag{2.2.7}$$

In terms of the period vector $\mathbf{\Pi}$, under our convention, we have

$$\mathbf{\Pi}(\ldots, e^{2\pi \mathbf{i}} z^k, \ldots) = T_k^{-1}\ \mathbf{\Pi}(\ldots, z^k, \ldots)\ . \tag{2.2.8}$$

The monodromy matrices are shown to be quasi-unipotent [75, 123], i.e. they satisfy an equation of the form $(T^m - \mathrm{Id})^{n+1} = 0$ for some positive integers m, n. Furthermore, the monodromies arising from intersecting divisors Δ_k, Δ_l commute $[T_k, T_l] = 0$. This fact remains true for each pair of monodromy matrices if one considers higher intersections. Collecting all T_k from all components of Δ one obtains a group Γ known as the monodromy group. It preserves the pairing η, such that by (2.2.5) we have

$$\Gamma \subset \mathrm{Sp}(2h^{2,1} + 2, \mathbb{R})\ . \tag{2.2.9}$$

More abstractly, the monodromy group can be defined by considering representations of the fundamental group $\pi_1(\mathcal{M}_{\mathrm{cs}})$ acting on the period vectors. In general, the elements of Γ will not commute. However, in this chapter we will restrict ourselves to the commuting monodromies arising at intersections of divisors Δ_k.

In the next section we will have a closer look at the singularities occurring along the Δ_k and their intersections. In order to do that it will be important to extract the unipotent part $T_k^{(u)}$ of each T_k. We define

$$N_k = \frac{1}{m_k} \log(T_k^{m_k}) \equiv \log\Big(T_k^{(u)}\Big)\ , \tag{2.2.10}$$

where m_k is the smallest integer that satisfies $(T_k^{m_k} - \mathrm{Id})^{n_k+1} = 0$. This implies that the N_k are nilpotent, i.e. that there exist integers n_k such that

$$N_k^{n_k+1} = 0\ . \tag{2.2.11}$$

Since each T_k preserves the bilinear form S introduced in (2.2.4), i.e. $S(T_k\cdot, T_k\cdot) = S(\cdot,\cdot)$ one finds

$$S(N_k\mathbf{v}, \mathbf{w}) = -S(\mathbf{v}, N_k\mathbf{w})\ , \tag{2.2.12}$$

and since $T_k^{(u)} \in \mathrm{Sp}(2h^{2,1}+2,\mathbb{R})$ we have $N_k \in \mathfrak{sp}(2h^{2,1}+2,\mathbb{R})$, where $\mathfrak{sp}(n,\mathbb{R})$ is the Lie algebra of $\mathrm{Sp}(n,\mathbb{R})$. The nilpotent elements N_k will be the key players in much of the following discussion. Therefore, it is convenient to make a base transformation and pick right away coordinates for which the monodromies are unipotent. This can be achieved by sending $z^k \to (z^k)^{m_k}$. We should stress that this implies that we lose information about certain types of singularities, such as orbifold singularities. We will see below that it is the unipotent part of T_k that encodes whether or not a point on Δ is at finite or infinite distance. In fact, one checks that the above coordinate change does not alter the discussion relevant to this chapter.

2.2.2 Approximating the periods: Nilpotent orbits

In this section we discuss the first important tool which is used in establishing the mathematical structure that we will explore throughout this chapter. The general important question one wants to address is: Are there simpler functions that approximate the periods $\mathbf{\Pi}$ introduced in (2.2.2) and capture some of their key features? In the following we will introduce a set of such functions known as *nilpotent orbits* following [75]. These not only approximate the periods, but also share their transformation behaviour (2.2.8) under local monodromy transformations. We will also comment on the importance of nilpotent orbits in the context of variations of Hodge structures.

To begin with, let us note that the periods $\mathbf{\Pi}$ of Ω are in general very complicated functions on the moduli space $\mathcal{M}_{\rm cs}$. This can be already expected from the figure 2.2. Hence, at best one can hope to approximate the $\mathbf{\Pi}$ locally. The nilpotent orbits approximate $\mathbf{\Pi}$ in a local patch denoted by $\mathcal{E}$ containing points of the discriminant locus Δ. The local patch is chosen to be of the form

$$\mathcal{E} = (\mathbb{D}^*)^{n_\mathcal{E}} \times \mathbb{D}^{h^{2,1}-n_\mathcal{E}} \ , \tag{2.2.13}$$

i.e. a product of punctured disks $\mathbb{D}^* = \{z \in \mathbb{C} \mid 0 < |z| < 1\}$ and unit disks $\mathbb{D} = \{\zeta \in \mathbb{C} \mid |\zeta| < 1\}$ so that the singular point "lies in the puncture". In other words, we approximate the periods near points at the intersection of $n_\mathcal{E}$ discriminant divisors Δ_i, $i = 1, \ldots, n_\mathcal{E}$, but away from any further intersection. The introduced local coordinates $z^I = (z^i, \zeta^\kappa)$ parametrize the $n_\mathcal{E}$ intersecting discriminant divisors Δ_i given by $z^i = 0$. The coordinates ζ^κ parametrize additional complex directions and do not play an important role in the following discussion. We have introduced the nilpotent matrices N_i in (2.2.10). It was then shown by Schmid [75] that locally

around the point P with $z^i = 0$ the periods take the form

$$\begin{aligned}\mathbf{\Pi}(z,\zeta) &= \exp\Big[\sum_{j=1}^{n_\mathcal{E}} -\frac{1}{2\pi\mathbf{i}}(\log z^j)N_j\Big]\mathbf{A}(z,\zeta)\ , \\ &\equiv \exp\Big[\sum_{j=1}^{n_\mathcal{E}} -t^j N_j\Big]\mathbf{A}\big(e^{2\pi\mathbf{i}t},\zeta\big)\ ,\end{aligned} \tag{2.2.14}$$

with $\mathbf{A}$ being holomorphic in z^i, ζ^κ near P. Here we have also expressed the result in the coordinates

$$t^j \equiv x^j + \mathbf{i}\, y^j = \frac{1}{2\pi\mathbf{i}}\log z^j\ . \tag{2.2.15}$$

This implies that crucial information about the *singular behaviour* of the periods $\mathbf{\Pi}$ near the point P is in the matrices N_j. Furthermore, the second essential information is the leading term in the vector $\mathbf{A}(z,\zeta)$. Since it is holomorphic it admits an expansion

$$\mathbf{A}(z,\zeta) = \mathbf{a}_0(\zeta) + \mathbf{a}_j(\zeta)z^j + \mathbf{a}_{jl}(\zeta)z^j z^l + \mathbf{a}_{jlm}(\zeta)z^j z^l z^m + \dots\ , \tag{2.2.16}$$

with the $\mathbf{a}_0(\zeta),\ \mathbf{a}_j(\zeta)\ ,\dots$ being holomorphic functions of ζ^κ. The nilpotent orbit theorem underlies the statement (2.2.14). Namely, it establishes the fact that the periods $\mathbf{\Pi}$ are well-approximated by the nilpotent orbit

$$\mathbf{\Pi}_{\rm nil} = \exp\Big[\sum_{j=1}^{n_\mathcal{E}} -\frac{1}{2\pi\mathbf{i}}(\log z^j)N_j\Big]\mathbf{a}_0(\zeta) \equiv \exp\Big[\sum_{j=1}^{n_\mathcal{E}} -t^j N_j\Big]\mathbf{a}_0(\zeta)\ , \tag{2.2.17}$$

where an estimate how well the orbit (2.2.17) approximates the actual period $\mathbf{\Pi}$ was given in [75] and [76]. We stress that the nilpotent orbit drops the exponential corrections in the coordinates t, i.e.

$$\mathbf{\Pi}(t,\zeta) = \underbrace{\exp\Big[\textstyle\sum_{j=1}^{n_\mathcal{E}} - t^j N_j\Big]\Big(\mathbf{a}_0(\zeta)}_{\text{nilpotent orbit } \mathbf{\Pi}_{\rm nil}} + \mathcal{O}(e^{2\pi\mathbf{i}t})\Big)\ . \tag{2.2.18}$$

This result is crucial, for example, in evaluating the leading form of the Kähler potential (2.2.1).

Having defined the nilpotent orbit, one immediately sees that it shares the transformation behaviour of the periods under the shifts $t^i \to t^i - \delta^i_k$, i.e.

$$\mathbf{\Pi}_{\rm nil}(\dots, t^k - 1, \dots) = e^{N_k}\,\mathbf{\Pi}_{\rm nil}(\dots, t^k, \dots) = T_k^{(\rm u)}\ \mathbf{\Pi}_{\rm nil}(\dots, t^k, \dots)\ . \tag{2.2.19}$$

Here we stress again that N_k defined via (2.2.10) only captures the unipotent part of the monodromy transformation, which is the only relevant part since we assume

a coordinate transformation $t^k \to m_k t^k$ as at the end of subsection 2.2.1 have been performed.

Let us close this section by recalling some basic facts about Hodge structures and Hodge filtrations and their relation to nilpotent orbit. Recall, that the third cohomology group splits for a given complex structure as

$$H^3(Y_3, \mathbb{C}) = H^{3,0} \oplus H^{2,1} \oplus H^{1,2} \oplus H^{0,3} \ . \tag{2.2.20}$$

This (p,q)-split for a smooth geometry Y_3 defines a so-called *pure Hodge structure* of weight 3 (see appendix 2.A, for some additional details). The changes of this split as one moves in complex structure moduli space are captured by the study of variations of Hodge structures. In order to make this more explicit, we first combine the $H^{p,q}$ as

$$\begin{aligned} F^3 &= H^{3,0}\,, & F^2 &= H^{3,0} \oplus H^{2,1}\,, \\ F^1 &= H^{3,0} \oplus H^{2,1} \oplus H^{1,2}\,, & F^0 &= H^{3,0} \oplus H^{2,1} \oplus H^{1,2} \oplus H^{0,3}\,. \end{aligned} \tag{2.2.21}$$

These complex spaces vary holomorphically with the complex structure moduli z^I. Introducing a flat connection $\nabla_I \equiv \nabla_{\partial/\partial z^I}$, known as the Gauss-Manin connection, one has $\nabla_I F^p \subset F^{p-1}$. For Calabi-Yau threefolds one furthermore finds that all elements of the lower F^p, $p < 3$ are obtained as derivatives of F^3 spanned by the holomorphic $(3,0)$-form. Roughly speaking this implies that all information about the filtration $F \equiv (F^3, F^2, F^1, F^0)$ is encoded by Ω.

Since the periods of Ω are approximated by the nilpotent orbit given in (2.2.17), we can also obtain a filtration by taking derivatives of $\mathbf{\Pi}_{\rm nil}$ when $\mathbf{\Pi}_{\rm nil}$ is represented in a flat frame. Concretely, we evaluate

$$\mathbf{\Pi}_{\rm nil} \xrightarrow{\partial_{t^i}} N_i \mathbf{\Pi}_{\rm nil} \xrightarrow{\partial_{t^j}} N_i N_j \mathbf{\Pi}_{\rm nil} \ \to \ \dots \ , \tag{2.2.22}$$

and note that the derivatives with respect to ζ^κ are encoded by $\nabla_\kappa \mathbf{a}_0, \nabla_\kappa \nabla_\lambda \mathbf{a}_0$, etc. Due to the nilpotent orbit theorem the derivatives of $\mathbf{\Pi}_{\rm nil}$ approximate the elements in spaces F^2, F^1, F^0 up to corrections proportional to $z^j = e^{2\pi \mathbf{i} t^j}$. Clearly, when moving to the points on Δ by sending $t^i \to \mathbf{i}\infty$ the elements (2.2.22) are singular. However, this singularity arises in $\mathbf{\Pi}_{\rm nil}$ and all its derivatives only via the exponential prefactor $\exp(\sum_i t^i N_i)$. As we discuss in the next subsection, we can characterize singularities after dropping the singular prefactor, e.g. by replacing (2.2.22) with

$$\mathbf{a}_0 \longrightarrow N_i \mathbf{a}_0 \longrightarrow N_i N_j \mathbf{a}_0 \ \to \ \dots \ , \tag{2.2.23}$$

and considering in the ζ^κ-directions the derivatives $\nabla_\kappa \mathbf{a}_0, \nabla_\lambda \mathbf{a}_0$, etc. The limiting Hodge filtrations F^p_Δ spanned by these vectors will be discussed in more detail in the next subsection.

2.2.3 Characterizing Singularities in Calabi-Yau Threefolds

We now have a closer look at the arising singularities at the divisors Δ_i and their intersections. In subsections 2.3.1 and 2.3.2 we summarize a recent classification of singularities and allowed enhancements carried out in [113]. This chapter builds on many important and deep mathematical results about so-called limiting mixed Hodge structures. This subsection aims to give the reader a somewhat condensed summary of the underlying mathematical tools with some additional details deferred to appendix 2.A.

The basic object that one associates to the points on Δ is a limiting mixed Hodge structure. For our purposes, rather then introducing in detail the concept of a mixed Hodge structure, it turns out to be useful to directly work with the so-called *Deligne splitting*. We will introduce this splitting in the following. Roughly speaking it captures a finer split $I^{p,q}$, $p,q = 0,\ldots,3$ of the third cohomology group $H^3(Y_3,\mathbb{C})$ as one moves to a singularity of Y_3. In other words the (p,q)-split (2.2.20) for a smooth geometry Y_3 splits into this finer Deligne splitting schematically depicted as

$$(H^{3,0},\ H^{2,1},\ H^{1,2},\ H^{0,3}) \quad \xrightarrow{\text{move to } \Delta} \quad \begin{array}{ccccccc} & & & I^{3,3} & & & \\ & & I^{3,2} & & I^{2,3} & & \\ & I^{3,1} & & I^{2,2} & & I^{1,3} & \\ I^{3,0} & & I^{2,1} & & I^{1,2} & & I^{0,3} \\ & I^{2,0} & & I^{1,1} & & I^{0,2} & \\ & & I^{1,0} & & I^{0,1} & & \\ & & & I^{0,0} & & & \end{array} \ . \tag{2.2.24}$$

To introduce this splitting we follow the filtration $F \equiv (F^3, F^2, F^1, F^0)$ given in (2.2.21) to a point in Δ. As pointed out already in the previous subsection the form will become singular in this limit. However, we can remove these singularities as we discuss in the following.

We begin our consideration with the simplest situation, namely consider points on a divisor Δ_1 that are not elements of any other Δ_l, i.e. we are away from any intersection locus $\Delta_{1l} = \Delta_1 \cap \Delta_l$. We denote this set of points by Δ_1°, generally setting

$$\Delta_k^\circ = \Delta_k - \bigcup_{l\neq k} \Delta_{kl} \ . \tag{2.2.25}$$

To reach the locus Δ_1 we have to send $z^1 \to 0$, which by (2.2.15) is equivalent to

$t^1 \to \mathbf{i}\infty$. For points on Δ_1° one shows that

$$F^p(\Delta_1^\circ) = \lim_{t^1 \to \mathbf{i}\infty} \exp\left[-t^1 N_1\right] F^p \ , \tag{2.2.26}$$

is well-behaved. In this expression we let N_k act on the basis $\gamma_{\mathcal{I}}$ in which all elements of F^p can be expanded. Clearly, $F^p(\Delta_1^\circ)$ is defined on Δ_1° and still depends homomorphically on the other $h^{2,1} - 1$ complex structure moduli.

Let us next move towards the intersection of Δ_1 with another divisor, say Δ_2 in Δ, i.e. let us consider the surface $\Delta_{12} = \Delta_1 \cap \Delta_2$. This requires to send both $z^1, z^2 \to 0$ or $t^1, t^2 \to \mathbf{i}\infty$ and one shows that the spaces $F^p(\Delta_1^\circ)$ are also not generally well-behaved in this limit. To remedy this problem, we consider the locus Δ_{12}°, generally defining defined as

$$\Delta_{kl}^\circ = \Delta_{kl} - \bigcup_{m \neq k,l} \Delta_{klm} \ . \tag{2.2.27}$$

Hence, Δ_{12}° consists of points on Δ_{12} away from any further intersection. On this locus one considers

$$F^p(\Delta_{12}^\circ) = \lim_{t^1, t^2 \to \mathbf{i}\infty} \exp\left[-t^1 N_1 - t^2 N_2\right] F^p \ . \tag{2.2.28}$$

The $F^p(\Delta_{12}^\circ)$ now depend on the remaining $h^{2,1} - 2$ coordinates and are non-singular. We have depicted the assignment of the $F^p(\Delta_1^\circ)$ and $F^p(\Delta_{12}^\circ)$ to the points in Δ in figure 2.6. From this discussion it should be clear that one can proceed in a similar fashion for higher intersections.

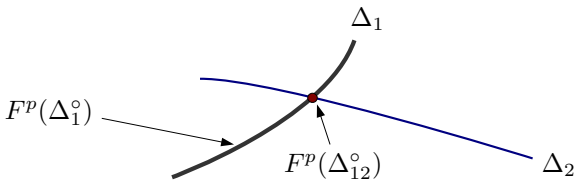

Figure 2.6: Association of a limiting F^p to the points on the discriminant locus.

Let us now turn to the finer split arising at the points of the discriminate locus Δ. This is known as the *Deligne splitting* and encoded by complex vector spaces $I^{r,s}$ with $r + s \in \{0, \ldots, 6\}$. The data defining the splitting at each point of Δ are a limiting F^p, such as $F^p(\Delta_1^\circ)$ and $F^p(\Delta_{12}^\circ)$ introduced in (2.2.26) and (2.2.28),

and an associated nilpotent matrix. The simplest case are again points that are on Δ_1° defined in (2.2.25). The associated nilpotent element is simply N_1. In other words, one associates

$$(F(\Delta_1^\circ), N_1) \quad \mapsto \quad \{I^{p,q}(\Delta_1^\circ)\}_{p,q=0,\ldots,3} \ , \tag{2.2.29}$$

where we denote $F(\Delta_1^\circ) \equiv (F^3(\Delta_1^\circ), \ldots, F^0(\Delta_1^\circ))$ More involved are points that lie on the intersection locus Δ_{12}° of two divisors, since here the immediate question for the associated nilpotent matrix arises. It turns out [75] that one is actually free to choose any N_{12} in the cone

$$\sigma(N_1, N_2) = \{a_1 N_1 + a_2 N_2 \mid a_i > 0\} \ . \tag{2.2.30}$$

It is crucial to note that each choice of a_1, a_2 in (2.2.30) yields the same $I^{p,q}(\Delta_{12}^\circ)$ and we can pick the most convenient combination, such as $N_1 + N_2$. In summary, at the intersection Δ_{12}° and away from any further intersection, one associates

$$(F(\Delta_{12}^\circ), N_1 + N_2) \quad \mapsto \quad \{I^{p,q}(\Delta_{12}^\circ)\}_{p,q=0,\ldots,3} \ . \tag{2.2.31}$$

It should be clear how to generalize this discussion to even higher intersection loci $\Delta_{k_1\ldots k_l}$ introduced in (2.2.6). The associated nilpotent element are now elements of the cone

$$\sigma(N_{k_1}, \ldots, N_{k_l}) = \{a_{k_1} N_{k_1} + \ldots + a_{k_l} N_{k_l} \mid a_i > 0\} \ . \tag{2.2.32}$$

For example, let us consider the intersection of Δ_i, $i = 1, \ldots, l$, away from any further intersection and denote this space by $\Delta_{1\ldots l}^\circ$. By an appropriate relabelling this is the general situation. The limiting Hodge filtration for points on such intersections are given by

$$F^p(\Delta_{1\ldots l}^\circ) = \lim_{t^1,\ldots,t^l \to \mathbf{i}\infty} \exp\left[- \textstyle\sum_{i=1}^l t^i N_i \right] F^p \ . \tag{2.2.33}$$

Then the map to the Deligne splitting is

$$(F(\Delta_{1\ldots l}^\circ), N_{(l)}) \quad \mapsto \quad \{I^{p,q}(\Delta_{1\ldots l}^\circ)\}_{p,q=0,\ldots,3} \ . \tag{2.2.34}$$

Here $N_{(l)}$ is an element of (2.2.32) and we have chosen a simple representative by picking

$$N_{(l)} = \sum_{i=1}^{l} N_i \ . \tag{2.2.35}$$

This also allows us to introduce a notation which will be used throughout the chapter, namely that an index (l) in brackets on a matrix indicates that we add the first l elements of an ordered set, i.e. $(N_1, \ldots, N_l, \ldots)$. Indeed, we will often denote (2.2.34) this way

$$I^{p,q}_{(l)} \equiv I^{p,q}(\Delta^\circ_{1\ldots l}) \ . \tag{2.2.36}$$

With this information at hand we are now in the position to introduce the Deligne splitting $I^{p,q}$ and discuss its properties. To keep the notation simple we will study the map

$$(F_\Delta, N) \quad \mapsto \quad \{I^{p,q}\}_{p,q=0,\ldots,3} \ , \tag{2.2.37}$$

with $F_\Delta = (F^3_\Delta, \ldots, F^0_\Delta)$. The F^p_Δ is the limiting F^p and the N stands for the nilpotent element associated to the considered point on Δ. In other words (2.2.37) can correspond to the cases (2.2.29) and (2.2.31) or any higher intersection. In order to define the $I^{p,q}$ we first note that there is a natural set of vector spaces associated to a nilpotent N known as the *monodromy filtration* W_i, $i = 0, \ldots, 6$. The most natural spaces associated to a given N acting on $H^3(Y_3, \mathbb{C})$ are constructed from the images $\mathrm{Im}\, N^p$ and kernels $\mathrm{Ker}\, N^q$. These allow us to define

$$\begin{array}{ccl}
W_6 & = & V, \\
\cup & & \\
W_5 & = & \mathrm{Ker}\, N^3, \\
\cup & & \\
W_4 & = & \mathrm{Ker}\, N^2 + \mathrm{Im}\, N, \\
\cup & & \\
W_3 & = & \mathrm{Ker}\, N + \mathrm{Im}\, N \cap \mathrm{Ker}\, N^2, \\
\cup & & \\
W_2 & = & \mathrm{Im}\, N \cap \mathrm{Ker}\, N + \mathrm{Im}\, N^2, \\
\cup & & \\
W_1 & = & \mathrm{Im}\, N^2 \cap \mathrm{Ker}\, N, \\
\cup & & \\
W_0 & = & \mathrm{Im}\, N^3.
\end{array} \tag{2.2.38}$$

The properties of the so-defined W_i will be discussed in more detail in appendix 2.A. It is a crucial fact that this filtration W_i associated to higher intersections does not depend on the precise element chosen among the $\sum_i a_i N_i$ with $a_i > 0$ [115]. For example, on Δ°_{12}, the associated spaces W do not depend on which element N_{12} in (2.2.30) one picks.

We now have all the required information to define the Deligne splitting

$$I^{p,q} = F^p_\Delta \cap W_{p+q} \cap \left(\bar{F}^q_\Delta \cap W_{p+q} + \sum_{j\geq 1} \bar{F}^{q-j}_\Delta \cap W_{p+q-j-1} \right) . \tag{2.2.39}$$

At first, this definition looks rather involved and somewhat arbitrary. However, it has many remarkable features, such as being the unique definition satisfying

$$F^p_\Delta = \bigoplus_{r\geq p} \bigoplus_s I^{r,s} , \qquad W_l = \bigoplus_{p+q\leq l} I^{p,q} , \qquad \overline{I^{p,q}} = I^{q,p} \bmod \bigoplus_{r<q, s<p} I^{r,s} . \tag{2.2.40}$$

While the details of this definition are important in our explicit constructions, within this section it often suffices to view $I^{p,q}$ as spaces obtained from F^p_Δ, N and use the features that we will discuss next. Let us note that it is often convenient to use the shorthand notation (F, W) to summarize the relevant data for the map (2.2.39). Here F is a vector containing the spaces $F^3, \ldots, F^0$ relevant at the point in Δ, and W is the weight filtration relevant at this point. This data (F, W) also determines a limiting mixed Hodge structure as described in appendix 2.A. However, it will be more convenient in the following to work with the Deligne splitting.

As a first important property of (2.2.39) one checks that the spaces indeed define a splitting of the total vector space. In fact, at any point of Δ one needs to replace the split (2.2.20) by

$$H^3(Y_3, \mathbb{C}) = \bigoplus_{p,q=0}^{3} I^{p,q} , \tag{2.2.41}$$

where we remind the reader that the $I^{p,q}$ crucially depend on the location of the point, as indicated in (2.2.29) and (2.2.31). One of the most important features of the Deligne splitting arises from the fact that N acts as $NF^p_\Delta \subset F^{p-1}_\Delta$ and $NW_i \subset W_{i-2}$. Applied to (2.2.39) we find

$$NI^{p,q} \subset I^{p-1,q-1} . \tag{2.2.42}$$

We note that this does not mean that the whole lower (p, q)-spaces are obtained by acting with N. In fact, there is a natural way to split each $I^{p,q}$ into a primitive part $P^{p,q}$ that is not obtained by acting with N on a $(p+i, q+i)$-element and a non-primitive part. Explicitly one defines the *primitive* parts to be

$$P^{p,q} = I^{p,q} \cap \operatorname{Ker} N^{p+q-2} . \tag{2.2.43}$$

Clearly, the primitive part $P^{p,q}$ of $I^{p,q}$ contains the core information in the Deligne splitting, since all other elements are obtained by the action of N_k. One shows

that

$$I^{p,q} = \bigoplus_{i\geq 0} N^i(P^{p+i,q+i}) \ . \tag{2.2.44}$$

The primitive elements satisfy another remarkable feature, namely, their norm is positive and non-vanishing for non-vanishing elements. More explicitly, one has

$$S(P^{p,q}, N^l P^{r,s}) = 0 \text{ for } p+q = r+s = l+3 \text{ and } (p,q) \neq (s,r), \tag{2.2.45}$$

$$\mathbf{i}^{p-q} S(v, N^{p+q-3}\bar{v}) > 0 \text{ for } v \in P^{p,q}\,, v \neq 0\,, \tag{2.2.46}$$

where we use the bilinear form introduced in (2.2.4). These properties give us a powerful tool to analyse positivity and vanishing properties of forms at Δ. As we will discuss in the next subsection they are actually key in systematically classifying the allowed singularities and enhancement patterns.

In summary, we have now explained the following picture. As we change the complex structure moduli from a smooth Calabi-Yau threefold to a singular threefold on the discriminant locus on Δ, we need to replace the splitting of $H^3(Y_3, \mathbb{C})$ as in (2.2.24) with the $I^{p,q}$ defined via (2.2.39) or (2.2.40). The occurring splits characterize the singularity at $P \in \Delta$. In subsection 2.3.1 we will focus in detail on such splits and explain how these can be classified systematically for Calabi-Yau threefolds.

From the above construction it is clear that the precise form of $I^{p,q}$ depends on the considered point on Δ and will generally differ for points, for example, on Δ_1° and points on the intersection Δ_{12}°. This implies that we could also move from a generic point on Δ_1° to the intersection locus Δ_{12}°. In this case we expect that the $I^{p,q}(\Delta_1^\circ)$ change to the $I^{p,q}(\Delta_{12}^\circ)$. We write this as

$$I^{p,q}(\Delta_1^\circ) \quad \longrightarrow \quad I^{p,q}(\Delta_{12}^\circ)\ , \tag{2.2.47}$$

with an arrow indicating the enhancement direction. It is crucial in this step to ensure that the polarization conditions (2.2.45), (2.2.46) are transmitted correctly, which in fact imposes severe constraints on the form of the enhancement. As stressed in the introduction it is crucial for us not only to classify all the allowed splittings $I^{p,q}$, but also all the allowed enhancement. This formidable task was carried out in [113] and will be the subject of the next two subsections.

2.2.4 Commuting $\mathfrak{sl}(2)$s and the Sl(2)-orbit

While the nilpotent orbits are useful, for example, in approximating the periods they are, in general, not a simple representation encoding the information about

the asymptotic limit when approaching Δ. However, there is a foundational result of Cattani, Kaplan, and Schmid [76], which shows that there is asymptotically a special representation of the data contained in the nilpotent orbit (2.2.17). Roughly speaking, one is able to replace $(N_i, \mathbf{a}_0)$ with $(N_i^-, \tilde{\mathbf{a}}_0)$ such that the N_i^- are part of commuting $\mathfrak{sl}(2,\mathbb{C})$ algebras and $\tilde{\mathbf{a}}_0$ splits into subvectors affected by the action of these $\mathfrak{sl}(2,\mathbb{C})$. In this representation many of the asymptotic properties of the setting are rather easy to show and can then be translated back into the representation $(N_i, \mathbf{a}_0)$. For example, the growth properties of the Hodge norm discussed in subsection 2.2.5 are proved in this way. For us the existence of the commuting $\mathfrak{sl}(2,\mathbb{C})$ algebras will be of crucial importance when constructing the infinite charge orbit relevant for the Swampland Distance Conjecture as we describe in detail in section 2.4.

We begin our exposition by introducing the commuting $\mathfrak{sl}(2,\mathbb{C})$ algebras in more detail and introduce the steps required to explicitly construct them. In order to do that we consider a local patch $\mathcal{E}$ of the complex structure moduli space that intersects $n_{\mathcal{E}}$ discriminant divisors Δ_i, $i = 1, \ldots, n_{\mathcal{E}}$, which non-trivially intersect each other. In other words, we assume that the highest intersection in $\mathcal{E}$ is $\Delta_{1\ldots n_{\mathcal{E}}}$ which is obtained by intersecting all $n_{\mathcal{E}}$ divisors. Clearly, all other intersections of a smaller number of Δ_i can also be considered. As usual we denote the monodromy logarithms associated to Δ_i by N_i. Crucially, we will choose an ordering of the N_i: $(N_1, \ldots, N_{n_{\mathcal{E}}})$, and all the results presented below will depend on this ordering. Clearly, one still is free to pick any other ordering, but then has to adjust the statements below accordingly. Furthermore, we will assume that the patch $\mathcal{E}$ is chosen such that the nilpotent orbit

$$\mathbf{\Pi}_{\text{nil}} = \exp\Big[\sum_{j=1}^{n_{\mathcal{E}}} -t^j N_j\Big]\mathbf{a}_0^{(n_{\mathcal{E}})} \ , \tag{2.2.48}$$

approximates the periods in $\mathcal{E}$. Starting from this data we want to construct associated commuting $\mathfrak{sl}(2,\mathbb{C})$ algebras. Each of these algebras $\mathfrak{sl}(2,\mathbb{C})_i$ is generated by three elements, and we denote these triples by

$$\text{commuting } \mathfrak{sl}(2,\mathbb{C})_i \text{ triple:} \quad (N_i^-, N_i^+, Y_i) \ . \tag{2.2.49}$$

These elements satisfy the standard $\mathfrak{sl}(2)$-commutation relations $[Y_i, N_i^\pm] = \pm 2 N_i^\pm$ and $[N_i^+, N_i^-] = Y_i$. Furthermore, the triples are pairwise commuting, i.e. all elements in the ith triple commute with all elements of the jth triple for $i \neq j$. Together these triples define a Lie algebra homomorphism

$$\rho_* : \bigoplus_i \mathfrak{sl}(2,\mathbb{C})_i \ \longrightarrow \ \mathfrak{sp}(2h^{2,1}+2,\mathbb{C}) \ , \tag{2.2.50}$$

where ρ gives the map of the corresponding Lie groups. The Sl(2)-orbit theorem of [76] states the properties of the triples in relation to a given nilpotent orbit.

Given a nilpotent orbit (2.2.48) around the highest intersection $\Delta_{1\ldots n_\mathcal{E}}$ one can read off the filtrations (F_Δ, W) with F^p_Δ defined in (2.2.33) and $W_i(N_{(n_\mathcal{E})})$ discussed in (2.2.38). Here we recall that the W_i are induced by $N_{(n_\mathcal{E})} = \sum_{i=1}^{n_\mathcal{E}} N_i$ or any other positive linear combination of the N_i. The corresponding Deligne splitting $I^{p,q}(\Delta_{1\ldots n_\mathcal{E}})$ is determined via (2.2.39) or (2.2.40). A splitting $I^{p,q}$ is called $\mathbb{R}$-split, if it obeys

$$\overline{I^{p,q}} = I^{q,p}, \text{ for all } p, q \ . \tag{2.2.51}$$

It is crucial that the limiting F^p_Δ do not generally induce an $\mathbb{R}$-split Deligne splitting. The SL(2)-orbit theorem of [76][4] remedies this problem by assigning two matrices δ, ζ and a Hodge filtration $\hat{F} = e^{\zeta} e^{-\mathbf{i}\delta} F$ to (F, W) such that the new Deligne splitting $\tilde{I}^{p,q}$ derived from $(\hat{F}, W)$ is $\mathbb{R}$-split. This new structure $(\hat{F}, W)$ is called the Sl(2)-splitting of (F, W). We will review its construction in appendix 2.B. The Sl(2)-splitting is central to the construction of commuting $\mathfrak{sl}(2)$-triples as we discuss in appendix 2.C. In particular, both are linked via the relation

$$Y_{(k)}\, \tilde{I}^{p,q}(\Delta^\circ_{1\ldots k}) = (p+q-3)\, \tilde{I}^{p,q}(\Delta^\circ_{1\ldots k}) \ , \tag{2.2.52}$$

where $Y_{(k)} = Y_1 + \ldots + Y_k$ and $\tilde{I}^{p,q}(\Delta^\circ_{1\ldots k})$ is the Sl(2)-splitting associated to $\Delta^\circ_{1\ldots k}$.

Note that for Calabi-Yau threefolds we have discussed after (2.2.22) that all information contained in F^p_Δ can be inferred from $\mathbf{a}_0$ and its ζ^κ-derivatives and the nilpotent elements. Hence, the existence of an Sl(2)-splitting can be reformulated to the statement that there exists a special

$$\tilde{\mathbf{a}}_0 = e^{\zeta} e^{-\mathbf{i}\delta} \mathbf{a}_0 \ . \tag{2.2.53}$$

The $\tilde{\mathbf{a}}_0$ for the highest point of intersection $\Delta_{1\ldots n_\mathcal{E}}$ will serve as a starting point for the construction of the $\mathfrak{sl}(2)$-triples (2.2.49). Let us denote this by

$$\tilde{\mathbf{a}}_0^{(n_\mathcal{E})} \equiv \tilde{\mathbf{a}}_0(\Delta^\circ_{1\ldots n_\mathcal{E}}) \ . \tag{2.2.54}$$

One then constructs the $\tilde{\mathbf{a}}_0$ relevant at the lower intersections stepwise as we summarize in appendix 2.C. The crucial point for our later discussion is the fact that the initial step for constructing the commuting Sl(2)-triples always requires to start at the highest intersection. The $\tilde{\mathbf{a}}_0^{(n_P)} \equiv \tilde{\mathbf{a}}_0(\Delta^\circ_{1\ldots n_P})$ relevant for a point $P \in \Delta^\circ_{1\ldots n_P}$

[4] More precisely Proposition 2.20 and Theorem 3.25 of [76].

is given by [76] [5]

$$\tilde{\mathbf{a}}_0^{(n_P)} = \exp\left(-\mathbf{i}N^-_{n_P+1}\right)\ \tilde{\mathbf{a}}_0^{(n_P+1)} = \ \ldots\ = \exp\left(-\mathbf{i}\sum_{i=n_P+1}^{n_\mathcal{E}} N_i^-\right)\ \tilde{\mathbf{a}}_0^{(n_\mathcal{E})}\ . \tag{2.2.55}$$

This implies that considering such a point P on a lower intersection also the data of the highest intersection $\Delta^\circ_{1\ldots n_\mathcal{E}}$ is relevant. This non-local information will be crucial in section 2.4 when constructing an infinite charge orbit. An explicit construction of the triples (N_i^-, N_i^+, Y_i) for a two-parameter example is presented in appendix 2.D.

Another important statement of the Sl(2)-orbit theorem is that the nilpotent orbit can be written in terms of yet another orbit, namely the Sl(2)-orbit $\mathbf{\Pi}_{\text{Sl}(2)}$. However, in contrast to the above discussion of the nilpotent orbit approximating the periods, the Sl(2)-orbit should be viewed as an alternative description capturing the main structure of the limiting variation of Hodge structure. Explicitly the relation between the nilpotent orbits and the Sl(2)-orbit are given by

$$\mathbf{\Pi}_{\text{nil}} \equiv \exp\Big[\sum_{j=1}^{n_\mathcal{E}} -t^j N_j\Big]\mathbf{a}_0(\zeta) = \exp\Big[\sum_{j=1}^{n_\mathcal{E}} -x^j N_j\Big]\cdot M(y)\cdot \mathbf{\Pi}_{\text{Sl}(2)} \tag{2.2.56}$$

where the Sl(2)-orbit is given by

$$\mathbf{\Pi}_{\text{Sl}(2)} \equiv \exp\Big[\sum_{j=1}^{n_\mathcal{E}} -\mathbf{i}\,y^j N_j^-\Big]\tilde{\mathbf{a}}_0^{(n_\mathcal{E})}(\zeta)\ , \tag{2.2.57}$$

and we recall the notation $t^i = x^i + \mathbf{i}y^i$. It is crucial here to introduce the y^i-dependent matrix $M(y)$. The Sl(2)-orbit theorem states that $M(y)$ can be written as

$$M(y) = \prod_{r=n}^{1} g_r\left(\frac{y^1}{y^{r+1}}, \ldots, \frac{y^r}{y^{r+1}}\right)\ , \tag{2.2.58}$$

where $g_r(y^1,\ldots,y^r)$ are $\text{Sp}(2h^{2,1}+2,\mathbb{R})$-valued functions. Furthermore, functions $g_r(y^1,\ldots,y^r)$ and $g_r^{-1}(y^1,\ldots,y^r)$ have power-series expansions in non-positive powers of y^1/y^2, y^2/y^3, $\ldots$, y^r with constant term 1 and convergent in a region

$$\hat{\mathcal{R}}_{1\ldots r} = \left\{\frac{y^1}{y^2} > \lambda\ ,\quad \frac{y^2}{y^3} > \lambda\ ,\ldots,\quad y^r > \lambda\right\}\ , \tag{2.2.59}$$

for some $\lambda > 0$. In other words, writing $\mathbf{\Pi}_{\text{nil}}$ in terms of an Sl(2)-orbit $\mathbf{\Pi}_{\text{Sl}(2)}$ depends on the considered region $\hat{\mathcal{R}}_{1\ldots r}$ in moduli space. Of course, we can always

[5] Note that there is an additional minus sign in the exponent compared to (4.56) of [76]. This arises from the fact that we let N_i^- act on the coefficients in an integer basis, rather then the basis itself.

reorder the y^i sending $y^i \to y^{\sigma(i)}$ to be in a region $\hat{\mathcal{R}}_{\sigma(1)\ldots\sigma(r)}$ that satisfies the above conditions. This implies that the Sl(2)-orbit will then be adapted to this ordering.

2.2.5 Growth of the Hodge norm

In this subsection we introduce an important result that follows from the correspondence between nilpotent orbits and commuting Sl(2)s. Namely, we discuss the asymptotic behaviour of the Hodge norm of general three-forms near the discriminant locus Δ. The Hodge norm on a smooth space Y_3 is defined as

$$||v||^2 \equiv ||\mathbf{v}||^2 = \int_{Y_3} v \wedge *\bar{v} \equiv S(C\mathbf{v}, \bar{\mathbf{v}}) \ , \tag{2.2.60}$$

where v is a complex 3-form, $*$ is the Hodge star operator, and $\mathbf{v}$ are the components of v in the integral basis γ_I. In the pure Hodge decomposition (2.2.20) the Hodge operator acts as $*v = \mathbf{i}^{p-q} v$ for $v \in H^{p,q}(Y_3)$. Let us note that the Hodge norm can also be written in terms of the bilinear form S defined in (2.2.4) and the Weil operator C. The Weil operator acts as $\mathbf{i}^{p-q}$ on (p,q)-forms and is used in [75, 76]. The definition (2.2.60) implies, for example, that the Hodge norm of the unique $(3,0)$-form Ω on Y_3 is given by

$$||\Omega||^2 \equiv ||\mathbf{\Pi}||^2 = \mathbf{i} \int_{Y_3} \Omega \wedge \bar{\Omega} = e^{-K} \ , \tag{2.2.61}$$

where we have expressed the result using the Kähler potential (2.2.1) on the complex structure moduli space.

Extracting the behaviour of $||v||^2$ when approaching a point on Δ is, of course, a very non-trivial task. In fact, at first, it seems impossible that this can be done at all, since it appears to be a highly *path-dependent* question. To highlight this point further, let us consider a two-dimensional moduli space, locally parameterized by two coordinates z^1, z^2. We consider two divisors Δ_1 and Δ_2 intersecting in a point (see also subsection 2.2.3). Clearly an intersection point $P = \Delta_1 \cap \Delta_2$ can be approached on many different paths, as indicated in figure 2.7. Recalling the discussion of subsection 2.3.3 the points on Δ_1° and Δ_2° can be at finite or infinite distance, and one expects that the growth of the norm $||v||^2$ can differ greatly when approaching a finite or an infinite distance point. Considering, for example, $||\Omega||^2$ the growth of the Hodge norm corresponds to the growth of the Kähler potential which clearly is connected to the distance of the point. The issue becomes particularly eminent when P is at this intersection of divisors with Δ_1° of type I and

Δ_2° of type IV, i.e. using (2.3.11) one at finite distance and one at infinite distance. The growth of the Hodge norm along the paths in figure 2.7 then should differ significantly. Remarkably, the growth theorem proven in [76] takes into account this path dependence and nevertheless gives a universal result. We present this results for v being a flat section under the Gauss-Manin connection ∇ briefly discussed at the end of subsection 2.2.2 and briefly comment on generalizations in (2.2.74).

To begin with let us state the growth theorem for the case that we consider points at a single divisor Δ_1° at $t^1 = \mathbf{i}\infty$, i.e. a point on Δ_1 away from any intersection. We consider a three-form v that satisfies

$$v \in W_j(N_1) , \qquad W_j(N_1) = \bigoplus_{p+q\leq j} I^{p,q}(\Delta_1^\circ) , \tag{2.2.62}$$

where we recalled that W_j, defined in (2.2.38), can be decomposed into the Deligne splitting $I^{p,q}$ associated to the locus Δ_1° (see (2.2.40)). Here j is corresponding to the smallest value $0, 1, \ldots, 6$ such that (2.2.62) holds. This is relevant due to the fact that we have $W_{j+1} \subset W_j$. Then the growth theorem [75] states, that for $\mathrm{Im}\, t^1 > \lambda$ and $\mathrm{Re}\, t^1 < \delta$, with λ, δ being sufficiently large constants, one finds the dominant growth

$$||v||^2 \sim c\,(\mathrm{Im}\, t^1)^{j-3} , \qquad c > 0 . \tag{2.2.63}$$

Here and below the $\sim$ indicates that there are generally terms that grow slower than this leading term. In particular, one can have terms proportional to $(\mathrm{Im}\, t^1)^{j-3-k}$ for $k > 0$ or exponentially suppressed terms proportional to $e^{-\mathrm{Im}\, t^1}$. Clearly, in this one-parameter case, path dependence is not an issue.

Let us next consider the two-parameter situation, i.e. we consider a point P on the intersection of Δ_1 and Δ_2, located at $t^1 = \mathbf{i}\infty$ and $t^2 = \mathbf{i}\infty$, but away from any further intersection within Δ. Then the growth theorem depends on the path taken towards the point P at $t^1 = t^2 = \mathbf{i}\infty$. We can think of this as corresponding to the two ways we can reach the singularity type at point P. Namely, we can first enhance to the singularity at Δ_1° and then move to Δ_{12}° or we can first enhance to the singularity at Δ_2° and then to Δ_{12}°. This corresponds to paths 1 and 3 in figure 2.7. The relevant nilpotent elements are then

$$\begin{aligned} &(1) \quad \Delta_1^\circ \;\to\; \Delta_{12}^\circ : \qquad (N_1, N_1 + N_2) , \\ &(2) \quad \Delta_2^\circ \;\to\; \Delta_{12}^\circ : \qquad (N_2, N_1 + N_2) . \end{aligned} \tag{2.2.64}$$

Let us start with the case (1) and consider a three-form v satisfying

$$v \in W_{l_1}(N_1) \cap W_{l_2}(N_1 + N_2) , \tag{2.2.65}$$

where $W_{l_1}(N_1)$ can be split as in (2.2.62), while $W_{l_2}(N_1+N_2)$ is associated to N_1+N_2 and hence splits into the Deligne splitting on Δ_{12}° as $W_{l_2}(N_1+N_2) = \bigoplus_{p+q\leq l_2} I^{p,q}(\Delta_{12}^\circ)$. Note that here l_1 and l_2 are the lowest values for which (2.2.65) is satisfied. The growth theorem of [76] now states that this v has the leading growth

$$||v||^2 \sim c\left(\frac{\text{Im } t^1}{\text{Im } t^2}\right)^{l_1-3} (\text{Im } t^2)^{l_2-3}\ , \qquad c>0\ , \tag{2.2.66}$$

when approaching the intersection point $t^1=t^2=\mathbf{i}\infty$. In order for this to be true, however, one has to restrict to paths in the region

$$\mathcal{R}_{12} = \left\{ \frac{\text{Im } t^1}{\text{Im } t^2} > \lambda\ ,\ \ \text{Im } t^2 > \lambda \right\}\ , \tag{2.2.67}$$

for any constant $\lambda>0$ and demand that $\text{Re } t^1, \text{Re } t^2$ are bounded by some constant. We will denote such a restriction as a *growth sector*, so that all paths in $\mathcal{R}_{12}$ are in the same growth sector. We have depicted this condition in figure 2.7. Let us stress that the growth in (2.2.66) is polynomial as long as $l_1\leq l_2$. This will always happen, for example, for the growth of the Kähler potential e^{-K} as we will see below.

Clearly, in order to discuss the case (2) we simply have to exchange N_1 and N_2 and t^1 and t^2 in all formulas. One thus finds that for

$$v\ \in\ W_{l_1}(N_2)\cap W_{l_2}(N_1+N_2)\ , \tag{2.2.68}$$

one has the leading growth of the Hodge norm

$$||v||^2 \sim c\left(\frac{\text{Im } t^2}{\text{Im } t^1}\right)^{l_1-3} (\text{Im } t^1)^{l_2-3} \quad \text{in} \quad \mathcal{R}_{21} = \left\{ \frac{\text{Im } t^2}{\text{Im } t^1} > \lambda\,,\ \text{Im } t^1 > \lambda \right\}\ , \tag{2.2.69}$$

for any constant $\lambda>0$ and bounded $\text{Re } t^1, \text{Re } t^2$.

While having only discussed the two-parameter case, the reader might anticipate the form of the general growth theorem for any number of intersecting divisors. We summarize this important result of Cattani, Kaplan, and Schmid [76] and Kashiwara [107] in the following. Let us consider the leading growth when approaching a point P on the intersection of n_P divisors $\Delta_1,\ldots,\Delta_{n_P}$ in Δ located at $t^1=\ldots=t^{n_P}=\mathbf{i}\infty$. To simplify the notation we recall that we introduced in (2.2.15) that $t^i=x^i+\mathbf{i}y^i$. The sectors are specified for fixed $\lambda,\delta>0$. The $n_P!$ orderings give different overlapping sectors. We pick for the N_i the ordering

$$\text{chosen ordering:} \qquad N_1,\ N_2,\ \ldots,\ N_{n_P}\ , \tag{2.2.70}$$

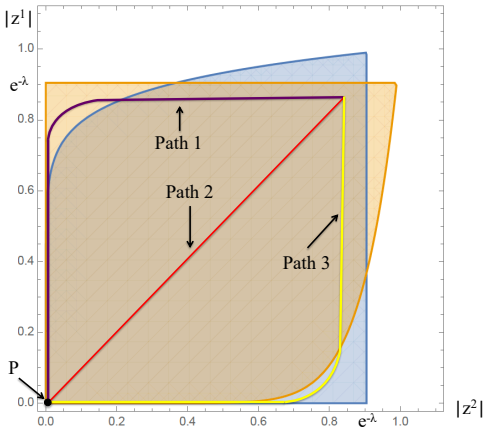

Figure 2.7: Real slice through two intersecting divisors located at $z^1 = e^{2\pi i t^1} = 0$ and $z^2 = e^{2\pi i t^2} = 0$. The intersection point is the origin $P = \{|z^1| = |z^2| = 0\}$. The shaded areas show the two overlapping regions (2.2.67), (2.2.69) a path to the singularity at the origin can pass through, in order that the growth can be evaluated using (2.2.66), (2.2.69) for the constant λ set to $\lambda = 0.1$. Three paths of different nature with respect to this are shown.

with all other orderings obtained by exchanging N_i and t^i in the following formulas. Next we consider a v with

$$v \in W_{l_1}\big(N_{(1)}\big) \cap W_{l_2}\big(N_{(2)}\big) \cap \ldots \cap W_{l_{n_P}}\big(N_{(n_P)}\big) \tag{2.2.71}$$

where $N_{(j)} = \sum_{i=1}^{j} N_i$ and l_i are the lowest values for which this is true. The leading growth of the Hodge norm is then

$$||v||^2 \sim c \left(\frac{y^1}{y^2}\right)^{l_1-3} \cdots \left(\frac{y^{n_P-1}}{y^{n_P}}\right)^{l_{n_P-1}-3} (y^{n_P})^{l_{n_P}-3} \tag{2.2.72}$$

for some $c > 0$. Associated to the ordering (2.2.70) the growth sector for the allowed paths takes the form

$$\mathcal{R}_{1\ldots n_P} = \left\{ t^i : \quad \frac{y^1}{y^2} > \lambda, \ldots, \frac{y^{n_P-1}}{y^{n_P}} > \lambda, \; y^{n_P} > \lambda, \quad x^i < \delta \right\}. \tag{2.2.73}$$

It might be interesting to stress that the proof in [76] of this theorem uses fundamentally the Sl(2)-orbit theorem briefly discussed in subsection 2.2.4 and much of

the technology reviewed in this section. In particular, the relevant sector (2.2.73) for allowed paths arises due to the convergence properties of the Sl(2)-orbit and agrees with (2.2.59) in its y^i-part.

As an application of this growth theorem, let us evaluate the growth of $||\Omega||^2$ and hence via (2.2.61) of the Kähler potential e^{-K}. The first step is to approximate the periods $\mathbf{\Pi}$ by the nilpotent orbit $\mathbf{\Pi}_{\rm nil}$. The nilpotent orbit $\mathbf{\Pi}_{\rm nil}$ then can be approximated by the Sl(2)-orbit as in (2.2.56), when restricting to the appropriate sector (2.2.59). The latter is defined using the $\tilde{\mathbf{a}}_0^{(n_\varepsilon)}$ introduced in subsection 2.2.4. While the relation between the nilpotent and Sl(2)-orbit contains non-trivial y^i-dependent terms, one can show that they are bounded and do not alter the growth. In fact, one has that the growth of both $\mathbf{\Pi}_{\rm nil}$ and $\tilde{\mathbf{a}}_0^{(n_\varepsilon)}$ agree such that [76][6]

$$||\mathbf{\Pi}||^2 \;\sim\; ||\mathbf{\Pi}_{\rm nil}||^2 \;\sim\; \big|\big|\tilde{\mathbf{a}}_0^{(n_\varepsilon)}\big|\big|^2 \;, \tag{2.2.74}$$

where the symbol $\sim$ as above indicates that we are only considering the leading growth near the point P on the discriminant locus. We can now infer the growth by using the location of $\mathbf{a}_0$ in the filtrations $W_l(N^-_{(k)})$, where $N^-_{(k)} = \sum_{i=1}^k N^-_i$ in analogy to (2.2.35). We note that [7]

$$\tilde{\mathbf{a}}_0^{(n_\varepsilon)} \;\in\; W_{d_1+3}\big(N^-_{(1)}\big) \cap W_{d_2+3}\big(N^-_{(2)}\big) \cap \ldots \cap W_{d_{n_P}+3}\big(N^-_{(n_P)}\big) \;. \tag{2.2.75}$$

The integer d_i is defined by

$$\big(N^-_{(i)}\big)^{d_i}\tilde{\mathbf{a}}_0^{(n_\varepsilon)} \neq 0 \;, \qquad \big(N^-_{(i)}\big)^{d_i+1}\tilde{\mathbf{a}}_0^{(n_\varepsilon)} = 0 \;. \tag{2.2.76}$$

In other words it labels in which $\tilde{I}^{p,q}$ the $\tilde{\mathbf{a}}_0^{(n_\varepsilon)}$ resides at the various intersection loci. Denoting the Sl(2)-split Deligne splitting on $\Delta^\circ_{1\ldots k}$ by $\tilde{I}^{p,q}(\Delta^\circ_{1..k})$ one has $\tilde{\mathbf{a}}_0^{(n_\varepsilon)} \in \tilde{I}^{3,d_k}(\Delta^\circ_{1\ldots k})$ for $k = 1, \ldots, n_P$. Later on in subsection 2.3.1 we will also see that d_i labels the type of the singularity at the intersection, i.e. one has

$$\text{singularity on } \Delta^\circ_{1\ldots k} \text{ is Type I, II, III, IV} \quad\Longleftrightarrow\quad d_k = (0,1,2,3) \;. \tag{2.2.77}$$

This will become more clear with the classification of singularities that we will present in the next section. We will also show that there are restrictions on the

[6] In fact, it was shown generally in [76] that the growth result (2.2.72) also hold if one multiplies v by either $\exp(\sum_i x^i N_i)$, $\exp(\sum_i t^i N_i)$, or even the matrix relating $\mathbf{\Pi}$ and $\mathbf{a}_0$.

[7] This can be inferred by using (2.2.55) extended to all $\mathbf{a}_0^{(i)}$. The $\mathbf{a}_0^{(i)}$ are the vectors spanning the Sl(2)-split $\hat{F}^3 = \tilde{I}^{3,d_i}$ on the intersection loci $\Delta^\circ_{1\ldots i}$. The fact, that the location of $\mathbf{a}_0^{(i)}$ and $\mathbf{a}_0^{(n_\varepsilon)}$ follows from the commutativity of the $\mathfrak{sl}(2)$-triples, as we will discuss in a slightly different context when we study the charge orbit below.

allowed enhancements and in particular that $d_i \leq d_{i+1}$. Using (2.2.75), together with the fact $W(N^-_{(i)}) = W(N_{(i)})$ in the Sl(2)-orbit theorem of [76], and the general growth result (2.2.72) we thus find

$$e^{-K} \sim \left|\left|\tilde{\mathbf{a}}_0^{(n\varepsilon)}\right|\right|^2 \sim c\, \left(y^1\right)^{d_1} \left(y^2\right)^{d_2-d_1} \cdots (y^{n_P})^{d_{n_P}-d_{n_P-1}} \,. \tag{2.2.78}$$

This expression gives the general growth of the Kähler potential for any path approaching P in the sector (2.2.73). Other sectors can be obtained by exchanging the N_i and y^i.

2.3 Classifying Singularities in Calabi-Yau Moduli Spaces

In this section we summarize some general classification results that highlight the power of the mathematical tools introduced in section 2.2. More precisely, we will discuss a classification of Calabi-Yau threefold singularities in subsection 2.3.1, their allowed enhancement patterns in subsection 2.3.2, and make some comments on the classification of infinite distance points in subsection 2.3.3. A special emphasis is given to the discussion of the large complex structure and large volume configurations, where the presented tools and classifications are of immediate use. We stress that the results of this section are relevant in many different contexts that are not related to a discussion of the Swampland Distance Conjecture. Therefore, this section can also be read independently of the main motivation of this chapter.

2.3.1 A Classification of Calabi-Yau Threefold Singularities

Having summarized the relevant mathematical background we are now in the position to present a classification of Calabi-Yau threefold singularities and allowed enhancement patterns. While we will mostly discuss the results of [113], we will add some additional new insights that are particularly useful for explicit computations.

The basic idea to classify the arising singularities of Y_3 is to classify the allowed Deligne splittings $I^{p,q}$. As we described in subsection 2.2.3 these Deligne splittings non-trivially depend on the objects F^p_Δ and N associated to the considered point on Δ. The $I^{p,q}$ package this information in an intuitive and useful way. In particular, one can introduce to each point of Δ a *limiting Hodge diamond* containing the

dimensions of the $I^{p,q}$ given by

$$\begin{array}{ccccccc} & & & i^{3,3} & & & \\ & & i^{3,2} & & i^{2,3} & & \\ & & i^{3,1} & & i^{2,2} & & i^{1,3} \\ & i^{3,0} & & i^{2,1} & & i^{1,2} & & i^{0,3} \\ & & i^{2,0} & & i^{1,1} & & i^{0,2} \\ & & & i^{1,0} & & i^{0,1} & \\ & & & & i^{0,0} & & \end{array} \quad , \qquad i^{p,q} = \dim_{\mathbb{C}} I^{p,q} \ . \tag{2.3.1}$$

Since the $I^{p,q}$ represent a finer split of the cohomology near the singularity, we can decompose original Hodge numbers for the smooth geometry at the considered point on Δ into the Hodge-Deligne numbers as

$$h^{p,3-p} = \sum_{q=0}^{3} i^{p,q} \ , \qquad p = 0, \ldots, 3. \tag{2.3.2}$$

Furthermore, one can deduce several properties of a limiting Hodge diamond [8]

$$i^{p,q} = i^{q,p} = i^{3-q,3-p} \ , \qquad \text{for all } p, q \ , \tag{2.3.3}$$

$$i^{p-1,q-1} \leq i^{p,q}, \qquad \text{for } p+q \leq 3 \ . \tag{2.3.4}$$

Given these properties, a first step in classifying singularities is to classify all possible Hodge-Deligne diamonds.

For Calabi-Yau threefolds the classification of limiting Hodge diamonds is greatly simplified by the fact that one has $h^{3,0} = 1$. Using (2.3.2) that there are four possible cases $i^{3,d} = 1$, $d = 0, 1, 2, 3$, which we label by Latin numbers following [113], I, II, III, IV. Furthermore, due to the symmetries (2.3.3) there are just two independent Hodge-Deligne numbers, which we pick to be $i^{2,1}$ and $i^{2,2}$. In table 2.1 we will use a more pictorial way to represent the limiting Hodge diamonds. For example, the limiting Hodge diamond for $d = 2$ is depicted as

$$\begin{array}{ccccccc} & & & 0 & & & \\ & & 1 & & 1 & & \\ & 0 & & i^{2,2} & & 0 & \\ 0 & & i^{2,1} & & i^{2,1} & & 0 \\ & 0 & & i^{2,2} & & 0 & \\ & & 1 & & 1 & & \\ & & & 0 & & & \end{array} \qquad \cong \qquad$$

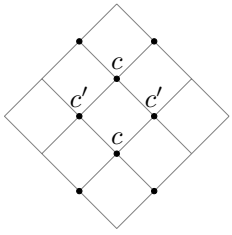

$$c = i^{2,2}$$
$$c' = i^{2,1}$$

[8] A detailed discussion of these properties can be found in section 5.2 of [113].

Furthermore, we will index the singularity type with $i^{2,2}$ writing

$$\mathrm{I}_{i^{2,2}}\,, \quad \mathrm{II}_{i^{2,2}}\,, \quad \mathrm{III}_{i^{2,2}}\,, \quad \mathrm{IV}_{i^{2,2}}\,. \tag{2.3.5}$$

The allowed values for $i^{2,2}$ are obtained form (2.3.2) and differ for the different singularity types as summarized in the third column of table 2.1. In total we thus find $4h^{2,1}$ possible limiting Hodge diamonds depicted in the second column of table 2.1.

name	Hodge diamond	labels	Young diagram	rank$(N, N^2, N^3), \eta$
I_a	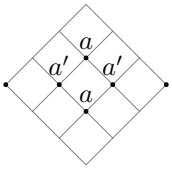	$a + a' = m$ $0 \leq a \leq m$	$\begin{array}{\|c\|c\|}\hline + & - \\ \hline \end{array} \otimes a$ $\otimes 2a' + 2$	$(a, 0, 0)\,,$ ηN has a negative eigenvalues
II_b	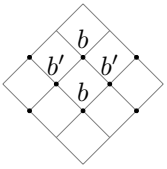	$b + b' = m - 1$ $0 \leq b \leq m - 1$	$\begin{array}{\|c\|c\|}\hline + & - \\ \hline - & + \\ \hline \end{array} \otimes b$ $\otimes 2$ $\otimes 2b'$	$(2 + b, 0, 0)\,,$ ηN has b negative and 2 positive eigenvalues
III_c	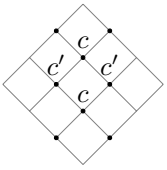	$c + c' = m - 1$ $0 \leq c \leq m - 2$	$\begin{array}{\|c\|c\|c\|}\hline & & \\ \hline + & - & \\ \hline \end{array} \otimes 2$ $\otimes c$ $\otimes 2c' - 2$	$(4 + c, 2, 0)$
IV_d	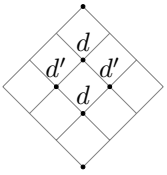	$d + d' = m$ $1 \leq d \leq m$	$\begin{array}{\|c\|c\|c\|c\|}\hline - & + & - & + \\ \hline + & - & & \\ \hline \end{array} \otimes 1$ $\otimes d - 1$ $\otimes 2d'$	$(2 + d, 2, 1)$

Table 2.1: The $4m$ possible limiting Hodge diamonds with Hodge numbers $h^{2,1} = m$. The label next to a dot at a point (p, q) represents the value of $i^{p,q}$. A dot at (p, q) without a label represents $i^{p,q} = 1$.

In addition to enumerating the allowed limiting Hodge diamonds one can also characterize the associated nilpotent elements N. In order to do that one has

to classify conjugacy classes of nilpotent elements that are invariant under basis transformations. Recall that N is an element of the Lie algebra $\mathfrak{sp}(2h^{2,1}+2,\mathbb{R})$ as discussed after (2.2.12). The Lie group $\mathrm{Sp}(2h^{2,1}+2,\mathbb{R})$ acts on its Lie algebra $\mathfrak{sp}(2h^{2,1}+2,\mathbb{R})$ via the adjoint action, i.e. $N \mapsto gNg^{-1}$ for $g \in \mathrm{Sp}(2h^{2,1}+2,\mathbb{R})$. Classifying the conjugacy classes of nilpotent elements obtained by this equivalence is a well-known problem and it was shown in [124, 125] that it is equivalent to classifying signed Young diagrams. While not very involved, we will refrain from presenting the details of this classification here, but only list the relevant result in the fourth column of table 2.1. The result is that to each singularity type I_a, II_b, III_a, IV_d there is a unique associated signed Young diagram which characterizes the form of N and η. This information allows one, for example, to associate a simple normal form of N, η to the singularity type. In order that the reader gets an intuition for such normal forms, we give a possible choice in table 2.2. In order to obtain the complete N, η one needs to use the building blocks of table 2.2 and combine them in the canonical way to a higher-dimensional matrix.

We should stress that in many of the applications and explicit computations the normal forms of table 2.2 play no role. Rather, it is often useful to have a more basis independent way to determine the singularity type for a given N, η. In the last column of table 2.1 we have included such a distinguishing criterion. To begin with we note that the ranks of N^k, $k = 1, 2, 3$, often differ for the various singularity types, as one deduces from (2.2.42), (2.2.44) and the polarization condition (2.2.45), (2.2.46). However, there are $(h^{2,1}-1)$ pairs of I_a and II_{a-2} that cannot be distinguished by only comparing the ranks. In this case one can use again the polarization condition to show that these cases differ by the sign of the eigenvalues of ηN. Taking this feature into account indeed the singularity type for a given N, η is uniquely fixed. Clearly, the same conclusion can be reached from using the normal forms combining table 2.1 and 2.2.

2.3.2 A Classification of allowed Singularity Enhancements

Having classified the allowed singularity types, we next turn to the discussion of allowed singularity enhancements. More precisely, let us assume that on the locus Δ_1° the singularity type is specified by $\mathrm{Type}_a(\Delta_1^\circ)$. We then want to answer the question to which singularity types $\mathrm{Type}_b(\Delta_{12'}^\circ)$ this type can enhance further when moving to Δ_{12}°, i.e. we consider

$$\mathrm{Type}_a(\Delta_1^\circ) \quad \longrightarrow \quad \mathrm{Type}_{\hat{a}}(\Delta_{12}^\circ)\ , \tag{2.3.6}$$

(signed) Young diagram	N	η
	$\begin{pmatrix} 0 & 0 \\ 0 & 0 \end{pmatrix}$	$\begin{pmatrix} 0 & -1 \\ 1 & 0 \end{pmatrix}$
	$\begin{pmatrix} 0 & 0 \\ 1 & 0 \end{pmatrix}$	$\begin{pmatrix} 0 & -1 \\ 1 & 0 \end{pmatrix}$
	$\begin{pmatrix} 0 & 0 \\ 1 & 0 \end{pmatrix}$	$\begin{pmatrix} 0 & 1 \\ -1 & 0 \end{pmatrix}$
	$\begin{pmatrix} 0 & 0 & 0 & 0 & 0 & 0 \\ 1 & 0 & 0 & 0 & 0 & 0 \\ 0 & 1 & 0 & 0 & 0 & 0 \\ 0 & 0 & 0 & 0 & 0 & 0 \\ 0 & 0 & 0 & -1 & 0 & 0 \\ 0 & 0 & 0 & 0 & -1 & 0 \end{pmatrix}$	$\begin{pmatrix} 0 & 0 & 0 & 0 & 0 & -1 \\ 0 & 0 & 0 & 0 & -1 & 0 \\ 0 & 0 & 0 & -1 & 0 & 0 \\ 0 & 0 & 1 & 0 & 0 & 0 \\ 0 & 1 & 0 & 0 & 0 & 0 \\ 1 & 0 & 0 & 0 & 0 & 0 \end{pmatrix}$
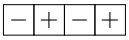	$\begin{pmatrix} 0 & 0 & 0 & 0 \\ 1 & 0 & 0 & 0 \\ 0 & 1 & 0 & 0 \\ 0 & 0 & -1 & 0 \end{pmatrix}$	$\begin{pmatrix} 0 & 0 & 0 & 1 \\ 0 & 0 & 1 & 0 \\ 0 & -1 & 0 & 0 \\ -1 & 0 & 0 & 0 \end{pmatrix}$

Table 2.2: List of all relevant signed Young diagrams and their associated N, η in some normal form. The complete signed Young diagram and N, η that classify a singularity type are composed out of these building blocks.

where in the following we will denote the allowed enhancements by an arrow. It was argued in [113] that imposing consistency of the polarization conditions (2.2.45), (2.2.46) on Δ_1° and Δ_{12}° leads to non-trivial constraints on possible enhancements. The resulting rules are shown in table 2.3, and their derivation is outlined later in this section and in appendix 2.E. It should be stressed that the enhancement rules are actually general and apply to any higher intersection and not only to the case of two divisors Δ_1, Δ_2 intersecting in Δ_{12}°.

starting singularity type	enhance singularity type
I_a	$\mathrm{I}_{\hat{a}}$ for $a \leq \hat{a}$
	$\mathrm{II}_{\hat{b}}$ for $a \leq \hat{b}$, $a < h^{2,1}$
	$\mathrm{III}_{\hat{c}}$ for $a \leq \hat{c}$, $a < h^{2,1}$
	$\mathrm{IV}_{\hat{d}}$ for $a < \hat{d}$, $a < h^{2,1}$
II_b	$\mathrm{II}_{\hat{b}}$ for $b \leq \hat{b}$
	$\mathrm{III}_{\hat{c}}$ for $2 \leq b \leq \hat{c}+2$
	$\mathrm{IV}_{\hat{d}}$ for $1 \leq b \leq \hat{d}-1$
III_c	$\mathrm{III}_{\hat{c}}$ for $c \leq \hat{c}$
	$\mathrm{IV}_{\hat{d}}$ for $c+2 \leq \hat{d}$
IV_d	$\mathrm{IV}_{\hat{d}}$ for $d \leq \hat{d}$

Table 2.3: List of all allowed enhancements obtained by imposing consistency of the polarization conditions (2.2.45), (2.2.46). These have been shown in [113] and the details of their derivation are given in appendix 2.E.

Using the enhancement rules of table 2.3 one obtains an instructive picture of the singularity structure of a Calabi-Yau threefold Y_3 for a given $h^{2,1}$. In figure 2.4 we display the two cases $h^{2,1} = 2$ and $h^{2,1} = 3$. It is interesting to note that, as of now, it is not known whether all allowed enhancements of table 2.3 are actually realized in some Calabi-Yau threefold.

In order to deduce the allowed enhancements one has to use a substantial amount

of mathematics. We will limit ourselves to some essential facts and refer the reader to appendix 2.E, where further details on the underlying constructions are presented. The main focus of this investigation lies on the primitive parts $P^{p,q} \subset I^{p,q}$ that were defined in (2.2.43). We note that by using (2.2.43) one deduces that $I^{3,j} = P^{3,j}$ and $I^{j,3} = P^{j,3}$ for $j = 0, 1, 2, 3$. Furthermore, we can apply (2.2.44) to infer that the $I^{p,q}$ split into the $P^{p,q}$ as

$$\begin{array}{ccccccc} & & & P^{3,3} & & & \\ & & P^{3,2} & & P^{2,3} & & \\ & P^{3,1} & & P^{2,2} \oplus NP^{3,3} & & P^{1,3} & \\ P^{3,0} & & P^{2,1} \oplus NP^{3,2} & & P^{1,2} \oplus NP^{2,3} & & P^{0,3} \\ & NP^{3,1} & & NP^{2,2} \oplus N^2P^{3,3} & & NP^{1,3} & \\ & & N^2P^{3,2} & & N^2P^{2,3} & & \\ & & & N^3P^{3,3} & & & \end{array} \ . \tag{2.3.7}$$

The primitive subspaces are thus given by

$$\begin{aligned} P^6 &= P^{3,3} \ , & P^5 &= P^{3,2} \oplus P^{2,3} \ , \\ P^4 &= P^{3,1} \oplus P^{2,2} \oplus P^{1,3} \ , & P^3 &= P^{3,0} \oplus P^{2,1} \oplus P^{1,2} \oplus P^{0,3} \ , \end{aligned} \tag{2.3.8}$$

where the single superscript on P^r is the weight $r = p + q$ of the contained $P^{p,q}$. One of the most fundamental results about this construction is that each P^j with $j = 3, \ldots, 6$ can be shown to define a pure Hodge structure of weight j. Recall that also the decomposition (2.2.20) on a smooth Y_3 provided a pure Hodge structure, which was the starting point of the construction of the splittings relevant at the singularities. The main idea for looking at enhancements moving from Δ_1° to an intersection Δ_{12}° is to view $P^j(\Delta_1^\circ)$ as defining the starting pure Hodge structures that then splits into even finer mixed Hodge structures. Representing the mixed Hodge structures by Deligne splittings, one thus has

$$P^j(\Delta_1^\circ) \quad \longrightarrow \quad [I^{p,q}]^j\,(\Delta_{12}^\circ) \text{ with } 0 \leq p + q \leq 2j \ . \tag{2.3.9}$$

One can rearrange the spaces $[I^{p,q}]^j\,(\Delta_{12}^\circ)$ to form the Deligne splitting $I^{p,q}(\Delta_{12}^\circ)$ of the enhanced type. To identify the rules when this is possible makes it necessary to use the full technology of the Sl(2)-orbit theorem [76] as done in [113] and outlined in appendix 2.E.

As a rather simple application of the classification we can evaluate the growth of the Kähler potential e^{-K} for the 10 possible enhancements of table 2.3. Using the general result (2.2.78) and the link (2.2.77) of d_i to the singularity type one reads of table 2.4.

Type	d_1	d_2	Leading behaviour of e^{-K}
$\mathrm{I}_a \to \mathrm{I}_b$	0	0	const. or $e^{-\mathrm{Im}\, t}$
$\mathrm{II}_a \to \mathrm{II}_b$	1	1	$\mathrm{Im}\ t^1$
$\mathrm{III}_a \to \mathrm{III}_b$	2	2	$\left(\mathrm{Im}\ t^1\right)^2$
$\mathrm{IV}_a \to \mathrm{IV}_b$	3	3	$\left(\mathrm{Im}\ t^1\right)^3$
$\mathrm{I}_a \to \mathrm{II}_b$	0	1	$\mathrm{Im}\ t^2$
$\mathrm{I}_a \to \mathrm{III}_b$	0	2	$\left(\mathrm{Im}\ t^2\right)^2$
$\mathrm{I}_a \to \mathrm{IV}_b$	0	3	$\left(\mathrm{Im}\ t^2\right)^3$
$\mathrm{II}_a \to \mathrm{III}_b$	1	2	$\left(\mathrm{Im}\ t^1\right)\left(\mathrm{Im}\ t^2\right)$
$\mathrm{II}_a \to \mathrm{IV}_b$	1	3	$\left(\mathrm{Im}\ t^1\right)\left(\mathrm{Im}\ t^2\right)^2$
$\mathrm{III}_a \to \mathrm{IV}_b$	2	3	$\left(\mathrm{Im}\ t^1\right)^2\left(\mathrm{Im}\ t^2\right)$

Table 2.4: Leading growth terms of e^{-K} when approaching the singular locus $t^1 = t^2 = \mathbf{i}\infty$ obtained by using (2.2.77) and (2.2.78).

2.3.3 On the Classification of Infinite Distance Points

Having introduced a classification of singularities and singularity enhancements arising in general Calabi-Yau threefold geometries, we next turn to the discussion of infinite distance points. To define such points let us pick a point P in the complex structure moduli space $\mathcal{M}_{\mathrm{cs}}$ including Δ. P is said to be an *infinite distance point*, if the length measured with the Weil-Petersson metric g_{WP} of *every* path to this point is infinite. Accordingly, we would call P a *finite distance point* if there exists at least one path to this point that has finite length in the metric g_{WP}. In the following we will discuss the classification of finite and infinite distance points using the classification of singularities presented in subsection 2.3.1.

To begin with, we note that any two points P, Q that are not on the discriminant locus Δ are connected by a path of finite distance in the Weil-Petersson metric. This implies that in order to have an infinite distance point, at least one of the points has to lie on Δ and we chose this to be P. One then has to distinguish

two situations: (1) P lies on a divisor Δ_k away from any intersection locus, (2) P lies on an intersection locus $\Delta_{kk'}$ of two (or more) divisors Δ_k and $\Delta_{k'}$. In the following we will discuss the two cases in turn.

Considering a point P on a divisor Δ_k that does not lie on any intersection with other divisors corresponds to considering a one-parameter degeneration of the Calabi-Yau manifold Y_3. In this case one can prove a simple criterion when such a point is at infinite distance. More precisely, it was shown in [126] that a point on Δ_k° is at finite distance if and only if $NF^3(\Delta_k^\circ) = 0$. Using the nilpotent orbit (2.2.17) this is nothing else then the condition

$$P \in \Delta_k^\circ \text{ at finite distance} \quad \Longleftrightarrow \quad N\mathbf{a}_0 = 0 \ . \tag{2.3.10}$$

It is not difficult to translate this condition to the statement that the singularity on Δ_k° is Type I. Thus one concludes

$$\begin{aligned} P \in \Delta_k^\circ \text{ is finite distance point} \quad &\Longleftrightarrow \quad \text{Type I} \ , \\ P \in \Delta_k^\circ \text{ is infinite distance point} \quad &\Longleftrightarrow \quad \text{Type II} \, , \ \text{Type III} \, , \ \text{Type IV} \ . \end{aligned} \tag{2.3.11}$$

This shows that the classification of singularities is sufficiently fine to separate infinite and finite distance points Δ_k°. In fact, it clearly contains more information, since the index on the type, as introduced in (2.3.5), is not relevant for this distinction.

Let us now turn to the more involved case that the considered point lies on an intersection locus $\Delta_{kk'}^\circ$. This implies that one is not considering a one-parameter degeneration and path-dependence becomes a very important issue. It is currently not known an equivalent condition to (2.3.11) is true. The directions that are not difficult to prove are

$$\begin{aligned} P \in \Delta_{kk'}^\circ \text{ is finite distance point} \quad &\Longleftarrow \quad \text{Type I} \ , \\ P \in \Delta_{kk'}^\circ \text{ is infinite distance point} \quad &\Longrightarrow \quad \text{Type II} \, , \ \text{Type III} \, , \ \text{Type IV} \ . \end{aligned} \tag{2.3.12}$$

To see this we note that in order to show that Type I implies that the point is finite distance, it suffices to find a single path that is at finite distance. This path can be easily chosen such that the question reduces to a one-parameter degeneration with nilpotent operator $N_k + N_{k'}$ and one can use (2.3.11). Clearly, the statement in the second line in (2.3.12) is just equivalent to the statement in the first line. Note that (2.3.12), and its obvious higher-dimensional generalizations, can also be stated as [127]

$$P \text{ is infinite distance point} \quad \Longrightarrow \quad \exists \, N_i \mathbf{a}_0 \neq 0 \ , \tag{2.3.13}$$

where $\mathbf{a}_0$ is associated via (2.2.17) to the point on $\Delta_{i_1\ldots i_l}$. Attempting to prove a one-to-one correspondence as in (2.3.11) requires to carefully deal with a path dependence.[9] We believe that this is a very important problem that, however, goes beyond the scope of the current chapter.

2.3.4 The Large Complex Structure and Large Volume Point

A prime example of an infinite distance point in complex structure moduli space is the so-called *large complex structure point*. To begin with, we first have to more formally define such points. General definitions have been discussed in [128]. However, with the classification of singularities presented in subsection 2.3.1, we can give a very elegant general definition. We call a point a large complex structure point if it is a type $\mathrm{IV}_{h^{2,1}(Y_3)}$ point on Δ that arises from the intersection of $h^{2,1}(Y_3)$ divisors Δ_I, $I = 1, \ldots, h^{2,1}(Y_3)$ each being of type II, III, or IV. By this we mean that a generic point, i.e. a point on Δ_I°, on these Δ_I has these types. While we did not show the equivalence of this definition with the ones in [128], we will see that it is in perfect match with the expectations from mirror symmetry.

The large complex structure points are of crucial importance in the first mirror symmetry proposals [129]. More precisely, mirror symmetry states that the large complex structure point is mapped to large volume point by identifying complex structure and complexified Kähler structure deformations in Type IIA and Type IIB compactifications. One thus has a mirror Calabi-Yau threefold geometry $\tilde{Y}_3$ associated to Y_3. On this mirror one defines the complexified Kähler coordinates t^I, $I = 1, \ldots, h^{1,1}(\tilde{Y}_3)$ by

$$B_2 + \mathbf{i}J = t^I \omega_I \ , \tag{2.3.14}$$

where B_2 is the NS-NS two-form field and J is the Kähler form. The large volume point is given by

$$t^I \ \rightarrow \ \mathbf{i}\infty \ , \quad I = 1, \ldots, h^{1,1}(\tilde{Y}_3) \ . \tag{2.3.15}$$

In other words the large volume point arises from the intersection of $h^{1,1}(\tilde{Y}_3)$ divisors in the Kähler moduli space that are individually given by $t^I = \mathbf{i}\infty$. We depict this in figure 2.8. Clearly, in order to consider the complete mirror moduli space to $\mathcal{M}_{\mathrm{cs}}$ we have to investigate the allowed values of t^I. These are encoded by the Kähler cone, which we will briefly introduce next.

In order to define the Kähler cone it is easiest to first introduce the dual Mori cone. The Mori cone is spanned by equivalence classes of the irreducible, proper

[9] It was conjectured in [127] that a statement equivalent to (2.3.11) is true.

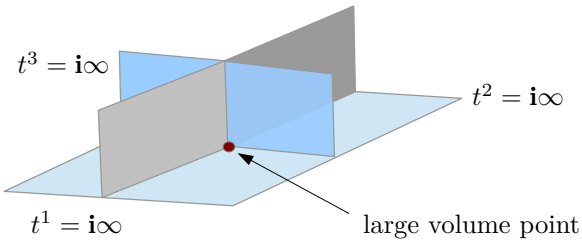

Figure 2.8: The large volume point arises on the discriminant locus of the Kähler moduli space at the intersection of $h^{1,1}(\tilde{Y}_3) = 3$ divisors $t^I = \mathbf{i}\infty$.

curves on $\tilde{Y}_3$, i.e. one can form positive linear combinations $\sum_i a_i[C^i]$, $a_i > 0$ of homology classes $[C^i]$ of such curves. The dual cone is obtained by

$$J \in H^{1,1}(Y_3): \quad \int_C J \geq 0 \ , \tag{2.3.16}$$

for all curves C in the (closure of the) Mori cone. Hence, when picking a Kähler form inside the Kähler cone one ensures that all proper curves have positive volume. For the following discussion it is important to point out that the Kähler cone is in general not simplicial. Roughly speaking this implies that we cannot represent the cone by picking $h^{1,1}(Y_3)$ generating two-forms ω_I and consider the linear combination $a^I\omega_I$, $a^I \geq 0$. In order to connect to the discussion of the previous subsections, we will now make a crucial simplifying assumption. More precisely, we will consider only situations that admit a *simplicial Kähler cone*. While many of our formulas are valid generally, this assumption will help us to interpret our results more easily.

Our starting point will be the local form of the mirror periods at the large volume point. These can be computed in various different ways, for example, by evaluating the central charges for a set of D0-, D2-, D3-, D4-branes by using the Γ-class (see, e.g. refs. [35–38, 130]). For these branes one can introduce an appropriate K-theory basis

$$(\mathcal{O}_{\tilde{Y}_3}, \mathcal{O}_{D_I}, \mathcal{C}^J, \mathcal{O}_p), \tag{2.3.17}$$

where D_J are $h^{1,1}(\tilde{Y}_3)$ divisors, p are points and, for $h^{1,1}(\tilde{Y}_3)$ curves C^I, the K-theory basis are $\mathcal{C}^J := \iota_! \mathcal{O}_{C^J}\left(K_{C^J}^{1/2}\right)$ (see [36], section 2.3 for their precise definition).

We require that the curves and divisors are dual, i.e. that $C^J \cdot D_I = \delta_I^J$, and that the Poincaré dual two-forms ω_I to D_I span the Kähler cone. Furthermore, we define

$$K_{IJK} = \int_{\tilde{Y}_3} \omega_I \wedge \omega_J \wedge \omega_K \ , \qquad b_I = \frac{1}{24} \int_{\tilde{Y}_3} \omega_I \wedge c_2(\tilde{Y}_3) \ , \tag{2.3.18}$$

where K_{IJK} are the triple intersection numbers and $c_2(\tilde{Y}_3)$ is the second Chern class of $\tilde{Y}_3$. Using these abbreviations one finds the mirror period vector

$$\Pi^{\Omega}(t^I) = \begin{pmatrix} 1 \\ t^I \\ \frac{1}{2}K_{IJK}t^J t^K + \frac{1}{2}K_{IJJ}t^J - b_I + \mathcal{O}(e^{2\pi \mathbf{i} t}) \\ \frac{1}{6}K_{IJK}t^I t^J t^K - (\frac{1}{6}K_{III} + b_I)t^I + \frac{\mathbf{i}\zeta(3)\chi(\tilde{Y}_3)}{8\pi^3} + \mathcal{O}(e^{2\pi \mathbf{i} t}) \end{pmatrix}, \tag{2.3.19}$$

where $\chi(\tilde{Y}_3) = \int_{\tilde{Y}_3} c_3(\tilde{Y}_3)$ is the Euler number of $\tilde{Y}_3$.

Having determined the local form of the periods near the large volume point, we use them to compute the monodromy matrix T_A. Note that by (2.2.8) the action of T_A is induced by sending $t^A \mapsto t^A - 1$, when taking $z^A = e^{2\pi \mathbf{i} t^A}$. Explicitly we find the $(2h^{1,1}+2) \times (2h^{1,1}+2)$-matrix

$$T_A = \begin{pmatrix} 1 & 0 & 0 & 0 \\ -\delta_{AI} & \delta_{IJ} & 0 & 0 \\ 0 & -K_{AIJ} & \delta_{IJ} & 0 \\ 0 & \frac{1}{2}(K_{AAJ} + K_{AJJ}) & -\delta_{AJ} & 1 \end{pmatrix}, \tag{2.3.20}$$

where the upper left corner corresponds to the element $\mathcal{O}_{\tilde{Y}_3} - \mathcal{O}_{\tilde{Y}_3}$ in the basis (2.3.17). It is interesting to point out that due to the basis choice (2.3.17) the T_A only depends on the intersection numbers with no b_I appearing. Given these monodromies one checks that they are unipotent and we can determine the log-monodromies N_A by simply evaluating $N_A = \log T_A$ following their definition (2.2.10). We thus find

$$N_A = \begin{pmatrix} 0 & 0 & 0 & 0 \\ -\delta_{AI} & 0 & 0 & 0 \\ -\frac{1}{2}K_{AAI} & -K_{AIJ} & 0 & 0 \\ \frac{1}{6}K_{AAA} & \frac{1}{2}K_{AJJ} & -\delta_{AJ} & 0 \end{pmatrix} . \tag{2.3.21}$$

This rather simple expression determines all large complex volume log-monodromies about single divisors in the discriminant locus of the Kähler moduli space specified by $t^A = \mathbf{i}\infty$. As discussed above in (2.2.30), log-monodromies around intersecting

divisors are determined by positive linear combinations of these N_A. For example, the log-monodromies relevant for the discriminant locus given by $t^A = \mathbf{i}\infty$, $t^{A'} = \mathbf{i}\infty$ are given by $aN_A + bN_{A'}$ with $a, b > 0$.

In order to also classify the corresponding singularity types using table 2.1, we still need to determine the polarisation η. This can be done by evaluating the negative of the Mukai pairing [35, 37, 38, 130]. On the K-theory space the Mukai pairing of branes ξ and ξ' is defined by

$$\langle \xi, \xi' \rangle = \int_{\tilde{Y}_3} \mathrm{ch}(\xi^\vee)\mathrm{ch}(\xi')\mathrm{Td}(\tilde{Y}_3)\,, \tag{2.3.22}$$

where $-^\vee$ is the dual operation, $\mathrm{ch}(-)$ is the Chern character and $\mathrm{Td}(-)$ is the Todd class. In the basis (2.3.17) one finds

$$\eta = \begin{pmatrix} 0 & -\frac{1}{6}K_{JJJ} - 2b_J & 0 & -1 \\ \frac{1}{6}K_{III} + 2b_I & \frac{1}{2}(K_{IIJ} - K_{IJJ}) & \delta_{IJ} & 0 \\ 0 & -\delta_{IJ} & 0 & 0 \\ 1 & 0 & 0 & 0 \end{pmatrix}\,, \tag{2.3.23}$$

and it always satisfies $\det \eta = 1$. The inverse of η is also computed

$$\eta^{-1} = \begin{pmatrix} 0 & 0 & 0 & 1 \\ 0 & 0 & -\delta_{IJ} & 0 \\ 0 & \delta_{IJ} & \frac{1}{2}(K_{IIJ} - K_{IJJ}) & -\frac{1}{6}K_{III} - 2b_I \\ 1 & 0 & \frac{1}{6}K_{JJJ} + 2b_J & 0 \end{pmatrix}\,. \tag{2.3.24}$$

These expressions now depends both on the intersection numbers, as well as the second Chern class. As a side remark, let us note that the complete set of N_A's together with η and the Hodge numbers $h^{2,1}(\tilde{Y}_3)$, $h^{1,1}(\tilde{Y}_3)$ contain the relevant information for Wall's classification theorem of homotopy types of complex compact Calabi-Yau threefolds [131]. It is interesting to combine this fact with the following classification of singularities.

Given the explicit forms (2.3.21) and (2.3.23) of N_A, η it is now straightforward to determine the singularity type using the last column table 2.1. Due to the lower-triangular form of N_A its powers N_A^2 and N_A^3 are easily computed. We immediately see that N_A^3 is only non-zero if K_{AAA} is non-vanishing. This is thus precisely the condition for a type IV_d singularity. Similarly, if and only if K_{AAI} is non-vanishing for one or more I we find that N_A^2 is non-vanishing. Hence, the N_A is of type III_c if $K_{AAA} = 0$ and K_{AAI} non-vanishing for some $I \neq A$. The precise type III_c and IV_d are now determined by evaluating the rank of the matrix K_{AIJ} with the result listed in table 2.5.

It remains to discuss the cases I_a and II_b that occur if all $K_{AAI} = 0$. As we have discussed in subsection 2.3.1 they can, in general, only be distinguished if we also consider η. In fact, we can compute ηN_A and determine its number of positive and negative eigenvalues. Explicitly, we find that

$$\eta N_A = \begin{pmatrix} 2b_A & -\frac{1}{2}K_{AJJ} & \delta_{AJ} & 0 \\ \frac{1}{2}(K_{IAA} - K_{IIA}) & -K_{AIJ} & 0 & 0 \\ \delta_{AI} & 0 & 0 & 0 \\ 0 & 0 & 0 & 0 \end{pmatrix} , \tag{2.3.25}$$

where we need to impose $K_{AAI} = 0$ for all I. It can be now easily seen that this matrix has positive eigenvalues. In fact, evaluating $V^{\mathrm{T}}\eta N_A V = 2$ for $V = (1, 0, \ldots, 0, (1 - b_A)\delta_{AI}, 0)^{\mathrm{T}}$ we find a positive direction. Hence, the case I_a is actually never realized for the N_A, η given in (2.3.21), (2.3.23). We thus conclude that we can distinguish also the precise type II_b by evaluating the rank of the matrix K_{AIJ} as listed in table 2.5.

name	$\mathrm{rank}(K_{AAA})$	$\mathrm{rank}(K_{AAI})$	$\mathrm{rank}(K_{AIJ})$
II_b	0	0	b
III_c	0	1	$c+2$
IV_d	1	1	d

Table 2.5: This table list the conditions on N_A, η given in (2.3.21) and (2.3.23) that ensure a certain singularity type on the discriminant divisor $t^A = \mathbf{i}\infty$ for a single coordinate. Note that $\mathrm{rank}(K_{AAA})$ and $\mathrm{rank}(K_{AAJ})$ are either 0, 1 depending on whether these quantities are trivially zero or non-zero.

To conclude this section, let us note that the large volume point $t^A = \mathbf{i}\infty$ for all $A = 1, \ldots, h^{1,1}(\tilde{Y}_3)$ has precisely the properties mirror dual to a large complex structure point defined at the beginning of this subsection. To see this, let us first show that it is a point of type $\mathrm{IV}_{h^{1,1}}$. In order to do that we have to analyse the sum of all N_A with positive coefficients. A convenient choice is to pick the Kähler coordinates $v^A = \mathrm{Im}\ t^A$, which are positive in a simplicial Kähler cone. Hence we consider

$$N = \sum_A v^A N_A = \begin{pmatrix} 0 & 0 & 0 & 0 \\ -v^I & 0 & 0 & 0 \\ -\frac{1}{2}v^A K_{AAI} & -v^A K_{AIJ} & 0 & 0 \\ \frac{1}{6}v^A K_{AAA} & \frac{1}{2}K_{AJJ} & -v^J & 0 \end{pmatrix} . \tag{2.3.26}$$

If we now compute N^3, we simply find a matrix which only has a single entry proportional to the volume $\frac{1}{6}\,K_{IJK}v^Iv^Jv^K$. Hence, the rank of N^3 is 1 and we conclude from the last column in table 2.5 that the singularity is type IV_d. To determine d we need to evaluate the rank of N itself. However, the contraction v^AK_{AIJ} is crucial in defining the metric on Kähler moduli space and is full rank [33]. So indeed, we find that the singularity $t^A = \mathbf{i}\infty$ is of type $\text{IV}_{h^{1,1}(\tilde{Y}_3)}$. Furthermore, all the intersecting divisors have type II, III, or type IV as discussed above.

2.4 Charge orbits and the Swampland Distance Conjecture

In this section we analyse the Swampland Distance Conjecture (SDC) using the powerful geometric tools about the complex structure moduli space introduced so far. To begin with, let us first recall the statement of the SDC adapted to our setting. It implies that when approaching any infinite distance point P along any path γ one should encounter a universal behaviour of infinitely many states of the theory sufficiently close to P. More precisely, picking a point Q' in a sufficiently small neighbourhood of the infinite distance point P, and then moving along the geodesic towards P onto a point P', the SDC asserts that one should be able to identify an infinite tower of states with masses M_m, $m = 1, \ldots, \infty$, behaving as

$$M_m\left(P'\right) \approx M_m\left(Q'\right)\, e^{-\gamma d\left(Q',P'\right)}\ , \tag{2.4.1}$$

where $M_m\left(P'\right)$ and $M_m\left(Q'\right)$ are the masses of the states at P' and Q', respectively. Here $d(Q', P')$ is the distance along the geodesic in the Weil-Petersson metric determined from the Kähler potential (2.2.1) and γ is some positive constant. In other words, the SDC not only asserts that there is an infinite tower of states becoming massless at P, but also that this has to happen exactly in an exponentially suppressed way (2.4.1).

The goal of this section is to identify such a candidate set of states. As in [5], we propose that these states arise from BPS D3-branes wrapped on certain three-cycles in the Calabi-Yau space Y_3. In the case of one-modulus degenerations studied in [5] arguments were presented, by using walls of marginal stability, that the proposed tower is actually populated by BPS states. In this chapter, we will focus solely on identifying the tower of states, and will not be able to show that they are indeed populated by BPS states. We leave such an analysis for future work, and for now will assume that the identified tower of states is indeed populated by BPS states.

Asserting that the constructed tower indeed consists of BPS states with charges $\mathbf{Q}$, we can use the central charge $Z(\mathbf{Q})$ to compute their mass $M = |Z(\mathbf{Q})|$. The explicit form of $Z(\mathbf{Q})$ is given by [10]

$$Z(\mathbf{Q}) = e^{\frac{K}{2}} \int_{Y_3} H \wedge \Omega = e^{\frac{K}{2}} \; S(\mathbf{\Pi}, \mathbf{Q}) \; , \tag{2.4.2}$$

where H is the three-form with coefficients $\mathbf{Q}$ in the integral basis γ_I, the Ω is the (3,0)-form introduced in (2.2.2) with periods $\mathbf{\Pi}$, and K is the Kähler potential given in (2.2.1).

We construct the infinite set of states relevant for the SDC by introducing, what we call a *charge orbit*. In the one-parameter case this is the same as the monodromy orbit of [5]. It will be obtained by acting on a seed charge vector $\mathbf{q}_0$ with the monodromy matrices relevant in a local patch around the infinite distance point P. Due to the multi-parameter nature of our analysis, we will change notation with respect to reference [5] and denote the infinite charge orbit by

$$\mathbf{Q}\left(\mathbf{q}_0 | m_1, \ldots, m_n\right) \; , \tag{2.4.3}$$

where $m_1, \ldots, m_n$ is a set of integers labelling the considered states, as we discuss below. The charge orbit will be infinite, if there are infinitely many allowed values for $m_1, \ldots, m_n$.

2.4.1 Single parameter charge orbits

To give a comprehensive introduction of the charge orbit, we will first discuss a single parameter degeneration $t^1 \to \mathbf{i}\infty$, where we consider only the divisor $\Delta_1 \subset \Delta$ disregarding any further intersections. In other words we consider a local patch $\mathcal{E}$ intersecting Δ_1, but not containing any other component of the discriminant locus (see figure 2.9). Such one-parameter degenerations have been discussed at length in [5]. We will introduce a slightly modified description in the following which will then match more seamlessly unto the multi-parameter analysis.

In analogy to a one-parameter nilpotent orbit (2.2.17) and a one-parameter Sl(2)-orbit (2.2.57), we define the charge orbit as

$$\mathbf{Q}(\mathbf{q}_0 | m_1) \equiv \exp\left[m_1 N_1\right] \mathbf{q}_0 \; , \tag{2.4.4}$$

where m_1 is an integer. Note that since the monodromy matrix $T_1 = \exp\left[N_1\right]$ the Q are simply the charges obtained by acting with the monodromy matrix $T_1^{m_1}$.

[10] Note that we have exchanged $\mathbf{\Pi}$ and $\mathbf{Q}$ in S in order to absorb the minus sign in (2.2.4).

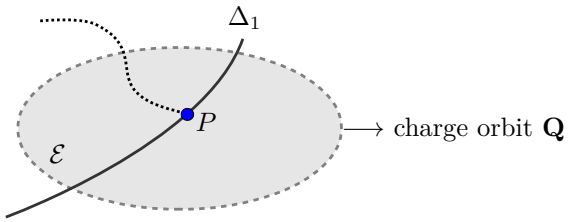

Figure 2.9: Associating a charge orbit to a point $P \in \Delta_1$ in local patch $\mathcal{E}$ in moduli space. In this single parameter degeneration no intersection locus of Δ_1 within Δ is in $\mathcal{E}$.

Since we consider an infinite distance point P the results of subsection 2.3.3 imply that N_1 is non-trivial and thus T_1 is of infinite order, i.e. there exists no m such that $T_1^m = T_1$. In order that the orbit is actually infinite, we further have to demand that

$$N_1 \mathbf{q}_0 \neq 0 \ . \tag{2.4.5}$$

Hence the definition of an infinite charge orbit agrees with the one in [5].

Let us next consider the second crucial part of the distance conjecture, namely that the infinite tower of states becomes exponentially light towards the infinite distance point. As mentioned above, we will assume that the considered states are BPS D3-branes, such that their masses are measured by $|Z|$, with the central charge Z given in (2.4.2). Near the point P we can use the one-variable nilpotent orbit $\mathbf{\Pi}_{\text{nil}} = \exp\left[t^1 N_1\right] \mathbf{a}_0$, to approximate the behaviour of the central charge

$$Z_{\text{asy}}(\mathbf{Q}) = e^{\frac{K}{2}} \ S(\mathbf{\Pi}_{\text{nil}}, \mathbf{Q}) \ . \tag{2.4.6}$$

Note that using the results of subsection 2.2.2 the asymptotic central charge $Z_{\text{asy}}(\mathbf{Q})$ differs from $Z(\mathbf{Q})$ by terms proportional to the exponential $e^{2\pi \mathbf{i} t^1}$, which are strongly suppressed in the limit $\text{Im}\ t^1 \to \infty$. Inserting (2.4.4) into (2.4.6), we realize that $|Z(\mathbf{Q})| \approx |Z_{\text{asy}}(\mathbf{Q})| \to 0$ is equivalent to demanding

$$|Z_{\text{asy}}(\mathbf{q}_0)| \to 0 \ . \tag{2.4.7}$$

This can be deduced by moving the exponential $e^{m_1 N_1}$ onto $\mathbf{\Pi}_{\text{nil}}$ and absorbing it by a shift $\text{Re}\{t^1\} \to \text{Re}\{t^1\} - 1$. Hence, in order to find an *infinite massless charge orbit* $\mathbf{Q}$ we have to demand that the seed charge $\mathbf{q}_0$ satisfies (2.4.5) and (2.4.7).

Let us now construct the seed $\mathbf{q}_0$ for an infinite massless charge orbit $\mathbf{Q}$. We first note that there is a particular set of charges that is massless which in [5] were

termed to be of type II. They are obtained as elements of the space

$$\mathcal{M}_{\rm II}(\mathbf{\Pi}_{\rm nil}) = \left\{ \mathbf{q}^{\mathcal{I}} \gamma_{\mathcal{I}} \in H^3(Y_3, \mathbb{Z}) : \quad S(\mathbf{q}, N_1^k \mathbf{a}_0) = 0 \,,\ \forall\, k \right\} , \tag{2.4.8}$$

where we have considered vectors $\mathbf{q}$ over the integers $\mathbb{Z}$. Note that this space depends on the data $(N_1, \mathbf{a}_0)$ defining the nilpotent orbit. Stated differently, these are precisely the states that are orthogonal to the nilpotent orbit $\mathbf{\Pi}_{\rm nil}$. Their asymptotic central charge (2.4.6) vanishes trivially, which implies that the full central charge Z vanishes by exponentially suppressed terms $e^{2\pi \mathbf{i} t^1}$.

BPS states which become massless as Im $t^1 \to \infty$, but which are not of type II, are called type I states. In [5] arguments were presented for why, given a one-parameter degeneration, the populated BPS states are of type I, and therefore the tower of states of the distance conjecture should be composed of an infinite number of type I states.

It was also shown in [5] that the mass of type I states decreases exponentially fast for one-parameter variations approaching infinite distance. This can be easily seen since the states become massless as a power law in Im t^1, while the leading behaviour of the Kähler potential (2.2.63) is logarithmic in Im t^1. This matches the behaviour predicted by the distance conjecture.

Let us now determine a the set of states that become massless at P. To begin with we give a sufficient condition for a charge $\mathbf{q}$ to become massless at P. In order to do that we note that the central charge $Z(\mathbf{q})$ can also be written with the help of the Hodge inner product $S(C\mathbf{a}, \bar{\mathbf{b}}) = \int_{Y_3} a \wedge * \bar{b}$, which is the inner product associated to the Hodge norm (2.2.60). Using the fact that $C\mathbf{\Pi} = -\mathbf{i}\,\mathbf{\Pi}$ together with (2.2.61) we find that $Z(\mathbf{q})$ can be written as

$$|Z(\mathbf{q})| = \frac{|S(C\mathbf{\Pi}, \mathbf{q})|}{||\mathbf{\Pi}||} \leq ||\mathbf{q}|| \,, \tag{2.4.9}$$

where we have used the Cauchy-Schwarz inequality $|S(C\mathbf{v}, \bar{\mathbf{u}})| \leq ||\mathbf{v}||\,||\mathbf{u}||$. We thus conclude that if the norm $||\mathbf{q}||$ goes to zero at the singularity, the charge $\mathbf{q}$ yields a massless state. Now we can use the growth theorem (2.2.62), (2.2.63) to infer that

$$||\mathbf{q}|| \to 0 \quad \Longleftrightarrow \quad \mathbf{q} \in W_i^{\mathbb{Q}} \text{ for } i \leq 2 \,, \tag{2.4.10}$$

which identifies vector spaces that contain massless states. It is important to stress that the condition (2.4.10) is a sufficient, but not necessary condition that a charge $\mathbf{q}$ is massless.

Finally, we relate the result (2.4.10) to the classification of singularities discussed in subsection 2.3.1. We use the fact that $W_j^{\mathbb{C}} = \bigoplus_{p+q \leq j} I^{p,q}$ and apply the clas-

sification of Hodge diamonds for the singularity Types I, II, III, and IV given in table 2.1. Using (2.3.7) and (2.3.8) we realize that

$$\begin{aligned}
&\text{Type I}: W_2^{\mathbb{C}} \subset \mathcal{M}_{\text{II}}\,, && W_1^{\mathbb{C}} = 0\,, && W_0^{\mathbb{C}} = 0\,,\\
&\text{Type II}: W_2^{\mathbb{C}} = N_1 P^4\,, && W_1^{\mathbb{C}} = 0\,, && W_0^{\mathbb{C}} = 0\,,\\
&\text{Type III}: W_2^{\mathbb{C}} = N_1 P^4 \oplus N_1^2 P^5\,, && W_1^{\mathbb{C}} = N_1^2 P^5\,, && W_0^{\mathbb{C}} = 0\,,\\
&\text{Type IV}: W_2^{\mathbb{C}} = N_1 P^4 \oplus N_1^2 P^6 \oplus N_1^3 P^6\,, && W_1^{\mathbb{C}} = N_1^3 P^6\,, && W_0^{\mathbb{C}} = N_1^3 P^6\,.
\end{aligned} \tag{2.4.11}$$

We stress that only for the Type IV singularities all spaces $W_2^{\mathbb{C}}$, $W_1^{\mathbb{C}}$ and $W_0^{\mathbb{C}}$ are always non-zero due to the existence of the non-trivial vectors $N^j\mathbf{a}_0$, $j \leq 3$. Finally, combining this with the requirement that $N\mathbf{q}_0 \neq 0$ as well as the fact that $N_1 W_i \subset W_{i-2}$ we find that only Type IV singularities straightforwardly admit an infinite massless charge orbit $\mathbf{Q}$.

Let us have a closer look at the $\mathbf{q}_0$ in the case of a Type IV singularity. From the above discussion we require $\mathbf{q}_0 \in W_2^{\mathbb{Q}}$. Furthermore, we note that $W_2^{\mathbb{C}} = I^{1,1} \oplus I^{0,0} = N_1 P^{2,2} \oplus N_1^2 P^{3,3}$ and stress that

$$S(N_1 P^{2,2}, N_1^k \mathbf{a}_0) = 0\ , \tag{2.4.12}$$

for all k, since $\mathbf{a}_0$ spans $P^{3,3}$. The latter condition shows that $N_1 P^{2,2}$ is a type II state. Since we require the orbit to be composed of type I states, we can therefore determine that $\mathbf{q}_0$ must have a non-trivial component in $N_1^2 P^{3,3}$, so $\mathbf{q}_0 \notin N_1 P^{2,2}$. In fact, we propose a particular element of the $\mathbb{R}$-split $P^{3,3}$, which can be written as

$$\mathbf{q}_0 \sim_{\mathbb{Z}} N_1^2 \tilde{\mathbf{a}}_0^{(1)}\ . \tag{2.4.13}$$

Here we have introduced new notation $\sim_{\mathbb{Z}}$ which is rather involved but has a precise definition as follows.

Consider an element $\mathbf{a}$ in $W_l^{\mathbb{C}}$, where l is the smallest possible index. If it is possible to add to $\mathbf{a}$ some other elements in $W_l^{\mathbb{C}} \cap \operatorname{Ker} N$ such that one obtains an element in $W_l^{\mathbb{Q}}$, then $\sim_{\mathbb{Z}} \mathbf{a}$ is defined as the associated element of $W_l^{\mathbb{Q}}$. If it is not possible, then $\sim_{\mathbb{Z}} \mathbf{a}$ is defined to vanish.

In utilising $\sim_{\mathbb{Z}}$ in (2.4.13), we will *assume* that defined this way $\mathbf{q}_0$ is non-vanishing. This is true in any example we have studied, but we have no proof that it is always the case. Note that for the particular case of the one-parameter example (2.4.13), acting with N_1 on $\mathbf{q}_0$ will only receive a contribution from the piece $N_1^2 \tilde{\mathbf{a}}_0$, but the other components may be necessary in general for quantisation purposes. Note also that we have utilised $\tilde{\mathbf{a}}_0$, rather than $\mathbf{a}_0$, as introduced in subsection 2.2.4. Finally, it is important to emphasise that in general $\tilde{\mathbf{a}}_0$ may depend on the

coordinates along the singular locus $\tilde{\mathbf{a}}_0(\xi)$, and so the combination of elements involved in defining $\sim_{\mathbb{Z}}$ can vary with ξ.

This conclusion seems to imply that the SDC cannot be shown using this construction for the cases Type II and Type III. We know from the discussion of subsection 2.3.3 that points on these loci are at infinite distance. In examples with $h^{2,1} = 1$ the classification of table 2.1 shows that Type III can never be realized. However, Type II singularities do occur in explicit examples and have been discussed in more detail in [5]. These constitute interesting cases that require further investigation. For higher-dimensional moduli spaces, we will now show that the above construction can be generalized yielding a remarkable way to satisfy the SDC if intersection loci of divisor Δ_i appear.

2.4.2 Defining the general charge orbit

Having discussed the one-parameter degenerations, we next propose a general form of the charge orbit $\mathbf{Q}(\mathbf{q}_0|m_1,\ldots,m_n)$ labelling the states relevant for the SDC close to an infinite distance point P. We stress that this requires that $\mathbf{Q}$ labels *infinitely many* states that become *massless* at the point P. Hence we have to carefully define an appropriate orbit that ensures these properties. We first give the general expression and then show that it has the desired features.

To begin with, let us stress that the definition of $\mathbf{Q}$ is, at first, not global on $\mathcal{M}_{\rm cs}$. Rather we have to adjust the orbit according to the location of P in the discriminant Δ. Nevertheless, the definition of $\mathbf{Q}$ also is not only depending on the location of P, but rather takes into account two additional features:

(1) the intersecting patterns and singularity enhancements of the Δ_i in some sufficiently small neighbourhood $\mathcal{E}$ containing P,

(2) the sector $\mathcal{R}$ of the path that is traversed when approaching the point P.

While the first condition will be used in showing when $\mathbf{Q}$ labels infinitely many states, the second condition is crucial to ensure that they become massless. It will be an important task to carefully spell out these two properties of $\mathbf{Q}$ in the following. The reason that these features occur stems from our construction of $\mathbf{Q}$ using the Sl(2)-orbit theorem introduced in subsection 2.2.4 and the growth theorem discussed in subsection 2.2.5.

To display our proposal for the charge orbit, it is convenient to recall some more notation from subsections 2.2.2 and 2.2.4. We consider a patch $\mathcal{E}$ around the point $P \in \Delta$ which might contain any type of higher intersections of divisors Δ_i. This patch is defined by requiring that the nilpotent orbit (2.2.17) provides

a good approximation in $\mathcal{E}$ to the full periods. In other words, we can drop the exponential corrections in $\mathcal{E}$ as discussed in detail in subsection 2.2.2. Let us denote the divisors intersecting in the patch $\mathcal{E}$ by Δ_i with $i = 1, \ldots, n_{\mathcal{E}}$. As usual we denote the monodromy logarithms associated to Δ_i by N_i. Furthermore, we will consider a point P on the intersection of the first n_P divisors Δ_k, i.e.

$$P \in \Delta^{\circ}_{1\ldots n_P} \ , \tag{2.4.14}$$

where we recall that $^{\circ}$ indicates that we consider points away from any further intersection as introduced in subsection 2.2.3. In order to use the growth theorem for the norm of $\mathbf{Q}$ when approaching P we introduce the sectors $\mathcal{R}_{r_1\ldots r_{n_P}}$ as before. They are defined by first setting

$$\mathcal{R}_{1\ldots n_P} \equiv \left\{ t^i : \quad \frac{\text{Im } t^1}{\text{Im } t^2} > \lambda, \ldots, \ \frac{\text{Im } t^{n_P-1}}{\text{Im } t^{n_P}} > \lambda, \ \text{Im } t^{n_P} > \lambda, \quad \text{Re } t^i < \delta \right\}, \tag{2.4.15}$$

for some fixed $\lambda, \delta > 0$. The other orderings of the indices on $\mathcal{R}_{1\ldots n_P}$ are defined by simple permutations of the indices in all of (2.4.15). In this chapter we will only consider paths that traverse a single sector $\mathcal{R}_{r_1\ldots r_{n_P}}$. Completely arbitrary paths cannot be analysed so easily and might require to patch together sectors of the form (2.4.15). It should, however, be stressed that this is a very mild path dependence. We do not expect that our conclusions change for more general paths. The setup is illustrated in figure 2.10.

Let us now turn to the proposal for the charge orbit $\mathbf{Q}$. Given a path towards P that traverses a single sector $\mathcal{R}_{r_1\ldots r_{n_P}}$ we fix an ordering of n_P matrices N_i as $(N_{r_1}, \ldots, N_{r_{n_P}})$. By a simple relabelling we can pick this ordering to be $(N_1, \ldots, N_{n_P})$ without loss of generality. The ordering of the remaining N_i, $i = n_P, \ldots, n_{\mathcal{E}}$ does not need to be fixed as of now. For convenience we will pick the simplest ordering such that we have in total $(N_1, \ldots, N_{n_{\mathcal{E}}})$. In analogy the Sl(2)-orbit (2.2.57) we now define the charge orbit as

$$\mathbf{Q}(\mathbf{q}_0 | m_1, \ldots, m_{\mathcal{E}}) \equiv \exp\Big(\sum_{i=1}^{n_{\mathcal{E}}} m_i N_i^- \Big) \mathbf{q}_0 \ , \tag{2.4.16}$$

with integers m_i. The first non-trivial part of the construction is the use of the matrices N_i^- in (2.4.16). These are part of the commuting $\mathfrak{sl}(2)$s discussed in subsection 2.2.4 and are non-trivially constructed from the N_i given in a particular ordering. Clearly, we pick the ordering introduced before, which was partly dictated by the considered path towards P. Note that the construction of N_i^- depends on all other N_j with $j \geq i$. If one considers situations with $n_P < n_{\mathcal{E}}$ this implies that

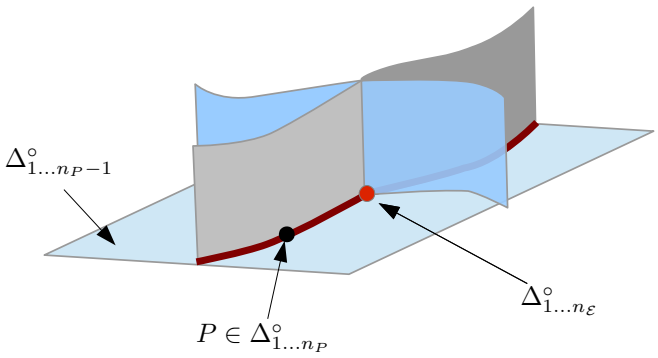

Figure 2.10: Illustration of the general setup showing a patch $\mathcal{E}$ around a point P which lies on the intersection of n_P singular divisors, but away from any further intersections $P \in \Delta^\circ_{1\ldots n_P}$. Within the patch, there is also a further enhancement due to an intersection of additional divisors at $\Delta^\circ_{1\ldots n_\mathcal{E}}$.

they contain information about the other divisors intersection in $\mathcal{E}$ even though P can be away from them. Also note that for a one-parameter case one trivially has $N_1 = N_1^-$, such that (2.4.16) is a natural generalization of (2.4.4).

In order to fully specify the charge orbit (2.4.16) it is crucial to determine the properties of the intersections in $\mathcal{E}$ such that a seed charge $\mathbf{q}_0$ exists that ensures that $\mathbf{Q}(\mathbf{q}_0|m_1,\ldots,m_\mathcal{E})$ yields an infinite set of charges that become massless when approaching P. Let us thus consider a general enhancement chain within $\mathcal{E}$ of the form

$$\text{Type } \mathsf{A}_1 \to \ldots \to \underbrace{\boxed{\text{Type } \mathsf{A}_{n_P}}}_{\text{location of } P} \to \ldots \to \text{Type } \mathsf{A}_{n_\mathcal{E}} \ , \tag{2.4.17}$$

where we list the singularity types on the intersection loci Δ°_1, Δ°_{12}, $\ldots$,$\Delta^\circ_{1\ldots n_P}$, $\ldots$, $\Delta^\circ_{1\ldots n_\mathcal{E}}$ and indicated by a box singularity of the locus $\Delta^\circ_{1\ldots n_P}$ containing P. Note that we have fixed an ordering of the first n_P elements N_i according to the considered path.

Let us now summarize the results that we will show in this section.

Existence and construction of a charge orbit. We find an *infinite* charge orbit $\mathbf{Q}$ that becomes *massless* at the location of a point $P \in \Delta^\circ_{1\ldots n_P}$ if one of the two conditions are satisfied:

(R1) P is on a locus $\Delta^\circ_{1\ldots n_P}$ carrying a Type IV singularity. In other words, if $\text{Type } \mathsf{A}_{n_P} = \text{IV}$ in the enhancement chain (2.4.17).

(R2) P is on a locus $\Delta^\circ_{1\ldots n_P}$ carrying a Type II or Type III singularity and there exists a higher intersection, $\Delta^\circ_{1\ldots n_P+1}, \ldots, \Delta^\circ_{1\ldots n_\mathcal{E}}$, on which the singularity type increases. In other words, we have $\boxed{\text{Type A}_{n_P}} = \text{II or III}$ and the enhancement chain (2.4.17) contains either one of the enhancements II $\to$ III, II $\to$ IV or III $\to$ IV after the singularity type at P.

Importantly, as indicated at the beginning of this section, these results are true for *any path* approaching P that stays within the growth sector (2.4.15). We will generally show these statements employing the full power of the mathematical machinery introduced in section 2.2 and section 2.3. Furthermore, we will explicitly construct the seed charge $\mathbf{q}_0$ for all of the enhancement chains allowed by (R1) and (R2). Given a chain (2.4.17) satisfying (R1) and (R2), we show the existence of a seed charge $\mathbf{q}_0$ with the following simple features:

$$\begin{aligned}
\boxed{\text{Type A}_{n_P}} \neq \text{IV}: &\quad \begin{cases} N^-_{(i)}\mathbf{q}_0 = 0 & \text{for all } i \text{ with } 1 \leq i \leq n_P\ , \\ N^-_{(j)}\mathbf{q}_0 \neq 0 & \text{for some } j \text{ with } n_P < j \leq n_\mathcal{E}\ , \end{cases} \\
\boxed{\text{Type A}_{n_P}} = \text{IV}: &\quad \begin{cases} N^-_{(i)}\mathbf{q}_0 = 0 & \text{for all } i \text{ with } 1 \leq i < n_P\ , \\ N^-_{(n_P)}\mathbf{q}_0 \neq 0, \quad \big(N^-_{(n_P)}\big)^2\mathbf{q}_0 = 0. \end{cases}
\end{aligned} \tag{2.4.18}$$

We will show that together with the fact that P is on an infinite distance locus, this ensures that $\mathbf{q}_0$ is massless along any path within the growth sector (2.4.15).

To systematically establish these claims we first discuss in subsection 2.4.3 some general facts about the mass of the states associated to $\mathbf{Q}$ and $\mathbf{q}_0$ when approaching P. We then turn to our main tool and discuss in detail in subsection 2.4.4 configurations which consists of two intersecting divisors in $\mathcal{E}$, i.e. we will study the general $n_\mathcal{E} = 2$ configuration. We will not only see that (R1) and (R2) are true in this case, but also describe how a given $\mathbf{q}_0$ can be tracked through an enhancement. Concretely we will consider two types of enhancement chains

$$n_P = 1 \quad : \qquad \boxed{\text{Type A}} \to \text{Type B}\ , \tag{2.4.19}$$

$$n_P = 2 \quad : \qquad \text{Type A} \to \boxed{\text{Type B}}\ , \tag{2.4.20}$$

where, as above, the box indicates the location of the point P. In this simpler situation we will easier to construct the relevant seed charges $\mathbf{q}_0$ and explain how in the cases stated above induce an infinite, massless orbit when approaching P. The general case of having an arbitrary enhancement chain (2.4.17) will be subsequently studied in subsection 2.4.5.

Note that while this covers many possible singularities and singularity enhancements in the Calabi-Yau moduli space, there are a number of enhancements that

do not lead to a simple charge orbit that is both infinite and massless for any path in a sector. For example, we will see that if the chain (2.4.17) ends on an enhancement II $\to$ III with P being at the Type III locus, a natural candidate orbit with the desired features exists only if one excludes certain paths in the sector. More generally, we find that all chains (2.4.17) of the form

$$\text{Type } \mathsf{A}_1 \to \ldots \to \text{Type } \mathsf{A}_{n_{\mathcal{E}}-1} \to \boxed{\text{Type II or Type III}} \,, \tag{2.4.21}$$

do not lead to a natural infinite and massless orbit that is path-independent within a sector by using the methods presented in this chapter. We will discuss possible extensions to tackle these cases in more detail in subsection 2.4.7.

2.4.3 Masslessness of the charge orbit

Let us first discuss the conditions on the charge orbit $\mathbf{Q}$ defined in (2.4.16) such that it consists of states that become light at P and can serve as the states of SDC. To do that we have to determine the behaviour of the central charge $|Z(\mathbf{Q})|$ when approaching the point P. In other words we have to ensure that

$$M(\mathbf{Q}) = |Z(\mathbf{Q})| \;\longrightarrow\; 0 \,. \tag{2.4.22}$$

To identify sufficient conditions for (2.4.22) we use the general growth theorem (2.2.72) for the Hodge norm $||\mathbf{Q}||$. In order to do that we note that the central charge $Z(\mathbf{Q})$ can also be written with the help of the Hodge inner product $S(C\mathbf{a}, \bar{\mathbf{b}})$ associated to the Hodge norm (2.2.60). Using the fact that $C\mathbf{\Pi} = -\mathbf{i}\mathbf{\Pi}$ together with (2.2.61) we find that $|Z(\mathbf{Q})|$ can be written as

$$|Z(\mathbf{Q})| = \frac{|S(C\mathbf{\Pi}, \mathbf{Q})|}{||\mathbf{\Pi}||} \leq ||\mathbf{Q}|| \,. \tag{2.4.23}$$

where we have used the Cauchy-Schwarz inequality $|S(C\mathbf{v}, \bar{\mathbf{u}})| \leq ||\mathbf{v}||\,||\mathbf{u}||$. We thus conclude that if the norm $||\mathbf{Q}||$ goes to zero at the singularity, the charge orbit $\mathbf{Q}$ yields massless states.

The general discussion of subsection 2.2.5 provides us with a powerful tool to determine the behaviour of $||\mathbf{Q}||$ near the point P. More precisely, we introduced the multi-variable growth theorem, which allows us to evaluate the asymptotic behaviour of $\mathbf{Q}$ from its location in

$$W_{l_1}\big(N_{(1)}\big) \cap W_{l_2}\big(N_{(2)}\big) \cap \ldots \cap W_{l_{n_P}}\big(N_{(n_P)}\big) \,, \tag{2.4.24}$$

with the $N_{(i)}$ introduced in (2.2.35). Given our definition of $\mathbf{Q}$, the restriction to a growth sector and ordering as discussed in subsection 2.4.2, we would rather like

to work with the $N^-_{(i)}$ constructed from the commuting $\mathfrak{sl}(2)$s containing N^-_i. Here another fact from the Sl(2)-orbit theorem of [76] can be applied, which states that

$$W_l\big(N_{(i)}\big) = W_l\big(N^-_{(i)}\big) \ . \tag{2.4.25}$$

Hence, we can apply the results of subsection (2.2.5) by simply replacing $N_{(i)} \to N^-_{(i)}$ when staying in the ordering of the N_i used to determine N^-_i.

The next step is to establish that the growth of $||\mathbf{Q}||$ is identical to this of $||\mathbf{q}_0||$. In order to do that we have to show that the location of $\mathbf{Q}$ and $\mathbf{q}_0$ in the spaces

$$W_{l_1}\big(N^-_{(1)}\big) \cap W_{l_2}\big(N^-_{(2)}\big) \cap \ldots \cap W_{l_{n_P}}\big(N^-_{(n_P)}\big) \ , \tag{2.4.26}$$

agree, where we recall the notation $N^-_{(n)} = \sum_{i=1}^n N^-_i$. Now the existence of $n_\mathcal{E}$ *commuting* $\mathfrak{sl}(2)$-triples (2.2.49) containing the N^-_i becomes relevant. In fact, each of these triples contain the operators Y_i that gives the location of a vector $\mathbf{v}$ in $W_l\big(N^-_{(j)}\big)$. Using (2.2.52) and (2.2.40) one has

$$Y_{(j)}\mathbf{v} = l_j\mathbf{v} \quad \Rightarrow \quad \mathbf{v} \in W_{l_j+3}(N^-_{(j)}) \ , \tag{2.4.27}$$

where $Y_{(j)} = Y_1 + \ldots + Y_j$ as in (2.2.52). Crucially, the location of $\mathbf{q}_0$ and $N^-_j\mathbf{q}_0$ agree, which implies that if $\mathbf{q}_0$ is massless also $\exp(m_{n_P+1}N^-_{n_P+1}+\ldots+m_{n_\mathcal{E}}N^-_{n_\mathcal{E}})\mathbf{q}_0$ is massless. Concerning the growth and the masslessness thus only the terms $\exp(m_1N^-_1 + \ldots + m_{n_P}N^-_{n_P})$ are relevant. However, due to the exponential the location of the highest l_i-components of $\mathbf{Q}$ and $\mathbf{q}_0$ agree. In fact, it was already shown in [76] that the growth does not change upon multiplying by this exponential term. We hence conclude that with respect to the leading growth one has

$$||\mathbf{Q}|| \sim ||\mathbf{q}_0|| \ , \tag{2.4.28}$$

and hence $\mathbf{Q}$ is massless for all values of $m_1, \ldots, m_\mathcal{E}$ as long as $\mathbf{q}_0$ is massless.

Let us finally give a *sufficient* condition for having $||\mathbf{q}_0|| \to 0$ along any path in the considered growth sector. Using the general growth theorem (2.2.72) with (2.2.71), it is not hard show that $||\mathbf{q}_0|| \to 0$ is true if one has

$$\begin{aligned} \mathbf{q}_0 \quad \in \quad & W_{l_1}\big(N^-_{(1)}\big) \cap W_{l_2}\big(N^-_{(2)}\big) \cap \ldots \cap W_{l_{n_P}}\big(N^-_{(n_P)}\big) \ , \\ & \text{with} \ \ l_{n_P} < 3, \quad l_1, \ldots, l_{n_P-1} \leq 3 \ . \end{aligned} \tag{2.4.29}$$

This condition uses that if $l_i \leq 3$, $i = 1, \ldots, n_P - 1$ then we can estimate $\frac{\text{Im } t^{i+1}}{\text{Im } t^i} < \lambda^{-1}$ in (2.4.15) and hence find that $||\mathbf{q}_0||$ vanishes for any path. Let us stress that this statement of masslessness can only be obtained on the sector $\mathcal{R}_{1\ldots n_P}$ defined in (2.4.15), due to the path dependence in the growth theorem.

While we have discussed in detail the masslessness of the orbit at infinite distance, the distance conjecture further states that the states in the orbit should become massless exponentially fast in the geodesic proper distance. This is much more difficult to prove generally for multi-parameter settings since one must calculate geodesics. We leave a detailed analysis of this for future work, but will give some evidence that it is natural to expect that the exponential behaviour is universal. First we note that the masses of the BPS states are still power-law in the Im t^i, as was the case for the one-parameter case. Therefore, if the geodesic proper distance grows only logarithmically in the Im t^i the states will becomes massless exponentially fast.

To see evidence for the logarithmic behaviour in the multi-parameter cases we can approximate the behaviour of the field space metric through the leading behaviour of the Kähler potential. The growth theorem applied to the Kähler potential implies as shown in (2.2.78) that the asymptotic leading behaviour within a given growth sector takes the form

$$K_{\text{asy}} = -\sum_i r_i \log\left(\text{Im } t^i\right) \ , \tag{2.4.30}$$

where the $r_i = d_i - d_{i-1}$, with $d_0 = 0$, are positive integers no larger than 3. The Kähler metric derived from this asymptotic Kähler potential, which we emphasise may not necessarily be the leading behaviour of the metric, takes the form

$$g_{i\bar{\jmath}} \sim \text{diag}\left(\frac{r_i}{(\text{Im } t^i)^2}\right) \ . \tag{2.4.31}$$

The proper distance $d_\gamma(P,Q)$ along a path γ in field space with affine parameter s then take the form

$$d_\gamma(P,Q) = \int_\gamma \sqrt{g_{i\bar{\jmath}} \frac{dt^i}{ds}\frac{d\bar{t}^{\bar{\jmath}}}{ds}} ds \ . \tag{2.4.32}$$

If we restrict to a path with fixed Re t^i we can write this as

$$d_\gamma(P,Q) = \int_\gamma \left[\sum_i r_i \left(\frac{d \log \text{Im } t^i}{ds}\right)^2\right]^{\frac{1}{2}} ds \ . \tag{2.4.33}$$

For sufficiently simple paths this manifestly grows logarithmically. The distance $d(P,Q)$ along a geodesic path is relevant for the exponential behaviour (2.4.1) of the SDC and we expect that it shares the logarithmic behaviour in the asymptotic regime.

2.4.4 The two-divisor analysis

Most of our general arguments about enhancement chains and charge orbits will be built on the case of just two singularity loci intersecting. To study this canonical situation, we will consider a patch $\mathcal{E}$ in which two discriminant divisors Δ_1, Δ_2 with associated monodromy logarithms N_1, N_2 intersect. This is depicted in figure 2.11. The point P under consideration now can be at different locations in this configuration. We can have either $P \in \Delta_1^\circ$, $P \in \Delta_2^\circ$, or $P \in \Delta_{12}^\circ = (\Delta_1 \cap \Delta_2)^\circ$.

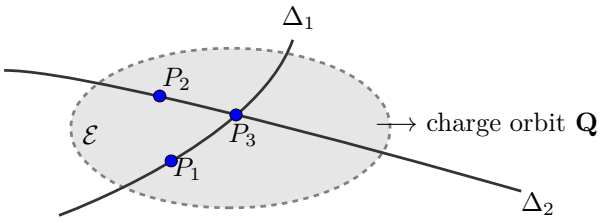

Figure 2.11: The canonical case of two singular divisors intersecting on a local patch $\mathcal{E}$ in moduli space. The considered infinite distance points P can be located either on Δ_1°, Δ_2° or Δ_{12}° as exemplified by P_1, P_2, and P_3.

The restriction of (2.4.16) to the two-dimensional case $n_{\mathcal{E}} = 2$ is given by

$$\mathbf{Q}(\mathbf{q}_0|m_1, m_2) \equiv \exp\Big(m_1 N_1^- + m_2 N_2^-\Big)\mathbf{q}_0 \ . \tag{2.4.34}$$

Recall that the definition of N_1^-, N_2^- requires to fix an ordering. We thus distinguish three cases

$$\begin{aligned} &(1) \quad P \in \Delta_1^\circ : && \text{ordering } (N_1, N_2) \ \to \ (N_1^- = N_1, N_2^-) \ , \\ &(2) \quad P \in \Delta_2^\circ : && \text{ordering } (N_2, N_1) \ \to \ (N_1^- = N_2, N_2^-) \ , \end{aligned} \tag{2.4.35}$$

and the sector-dependent case

$$(3) \quad P \in \Delta_{12}^\circ : \begin{cases} (N_1, N_2) \ \to \ (N_1^- = N_1, N_2^-) & \text{path } \left\{ \frac{\text{Im } t^1}{\text{Im } t^2},\ \text{Im } t^2 > \lambda \right\} , \\ (N_2, N_1) \ \to \ (N_1^- = N_2, N_2^-) & \text{path } \left\{ \frac{\text{Im } t^2}{\text{Im } t^1},\ \text{Im } t^1 > \lambda \right\} . \end{cases} \tag{2.4.36}$$

Note that the construction of N_2^- is a rather non-trivial task, as outlined in the appendices. Our aim is to identify the possible enhancements for which a $\mathbf{q}_0$ exists such that the charge orbit is massless and infinite.

We can choose, with generality, to focus on the ordering (1) above and correspondingly focus only on the upper growth sector in (2.4.36). We go through each enhancement chain Type A $\to$ Type B and track candidate charges $\mathbf{q}_0$ through the enhancement. In particular, we will check the conditions (R1) and (R2) and identify the $\mathbf{q}_0$ that induces an infinite massless orbit. Moreover, we will show how our construction does not necessarily yield an infinite orbit that is massless on any path within a sector if (R1) and (R2) are violated. We show that the enhancement of type $\boxed{\mathrm{I}_a}$ $\to$ Type B do not admit infinite orbits by examining the example $\mathrm{I}_a \to \mathrm{IV}_d$. The path dependence will be discussed for the example $\mathrm{II}_b \to \boxed{\mathrm{III}_c}$. Finally, we will also examine chains with no type enhancement by discussing the example $\mathrm{II}_b \to \mathrm{II}_c$.

For every enhancement Type A $\to$ Type B, we denote the Sl(2)-splitting of the limiting mixed Hodge structure of Type A and Type B by $(F_{(1)}, W^{(1)})$ and $(F_{(2)}, W^{(2)})$, respectively. Then we have a pair of commuting $\mathfrak{sl}(2)$-operators (N_1^-, N_1^+, Y_1) and (N_2^-, N_2^+, Y_2). The Deligne splitting of $(F_{(i)}, W^{(i)})$ is denoted by

$$H^3(Y_3, \mathbb{C}) = \bigoplus_{p,q} I_{(i)}^{p,q}, \qquad I_{(i)}^{p,q} = \bigoplus_{k\geq 0} \left(N_{(i)}^-\right)^k P^{p+k,q+k}(N_{(i)}^-)\,, \tag{2.4.37}$$

where we have also displayed the decomposition (2.2.44) into primitive parts. The bracket notation matches that introduced in (2.2.35) and (2.2.36), so for example $W_l^{(2)} \equiv W_l\left(N_1^- + N_2^-\right)$.

2.4.4.1 The enhancement $\mathrm{I}_a \to \mathrm{IV}_d$

Let us first discuss the enhancement chains $\boxed{\mathrm{I}_a} \to \mathrm{IV}_d$ and $\mathrm{I}_a \to \boxed{\mathrm{IV}_d}$, i.e. where we consider P at either on a I_a locus or a IV_d locus. This will also allow us to introduce the strategy on how we relate the Hodge-Deligne diamonds along enhancements.

Focusing first on $\boxed{\mathrm{I}_a} \to \mathrm{IV}_d$, we recall that the conditions (2.3.12) imply that a divisor of type I_a is at finite distance. Hence we do not necessarily expect any infinite tower of massless states as we approach the type I_a divisor in our formalism. We will check that we can indeed not identify an infinite charge orbit associated to this locus.

We first spell out the decomposition into primitive parts (2.3.7) associated with the mixed Hodge structure $\left(F_{(1)}, W^{(1)}\right)$ of type I_a

$$H^3(Y_3, \mathbb{C}) = P^3(N_1^-) \oplus \left[P^4(N_1^-) \oplus N_1^- P^4(N_1^-)\right]\,, \tag{2.4.38}$$

where the $P^i(N_1^-)$ are the primitive spaces defined in (2.3.8). Note the we have used different colours for later expositional convenience. We depict the decomposition into primitive parts also in the Hodge-Deligne diamond in figure 2.12.

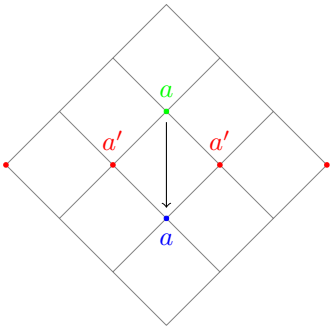

Figure 2.12: The Hodge-Deligne diamond of type I_a with its decomposition into primitive parts (2.4.38). The action of N_1^- are labelled by arrows, and we use colours to highlight the primitive subspaces $P^3(N_1^-)$, $P^4(N_1^-)$ and their images under the action of N_1^-. Since the two $\mathfrak{sl}(2)$-triples are commuting, the primitive subspace $P^3(N_1^-)$, $P^4(N_1^-)$ and their images under N_1^- are preserved by N_2^-.

As discussed in section 2.3.2, the $P^k(N_1^-)$ carry a pure Hodge structure of weight k on Δ_1°, while at Δ_{12}° these degenerate into mixed Hodge structures. Specifically, we have a pure Hodge structure of weight 3 with Hodge number $(0, a', a', 0)$ on $P^3(N_1^-)$, and a pure Hodge structure of weight 4 with Hodge number $(0, 0, a, 0, 0)$ on $P^4(N_1^-)$. Then the second $\mathfrak{sl}(2)$-triple (N_2^-, N_2^+, Y_2) induces polarised mixed Hodge structures polarised by N_2^- coming from variation of Hodge structures on $P^3(N_1^-)$ and $P^4(N_1^-)$. We show the Deligne splitting of these two mixed Hodge structures and their images under the action of N_1^- in the figure 2.13.[11] The sum (2.4.38) of the mixed Hodge structures then gives a mixed Hodge structure, $I^{p,q}_{(2)}$, of type IV_d with $d = r + a$ where $r \geq 1$ is an integer.

We can now identify an element $\mathbf{q}_0$ in $I^{p,q}_{(2)}$ that looks similar to the one occurring in the one-parameter case (2.4.13). The relevant $\mathbf{q}_0$ is shown in figure 2.13, and it can be written as

$$\mathbf{q}_0 \sim_{\mathbb{Z}} \left(N^-_{(2)}\right)^2 \tilde{\mathbf{a}}^{(2)}_0 \ . \tag{2.4.39}$$

We can see also from figure 2.13 that $\mathbf{q}_0$ is not in the kernel of N_2^-, and so the

[11] Note that we do not depict the full grid for the higher weight Hodge structures, see for example appendix 2.E for this.

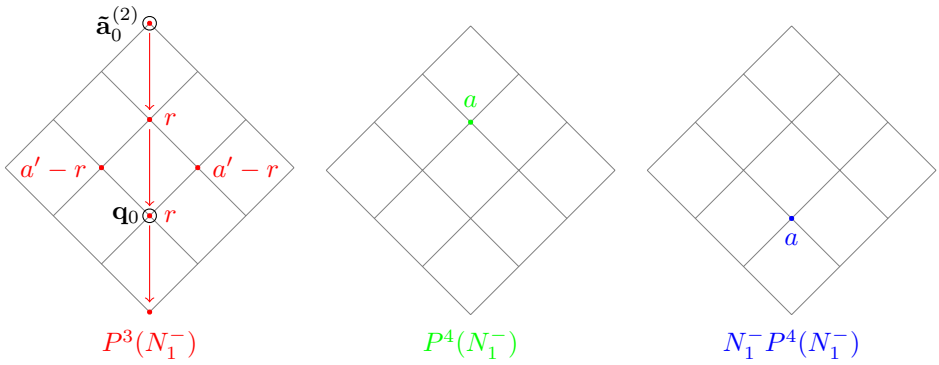

Figure 2.13: The left picture shows a mixed Hodge structure, determined by some integer $r \geq 1$, on $P^3(N_1^-)$. The middle picture shows a mixed Hodge structure on $P^4(N_1^-)$. The right picture shows the image of the middle picture under the action of N_1^-. In these diamonds, the coloured arrows label the action of N_2^-. The colourings are in agreement with equation (2.4.38) and figure 2.12. The sum of these three Hodge-Deligne diamonds is the diamond of $\left(F_{(2)}, W^{(2)}\right)$, associated to the mixed Hodge structure $I^{p,q}_{(2)}$, of type IV_d. The circles around the dots in the first diamond indicate the location of $\mathbf{q}_0$ and $\tilde{\mathbf{a}}_0^{(2)}$.

charge orbit (2.4.34) is indeed infinite and given by

$$\mathbf{Q}(\mathbf{q}_0|m_1,m_2) = \mathbf{q}_0 + m_2 N_2^- \mathbf{q}_0, \text{ for } m_1, m_2 \in \mathbb{Z}. \tag{2.4.40}$$

Next we would like to check if this infinite orbit is indeed massless on Δ_1°. This can of course be checked by using condition (2.4.29), but in this section of two-divisor analysis we will also spell out the growths of Hodge norm explicitly to familiarise the reader with the formalism. To do this we follow a similar procedure to the one-parameter case in section 2.4.1. We first determine the location of $\mathbf{q}_0$, i.e. $\mathbf{q}_0 \in W_{l_1}\left(N_1^-\right) \cap W_{l_2}\left(N_{(2)}^-\right)$. The grades l_1 and l_2 can be read off from figures 2.12 and 2.13 as the height of the position of $\mathbf{q}_0$. This then readily gives

$$\mathbf{q}_0 \in W_3\left(N_1^-\right) \cap W_2\left(N_{(2)}^-\right) . \tag{2.4.41}$$

Since approaching a point $P \in \Delta_1^\circ$ requires to send $\mathrm{Im}\, t^1 \to \infty$ while keeping $\mathrm{Im}\, t^2$ finite we use the growth theorem (2.2.63) to read off that

$$||\mathbf{q}_0|| \sim c\,(\mathrm{Im}\, t^1)^0 , \tag{2.4.42}$$

which implies that $||\mathbf{q}_0||$ does not tend to 0 at P. Hence $\mathbf{Q}(\mathbf{q}_0|m_1,m_2)$, the charge orbit, is not necessarily massless. In terms of the condition (2.4.29), we see that

the grade relevant to the type I_a divisor is $l_1 = 3$ and it obviously does not satisfy (2.4.29).

Let us now turn to the enhancement $\mathrm{I}_a \to \boxed{\mathrm{IV}_d}$, i.e. to the case that P is located at Δ_{12}°. We now have to utilize the multi-parameter growth theorem as outlined in section 2.2.5. Using the location (2.4.41) in the two-parameter growth (2.2.66) we find

$$||\mathbf{q}_0|| \sim c\,\frac{1}{\mathrm{Im}\,t^2}\ . \tag{2.4.43}$$

From this growth we can easily see that the $\mathbf{q}_0$ defined in (2.4.39) indeed generates a massless charge orbit, which is infinite due to (2.4.40). In order to discuss the path dependence of this result, we first recall that we have fixed the upper sector in (2.4.36). It is now obvious form (2.4.43) that $\mathbf{q}_0$ is massless along any path in this sector approaching P at $t^1 = t^2 = \mathbf{i}\infty$. This confirms that (R1) applies in this case.

2.4.4.2 The enhancement $\mathrm{II}_b \to \mathrm{IV}_d$

The other enhancement cases where the type increases can be analysed in the same way. The case we discuss next is the enhancement $\mathrm{II}_b \to \mathrm{IV}_d$, again considering the two possible locations for P.

We first consider placing the P on the type II_b divisor, i.e. $\boxed{\mathrm{II}_b} \to \mathrm{IV}_d$. The decomposition into primitive parts of the type II_b mixed Hodge structure $\left(F_{(1)}, W^{(1)}\right)$ is

$$H^3\left(Y_3, \mathbb{C}\right) = P^3(N_1^-) \oplus \left[P^4(N_1^-) \oplus N_1^- P^4(N_1^-)\right]\ . \tag{2.4.44}$$

We depict this decomposition in the Hodge-Deligne diamond of II_b in figure 2.14. The enhancement $\mathrm{II}_b \to \mathrm{IV}_d$ is equivalent to a decomposition of the Hodge diamond of IV_d as shown in figure 2.15.

We can now identify the element in $I_{(2)}^{p,q}$ which gives $\mathbf{q}_0$ as

$$\mathbf{q}_0 \sim_{\mathbb{Z}} N_{(1)}^- \tilde{\mathbf{a}}_0^{(2)}\ . \tag{2.4.45}$$

Again from figure 2.15 we see that $\mathbf{q}_0$ is not in the kernel of N_2^- and so we have an infinite orbit

$$\mathbf{Q}(\mathbf{q}_0|m_1, m_2) = \mathbf{q}_0 + m_2 N_2^- \mathbf{q}_0 + \frac{1}{2} m_2^2 \left(N_2^-\right)^2 \mathbf{q}_0,\ \text{for } m_1, m_2 \in \mathbb{Z}\ . \tag{2.4.46}$$

The location of $\mathbf{q}_0$ is determined as well from figure 2.15 to be

$$\mathbf{q}_0 \in W_2\left(N_1^-\right) \cap W_4\left(N_{(2)}^-\right)\ . \tag{2.4.47}$$

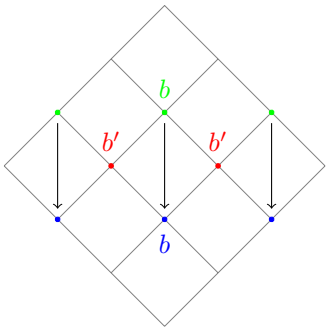

Figure 2.14: The Hodge-Deligne diamond of type II_b with its decomposition into primitive parts (2.4.44). The action of N_1^- are labelled by arrows, and we use colours to highlight the primitive subspaces $P^3(N_1^-)$, $P^4(N_1^-)$ and their images under the action of N_1^-. Since the two $\mathfrak{sl}(2)$-triples are commuting, the primitive subspaces $P^3(N_1^-)$, $P^4(N_1^-)$ and their images under N_1^- are preserved by N_2^-.

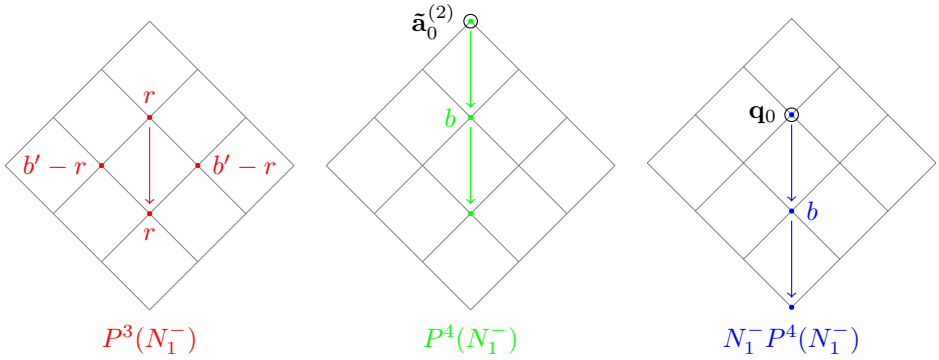

Figure 2.15: The left picture shows a mixed Hodge structure on $P^3(N_1^-)$, the middle picture a mixed Hodge structure on $P^4(N_1^-)$, and the right picture shows the image of the middle picture under the action of N_1^-. In these diamonds, the arrows label the action of N_2^-. The colourings are in agreement with equation (2.4.44) and figure 2.14. The sum of these three Hodge-Deligne diamonds is the diamond of $\left(F_{(2)}, W^{(2)}\right)$ of type IV_d. Again, $\mathbf{q}_0$ and $\tilde{\mathbf{a}}_0^{(2)}$ are denoted explicitly.

Considering a path towards P in the Type II locus Δ_1° amounts to keeping t^2 finite and sending $t^1 = \mathbf{i}\infty$. The growth theorem (2.2.63) thus implies $\|\mathbf{q}_0\| \sim c\,\frac{1}{\mathrm{Im}\,t^1}$. In accord with the condition (2.4.29) we thus find that $\mathbf{q}_0$ is massless at P. We

therefore deduce that the full infinite charge orbit is massless on Δ_1°. This case belongs to the condition (R2) in section 2.4.2 and exemplifies one of the key results of our work.

Having identified the orbit we can return to the point discussed in section 2.4.1, that the orbit should not only contain an infinite number of type II states. This can be easily checked to be the case. In particular, the orbit contains an infinite number of elements with non-vanishing components in $P^{0,2}(\Delta_1^\circ)$, which have non-trivial contraction with $\tilde{\mathbf{a}}_0^{(1)}$. The fact that the orbit is still infinite, even after a quotient by type II charges as proposed in [5], will hold for all the cases where we identify such an orbit.

We can also change the position of P, considering $\mathrm{II}_b \to \boxed{\mathrm{IV}_d}$ instead. Following a similar analysis as above, we find that the choice of seed charge

$$\mathbf{q}_0 \sim_{\mathbb{Z}} N^-_{(1)} N^-_{(2)} \tilde{\mathbf{a}}_0^{(2)} \,, \tag{2.4.48}$$

yields an infinite massless charge orbit $\mathbf{Q}(\mathbf{q}_0|m_1,m_2)$ at Δ_{12}°. It is useful to notice that we have used the $N^-_{(2)}$ which is at the type IV_d divisor, and the $N^-_{(1)}$ which is at the type II_b divisor just before the enhancement. This fact is crucial in defining the corresponding general version of the charge orbit in table 2.6. We also remark that such a $\mathbf{q}_0$ always exists, because the enhancement condition (2.3) for $\mathrm{II}_b \to \mathrm{IV}_d$ requires that $b \geq 1$. This case belongs to the condition (R1) in section 2.4.2.

2.4.4.3 The enhancement $\mathrm{III}_c \to \mathrm{IV}_d$

Turning to the case $\mathrm{III}_c \to \mathrm{IV}_d$ we follow the same procedure as the previous two cases, first considering $\boxed{\mathrm{III}_c} \to \mathrm{IV}_d$. The decomposition into primitive parts of the type III_c mixed Hodge structure $\left(F_{(1)}, W^{(1)}\right)$ is

$$\begin{aligned} H^3(Y_3,\mathbb{C}) = {} & P^3(N_1^-) \oplus \left[P^4(N_1^-) \oplus N_1^- P^4(N_1^-)\right] \\ & \oplus \left[P^5(N_1^-) \oplus N_1^- P^5(N_1^-) \oplus \left(N_1^-\right)^2 P^5(N_1^-)\right] . \end{aligned} \tag{2.4.49}$$

We depict this decomposition in the Hodge-Deligne diamond of III_c in figure 2.16. The enhancement $\mathrm{III}_c \to \mathrm{IV}_d$ is equivalent to a decomposition of the Hodge diamond of IV_d as shown in figure 2.17.

In this case we have that $\mathbf{q}_0$ is given by

$$\mathbf{q}_0 \sim_{\mathbb{Z}} \left(N^-_{(1)}\right)^2 \tilde{\mathbf{a}}_0^{(2)} \,. \tag{2.4.50}$$

and we see that there is an infinite orbit

$$\mathbf{Q}(\mathbf{q}_0|m_1,m_2) = \mathbf{q}_0 + m_2 N_2^- \mathbf{q}_0, \text{ for } m_1,m_2 \in \mathbb{Z} \,. \tag{2.4.51}$$

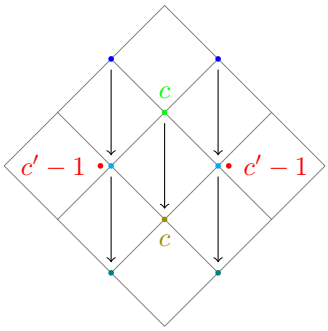

Figure 2.16: The Hodge-Deligne diamond of type III_c with its decomposition into primitive parts (2.4.49). The action of N_1^- are labelled by arrows, and we use colours to highlight the primitive subspaces $P^3(N_1^-)$, $P^4(N_1^-)$, $P^5(N_1^-)$ and their images under the action of N_1^-. Since the two $\mathfrak{sl}(2)$-triples are commuting, the primitive subspaces $P^3(N_1^-)$, $P^4(N_1^-)$, $P^5(N_1^-)$ and their images under N_1^- are preserved by N_2^-.

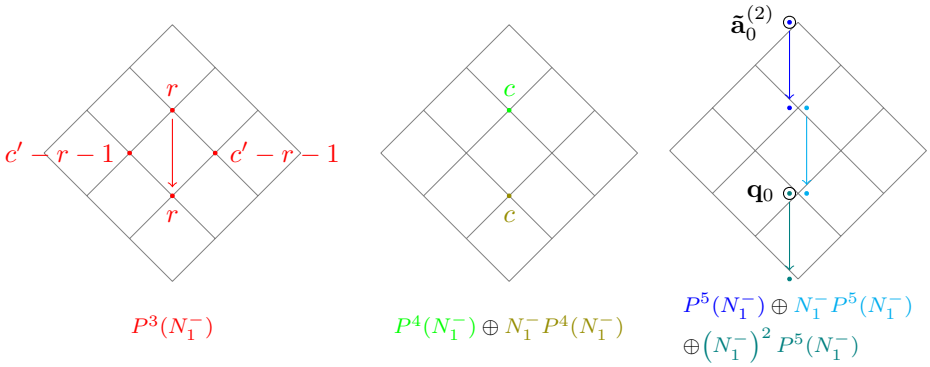

Figure 2.17: Pictures showing the mixed Hodge structures induced on $P^3(N_1^-)$, $P^4(N_1^-)$ and $P^5(N_1^-)$, together with their images under the action of N_1^- and $(N_1^-)^2$. In these diamonds, the coloured arrows label the action of N_2^-. The colourings are in agreement with (2.4.49) and figure 2.16. The sum of these three Hodge-Deligne diamonds is the diamond of $(F_{(2)}, W^{(2)})$ of type IV_d. As before, $\mathbf{q}_0$ and $\tilde{\mathbf{a}}_0^{(2)}$ are denoted explicitly.

The location $\mathbf{q}_0 \in W_1(N_1^-) \cap W_2(N_{(2)}^-)$ implies by using (2.2.63) the asymptotics $\|\mathbf{q}_0\| \sim c \left(\operatorname{Im} t^1\right)^{-2}$ in the limit $t^1 \to \mathbf{i}\infty$. Therefore, again for $P \in \Delta_1^\circ$ we have an infinite massless charge orbit. This case belongs to the condition (R2) in section 2.4.2.

We can also explore the candidate $\mathbf{q}_0$ for the enhancement $\mathrm{III}_c \to \boxed{\mathrm{IV}_d}$ and we find the same seed $\mathbf{q}_0$ as in (2.4.50). The orbit stays massless approaching Δ_{12} along any path in the considered growth sector. It is useful to notice that in defining the seed charge $\mathbf{q}_0$ around IV_d, we are using the $N^-_{(1)}$ which is at the type III_c divisor just before the enhancement. This fact is crucial in defining the corresponding general charge orbit in table 2.6. This case belongs to condition (R1) in section 2.4.2.

2.4.4.4 The enhancement $\mathrm{II}_b \to \mathrm{III}_c$

Let us next consider $\mathrm{II}_b \to \mathrm{III}_c$ and first focus on $\boxed{\mathrm{II}_b} \to \mathrm{III}_c$. Following the same procedure as the previous cases, we refer to equation (2.4.44) and figure 2.14 for the decomposition into primitive parts of the type II_b mixed Hodge structure $\left(F_{(1)}, W^{(1)}\right)$. Then the enhancement $\mathrm{II}_b \to \mathrm{III}_c$ is equivalent to a decomposition of the Hodge diamond of III_c as shown in figure 2.18.

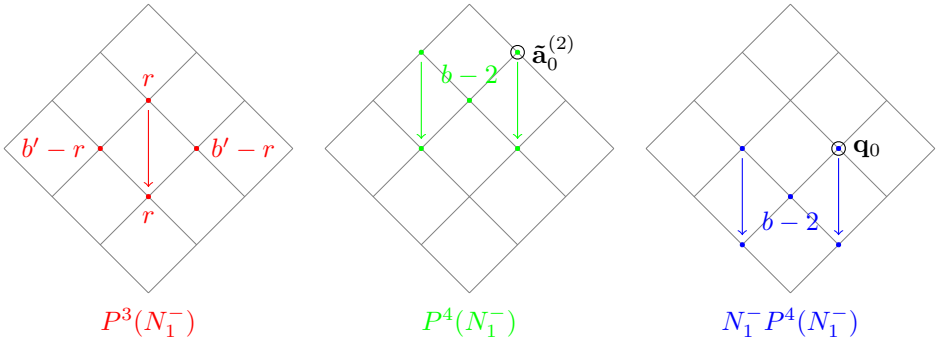

Figure 2.18: The left picture shows a mixed Hodge structure, determined by some non-negative integer r, on $P^3(N_1^-)$. The middle picture shows a mixed Hodge structure on $P^4(N_1^-)$. The right picture shows the image of the middle picture under the action of N_1^-. In these diamonds, the coloured arrows label the action of N_2^-. The colourings are in agreement with equation (2.4.44) and figure 2.14. The sum of these three Hodge-Deligne diamonds is the diamond of $\left(F_{(2)}, W^{(2)}\right)$, associated to the mixed Hodge structure $I^{p,q}_{(2)}$, of type III_c. The circle around the dot in the last diamond indicates the location of $\mathbf{q}_0$, and the circle around the dot in the middle diamond indicates the location of $\tilde{\mathbf{a}}_0^{(2)}$.

In this case, the $\mathbf{q}_0$ is chosen to be

$$\mathbf{q}_0 \sim_{\mathbb{Z}} N^-_{(1)} \tilde{\mathbf{a}}_0^{(2)} \ . \tag{2.4.52}$$

and we see that the orbit

$$\mathbf{Q}(\mathbf{q}_0|m_1,m_2) = \mathbf{q}_0 + m_2 N_2^- \mathbf{q}_0, \text{ for } m_1,m_2 \in \mathbb{Z} \tag{2.4.53}$$

is indeed infinite.

The location of $\mathbf{q}_0$ is determined to be

$$\mathbf{q}_0 \in W_2\left(N_1^-\right) \cap W_3\big(N_{(2)}^-\big). \tag{2.4.54}$$

This implies that for P on Δ_1°, i.e. when taking the limit $t^1 \to \mathbf{i}\infty$, we find by using (2.2.63) that $||\mathbf{q}_0|| \sim c\,(\text{Im}\ t^1)^{-1}$. Together with (2.4.53) we have an infinite massless charge orbit. This case belongs to the condition (R2) in section 2.4.2.

We now turn to the situation $\text{II}_b \to \boxed{\text{III}_c}$. As we will show, in this case, the masslessness of the charge orbit around the type III_c divisor will depend on the path along which we approach it. For concreteness our choice of $\mathbf{q}_0$ is still (2.4.52), but it is important to note that one cannot find any other $\mathbf{q}_0$ that generates an infinite orbit and is path-independently massless. The fate of the orbit as we approach the point P on the type III_c divisor is different from the previous cases. In fact, using the growth theorem (2.2.66) for the $\mathbf{q}_0$-locations (2.4.54) one finds

$$||\mathbf{q}_0|| \sim c\,\frac{\text{Im}\ t^2}{\text{Im}\ t^1} \tag{2.4.55}$$

in the upper growth region in (2.4.36). We thus conclude that the charge orbit remains massless at P if we approach it with a path satisfying

$$\text{Massless Path}\ :\ \text{Im}\ t^2 \to \infty,\ \text{Im}\ t^1 \to \infty\ ,\ \text{ such that } \frac{\text{Im}\ t^2}{\text{Im}\ t^1} \to 0\ . \tag{2.4.56}$$

The only other possible path, compatible with the considered growth sector, is

$$\text{Massive Path}\ :\ \text{Im}\ t^2 \to \infty,\ \text{Im}\ t^1 \to \infty\ ,\ \text{ such that } \frac{\text{Im}\ t^2}{\text{Im}\ t^1} \to \lambda > 0\ . \tag{2.4.57}$$

In other words, we cannot claim that the considered $\mathbf{q}_0$ is actually massless independent of the path. Therefore, this case was excluded from the conditions (R1), (R2) specifying our general construction. Clearly, in this case also the location (2.4.54) of $\mathbf{q}_0$ does not satisfy the condition (2.4.29). This case belongs to the situation described at the end of section 2.4.2.

2.4.4.5 A case without type enhancement $\mathbf{II}_b \to \mathbf{II}_c$

To end our two-divisor analysis let us explore a case where no type enhancement is present. As usual, the decomposition into primitive parts of the type II_b mixed

Hodge structure $\left(F_{(1)}, W^{(1)}\right)$ is given by equation (2.4.44), and it is depicted in figure 2.14. Then $\mathrm{II}_b \to \mathrm{II}_c$ is equivalent to a decomposition of the Hodge-Deligne diamond of type II_c shown in figure 2.19.

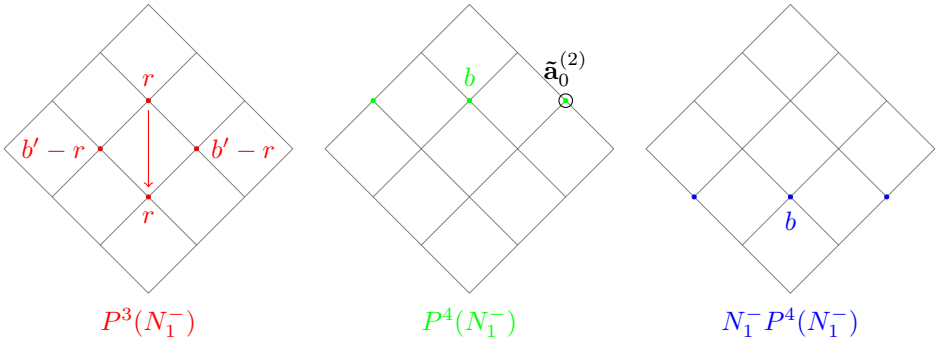

Figure 2.19: The left picture shows a mixed Hodge structure on $P^3(N_1^-)$ of weight 3 with Hodge numbers $(0, b', b', 0)$. The middle picture shows a mixed Hodge structure on $P^4(N_1^-)$ of weight 4 with Hodge numbers $(0, 1, b, 1, 0)$. The right picture shows the image of the middle picture under the action of N_1^-. In these diamonds, the coloured arrows label the action of N_2^-. The colourings are in agreement with equation (2.4.44) and figure 2.14. The sum of these three Hodge-Deligne diamonds is the diamond of $(F_{(2)}, W^{(2)})$ of type II_c. The circle around the dot in the middle diamond indicates the location of $\tilde{\mathbf{a}}_0^{(2)}$.

If we try to find a $\mathbf{q}_0$ such that the generated orbit is infinite and massless at either II_b or II_c following the methods in previous cases, then we realise that such a $\mathbf{q}_0$ does not exist. In particular if $b = c$, meaning that there is no enhancement at all, then the second $\mathfrak{sl}(2)$-triple is trivial

$$(N_2^-, N_2^+, Y_2) = (0, 0, 0). \tag{2.4.58}$$

Nevertheless, this case is relevant in the discussion of multi-divisor enhancements in the following section. To exemplify this we consider the following simple case of a 3-term enhancement chain

$$\mathrm{II}_a \to \boxed{\mathrm{II}_b} \to \mathrm{III}_c\,. \tag{2.4.59}$$

In this chain we have already considered in (2.4.52) a $\mathbf{q}_0$ from the last step of type enhancement. The next step is to estimate the Hodge norm of $\mathbf{q}_0$ and this requires the location of $\mathbf{q}_0$ in every monodromy weight filtration of the mixed Hodge structures of type $\mathrm{II}_a, \mathrm{II}_b$ and III_c. According to the analysis in subsection

2.4.4.4, we have $\mathbf{q}_0$ staying in $W_2(N^-_{(2)})$ and $W_3(N^-_{(3)})$. Then the analysis in this section tells us that generally $\mathbf{q}_0 \in W_3(N^-_{(1)})$. It could still be possible that we have $\mathbf{q}_0 \in W_2(N^-_{(1)})$. However, either of these two possible locations satisfies the massless condition (2.4.29) and hence implies that the charge orbit generated by $\mathbf{q}_0$ is massless at P located at the type II_b singular locus. Analogously we can also analyse the other cases without type enhancements $\mathrm{I}_a \to \mathrm{I}_b$, $\mathrm{III}_a \to \mathrm{III}_b$ and $\mathrm{IV}_a \to \mathrm{IV}_b$. The results of this analysis are similar to the $\mathrm{II}_a \to \mathrm{II}_b$ case and will be used to justify the analysis in the next section. In particular, it will allow us to introduce the notation (2.4.67), which indicates that all enhancements of non-changing type will not influence our constructions.

This completes our two-divisor analysis. We will now use these results to perform the general multi-divisor analysis.

2.4.5 The general multi-divisor analysis

In the previous subsection we have shown when in the case of two intersecting divisors it is possible to identify an infinite massless charge orbit depending on the type of singularity of the divisors and at the intersection as well as the location of P. In this subsection we will generalise the analysis to multiple intersecting divisors. We will first give all possible enhancement chains and then stepwise apply the two-divisor result by treating the two intersecting divisors which themselves are loci of intersection of an arbitrary number of divisors. This is the general setup described in subsection 2.4.2. By explicitly constructing $\mathbf{q}_0$ we will thus be able to show the conditions (R1), (R2) for it to generate an infinite massless charge orbit when approaching P.

2.4.5.1 Masslessness of the general charge orbit

In this subsection we show that one can construct for each enhancement chain (2.4.17) an appropriate seed charge $\mathbf{q}_0$ that defines a massless state when approaching P along any path in a fixed growth sector (2.4.15). Crucially, as stated already in subsection 2.4.2, such a $\mathbf{q}_0$ only exists if the singularity type at the location of P is either II, III, IV. These are also the singularities that occur if we demand P to be at infinite distance.

We thus have to consider the three following general enhancement chains

$$\mathrm{I}_{a_1} \to ... \to \mathrm{I}_{a_k} \to \mathrm{II}_{b_1} \to ... \to \boxed{\mathrm{II}_{b_m}} \to ... \tag{2.4.60}$$

$$\mathrm{I}_{a_1} \to ... \to \mathrm{I}_{a_k} \to \mathrm{II}_{b_1} \to ... \to \mathrm{II}_{b_m} \to \mathrm{III}_{c_1} \to ... \to \boxed{\mathrm{III}_{c_n}} \to ... \tag{2.4.61}$$

$$\mathrm{I}_{a_1} \to ... \to \mathrm{I}_{a_k} \to \mathrm{II}_{b_1} \to ... \to \mathrm{II}_{b_m} \to \mathrm{III}_{c_1} \to ... \to \mathrm{III}_{c_n} \to \mathrm{IV}_{d_1} \to ... \to \boxed{\mathrm{IV}_{d_r}} \to ... \ , \tag{2.4.62}$$

where the box indicates the singularity at the location of P. Note that k, m, n, and r are integers and we allow for chains that do not admit all types. For example, in (2.4.60), (2.4.61), and (2.4.62) we can have $k = 0$, i.e. start the enhancement at type II. Furthermore, let us stress that we have only displayed the enhancement chains until the singularity at P. This part will be relevant in studying the masslessness of the associated $\mathbf{q}_0$ as we will see below. In order to show that the full orbit $\mathbf{Q}$ is infinite, the enhancements after the singularity at P become relevant. We will discuss these parts in subsection 2.4.5.2.

It will turn out to be sufficient to only focus on the type I, II, III, IV without having information about the index required in the complete classification of subsection 2.3.1. Since we also want to simplify the expressions, we thus introduce the shorthand notation

$$\begin{aligned} \mathrm{I} &\equiv \mathrm{I}_{a_1} \to \ldots \to \mathrm{I}_{a_k} \ , \\ \mathrm{II} &\equiv \mathrm{II}_{b_1} \to \ldots \to \mathrm{II}_{b_m} \ , \\ \mathrm{III} &\equiv \mathrm{III}_{c_1} \to \ldots \to \mathrm{III}_{c_n} \ , \\ \mathrm{IV} &\equiv \mathrm{IV}_{d_1} \to \ldots \to \mathrm{IV}_{d_p} \ . \end{aligned} \tag{2.4.63}$$

Now it is straightforward to display all appearing enhancement chains that can occur before the singularity at P. We list them in the first column of table 2.6.

The second column of table 2.6 lists the seed charge $\mathbf{q}_0$ that we propose for the corresponding chain. This charge has been constructed such that it has a universal location in the spaces $W(N^-_{(k)})$ relevant in the growth theorem of subsection 2.2.5. In fact, tracking $\mathbf{q}_0$ through the various enhancements as in subsection 2.4.4 we find for the three general chains (2.4.60)-(2.4.62) the locations

$$P \in \text{Type II locus}: \qquad \mathbf{q}_0 \in W_3\big(N^-_{(\mathrm{I})}\big) \cap W_2\big(N^-_{(\mathrm{II})}\big) \tag{2.4.64}$$

$$P \in \text{Type III locus}: \qquad \mathbf{q}_0 \in W_3\big(N^-_{(\mathrm{I})}\big) \cap W_2\big(N^-_{(\mathrm{II})}\big) \cap W_1\big(N^-_{(\mathrm{III})}\big) \tag{2.4.65}$$

$$P \in \text{Type IV locus}: \qquad \mathbf{q}_0 \in W_3\big(N^-_{(\mathrm{I})}\big) \cap W_2\big(N^-_{(\mathrm{II})}\big) \cap W_1\big(N^-_{(\mathrm{III})}\big) \cap W_2\big(N^-_{(\mathrm{IV})}\big) \ , \tag{2.4.66}$$

Chain	$\mathbf{q}_0$	location of $\mathbf{q}_0$
$\boxed{\text{II}} \to \cdots$	$N^-_{(n_P)}\tilde{\mathbf{a}}_0^{(n\mathcal{E})}$	$W_2\big(N^-_{(\text{II})}\big)$
$\text{I} \to \boxed{\text{II}} \to \cdots$	$N^-_{(n_P)}\tilde{\mathbf{a}}_0^{(n\mathcal{E})}$	$W_3\big(N^-_{(\text{I})}\big) \cap W_2\big(N^-_{(\text{II})}\big)$
$\boxed{\text{III}} \to \cdots$	$\big(N^-_{(n_P)}\big)^2\tilde{\mathbf{a}}_0^{(n\mathcal{E})}$	$W_1\big(N^-_{(\text{III})}\big)$
$\text{I} \to \boxed{\text{III}} \to \cdots$	$\big(N^-_{(n_P)}\big)^2\tilde{\mathbf{a}}_0^{(n\mathcal{E})}$	$W_3\big(N^-_{(\text{I})}\big) \cap W_1\big(N^-_{(\text{III})}\big)$
$\text{II} \to \boxed{\text{III}} \to \cdots$	$\big(N^-_{(n_P)}\big)^2\tilde{\mathbf{a}}_0^{(n\mathcal{E})}$	$W_2\big(N^-_{(\text{II})}\big) \cap W_1\big(N^-_{(\text{III})}\big)$
$\text{I} \to \text{II} \to \boxed{\text{III}} \to \cdots$	$\big(N^-_{(n_P)}\big)^2\tilde{\mathbf{a}}_0^{(n\mathcal{E})}$	$W_3\big(N^-_{(\text{I})}\big) \cap W_2\big(N^-_{(\text{II})}\big) \cap W_1\big(N^-_{(\text{III})}\big)$
$\boxed{\text{IV}} \to \cdots$	$\big(N^-_{(n_P)}\big)^2\tilde{\mathbf{a}}_0^{(n\mathcal{E})}$	$W_2\big(N^-_{(\text{IV})}\big)$
$\text{I} \to \boxed{\text{IV}} \to \cdots$	$\big(N^-_{(n_P)}\big)^2\tilde{\mathbf{a}}_0^{(n\mathcal{E})}$	$W_3\big(N^-_{(\text{I})}\big) \cap W_2\big(N^-_{(\text{IV})}\big)$
$\text{II} \to \boxed{\text{IV}} \to \cdots$	$N^-_{(n_P-r)}N^-_{(n_P)}\tilde{\mathbf{a}}_0^{(n\mathcal{E})}$	$W_2\big(N^-_{(\text{II})}\big) \cap W_2\big(N^-_{(\text{IV})}\big)$
$\text{III} \to \boxed{\text{IV}} \to \cdots$	$\big(N^-_{(n_P-r)}\big)^2\tilde{\mathbf{a}}_0^{(n\mathcal{E})}$	$W_1\big(N^-_{(\text{III})}\big) \cap W_2\big(N^-_{(\text{IV})}\big)$
$\text{I} \to \text{II} \to \boxed{\text{IV}} \to \cdots$	$N^-_{(n_P-r)}N^-_{(n_P)}\tilde{\mathbf{a}}_0^{(n\mathcal{E})}$	$W_3\big(N^-_{(\text{I})}\big) \cap W_2\big(N^-_{(\text{II})}\big) \cap W_2\big(N^-_{(\text{IV})}\big)$
$\text{I} \to \text{III} \to \boxed{\text{IV}} \to \cdots$	$\big(N^-_{(n_P)}\big)^2\tilde{\mathbf{a}}_0^{(n\mathcal{E})}$	$W_3\big(N^-_{(\text{I})}\big) \cap W_1\big(N^-_{(\text{III})}\big) \cap W_2\big(N^-_{(\text{IV})}\big)$
$\text{II} \to \text{III} \to \boxed{\text{IV}} \to \cdots$	$\big(N^-_{(n_P-r)}\big)^2\tilde{\mathbf{a}}_0^{(n\mathcal{E})}$	$\big(N^-_{(\text{II})}\big) \cap W_1\big(N^-_{(\text{III})}\big) \cap W_2\big(N^-_{(\text{IV})}\big)$
$\text{I} \to \text{II} \to \text{III} \to \boxed{\text{IV}} \to \cdots$	$\big(N^-_{(n_P-r)}\big)^2\tilde{\mathbf{a}}_0^{(n\mathcal{E})}$	$W_3\big(N^-_{(\text{I})}\big) \cap W_2\big(N^-_{(\text{II})}\big)$ $\cap W_1\big(N^-_{(\text{III})}\big) \cap W_2\big(N^-_{(\text{IV})}\big)$

Table 2.6: The table contains all possible enhancement chains that can arise before the singularity at P. We use the notation (2.4.63) in the first column. The $\mathbf{q}_0$ associated to each chain is listed in the second column. Note that $N^-_{(n_P-r)}$ is the element associated to the last type III singularity in the locus, with r as in (2.4.62). The third column lists the location of $\mathbf{q}_0$ using the notation introduced in (2.4.67).

where we have introduced the shorthand notation [12]

[12] Note the unusual pattern in $W_2\big(N^-_{(\text{II})}\big)$, which contains an additional parameter k' with $k+1 \leq k' \leq k+m$. The crucial information here is that if $\mathsf{Type}\ \mathsf{A}_{n_P} = \text{II}$, then we must have $\mathbf{q}_0 \in W_2\big(N^-_{(n_P)}\big)$ to ensure masslessness. Before the end of the type II chain, the location of an $\mathbf{q}_0$ could be pushed up by 1 to W_3 but this will not affect the masslessness. In $W\big(N^-_{(\text{I})}\big), W\big(N^-_{(\text{III})}\big)$ and $W\big(N^-_{(\text{IV})}\big)$, such a phenomenon is not present. This justifies the shorthand notation (2.4.67).

$$
\begin{aligned}
W_3\big(N^-_{(\mathrm{I})}\big) &\equiv W_3\big(N^-_{(1)}\big) \cap \ldots \cap W_3\big(N^-_{(k)}\big)\,, \\
W_2\big(N^-_{(\mathrm{II})}\big) &\equiv W_3\big(N^-_{(k+1)}\big) \cap \ldots \cap W_3\big(N^-_{(k')}\big) \\
&\quad \cap W_2\big(N^-_{(k'+1)}\big) \cap \ldots \cap W_2\big(N^-_{(k+m)}\big)\,, \\
W_1\big(N^-_{(\mathrm{III})}\big) &\equiv W_1\big(N^-_{(k+m+1)}\big) \cap \ldots \cap W_1\big(N^-_{(k+m+n)}\big)\,, \\
W_2\big(N^-_{(\mathrm{IV})}\big) &\equiv W_2\big(N^-_{(k+m+n+1)}\big) \cap \ldots \cap W_2\big(N^-_{(k+m+n+r)}\big)\,.
\end{aligned}
\tag{2.4.67}
$$

Note that the $W_l(N^-_{(i)})$ in each line (2.4.64)-(2.4.66) is always $W_l\big(N^-_{(n_P)}\big)$ corresponding to the location of P. The shorthand notation (2.4.67) is also used in the last column of table 2.6 giving the location of the listed $\mathbf{q}_0$.

We now collected all the information to show that $\mathbf{q}_0$ becomes massless along any path approaching P within a growth sector. This is straightforward since we have already established the general result (2.4.29), which gives a sufficient condition for this behaviour. It is easy to check using the last column of table 2.6 that (2.4.29) is satisfied.

2.4.5.2 Infiniteness of the general charge orbit

Having shown the masslessness of the charge orbit $\mathbf{Q}(\mathbf{q}_0|m_1,\ldots,m_{n_\mathcal{E}})$, we will in this subsection check its infiniteness. The procedure is similar to the one used in subsection 2.4.4. Let us first repeat the definition of the charge orbit (2.4.16) and expand the exponential

$$
\begin{aligned}
\mathbf{Q}(\mathbf{q}_0|m_1,\ldots,m_{n_\mathcal{E}}) &= \exp\Big(\sum_{i=1}^{n_\mathcal{E}} m_i N_i^-\Big)\mathbf{q}_0 \\
&= \mathbf{q}_0 + \sum_{i=1}^{n_\mathcal{E}} m_i N_i^- \mathbf{q}_0 + \ldots\,,
\end{aligned}
\tag{2.4.68}
$$

where each m_i is an integer, and the $\ldots$ indicate terms that are at least quadratic in m_i.

Furthermore, we notice that if there exists an $N^-_{(k)}$ with k taking any value $k = 1,\ldots,n_\mathcal{E}$ which does not annihilate $\mathbf{q}_0$ then the orbit is infinite. To see this, we set $m_1 = \cdots = m_{k-1} = m_k = m$ and $m_{k+1} = \cdots = m_{n_\mathcal{E}} = 0$. The orbit reduces to

$$
\mathbf{Q}(\mathbf{q}_0|m,\ldots,m,0,\ldots,0) = \mathbf{q}_0 + m\,N^-_{(k)}\mathbf{q}_0 + \frac{1}{2}m^2\big(N^-_{(k)}\big)^2\mathbf{q}_0 + \frac{1}{6}m^3\big(N^-_{(k)}\big)^3\mathbf{q}_0,
\tag{2.4.69}
$$

where we have used $\left(N^-_{(k)}\right)^4\mathbf{q}_0 = 0$. If the orbit $\mathbf{Q}(\mathbf{q}_0|m,\dots,m,0,\dots,0)$ is not infinite, then there is an $m' \neq m$ such that

$$\mathbf{Q}(\mathbf{q}_0|m',\dots,m',0,\dots,0) = \mathbf{Q}(\mathbf{q}_0|m,\dots,m,0,\dots,0)\,,$$

hence $N^-_{(k)}\mathbf{q}_0 = 0$. This contradiction implies that the orbit $\mathbf{Q}(\mathbf{q}_0|m_1,\dots,m_{n_\mathcal{E}})$ is infinite, provided the existence of an $N^-_{(k)}$ that does not annihilate $\mathbf{q}_0$.

Let us now show that such an $N^-_{(k)}$ exists for the enhancement chains (2.4.17) satisfying the conditions (R1) or (R2) of subsection 2.4.2. The simpler condition to show is (R1), which considers enhancement chains for in which P is at a Type IV locus. In this case the $N^-_{(k)}$ not annihilating the seed charge $\mathbf{q}_0$ is simply $N^-_{(k)} = N^-_{(n_P)}$. This immediately follows from the fact that in the Type IV case one has $\left(N^-_{(n_P)}\right)^3\tilde{\mathbf{a}}_0^{(n_\mathcal{E})} \neq 0$, which implies that the relevant $\mathbf{q}_0$s given in table 2.6 satisfy $N^-_{(n_P)}\mathbf{q}_0 \neq 0$.

Turning to condition (R2), we recall that it states that for every enhancement chain with P at a Type II or Type III locus at least one further enhancement has to occur after the location of P. Considering this enhancement to occur from the (n_P+j-1)-term to (n_P+j)-term the general expressions of the relevant chains are

$$\begin{aligned}
&\cdots \to \mathrm{II}_{b_1} \to \cdots \to \underset{\text{at } n_P}{\boxed{\mathrm{II}_b}} \to \cdots \to \mathrm{II}_{b_m} \to \underset{\text{at } (n_P+j)}{\mathrm{III}_{c_1}} \to \cdots\,,\\
&\cdots \to \mathrm{II}_{b_1} \to \cdots \to \underset{\text{at } n_P}{\boxed{\mathrm{II}_b}} \to \cdots \to \mathrm{II}_{b_m} \to \underset{\text{at } (n_P+j)}{\mathrm{IV}_{d_1}} \to \cdots\,,\\
&\cdots \to \mathrm{III}_{c_1} \to \cdots \to \underset{\text{at } n_P}{\boxed{\mathrm{III}_c}} \to \cdots \to \mathrm{III}_{c_n} \to \underset{\text{at } (n_P+j)}{\mathrm{IV}_{d_1}} \to \cdots\,.
\end{aligned} \tag{2.4.70}$$

We claim that in these cases the $N^-_{(k)}$ not annihilating $\mathbf{q}_0$ is given by $N^-_{(k)} = N^-_{(n_P+j)}$. Indeed, since the type of the singularity increases, also the highest power of $N^-_{(i)}$ not annihilating $\tilde{\mathbf{a}}_0^{(n_\mathcal{E})}$ increases. Using the relevant definitions of $\mathbf{q}_0$ of table 2.6 this implies that $N^-_{(n_P+j)}$ does not annihilate $\mathbf{q}_0$. In conclusion we have found for chains satisfying (R1) and (R2) relevant $N^-_{(k)}$ that do not annihilate the seed charge $\mathbf{q}_0$ and thus have shown the infiniteness of the charge orbit $\mathbf{Q}(\mathbf{q}_0|m_1,\dots,m_{n_\mathcal{E}})$.

2.4.6 A two parameter example: mirror of $\mathbb{P}^{(1,1,1,6,9)}[18]$

The discussions so far have been general, but rather abstract. In this section we show how to explicitly realise our approach to identifying the orbit. We consider the

degree-18 Calabi-Yau hypersurface inside the weighted projective space $\mathbb{P}^{(1,1,1,6,9)}$. This hypersurface is denoted by $\tilde{Y}_3 = \mathbb{P}^{(1,1,1,6,9)}[18]$ and has $h^{1,1}(\tilde{Y}_3) = 2$. The Calabi-Yau hypersurface of which we will consider the complex structure moduli space is the mirror Y_3 of $\tilde{Y}_3$. Note that the geometry and the periods of the pair $(\tilde{Y}_3, Y_3)$ have been studied in detail in [119] as one of the early applications of mirror symmetry.

We will consider a patch $\mathcal{E}$ containing the large complex structure point of Y_3, which by mirror symmetry corresponds to the large volume point of $\tilde{Y}_3$. Hence we can use the formulas of subsection 2.3.4 to derive the monodromy logarithms N_1, N_2 and determine the corresponding singularity type. The Calabi-Yau threefold $\tilde{Y}_3$ sits inside the toric ambient space with toric data

						$l^{(1)}$	$l^{(2)}$
K	1	0	0	0	0	−6	0
D_0	1	0	0	−1	−1	1	−3
D_1	1	1	0	−1	−1	0	1
D_2	1	0	1	−1	−1	0	1
D_3	1	−1	−1	−1	−1	0	1
D'	1	0	0	2	−1	2	0
D''	1	0	0	−1	1	3	0

(2.4.71)

where the first column labels the toric divisors. Restricting all divisors to the hypersurface $\tilde{Y}_3$ in this ambient space, the generators of the Kähler cone are chosen to be

$$J_1 = D_0 + 3D_1\,, \qquad J_2 = D_1\,. \tag{2.4.72}$$

The intersection numbers $K_{ijk} = J_i \cdot J_j \cdot J_k$ in this bases are determined to be [13]

$$K_{111} = 9\,, \qquad K_{112} = 3\,, \qquad K_{122} = 1\,, \qquad K_{222} = 0\,. \tag{2.4.73}$$

[13] While not relevant later on, we note that the second Chern class for this example yields $b_1 = \frac{1}{24} c_2 \cdot J_1 = \frac{17}{4}$, $b_2 = \frac{1}{24} c_2 \cdot J_2 = \frac{3}{2}$.

Inserting (2.4.73) into the general expression (2.3.21) we derive

$$N_1 = \begin{pmatrix} 0 & 0 & 0 & 0 & 0 & 0 \\ -1 & 0 & 0 & 0 & 0 & 0 \\ 0 & 0 & 0 & 0 & 0 & 0 \\ -\frac{9}{2} & -9 & -3 & 0 & 0 & 0 \\ -\frac{3}{2} & -3 & -1 & 0 & 0 & 0 \\ \frac{3}{2} & \frac{9}{2} & \frac{1}{2} & -1 & 0 & 0 \end{pmatrix}, \qquad N_2 = \begin{pmatrix} 0 & 0 & 0 & 0 & 0 & 0 \\ 0 & 0 & 0 & 0 & 0 & 0 \\ -1 & 0 & 0 & 0 & 0 & 0 \\ -\frac{1}{2} & -3 & -1 & 0 & 0 & 0 \\ 0 & -1 & 0 & 0 & 0 & 0 \\ 0 & \frac{3}{2} & 0 & 0 & -1 & 0 \end{pmatrix}. \tag{2.4.74}$$

Furthermore, using table 2.5 we immediately determine the singularity types

$$\begin{aligned} &\Delta_1 = \left\{t^1 = \mathbf{i}\infty\right\} : && N_1 && \text{Type IV}_1 \ , \\ &\Delta_2 = \left\{t^2 = \mathbf{i}\infty\right\} : && N_2 && \text{Type III}_0 \ , \\ &\Delta_{12} = \left\{t^1 = \mathbf{i}\infty, t^2 = \mathbf{i}\infty\right\} : && N_1 + N_2 && \text{Type IV}_2 \ , \end{aligned} \tag{2.4.75}$$

where we note that Δ_{12} is nothing else then the large complex structure or large volume point and hence has the maximal enhancement $\text{IV}_{h^{2,1}}$.

In order to construct the charge orbits, we next have to explicitly construct the vector $\tilde{\mathbf{a}}_0^{(2)}$, i.e. the limiting vector at Δ_{12}, and the two nilnegative elements N_1^-, N_2^- in the commuting $\mathfrak{sl}(2)$-pair associated to the enhancements $\text{III}_0 \ \to \text{IV}_2$ and $\text{IV}_1 \ \to \text{IV}_2$. The corresponding derivation is lengthy, but follows the steps outlined in subsection 2.2.4. The details of this computation are presented in the appendices 2.B, 2.C and 2.D. Firstly, one uses the large complex structure periods rotated to an $\mathbb{R}$-split representation to derive

$$\tilde{\mathbf{a}}_0^{(2)} = \left(1, 0, 0, -\frac{17}{4}, -\frac{3}{2}, 0\right)^{\mathrm{T}}. \tag{2.4.76}$$

The commuting $\mathfrak{sl}(2)$-pair for the enhancement $\text{IV}_1 \ \to \text{IV}_2$ are then shown to be

$$N_1^- = \begin{pmatrix} 0 & 0 & 0 & 0 & 0 & 0 \\ -1 & 0 & 0 & 0 & 0 & 0 \\ 0 & 0 & 0 & 0 & 0 & 0 \\ -\frac{9}{2} & -9 & -3 & 0 & 0 & 0 \\ -\frac{3}{2} & -3 & -1 & 0 & 0 & 0 \\ \frac{3}{2} & \frac{9}{2} & \frac{1}{2} & -1 & 0 & 0 \end{pmatrix}, \qquad N_2^- = \begin{pmatrix} 0 & 0 & 0 & 0 & 0 & 0 \\ 0 & 0 & 0 & 0 & 0 & 0 \\ 0 & 0 & 0 & 0 & 0 & 0 \\ 0 & 0 & 0 & 0 & 0 & 0 \\ 0 & 0 & \frac{1}{3} & 0 & 0 & 0 \\ 0 & 0 & 0 & 0 & 0 & 0 \end{pmatrix}. \tag{2.4.77}$$

In contrast, for the enhancement $\mathrm{III}_0 \to \mathrm{IV}_2$ we find the $\mathfrak{sl}(2)$-pair

$$N_1^- = \begin{pmatrix} 0 & 0 & 0 & 0 & 0 & 0 \\ 0 & 0 & 0 & 0 & 0 & 0 \\ -1 & 0 & 0 & 0 & 0 & 0 \\ -\frac{1}{2} & -3 & -1 & 0 & 0 & 0 \\ 0 & -1 & 0 & 0 & 0 & 0 \\ 0 & \frac{3}{2} & 0 & 0 & -1 & 0 \end{pmatrix}, \quad N_2^- = \begin{pmatrix} 0 & 0 & 0 & 0 & 0 & 0 \\ -1 & 0 & 0 & 0 & 0 & 0 \\ \frac{3}{2} & 0 & 0 & 0 & 0 & 0 \\ -\frac{15}{4} & -\frac{9}{4} & -\frac{3}{2} & 0 & 0 & 0 \\ -\frac{3}{2} & -\frac{3}{2} & -1 & 0 & 0 & 0 \\ \frac{3}{2} & \frac{9}{4} & \frac{1}{2} & -1 & \frac{3}{2} & 0 \end{pmatrix}. \tag{2.4.78}$$

With these results we immediately compute the infinite charge orbits for this patch in moduli space. Using (2.4.34) for the cases (2.4.35), (2.4.36) and inserting $\mathbf{q}_0$ proposed in table 2.6 we find

$$\begin{aligned} &(1)\ P \in \Delta_1^\circ: && \mathbf{Q} = (0,0,0,9,3,-9m_1)^{\mathrm{T}}\ , \\ &(2)\ P \in \Delta_2^\circ: && \mathbf{Q} = (0,0,0,1,0,-m_2)^{\mathrm{T}}\ , \\ &(3)\ P \in \Delta_{12}^\circ: && \begin{cases} \mathbf{Q} = (0,0,0,9,3,-9m_1)^{\mathrm{T}} & \text{for } \left\{ \frac{\mathrm{Im}\ t^1}{\mathrm{Im}\ t^2},\ \mathrm{Im}\ t^2 > \lambda \right\}, \\ \mathbf{Q} = (0,0,0,1,0,-m_2)^{\mathrm{T}} & \text{for } \left\{ \frac{\mathrm{Im}\ t^2}{\mathrm{Im}\ t^1},\ \mathrm{Im}\ t^1 > \lambda \right\}. \end{cases} \end{aligned} \tag{2.4.79}$$

Let us stress that by our general arguments all three orbits are infinite and massless at the location of the P under consideration. The infiniteness is immediate due to the dependence on m_1, m_2, while the masslessness can alternatively be explicitly checked by a tedious but straightforward computation using the results of appendix 2.D. It is also nice to see that the charges are actually quantized. This is non-trivial, since $\tilde{\mathbf{a}}_0^{(2)}$ as well as N_1^-, N_2^- contain rational entries.

We close this section by discussing how the general properties and ideas we have outlines are realised in the charge orbits (2.4.79). Firstly, we recall that Δ_2° is a Type III locus and hence the one parameter arguments of subsection 2.4.1 and reference [5] would suggest that there is no infinite orbit. Indeed the orbit $\mathbf{Q}$ is independent of m_1 and hence not generated by the $N_1^- = N_2$ associated to Δ_2°. However, we see in (2.4.79) that this orbit is 'inherited' from the enhancement locus, i.e. induced by the second monodromy logarithm N_2^- not directly associated to Δ_2°. Secondly, we stress that the expression for $\mathbf{Q}$ in case (3) is indeed path dependent. If one approaches Δ_{12}° via a path almost touching Δ_1°, we find that the orbit agrees with the one of case (1). This is not surprising, since this is the infinite orbit of the Type IV_1 singularity along Δ_1° which is transferred to Δ_{12}°. Moving towards Δ_{12}° along a path almost touching Δ_2° we find a completely different charge orbit depending on m_2.

2.4.7 Discussion on properties of the charge orbit

To summarise, in this section we have shown how to identify infinite massless charge orbits using data which is not completely local but rather associated to a patch where singular divisors can intersect. In particular, this significantly extends the infinite charge orbits that were identified in [5]. It also forms a starting point towards a global understanding of the infinite towers of states associated to the monodromies in the full moduli space.

A first point to stress is that our current definition of $\mathbf{Q}$ and $\mathbf{q}_0$ vitally uses the commuting $\mathfrak{sl}(2)$ algebras (2.2.49). In particular, this fact has been exploited in subsection 2.4.3 to show that $\mathbf{Q}$ and $\mathbf{q}_0$ have the same Hodge norm growth. However, the usage of the commuting $\mathfrak{sl}(2)$ basis containing N_i^- could be just an intermediate step to show the desired results. In fact, it is an important strategy of [76, 113] to translate the final statement back to the formulation with the N_i. It may be that a similar result can be shown for our constructions. Therefore, a natural candidate charge orbit is then

$$\tilde{\mathbf{Q}}(\tilde{\mathbf{q}}_0|m_1,\dots,m_{n_\mathcal{E}}) \equiv \exp\Big(\sum_{i=1}^{n_\mathcal{E}} m_i N_i\Big)\tilde{\mathbf{q}}_0 \ , \tag{2.4.80}$$

which is the natural analogue to (2.4.16). In order to identify the seed charge $\tilde{\mathbf{q}}_0$, we would then require that it satisfies the massless condition (2.4.29) within the monodromy weight filtration $W\big(N_{(i)}\big)$ in order to generate an orbit that becomes massless when approaching P within a growth sector. This requirement is natural due to the fact that $W\big(N_{(i)}^-\big) = W\big(N_{(i)}\big)$ as already stated in (2.4.25). More concretely, unpacking the filtration $W\big(N_{(i)}\big)$ with definition (2.2.38) and using the concrete Hodge-Deligne diamonds of singularity types shown in table 2.1, we see that the seed charge has to obey, for every $i = 1,\dots,n_P-1$:

- If Type A_i = I or II, then $N_{(i)}\tilde{\mathbf{q}}_0 = 0$;
- If Type A_i = III, then there exists charge vectors $\mathbf{b}_i$ and $\mathbf{u}_i$ with $N_{(i)}\mathbf{u}_i = 0$ such that $\tilde{\mathbf{q}}_0 = N_{(i)}\mathbf{b}_i + \mathbf{u}_i$;
- If Type A_i = IV, then there exists charge vectors $\mathbf{w}_i$ and $\mathbf{x}_i$ with $N_{(i)}\mathbf{w}_i = 0$ and $\big(N_{(i)}\big)^3\mathbf{x}_i = 0$ such that $\tilde{\mathbf{q}}_0 = \mathbf{w}_i + N_{(i)}\mathbf{x}_i$.

Furthermore, the following conditions are imposed at position n_P:

- If Type A_{n_P} = II, then there is a charge vector $\mathbf{a}$ such that $\tilde{\mathbf{q}}_0 = N_{(n_P)}\mathbf{a}$;
- If Type A_{n_P} = III, then there is a charge vector $\mathbf{u}_{n_P}$ with $\big(N_{(n_P)}\big)^2\mathbf{u}_{n_P} = 0$ such that $\tilde{\mathbf{q}}_0 = N_{(n_P)}\mathbf{u}_{n_P}$;

- If Type $\mathsf{A}_{n_P} = \text{IV}$, then there are charge vectors $\mathbf{c}$ and $\mathbf{w}_{n_P}$ with $\left(N_{(n_P)}\right)^2 \mathbf{w}_{n_P} = 0$, such that $\tilde{\mathbf{q}}_0 = \left(N_{(n_P)}\right)^2 \mathbf{c} + N_{(n_P)} \mathbf{w}_{n_P}$.

Finally to ensure infiniteness, we require the existence of an $N_{(j)}$ with $n_P \leq j \leq n_\mathcal{E}$ such that $N_{(j)} \tilde{\mathbf{q}}_0 \neq 0$. Applying the growth theorem as before we see that the seed charge $\tilde{\mathbf{q}}_0$ satisfying the above properties becomes massless when approaching P within a growth sector if either of the two conditions (R1), (R2) of subsection 2.4.2 are satisfied. Moreover the resulting $\tilde{\mathbf{Q}}$ is infinite by the same reasoning in subsection 2.4.5.2. We would then claim that this $\tilde{\mathbf{Q}}$ becomes massless when approaching P within the same growth sector as $\tilde{\mathbf{q}}_0$. Let us stress, however, that establishing full equivalent to the results of subsections 2.4.3 and 2.4.5, including the explicit constructions of table 2.6, without using the commuting basis would require more work and will be left for the future.

We have discussed how the intersection points can be utilised to build the infinite distance networks in moduli space, which follow the rules of enhancement in table 2.3. If we consider such a network we can identify orbits in patches which contain type IV loci or intersections which enhance the singularity type.[14] Once such an orbit is identified, it will retain its identity along any finite distance along the singularity curve moving away from this local patch. This is because the limiting Hodge structure is defined over the full singular locus. If we move an infinite distance away, so towards a different intersection with some other infinite distance locus, then it is more difficult to track this orbit. We actually expect that the charge orbit can be 'transferred' between singular divisors which intersect even when there is no enhancement of the singularity type. By this we mean that a set of charges identified by a charge orbit on one divisor has a corresponding set on the divisor which intersects it. This is supported by tracking the Hodge-Deligne diamonds from one divisor to the other through the intersection. Should we be able to track the orbit this way, we would be able to identify an infinite charge orbit over a full intersecting infinite distance network. However, we leave a detailed study of this possibility for future work.

In [5] it was shown that the monodromy charge orbit is fully populated by BPS states as long as one of the charges corresponds to a BPS state. This was shown for the only case where such an orbit could be identified, which is for type IV singularities. In this chapter, we are not able to show such a connection between the charge orbit and BPS states. This is not unexpected, the argument of [5] was based on walls of marginal stability. While being away from a wall of marginal

[14] Note that this implies the identification always holds in the large volume regime of the mirror.

stability ensures that a BPS state remains in the spectrum, this is not a necessary condition, i.e. there are many examples of BPS states which by, charge and energy conservation alone, could decay to other BPS states. So one expects that the spectrum of BPS states has some finer underlying structure. The utilisation of the charge orbits in this chapter amounts to a proposal that this finer structure includes the population of charge orbits by BPS states, at least asymptotically towards infinite distance.

2.5 Conclusions

In this chapter we studied aspects of the Swampland Distance Conjecture in the complex structure moduli space of Calabi-Yau manifolds. In this context, the set of infinite distance loci in field space can be understood both generally and precisely. We utilised the powerful mathematical tools of the orbit theorems and mixed Hodge structures to analyse infinite distance points in complete generality, so any infinite distance point in any Calabi-Yau threefold. We showed that any infinite distance point is part of a locus in moduli space to which we can associate a set of discrete topological data, its Hodge-Deligne diamond, that defines its key characteristics. We also showed how to extract this data from the monodromy, associated to axion-type shifts, about the infinite distance locus. The data can be used to completely classify infinite distance loci in the moduli space, and this classification includes an understanding of how different infinite distance loci can intersect and change their type. In this way, the different types of infinite distance loci form a rich intersecting infinite distance network. We showed that there are rules for how such intersections can occur and so for which kinds of infinite distance networks can be built. These rules and networks therefore are uncovering a new perspective on the distance conjecture where global structures in the field space are emerging.

The intersections between different types of infinite distance loci are clearly central to this global perspective, and so naturally most of the investigation was focused on them. Within a local patch in field space containing such an intersection, we were able to reach a significant number of results regarding the nature of the infinite tower of states of the distance conjecture. More precisely, to each infinite distance locus one can associate a nilpotent matrix N, and when the loci intersect the different matrices commute. However, a remarkable result of [76], known as the general Sl(2)-orbit theorem, shows that the nilpotent matrices can further be completed into fully commuting $\mathfrak{sl}(2)$ algebras. This can be thought of as a type of

factorisation of the infinite distance loci, and greatly simplifies the analysis of the intersections. In particular, it allows for a rather precise identification of an infinite tower of states in terms of a *charge orbit*. This orbit generalises the monodromy orbits presented in [5] by utilising the commuting structure of the $\mathfrak{sl}(2)$ algebras. Importantly, it can be generalised recursively to any number of intersecting infinite distance loci. We then established general conditions when such a charge orbit can define an infinite tower of states that become massless when approaching the infinite distance point. More specifically, we have explicitly constructed a candidate charge orbit for any infinite distance point that has another infinite distance locus of higher type in its vicinity. This non-local construction allowed us to identify the tower of states of the distance conjecture for a more general set of infinite distance loci than was done in [5], thereby making progress towards a complete identification of the tower of states globally on the moduli space. However, it is important to state that in [5], by utilising walls of marginal stability, the monodromy orbits were shown to be populated by actual BPS states in the spectrum. We are not able to reach such a result for the more general charge orbits introduced in this chapter. We therefore leave a study of the precise relation between charge orbits and BPS states for future work.

One particularly interesting new aspect of the distance conjecture in the context of intersecting infinite distance loci is that the mass spectrum of BPS states picks up a dependence on the path of approach to the intersection. The results of [76] allowed us to quantify this path dependence rather precisely, showing how to classify paths into different growth sectors, and to determine how the masses of the tower of states behave within each growth sector. We find the encouraging result that the particular form of the infinite charge orbit of states is such that the states become massless independently of the path of approach, within a given growth sector. This lends further evidence to the proposal in [5] that the tower of states associated to the monodromy action induces the infinite distance divergence, since there are no infinite distance paths of approach whereby the tower remains massive.

Our results show that there is a rich structure at infinite distances in field spaces of theories of quantum gravity. While we made significant progress at uncovering some of this structure, we believe that there is much more to discover. The close ties to the existing rich and deep mathematical framework of nilpotent orbits suggest that much of this structure is general. By this we mean that many of the results can be formulated just by an association of a nilpotent matrix to an infinite distance point. Such an association is rather natural from the perspective of quantum

gravity as discussed in [5]. There are two ways to motivate this. The first is that the nilpotent matrix is associated to a discrete gauge symmetry, an axion shift, which is promoted to a continuous global symmetry at infinite distance. The infinite distance and infinite tower of states can then be understood as a quantum gravity obstruction to the global symmetry limit. The second way is in the context of emergence of infinite distances, so the idea that the infinite distance is itself induced by integrating out the tower of states. Then the nilpotent matrix associated to it is a remnant of the structure of this tower. The appearance of nilpotent matrices, associated to axion transformations, was also found in [132]. This ties in nicely also to the ideas of [63] where potentials on field spaces are also controlled by the towers of states. Motivated by these results, we believe that it is a natural expectation that nilpotent elements, and the rich structure associated to them which we have been exploring in this chapter, may underlie much of the universal behaviour of quantum gravity theories at large distances in field space.

While our work was motivated by the distance conjecture, the results are significant also purely as a study of Calabi-Yau moduli spaces. We have adapted the recent results on relations between polarised mixed Hodge structures [113] to the moduli space, expanded on them and developed their connection to distances in the space. We have also presented the first, to our knowledge, computation of the commuting $\mathfrak{sl}(2)$ triples of matrices at intersections of infinite distance loci, or from the Hodge-theoretic perspective, at degenerations of polarized mixed Hodge structures.

Our analysis was focused on the complex structure moduli space, but we have also discussed the mirror dual configuration in some detail. More precisely, we have explicitly determined the monodromy matrices relevant in the complexified Kähler cone when encircling the large volume point in a higher-dimensional moduli space. We showed that by only using the triple intersection numbers and the second Chern class of the mirror threefold one is able to classify the monodromies and the arising infinite distance singularity types in this large volume regime. In this large volume regime we can then directly apply our findings on the charge orbit. They immediately imply that we have shown that to every infinite distance point in the large volume regime we can identify an infinite charge orbit that becomes massless at this point. Crucially the considered point does not have to be the large volume point itself, but rather any partial limit will also share this feature. Let us stress that we expect that our construction of the charge orbit is also valid relevant in string compactifications that are not directly the mirror to the considered Type IIB configurations [81]. Moreover, it is interesting to point out that this

perspective gives a new way to systematically classify allowed triple intersection numbers and hence allowed Kähler potentials. In fact, the associated polarized mixed Hodge structure incorporates more canonically the positivity conditions on various couplings, while the growth theorem ensures that possible cancellations are ruled out. It would be very interesting to systematically explore the power of this new perspective for questions beyond the distance conjecture.

Appendices

2.A Monodromy filtrations and mixed Hodge structures

In this appendix we give a short review of some further mathematical concepts relevant for this chapter. We first introduce a *pure* Hodge structure and its associated Hodge filtration. A pure Hodge structure of weight w provides a splitting of the complexification $V_{\mathbb{C}} = V \otimes \mathbb{C}$ of a rational vector space V by the Hodge decomposition

$$V_{\mathbb{C}} = \mathcal{H}^{w,0} \oplus \mathcal{H}^{w-1,1} \oplus \ldots \oplus \mathcal{H}^{1,w-1} \oplus \mathcal{H}^{0,w} \ , \tag{2.A.1}$$

with the subspaces satisfying $\mathcal{H}^{p,q} = \overline{\mathcal{H}^{q,p}}$ with $w = p + q$, where the complex conjugation on $V_{\mathbb{C}}$ is defined with respect to the rational vector space V. Using the $\mathcal{H}^{p,q}$ one can also define a Hodge filtration as $F^p = \oplus_{i \geq p} \mathcal{H}^{i,w-i}$ satisfying

$$V_{\mathbb{C}} = F^0 \ \supset \ F^1 \ \supset \ \ldots \ \supset \ F^{w-1} \ \supset \ F^w = \mathcal{H}^{w,0} \ , \tag{2.A.2}$$

such that $\mathcal{H}^{p,q} = F^p \cap \bar{F}^q$. A *polarized* pure Hodge structure requires additionally the existence of a bilinear form $S(\cdot, \cdot)$ on $V_{\mathbb{C}}$, such that the conditions $S(\mathcal{H}^{p,q}, \mathcal{H}^{r,s}) = 0$ for $p \neq s, \ q \neq r$ and $\mathbf{i}^{p-q} S(v, \bar{v}) > 0$ for any non-zero $v \in \mathcal{H}^{p,q}$ are satisfied.

The crucial extra ingredient relevant to define a (limiting) mixed Hodge structure, is the so-called *monodromy weight filtration* W_i. It was defined in (2.2.38) using the kernels and images of the nilpotent matrix N. The rational vector subspaces $W_j(N) \subset V$ can alternatively be defined by requiring that they form a filtration

$$W_{-1} \equiv 0 \ \subset \ W_0 \ \subset \ W_1 \ \subset \ \ldots \ \subset \ W_{2w-1} \ \subset \ W_{2w} = V \ , \tag{2.A.3}$$

with the properties

$$1.) \quad NW_i \subset W_{i-2} \tag{2.A.4}$$

$$2.) \quad N^j : Gr_{w+j} \to Gr_{w-j} \text{ is an isomorphism}, \quad Gr_j \equiv W_j/W_{j-1} \ . \tag{2.A.5}$$

The quotients Gr_i contain equivalence classes of elements of W_i that differ by elements of W_{i-1}. When $V_{\mathbb{C}}$ also admits a Hodge filtration F^p as in (2.A.2), we require that N is compatible with this structure and acts on it horizontally, i.e. $NF^p \subset F^{p-1}$.

We are now in the position to define a *mixed Hodge structure* (V, W, F), induced by the filtrations W_i and F^q on the vector space V. The defining feature of this structure is that each Gr_j defined in (2.A.5) admits an induced Hodge filtration

$$F^p Gr_j^{\mathbb{C}} \equiv (F^p \cap W_j^{\mathbb{C}})/(F^p \cap W_{j-1}^{\mathbb{C}}) \ , \tag{2.A.6}$$

where $Gr_j^{\mathbb{C}} = Gr_j \otimes \mathbb{C}$ and $W_i^{\mathbb{C}} = W_i \otimes \mathbb{C}$ are the complexification. In other words, in the notation of (2.A.1) we spilt each Gr_j into a pure Hodge structure $\mathcal{H}^{p,q}$ as

$$Gr_j = \bigoplus_{p+q=j} \mathcal{H}^{p,q} \ , \qquad \mathcal{H}^{p,q} = F^p Gr_j \cap \overline{F^q Gr_j} \ , \tag{2.A.7}$$

where we recall that $w = p + q$ is the weight of the corresponding pure Hodge structure. The operator N is a morphism among these pure Hodge structures. Using the action of N on W_i and F^p, we find $NGr_j \subset Gr_{j-2}$ and $N\mathcal{H}^{p,q} \subset \mathcal{H}^{p-1,q-1}$. Note that this induces a jump in the weight of the pure Hodge structure by -2, while the mixed Hodge structure is preserved by N.

2.B Construction of the SL(2)-splitting

In this appendix we review the construction of the matrices δ and ζ that are used to construct a special $\mathbb{R}$-split mixed Hodge structure $(V, \hat{F}, W)$, first discussed in subsection 2.2.4, via

$$\hat{F} = e^{\zeta} e^{-\mathbf{i}\delta} F \ . \tag{2.B.1}$$

The mixed Hodge structure $(V, \hat{F}, W)$ is called the SL(2)-splitting of the limiting mixed Hodge structure (V, F, W). Here we denote by (V, F, W) a vector space V with filtrations F^p and W_i, see appendix 2.A. As in subsection 2.2.3 the latter is induced by some nilpotent N. Using (2.2.39) and (2.2.40) we can determine a Deligne splitting $V_{\mathbb{C}} = \bigoplus I^{p,q}$ from the data (F, W). On this splitting there is a semisimple operator T, called the grading operator, that acts on the subspace

$\bigoplus_{p+q=l} I^{p,q}$ as multiplication by l. Let $\overline{T}$ be the complex conjugate of the grading operator T defined by

$$\overline{T}(v) := \overline{T(\overline{v})}, \tag{2.B.2}$$

for all $v \in V_{\mathbb{C}}$. Then $\overline{T}$ and T are related by a conjugation by $e^{-2\mathbf{i}\delta}$

$$\overline{T} = e^{-2\mathbf{i}\delta} T e^{2\mathbf{i}\delta}, \tag{2.B.3}$$

where the real operator δ sends every $I^{p,q}$ to its "lower parts":

$$\delta(I^{p,q}) \subset \bigoplus_{\substack{r<p \\ s<q}} I^{r,s}, \text{ for all } p, q. \tag{2.B.4}$$

Thus we can solve equation (2.B.3) with an Ansatz satisfying (2.B.4) for the operator δ. Furthermore δ commutes with N and preserves the polarisation $\delta^{\mathrm{T}}\eta + \eta\delta = 0$. Such an operator δ is unique. Let

$$\tilde{F} := e^{-\mathbf{i}\delta} F, \tag{2.B.5}$$

and the mixed Hodge structure $(V, \tilde{F}, W)$ is $\mathbb{R}$-split. For a mathematically precise discussion we refer to Proposition 2.20 of [76].

The second operator ζ further builds another $\mathbb{R}$-split mixed Hodge structure out of $(V, \tilde{F}, W)$. Its construction is indirect and we refer to section 3 and Lemma 6.60 of [76] for the full original discussion. Also section 1 of [133] contains a good review of the ζ operator and in its Appendix the authors worked out some explicit expressions that will be used in our computation.

To find ζ, we first compute a 'Deligne splitting' of the operator δ: Let $V_{\mathbb{C}} = \bigoplus \tilde{I}^{p,q}$ be the Deligne splitting of the $\mathbb{R}$-split mixed Hodge structure $(V, \tilde{F}, W)$, then this Deligne splitting induces a decomposition of δ

$$\delta = \sum_{p,q>0} \delta_{-p,-q}, \tag{2.B.6}$$

where each component $\delta_{-p,-q}$ precisely does the following:

$$\delta_{-p,-q}(\tilde{I}^{r,s}) \subset \tilde{I}^{r-p,s-q}, \text{ for all } r, s. \tag{2.B.7}$$

The operator ζ admits the same kind of decomposition

$$\zeta = \sum_{p,q>0} \zeta_{-p,-q}, \tag{2.B.8}$$

and its relation with δ is given by the equation in Lemma 6.60 of [76]

$$e^{\mathbf{i}\delta} = e^{\zeta}\left(\sum_{k\geq 0}\frac{(-\mathbf{i})^k}{k!}\mathrm{ad}_N^k(\tilde{g}_k)\right), \tag{2.B.9}$$

where every $\tilde{g}_k$ is an real operator preserving the polarisation η of the real vector space V and $\mathrm{ad}_N(-) = [N,-]$ is the adjoint action. The main outcome of this formula useful for us is that, upon decomposing δ and ζ into their $(-p,-q)$ components and solving for $\zeta_{-p,-q}$, we get a polynomial in $\delta_{-p,-q}$ and the iterated commutators among various components $\delta_{-p,-q}$.

Specialising to weight-3 degenerating variation of Hodge structures, the possible non-vanishing components of $\zeta_{-p,-q}$ are restricted to $1\leq p,q\leq 3$. Then according to the Appendix of [133], we have the following explicit expressions

$$\begin{aligned}&\zeta_{-1,-1}=0,\quad \zeta_{-1,-2}=-\frac{\mathbf{i}}{2}\delta_{-1,-2},\quad \zeta_{-1,-3}=-\frac{3\mathbf{i}}{4}\delta_{-1,-3},\quad \zeta_{-2,-2}=0,\\ &\zeta_{-2,-3}=-\frac{3\mathbf{i}}{8}\delta_{-2,-3}-\frac{1}{8}[\delta_{-1,-1},\delta_{-1,-2}],\quad \zeta_{-3,-3}=-\frac{1}{8}[\delta_{-1,-1},\delta_{-2,-2}],\end{aligned} \tag{2.B.10}$$

while the remaining $\zeta_{-q,-p}$ are obtained from $\zeta_{-p,-q}$ by replacing all $\mathbf{i}$ by $-\mathbf{i}$ and $\delta_{-r,-s}$ by $\delta_{-s,-r}$. Summing all $\zeta_{-p,-q}$, we get a formula for ζ that is valid in weight-3 degenerating variation of Hodge structures given by

$$\begin{aligned}\zeta =&\frac{\mathbf{i}}{2}(\delta_{-2,-1}-\delta_{-1,-2})+\frac{3\mathbf{i}}{4}(\delta_{-3,-1}-\delta_{-1,-3})+\frac{3\mathbf{i}}{8}(\delta_{-3,-2}-\delta_{-2,-3})\\ &-\frac{1}{8}[\delta_{-1,-1},\delta_{-1,-2}+\delta_{-2,-1}+\delta_{-2,-2}].\end{aligned} \tag{2.B.11}$$

2.C General procedure to construct the commuting $\mathfrak{sl}(2)$s

The construction of commuting $\mathfrak{sl}(2)$s is part of the multi-variable SL(2)-orbit theorem in [76]. We summarise its construction in this section for completeness.

Finding the commuting $\mathfrak{sl}(2)$-triples associated to the intersection $\Delta_{1,\dots,n_{\mathcal{E}}}$ needs $n_{\mathcal{E}}$-times iteration. One starts with the mixed Hodge structure $(F_\infty, W^{n_{\mathcal{E}}})$, where F_∞ is the limiting Hodge filtration extracted by nilpotent orbit theorem, and $W^{n_{\mathcal{E}}}$ is the monodromy weight filtration associated to the nilpotent cone $\sigma(N_1,\dots,N_{n_{\mathcal{E}}})$ generated by the monodromies $N_1,\dots,N_{n_{\mathcal{E}}}$, i.e.,

$$W^{n_{\mathcal{E}}} = W(N_1+\cdots+N_{n_{\mathcal{E}}}). \tag{2.C.1}$$

The limiting mixed Hodge structure $(F_\infty, W^{n_\mathcal{E}})$ will be used as the input of the first iteration of the construction. Let the index $k = n_\mathcal{E}$, which will be counted downwards after each iteration.

For each iteration with index k, we denote the input mixed Hodge structure by (F', W^k). Then one computes the SL(2)-splitting (F_k, W^k) of (F', W^k). Furthermore, one finds the Deligne splitting of the mixed Hodge structure (F_k, W^k)

$$V_\mathbb{C} = \bigoplus_{p,q} I^{p,q}_{(F_k, W^k)}. \tag{2.C.2}$$

Record the semisimple grading operator $Y_{(k)}$ which acts on each subspace by multiplication

$$Y_{(k)} v = (p + q - 3)v, \text{ for every } v \in I^{p,q}_{(F_k, W^k)}. \tag{2.C.3}$$

And set the mixed Hodge structure $(e^{\mathbf{i}N_k} F_k, W^{k-1})$ as the input of the next iteration, which carries index $k - 1$.

The loop stops once $k = 0$. In the end, we get a bunch of grading operators $Y_{(n_\mathcal{E})}, \ldots, Y_{(1)}$ associated with $\mathbb{R}$-split mixed Hodge structures

$$(F_{n_\mathcal{E}}, W^{n_\mathcal{E}}), \ldots, (F_1, W^1)\,.$$

For convenience, set $Y_{(0)} = 0$.

The next step is to find the nilpotent elements N_i^- in each triple (N_i^-, N_i^+, Y_i). Every N_i^- is determined by diagonalising the adjoint action of $Y_{(i-1)}$: Decompose N_i into eigenvectors of the adjoint action of $Y_{(i-1)}$

$$N_i = \sum_\alpha N_i^\alpha, \tag{2.C.4}$$

where N_i^α satisfies $[Y_{(i-1)}, N_i^\alpha] = \alpha N_i^\alpha$. Then the nilnegative element is extracted $N_i^- := N_i^0$. Note that one always has $N_1^- = N_1$ since $Y_{(0)} = 0$.

The neutral elements are set to be

$$Y_i = Y_{(i)} - Y_{(i-1)}. \tag{2.C.5}$$

Since $Y_{(0)} = 0$, we have $Y_0 = Y_{(0)}$.

Finally, we complete the triples by solving the equations defining an $\mathfrak{sl}(2)$-triple

$$[Y_i, N_i^+] = 2N_i^+, \qquad [N_i^+, N_i^-] = Y_i, \tag{2.C.6}$$

for the nilpositive element N_i^+, which is required to also preserve the polarisation

$$(N_i^+)^\mathrm{T} \eta + \eta N_i^+ = 0. \tag{2.C.7}$$

We have thus found the commuting $\mathfrak{sl}(2)$-triples (N_i^-, N_i^+, Y_i) for $i = 1, \ldots, n_\mathcal{E}$ according to theorem (4.20) of [76].

2.D An example: commuting $\mathfrak{sl}(2)$s in the mirror of $\mathbb{P}^{(1,1,1,6,9)}[18]$

This section aims to exemplify the structures of section 2.2 and 2.4, by analysing the periods and Hodge structure of an explicit Calabi-Yau threefold geometry. More precisely, we will denote by $\tilde{Y}_3$ the degree-18 Calabi-Yau hypersurface inside the weighted projective space $\mathbb{P}^{(1,1,1,6,9)}$ and denote by Y_3 its mirror. We show in detail how the associated commuting $\mathfrak{sl}(2)$-pair for the variation of Hodge structure on Y_3 arises from the study of its complex structure moduli space. We also illustrate several abstract constructions introduced in the previous sections, including the Deligne splitting (2.2.39) and the associated canonical SL(2)-splitting MHS in SL(2)-orbit theorem of appendix 2.B. Note that the geometry and the periods of the pair $(\tilde{Y}_3, Y_3)$ have been studied in detail in [119] as one of the first applications of mirror symmetry.

2.D.1 Introduction to the example

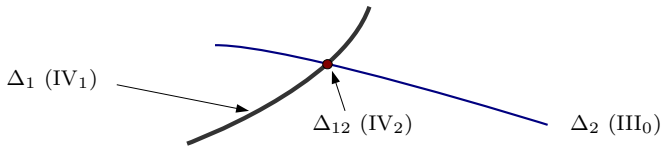

Figure 2.20: Two singular divisors Δ_1 and Δ_2 intersect at the large complex structure point Δ_{12}, where the corresponding types of degenerations are also labelled. The coloured divisor shows one of the possible ways of approaching the large complex structure point, namely moving along the type-III$_0$ divisor towards the type-IV$_2$ intersection. This choice is equivalent to a choice of the ordering of the monodromies as (N_2, N_1), so that we have the singularity enhancement from Δ_2° to Δ_{12}°.

We focus on 2-moduli degeneration in this section. The geometric setup is that we sit near the large complex structure point, where locally the moduli space contains two copies of punctured disk as shown in figure 2.20. From the period vector around the large complex structure point, we extract the limiting Hodge filtration $F(\Delta_{12}^\circ)$, whose top component $F^3(\Delta_{12}^\circ)$ is generated by $\mathbf{a}_0^{(2)}$. Then $(F(\Delta_{12}^\circ), W(N_1 + N_2))$ is a limiting mixed Hodge structure. In accordance with

appendix 2.C, we denote $F_\infty := F(\Delta_{12}^\circ)$ and $W^2 := W(N_1 + N_2)$ in the following discussion.

2.D.1.1 The periods of Y_3 around the large complex structure point

In this section we give the periods of Y_3 around the large complex structure point following the method described in section 2.3.4. The toric and relevant topological data of $\tilde{Y}_3$ is given in section 2.4.6 and we remark that the Euler characteristic of $\tilde{Y}_3$ is $\chi(\tilde{Y}_3) = -540$.

Furthermore, the generators of the Mori cone C_1, C_2 dual to J_1, J_2 are chosen to be

$$C_1 = J_2 \cap J_2, \qquad C_2 = D_0 \cap J_2, \tag{2.D.1}$$

so that the following K-theory basis for branes

$$(\mathcal{O}_{X^\circ}, \mathcal{O}_{J_1}, \mathcal{O}_{J_2}, \mathcal{C}_1, \mathcal{C}_2, \mathcal{O}_p) \tag{2.D.2}$$

yields the asymptotic period vector around the large complex structure point and the polarisation matrix:

$$\mathbf{\Pi}^{\mathbf{\Omega}}(t^1, t^2) = \begin{pmatrix} 1 \\ t^1 \\ t^2 \\ \frac{9}{2}(t^1)^2 + 3t^1t^2 + \frac{1}{2}(t^2)^2 + \frac{9}{2}t^1 + \frac{1}{2}t^2 - \frac{17}{4} + \cdots \\ \frac{3}{2}(t^1)^2 + t^1t^2 + \frac{3}{2}t^1 - \frac{3}{2} + \cdots \\ \frac{3}{2}(t^1)^3 + \frac{3}{2}(t^1)^2t^2 + \frac{1}{2}t^1(t^2)^2 - \frac{23}{4}t^1 - \frac{3}{2}t^2 - \frac{135\mathbf{i}\zeta(3)}{2\pi^3} + \cdots \end{pmatrix}, \tag{2.D.3}$$

$$\eta = \begin{pmatrix} 0 & -10 & -3 & 0 & 0 & -1 \\ 10 & 0 & 1 & 1 & 0 & 0 \\ 3 & -1 & 0 & 0 & 1 & 0 \\ 0 & -1 & 0 & 0 & 0 & 0 \\ 0 & 0 & -1 & 0 & 0 & 0 \\ 1 & 0 & 0 & 0 & 0 & 0 \end{pmatrix}, \tag{2.D.4}$$

where t^i is the coordinate on the Kähler moduli space of $\tilde{Y}_3$, under the mirror map it corresponds to the coordinates z^i on the complex structure moduli space of Y_3 via $t^i = \frac{1}{2\pi\mathbf{i}} \log z^i + \cdots$. The full period can be acquired by solving the Picard-Fuchs equation on the space Y_3 and matching the leading logarithmic behaviour of

the solution with the above asymptotic period. We do not give the full instanton-corrected period vector since it is not relevant to our discussion.

The monodromy operator T_i is then induced by sending $t^i \mapsto t^i - 1$:

$$T_1 = \begin{pmatrix} 1 & 0 & 0 & 0 & 0 & 0 \\ -1 & 1 & 0 & 0 & 0 & 0 \\ 0 & 0 & 1 & 0 & 0 & 0 \\ 0 & -9 & -3 & 1 & 0 & 0 \\ 0 & -3 & -1 & 0 & 1 & 0 \\ 0 & 9 & 2 & -1 & 0 & 1 \end{pmatrix}, \qquad T_2 = \begin{pmatrix} 1 & 0 & 0 & 0 & 0 & 0 \\ 0 & 1 & 0 & 0 & 0 & 0 \\ -1 & 0 & 1 & 0 & 0 & 0 \\ 0 & -3 & -1 & 1 & 0 & 0 \\ 0 & -1 & 0 & 0 & 1 & 0 \\ 0 & 2 & 0 & 0 & -1 & 1 \end{pmatrix}, \tag{2.D.5}$$

and they are already unipotent. Their corresponding logarithms $N_i := \log T_i$ are given by

$$N_1 = \begin{pmatrix} 0 & 0 & 0 & 0 & 0 & 0 \\ -1 & 0 & 0 & 0 & 0 & 0 \\ 0 & 0 & 0 & 0 & 0 & 0 \\ -\frac{9}{2} & -9 & -3 & 0 & 0 & 0 \\ -\frac{3}{2} & -3 & -1 & 0 & 0 & 0 \\ \frac{3}{2} & \frac{9}{2} & \frac{1}{2} & -1 & 0 & 0 \end{pmatrix}, \qquad N_2 = \begin{pmatrix} 0 & 0 & 0 & 0 & 0 & 0 \\ 0 & 0 & 0 & 0 & 0 & 0 \\ -1 & 0 & 0 & 0 & 0 & 0 \\ -\frac{1}{2} & -3 & -1 & 0 & 0 & 0 \\ 0 & -1 & 0 & 0 & 0 & 0 \\ 0 & \frac{3}{2} & 0 & 0 & -1 & 0 \end{pmatrix}. \tag{2.D.6}$$

According to the classification in table 2.1, we especially find that the degeneration types shown in figure 2.20.

To find the commuting $\mathfrak{sl}(2)$-triples, we need the full characterisation of the Hodge filtration $0 \subset F^3 \subset F^2 \subset F^1 \subset F^0 = V_{\mathbb{C}}$. According to special geometry, the period generating Hodge flags lower than F^3 can be obtained by taking various derivatives with respect to t^i. We make the following choice

$$\Pi(t^1, t^2) = \left(\mathbf{\Pi^\Omega}, \partial_{t^1} \mathbf{\Pi^\Omega}, \partial_{t^2} \mathbf{\Pi^\Omega}, \frac{1}{9}\partial_{t^1}^2 \mathbf{\Pi^\Omega}, \partial_{t^2}^2 \mathbf{\Pi^\Omega}, \frac{1}{9}\partial_{t^1}^3 \mathbf{\Pi^\Omega} \right), \tag{2.D.7}$$

where the coefficient $\frac{1}{9}$ is chosen for convenience. Each entry in $\Pi(t^1, t^2)$ is understood to be a column vector, representing the Hodge basis in terms of the multi-valued integral basis $\{\gamma_i\}$. Further explanation of the period matrix representation can be found in the next subsection.

2.D.2 The commuting $\mathfrak{sl}(2)$-pair associated to $\mathrm{III}_0 \to \mathrm{IV}_2$

In this subsection, we compute the commuting $\mathfrak{sl}(2)$-pair arising from a degeneration from type III_0 to IV_2, which amounts to an ordering (N_2, N_1). We also denote $N_{(2)} = N_2 + N_1$.

2.D.2.1 Initial data: the mixed Hodge structure around the large volume point

Let $(\gamma_5, \gamma_4, \gamma_3, \gamma_2, \gamma_1, \gamma_0)$ be the multi-valued integral basis in terms of which the Hodge basis are represented as the period matrix. Upon looping $z^i \mapsto e^{2\pi \mathbf{i}} z^i$ counterclockwise, they experience the monodromy transformation $(\gamma_5, \ldots, \gamma_0) \mapsto (\gamma_5, \ldots, \gamma_0) T_i$ which is equivalent to sending $t^i \mapsto t^i - 1$ in the period matrix. We first define a set of untwisted basis elements by setting

$$(e_5, e_4, \ldots, e_0)_{t^1, t^2} := (\gamma_5, \gamma_4, \ldots, \gamma_0)_{t^1, t^2} e^{-t^1 N_1 - t^2 N_2} \tag{2.D.8}$$

where the subscript t^1, t^2 reminds us that all the base vectors are (t^1, t^2)-dependent. The basis $\{e_i(t^1, t^2)\}$ are invariant under the monodromy transformation. Then the limiting Hodge filtration is extracted by sending $t^1, t^2 \to \mathbf{i}\infty$:

$$\begin{aligned} \Pi_\infty &= \lim_{\substack{t^1 \to \mathbf{i}\infty \\ t^2 \to \mathbf{i}\infty}} e^{t^1 N_1 + t^2 N_2} \Pi(t^1, t^2) \\ &= \left(\begin{array}{c|c|cc|cc|c} & w_3 & w_{21} & w_{22} & w_{11} & w_{12} & w_0 \\ \hline e_5 & 1 & 0 & 0 & 0 & 0 & 0 \\ e_4 & 0 & 1 & 0 & 0 & 0 & 0 \\ e_3 & 0 & 0 & 1 & 0 & 0 & 0 \\ e_2 & -\frac{17}{4} & \frac{9}{2} & \frac{1}{2} & 1 & 1 & 0 \\ e_1 & -\frac{3}{2} & \frac{3}{2} & 0 & \frac{1}{3} & 0 & 0 \\ e_0 & -\frac{135\mathbf{i}\zeta(3)}{2\pi^3} & -\frac{23}{4} & -\frac{3}{2} & 0 & 0 & 1 \end{array} \right), \end{aligned} \tag{2.D.9}$$

where the constant $\{e_i\}$ basis are now understood as the limit of the untwisted basis $\{e_i(t^1, t^2)\}$ as $t^1, t^2 \to \mathbf{i}\infty$.

For clarity, we explain the meaning of the period matrix: A Hodge filtration $0 \subset F^3 \subset F^2 \subset F^1 \subset F^0 = V_{\mathbb{C}}$ is characterised by a Hodge basis $(w_3, \ldots, w_0)$ generating the Hodge flags. In our 2-moduli example whose Hodge numbers of the middle cohomology $H^3(Y_3, \mathbb{C})$ are always $(1, 2, 2, 1)$, we have

$$\begin{aligned} &F^3 = \mathrm{span}_{\mathbb{C}}\{w_3\}, \quad F^2 = \mathrm{span}_{\mathbb{C}}\{w_3, w_{21}, w_{22}\}, \\ &F^1 = \mathrm{span}_{\mathbb{C}}\{w_3, w_{21}, w_{22}, w_{11}, w_{12}\}, \quad F^0 = \mathrm{span}_{\mathbb{C}}\{w_3, w_{21}, w_{22}, w_{11}, w_{12}, w_0\}. \end{aligned} \tag{2.D.10}$$

Then the period matrix representing a Hodge flag consists of column vectors expressing the Hodge basis $\{w_i\}$ in terms of the single-valued integral basis $\{e_i\}$. For example, in the above period matrix Π_∞, the basis $w_{22} = e_3 + \frac{1}{2} e_2 - \frac{3}{2} e_0$. In the following, every operator acting on F will be regarded as transforming the $\{w_i\}$ vectors, whose action is computed as right multiplication on the period matrix.

While the above usage of nilpotent orbit theorem is regraded as a change of the integral basis so we have the (inverse) action of $e^{-t^1 N_1 - t^2 N_2}$ on the left. For clarity, we have labelled the column and rows in every period matrix representing the Hodge filtration in a limiting mixed Hodge structure.

We also need the monodromy weight filtration $W^2 := W\left(N_{(2)}\right)$ associated to the cone $\sigma(N_1, N_2)$. It is simply given by

$$\begin{array}{ccccc} & & W_6^2 & = & \mathrm{span}_{\mathbb{R}}\{e_5, e_4, e_3, e_2, e_1, e_0\} \\ & & \cup & & \\ W_5^2 & = & W_4^2 & = & \mathrm{span}_{\mathbb{R}}\{e_4, e_3, e_2, e_1, e_0\} \\ & & \cup & & \\ W_3^2 & = & W_2^2 & = & \mathrm{span}_{\mathbb{R}}\{e_2, e_1, e_0\} \\ & & \cup & & \\ W_1^2 & = & W_0^2 & = & \mathrm{span}_{\mathbb{R}}\{e_0\} \end{array} \tag{2.D.11}$$

One can check that this filtration indeed satisfies the following conditions:

$$\begin{aligned} &N_{12} : W_i^2 \to W_{i-2}^2 \text{ for every } i, \\ &N_{12}^k : \mathrm{Gr}_{3+k}^{W^2} \to \mathrm{Gr}_{3-k}^{W^2} \text{ is an isomorphism for every } k. \end{aligned}$$

From now on, it is helpful to forget the geometric origin of this limiting mixed Hodge structure and only regard it as a construction in linear algebra. To clarify: We fix a 6-dimensional real vector space V with a distinguished real basis $(e_5, \ldots, e_0)$ and two nilpotent matrices N_1, N_2 expressed in the $\{e_i\}$-basis. The mixed Hodge structure to work with is then (V, F_∞, W^2).

2.D.2.2 First round: finding the SL(2)-splitting of (V, F_∞, W^2)

Firstly we need to find the Deligne splitting of (V, F_∞, W^2). Denote the Deligne splitting by $V_{\mathbb{C}} = \bigoplus I_\infty^{p,q}$ and it can be computed by directly applying the definition (2.2.39). The result is given in the Hodge diamond in figure 2.21 and we note that the shape of the Hodge diagram clearly shows that at the large complex structure point Δ_{12} the degeneration type is IV_2.

We can further check that the splitting satisfies the conjugation property that $I_\infty^{p,q} = \overline{I_\infty^{q,p}}$ for all p, q except

$$I_\infty^{3,3} = \overline{I_\infty^{3,3}} \mod I_\infty^{0,0},$$

hence the mixed Hodge structure (F_∞, W^2) is not $\mathbb{R}$-split.

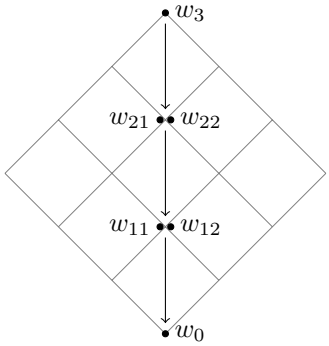

Figure 2.21: The Hodge diamond of the mixed Hodge structure (V, F_∞, W^2), in which each dot near the (p,q)-site represents a base vector of the corresponding subspace $I_\infty^{p,q}$. The arrows show the action of $N_{(2)}$.

The grading operator T and its complex conjugate $\overline{T}$ defined in appendix 2.B expressed in the Hodge basis $(w_3, \ldots, w_0)$ can be directly read out from figure 2.21

$$T = \begin{pmatrix} 6 & 0 & 0 & 0 & 0 & 0 \\ 0 & 4 & 0 & 0 & 0 & 0 \\ 0 & 0 & 4 & 0 & 0 & 0 \\ 0 & 0 & 0 & 2 & 0 & 0 \\ 0 & 0 & 0 & 0 & 2 & 0 \\ 0 & 0 & 0 & 0 & 0 & 0 \end{pmatrix}, \qquad \overline{T} = \begin{pmatrix} 6 & 0 & 0 & 0 & 0 & 0 \\ 0 & 4 & 0 & 0 & 0 & 0 \\ 0 & 0 & 4 & 0 & 0 & 0 \\ 0 & 0 & 0 & 2 & 0 & 0 \\ 0 & 0 & 0 & 0 & 2 & 0 \\ \frac{810\mathbf{i}\zeta(3)}{\pi^3} & 0 & 0 & 0 & 0 & 0 \end{pmatrix}. \tag{2.D.12}$$

Then the δ operator written in the $\{w_i\}$ basis is solved to be

$$\delta = \begin{pmatrix} 0 & 0 & 0 & 0 & 0 & 0 \\ 0 & 0 & 0 & 0 & 0 & 0 \\ 0 & 0 & 0 & 0 & 0 & 0 \\ 0 & 0 & 0 & 0 & 0 & 0 \\ 0 & 0 & 0 & 0 & 0 & 0 \\ -\frac{135\zeta(3)}{2\pi^3} & 0 & 0 & 0 & 0 & 0 \end{pmatrix}. \tag{2.D.13}$$

It is easily seen that the δ operator only has the $\delta_{-3,-3}$ component, hence the ζ operator is simply $\zeta = 0$.

Computing $F_2 = e^{-\mathbf{i}\delta} F_\infty$ we have found the SL(2)-splitting (F_2, W^2) of (F_∞, W^2).

The filtration F_2 is represented by its period matrix

$$\Pi_2 = \left(\begin{array}{c|c|cc|cc|c} & w_3^{(2)} & w_{21}^{(2)} & w_{22}^{(2)} & w_{11}^{(2)} & w_{12}^{(2)} & w_0^{(2)} \\ \hline e_5 & 1 & 0 & 0 & 0 & 0 & 0 \\ e_4 & 0 & 1 & 0 & 0 & 0 & 0 \\ e_3 & 0 & 0 & 1 & 0 & 0 & 0 \\ e_2 & -\frac{17}{4} & \frac{9}{2} & \frac{1}{2} & 1 & 1 & 0 \\ e_1 & -\frac{3}{2} & \frac{3}{2} & 0 & \frac{1}{3} & 0 & 0 \\ e_0 & 0 & -\frac{23}{4} & -\frac{3}{2} & 0 & 0 & 1 \end{array}\right). \tag{2.D.14}$$

And it is clear that this mixed Hodge structure (F_2, W^2) is $\mathbb{R}$-split

2.D.2.3 The second round: finding the SL(2)-splitting of (F', W^1)

We now proceed to the second round of the computation. The starting point of this round is the mixed Hodge structure (F', W^1), where $W^1 = W(N_2)$ is the monodromy weight filtration associated to N_2, and $F' = e^{\mathbf{i}N_1}F_2$. One can check that the weight filtration is now given by

$$\begin{array}{ccccc} W_6^1 & = & W_5^1 & = & \mathrm{span}_{\mathbb{R}}\{e_5, e_4, e_3, e_2, e_1, e_0\} \\ & & \cup & & \\ W_4^1 & = & W_3^1 & = & \mathrm{span}_{\mathbb{R}}\{e_3, e_2, e_1, e_0\} \\ & & \cup & & \\ W_2^1 & = & W_1^1 & = & \mathrm{span}_{\mathbb{R}}\{e_2, e_0\} \\ & & \cup & & \\ & & W_0^1 & = & 0 \end{array} \tag{2.D.15}$$

and the period matrix Π' representing F' is

$$\Pi' = \left(\begin{array}{c|c|cc|cc|c} & w_3' & w_{21}' & w_{22}' & w_{11}' & w_{12}' & w_0' \\ \hline e_5 & 1 & 0 & 0 & 0 & 0 & 0 \\ e_4 & \mathbf{i} & 1 & 0 & 0 & 0 & 0 \\ e_3 & 0 & 0 & 1 & 0 & 0 & 0 \\ e_2 & -\frac{35}{4} + \frac{9\mathbf{i}}{2} & \frac{9}{2} + 9\mathbf{i} & \frac{1}{2} + 3\mathbf{i} & 1 & 1 & 0 \\ e_1 & -3 + \frac{3\mathbf{i}}{2} & \frac{3}{2} + 3\mathbf{i} & \mathbf{i} & \frac{1}{3} & 0 & 0 \\ e_0 & -\frac{29\mathbf{i}}{4} & -\frac{41}{4} & -3 & \mathbf{i} & \mathbf{i} & 1 \end{array}\right). \tag{2.D.16}$$

Denote the Deligne splitting of (F', W^1) by $V_{\mathbb{C}} = \bigoplus I'^{p,q}$. Using the formula (2.2.39) we find the Deligne splitting of (V, F', W^1) shown in figure 2.22.

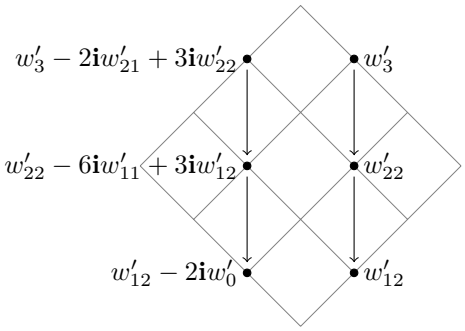

Figure 2.22: The Hodge diamond of the mixed Hodge structure (V, F', W^1), in which each dot near the (p,q)-site represents a base vector of the corresponding subspace $I'^{p,q}$. The arrows show the action of N_2. The diamond is clearly of type III_0.

We further remark that this splitting satisfies $I'^{p,q} = \overline{I'^{q,p}}$ for all p, q except

$$\begin{aligned} I'^{3,2} &= \overline{I'^{2,3}} \mod I'^{2,1} \oplus I'^{1,0} \oplus I'^{0,1}, \\ I'^{2,1} &= \overline{I'^{1,2}} \mod I'^{1,0}. \end{aligned}$$

The Deligne splitting in figure 2.22 yields the following grading operator T' and its complex conjugate $\overline{T}'$ expressed in the Hodge basis $(w'_3, \ldots, w'_0)$

$$T' = \begin{pmatrix} 5 & 0 & 0 & 0 & 0 & 0 \\ 0 & 5 & 0 & 0 & 0 & 0 \\ 0 & -3 & 3 & 0 & 0 & 0 \\ 0 & 0 & 0 & 3 & 0 & 0 \\ 0 & 0 & 0 & -1 & 1 & 0 \\ 0 & 0 & 0 & 0 & 0 & 1 \end{pmatrix}, \quad \overline{T}' = \begin{pmatrix} 5 & 0 & 0 & 0 & 0 & 0 \\ 0 & 5 & 0 & 0 & 0 & 0 \\ -6\mathbf{i} & -3 & 3 & 0 & 0 & 0 \\ 0 & -18\mathbf{i} & 0 & 3 & 0 & 0 \\ 18 & -18\mathbf{i} & -6\mathbf{i} & -1 & 1 & 0 \\ -24\mathbf{i} & -18 & 0 & -2\mathbf{i} & 0 & 1 \end{pmatrix}. \tag{2.D.17}$$

The operator δ' written in the Hodge basis $(w'_3, \ldots, w'_0)$ is solved to be

$$\delta' = \begin{pmatrix} 0 & 0 & 0 & 0 & 0 & 0 \\ 0 & 0 & 0 & 0 & 0 & 0 \\ \frac{3}{2} & 0 & 0 & 0 & 0 & 0 \\ 0 & \frac{9}{2} & 0 & 0 & 0 & 0 \\ \frac{9\mathbf{i}}{4} & \frac{9}{4} & \frac{3}{2} & 0 & 0 & 0 \\ 3 & -\frac{9\mathbf{i}}{4} & 0 & \frac{1}{2} & 0 & 0 \end{pmatrix}. \tag{2.D.18}$$

This matrix does not seem to be real because we are working in the complex basis

$\{w'_i\}$. If we transform it into the $(e_5, \ldots, e_0)$ basis using the period matrix Π' then all of its entries are real numbers. Hence δ' is indeed a real operator.

Let $\tilde{F}' = e^{-\mathbf{i}\delta'}F'$, and we have found the first $\mathbb{R}$-split mixed Hodge structure associated with (F', W^1). Let $(\tilde{w}'_3, \ldots, \tilde{w}'_0) = (w_3, \ldots, w_0)e^{-\mathbf{i}\delta'}$ and we have a new set of Hodge basis $\{\tilde{w}'_i\}$. The Deligne splitting of (F', W^1) is the same as in figure 2.22 with all w'_i replaced by $\tilde{w}'_i$. Then the decomposition of the operator δ' is found to be

$$\delta' = \delta'_{-1,-1} + \delta'_{-2,-2} + \delta'_{-3,-1} + \delta'_{-1,-3}, \tag{2.D.19}$$

where $\delta'_{-p,-q}$ maps $\tilde{I}'^{r,s}$ to $\tilde{I}'^{r-p,s-q}$. The components are given by, in the $\tilde{w}'_i$ basis,

$$\delta'_{-1,-1} = \begin{pmatrix} 0 & 0 & 0 & 0 & 0 & 0 \\ 0 & 0 & 0 & 0 & 0 & 0 \\ \frac{3}{2} & 0 & 0 & 0 & 0 & 0 \\ 0 & \frac{9}{2} & 0 & 0 & 0 & 0 \\ 0 & 0 & \frac{3}{2} & 0 & 0 & 0 \\ 0 & 0 & 0 & \frac{1}{2} & 0 & 0 \end{pmatrix}, \qquad \delta'_{-2,-2} = \begin{pmatrix} 0 & 0 & 0 & 0 & 0 & 0 \\ 0 & 0 & 0 & 0 & 0 & 0 \\ 0 & 0 & 0 & 0 & 0 & 0 \\ 0 & 0 & 0 & 0 & 0 & 0 \\ \frac{3\mathbf{i}}{4} & \frac{3}{4} & 0 & 0 & 0 & 0 \\ 0 & -\frac{3\mathbf{i}}{4} & 0 & 0 & 0 & 0 \end{pmatrix}, \tag{2.D.20}$$

$$\delta'_{-3,-1} = \begin{pmatrix} 0 & 0 & 0 & 0 & 0 & 0 \\ 0 & 0 & 0 & 0 & 0 & 0 \\ 0 & 0 & 0 & 0 & 0 & 0 \\ 0 & 0 & 0 & 0 & 0 & 0 \\ \frac{3\mathbf{i}}{2} & \frac{3}{4} & 0 & 0 & 0 & 0 \\ 3 & -\frac{3\mathbf{i}}{2} & 0 & 0 & 0 & 0 \end{pmatrix}, \qquad \delta'_{-1,-3} = \begin{pmatrix} 0 & 0 & 0 & 0 & 0 & 0 \\ 0 & 0 & 0 & 0 & 0 & 0 \\ 0 & 0 & 0 & 0 & 0 & 0 \\ 0 & 0 & 0 & 0 & 0 & 0 \\ 0 & \frac{3}{4} & 0 & 0 & 0 & 0 \\ 0 & 0 & 0 & 0 & 0 & 0 \end{pmatrix}. \tag{2.D.21}$$

Furthermore, all components are commuting with each other $[\delta'_{-p,-q}, \delta'_{-r,-s}] = 0$.

The operator ζ' given in terms of its decomposition $\zeta' = \sum \zeta'_{-p,-q}$ only has two non-vanishing components $\zeta'_{-1,-3}$ and $\zeta'_{-3,-1}$, hence, written in the $(\tilde{w}'_3, \ldots, \tilde{w}'_0)$ basis

$$\zeta' = \frac{3\mathbf{i}}{4}(\delta'_{-3,-1} - \delta'_{-1,-3}) = \begin{pmatrix} 0 & 0 & 0 & 0 & 0 & 0 \\ 0 & 0 & 0 & 0 & 0 & 0 \\ 0 & 0 & 0 & 0 & 0 & 0 \\ 0 & 0 & 0 & 0 & 0 & 0 \\ -\frac{9}{8} & 0 & 0 & 0 & 0 & 0 \\ \frac{9\mathbf{i}}{4} & \frac{9}{8} & 0 & 0 & 0 & 0 \end{pmatrix}. \tag{2.D.22}$$

Finally, applying the operator $e^{\zeta'}$ to $\tilde{F}'$, we arrive at the SL(2)-splitting (F_1, W^1) associated to (F', W^1). The period matrix Π_1 representing the Hodge filtration

$F_1 = e^{\zeta'} e^{-\mathbf{i}\delta'} F'$ is

$$\Pi_1 = \left(\begin{array}{c|c|cc|cc|c} & w_3^{(1)} & w_{21}^{(1)} & w_{22}^{(1)} & w_{11}^{(1)} & w_{12}^{(1)} & w_0^{(1)} \\ \hline e_5 & 1 & 0 & 0 & 0 & 0 & 0 \\ e_4 & \mathbf{i} & 1 & 0 & 0 & 0 & 0 \\ e_3 & -\frac{3\mathbf{i}}{2} & 0 & 1 & 0 & 0 & 0 \\ e_2 & -\frac{17}{4} + \frac{15\mathbf{i}}{4} & \frac{9}{2} + \frac{9\mathbf{i}}{4} & \frac{1}{2} + \frac{3\mathbf{i}}{2} & 1 & 1 & 0 \\ e_1 & -\frac{3}{2} + \frac{3\mathbf{i}}{2} & \frac{3}{2} + \frac{3\mathbf{i}}{2} & \mathbf{i} & \frac{1}{3} & 0 & 0 \\ e_0 & -\frac{7\mathbf{i}}{2} & -\frac{23}{4} & -\frac{3}{2} & \frac{\mathbf{i}}{2} & \mathbf{i} & 1 \end{array}\right) \tag{2.D.23}$$

2.D.2.4 Final output: the commuting $\mathfrak{sl}(2)$-pair

With the two SL(2)-splittings (F_i, W^i) we can now compute the commuting $\mathfrak{sl}(2)$-pair. First we read out the semisimple grading $Y_{(i)}$ which acts on $I^{p,q}_{(F_i,W^i)}$ as multiplication by $p+q-3$. Writing now everything in the real basis $(e_5, \ldots, e_0)$ for convenience, we have

$$\begin{aligned} Y_{(1)} &= \begin{pmatrix} 2 & 0 & 0 & 0 & 0 & 0 \\ 0 & 2 & 0 & 0 & 0 & 0 \\ 0 & -3 & 0 & 0 & 0 & 0 \\ -\frac{25}{2} & 12 & 1 & -2 & 3 & 0 \\ -3 & 3 & 0 & 0 & 0 & 0 \\ 0 & -\frac{37}{2} & -3 & 0 & 0 & -2 \end{pmatrix}, \\ Y_{(2)} &= \begin{pmatrix} 3 & 0 & 0 & 0 & 0 & 0 \\ 0 & 1 & 0 & 0 & 0 & 0 \\ 0 & 0 & 1 & 0 & 0 & 0 \\ -17 & 9 & 1 & -1 & 0 & 0 \\ -6 & 3 & 0 & 0 & -1 & 0 \\ 6 & -23 & -6 & 0 & 0 & -3 \end{pmatrix}, \end{aligned} \tag{2.D.24}$$

so the neutral elements in the $\mathfrak{sl}(2)$-pair are

$$Y_1 = Y_{(1)}, \quad Y_2 = Y_{(2)} - Y_{(1)} = \begin{pmatrix} 1 & 0 & 0 & 0 & 0 & 0 \\ 0 & -1 & 0 & 0 & 0 & 0 \\ 0 & 3 & 1 & 0 & 0 & 0 \\ -\frac{9}{2} & -3 & 0 & 1 & -3 & 0 \\ -3 & 0 & 0 & 0 & -1 & 0 \\ 0 & -\frac{9}{2} & -3 & 0 & 0 & -1 \end{pmatrix}. \tag{2.D.25}$$

In addition, $N_1^- = N_2$ is already one of the nilnegative elements. We kindly remind the reader that the particular ordering (N_2, N_1) of the monodromies is adopted so as to study the degeneration $\mathrm{III}_0 \to \mathrm{IV}_2$.

To find the other nilnegative element N_2^-, we compute the decomposition of N_1 into the eigenvectors of the adjoint representation $[Y_{(1)}, -]$. Denote the decomposition $N_1 = \sum N_1^\alpha$, where $[Y_{(1)}, N_1^\alpha] = \alpha N_1^\alpha$ is the component corresponding to the eigenvalue α. Bearing in mind that any component N_1^α must also preserve the polarisation $(N_1^\alpha)^{\mathrm{T}}\eta + \eta N_1^\alpha = 0$, we find that

$$N_1 = N_1^{-4} + N_1^{-2} + N_1^0, \tag{2.D.26}$$

where

$$N_1^{-4} = \begin{pmatrix} 0 & 0 & 0 & 0 & 0 & 0 \\ 0 & 0 & 0 & 0 & 0 & 0 \\ 0 & 0 & 0 & 0 & 0 & 0 \\ 0 & -\frac{9}{4} & 0 & 0 & 0 & 0 \\ 0 & 0 & 0 & 0 & 0 & 0 \\ 0 & 0 & 0 & 0 & 0 & 0 \end{pmatrix}, \qquad N_1^{-2} = \begin{pmatrix} 0 & 0 & 0 & 0 & 0 & 0 \\ 0 & 0 & 0 & 0 & 0 & 0 \\ -\frac{3}{2} & 0 & 0 & 0 & 0 & 0 \\ -\frac{3}{4} & -\frac{9}{2} & -\frac{3}{2} & 0 & 0 & 0 \\ 0 & -\frac{3}{2} & 0 & 0 & 0 & 0 \\ 0 & \frac{9}{4} & 0 & 0 & -\frac{3}{2} & 0 \end{pmatrix}, \tag{2.D.27}$$

and the N_1^0 is what we need for the nilnegatives

$$N_1^- = N_2, \quad N_2^- = N_1^0 = \begin{pmatrix} 0 & 0 & 0 & 0 & 0 & 0 \\ -1 & 0 & 0 & 0 & 0 & 0 \\ \frac{3}{2} & 0 & 0 & 0 & 0 & 0 \\ -\frac{15}{4} & -\frac{9}{4} & -\frac{3}{2} & 0 & 0 & 0 \\ -\frac{3}{2} & -\frac{3}{2} & -1 & 0 & 0 & 0 \\ \frac{3}{2} & \frac{9}{4} & \frac{1}{2} & -1 & \frac{3}{2} & 0 \end{pmatrix}. \tag{2.D.28}$$

The last step is to find the nilpositive element N_i^+. Solving the equations

$$[Y_i, N_i^+] = 2N_i^+, \quad [N_i^+, N_i^-] = Y_i, \quad (N_i^+)^{\mathrm{T}}\eta + \eta N_i^+ = 0,$$

simply yields the following unique pair of matrices

$$N_1^+ = \begin{pmatrix} 0 & -3 & -2 & 0 & 0 & 0 \\ -3 & 3 & 0 & 0 & -2 & 0 \\ \frac{1}{2} & 0 & 1 & -2 & 6 & 0 \\ -\frac{53}{4} & 9 & \frac{9}{2} & -1 & -6 & -3 \\ -\frac{9}{2} & -\frac{5}{2} & 0 & 0 & -3 & -2 \\ \frac{33}{2} & -\frac{69}{4} & -\frac{3}{2} & 3 & \frac{5}{2} & 0 \end{pmatrix},$$
$$N_2^+ = \begin{pmatrix} 0 & -1 & 0 & 0 & 0 & 0 \\ 0 & 0 & 0 & 0 & 0 & 0 \\ -\frac{3}{2} & \frac{3}{2} & 0 & 0 & -1 & 0 \\ -\frac{3}{4} & -\frac{3}{4} & -\frac{3}{2} & 0 & -\frac{1}{2} & -1 \\ 0 & \frac{3}{2} & 0 & 0 & 0 & 0 \\ \frac{9}{4} & -\frac{9}{4} & 0 & 0 & \frac{3}{2} & 0 \end{pmatrix}. \tag{2.D.29}$$

One can finally check that the (N_i^-, N_i^+, Y_i) with matrices in the $(e_5, \ldots, e_0)$ basis given by (2.D.28), (2.D.29), (2.D.25) are indeed two sets of $\mathfrak{sl}(2)$-Lie algebra elements and the two sets of operators commute with each other. This completes our computation of the commuting $\mathfrak{sl}(2)$-pair arising from the $\mathrm{III}_0 \to \mathrm{IV}_2$ degeneration in the complex structure moduli space of the Calabi-Yau threefold Y_3.

2.D.3 The commuting $\mathfrak{sl}(2)$-pair associated to $\mathrm{IV}_1 \to \mathrm{IV}_2$

The other singularity locus Δ_1 in the moduli space of Y_3 has the type IV_1. In this subsection we also work out the commuting $\mathfrak{sl}(2)$-pair as we move along Δ_1 towards the large complex structure point of type IV_2. This amounts to switch the ordering of the monodromy cone to (N_1, N_2). The computation is essentially the same as the $\mathrm{III}_0 \to \mathrm{IV}_2$ degeneration, so we only list the results here without explanation.

2.D.3.1 The two SL(2)-splittings

The starting point (F_∞, W^2) is the same as the starting point of $\mathrm{III}_0 \to \mathrm{IV}_2$, hence also its SL(2)-splitting is the same (F_2, W^2) with the period matrix (2.D.14). Now, we consider the limiting mixed Hodge structure (F', W^1) where $F' = e^{\mathbf{i}N_2} F_2$ and

$W^1 = W(N_1)$. The period matrix of F' is now given by

$$\Pi' = \left(\begin{array}{c|c|cc|cc|c} & w'_3 & w'_{21} & w'_{22} & w'_{11} & w'_{12} & w'_0 \\ \hline e_5 & 1 & 0 & 0 & 0 & 0 & 0 \\ e_4 & 0 & 1 & 0 & 0 & 0 & 0 \\ e_3 & \mathbf{i} & 0 & 1 & 0 & 0 & 0 \\ e_2 & -\frac{19}{4}+\frac{\mathbf{i}}{2} & \frac{9}{2}+3\mathbf{i} & \frac{1}{2}+\mathbf{i} & 1 & 1 & 0 \\ e_1 & -\frac{3}{2} & \frac{3}{2}+\mathbf{i} & 0 & \frac{1}{3} & 0 & 0 \\ e_0 & -\frac{3\mathbf{i}}{2} & -\frac{25}{4} & -\frac{3}{2} & \frac{\mathbf{i}}{3} & 0 & 1 \end{array}\right), \tag{2.D.30}$$

and the monodromy weight filtration W^1 has now the form

$$\begin{array}{ccccc} & & W^1_6 & = & \mathrm{span}_{\mathbb{R}}\{e_5, e_4, e_3, e_2, e_1, e_0\} \\ & & \cup & & \\ W^1_5 & = & W^1_4 & = & \mathrm{span}_{\mathbb{R}}\{e_4, e_3, e_2, e_1, e_0\} \\ & & \cup & & \\ & & W^1_3 & = & \mathrm{span}_{\mathbb{R}}\{-e_4+3e_3, e_2, e_1, e_0\} \\ & & \cup & & \\ & & W^1_2 & = & \mathrm{span}_{\mathbb{R}}\{3e_2+e_1, e_0\} \\ & & \cup & & \\ W^1_1 & = & W^1_0 & = & \mathrm{span}_{\mathbb{R}}\{e_0\} \end{array} \tag{2.D.31}$$

So the Deligne splitting $V_{\mathbb{C}} = \bigoplus I'^{p,q}$ is found to be in the figure 2.23.

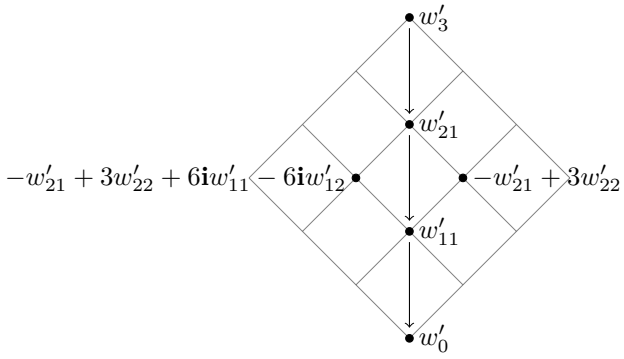

Figure 2.23: The Hodge diamond of the mixed Hodge structure (V, F', W^1), in which each dot near the (p,q)-site represents a base vector of the corresponding subspace $I'^{p,q}$. The arrows show the action of N_1. The diamond is clearly of type IV_1.

This structure is again far from $\mathbb{R}$-split, and we can check that $I^{p,q} = \overline{I^{q,p}}$ for all p, q except

$$\begin{aligned} I'^{3,3} &= \overline{I'^{3,3}} \mod I'^{2,2} \oplus I'^{1,2} \oplus I'^{2,1} \oplus I'^{1,1}, \\ I'^{2,2} &= \overline{I'^{2,2}} \mod I'^{1,1} \oplus I'^{0,0}, \\ I'^{2,1} &= \overline{I'^{1,2}} \mod I'^{0,0}, \\ I'^{1,1} &= \overline{I'^{1,1}} \mod I'^{0,0}. \end{aligned} \tag{2.D.32}$$

Reading out the grading and solving for δ', we find, in the $(w'_3, \ldots, w'_0)$ basis

$$\delta' = \begin{pmatrix} 0 & 0 & 0 & 0 & 0 & 0 \\ 0 & 0 & 0 & 0 & 0 & 0 \\ 1 & 0 & 0 & 0 & 0 & 0 \\ \mathbf{i} & 3 & 1 & 0 & 0 & 0 \\ -\mathbf{i} & 0 & 0 & 0 & 0 & 0 \\ \frac{2}{9} & 0 & -\frac{\mathbf{i}}{3} & \frac{1}{3} & 0 & 0 \end{pmatrix}, \tag{2.D.33}$$

which consists of real elements once we transform back to the $\{e_i\}$ basis.

The operator δ' now admits the following Deligne splitting

$$\delta' = \delta'_{-3,-3} + \delta'_{-2,-1} + \delta'_{-1,-1} + \delta'_{-1,-2}, \tag{2.D.34}$$

where various components are given by

$$\delta'_{-3,-3} = \begin{pmatrix} 0 & 0 & 0 & 0 & 0 & 0 \\ 0 & 0 & 0 & 0 & 0 & 0 \\ 0 & 0 & 0 & 0 & 0 & 0 \\ 0 & 0 & 0 & 0 & 0 & 0 \\ 0 & 0 & 0 & 0 & 0 & 0 \\ \frac{2}{9} & 0 & 0 & 0 & 0 & 0 \end{pmatrix}, \qquad \delta'_{-2,-1} = \begin{pmatrix} 0 & 0 & 0 & 0 & 0 & 0 \\ -\frac{1}{6} & 0 & 0 & 0 & 0 & 0 \\ \frac{1}{2} & 0 & 0 & 0 & 0 & 0 \\ \mathbf{i} & 0 & 0 & 0 & 0 & 0 \\ -\mathbf{i} & 0 & 0 & 0 & 0 & 0 \\ 0 & 0 & -\frac{\mathbf{i}}{3} & 0 & -\frac{1}{6} & 0 \end{pmatrix},$$

$$\delta'_{-1,-1} = \begin{pmatrix} 0 & 0 & 0 & 0 & 0 & 0 \\ \frac{1}{3} & 0 & 0 & 0 & 0 & 0 \\ 0 & 0 & 0 & 0 & 0 & 0 \\ 0 & 3 & 1 & 0 & 0 & 0 \\ 0 & 0 & 0 & 0 & 0 & 0 \\ 0 & 0 & 0 & \frac{1}{3} & \frac{1}{3} & 0 \end{pmatrix}, \qquad \delta'_{-1,-2} = \begin{pmatrix} 0 & 0 & 0 & 0 & 0 & 0 \\ -\frac{1}{6} & 0 & 0 & 0 & 0 & 0 \\ \frac{1}{2} & 0 & 0 & 0 & 0 & 0 \\ 0 & 0 & 0 & 0 & 0 & 0 \\ 0 & 0 & 0 & 0 & 0 & 0 \\ 0 & 0 & 0 & 0 & -\frac{1}{6} & 0 \end{pmatrix}, \tag{2.D.35}$$

with the only non-vanishing commutator

$$[\delta'_{-2,-1}, \delta'_{-1,-2}] = -\frac{3\mathbf{i}}{2}\delta'_{-3,-3}. \tag{2.D.36}$$

Then the only non-vanishing components of ζ' are $\zeta'_{-1,-2}$ and $\zeta'_{-2,-1}$, hence they sum to the ζ' operator

$$\zeta' = \frac{\mathbf{i}}{2}(\delta'_{-2,-1} - \delta'_{-1,-2}) = \begin{pmatrix} 0 & 0 & 0 & 0 & 0 & 0 \\ 0 & 0 & 0 & 0 & 0 & 0 \\ 0 & 0 & 0 & 0 & 0 & 0 \\ -\frac{1}{2} & 0 & 0 & 0 & 0 & 0 \\ \frac{1}{2} & 0 & 0 & 0 & 0 & 0 \\ 0 & 0 & \frac{1}{6} & 0 & 0 & 0 \end{pmatrix}, \tag{2.D.37}$$

where the matrix is written in the $\{w'\}$ basis.

The Hodge filtration $F_1 = e^{\zeta'} e^{-\mathbf{i}\delta'} F_2$ is given by its period matrix Π_1

$$\Pi_1 = \left(\begin{array}{c|c|cc|cc|c} & w_3^{(1)} & w_{21}^{(1)} & w_{22}^{(1)} & w_{11}^{(1)} & w_{12}^{(1)} & w_0^{(1)} \\ \hline e'_5 & 1 & 0 & 0 & 0 & 0 & 0 \\ e'_4 & 0 & 1 & 0 & 0 & 0 & 0 \\ e'_3 & 0 & 0 & 1 & 0 & 0 & 0 \\ e'_2 & -\frac{17}{4} & \frac{9}{2} & \frac{1}{2} & 1 & 1 & 0 \\ e'_1 & -\frac{3}{2} & \frac{3}{2} & -\frac{\mathbf{i}}{3} & \frac{1}{3} & 0 & 0 \\ e'_0 & 0 & -\frac{23}{4} & -\frac{3}{2} & 0 & 0 & 1 \end{array}\right), \tag{2.D.38}$$

thus we have arrived at the SL(2)-splitting (F_1, W^1) of (F', W^1).

2.D.3.2 The commuting $\mathfrak{sl}(2)$-pair

For convenience we express everything in the $(e_5, \ldots, e_0)$ basis in this subsection. We read out the grading elements

$$Y_{(1)} = \begin{pmatrix} 3 & 0 & 0 & 0 & 0 & 0 \\ 0 & 1 & \frac{1}{3} & 0 & 0 & 0 \\ 0 & 0 & 0 & 0 & 0 & 0 \\ -17 & 9 & 2 & -1 & 0 & 0 \\ -\frac{71}{12} & 3 & \frac{2}{3} & -\frac{1}{3} & 0 & 0 \\ 0 & -23 & -\frac{77}{12} & 0 & 0 & -3 \end{pmatrix},$$

$$Y_{(2)} = \begin{pmatrix} 3 & 0 & 0 & 0 & 0 & 0 \\ 0 & 1 & 0 & 0 & 0 & 0 \\ 0 & 0 & 1 & 0 & 0 & 0 \\ -17 & 9 & 1 & -1 & 0 & 0 \\ -6 & 3 & 0 & 0 & -1 & 0 \\ 0 & -23 & -6 & 0 & 0 & -3 \end{pmatrix}, \tag{2.D.39}$$

so that the neutral elements are given by

$$Y_1 = Y_{(1)}, \quad Y_2 = Y_{(2)} - Y_{(1)} = \begin{pmatrix} 0 & 0 & 0 & 0 & 0 & 0 \\ 0 & 0 & -\frac{1}{3} & 0 & 0 & 0 \\ 0 & 0 & 1 & 0 & 0 & 0 \\ 0 & 0 & -1 & 0 & 0 & 0 \\ -\frac{1}{12} & 0 & -\frac{2}{3} & \frac{1}{3} & -1 & 0 \\ 0 & 0 & \frac{5}{12} & 0 & 0 & 0 \end{pmatrix}. \tag{2.D.40}$$

Decompose $N_2 = \sum N_2^\alpha$ into the eigen-components of the action $[Y_{(1)}, -]$ and we have

$$N_2 = N_2^{-3} + N_2^{-2} + N_2^0, \tag{2.D.41}$$

where

$$N_2^{-3} = \begin{pmatrix} 0 & 0 & 0 & 0 & 0 & 0 \\ \frac{1}{3} & 0 & 0 & 0 & 0 & 0 \\ -1 & 0 & 0 & 0 & 0 & 0 \\ 1 & 0 & 0 & 0 & 0 & 0 \\ \frac{1}{2} & 0 & 0 & 0 & 0 & 0 \\ -\frac{1}{2} & 0 & -\frac{1}{6} & \frac{1}{3} & -1 & 0 \end{pmatrix}, \; N_2^{-2} = \begin{pmatrix} 0 & 0 & 0 & 0 & 0 & 0 \\ -\frac{1}{3} & 0 & 0 & 0 & 0 & 0 \\ 0 & 0 & 0 & 0 & 0 & 0 \\ -\frac{3}{2} & -3 & -1 & 0 & 0 & 0 \\ -\frac{1}{2} & -1 & -\frac{1}{3} & 0 & 0 & 0 \\ \frac{1}{2} & \frac{3}{2} & \frac{1}{6} & -\frac{1}{3} & 0 & 0 \end{pmatrix}, \tag{2.D.42}$$

and the remaining N_2^0 together with N_1 constitute the nilnegative elements

$$N_1^- = N_1, \quad N_2^- = N_2^0 = \begin{pmatrix} 0 & 0 & 0 & 0 & 0 & 0 \\ 0 & 0 & 0 & 0 & 0 & 0 \\ 0 & 0 & 0 & 0 & 0 & 0 \\ 0 & 0 & 0 & 0 & 0 & 0 \\ 0 & 0 & \frac{1}{3} & 0 & 0 & 0 \\ 0 & 0 & 0 & 0 & 0 & 0 \end{pmatrix}. \tag{2.D.43}$$

Finally we can complete the (N_i^-, Y_i) into the complete $\mathfrak{sl}(2)$-triples (N_i^-, N_i^+, Y_i)

with nilpositive elements

$$N_1^+ = \begin{pmatrix} 0 & -3 & -1 & 0 & 0 & 0 \\ -\frac{17}{9} & 2 & \frac{2}{9} & -\frac{4}{9} & 0 & 0 \\ 0 & 0 & 0 & 0 & 0 & 0 \\ -\frac{17}{2} & \frac{9}{2} & \frac{3}{4} & -2 & 0 & -3 \\ -\frac{17}{6} & \frac{7}{4} & \frac{1}{3} & -\frac{2}{3} & 0 & -1 \\ \frac{391}{36} & -\frac{23}{2} & -\frac{23}{18} & \frac{23}{9} & 0 & 0 \end{pmatrix},$$
$$N_2^+ = \begin{pmatrix} 0 & 0 & 0 & 0 & 0 & 0 \\ -\frac{1}{12} & 0 & -\frac{1}{6} & \frac{1}{3} & -1 & 0 \\ \frac{1}{4} & 0 & \frac{1}{2} & -1 & 3 & 0 \\ -\frac{1}{4} & 0 & -\frac{1}{2} & 1 & -3 & 0 \\ -\frac{1}{8} & 0 & -\frac{1}{4} & \frac{1}{2} & -\frac{3}{2} & 0 \\ \frac{5}{48} & 0 & \frac{5}{24} & -\frac{5}{12} & \frac{5}{4} & 0 \end{pmatrix}. \tag{2.D.44}$$

This completes our computation of the commuting $\mathfrak{sl}(2)$-pair for the degeneration from IV_1 to IV_2.

2.E Deriving the polarised relations

In this section we summarise the definition of polarised relation proposed in [113] and exemplify the derivation of the relation $\mathrm{III}_c \to \mathrm{IV}_{\hat{d}}$ in table 2.3.

For the ease of notation, we follow [113] to consider an entire Hodge-Deligne diamond at once. Given a Hodge-Deligne diamond consisting of Hodge-Deligne numbers $\{i^{p,q}\}$, we can define an integer-valued function $\lozenge(p,q) := i^{p,q}$ on the lattice $\mathbb{Z}\times\mathbb{Z}$. On the other hand, we define a Hodge-Deligne diamond of a variation of weight-w Hodge structure polarised by N with Hodge numbers $(h^{w,0}, h^{w-1,1}, \ldots, h^{0,w})$ to be any integer-valued function $\lozenge(p,q)$ on the lattice $\mathbb{Z}\times\mathbb{Z}$ such that

$$\sum_{q=0}^{w} \lozenge(p,q) = h^{p,w-p}, \text{ for all } p, \tag{2.E.1}$$

and satisfying the usual symmetry properties

$$\lozenge(p,q) = \lozenge(q,p) = \lozenge(w-q, w-p), \text{ for all } p,q, \tag{2.E.2}$$
$$\lozenge(p-1,q-1) \leq \lozenge(p,q), \text{ for } p+q \leq w. \tag{2.E.3}$$

In this fashion the sum $\lozenge = \lozenge_1 + \lozenge_2$ of two Hodge-Deligne diamonds $\lozenge_1$ and $\lozenge_2$ is naturally defined pointwise

$$\lozenge(p,q) := \lozenge_1(p,q) + \lozenge_2(p,q). \tag{2.E.4}$$

And also the shifted Hodge-Deligne diamond $\lozenge[a]$ of $\lozenge$ is defined to be

$$\lozenge[a](p,q) = \lozenge(p+a, q+q). \tag{2.E.5}$$

Now it comes to the enhancement relation [113]. Let (F_1, N_1) and (F_2, N_2) be two nilpotent orbits with limiting mixed Hodge structures $(F_1, W(N_1))$ and $(F_2, W(N_2))$. Denote $\lozenge(F_1, N_1)$ and $\lozenge(F_2, N_2)$ respectively their Hodge-Deligne diamonds. Considering a possible degeneration relation $(F_1, N_1) \to (F_2, N_2)$ there is the following equivalent condition:

Every primitive subspace $P^k(N_1)$ $(3 \leq k \leq 6)$ of $(F_1, W(N_1))$ carries a weight-k Hodge structure $P^k(N_1) = \bigoplus_{p+q=k} P^{p,q}(N_1)$. Denote its Hodge numbers by $j_1^{p,q} := \dim_{\mathbb{C}} P^{p,q}(N_1)$. Let $\lozenge(F_k', N_k')$ be a Hodge-Deligne diamond of the variation of weight-k Hodge structure polarised by $S(\cdot, N_1^k \cdot)$ on $P^k(N_1)$ with Hodge numbers $(j^{k,0}, j^{k-1,1}, \ldots, j^{0,k})$ where S is the polarisation bilinear form (2.2.4). If one can decompose $\lozenge(F_2, N_2)$ as

$$\lozenge(F_2, N_2) = \sum_{\substack{3 \leq k \leq 6 \\ 0 \leq a \leq k-3}} \lozenge(F_k', N_k')[a], \tag{2.E.6}$$

where $\lozenge(F_k', N_k')[a]$ is the shifted Hodge-Deligne diamond defined above, then the degeneration relation

$$(F_1, N_1) \to (F_2, N_2) \tag{2.E.7}$$

holds. The converse is also true.

We refer the reader to [113] for details.

We exemplify the above condition on the relation $\mathrm{III}_c \to \mathrm{IV}_{\hat{d}}$. Firstly we list the primitive Hodge-Deligne sub-diamond of III_c containing only primitive Hodge-Deligne numbers $j_1^{p,q}$ and the Hodge-Deligne diamond of $\mathrm{IV}_{\hat{d}}$:

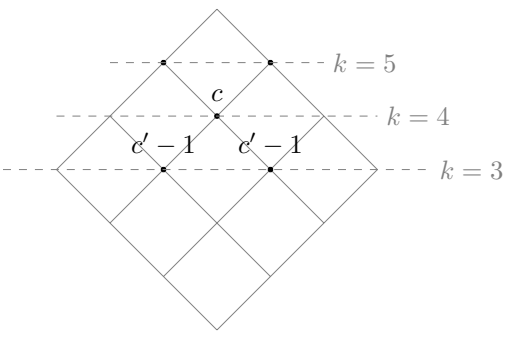

$\mathrm{III}_c^{\mathrm{prim}}$

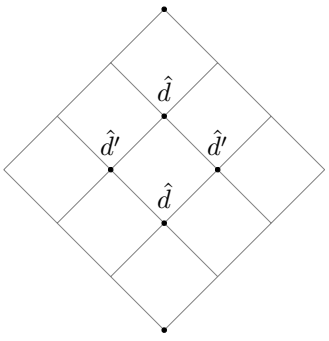

$\mathrm{IV}_{\hat{d}}$

For the relation $\mathrm{III}_c \to \mathrm{IV}_{\hat{d}}$ to hold, we need to find three Hodge-Deligne diamonds with Hodge numbers $(0, c'-1, c'-1, 0)$, $(0, 0, c, 0, 0)$ and $(0, 0, 1, 1, 0, 0)$ that sums (with proper shifts) to $\mathrm{IV}_{\hat{d}}$. The following are three such Hodge-Deligne diamonds

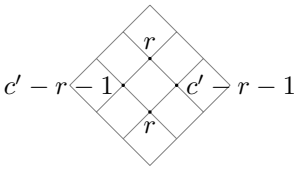

$\Diamond(F_3', N_3')$ with $r \geq 0$ for $(0, c'-1, c'-1, 0)$.

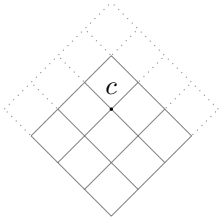

$\Diamond(F_4', N_4')$ for $(0, 0, c, 0, 0)$.

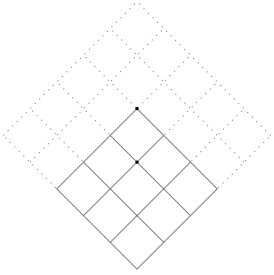

$\Diamond(F_5', N_5')$ for $(0, 0, 1, 1, 0, 0)$.

Then we consider the sum

$$\Diamond(F_3', N_3') + \Diamond(F_4', N_4') + \Diamond(F_4', N_4')[1] + \Diamond(F_5', N_5') + \Diamond(F_5', N_5')[1] + \Diamond(F_5', N_5')[2] \tag{2.E.8}$$

which can be depicted as

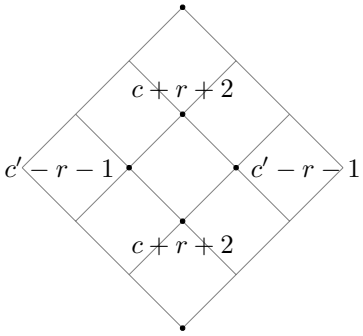

and we expect that this diamond agrees with the Hodge-Deligne diamond of $\mathrm{IV}_{\hat{d}}$. This is possible if the condition

$$\hat{d} = c + r + 2, \tag{2.E.9}$$

together with the usual $r \geq 0$, $0 \leq c \leq h^{2,1} - 2$ and $1 \leq \hat{d} \leq h^{2,1}$ are satisfied. Hence we have derived the condition $c + 2 \leq \hat{d}$ for the relation $\mathrm{III}_c \to \mathrm{IV}_{\hat{d}}$ in table 2.3.

3 Asymptotic Flux Compactifications and the Swampland

This chapter is based on: T. W. Grimm, C. Li and I. Valenzuela, *Asymptotic Flux Compactifications and the Swampland*, JHEP **06** (2020), 009, [erratum: JHEP **01** (2021), 007], [arXiv:1910.09549].

In this chapter, we initiate the systematic study of flux scalar potentials and their vacua by using asymptotic Hodge theory. To begin with, we consider F-theory compactifications on Calabi-Yau fourfolds with four-form flux. We argue that a classification of all scalar potentials can be performed when focusing on regions in the field space in which one or several fields are large and close to a boundary. To exemplify the constraints on such asymptotic flux compactifications, we explicitly determine this classification for situations in which two complex structure moduli are taken to be large. Our classification captures, for example, the weak string coupling limit and the large complex structure limit. We then show that none of these scalar potentials admits de Sitter critical points at parametric control, formulating a new no-go theorem valid beyond weak string coupling. We also check that the recently proposed asymptotic de Sitter conjecture is satisfied near any infinite distance boundary. Extending this strategy further, we generally identify the type of fluxes that induce an infinite series of Anti-de Sitter critical points, thereby generalizing the well-known Type IIA settings. Finally, we argue that also the large field dynamics of any axion in complex structure moduli space is universally constrained. Displacing such an axion by large field values will generally lead to severe backreaction effects destabilizing other directions.

3.1 Introduction

The asymptotic de Sitter conjecture [63] (see [62, 134] for previous formulations) reviewed in Section 1.3.2 claims a universal bound on the potential that forbids de Sitter vacua when approaching any infinite distance limit in field space and hence implies that there is a sort of Dine-Seiberg problem [135] for any scalar field

near any infinite distance limit. The universality claim is motivated in [63] by a connection to another conjecture, the so-called Swampland Distance Conjecture [4, 57], which asserts the universal existence of an infinite tower of massless states at any infinite field distance limit. Crucial to this present chapter will be the fact that in the search of evidence for the Swampland Distance Conjecture the works [5,81,136] uncovered a universal structure in any large field limit in geometric moduli spaces. It turns out that this structure also constraints the form of the flux-induced scalar potentials and provides us a tool to systematically classify such potentials at any large field limit and promote the above conjectures into precise statements linked to this universal structure. We will not only provide significant evidence for the asymptotic de Sitter conjecture [63], but also bring a new angle to the origin of the set of seemingly infinite number of Anti-de Sitter vacua of [137] and get general constraints on axion scalar potentials relevant for backreaction issues in axion monodromy [138–140] that are related to the refined Distance Conjecture [57, 58].

To answer systematically questions about the scalar potentials arising in string theory, we initiate the general study of flux compactifications in any region of field space that involves a large field limit. We call such settings *asymptotic flux compactifications* in the following. These compactifications will share the common feature that they capture limits that occur when approaching the boundary of the field space which, however, is not constrained to be of infinite distance in the field space metric. Asymptotic flux compactifications often describe an effective theory in which, at least in a dual description, a small coupling constant ensures that the leading perturbative expansion suffices to study the properties of the system. Two famous examples are Type IIB orientifold flux compactifications carried out at small string coupling, and Type IIA flux compactifications studied in the large volume regime [7, 8, 41]. We argue in this chapter that also the flux scalar potential in more general asymptotic limits can be systematically studied by using F-theory compactified on a Calabi-Yau fourfold with G_4-form flux. The complex structure moduli space of such fourfolds has a very rich structure, which allows us, among others, to recover flux potentials encountered at weak string coupling or large volume. Clearly, interpreting the various limits might require to move to a dual frame, as we will show by relating the flux scalar potentials in F-theory, Type IIB orientifolds and Type IIA orientifolds via mirror symmetry. Although, in general, such a dual description does not necessarily correspond to a perturbative string theory. It turns out that considering all possible asymptotic flux compactifications of F-theory goes beyond these well-known settings and yields a

set of new characteristic scalar potentials. These insights then allow us to generalize the no-go theorems for flux-induced de Sitter vacua to more general asymptotic regimes beyond string weak coupling. Let us remark that our results also go beyond the Maldacena-Nuñez no-go theorem [141] as the F-theory potential also includes the contribution from higher derivative terms and more exotic seven-branes, such as the ones combining into orientifold planes.

The mathematical machinery that we will employ is part of asymptotic Hodge theory, which in particular implies that there exists a so-called limiting mixed Hodge structure at any asymptotic limit to the boundary of the moduli space. These mixed Hodge structures encode crucial information about the behavior of the (p,q)-decomposition of forms on the compactification manifold in the asymptotic limits in complex structure moduli space. In particular, asymptotic Hodge theory provides an asymptotic expression of the Hodge norm [76] that we will use heavily in this chapter. It also allow us to discuss the conditions on self-dual fluxes in the asymptotic regime. Furthermore, it is crucial that all allowed limiting mixed Hodge structures can be classified by using the underlying $\mathfrak{sl}(2)$-representation theory [113], as has been done for Calabi-Yau threefolds in [136]. Our analysis aims to give the first steps towards a classification of asymptotic regimes in Calabi-Yau fourfolds and subsequently all asymptotic flux-induced scalar potentials induced by G_4-flux. Let us note that this machinery has been proven useful to test the Swampland Distance Conjecture and the Weak Gravity Conjecture [142] in Calabi-Yau string compactifications [5, 81, 82, 136, 143][1].

In this chapter we will study asymptotic flux compactifications with G_4 with a focus on asymptotic limits given by only two fields becoming large. In other words, we will consider regions near codimension-two boundary loci in the complex structure moduli space and leave the generalization to higher codimensions for future work. We classify all possible asymptotic two-variable large field limits in general Calabi-Yau fourfolds, both at finite and infinite field distance. We then focus on the *strict asymptotic regime* in which two fields and their ratio are large. Physically this implies a suppression of certain perturbative corrections, while mathematically it corresponds to using the so-called sl(2)-orbit approximation. It is then possible to explicitly derive the asymptotic scalar potential for all such strict asymptotic regimes (see table 3.5). This allows us to study the structure of flux vacua and obtain a no-go theorem that forbids the presence of de Sitter vacua at parametric control near any large field limit of two fields parametrizing

[1] See [60, 116, 117, 138–140, 143–153] for other works testing the Swampland Distance Conjecture in the context of asymptotic string compactifications.

complex structure deformations. The details of the no-go and assumptions can be found in section 3.6.4. The list of scalar potentials also allows us to explicitly test the asymptotic Sitter conjecture of [63] and to show that it is satisfied if we are dealing with infinite distance limits. Note that we do not discuss the stabilization of Kähler structure moduli. Remarkably, our findings can be interpreted as stating that a subsector of moduli, which one aims to stabilize near the boundary, already imposes strong constraints on the vacuum structure. This becomes more apparent when considering the flux scalar potentials in a more general context in which it yields a generalization of the Type IIA no-go of [154].

Crucially, we therefore also consider a more general class of flux scalar potentials that capture, in particular, the potentials found in Type IIA flux compactifications [16]. These potentials are, in contrast to the standard F-theory flux potentials not positive definite and hence can admit Anti-de Sitter vacua. In particular, it was argued in [137] that a seemingly infinite series of flux vacua exists in Type IIA at weak string coupling and large volume. We identify the special fluxes that are necessary to generate such sequences and check if they can exist at the various limits in moduli space. More precisely, such fluxes are necessarily having vanishing Hodge norm in the asymptotic limit and drop out from the tadpole constraint. This implies that they cannot correspond to self-dual fluxes and hence would induce a backreaction on the geometry in the F-theory context. Remarkably, their construction and existence seems deeply related to the infinite charge orbits presented in [5, 136] in the study of the Swampland Distance Conjecture.

Our approach also allows us to generally analyze the backreaction effects of axion monodromy inflationary models in Calabi-Yau manifolds, in which the role of the inflaton is played by an axion with a flux-induced potential. It was shown in [138–140] for particular examples that displacing an axion for large field values implies in turn a displacement of the saxionic fields which backreacts on the kinetic term of the axion such that the proper field distance grows only logarithmically with the inflaton vev. This further implies that the cut-off scale set by the infinite tower of states of the Distance Conjecture also decreases exponentially in terms of the axionic field distance and invalidates the effective theory. It was argued [138–140] that for closed string axions with a flux-induced potential generated at weak coupling and large volume, these backreaction effects cannot be delayed but become important at transplanckian field values, disfavoring certain models of large field inflation. However, it remained as an open question if the backreaction can be delayed in other setups by generating a mass hierarchy between the axion and the saxions [139, 155] (see also [156, 157]). Here, we will show with complete

generality that the backreaction cannot be delayed for any axion belonging to the complex structure moduli space of F-theory Calabi-Yau compactifications in the asymptotic regimes analyzed in this chapter, as long as we move along a gradient flow trajectory. The reason is that the parameter that controls the backreaction becomes independent of the fluxes at large field for any two-moduli asymptotic limit of the moduli space of a Calabi-Yau fourfold. Interpreted in the Type IIB context this result implies that neither closed string complex structure deformations, nor open-string seven-brane deformations can provide axions where backreaction effects can be made small. This provides new evidence for the refined Distance Conjecture [57, 58].

The outline of the chapter goes as follows. We start in section 3.2 by reviewing the scalar potential of $\mathcal{N} = 1$ compactifications of M/F-theory on a Calabi-Yau fourfold with G_4 flux, and the chain of dualities that reduce the setting to four dimensional Type IIB and IIA flux compactifications. In section 3.3, we will introduce the machinery to study these flux compactifications in the asymptotic regimes of the moduli space. Key results are the asymptotic decomposition of the fluxes adapted to the different limits and the asymptotic behavior of the Hodge norm, which allow us to determine the universal leading behavior of the flux-induced scalar potential at the asymptotic limits. In section 3.4 we explain this structure in the context of an $\mathcal{N} = 1$ supergravity embedding and its relation to the dual description of the scalar potential in terms of three-form gauge fields. A complete classification of all possible two-moduli asymptotic limits in the Calabi-Yau fourfold is performed in section 3.5 together with the flux-induced scalar potential arising in each case. In section 3.6 we analyze the vacua structure of this potential and get a new no-go theorem for de Sitter as well as new insights regarding infinite sets of families of AdS vacua. The analysis of the axion dependence of the scalar potential and the implications for axion monodromy models are discussed in section 3.7, while section 3.8 contains our conclusions.

3.2 Flux compactifications on Calabi-Yau fourfolds

In this section we introduce the setup that we investigate in detail in this chapter. Concretely, we will be interested in flux compactifications of F-theory and Type IIB orientifolds that can be studied via the duality to M-theory. We will thus first recall in subsection 3.2.1 the scalar potential $V_{\rm M}$ of M-theory compactified on a Calabi-Yau fourfold with G_4 flux and introduce the tadpole cancellation condition [158, 159]. We briefly comment on how $V_{\rm M}$ lifts to a four-dimensional

scalar potential of an $\mathcal{N} = 1$ compactification of F-theory on an elliptically fibered Y_4. In subsection 3.2.2 we then recall how the F-theory setting reduces to a four-dimensional flux compactified Type IIB on an orientifold background. Restricting the allowed background fluxes we also show how a specific scalar potential (3.2.16) in Type IIA flux compactification can be described within this setting and we will later on analyze generalizations of such potential by loosening the correlation between the coefficients in the remaining sections.

3.2.1 Four-form flux and the scalar potential

In this section, we elaborate on the contents reviewed in Section 1.2.4. As recalled in Section 1.2.4, compactifications for M-theory, or rather eleven-dimensional supergravity, on a Calabi-Yau fourfold leads to a three-dimensional effective supergravity theory with $\mathcal{N} = 2$ supersymmetry. This theory is characterized by a Kähler potential, determining the metric of the dynamical scalars, and a superpotential, inducing a non-trivial scalar potential for these fields. In case one is considering a smooth Calabi-Yau fourfold the superpotential is only induced by four-form fluxes G_4, which parametrize non-vanishing vacuum expectation values of the field-strength $\hat{G}_4$ of the M-theory three-form $\hat{C}_3$ through four-cycles of the internal space Y_4. Such fluxes $\hat{G}_4$ can also induce a gauging of the theory [44,160], but we will not discuss this part of the effective action in any detail in the following. We will also be not concerned with the quantization of fluxes, since this discreteness property will not be of significance in the later analysis.

Performing the dimensional reduction the three-dimensional scalar potential in the Einstein frame takes the form

$$V_{\mathrm{M}} = \frac{1}{\mathcal{V}_4^3}\Big(\int_{Y_4} G_4 \wedge \star G_4 - \int_{Y_4} G_4 \wedge G_4 \Big) \tag{3.2.1}$$

where $\mathcal{V}_4$ is the volume of Y_4 and $\star$ is the Hodge-star on Y_4. Note that the derivation of V_{M} requires to perform a dimensional reduction with a non-trivial warp-factor and higher-derivative terms [161–166]. The warp-factor equation integrated over Y_4 furthermore induces a non-trivial consistency condition linking flux and curvature. This tadpole cancellation condition takes the form

$$\frac{1}{2}\int_{Y_4} G_4 \wedge G_4 = \frac{\chi(Y_4)}{24} \ , \tag{3.2.2}$$

where $\chi(Y_4) = \int_{Y_4} c_4(Y_4)$ is the Euler characteristic of Y_4. The condition (3.2.2) has to be used crucially in the derivation of (3.2.1) and leads to the second term.

The scalar potential (3.2.1) depends via the Hodge-star and $\mathcal{V}_4$ both on the complex structure moduli and Kähler structure moduli of Y_4. Since our main target will be to investigate the vacua in complex structure moduli space, it is convenient to split the scalar potential with respect to these two sets of moduli. We will do that by demanding that the flux under consideration satisfies the primitivity condition

$$J \wedge G_4 = 0 \ , \tag{3.2.3}$$

which should hold in cohomology and defines the primitive cohomology $H^4_{\rm p}(Y_4, \mathbb{R})$. This condition forces the scalar potential induced by this flux to only depend on the complex structure moduli and the overall volume factor. In fact, one shows [167] that it then can be written as

$$V_{\rm M} = e^K G^{I\bar{J}} D_I W \overline{D_J W} \ , \tag{3.2.4}$$

where K is a Kähler potential, determining the metric $G_{I\bar{J}}$ and its inverse $G^{I\bar{J}}$, and W a holomorphic superpotential. The derivative appearing in (3.2.4) are given by $D_I W = \partial_I W + (\partial_I K) W$, with ∂_I are derivatives with respect to the complex structure moduli fields of Y_4. Note that a term proportional to $|W|^2$ does not arise due to the no-scale condition for the Kähler moduli.

Let us introduce the various quantities appearing in expression (3.2.4) in more detail. Firstly, we have introduced the Kähler potential $K = -3 \log \mathcal{V}_4 + K^{\rm cs}$, which absorbs the overall volume factor and depends on the Kähler potential $K^{\rm cs}$. The latter determines the metric $G_{I\bar{J}} = \partial_{z^I} \partial_{\bar{z}^J} K^{\rm cs}$ on the complex structure moduli space $\mathcal{M}^{\rm cs}$ of Y_4. In general, $K^{\rm cs}$ is a very non-trivial function of the complex structure moduli z^I, $I = 1, \ldots, h^{3,1}(Y_4)$. Explicitly it can be written as

$$K^{\rm cs}(z, \bar{z}) = -\log \int_{Y_4} \Omega(z) \wedge \bar{\Omega}(\bar{z}) \ , \tag{3.2.5}$$

where Ω is the, up to rescalings, unique $(4,0)$-form on Y_4. Note that Ω varies holomorphically in the fields z^J. Secondly, we have used that the superpotential depending on the complex structure moduli takes the form [51]

$$W(z) = \int_{Y_4} G_4 \wedge \Omega(z) \ . \tag{3.2.6}$$

In order to simplify the notation, let us introduce a bilinear form $\langle \cdot \, , \cdot \rangle$ and the Hodge norm $\| \cdot \|$ by defining

$$\langle v, v' \rangle \equiv \int_{Y_4} v \wedge v' \ , \qquad \|v\|^2 \equiv \int_{Y_4} v \wedge \star \bar{v} \ , \tag{3.2.7}$$

Note that $\langle \cdot , \cdot \rangle$ is symmetric for Calabi-Yau fourfolds. Using this notation one finds that (3.2.5) and (3.2.6) reduce to

$$K^{\rm cs} = -\log\langle \Omega, \bar{\Omega}\rangle = -\log \|\Omega\|^2 \ , \qquad W = \langle G_4, \Omega\rangle \ , \tag{3.2.8}$$

where we have used that $\star\Omega = \Omega$. Furthermore, we can write the scalar potential (3.2.1) elegantly as

$$V_{\rm M} = \frac{1}{\mathcal{V}_4^3}\Big(\|G_4\|^2 - \langle G_4, G_4\rangle\Big) = \frac{1}{2\mathcal{V}_4^3}\|G_4 - \star G_4\|^2 \ . \tag{3.2.9}$$

It will be crucial for our later discussion to recall some well-known features of the vacua of (3.2.1), (3.2.4). If we look for supersymmetric vacua one has to demand $D_I W = 0$ and $W = 0$, where the later condition arises when considering a W independent of the Kähler structure moduli. Hence, in the (p,q)-Hodge decomposition of the primitive cohomology $H^4_{\rm p}(Y_4, \mathbb{C})$, defined by the vanishing of the wedge product of these forms with J as in (3.2.3), supersymmetric fluxes are of type $(2,2)$. Clearly, the potential (3.2.4) is vanishing for these vacua. In fact, it is important to stress that if one demands that the equations of motion for a background solution are strictly satisfied, one has

$$G_4 = \star G_4 \ , \tag{3.2.10}$$

and the scalar potential (3.2.1) vanishes identically. Therefore, in order to obtain non-trivial Anti-de Sitter or de Sitter solutions we have to violate (3.2.10) in the vacuum. In order that this does not destabilize the solution, this has to be done in a controlled way, as we discuss in more detail below.

Let us close the recap of the fourfold compactifications by noting that the scalar potential (3.2.9) admits a lift to four-dimensional F-theory compactifications if Y_4 is elliptically fibered with a threefold base B_3 [40]. In order to discuss this up-lift in some more detail, we note that the restriction to primitive fluxes G_4 is important in the following discussion. In fact, in contrast to some of the Kähler moduli, the complex structure moduli of Y_4 will equally be complex scalar fields in a four-dimensional F-theory compactification. Therefore, for primitive flux the combination $\|G_4\|^2 - \langle G_4, G_4\rangle$ in (3.2.9) will lift directly to four dimensions. The overall volume, however, has to be split into a volume of the base B_3 denoted by $\mathcal{V}_{\rm b}$ and the volume of the fiber as discussed in [44]. Identifying the fiber volume with the radius of the circle connecting M-theory and F-theory, we then obtain the F-theory scalar potential

$$V_{\rm F} = \frac{1}{\mathcal{V}_{\rm b}^2}\Big(\|G_4\|^2 - \langle G_4, G_4\rangle\Big) \ . \tag{3.2.11}$$

Crucially, this result contains the volume $\mathcal{V}_{\rm b}$ of a Type IIB compactification performed in ten-dimensional Einstein frame and no further dilation factors appear in the overall prefactor. In the next subsection we will discuss how (3.2.11) reduces to the flux potential of a Type IIB orientifold compactification. The latter then relates to a Type IIA flux potential via mirror symmetry.

3.2.2 Relation to flux vacua in Type IIB and Type IIA orientifolds

In this section we briefly discuss how the G_4 flux compactifications introduced in section 3.2.1 are linked with flux compactifications of Type IIB and Type IIA orientifolds. In particular, we will recall the well-known results about Type IIA flux vacua following [16, 137, 154]. This will make it easier to compare later on our results to previous no-go theorems found in the literature.

Let us first discuss how the first term in the F-theory scalar potential (3.2.11) given by the Hodge norm of G_4 reduces to the well known flux induced scalar potential of Type IIB Calabi-Yau orientifold compactifications. This requires to perform Sen's weak coupling limit [168], which is a well-know limit in complex structure moduli space and will arise as a special case of the more general discussion introduced in the next section. Concretely, it requires to send the imaginary part of one of the complex structure moduli, namely the one corresponding to the complex structure modulus of the generic elliptic fiber of Y_4, to be very large. Denoting this modulus by S one then identifies $S = C_0 + ie^{-\phi_{\rm B}}$, where $\phi_{\rm B}$ is the ten-dimensional dilaton. This implies that $\text{Im}\, S \gg 1$ is indeed the weak string coupling limit. The flux G_4 splits as $G_4 = H_3 \wedge dy + F_3 \wedge dx$, where dx and dy are the two one-forms on the generic elliptic fiber and H_3 and F_3 are NS-NS and R-R fluxes in Type IIB, respectively. Inserting this form of G_4 into the F-theory potential (3.2.11) and using the standard torus metric, one finds that Type IIB orientifold flux potential takes the form

$$V_{\rm IIB} = \frac{e^{3\phi_{\rm B}}}{4(\mathcal{V}_s^{\rm B})^2}\Big[e^{-\phi_{\rm B}}\int_{Y_3} H_3 \wedge \star H_3 + e^{\phi_{\rm B}}\int_{Y_3} F_3 \wedge \star F_3 - \int_{Y_3} F_3 \wedge H_3\Big]\,. \quad (3.2.12)$$

Note that $\mathcal{V}_s^{\rm B}$ is the volume of the Calabi-Yau threefold emerging in the orientifold limit in the ten-dimensional string frame. The volume is related to $\mathcal{V}_{\rm b}$ via $\mathcal{V}_s^{\rm B} = \mathcal{V}_{\rm b} e^{3\phi_{\rm B}/2}$ and one has $B_3 = Y_3/\mathbb{Z}_2$. This implies also that the Hodge norm in (3.2.12) now only includes the dependence on the complex structure moduli of the threefold Y_3, which were part of the complex structure moduli of the fourfold Y_4. It is straightforward to express (3.2.12) in terms of the complex flux $F_3 - SH_3$ and then determine the well-known orientifold flux superpotential.

Let us now turn to discussing Type IIA orientifold compactifications with fluxes. Their effective action can also be determined by direct dimensional reduction from massive IIA supergravity [16]. However, we can alternatively use mirror symmetry to derive the effective theory of Type IIA on the mirror Calabi-Yau orientifold. By mirror symmetry, the complex structure moduli are mapped to Kähler moduli in Type IIA, while the four dimensional Type IIB dilaton $e^{D_{\rm B}} = e^{\phi_{\rm B}}/\sqrt{\mathcal{V}_s^{\rm B}}$ gets mapped to the Type IIA dilaton $e^{D_{\rm A}} = e^{\phi_{\rm A}}/\sqrt{\mathcal{V}_s^{\rm A}}$. It will be convenient for us to define [2]

$$s = e^{-\phi_{\rm A}} \frac{(\mathcal{V}_s^{\rm A})^{1/2}}{|\Omega^A|} \ , \qquad u = (\mathcal{V}_s^{\rm A})^{1/3} \ , \tag{3.2.13}$$

where we defined $|\Omega^A|^2 \equiv i \int_{\tilde{Y}_3} \bar{\Omega}^{\rm A} \wedge \Omega^{\rm A}$. The mirror identification of the fields implies

$$e^{-\phi_{\rm B}} \quad \leftrightarrow \quad s \ , \qquad \mathcal{V}_s^{\rm B} \quad \leftrightarrow \quad |\Omega^A|^2 \ , \qquad |\Omega^B|^2 \quad \leftrightarrow \quad \mathcal{V}_s^A \ , \tag{3.2.14}$$

with the definition $|\Omega^B|^2 \equiv i \int_{Y_3} \bar{\Omega}^{\rm B} \wedge \Omega^{\rm B}$.

The different components of the R-R three-form fluxes map to Type IIA R-R p-form fluxes with $p = 0, 2, 4, 6$. The NS-NS flux, though, can yield different components mapping to NS-NS flux, metric fluxes or non-geometric fluxes in IIA. For simplicity in this section, let us illustrate the result only for the R-R fluxes and the NS-NS component which maps to a NS-NS flux in IIA. Using (3.2.13) and (3.2.14) the Type IIA scalar potential dual to (3.2.12) reads

$$V_{\rm IIA} = \frac{1}{4 s^3 |\Omega^A|^4} \Big(\frac{s}{u^3} |\Omega^A|^2 \int_{\tilde{Y}_3} H_3 \wedge \star H_3 + \frac{1}{s u^3} \sum_p \int_{\tilde{Y}_3} F_p \wedge \star F_p - \int_{\rm O6/D6} F_0 H_3 \Big) \ . \tag{3.2.15}$$

In performing this duality one has to realize that also the Hodge star maps non-trivially under mirror symmetry (see e.g. [16, 169] for a more detailed discussion). Interestingly, not only all these fluxes have the same M-theory origin in terms of G_4, but also the contribution from O6-planes can be derived from the second term in (3.2.1). Since the orientifold planes are geometrised in M-theory, they will contribute to the Euler characteristic of the fourfold which appears in the tadpole cancellation condition (3.2.2). This term is topological so the only moduli dependence arises from the overall volume factor. Hence, there is an additional factor $1/s^3$ when comparing the Type IIB/F-theory scalar potential (3.2.11) and Type IIA scalar potential (3.2.15) arising from the change to the string frame and the use of the mirror map. For later reference it will be useful to write (3.2.15) in

[2] Note that $s = \mathrm{Re}\, CZ^0$ in the notation of [16]. The factor $i \int \Omega \wedge \bar{\Omega}$ was not included in [154].

a more compact form in the case one has only one volume modulus, namely u. In this case one show that $\int_{\tilde{Y}_3} F_p \wedge \star F_p \propto u^{6-2p}$ and (3.2.15) becomes

$$V_{\text{IIA}} = \frac{1}{4s^3}\Big(\frac{s}{u^3}\hat{A}_{H_3} + \frac{u^3}{s}\hat{A}_{F_0} + \frac{u}{s}\hat{A}_{F_2} + \frac{1}{su}\hat{A}_{F_4} + \frac{1}{su^3}\hat{A}_{F_6} - \hat{A}_{\text{loc}}\Big)\ , \qquad (3.2.16)$$

where we have absorbed $|\Omega^A|^4$ in the definitions in the coefficients $\hat{A}_{\text{loc}}$ and the non-negative $\hat{A}_{H_3}, \hat{A}_{F_0}, \ldots, \hat{A}_{F_6} \geq 0$.

The typical advantage of working using the M-theory language is that, as we have seen, Type II objects with different nature are described in a unified way in M-theory. However, this is not the only advantage. Notice that the volume and dilaton fields in Type IIA map to complex structure and dilaton in Type IIB respectively, and both lift to complex structure of the fourfold in M-theory. By studying different points in the complex structure moduli space of the fourfold we are, therefore, considering different limits for the volume and dilaton in Type IIA. Only a very special point in this complex structure moduli space corresponds to the large volume and small coupling limit in Type IIA, and only near this special point we can follow the chain of dualities by staying within the regime in which the Type IIA supergravity description is under control. Therefore, another clear advantage of studying these effective theories in the M-theory language, is that we can in fact move to other points in the complex structure moduli space of the fourfold in a controlled way, which allows us to study the effective theory beyond the large volume and weak coupling limit of Type IIA.

The question that drives our work is whether the conclusions and no-go's obtained from studying the structure of flux vacua at large volume and weak coupling limits are also valid when exploring other infinite distance limits of the moduli space. For this purpose, we will introduce a mathematical machinery that will allow us to compute the asymptotic splitting of G_4 into different components adapted to each type of infinite distance singularity. In the well known case of the large complex structure point, this asymptotic splitting of G_4 corresponds to the different components that map to the RR and NS fluxes in Type IIA. However, this may vary at other special points of the moduli space. Together with this asymptotic splitting we will provide the moduli dependence of each component, which will allow us to study the asymptotic structure of flux vacua in general grounds in section 3.6.

3.3 Asymptotic flux potential

In this section we discuss flux compactifications restricted to the asymptotic regime in the complex structure moduli space of a Calabi-Yau fourfold Y_4. The moduli space regions of interest are near limits in moduli space in which Y_4 becomes singular. To begin with, we first explain in section 3.3.1 how the moduli dependence of the the $(4,0)$-form Ω can be approximated in each asymptotic regime when knowing the monodromy matrices and a limiting four-form a_0 associated to the singular locus. We also briefly discuss how this data can be used to classify the limits. Furthermore, we then sketch in section 3.3.2 that the same data defines, very non-trivially, an orthogonal split of the fourth cohomology group, and hence the flux space, into smaller vector spaces $V_{\boldsymbol{\ell}}$ with certain remarkable properties. In fact, in section 3.3.3 we show that it can be used to give an asymptotic approximation to the Hodge norm in (3.2.1) and hence the flux scalar potential itself. Using these insights, we are then able to show in section 3.3.4 that self-dual fluxes take a particularly simple form in the strict asymptotic regime. In addition we define a certain new class of fluxes in section 3.3.5, which are relevant in determining the scaling limits of the scalar potential.

3.3.1 Asymptotic limits in Calabi-Yau fourfolds

In the following we will discuss the considered limits in the complex structure moduli space $\mathcal{M}^{\rm cs}(Y_4)$. The limits of interest are taken to reach the boundary of $\mathcal{M}^{\rm cs}(Y_4)$ at which Y_4 becomes singular. Of particular interest will be the ones which lead us to points that are of infinite geodesic distance in the metric $G_{I\bar{J}}$ derived from (3.2.5). A well-known example of such a degeneration point is the large complex structure point, but the following statements apply to all infinite distance points that can also lie on higher-dimensional degeneration loci. One describe the degeneration loci of Y_4 locally as the vanishing locus of n coordinates $z^1 = \cdots = z^{\hat{n}} = 0$.[3] We can also introduce new coordinates $t^j = \frac{1}{2\pi i}\log z^j$, such that the limits of interest are given by

$$t^j \;\to\; i\infty \;, \qquad j = 1, \ldots, \hat{n} \;, \tag{3.3.1}$$

with all other coordinates ζ^κ finite. In the following we will set

$$t^j = \phi^j + i s^j \;, \tag{3.3.2}$$

[3]This equation describes the intersection of $\hat{n}$ divisors in a blown-up version of the complex structure moduli space.

such that (3.3.1) corresponds to sending $s^j \to \infty$, while the ϕ^j approach any finite values.

Since we will be interested in the region close to the degeneration locus of Y_4, we will consider large values of $s^1, \ldots, s^{\hat{n}}$. In this case we can use a result of [75] that the limiting behavior of Ω is approximated by the so-called nilpotent orbit $\Omega_{\rm nil}$ which takes a much simpler form than the general Ω and will be introduced next. Firstly, $\Omega_{\rm nil}$ depends on the monodromy matrix T_j associated to the $t^j = i\infty$ point. To define the monodromy matrix, one needs to choose a flat basis for the four-form cohomology $H^4_{\rm p}(Y_4, \mathbb{R})$ and identify the $(4,0)$-form Ω with its period vector $\mathbf{\Pi}$ under such an integral basis. This period vector $\mathbf{\Pi}$ solves the Picard-Fuchs equations associated to the complex structure deformation. Then the monodromy matrix appears if one asks how the period vector $\mathbf{\Pi}$ transforms under $t^j \to t^j + 1$, i.e. it is defined via

$$\mathbf{\Pi}(\ldots, t^j + 1, \ldots) = T_j^{-1} \mathbf{\Pi}(\ldots, t^j, \ldots) \ , \tag{3.3.3}$$

where the appearance of the inverse of T_j is purely conventional. In the following we will use a shorthand notation writing a matrix action on a form. This is always understood as having the matrix acting on the integral basis of four-forms. For example, equation (3.3.3) is then expressed as

$$\Omega(\ldots, t^j + 1, \ldots) = T_j \Omega(\ldots, t^j, \ldots) \ , \tag{3.3.4}$$

where the inverse arises due to the action on the basis rather than on the coefficient vector.

If T_j possesses a non-trivial unipotent part, it defines a nilpotent matrix [4]

$$N_j = \log T_j \ . \tag{3.3.5}$$

The N_j form a commuting set of matrices and one has $\langle N_j \cdot, \cdot \rangle = -\langle \cdot, N_j \cdot \rangle$. The nilpotent orbit theorem of [75] states that Ω is approximated by the nilpotent orbit [5]

$$\Omega(t, \zeta) = \underbrace{e^{t^i N_i} a_0(\zeta)}_{\Omega_{\rm nil}(t,\zeta)} + \mathcal{O}(e^{2\pi i t^j}) \ , \tag{3.3.6}$$

[4] In the following we will assume that we have transformed the variables z^j and t^j, such that only the unipotent part of T_j is relevant in the transformation (3.3.3). This procedure causes us to lose some of the information about the monodromies of orbifold singularities, but the aspects crucial to the infinite distances are retained.

[5] Note that this statement is true up to an overall holomorphic rescaling of Ω. Such rescalings yield to a Kähler transformation of K given in (3.2.5). Unless otherwise indicated the following discussion is invariant under such rescalings.

where we sum in the exponential over $i = 1, \ldots, \hat{n}$. Here a_0 is a holomorphic function in the coordinates that are not send to a limit (3.3.1). Note here that the exponential yields a polynomial in t^i, since the N_i are nilpotent matrices. The important statement of (3.3.6) is that the vector $\Omega_{\rm nil}$ approximates Ω up to corrections that are suppressed by $e^{2\pi i t^j}$ in the limit of large $s^1, \ldots, s^{\hat{n}}$. The nilpotent orbit is the starting point for our analysis of the asymptotic regions in $\mathcal{M}^{\rm cs}$.

Let us note that all possible nilpotent matrices N, defined via (3.3.5), arising from the degeneration limits (3.3.1) of Calabi-Yau fourfolds can be classified systematically [113]. This classification proceeds analogously to the one of singularity types occurring for Calabi-Yau threefolds discussed in [113, 136]. In the fourfold case one distinguishes five general types denoted by I, II, III, IV, and V. Following a similar strategy as for Calabi-Yau threefolds we enumerate all singularity types of the primitive middle Hodge numbers $(1, h^{3,1}, \hat{m}, h^{3,1}, 1)$, where $\hat{m}$ denotes the dimension of the primitive part $H^{2,2}_{\rm p}(Y_4)$ of $H^{2,2}(Y_4)$.

One way of distinguishing these cases is by asking what the highest power of N is that does not annihilate a_0, i.e. one determines the integer d satisfying

$$N^d a_0 \neq 0 \ , \quad N^{d+1} a_0 = 0 \ . \tag{3.3.7}$$

Since $d \leq 4$, one finds exactly five cases, $d = 0, \ldots, 4$ corresponding to the singularity types $\mathrm{I}, \ldots, \mathrm{V}$. As for Calabi-Yau threefolds each of these types has further sub-types. For fourfolds one can label them by two indices and write:

$\mathrm{I}_{a,a'}$	$0 \leq a \leq a' \leq h^{3,1}$	$2a' - a \leq \hat{m}$
$\mathrm{II}_{b,b'}$	$0 \leq b \leq b' \leq h^{3,1} - 1$	$2b' - b \leq \hat{m}$
$\mathrm{III}_{c,c'}$	$0 \leq c \leq c' \leq h^{3,1} - 1$	$2c' - c \leq \hat{m} - 2$
$\mathrm{IV}_{d,d'}$	$1 \leq d + 1 \leq d' \leq h^{3,1} - 1$	$2d' - d \leq \hat{m}$
$\mathrm{V}_{e,e'}$	$1 \leq e \leq e' \leq h^{3,1}$	$2e' - e \leq \hat{m}$

(3.3.8)

The precise connection of N to the singularity type is summarized in table 3.1.

3.3.2 Asymptotic split of the flux space

In the following we want to introduce a basis of G_4 fluxes, which is adapted to the limits (3.3.1) discussed in the previous subsection. It turns out that in order to use the mathematical machinery that we will introduce next, one has to first divide

Type	Action on a_0 highest $d:\ N^d a_0 \neq 0$	N	Rank of N^2	N^3	N^4
$\mathrm{I}_{a,a'}$	$d=0$	$2a'-a$	a	0	0
$\mathrm{II}_{b,b'}$	$d=1$	$2b'-b+2$	b	0	0
$\mathrm{III}_{c,c'}$	$d=2$	$2c'+4$	$c+2$	0	0
$\mathrm{IV}_{d,d'}$	$d=3$	$2d'+4$	$d+4$	2	0
$\mathrm{V}_{e,e'}$	$d=4$	$2e'+2$	$e+2$	2	1

Table 3.1: Classification of the arising limits and singularities occurring in the complex moduli space of Calabi-Yau fourfolds.

the space into growth sectors. One such growth sector is given by

$$\mathcal{R}_{12\cdots\hat{n}} = \left\{ t^j = \phi^j + i s^j \Big| \frac{s^1}{s^2} > \gamma, \ldots, \frac{s^{\hat{n}-1}}{s^{\hat{n}}} > \gamma, s^{\hat{n}} > \gamma, \phi^j < \delta \right\} , \tag{3.3.9}$$

where we can chose arbitrary positive γ, δ. Other growth sectors can be obtained by the same expression but with permuted s^j.

Let us now introduce a basis for the G_4. It will depend on the following set of data: (1) the monodromy matrices N_i and the vector a_0 appearing in (3.3.6), (2) the growth sector (3.3.9) which one considers. Given this data it was shown in [76] that one can always find an associated set of

$$\text{commuting } \mathfrak{sl}(2,\mathbb{C})\text{-triples}: \qquad (N_i^-, N_i^+, Y_i) , \quad i = 1, \ldots, \hat{n} , \tag{3.3.10}$$

which captures the asymptotic behavior of the (3.3.6) and its derivatives. These triples satisfy the standard commutation relations

$$[Y_i, N_i^\pm] = \pm 2 N_i^\pm , \qquad [N_i^+, N_i^-] = Y_i . \tag{3.3.11}$$

In practice it it non-trivial to construct these $\mathfrak{sl}(2,\mathbb{C})$-triples starting with the data defining the nilpotent orbit (3.3.6). For Calabi-Yau threefolds an explicit example was worked out in [136]. In the following we will assume that the steps summarized in [136] have been performed and the commuting triples to the considered limit are known.

The $\mathfrak{sl}(2,\mathbb{C})$-triples can now be used to split the primitive cohomology group $H^4_{\rm p}(Y_4,\mathbb{R})$ into eigenspaces of Y_i. Let us introduce

$$H^4_{\rm p}(Y_4,\mathbb{R}) = \bigoplus_{\boldsymbol{\ell}\in\mathcal{E}} V_{\boldsymbol{\ell}} \ , \qquad \boldsymbol{\ell} = (\ell_1,\ldots,\ell_{\hat{n}}) \ , \tag{3.3.12}$$

where $\ell_i \in \{0,\ldots,8\}$ are integers representing the eigenvalues of $Y_{(i)} = Y_1+\cdots+Y_i$, i.e.

$$v_{\boldsymbol{\ell}} \in V_{\boldsymbol{\ell}} \quad \Longleftrightarrow \quad Y_{(i)} v_{\boldsymbol{\ell}} = (\ell_i - 4) v_{\boldsymbol{\ell}} \ . \tag{3.3.13}$$

In writing (3.3.12) we have introduced the set $\mathcal{E}$ of all possible vectors $\boldsymbol{\ell}$ labelling non-trivial $V_{\boldsymbol{\ell}}$ and collecting all eigenvalue combinations of $(Y_{(1)},\ldots,Y_{(\hat{n})})$. The allowed vectors in $\mathcal{E}$ are determined by investigating the properties of the singularity occurring in the limit (3.3.1) and we will see in more detail below. The $\mathfrak{sl}(2,\mathbb{C})$-algebra allows to derive several interesting properties of the vector spaces $V_{\boldsymbol{\ell}}$. For example, one finds that

$$\dim V_{\boldsymbol{\ell}} = \dim V_{\mathbf{8}-\boldsymbol{\ell}} \ , \tag{3.3.14}$$

where we abbreviated $\mathbf{8} = (8,\ldots,8)$, which implies that $V_{\boldsymbol{\ell}} \cong V_{\mathbf{8}-\boldsymbol{\ell}}$. Furthermore, the spaces $V_{\boldsymbol{\ell}}$ satisfy the orthogonality property

$$\langle V_{\boldsymbol{\ell}}, V_{\boldsymbol{\ell}'}\rangle = 0 \quad \text{unless} \quad \boldsymbol{\ell}+\boldsymbol{\ell}' = \mathbf{8} \ , \tag{3.3.15}$$

as can be inferred by using the fact that $\langle\, \cdot\, , Y_{(i)}\, \cdot\,\rangle = -\langle Y_{(i)}\, \cdot\, , \cdot\,\rangle$. In other words using (3.3.12) one finds a decomposition of an element $H^4_{\rm p}(Y_4,\mathbb{R})$ into sets of pairwise orthogonal components.

Applied to the fluxes $G_4 \in H^4_{\rm p}(Y_4,\mathbb{R})$, this decomposition implies an asymptotic split of the flux space into orthogonal components

$$G_4 = \sum_{\boldsymbol{\ell}\in\mathcal{E}} G_4^{\boldsymbol{\ell}}, \qquad \text{where } G_4^{\boldsymbol{\ell}} \in V_{\boldsymbol{\ell}} \text{ for every } \boldsymbol{\ell}\in\mathcal{E}. \tag{3.3.16}$$

This flux splitting will be the key of our starting program to classify possible flux scalar potentials in string compactifications.

3.3.3 The asymptotic behavior of the Hodge norm

In the following we will introduce one of the most non-trivial consequences of the splitting (3.3.12), by arguing that it determines the asymptotic behavior of the Hodge norm. To begin with let us recall some facts about the Hodge star operator

$\star$. To define its action on the primitive middle cohomology $H^4_{\rm p}(Y_4,\mathbb{C})$ we can introduce the Hodge decomposition

$$H^4_{\rm p}(Y_4,\mathbb{C}) = H^{4,0}\oplus H^{3,1}\oplus H^{2,2}_{\rm p}\oplus H^{1,3}\oplus H^{0,4}\ . \tag{3.3.17}$$

As long as the manifold Y_4 is non-singular the action of $\star$ is simply given by $\star v^{p,q} = i^{p-q}v^{p,q}$, for any element $v^{p,q}\in H^{p,q}$. Clearly, since the (p,q)-split in (3.3.17) depends on the choice of complex structure, it will vary when changing the complex structure moduli. This is the origin of the complex structure moduli dependence in (3.2.1). Close to a degeneration point of Y_4 we expect that also $\star$ takes a simplified form, just as the $(4,0)$-form Ω simplifies as discussed in section 3.3.1. In fact, we stated around (3.3.6) that Ω simplifies, when dropping exponentially suppressed corrections, to the nilpotent orbit $\Omega_{\rm nil}$. This approximation can also be applied to the Hodge star operator $\star$ as we will discuss in the following.

Let us start with a general element of $G_4\in H^4_{\rm p}(Y_4,\mathbb{R})$, which we can consider to be our G_4-flux. We want to evaluate the Hodge metric by using $\Omega_{\rm nil}$ rather than the complete $(4,0)$-form Ω. This can be done systematically, when extending the nilpotent orbit construction to the whole cohomology as we discuss in appendix 3.B. In this way one finds

$$\|G_4\|^2 = \int_{Y_4} G_4\wedge\star G_4 = \langle C_{\rm nil}G_4, G_4\rangle + \mathcal{O}(e^{2\pi i t^j})\ , \tag{3.3.18}$$

where $C_{\rm nil}(t,\zeta)$, the *Weil operator* associated to the nilpotent orbit, captures the moduli dependence on the fields t^j through terms involving $e^{t^i N_i}$ as appearing in the nilpotent orbit (3.3.6). We will introduce $C_{\rm nil}$ properly in appendix 3.B. Crucially, due to the fact that the t^j dependence of $C_{\rm nil}$ is simplified due to the nilpotent orbit approximation, we find that its dependence on the axions $\phi^i = {\rm Re}\, t^i$ can be made explicit by writing

$$C_{\rm nil}(t,\zeta) = e^{\phi^i N_i}\hat{C}_{\rm nil}e^{-\phi^i N_i}\ , \qquad \hat{C}_{\rm nil}\equiv C_{\rm nil}(\phi^i=0)\ . \tag{3.3.19}$$

We can use this identity by defining $\rho(G_4,\phi) = e^{-\phi^i N_i}G_4$ and deduce that (3.3.18) becomes

$$\|G_4\|^2 = \int_{Y_4} G_4\wedge\star G_4 = \langle \hat{C}_{\rm nil}\rho,\rho\rangle + \mathcal{O}(e^{2\pi i t^j})\ , \tag{3.3.20}$$

where crucially all ϕ^i dependence is now captured by $\rho(G_4,\phi)$ when neglecting the exponentially suppressed corrections. Let us note that we can expand the ϕ^i-dependent vectors ρ in any basis $v^A, A=1,\ldots,{\rm dim}H^4_{\rm p}(Y_4,\mathbb{R})$ as $\rho=\varrho_A v^A$. If we

also give the basis expression $Z^{AB} = \langle \hat{C}_{\text{nil}} v^A, v^B \rangle$ for the inner product, we can write (3.3.20) as

$$\|G_4\|^2 = Z^{AB} \varrho_A \varrho_B + \mathcal{O}(e^{2\pi i t^j}) \ . \tag{3.3.21}$$

It turns out that there is a clever choice of basis v^A, which allows us to also make the field dependence on the scalars $s^i = \text{Im}\, t^i$ explicit. This basis is adapted to the splitting (3.3.12) as we will discuss in the following.

Let us consider the real four-form G_4 and determine its split into vector spaces $V_{\boldsymbol{\ell}}$ by expanding $G_4 = \sum_{\boldsymbol{\ell} \in \mathcal{E}} G_4^{\boldsymbol{\ell}}$ as in (3.3.16). These vector spaces further satisfy to be orthogonal with respect to the inner product

$$\langle C_\infty V_{\boldsymbol{\ell}}, V_{\boldsymbol{\ell}'} \rangle = 0, \quad \text{for } \ \boldsymbol{\ell}' \neq \boldsymbol{\ell} \ . \tag{3.3.22}$$

where C_∞ is the Weil operator inducing a natural limiting Hodge norm

$$\|v\|_\infty = \langle C_\infty v, v \rangle \ , \tag{3.3.23}$$

which is defined using only the structure at the limiting locus (3.3.1). It is therefore independent of the coordinates $t^1, \ldots, t^{\hat{n}}$, while non-trivially varying with the remaining coordinates ζ^κ. The operator C_∞ will be introduced in more detail in appendix 3.B. We also point out that equation (3.3.15) and (3.3.22) imply the following behavior of this Weil operator

$$C_\infty : V_{\boldsymbol{\ell}} \to V_{\boldsymbol{8}-\boldsymbol{\ell}}, \tag{3.3.24}$$

for all $\boldsymbol{\ell}$, i.e., C_∞ exchanges $V_{\boldsymbol{\ell}}$ and $V_{\boldsymbol{8}-\boldsymbol{\ell}}$. For the purpose of this section, it is enough to remark that the flux norm satisfies the following direct sum decomposition on the split (3.3.12),

$$\|G_4\|_\infty^2 = \sum_{\boldsymbol{\ell} \in \mathcal{E}} \|G_4^{\boldsymbol{\ell}}\|_\infty^2 \ , \tag{3.3.25}$$

thanks to the orthogonality property (3.3.22) which forces all non-diagonal terms to vanish.

The next step is to move a bit away from the singular loci in order to recover the dependence on the scalar fields of the Hodge norm. First, in order to explicitly keep the axion dependence, we use (3.3.19) to also include the exponential $e^{-\phi^i N_i}$ and expand

$$\rho(G_4, \phi) \equiv e^{-\phi^i N_i} G_4 = \sum_{\boldsymbol{\ell} \in \mathcal{E}} \rho_{\boldsymbol{\ell}}(G_4, \phi) \ , \qquad \rho_{\boldsymbol{\ell}}(G_4, \phi^i = 0) = G_4^{\boldsymbol{\ell}} \ , \tag{3.3.26}$$

where $\rho_{\boldsymbol{\ell}}$ is the restriction of $e^{-\phi^i N_i} G_4$ to the vector space $V_{\boldsymbol{\ell}}$. Notice that the components $\rho_{\boldsymbol{\ell}}$ satisfy the same asymptotic orthogonality properties as $G_4^{\boldsymbol{\ell}}$, regardless

of the value of the axions. We can then use this expansion to get an asymptotic expression for the Hodge norm [76, 107] with all dependence on ϕ^i and s^i being explicit. More precisely, one has

$$\|G_4\|^2 \;\sim\; \|G_4\|^2_{\mathrm{sl}(2)} = \sum_{\boldsymbol{\ell}\in\mathcal{E}} \Big(\frac{s^1}{s^2}\Big)^{\ell_1-4} \cdots \Big(\frac{s^{\hat{n}-1}}{s^{\hat{n}}}\Big)^{\ell_{\hat{n}-1}-4} (s^{\hat{n}})^{\ell_{\hat{n}}-4}\, \|\rho_{\boldsymbol{\ell}}(G_4,\phi)\|^2_\infty \ . \tag{3.3.27}$$

where we have introduced the Weil operator $C_{\mathrm{sl}(2)}$ by setting

$$\|G_4\|^2_{\mathrm{sl}(2)} \equiv \langle C_{\mathrm{sl}(2)} G_4, G_4\rangle \ . \tag{3.3.28}$$

More detailed discussion on the operator $C_{\mathrm{sl}(2)}$ can be found in appendix 3.B. This operator captures the leading dependence on the saxionic coordinates s^i but neglects all sub-leading polynomial corrections of the form s^i/s^{i+1} for the corresponding growth sector (3.3.9). Hence, it is only a good approximation once a growth sector is selected and provides the asymptotic form of the Hodge norm along when considering the s^i in the growth sector with $\gamma \gg 1$. From now on, we will denote this regime of validity the *strict asymptotic regime*, in opposition to the *asymptotic regime* which captured all polynomial corrections and neglected only the exponentially suppressed terms of order $\mathcal{O}(e^{2\pi i t^j})$. In the mathematical terminology, the latter corresponds to the nilpotent orbit result while the strict asymptotic regime is given by the sl(2)-orbit approximation. We have summarized the different approximations of the Hodge operator and their regime of validity in table 3.2.

This strict asymptotic behavior of the Hodge norm is a very powerful result that will allow us to classify all possible flux scalar potentials and their vacua arising in the asymptotic regions of string compactifications. All we need is to provide a list of all possible values of the integer vector $\boldsymbol{\ell} = (\ell_1, \ell_2, \ldots, \ell_{\hat{n}}) \in \mathcal{E}$ associated to the different singular limits. This classification will be performed in section 3.5.2 for the case of two moduli becoming large in a Calabi-Yau fourfold. Notice also that the operator $C_{\mathrm{sl}(2)}$ still satisfies the same orthogonality properties as C_∞ with respect to the vector spaces $V_{\boldsymbol{\ell}}$, implying that the flux scalar potential will be simply given by a sum of squares, simplifying enormously the analysis of flux vacua.

We close this subsection by stressing that the symbol $\sim$ in (3.3.27) indicates that this expression displays the strict asymptotic behavior of the Hodge norm. In fact, this statement is actually well-defined. The expression (3.3.27) implies that for $s^1/s^2, \ldots, s^{\hat{n}-1}/s^{\hat{n}} > \gamma$, i.e. in a growth sector (3.3.9), there exist two positive

constants α, β such that

$$\alpha \|G_4\|^2_{\mathrm{sl}(2)} \;\leq\; \|G_4\|^2 \;\leq\; \beta \|G_4\|^2_{\mathrm{sl}(2)} \,. \tag{3.3.29}$$

The constants α, β do, in general, depend on γ, but are independent of G_4. Note that this inequality has the immediate consequence that we have to be careful when approximating the Hodge norm $\|G_4\|^2$ with $\|G_4\|^2_{\mathrm{sl}(2)}$, since it limits our ability to infer detailed information about $\|G_4\|^2$ from the much simpler norm $\|G_4\|^2_{\mathrm{sl}(2)}$. In general, only in the limit $\gamma \to \infty$ the constants $\alpha,\ \beta$ will approach each other and the norm $\|G_4\|^2$ converges to $\|G_4\|^2_{\mathrm{sl}(2)}$. However, there can be particular situations in which $\|G_4\|^2_{\mathrm{sl}(2)}$ provides the full result for the Hodge norm up to exponentially suppressed corrections, as we will explain more carefully when discussing the supergravity embedding in section 3.4.1.

Regime of validity:	Asymptotic s^i large	Strict asymptotic $\mathcal{R}_{1\cdots\hat{n}}$ with $\gamma \gg 1$	At boundary $s^i = \infty$
Approximating Hodge-operator:	C_{nil}	$C_{\mathrm{sl}(2)}$	C_∞
Corrections:	drop $\mathcal{O}(e^{2\pi i t^j})$	drop sub-leading $\frac{s^i}{s^{i+1}}$-polys	t^i-independent

Table 3.2: Weil operators and their regime of validity.

3.3.4 Self-dual fluxes in the strict asymptotic regime

In this subsection we discuss a first way of finding vacua of the potential (3.2.1) by restricting to asymptotically self-dual fluxes. Note that this potential is positive definite when written in the form (3.2.4) and vanishes when considering vacua in which the flux G_4 satisfies the self-duality condition (3.2.10). Recall that the self-duality condition is a necessity if we want the vacuum to solve the equations of motion of the eleven-dimensional supergravity. This condition fixes the moduli, since it involves the moduli-dependent Hodge star $\star$. As in the previous subsection, we can thus ask the question if, at least in the asymptotic regime, one can give an explicit moduli dependence of the self-duality condition and eventually fix the moduli explicitly.

In order to study moduli stabilization we thus replace $\star$ with its asymptotic counterparts C_{nil}, defined in (3.3.18), and $C_{\mathrm{sl}(2)}$, defined in (3.3.28). In the former case one neglects exponentially suppressed corrections in the variables t^i that are

taken to the limit. Using (3.3.19), we find that the self-duality condition (3.2.10) is approximated by

$$\hat{C}_{\rm nil}\,\rho(G_4,\phi) = \rho(G_4,\phi)\ . \tag{3.3.30}$$

Expanded into a basis this equation gives still a very complicated set of equations even in the t^i. To further decouple these equations we will move deeper into the asymptotic regime as in section 3.3.3. Let us thus consider the asymptotic expression of (3.2.10) using $C_{\rm sl(2)}$. In this case we can exploit the fact that everything splits into the $V_{\boldsymbol{\ell}}$ and we can extract the explicit t^i moduli dependence. We thus consider the asymptotic self-duality condition

$$C_{\rm sl(2)}G_4 = G_4\ . \tag{3.3.31}$$

In order to separate this condition into multiple equations we introduce a basis for the $V_{\boldsymbol{\ell}}$ as

$$v^{\boldsymbol{\ell}}_{i_{\boldsymbol{\ell}}}\ :\quad \mathrm{span}_{\mathbb{R}}\big\{v^{\boldsymbol{\ell}}_1,\ldots,v^{\boldsymbol{\ell}}_{\dim V_{\boldsymbol{\ell}}}\big\} = V_{\boldsymbol{\ell}}\ , \tag{3.3.32}$$

where $\boldsymbol{\ell}\in\mathcal{E}$ is a vector as before. We normalize these basis vectors with respect to the inner product, such that

$$\langle v^{\boldsymbol{\ell}}_{i_{\boldsymbol{\ell}}}, v^{\mathbf{8}-\boldsymbol{\ell}}_{j_{\mathbf{8}-\boldsymbol{\ell}}}\rangle = \delta_{i_{\boldsymbol{\ell}}j_{\mathbf{8}-\boldsymbol{\ell}}}\ ,\qquad \langle v^{\boldsymbol{\ell}}_{i_{\boldsymbol{\ell}}}, v^{\boldsymbol{\ell}'}_{j_{\boldsymbol{\ell}'}}\rangle = 0\ \ \text{for}\ \ \boldsymbol{\ell}\neq\mathbf{8}-\boldsymbol{\ell}'\ , \tag{3.3.33}$$

where we recall that the orthogonality (3.3.15) of the $V_{\boldsymbol{\ell}}$ enforces all other products to vanish. We also abbreviate the inner product between the basis vectors as

$$\mathcal{K}^{\boldsymbol{\ell}}_{i_{\boldsymbol{\ell}}j_{\boldsymbol{\ell}}} = \langle C_\infty v^{\boldsymbol{\ell}}_{i_{\boldsymbol{\ell}}}, v^{\boldsymbol{\ell}}_{j_{\boldsymbol{\ell}}}\rangle\ ,\qquad \langle C_\infty v^{\boldsymbol{\ell}}_{i_{\boldsymbol{\ell}}}, v^{\boldsymbol{\ell}'}_{j_{\boldsymbol{\ell}'}}\rangle = 0\ \ \text{for}\ \ \boldsymbol{\ell}\neq\boldsymbol{\ell}'\ , \tag{3.3.34}$$

where we note that $\langle C_\infty\,\cdot\,,\,\cdot\,\rangle$ is block-diagonal on the $V_{\boldsymbol{\ell}}$ as noted in (3.3.25). Now we can expand

$$G_4 = \sum_{\boldsymbol{\ell}\in\mathcal{E}} G_4^{\boldsymbol{\ell}} = \sum_{\boldsymbol{\ell}\in\mathcal{E}}\sum_{i_{\boldsymbol{\ell}}} g^{i_{\boldsymbol{\ell}}}_{\boldsymbol{\ell}}\, v^{\boldsymbol{\ell}}_{i_{\boldsymbol{\ell}}}\ , \tag{3.3.35}$$

with $g^{i_{\boldsymbol{\ell}}}_{\boldsymbol{\ell}}$ being the 'flux quanta' of the G_4.

With these preliminaries we can now split (3.3.31) into scalar equations. We first evaluate the product of (3.3.31) with the basis $\{v^{\mathbf{m}}_{i_{\mathbf{m}}}\}$ introduced in (3.3.32). Using the orthogonality conditions (3.3.33) and (3.3.34) we find

$$\Big(\frac{s^1}{s^2}\Big)^{m_1-4}\cdots\Big(\frac{s^{\hat{n}-1}}{s^{\hat{n}}}\Big)^{m_{\hat{n}-1}-4}(s^{\hat{n}})^{m_{\hat{n}}-4}\,\langle C_\infty\rho_{\mathbf{m}}, v^{i_{\mathbf{m}}}_{\mathbf{m}}\rangle = \langle\rho_{\mathbf{8}-\mathbf{m}}, v^{i_{\mathbf{m}}}_{\mathbf{m}}\rangle\ . \tag{3.3.36}$$

In order to interpret this expression, we set for the moment $\phi^i=0$, which implies that this expression reduces to

$$\Big(\frac{s^1}{s^2}\Big)^{4-m_1}\cdots\Big(\frac{s^{\hat{n}-1}}{s^{\hat{n}}}\Big)^{4-m_{\hat{n}-1}}(s^{\hat{n}})^{4-m_{\hat{n}}} = \frac{g^{i_{\mathbf{m}}}_{\mathbf{m}}\mathcal{K}^{\mathbf{m}}_{i_{\mathbf{m}}j_{\mathbf{m}}}}{g^{j_{\mathbf{m}}}_{\mathbf{8}-\mathbf{m}}},\quad \mathbf{m}\ \text{not summed}, \tag{3.3.37}$$

with $\mathcal{K}^{\mathbf{m}}_{i_{\mathbf{m}}j_{\mathbf{m}}}$ and $g^{i_{\mathbf{m}}}_{\mathbf{m}}$ defined in (3.3.34), (3.3.35), respectively. Note that the right-hand-side only depends on the fluxes $g^{i_{\mathbf{m}}}_{\mathbf{m}}$, $g^{i_{\mathbf{m}}}_{\mathbf{8-m}}$ and, via $\mathcal{K}^{\mathbf{m}}_{i_{\mathbf{m}}j_{\mathbf{m}}}(\zeta)$, the coordinates ζ^κ not taken to a limit. This implies that the combination of the s^i appearing on the left-hand side are fixed when imposing the asymptotic self-duality condition (3.3.31). Whether or not this fixes a particular s^i, or even all of them, depends on the vectors $\boldsymbol{\ell} \in \mathcal{E}$, and we will determine all possible sets for two s^1, s^2 in section 3.5.3.

3.3.5 Unbounded asymptotically massless fluxes

In this subsection we want to define a specific type of four-form flux that will be relevant in finding vacua in an asymptotic flux compactification. The basic idea is to identify a flux $\hat{G}_4$ that does not contribute to the tadpole cancellation condition (3.2.2) and thus, at lease taking into account only this constraint, can be made arbitrary large. However, it is clear that such a flux cannot satisfy the self-duality condition (3.2.10) and hence violates the equations of motion. We therefore also require the flux to have an asymptotically vanishing norm $||\hat{G}_4||^2$. As we will discuss in detail below, precisely such fluxes enable us to construct vacua that are under parametric control.

Let us stress that the complete flux under consideration will be of the form

$$G_4 = \hat{G}_4 + G_4^0. \tag{3.3.38}$$

Here the flux $\hat{G}_4$ is defined to have the following properties

$$\text{(1 a)} \quad \langle \hat{G}_4, \hat{G}_4 \rangle = 0 \ , \qquad \text{(1 b)} \quad \langle \hat{G}_4, G_4^0 \rangle = 0 \ , \tag{3.3.39}$$

$$\text{(2)} \quad \|\hat{G}_4\| \to 0 \quad \text{on every path with } t^1, \ldots, t^{\hat{n}} \to i\infty \text{ in (3.3.9).} \tag{3.3.40}$$

while the *rest* of the fluxes will be part of G_4^0. In the following we will call the fluxes satisfying (1 a) and (1 b) to be *unbounded*, since they are not restricted by the tadpole condition (3.2.2). The fluxes satisfying (2) will be called *asymptotically massless* in the following. As explained above, this latter condition has been introduced to ensure that the self-duality condition (3.2.10) is only violated mildly and restored in the limit. In fact, $\langle \hat{G}_4, \hat{G}_4 \rangle = 0$ implies that $\hat{G}_4$ cannot be self-dual at any finite value of the moduli, since otherwise $\langle \hat{G}_4, \hat{G}_4 \rangle = \|\hat{G}_4\|^2 > 0$. In the following, we will explain how to identify these unbounded asymptotically massless fluxes $\hat{G}_4$ in complete generality.

The split of the fourth cohomology into $V_{\boldsymbol{\ell}}$ as in (3.3.12) and the general growth property of the Hodge norm (3.3.27) gives us a powerful tool to specify the fluxes

that satisfy the condition (3.3.40). Recall that the asymptotic form of the Hodge norm was given in (3.3.27) and takes the form

$$\|G_4\|^2 \;\sim\; \sum_{\boldsymbol{\ell}\in\mathcal{E}} \Big(\frac{s^1}{s^2}\Big)^{\ell_1-4} \cdots \Big(\frac{s^{\hat{n}-1}}{s^{\hat{n}}}\Big)^{\ell_{\hat{n}-1}-4} (s^{\hat{n}})^{\ell_{\hat{n}}-4}\, A_{\boldsymbol{\ell}} \ , \tag{3.3.41}$$

where we have set

$$A_{\boldsymbol{\ell}} \equiv \|\rho_{\boldsymbol{\ell}}(G_4,\phi)\|^2_\infty > 0 \ . \tag{3.3.42}$$

Let us use this to identify the asymptotically massless part $\hat{G}_4$. Since by definition $\rho_{\boldsymbol{\ell}}(G_4,\phi) \in V_{\boldsymbol{\ell}}$ we directly infer from (3.3.41) that a sufficient condition that $\|\hat{G}_4\|^2 \to 0$ on all paths with $t^1,\dots,t^{\hat{n}} \to i\infty$ in (3.3.9) is that $\hat{G}_4$ has only components in the $V_{\boldsymbol{\ell}}$ with $\ell_1,\dots,\ell_{\hat{n}-1} \leq 4$ and $\ell_{\hat{n}} < 4$. To see this one can use that in (3.3.9) all fractions $(s^1/s^2)^{-1},\dots,(s^{\hat{n}-1}/s^{\hat{n}})^{-1}$ are bounded and the power $(s^{\hat{n}})^{\ell_{\hat{n}}-4}$ ensures that $\|\hat{G}_4\|^2$ vanishes asymptotically.

Note that this analysis suggests that it is natural to split the vector space $H^4_{\rm p}(Y_4,\mathbb{R})$ into three vector spaces as

$$H^4_{\rm p}(Y_4,\mathbb{R}) = V_{\rm light} \oplus V_{\rm heavy} \oplus V_{\rm rest} \ , \tag{3.3.43}$$

where we define

$$V_{\rm light} \;=\; \bigoplus_{\boldsymbol{\ell}\in\mathcal{E}_{\rm light}} V_{\boldsymbol{\ell}} \ , \qquad \mathcal{E}_{\rm light} = \{\ell_1,\dots,\ell_{\hat{n}-1}\leq 4, \ell_{\hat{n}}<4\} \ , \tag{3.3.44}$$

$$V_{\rm heavy} \;=\; \bigoplus_{\boldsymbol{\ell}\in\mathcal{E}_{\rm heavy}} V_{\boldsymbol{\ell}} \ , \qquad \mathcal{E}_{\rm heavy} = \{\ell_1,\dots,\ell_{\hat{n}-1}\geq 4, \ell_{\hat{n}}>4\} \ . \tag{3.3.45}$$

Using the growth result (3.3.27) one infers that $G_4 \in V_{\rm light}$ is equivalent to the statement that $\|G_4\| \to 0$ on every path with $t^1,\dots,t^{\hat{n}} \to i\infty$ in (3.3.9). Similarly, one sees that $G_4 \in V_{\rm heavy}$ is equivalent to demanding $\|G_4\| \to \infty$ on every path to the limit in the considered growth sector. It is not difficult to see from (3.3.15) and (3.3.14) that

$$\langle V_{\rm light}, V_{\rm light}\rangle = 0 \ , \qquad \langle V_{\rm heavy}, V_{\rm heavy}\rangle = 0 \ , \tag{3.3.46}$$

and that $V_{\rm light}$ and $V_{\rm heavy}$ can be identified as vector spaces. With these observations at hand the asymptotically massless fluxes satisfy

$$\hat{G}_4 \in V_{\rm light} \ . \tag{3.3.47}$$

Note that this identification immediately implies also condition (1 a). In contrast, condition (1 b) should be read as a constraint on both $\hat{G}_4$ and G^0_4. In fact, we will

see that for a given choice of fluxes in G_4^0 we will have to switch off components in $\hat{G}_4$ to select only those asymptotically massless fluxes $\hat{G}_4$ which have a vanishing inner product with G_4^0 to find a solution to both (1), (2).

Finally, let us notice that the condition (3.3.47) is equivalent to the condition imposed over the charge lattice of BPS states in [5,81,136] to find a tower of states that become massless at the singular loci, as predicted by the Swampland Distance Conjecture. Analogously, the condition to be unbounded resembles to the condition of stability [5]. A BPS state in a monodromy orbit cannot fragment into two BPS states if they are mutually local, i.e. if the inner product (1 b) vanishes. Therefore, the same element in $H^4_{\rm p}(Y_4,\mathbb{R})$ that generated a tower of massless stable BPS states at the singular loci gives rise here to an unbounded asymptotically massless flux which is necessary to construct vacua at parametric control. This puts manifest an intriguing relation between the Swampland Distance Conjecture and the presence of vacua at parametric control which deserves further investigation in the future.

3.4 Supergravity embedding and three-forms

In this section we will study the $\mathcal{N}=1$ supergravity embedding of the scalar potential at the asymptotic limits of the moduli space. We will provide the asymptotic form of the Kähler potential and superpotential arising in these limits in section 3.4.1 and explain what the strict asymptotic approximation taken in the previous section means for these supergravity quantities. In section 3.4.2, we will relate our results to the dual field theory description in terms of three-form gauge fields commonly used for axion monodromy models. This will allow us to provide a geometric meaning to the underlying structure revealed by the the three-form gauge fields in string flux compactifications. The reader only interested in the results of our analysis of flux vacua can safely skip this section.

3.4.1 Asymptotic limits and the $\mathcal{N}=1$ supergravity data

Equivalently to studying the asymptotic limits of the scalar potential we can also determine the asymptotic behavior of the Kähler potential (3.2.5) and flux superpotential (3.2.6). This analysis will highlight various properties of the asymptotic limits and clarify our approximation taken in the strict asymptotic regime.

Let us begin by investigating the Kähler potential (3.2.5), which can be written in a more compact form as indicated in (3.2.8). The moduli dependence in $K^{\rm cs}$ on t^i,ζ^κ arises through the appearance of Ω. As a first approximation when taking

the limit $t^i \to i\infty$, we will replace Ω with the nilpotent orbit $\Omega_{\rm nil}$ as discussed around (3.3.6). Inserting the expression for $\Omega_{\rm nil}$ we can use the properties of N_i in $\langle\,\cdot\,,\,\cdot\,\rangle$ to write

$$K^{\rm cs}_{\rm nil} = -\log\langle\Omega_{\rm nil},\bar\Omega_{\rm nil}\rangle = -\log\langle e^{2is^jN_j}a_0(\zeta),\bar a_0(\bar\zeta)\rangle\ . \tag{3.4.1}$$

Since N_j are nilpotent operators, the exponential in (3.4.1) can always be expanded to get a polynomial with a finite number of terms. This implies that $K^{\rm cs}$, in the nilpotent orbit approximation with all exponential corrections $e^{2\pi it^j}$ dropped, is the logarithm of a polynomial in the s^i and is independent of the axions ϕ^i. $K^{\rm cs}_{\rm nil}$ still depends on a considered variable s^i if $N_ia_0 \neq 0$. This latter condition is a necessary condition for the limit to be at infinite distance in the metric derived from $K^{\rm cs}$. The appearance of the continuous shift symmetries $\phi^i \to \phi^i + c^i$ at infinite distance singularities was recently discussed in [5] in the context of the Swampland Distance Conjecture. It is important to stress that $K^{\rm cs}_{\rm nil}$ given in (3.4.1) is not yet the strict asymptotic expression obtained by using the growth result (3.3.27). In fact, to apply this growth estimate one first has to fix a growth sector (3.3.9) and expand (3.4.1) in powers of the ratios s^i/s^{i+1} to obtain

$$K^{\rm cs}_{{\rm sl}(2)} \sim -\log\Big[\Big(\frac{s^1}{s^2}\Big)^{d_1}\cdots\Big(\frac{s^{\hat n-1}}{s^{\hat n}}\Big)^{d_{\hat n-1}}(s^{\hat n})^{d_{\hat n}}f(\zeta,\bar\zeta)\Big]\ , \tag{3.4.2}$$

where d_i is the highest power of $N_1+\cdots+N_i$ acting on a_0 that is non-zero as in (3.3.7). In other words, the estimate (3.4.2) extracts the leading power of the coordinates s^i from the general expression (3.4.1) in a sector (3.3.9). This implies that not only exponential corrections are omitted, but also sub-leading polynomial corrections in the coordinates s^i.

In a next step we look at the flux superpotential W introduced in (3.2.6). The approximation of neglecting exponential corrections is again implemented by replacing Ω with $\Omega_{\rm nil}$ in the asymptotic regime. Using the shorthand notation (3.2.8) we thus find

$$W_{\rm nil} = \langle G_4,\Omega_{\rm nil}\rangle = \langle\rho(G_4,\phi),e^{is^jN_j}a_0\rangle\ , \tag{3.4.3}$$

where $\rho(G_4,\phi)$ was defined in (3.3.26). Despite the fact that we have dropped exponential corrections, this expression captures the field dependence in a non-trivial way. Let us expand ρ into some basis. To be concrete we use the basis associated to the splitting of $H^4_{\rm p}(Y_4,\mathbb{R})$ given by the $V_{\boldsymbol{\ell}}$, and denote it by

$$v^{\boldsymbol{\ell}}_{i_{\boldsymbol{\ell}}}\ :\quad {\rm span}_{\mathbb{R}}\big\{v^{\boldsymbol{\ell}}_1,\ldots,v^{\boldsymbol{\ell}}_{\dim V_{\boldsymbol{\ell}}}\big\} = V_{\boldsymbol{\ell}}\ , \tag{3.4.4}$$

where $\boldsymbol{\ell} \in \mathcal{E}$ is a vector as before. We thus write $\rho = \varrho^{i_{\boldsymbol{\ell}}}_{\boldsymbol{\ell}} v^{\boldsymbol{\ell}}_{i_{\boldsymbol{\ell}}}$, such that (3.4.3) takes the form

$$W_{\rm nil} = \sum_{\boldsymbol{\ell}\in\mathcal{E}} \sum_{i_{\boldsymbol{\ell}}} \varrho^{i_{\boldsymbol{\ell}}}_{\boldsymbol{\ell}}(G_4,\phi)\, \Gamma^{\boldsymbol{\ell}}_{i_{\boldsymbol{\ell}}}(s,\zeta)\ , \qquad \Gamma^{\boldsymbol{\ell}}_{i_{\boldsymbol{\ell}}} = \langle v^{\boldsymbol{\ell}}_{i_{\boldsymbol{\ell}}}, e^{is^j N_j} a_0\rangle\ . \tag{3.4.5}$$

The remarkable fact about this expansion is, on the one hand, that we succeeded to separate the ϕ^i and s^i dependence. On the other hand, we have done this cleverly, such that the $\Gamma^{\boldsymbol{\ell}}_{i_{\boldsymbol{\ell}}}$ are polynomials of a highest s^i-power determined by $\boldsymbol{\ell}$, and the singularity type. Concretely they admit the expansion

$$\Gamma^{\boldsymbol{\ell}}_{i_{\boldsymbol{\ell}}} = (is^1)^{d_1-4+\ell_1}(is^2)^{d_2-d_1+\ell_2-\ell_1}\cdots(is^{\hat{n}})^{d_{\hat{n}}-d_{\hat{n}-1}+\ell_{\hat{n}}-\ell_{\hat{n}-1}}\ \widehat{\Gamma}^{\boldsymbol{\ell}}_{i_{\boldsymbol{\ell}}}\Big(\frac{s^1}{s^2},\frac{s^2}{s^3},\ldots,s^{\hat{n}}\Big)\,, \tag{3.4.6}$$

where $\widehat{\Gamma}^{\boldsymbol{\ell}}_{i_{\boldsymbol{\ell}}}\Big(\frac{s^1}{s^2},\frac{s^2}{s^3},\ldots,s^{\hat{n}}\Big)$ involves subleading polynomial corrections in the coordinates s^i. To determine the sl(2)-approximation, denoted for us as the strict asymptotic result, we have to further drop out the subleading polynomial corrections in the coordinates ratios s^i/s^{i+1} in (3.4.6), so that $\widehat{\Gamma}^{\boldsymbol{\ell}}_{i_{\boldsymbol{\ell}}}$ becomes just a constant $\widehat{\Gamma}^{\boldsymbol{\ell}}_{i_{\boldsymbol{\ell}}} \sim c^{\boldsymbol{\ell}}_{i_{\boldsymbol{\ell}}}$ and the superpotential reads[6]

$$W_{\rm sl(2)} = \sum_{\boldsymbol{\ell}\in\mathcal{E}} \sum_{i_{\boldsymbol{\ell}}} \varrho^{i_{\boldsymbol{\ell}}}_{\boldsymbol{\ell}}(G_4,\phi)\, c^{\boldsymbol{\ell}}_{i_{\boldsymbol{\ell}}}(s,\zeta)(is^1)^{d_1-4+\ell_1}(is^2)^{d_2-d_1+\ell_2-\ell_1}\cdots(is^{\hat{n}})^{d_{\hat{n}}-d_{\hat{n}-1}+\ell_{\hat{n}}-\ell_{\hat{n}-1}}. \tag{3.4.7}$$

This, together with (3.4.2), will give rise to the leading growth of the scalar potential given in (3.3.27). We will see in section 3.4.2 that this expansion also allows us to extract the crucial information when formulating the theory using Minkowski three-form gauge fields.

To sum up, the strict asymptotic approximation consists of neglecting, not only the exponentially suppressed corrections, but also subleading polynomial terms in the coordinates s^i. This can be done in a consistent way near any singular limit of the moduli space and provides the leading behavior of the scalar potential for each growth sector (3.3.9). In terms of the supergravity embedding, it corresponds to considering a factorizable Kähler potential that keeps only the leading term, i.e. the logarithm of a monomial of degree $d_{\hat{n}}$, and a superpotential where each axionic

[6] It is possible to get the same result for the superpotential if first extracting the leading dependence on the coordinates s^i and denoting

$$\varrho_{\boldsymbol{\ell}} \equiv \langle \rho(G_4,\phi), N_1^{(d_1-4+l_1)/2} N_2^{(d_2-d_1+l_2-l_1)/2}\cdots N_{\hat{n}}^{(d_{\hat{n}}-d_{\hat{n}-1}+l_n-l_{\hat{n}-1})/2} a_0\rangle\ .$$

function $\varrho_{\boldsymbol{\ell}}^{i_{\boldsymbol{\ell}}}$ is multiplied by a single saxionic monomial of degree $d_{\hat{n}} - 4 + l_{\hat{n}}$. This yields a scalar potential that can be expressed as a sum of squares as in (3.3.27).

Let us close this section by noting that the expressions arising in the strict asymptotic approximation can have a clear physical interpretation as neglecting some perturbative and non-perturbative corrections. This is for example the case in the famous Sen's weak coupling limit in Type IIB and the mirror Type IIA duals at large volume, in which the dependence on the dilaton can be factorized in the Kähler potential to leading order in α'. Hence, the sl(2)-norm provides the correct dilaton-dependence of the scalar potential at tree level and neglects α'-corrections that will mix the dilaton and the Kähler moduli. However, such an interpretation fails in other types of limits, where the subleading polynomial corrections have nothing to do with α'-corrections. It remains as an open question for the future to study how sensitive to this approximation our results are for the flux vacua presented in the next sections.

3.4.2 Relation to Minkowski three-form gauge fields

The asymptotic flux splitting and the nilpotent orbit result for the scalar potential at the large field limits derived in section 3.3 have a very intuitive physics interpretation in terms of the dual formulation of Minkowski three-form gauge fields, as we will explain in the following.

First, let us notice that each infinite distance limit of the form (3.3.1) is characterized by the appearance of some axions $\phi^i = \mathrm{Re}\, t^i$ whose discrete axionic shift symmetry is inherited from the monodromy transformation T_i around the singular locus located at $s^i = \mathrm{Im}\, t^i \to \infty$. In the context of the complex structure moduli space of Calabi-Yau compactifications, the axions can receive a flux-induced scalar potential which is multi-branched, i.e. only the combined discrete transformation of the axion and the fluxes leave invariant the effective theory.

The scalar potential of an axion can always be described in a dual picture by means of a coupling to the field strength of a space-time three-form gauge field $F_4 = dC_3$ [170–172]. Allowing for the presence of multiple axions and three-forms gauge fields, the scalar potential reads

$$V = -Z_{AB}(s^i) F_4^A F_4^B + F_4^A \varrho_A(\phi^i) \tag{3.4.8}$$

where A, B run over the number of three-form gauge fields. Here $Z_{AB}(s)$ is the kinetic matrix of the three-form gauge fields and is parametrized by the saxions, while all the dependence on the axion appears only through the shift symmetric

functions $\varrho_A(\phi)$. In particular, it has been shown in [173, 174] that the flux induced scalar potential of Type II compactifications can always be brought to the above form, where Z_{AB} and ϱ_A were derived by dimensional reduction from ten-dimensional Type II supergravity to four dimensions.[7] The functions ϱ_A are a shift symmetric combination of the internal fluxes and the axions that can be generically expressed [132] as

$$\varrho_A = (e^{-\phi^i N_i})^B_A \; q_B \tag{3.4.9}$$

where N_i are nilpotent matrices associated to the discrete axionic symmetries and q_B a vector of internal fluxes.

Upon integrating out the three-form gauge fields via their equations of motion,

$$\star F_4^A = Z^{AB} \varrho_B \tag{3.4.10}$$

the scalar potential becomes

$$V = Z^{AB}(s)\varrho_A(\phi)\varrho_B(\phi) \tag{3.4.11}$$

which corresponds to a quadratic form on ϱ_A. It was also shown in [173] (see also [132,174,178–182]) that the above scalar potential reproduces the usual form of the scalar potential derived from the $\mathcal{N} = 1$ supergravity formulae in four dimensional flux compactifications when combined with the contribution of localized sources.

Interestingly, the form (3.4.11) is the same expression for the scalar potential found in (3.3.21) upon applying the nilpotent orbit theorem in the asymptotic regime. Each flux component in (3.3.26) corresponds to the on-shell result of a four-form (3.4.10) and the nilpotent matrices in (3.4.9) are the same nilpotent operators $N_i = \log T_i$ of (3.3.5) in which the entire formalism is based on. This is expected from the fact that both formalisms rely on the presence of axionic shift symmetries inherited from the monodromy transformations and, therefore, become manifest in these asymptotic regimes. Let us remark that, even if the discrete shift symmetries are valid everywhere in the moduli space, the notion of an axion as a scalar field enjoying an approximate continuous shift symmetry is only valid in these asymptotic regimes. Let us also notice that this dual description in terms of four-form fields is independent of supersymmetry and can in principle even describe non-perturbative potentials [183]. It would be thus very interesting to further explore how the asymptotic Hodge theory approach can be interlinked with

[7] Note a three-form with action (3.4.8) naturally arises when computing the Type IIA scalar potential [16]. Furthermore, three-forms are essential when studying the couplings to D-branes [175–177].

the use of four-forms and how much of the structure derived with the four-forms has in fact a geometric counterpart. To give another example, the flux sublattice of dynamical fluxes found in [181] has a deep relation with the massless components in the asymptotic flux splitting of section 3.3.2 which would be interesting to further investigate in the future.

Finally, we would like to remark that the strict asymptotic approximation taken in (3.3.27) allows us to further express the potential as the sum of asymptotically orthogonal flux components at the large field limit. In other words, it is always possible to find a basis such that the kinetic matrix Z^{AB} of the four-forms is nearly block-diagonal in the sense that the non-diagonal terms are subleading with respect to the diagonal ones. The strict asymptotic approximation consists of neglecting these non-diagonal terms so that the potential becomes a sum of squares,

$$V = \sum_{\boldsymbol{\ell}\in\mathcal{E}} Z^{\boldsymbol{\ell}}(s)\|\rho_{\boldsymbol{\ell}}(G_4,\phi)\|^2 \ = \sum_{\boldsymbol{\ell}\in\mathcal{E}}\sum_{i_{\boldsymbol{\ell}},j_{\boldsymbol{\ell}}} Z^{\boldsymbol{\ell}}_{i_{\boldsymbol{\ell}}j_{\boldsymbol{\ell}}}(s)\ \varrho^{i_{\boldsymbol{\ell}}}_{\boldsymbol{\ell}}(\phi)\varrho^{j_{\boldsymbol{\ell}}}_{\boldsymbol{\ell}}(\phi) \tag{3.4.12}$$

with the exception of a possible remnant coming from tadpole cancellation. Here, we have used again the expansion (3.4.4) into a basis of vectors associated to the flux splitting into orthogonal $V_{\boldsymbol{\ell}}$ vector spaces, such that $\rho = \varrho^{i_{\boldsymbol{\ell}}}_{\boldsymbol{\ell}} v^{\boldsymbol{\ell}}_{i_{\boldsymbol{\ell}}}$. Using the growth theorem (3.3.27) we can infer the leading behavior of each block diagonal piece of the inverse metric $Z^{AB}(s)$,

$$Z^{\boldsymbol{\ell}}_{i_{\boldsymbol{\ell}}j_{\boldsymbol{\ell}}} \sim \left(\frac{s^1}{s^2}\right)^{\ell_1-4}\cdots\left(\frac{s^{\hat{n}-1}}{s^{\hat{n}}}\right)^{\ell_{\hat{n}-1}-4}(s^{\hat{n}})^{\ell_{\hat{n}}-4}\mathcal{K}^{\boldsymbol{\ell}}_{i_{\boldsymbol{\ell}}j_{\boldsymbol{\ell}}} \tag{3.4.13}$$

where $\mathcal{K}^{\boldsymbol{\ell}}_{i_{\boldsymbol{\ell}}j_{\boldsymbol{\ell}}}$ was defined in (3.3.34). This is something that could not be determined only in terms of the four-forms. Hence, our classification of the asymptotic flux splittings at the large field limits of Calabi-Yau manifolds can allow us to derive the three-form gauge field metrics and with them, the axionic monodromic potential, at other types of singularities beyond the typical case of the large complex structure limit. Furthermore, this monodromic potential written à la Dvali-Kaloper-Sorbo in terms of four-forms is useful to construct axion inflationary models and study the viability of large field ranges. In section 3.7 we will exploit our formalism to derive general conclusions about backreaction issues and large field ranges in axion monodromy models.

Let us finally mention that this bilinear form of the potential has been proven to be very useful to minimize the scalar potential of weakly coupled Type IIA flux compactifications and study the vacua structure in a systematic way [139, 182]. In fact, the ansatz assumed in [182] is precisely guaranteed by the strict asymptotic approximation yielding (3.4.13). In this chapter, we will exploit the algebraic

structure arising in the strict asymptotic regime to study the vacua structure at any asymptotic limit of the complex structure moduli space of a Calabi-Yau manifold.

3.5 General two-moduli limits

In this section we apply the machinery introduced in the previous sections for two-moduli families of Calabi-Yau fourfolds. More precisely, we investigate the limits (3.3.1) with $\hat{n} = 2$ in the complex structure moduli space of any Calabi-Yau fourfold Y_4 with $h^{3,1} = 2$. We first set up notations in order to get familiar with the asymptotic splitting of $H^4_{\rm p}(Y_4, \mathbb{R})$ in the two-moduli setting in subsection 3.5.1. Then, in subsection 3.5.2, we list all possible limits and corresponding singularity types that can occur in this moduli space. As a consequence, we are able to infer the asymptotic splitting of the flux space for each limit. To exemplify the use of these results, we focus in subsection 3.5.3 on a particular limit and discuss all possible decompositions $G_4 = \hat{G}_4 + G_4^0$, with $\hat{G}_4$ being an unbounded asymptotically massless flux. This data will be used in the next section to establish universal no-go results on flux vacua.

3.5.1 Asymptotic flux splitting and scalar potential

Let us consider the complex structure moduli space of a Calabi-Yau fourfold Y_4 with $h^{3,1} = 2$. We are interested in the case $\hat{n} = 2$ in (3.3.1) sending both coordinates to a limit. Around such a limit we introduce local coordinates t^1, t^2 denoted by

$$t^1 = \phi^1 + is \ , \qquad t^2 = \phi^2 + iu \ , \tag{3.5.1}$$

such that Y_4 becomes singular at $s, u \to \infty$. For any chosen positive γ, δ we can consider two growth sectors (3.3.9) given by

$$\mathcal{R}_{12} = \left\{ (t^1, t^2) \Big| \frac{s}{u} > \gamma, u > \gamma, \phi^i < \delta \right\} \ , \quad \mathcal{R}_{21} = \left\{ (t^1, t^2) \Big| \frac{u}{s} > \gamma, s > \gamma, \phi^i < \delta \right\} \ . \tag{3.5.2}$$

The first sector $\mathcal{R}_{12}$ can be interpreted as capturing paths in which s grows faster than u when approaching the limit $s, u \to \infty$, while $\mathcal{R}_{21}$ exchanges the roles of s and u. Let us consider $\mathcal{R}_{12}$, after possible renaming, and divide the limit into two steps. We first go to the singular locus $s \to \infty$ and call the arising singularity type Type A, where we necessarily find one of the types listed in (3.3.8). In a second step we send $u \to \infty$ arriving at singularity type Type B from the list (3.3.8). In this situation, we say that the sector $\mathcal{R}_{12}$ is associated to the singularity enhancement

$$\text{Type A} \ \to \text{Type B} \ . \tag{3.5.3}$$

Importantly, we are able to classify all possible singularity types, as already discussed in section 3.3.1, and determine all allowed enhancements, as discussed in section 3.5.2.

Associated to an enhancement Type A $\to$ Type B, there is an asymptotic splitting of $H^4_{\rm p}(Y_4,\mathbb{R})$ introduced in (3.3.12). In the two-moduli case it takes the form

$$H^4_{\rm p}(Y_4,\mathbb{R}) = \bigoplus_{\boldsymbol{\ell}=(m,n)\in\mathcal{E}} V_{mn} \ , \tag{3.5.4}$$

where we explicitly spelled out the indices on the subspaces V_{mn}. The set $\mathcal{E}$ depends on the enhancement Type A $\to$ Type B and will be given explicitly in subsection 3.5.2 for each possible enhancement. Using (3.5.4) a general flux G_4 can be decomposed as

$$G_4 = \sum_{(m,n)\in\mathcal{E}} G_4^{mn} \ , \qquad G_4^{mn}\in V_{mn} \ , \tag{3.5.5}$$

and we also introduce the expansion

$$e^{-\phi^i N_i} G_4 = \sum_{(m,n)\in\mathcal{E}} \rho_{mn} \ , \qquad \rho_{mn}\in V_{mn} \ , \tag{3.5.6}$$

Then the growth of the norm $\|G_4\|^2$ can be inferred from (3.3.41) and reads

$$\|G_4\|^2 \ \sim \sum_{(m,n)\in\mathcal{E}} \Big(\frac{s}{u}\Big)^{m-4} u^{n-4}\ A_{mn}(G_4,\phi) \ , \tag{3.5.7}$$

where we defined $A_{mn} = \|\rho_{mn}\|^2_\infty > 0$. Inserting this asymptotic growth into the M-theory scalar potential, we have

$$V_{\rm M} \sim \frac{1}{\mathcal{V}_4^3}\Big(\sum_{(m,n)\in\mathcal{E}} s^{m-4}u^{n-m}\, A_{mn} - A_{\rm loc}\Big), \tag{3.5.8}$$

where we have set $A_{\rm loc}\equiv\langle G_4, G_4\rangle$, which is independent of the moduli. The scalar potential (3.5.8) will be the starting point of our study of flux vacua in section 3.6.

In the next section we aim to establish no-go results for vacua of (3.5.8) that are under parametric control. This control is encoded in the fluxes and hence the coefficients A_{mn}. Whether or not a flux can be made very large is determined by the tadpole constraint (3.2.2). In section 3.3.5 we have introduced a type of flux, denoted by $\hat{G}_4$, that does not contribute to the tadpole constraint and has an asymptotically vanishing contribution to the scalar potential. Clearly, the determination of the allowed splits $\hat{G}_4$, G_4^0 depends crucially on the set of possible

indices $\mathcal{E}$ appearing in the asymptotic splitting (3.5.4). In particular, we recall from (3.3.47) that

$$\hat{G}_4 \in V_{\text{light}} = \bigoplus_{(m,n)\in\mathcal{E}_{\text{light}}} V_{mn} \,, \tag{3.5.9}$$

and hence the vectors in $\mathcal{E}_{\text{light}}$ crucially determine the allowed $\hat{G}_4$. It is the power of the used formalism that we can classify systematically all possible singularities and hence all possible splits (3.5.4). In the next subsection, we will show a full classification of singularity types of Calabi-Yau fourfolds with $h^{3,1} = 2$. We determine all possible singularity enhancements, the associated asymptotic splittings, and the form of the sets $\mathcal{E}$ and $\mathcal{E}_{\text{light}}$. For each of these cases one can then determine all possible $\hat{G}_4$ as we exemplify for an example in section 3.5.3.

3.5.2 Classification of two-moduli limits and enhancements therein

In this section we summarize the classification of all possible singularity types that can arise in a Calabi-Yau fourfold with $h^{3,1} = 2$, when both complex structure variables tend to a limit (3.3.1). Following a similar strategy as for Calabi-Yau threefolds, as discussed in detail in [113, 136], we enumerate all singularity types of the primitive middle Hodge numbers $(1, 2, \hat{m}, 2, 1)$. Here we denoted by $\hat{m}$ the dimension of the primitive part $H^{2,2}_{\text{p}}(Y_4)$ of $H^{2,2}(Y_4)$. As explained in section 3.3.1, there are five major types I, II, III, IV, and V. Each type is supplemented by two indices as shown in (3.3.8). The classification is summarized in table 3.3. In fact, the appearance of each type depends on the primitive Hodge number $\hat{m}$. When $0 \leq \hat{m} \leq 3$, not all types can occur. To avoid singling out special cases, we will assume $\hat{m} \geq 4$. The cases dropped with this assumption admit the same features as some of the cases we consider here and thus will not alter our conclusions.

I	$\mathrm{I}_{0,0},\ \mathrm{I}_{0,1},\ \mathrm{I}_{0,2},\ \mathrm{I}_{1,1},\ \mathrm{I}_{1,2},\ \mathrm{I}_{2,2}$
II	$\mathrm{II}_{0,0},\ \mathrm{II}_{0,1},\ \mathrm{II}_{1,1}$
III	$\mathrm{III}_{0,0},\ \mathrm{III}_{0,1},\ \mathrm{III}_{1,1}$
IV	$\mathrm{IV}_{0,1}$
V	$\mathrm{V}_{1,1},\ \mathrm{V}_{1,2},\ \mathrm{V}_{2,2}$

Table 3.3: Table showing all 16 singularity types that can occur in a two-moduli family of Calabi-Yau fourfolds with primitive Hodge number $\hat{m} \geq 4$.

Given the list of allowed singularity types in table 3.3, we can now check which singularities can occur in an enhancement where we send s, u to infinity successively. As in (3.5.3) we can send $s \to \infty$ to get a singularity type Type A and then $u \to \infty$ to get a singularity type Type B. We say Type A gets enhanced to Type B. There are intricate rules guarding the possible enhancements among different singularity types. And these rules determine the asymptotic splitting directly. These rules are described in [113] following the classic work [76], and its application in Calabi-Yau threefold degenerations can be found in [113, 136]. Following the same procedure as in [136], we determine the enhancement network among the types given in table 3.3. The result is shown in figure 3.1.[8]

[8]It was recently pointed out in [83] that this strategy, applied to the Kähler moduli side, can be employed to classify Calabi-Yau manifolds.

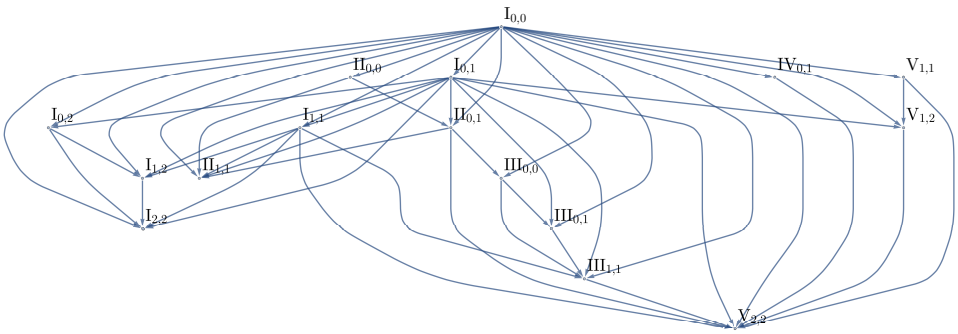

Figure 3.1: The enhancement network of Calabi-Yau fourfolds with primitive middle Hodge numbers $(1, 2, \hat{m}, 2, 1)$ with $\hat{m} \geq 4$. In this graph, an edge Type A $\rightarrow$ Type B indicates an enhancement of singularity type from Type A to Type B. Note that the enhancement relation is not transitive, as can be easily checked in, e.g., the enhancement chain $\mathrm{II}_{0,0} \rightarrow \mathrm{II}_{0,1} \rightarrow \mathrm{III}_{0,0}$.

It is worth pointing out that the type II enhancements occur, for example, at the Sen's weak coupling limit when the Calabi-Yau fourfold is used as an F-theory background. This has been discussed in detail in [184]. In a two-moduli limit as discussed here, one can combine the weak coupling limit with another limit in complex structure moduli space. In fact, as we will discuss below an example enhancement that occurs when combining Sen's weak coupling limit with another limit to reach the large complex structure point of Y_4. Concretely one finds in this case

$$\mathrm{II}_{0,1} \;\rightarrow\; \mathrm{V}_{2,2} \;, \tag{3.5.10}$$

where we have displayed the enhancement for which we first send $s \rightarrow \infty$ and then $u \rightarrow \infty$ as required for the growth sector $\mathcal{R}_{12}$ in (3.5.2). The limit $s \rightarrow \infty$ corresponds to the weak coupling limit.

Having determined all possible enhancements we can also compute for each case the associated asymptotic splitting (3.5.4). The results are shown in table 3.4. We will demonstrate the usage of this table in the following subsection in which we discuss one case in detail and determine the allowed unbounded asymptotically massless fluxes $\hat{G}_4$.

Given the data summarized in table 3.4 it is not hard to derive the corresponding scalar potentials V_{M} using (3.5.8). For completeness, we list the results in table 3.5. It is interesting to point out that all potentials obtained in this way actually come in pairs. There are two ways we find agreeing potentials, which we listed in table 3.5. Firstly, note that some of the sets $\mathcal{E}$ in table 3.4 are simply identical, as, for example,

Enhancements	$\mathcal{E}_{\text{light}}$	$\mathcal{E}_{\text{rest}}$	$\mathcal{E}_{\text{heavy}}$
$\mathrm{I}_{0,1} \to \mathrm{I}_{0,2}$	$(3,3),(4,3)$	$(\mathbf{4},\mathbf{4})$	$(\mathbf{4},\mathbf{5}),(\mathbf{5},\mathbf{5})$
$\mathrm{I}_{0,1} \to \mathrm{I}_{1,1}$	$(3,2)$	$(3,4),(\mathbf{4},\mathbf{4}),(5,4)$	$(\mathbf{5},\mathbf{6})$
$\mathrm{I}_{0,1} \xrightarrow{a} \mathrm{I}_{1,2}$	$(3,2),(4,3)$	$(3,4),(\mathbf{4},\mathbf{4}),(5,4)$	$(\mathbf{4},\mathbf{5}),(\mathbf{5},\mathbf{6})$
$\mathrm{I}_{0,1} \xrightarrow{b} \mathrm{I}_{1,2}$	$(3,3),(4,2)$	$(\mathbf{4},\mathbf{4})$	$(\mathbf{4},\mathbf{6}),(\mathbf{5},\mathbf{5})$
$\mathrm{I}_{0,1} \to \mathrm{I}_{2,2}$	$(3,2),(4,2)$	$(3,4),(\mathbf{4},\mathbf{4}),(5,4)$	$(\mathbf{4},\mathbf{6}),(\mathbf{5},\mathbf{6})$
$\mathrm{I}_{0,1} \to \mathrm{II}_{0,1}$	$(3,3),(4,3)$	$(\mathbf{4},\mathbf{4})$	$(\mathbf{4},\mathbf{5}),(\mathbf{5},\mathbf{5})$
$\mathrm{I}_{0,1} \to \mathrm{II}_{1,1}$	$(3,2),(4,3)$	$(3,4),(\mathbf{4},\mathbf{4}),(5,4)$	$(\mathbf{4},\mathbf{5}),(\mathbf{5},\mathbf{6})$
$\mathrm{I}_{0,1} \to \mathrm{III}_{0,1}$	$(3,3),(4,2)$	$(\mathbf{4},\mathbf{4})$	$(\mathbf{4},\mathbf{6}),(\mathbf{5},\mathbf{5})$
$\mathrm{I}_{0,1} \to \mathrm{III}_{1,1}$	$(3,2),(4,2)$	$(3,4),(\mathbf{4},\mathbf{4}),(5,4)$	$(\mathbf{4},\mathbf{6}),(\mathbf{5},\mathbf{6})$
$\mathrm{I}_{0,1} \to \mathrm{V}_{1,2}$	$(3,3),(4,0),(4,2)$	$(\mathbf{4},\mathbf{4})$	$(4,6),(\mathbf{4},\mathbf{8}),(\mathbf{5},\mathbf{5})$
$\mathrm{I}_{0,1} \to \mathrm{V}_{2,2}$	$(3,2),(4,0),(4,2)$	$(3,4),(\mathbf{4},\mathbf{4}),(5,4)$	$(4,6),(\mathbf{4},\mathbf{8}),(\mathbf{5},\mathbf{6})$
$\mathrm{I}_{0,2} \to \mathrm{I}_{1,2}$	$(3,2),(3,3)$	$(3,4),(\mathbf{4},\mathbf{4}),(5,4)$	$(\mathbf{5},\mathbf{5}),(\mathbf{5},\mathbf{6})$
$\mathrm{I}_{0,2} \to \mathrm{I}_{2,2}$	$(3,2)$	$(3,4),(\mathbf{4},\mathbf{4}),(5,4)$	$(\mathbf{5},\mathbf{6})$
$\mathrm{I}_{1,1} \to \mathrm{I}_{1,2}$	$(2,2),(4,3)$	$(\mathbf{4},\mathbf{4})$	$(\mathbf{4},\mathbf{5}),(\mathbf{6},\mathbf{6})$
$\mathrm{I}_{1,1} \to \mathrm{I}_{2,2}$	$(2,2),(4,2)$	$(\mathbf{4},\mathbf{4})$	$(\mathbf{4},\mathbf{6}),(\mathbf{6},\mathbf{6})$
$\mathrm{I}_{1,1} \to \mathrm{II}_{1,1}$	$(2,2),(4,3)$	$(\mathbf{4},\mathbf{4})$	$(\mathbf{4},\mathbf{5}),(\mathbf{6},\mathbf{6})$
$\mathrm{I}_{1,1} \to \mathrm{III}_{1,1}$	$(2,2),(4,2)$	$(\mathbf{4},\mathbf{4})$	$(\mathbf{4},\mathbf{6}),(\mathbf{6},\mathbf{6})$
$\mathrm{I}_{1,1} \to \mathrm{V}_{2,2}$	$(2,2),(4,0),(4,2)$	$(\mathbf{4},\mathbf{4})$	$(4,6),(\mathbf{4},\mathbf{8}),(\mathbf{6},\mathbf{6})$
$\mathrm{I}_{1,2} \to \mathrm{I}_{2,2}$	$(2,2),(3,2)$	$(3,4),(\mathbf{4},\mathbf{4}),(5,4)$	$(\mathbf{5},\mathbf{6}),(\mathbf{6},\mathbf{6})$
$\mathrm{II}_{0,0} \to \mathrm{II}_{0,1}$	$(3,3),(4,3)$	$(\mathbf{4},\mathbf{4})$	$(\mathbf{4},\mathbf{5}),(\mathbf{5},\mathbf{5})$
$\mathrm{II}_{0,0} \to \mathrm{II}_{1,1}$	$(3,3),(4,2)$	$(\mathbf{4},\mathbf{4})$	$(\mathbf{4},\mathbf{6}),(\mathbf{5},\mathbf{5})$
$\mathrm{II}_{0,1} \to \mathrm{II}_{1,1}$	$(3,2),(3,3)$	$(3,4),(\mathbf{4},\mathbf{4}),(5,4)$	$(\mathbf{5},\mathbf{5}),(\mathbf{5},\mathbf{6})$
$\mathrm{II}_{0,1} \to \mathrm{III}_{0,0}$	$(3,2)$	$(3,4),(\mathbf{4},\mathbf{4}),(5,4)$	$(\mathbf{5},\mathbf{6})$
$\mathrm{II}_{0,1} \to \mathrm{V}_{2,2}$	$(3,0),(3,2)$	$(3,4),(3,6),(\mathbf{4},\mathbf{4}),$ $(5,2),(5,4)$	$(5,6),(\mathbf{5},\mathbf{8})$
$\mathrm{III}_{0,0} \to \mathrm{III}_{0,1}$	$(2,2),(4,3)$	$(\mathbf{4},\mathbf{4})$	$(\mathbf{4},\mathbf{5}),(\mathbf{6},\mathbf{6})$
$\mathrm{III}_{0,0} \to \mathrm{III}_{1,1}$	$(2,2),(4,2)$	$(\mathbf{4},\mathbf{4})$	$(\mathbf{4},\mathbf{6}),(\mathbf{6},\mathbf{6})$
$\mathrm{III}_{0,1} \to \mathrm{III}_{1,1}$	$(2,2),(3,2)$	$(3,4),(\mathbf{4},\mathbf{4}),(5,4)$	$(\mathbf{5},\mathbf{6}),(\mathbf{6},\mathbf{6})$
$\mathrm{III}_{1,1} \to \mathrm{V}_{2,2}$	$(2,0),(2,2),(4,2)$	$(2,4),(\mathbf{4},\mathbf{4}),(6,4)$	$(4,6),(6,6),(\mathbf{6},\mathbf{8})$
$\mathrm{IV}_{0,1} \to \mathrm{V}_{2,2}$	$(1,0),(1,2),(3,2)$	$(3,4),(\mathbf{4},\mathbf{4}),(5,4)$	$(5,6),(7,6),(\mathbf{7},\mathbf{8})$
$\mathrm{V}_{1,1} \to \mathrm{V}_{1,2}$	$(0,0),(2,2),(4,3)$	$(\mathbf{4},\mathbf{4})$	$(\mathbf{4},\mathbf{5}),(6,6),(\mathbf{8},\mathbf{8})$
$\mathrm{V}_{1,1} \to \mathrm{V}_{2,2}$	$(0,0),(2,2),(4,2)$	$(\mathbf{4},\mathbf{4})$	$(\mathbf{4},\mathbf{6}),(6,6),(\mathbf{8},\mathbf{8})$
$\mathrm{V}_{1,2} \to \mathrm{V}_{2,2}$	$(0,0),(2,2),(3,2)$	$(3,4),(\mathbf{4},\mathbf{4}),(5,4)$	$(\mathbf{5},\mathbf{6}),(6,6),(\mathbf{8},\mathbf{8})$

Table 3.4: Asymptotic splittings of all enhancements shown in figure 3.1. We assume $\hat{m} \geq 4$, otherwise not all enhancements can occur. A boldface $(\mathbf{m},\mathbf{n})$ indicates that V_{mn} contains some highest weight form a^{mn}_{jmn} defined around equation (3.7.4). Note that we did not include the 16 cases $\mathrm{I}_{0,0} \to$ Type B, since these are simply the one-modulus enhancements with all elements in $\mathcal{E}$ of the form $(\mathbf{4},\mathbf{m})$. The enhancement $\mathrm{I}_{0,1} \to \mathrm{I}_{1,2}$ has two different $\mathcal{E}$ set configurations, and we distinguish them by adding small labels a and b on top of the arrows.

for the enhancements $\mathrm{I}_{0,1} \to \mathrm{III}_{0,1}$ and $\mathrm{II}_{0,0} \to \mathrm{II}_{1,1}$. Secondly, two potentials might agree if we exchange the names $s \leftrightarrow u$. This happens, for example, for the enhancements $\mathrm{II}_{0,1} \to \mathrm{V}_{2,2}$ and $\mathrm{IV}_{0,1} \to \mathrm{V}_{2,2}$. Recall that all enhancements in table 3.4 are determined for fixed growth sector $\mathcal{R}_{12}$ defined in (3.5.2), which allows for the limit of sending first $s \to \infty$ and then $u \to \infty$. However, we can also look at the other sector $\mathcal{R}_{21}$, in which the roles of s and u are exchanged. This implies that a certain form of a potential can arise from two different enhancements depending on the considered growth sector, the chosen names s, u, and thus the order of limits. The physical significance of such phenomenon is not completely clear, but it appears to be partially related to the possibility of realising the combinations of enhancements that yield identical scalar potentials in geometry. This topic will be studied more systematically in future works.

3.5.3 Main example: enhancement from type II singularity

In this subsection we focus on an enhancement from the type II singularity, i.e. $\mathrm{II}_{0,1} \to \mathrm{V}_{2,2}$. This is one case appearing in table 3.4 and we already noted around (3.5.10) that it plays a special role, since it involves Sen's weak coupling limit. In fact, we will see later that it precisely reproduces the potential and de Sitter no-go result of [154].

	V_{light}		V_{rest}					V_{heavy}	
$\mathcal{E}$	$(3,0)$	$(3,2)$	$(3,4)$	$(3,6)$	$(4,4)$	$(5,2)$	$(5,4)$	$(5,6)$	$(5,8)$
V_{mn}	V_{30}	V_{32}	V_{34}	V_{36}	V_{44}	V_{52}	V_{54}	V_{56}	V_{58}
$\dim V_{mn}$	1	1	1	1	$\hat{m}-2$	1	1	1	1
Basis	v_{30}	v_{32}	v_{34}	v_{36}	v^{κ}	v_{52}	v_{54}	v_{56}	v_{58}
Flux number	f_6	f_4	f_2	f_0	g_{κ}	h_0	h_1	h_2	h_3

Table 3.6: The data of the asymptotic splitting of the primitive middle cohomology $H^4_{\mathrm{p}}(Y_4, \mathbb{R})$ associated with the enhancement $\mathrm{II}_{0,1} \to \mathrm{V}_{2,2}$. The basis and flux numbers of the subspace V_{44} are denoted by g_{κ} and v^{κ} with $\kappa = 1, \ldots, \hat{m}-2$. Note that we assume $\hat{m} \geq 4$, so all the subspaces are present in the asymptotic splitting.

Let us first record the asymptotic splitting associated to this enhancement. According to table 3.4, we have $\mathcal{E}_{\text{light}} = \{(3,0),(3,2)\}$, $\mathcal{E}_{\text{heavy}} = \{(5,6),(5,8)\}$, and $\mathcal{E}_{\text{rest}} = \{(3,4),(3,6),(4,4),(5,2),(5,4)\}$. The asymptotic splitting is then explicitly

Enhancements	Potential $V_{\rm M}$
$\mathrm{I}_{0,1}$, $\mathrm{V}_{1,1}$ → $\mathrm{V}_{1,2}$	$\frac{c_1}{s}+\frac{c_2}{u^4}+\frac{c_3}{u^2}+c_4u^2+c_5u^4+c_6s-c_0$
$\mathrm{I}_{0,1}$, $\mathrm{V}_{1,2}$ → $\mathrm{V}_{2,2}$	$\frac{c_1}{us}+\frac{c_2}{u^4}+\frac{c_3}{u^2}+\frac{c_4u}{s}+\frac{c_5s}{u}+c_6u^2+c_7u^4+c_8us-c_0$
$\mathrm{I}_{1,1}$, $\mathrm{V}_{1,1}$ → $\mathrm{V}_{2,2}$	$\frac{c_1}{s^2}+\frac{c_2}{u^4}+\frac{c_3}{u^2}+c_4u^2+c_5u^4+c_6s^2-c_0$
$\mathrm{II}_{0,1}$, $\mathrm{IV}_{0,1}$ → $\mathrm{V}_{2,2}$	$\frac{c_1}{u^3s}+\frac{c_2}{us}+\frac{c_3u}{s}+\frac{c_4u^3}{s}+\frac{c_5s}{u^3}+\frac{c_6s}{u}+c_7us+c_8u^3s-c_0$
$\mathrm{I}_{0,1}$, $\mathrm{I}_{0,2}$ →[a] $\mathrm{I}_{1,2}$	$\frac{c_1}{us}+\frac{c_2}{u}+\frac{c_3u}{s}+\frac{c_4s}{u}+c_5u+c_6us-c_0$
$\mathrm{I}_{0,1}$, $\mathrm{II}_{0,1}$ → $\mathrm{II}_{1,1}$	
$\mathrm{I}_{0,1}$, $\mathrm{I}_{1,1}$ →[b] $\mathrm{I}_{1,2}$	$\frac{c_1}{s}+\frac{c_2}{u^2}+c_3u^2+c_4s-c_0$
$\mathrm{I}_{0,1}$, $\mathrm{III}_{0,0}$ → $\mathrm{III}_{0,1}$	
$\mathrm{II}_{0,0}$, $\mathrm{I}_{1,1}$ → $\mathrm{II}_{1,1}$	
$\mathrm{I}_{0,1}$, $\mathrm{I}_{1,2}$ → $\mathrm{I}_{2,2}$	$\frac{c_1}{us}+\frac{c_2}{u^2}+\frac{c_3u}{s}+\frac{c_4s}{u}+c_5u^2+c_6us-c_0$
$\mathrm{I}_{0,1}$, $\mathrm{III}_{0,1}$ → $\mathrm{III}_{1,1}$	
$\mathrm{I}_{0,1}$ ⇉ $\mathrm{I}_{0,2}$	$\frac{c_1}{s}+\frac{c_2}{u}+c_3u+c_4s-c_0$
$\mathrm{I}_{0,1}$ ⇉ $\mathrm{II}_{0,1}$	
$\mathrm{II}_{0,0}$ ⇉ $\mathrm{II}_{0,1}$	
$\mathrm{I}_{0,1}$, $\mathrm{II}_{0,0}$ → $\mathrm{II}_{0,1}$	
$\mathrm{I}_{0,1}$ ⇉ $\mathrm{I}_{1,1}$	$\frac{c_1}{us}+\frac{c_2u}{s}+\frac{c_3s}{u}+c_4us-c_0$
$\mathrm{I}_{0,2}$ ⇉ $\mathrm{I}_{2,2}$	
$\mathrm{II}_{0,1}$ ⇉ $\mathrm{III}_{0,0}$	
$\mathrm{I}_{1,1}$ ⇉ $\mathrm{I}_{2,2}$	$\frac{c_1}{s^2}+\frac{c_2}{u^2}+c_3u^2+c_4s^2-c_0$
$\mathrm{I}_{1,1}$ ⇉ $\mathrm{III}_{1,1}$	
$\mathrm{III}_{0,0}$ ⇉ $\mathrm{III}_{1,1}$	
$\mathrm{I}_{1,1}$, $\mathrm{III}_{0,0}$ → $\mathrm{III}_{1,1}$	
$\mathrm{III}_{1,1}$ ⇉ $\mathrm{V}_{2,2}$	$\frac{c_1}{u^2s^2}+\frac{c_2}{s^2}+\frac{c_3}{u^2}+\frac{c_4u^2}{s^2}+\frac{c_5s^2}{u^2}+c_6u^2+c_7s^2+c_8u^2s^2-c_0$

Table 3.5: Enhancements and their associated asymptotic scalar potential $V_{\rm M}$. In this table, we group together the enhancements that are simply identical or identical as we exchange the growth sector $\mathcal{R}_{12}$ and $\mathcal{R}_{21}$, i.e., exchange s with u. In each box there are two arrows with the upper one valid for the growth sector $\mathcal{R}_{12}$ and the lower one valid for the growth sector R_{21}. The double-arrow cases, e.g. $\mathrm{III}_{1,1}\to\mathrm{V}_{2,2}$ in the last row, have the scalar potential $V_{\rm M}$ symmetric in s and u. The coefficients c_i with $i>0$ are positive, while the sign of c_0 is undetermined.

given by

$$H^4_{\rm p}(Y_4,\mathbb{R}) = V_{30}\oplus V_{32}\oplus V_{34}\oplus V_{36}\oplus V_{44}\oplus V_{52}\oplus V_{54}\oplus V_{56}\oplus V_{58}\ , \qquad (3.5.11)$$

where the dimension and basis of each subspace is summarized in table 3.6 and we have also recorded our choice of notation for the flux numbers in the enhancement $\mathrm{II}_{0,1}\to \mathrm{V}_{2,2}$. The flux numbers are defined to be the coefficient of a flux G_4 in the basis shown in table 3.6 to the asymptotic splitting, i.e.

$$G_4 = f_6 v_{30}+f_4 v_{32}+f_2 v_{34}+f_0 v_{36}+g_\kappa v^\kappa+h_0 v_{52}+h_1 v_{54}+h_2 v_{56}+h_3 v_{58}\ . \qquad (3.5.12)$$

The particular names of flux numbers are chosen for convenience of our discussion in section 3.6.3 when we show that our formalism reproduces well-known existing no-go results. Furthermore, taking into account the orthogonality relation (3.3.15), we normalize the basis such that

$$\langle v_{30}, v_{58}\rangle = \langle v_{32}, v_{56}\rangle = \langle v_{34}, v_{54}\rangle = \langle v_{36}, v_{52}\rangle = 1. \qquad (3.5.13)$$

The pairing in the basis v^κ of V_{44} will be denoted by $\eta^{\kappa\lambda}$. It is positive, i.e. one has $\eta^{\kappa\lambda}g_\kappa g_\lambda > 0$ for non-zero g_κ.

Applying the asymptotic splitting of flux (3.5.12) and table 3.6 to the asymptotic behavior of the scalar potential (3.5.8), we have

$$V_{\rm M}\sim \tfrac{1}{\mathcal{V}_4^3}\left(\tfrac{A_{f_6}}{u^3 s}+\tfrac{A_{f_4}}{us}+\tfrac{A_{f_2}u}{s}+\tfrac{A_{f_0}u^3}{s}+\tfrac{A_{h_0}s}{u^3}+\tfrac{A_{h_1}s}{u}+A_{h_2}us+A_{h_3}u^3 s+A_{44}-A_{\rm loc}\right), \qquad (3.5.14)$$

where $A_{\rm loc}=\langle G_4, G_4\rangle$ and the coefficients in the growth terms are defined according to our notation of flux numbers in table 3.6 as follows

$$\begin{aligned} A_{f_6} &= \|\rho_{30}\|^2_\infty\,, \quad A_{f_4} = \|\rho_{32}\|^2_\infty\,, \quad A_{f_2} = \|\rho_{34}\|^2_\infty\,,\\ A_{f_0} &= \|\rho_{36}\|^2_\infty\,, \quad A_{h_0} = \|\rho_{52}\|^2_\infty\,, \quad A_{h_1} = \|\rho_{54}\|^2_\infty\,,\\ A_{h_2} &= \|\rho_{56}\|^2_\infty\,, \quad A_{h_3} = \|\rho_{58}\|^2_\infty\,, \quad A_{44} = \|\rho_{44}\|^2_\infty\,. \end{aligned}$$

Note that all A's are positive and still functions of the axions ϕ^1,ϕ^2 via the exponential in (3.5.6). Setting $\phi^i=0$ one finds that $A_{f_6}\propto (f_6)^2$, $A_{f_4}\propto (f_4)^2$ etc. With the asymptotic splitting (3.5.12) and the normalization (3.5.13), the tadpole condition (3.2.2) can be expressed as

$$\frac{\chi(Y_4)}{24} = \frac{1}{2}\langle G_4, G_4\rangle = f_6 h_3 + f_4 h_2 + f_2 h_1 + f_0 h_0 + \frac{1}{2}\eta^{\kappa\lambda}g_\kappa g_\lambda. \qquad (3.5.15)$$

Now we discuss the separation $G_4=\hat{G}_4+G_4^0$ of a flux G_4 into an unbounded part $\hat{G}_4$ and a remaining part G_4^0. First we deal with the unbounded component

$\hat{G}_4$ which belongs to V_{light}. By checking table 3.6, we see that the requirement $\hat{G}_4 \in V_{\text{light}}$ implies that an unbounded flux $\hat{G}_4$ can contain components f_6 or f_4. Also the first orthogonality in (3.3.39) and the massless condition (3.3.40) on $\hat{G}_4$ are automatically satisfied because we ask for $\hat{G}_4 \in V_{\text{light}}$.

Once an unbounded part G_4 is identified, the second condition in (3.3.39) can be used to restrict the remaining part G_4^0. The general results are displayed in table 3.7. We explain its derivation in an example where we take f_6 as the unbounded flux, i.e. we set $\hat{G}_4 = f_6 v_{30}$. Then, subtracting $\hat{G}_4$ from the splitting (3.5.12) we have the following form of $\widetilde{G}_4^0$ which needs further restriction

$$\widetilde{G}_4^0 = f_4 v_{32} + f_2 v_{34} + f_0 v_{36} + g_\kappa v^\kappa + h_0 v_{52} + h_1 v_{54} + h_2 v_{56} + h_3 v_{58}.$$

According to our normalization (3.5.13), it is readily computed that

$$\left\langle \hat{G}_4, \widetilde{G}_4^0 \right\rangle = 2 f_6 h_3. \tag{3.5.16}$$

Hence the second condition in (3.3.39) implies $h_3 = 0$, i.e.

$$G_4^0 = f_4 v_{32} + f_2 v_{34} + f_0 v_{36} + g_\kappa v^\kappa + h_0 v_{52} + h_1 v_{54} + h_2 v_{56}. \tag{3.5.17}$$

In this way, we have separated the flux components in G_4 into an unbounded flux component f_6 and the remaining flux components $f_4, \ldots, h_2$, with the condition that the flux component $h_3 = 0$ is absent. Inserting the condition $h_3 = 0$ into the tadpole condition (3.5.15), we see that the tadpole condition is then satisfied by the remaining components

$$f_4 h_2 + f_2 h_1 + f_0 h_0 + \frac{1}{2}\eta^{\kappa\lambda} g_\kappa g_\lambda = \frac{\chi(Y_4)}{24}. \tag{3.5.18}$$

We can now repeat this analysis for all combinations of possible unbounded fluxes f_6 and f_4, we obtain table 3.7. This data will be used in section 3.6 to determine the vacua of (3.5.14).

$\hat{G}_4$	G_4^0	Condition on G_4^0	Self-dual Pairs in G_4^0
f_6	$f_4, f_2, f_0, g_\kappa, h_0, h_1, h_2$	$h_3 = 0$	$(f_4, h_2), (f_2, h_1), (f_0, h_0)$
f_4	$f_6, f_2, f_0, g_\kappa, h_0, h_1, h_3$	$h_2 = 0$	$(f_6, h_3), (f_2, h_1), (f_0, h_0)$
f_6, f_4	$f_2, f_0, g_\kappa, h_0, h_1, h_2, h_3$	$f_6 h_3 + f_4 h_2 = 0$	$(f_2, h_1), (f_0, h_0)$

Table 3.7: All possible ways of separating G_4 into an unbounded flux $\hat{G}_4$ and a remaining part G_4^0. The third column, condition on the remaining part, is coming from the second orthogonality in (3.3.39). The tadpole condition can be found by applying the third column to (3.5.15) and it is satisfied by the remaining flux components. The forth column lists possible self-dual components inside G_4^0 which is introduced in section 3.3.4 and will be used in section 3.6.1.

3.6 Asymptotic structure of flux vacua

In this section we will analyze the vacua structure of the flux-induced scalar potential in the strict asymptotic regimes of the field space. We will focus on asymptotic two-moduli limits of the form (3.3.1) in the complex structure moduli space of a Calabi-Yau fourfold. These limits are characterized by two scalar fields, denoted as s, u, becoming large and the choice of a growth sector in (3.5.2), i.e. an order in the growth of the fields. We will select $\mathcal{R}_{12}$ describing paths in which s grows faster than u, but the results for the other growth sector can be trivially found after exchanging the roles of s and u and renaming the coordinates.

A complete classification of these two-moduli limits in the complex structure moduli space of a Calabi-Yau fourfold was performed in section 3.5 together with the scalar potential arising in each case (see table 3.5). Our starting point will, therefore, be the general asymptotic form of the flux potential derived in (3.5.8) and given by

$$V = \frac{1}{s^\alpha}\Big(\sum_{(m,n)\in\mathcal{E}} A_{mn} s^{m-4} u^{n-m} - A_{\rm loc}\Big) \equiv \frac{1}{s^\alpha}\Big(\sum_{i=1}^{\mathcal{N}} A_{m_i n_i} s^{m_i-4} u^{n_i-m_i} - A_{\rm loc}\Big)\,. \tag{3.6.1}$$

where the possible values for (m, n) are given in table 3.4 and depend on the type of limit under consideration. Recall that one just has to plug the values (m, n) of table 3.4 into eq. (3.6.1) to recover all possible potentials shown in table 3.5. For later convenience, we have re-labelled the elements of $\mathcal{E}$ as (m_i, n_i), $i = 1, \ldots, \mathcal{N}$, where $\mathcal{N}$ is the number of different pairs $(m, n) \in \mathcal{E}$ that can occur in each limit.

Notice that the coefficients A_{mn} are not arbitrary but depend on the integer fluxes and axions as in (3.3.42). However, we will leave them as free parameters in this section except for their sign, since they are restricted to be positive definite in the strict asymptotic regime (see eq.(3.3.42)). This way, we can keep our analysis more general and our results will also apply to higher dimensional moduli spaces with $h^{2,1} > 2$ in which there are more *spectator fields* in addition to the two moduli becoming large. In those situations, the coefficients A_{mn} will also be functions of these spectator fields, but the moduli scaling of s and u is expected to be the same. Interestingly, we will be able to formulate a no-go theorem for de Sitter only based on the scaling of s and u and independent of the concrete value of A_{mn} as long as they remain positive. Only in section 3.7 we will specify again the concrete values for A_{mn} to study axion stabilization and derive some universal results about backreaction effects in axion monodromy models.

The reader might have also noticed that we have included an additional overall factor $1/s^{\alpha}$ in (3.6.1) in comparison to (3.5.8). This will allow us to map our results to Type IIA flux compactifications, in which an additional factor of the dilaton appears upon performing mirror symmetry and going to the Einstein frame of Type IIA, as reviewed in section 3.2.2. This factor is known to be $1/s^3$ in the weak coupling limit, but we will leave the power also as a free parameter since its value is undetermined for any of the other limits of our list beyond weak coupling.

Therefore, the general potential (3.6.1) includes all the asymptotic potentials arising in M-theory flux compactifications in a Calabi-Yau fourfold (and their corresponding F-theory/Type IIB duals) if we set $\alpha = 0$, but can also describe other asymptotic string compactifications. The goal in this section is to take this general form of the asymptotic potential and analyze its vacuum structure. We will be particularly interested in whether this potential can admit any kind of vacuum at parametric control. Interestingly, since we have left the coefficients A_{mn} as arbitrary parameters, the above potential can also potentially yield AdS vacua. This is impossible in F-theory/Type IIB flux compactifications as the coefficients A_{mn} are correlated such that the potential is positive definite. However, it can occur in Type IIA flux compactifications where $A_{\rm loc}$ can receive contributions from other sources like metric fluxes or other components of NS flux which do not map to H_3 or F_3 fluxes in Type IIB. Hence, our general form of the potential will also allow us to study the conditions to get candidates for AdS vacua at parametric control. It is important to keep in mind, though, that they are only candidates in the sense that one should further check that the resulting values for A_{mn} are compatible with some top-down string construction.

Since this section contains many different interesting results about the structure of asymptotic flux vacua, let us add here a short outline of what comes next. In sections 3.6.1 and 3.6.2 we will describe our strategy to determine the (non-)existence of vacua at parametric control. We will then apply this strategy to a particular example corresponding to the familiar Sen's weak coupling limit and discuss the existence of dS and AdS vacua in section 3.6.3. Afterwards, we will apply the same methodology to all possible limits classified in section 3.5 and present the results for de Sitter in section 3.6.4 and for AdS vacua in section 3.6.5.

3.6.1 Flux ansatz and parametric control

In this chapter, we are interested in the presence of critical points at parametric control, i.e. for parametrically large field values of the scalars s, u. Let us recall that this is an additional constraint we need to impose as the asymptotic flux potential of (3.6.1) can in general yield vacua at finite values of s, u that are not necessarily large. Furthermore, we need to require to stay in a growth sector in order to be consistent with the strict asymptotic approximation, so the ratio s/u also needs to be large.

As it will become more clear through the following sections, we find that it is impossible to get any critical point at parametrically large field values of s, u if all fluxes are bounded by tadpole cancellation. Therefore, it becomes necessary to add some unbounded flux that can be adjusted to be large in the asymptotic limit. For this reason, we will assume the following general Ansatz for the fluxes,

$$G_4 = \hat{G}_4 + G_4^0 \tag{3.6.2}$$

where $\hat{G}_4$ is an asymptotically massless unbounded flux with respect to the remaining background fluxes in G_4^0. This special class of fluxes were introduced in section 3.3.5. We require them to be massless, in addition to unbounded, so that they only violate the self-duality condition mildly and it is restored in the limit. The fluxes in G_4^0 cannot be scaled to be large, but still must be consistent with generating a critical point at parametric control. We will consider two options, self-dual fluxes or more general fluxes with the same asymptotic scaling, as described in the following.

Self-dual fluxes G_4^0 :
Let us first consider in G_4^0 only fluxes that are self-dual in the strict asymptotic regime. The self-duality condition on the G_4-flux in the strict asymptotic regime was given in (3.3.31). In order to simplify the discussion and highlight the main

properties we assume that every subspace V_{mn} is one-dimensional, except for V_{44}. Because of the property (3.3.24) of the operator C_∞ and its relation to the $C_{\mathrm{sl}(2)}$ operator (3.3.27) (see also (3.B.14)), given an $(m,n) \in \mathcal{E}$, the minimal form of a non-vanishing self-dual flux should be

$$G_4 = g_{mn} v^{mn} + g_{8-m\,8-n} v^{8-m\,8-n} \ , \tag{3.6.3}$$

where v^{mn} is the basis vector of V_{mn} and no sum over m, n is taken in (3.6.3). The self-dual condition (3.3.37) on such G_4 further specializes for the case of two moduli into the following form

$$s^{m-4} u^{n-m} g_{mn} \mathcal{K}_{mn} = g_{8-m\,8-n} \ , \tag{3.6.4}$$

where $\mathcal{K}_{mn} = \|v^{mn}\|^2_\infty$. One realizes immediately that in most cases, if we impose two such conditions then both moduli s and u are fixed and one can find (finitely) many vacua by just imposing the self-duality conditions. All these vacua are Minkowski as the vacuum energy vanishes. It remains to check whether solving such self-dual conditions stabilizes the moduli inside the strict asymptotic regime, where s/u and u are required to be large. Since the product of flux components $g_{mn} g_{8-m\,8-n}$ contributes to the tadpole condition, we see that it is not possible to make both s/u and u parametrically large. So there are actually no vacua at parametric control using only self-dual fluxes.

We now turn on only one pair of self-dual components and allow for an unbounded massless flux as in (3.6.2). In this case, we can rewrite the self-dual condition (3.6.4) into

$$u = \left(\frac{g_{8-m\,8-n}}{g_{mn} \mathcal{K}_{mn}} \right)^{\frac{1}{n-m}} s^\beta , \tag{3.6.5}$$

where $\beta = \frac{4-m}{n-m}$. This actually imposes a correlation between two moduli in terms of fluxes that are bounded by tadpole condition. The possibilities for the exponent β are:

1. $\beta < 0$ The modulus u grows inversely with s, so it is not possible to get vacua at parametrically large field values of both s and u.

2. $\beta = 0$ The modulus u is completely fixed into a ratio of flux numbers bounded by the tadpole condition, so it is not possible to make it parametrically large.

3. $0 < \beta < 1$ In this case there is no obstruction to make s/u and u large, but only one combination is fixed.

4. $\beta \geq 1$ This case also includes $\beta = \infty$, where s is fixed into a ratio of flux numbers bounded by the tadpole condition. It is not possible to make s/u arbitrarily large to be consistent with the strict asymptotic approximation.

We can then see that only case 3 could yield vacua at parametric control. Since only one combination of s, u can be stabilized with the self-dual pair of fluxes, the other combination needs to be fixed by turning on some massless unbounded flux components so that we can dial both s/u and u into large values. To see this we substitute u given in terms of s by (3.6.5) back into the scalar potential and minimize the remaining one-variable potential with respect to s. The potential reads

$$V \propto \frac{1}{s^\alpha} \sum_{(\hat{m},\hat{n})\in\hat{\mathcal{E}}} \left(\hat{A}_{\hat{m}\hat{n}}\ s^{\hat{m}-4+\beta(\hat{n}-\hat{m})} - \hat{A}_{\rm loc} \right) , \tag{3.6.6}$$

where the sum only involves now unbounded massless fluxes. Recall that $\hat{m} \leq 4$ and $\hat{n} < 4$ are required for the flux to be massless. Interestingly, this potential can never yield de Sitter critical point for case 3 in which $0 < \beta < 1$, since all the terms involve negative powers of s. In F-theory/Type IIB flux compactifications, the contribution from $A_{\rm loc}$ cancels with the contribution from the pair of self-dual fluxes such that $\hat{A}_{\rm loc} = 0$. However, if we insist of keeping $\hat{A}_{\rm loc}$ as a free parameter so that it survives some negative contribution to the potential (as could occur in Type IIA flux compactifications), the potential (3.6.1) might also have AdS vacua. We check that, for all potentials in table 3.5, only the enhanced limit $\mathrm{II}_{0,1} \to \mathrm{V}_{2,2}$ could yield an AdS vacuum at parametric control with $0 < \beta < 1$. This case indeed corresponds to the famous large volume and weak coupling limit in IIA. We will explain in more detail this vacuum in section 3.6.3.

General flux G_4^0 :
Next, we will consider a more general situation in which any flux can appear in G_4^0, but still keeping the condition that the vacuum is at parametric control. Non self-dual fluxes can arise, for instance, from backreaction effects of localized sources in the string compactification. A way to implement the condition of parametric control is to require that all terms in the potential that are necessary to stabilize the moduli should scale in the same way as s, $u \to \infty$. In other words, we will look for solutions of the form

$$s \sim \lambda^p \ , \quad u \sim \lambda^q \ , \tag{3.6.7}$$

with p, q positive such that λ can be taken to be parametrically large. Each poten-

tial term will then scale as

$$V_i \sim A_i \lambda^{r_i} \ , \quad r_i = (m_i - 4 - \alpha)p + (n_i - m_i)q \ , \tag{3.6.8}$$

if A_i corresponds to a contribution from G_4^0. For massless unbounded fluxes in $\hat{G}_4$, there is no such a constraint as the flux can always be scaled up to yield the desired asymptotic scaling with λ.

We then require that a solution of the type (3.6.7) must be found only using unbounded massless fluxes and terms in G_4^0 yielding the same value for r and therefore scaling the same way with λ. This guarantees that the solution will still exist in the limit $\lambda \to \infty$, i.e. at parametrically large values of s, u. As a final check if a solution is found, we need to require that $p > q$ in order to have the ratio s/u large and be consistent with the strict asymptotic approximation. Similar scaling arguments to look for parametrically controlled vacua have also been recently used in [185, 186] for the weak string coupling limit in Type IIA compactifications. Let us stress that the non-trivial part of our analysis does not lie in applying such scaling arguments, but rather in identifying the asymptotic potentials that can arise in a valid flux compactification.

We will show the results for our main example in section 3.6.3, and then for all possible two-moduli limits in sections 3.6.4 and 3.6.5 in the case of dS and AdS vacua respectively. But first, let us discuss our method to solve the minimization equations in a systematic and convenient way.

3.6.2 Minimization conditions

In order to study the existence of extrema of the potential (3.6.1) we will translate the existence problem into a more convenient formulation using methods from linear optimization. To begin with, we note that the extrema of V are determined by the conditions

$$u\partial_u V = \sum_{i=1}^{\mathcal{N}} (n_i - m_i) V_i = 0 \ , \tag{3.6.9}$$

$$s\partial_s V = \sum_{i=1}^{\mathcal{N}} (m_i - 4 - \alpha) V_i + \alpha V_{\mathcal{N}+1} = 0 \ , \tag{3.6.10}$$

where we have defined

$$V_i \equiv \frac{A_{m_i n_i}}{s^\alpha} s^{m_i - 4} u^{n_i - m_i} \ , \quad V_{\mathcal{N}+1} = \frac{A_{\rm loc}}{s^\alpha} \ , \tag{3.6.11}$$

such that $V = \sum_{i=1}^{\mathcal{N}} V_i - V_{\mathcal{N}+1}$. We have introduced $V_{\mathcal{N}+1}$ in order to treat $A_{\rm loc}$ in analogy with other terms by associating it a scaling $m = n = 0$. We further define

$$V_0 \equiv |V|_{\partial V=0} \ , \tag{3.6.12}$$

i.e. introduce the absolute value of the potential at this extremum. The definition of V_0 implies that at the extremum one has

$$\sum_{i=1}^{\mathcal{N}} V_i - V_{\mathcal{N}+1} \pm V_0 = 0 \ , \tag{3.6.13}$$

where the positive sign implies an Anti-de Sitter extremum while the negative sign a de Sitter extremum. The equations (3.6.9), (3.6.10), and (3.6.13) can be packed into the following homogeneous system $Av = 0$ with

$$\mathcal{A} = \begin{pmatrix} m_1 - 4 - \alpha & m_2 - 4 - \alpha & \cdots & \alpha & 0 \\ n_1 - m_1 & n_2 - m_2 & \cdots & 0 & 0 \\ 1 & 1 & \cdots & -1 & \pm 1 \end{pmatrix} \tag{3.6.14}$$

and $v^T = (V_0, V_1, V_2, \ldots, V_{\mathcal{N}+1})$. Notice that we will have as many columns as contributions V_i to the potential with different m_i, n_i plus one.

We can now use Stiemke's theorem which states that either a linear homogeneous system $Av = 0$ possesses a solution with all variables positive or there exists a linear combination of the equations that has all non-negative coefficients, one or more of which are positive. Applied to our problem, one thus finds that either there exists a $v^T = (V_0, \ldots, V_{\mathcal{N}+1})$ such that

$$\mathcal{A}v = 0 \ , \quad V_\kappa > 0 \, , \ \kappa = 0, \ldots, \mathcal{N}+1 \ , \tag{3.6.15}$$

or there exists a $\pi^T = (a, b, c) \neq 0$ such that

$$(\mathcal{A}^T \pi)_\kappa \geq 0 \, , \ \kappa = 0, \ldots, \mathcal{N}+1 \ . \tag{3.6.16}$$

This second condition will be much easier to prove, and will allows us generalize some no-go theorems about de Sitter. Stiemke's theorem thus implies that (3.6.1) has no extremum with cosmological constant $\mp V_0$ if the following system of inequalities is feasible, i.e. has a non-trivial solution,

$$a(m_i - 4 - \alpha) + b(n_i - m_i) + c \ \geq \ 0 \ , \tag{3.6.17}$$

$$\alpha a - c \ \geq \ 0 \ , \tag{3.6.18}$$

$$\pm c \ \geq \ 0 \ , \tag{3.6.19}$$

where let us recall that + stands for AdS and − for dS. In other words, there will *not* be a dS (AdS) critical point if one can find $a, b \in \mathbb{R}$ such that (3.6.17) is satisfied for every pair (m_i, n_i) and $c \leq 0$ ($c \geq 0$). Notice that it only makes sense to impose the second inequality it if $V_{\mathcal{N}} \neq 0$. Analogously, if no non-trivial solution is found to (3.6.17), then the system has a critical point which is a solution of the minimization conditions (3.6.9). In order to determine whether it corresponds to a minimum or a maximum one would need to further study the Hessian matrix $\partial_i \partial_j V$. However, in this chapter, we will restrict ourselves to analyze the presence of critical points in general.

3.6.3 Parametrically controlled vacua for the main example

In this section we will analyze the presence of asymptotic flux vacua at parametric control for a particular example: the enhancement $\mathrm{II}_{0,1} \to \mathrm{V}_{2,2}$ in a two-dimensional moduli space. This enhancement is one of the possible limits appearing in table 3.4 and served as our main example in section 3.5.3. The importance of this example arises from the fact that it corresponds to the well known Sen's weak coupling limit and large complex structure limit in Type IIB. It can also be mapped to Type IIA at weak coupling and large volume, which will allow us to recover some no-go theorems for de Sitter vacua found in Type IIA compactifications [154, 187]. We will not find new results in this section, but it will serve us to exemplify the methodology that we will later apply to the other asymptotic limits of the moduli space of a Calabi-Yau fourfold.

The Sen weak coupling limit ($s \to \infty$) corresponds to a Type $\mathrm{II}_{0,1}$ singular divisor [184, 188]. When intersecting with a Type $\mathrm{IV}_{0,1}$ corresponding the large complex structure point ($u \to \infty$), it enhances to a Type $\mathrm{V}_{2,2}$ singularity of codimension-two at the intersection. The values of m, n consistent with this type of singularity are given in table 3.4 and imply a scalar potential of the form

$$V \sim \frac{1}{s^\alpha}\left(\frac{A_{f_6}}{u^3 s} + \frac{A_{f_4}}{us} + \frac{A_{f_2} u}{s} + \frac{A_{f_0} u^3}{s} + \frac{A_{h_0} s}{u^3} + \frac{A_{h_1} s}{u} + A_{h_2} us + A_{h_3} u^3 s \pm A_{\mathrm{loc}}\right), \tag{3.6.20}$$

as already stated in (3.5.14). From the perspective of Type IIB perturbative string theory ($\alpha = 0$), the fluxes denoted as f_p (h_p) correspond to different components of R-R flux F_3 (NS-NS flux H_3). as discussed in section 3.2.2. When mapping the potential to Type IIA flux compactifications at weak coupling and large volume (so $\alpha = 3$), it is important that we stay in the growth sector with s/u large, so that the 10d string coupling g_s remains small (see (3.2.13)). The R-R flux F_3 maps to R-R fluxes F_p in Type IIA (that is why we have chosen the notation), while

only h_0 maps to a NS flux in Type IIA. The other components have a more exotic interpretation in terms of geometric h_1 and non-geometric h_2, h_3 fluxes in Type IIA . In fact, the moduli dependence of the term proportional to h_1 can also arise as a contribution from the six-dimensional Ricci scalar in case the manifold has positive curvature, or from KK monopoles. The term $A_{\rm loc}$ has the right moduli dependence of a contribution from O6-planes. Since only the moduli dependence matters and not the specific value of the coefficients A_{mn}, our results will apply to compactifications involving any of these ingredients or any other object exhibiting the same moduli dependence as the above terms. See e.g. [189–198] for works attempting to construct classical de Sitter vacua using these ingredients. Notice that other types Oq-planes or NS5-branes are not captured in this setup, as their moduli dependence does not have a geometric interpretation in terms of G_4-fluxes in M/F-theory.

First of all, let us prove that in case that all fluxes are bounded, i.e. cannot take arbitrarily large values, it is impossible to have any AdS or dS extrema at parametric control. In order to get a solution at parametric control, we will apply Stiemke's theorem only to those terms that can scale with the same power of λ in (3.6.8). The groups of terms that give rise to the same asymptotic scaling are:

$$p = q \ : \qquad (f_4, h_0)\,, \quad (f_2, h_1, A_{\rm loc})\,, \quad (f_0, h_2)\ , \tag{3.6.21}$$

$$p = 2q \ : \qquad (f_2, h_0)\,, \quad (f_0, h_1)\ , \tag{3.6.22}$$

$$p = 3q \ : \qquad (f_0, h_0, A_{\rm loc})\ . \tag{3.6.23}$$

In particular, the pairs (f_0, h_0) and (f_2, h_1) correspond to self-dual pair of fluxes that exhibit the same asymptotic scaling that the negative term $A_{\rm loc}$. We can now check whether (3.6.17) can be satisfied for any of the above groups. The answer is that we can always find a solution to Stiemke's problem, meaning that there is no way to solve the minimization conditions at parametric control. Hence, there is nor AdS or dS minimum at parametric control if all fluxes are bounded.

It is not hard to see, however, that the preceding analysis is too restrictive to establish a general no-go statement, since it neglects the possibility to also adjust the fluxes to become large in the asymptotic limit. As explain in section 3.3.5, fluxes are expected to be bounded if they contribute to the tadpole cancellation condition. However, there is a special class of fluxes, namely the unbounded massless fluxes introduced in section 3.3.5, that do not contribute to the tadpole condition and violate the self-duality mildly. For this reason, in section 3.5.3, we identified all possible unbounded massless fluxes compatible with the singular limit taken for our main example (see table 3.7). In the following, we will consider a total flux

of the form (3.6.2) where we allow for unbounded massless fluxes $\hat{G}_4$ in addition to the group of flux terms (3.6.21)-(3.6.23) denoted as G_4^0. This means that we can always scale up $\hat{G}_4$ to achieve the desired asymptotic scaling on λ fixed by the scaling of the fluxes in G_4^0. Schematically, the procedure to find an AdS or dS minimum at parametric control goes as follows:

1. We select the fluxes in G_4^0 such that all of them exhibit the same asymptotic scaling. This imposes an extra constraint in table 3.7. In this case, there are six possibilities given by equations (3.6.21)-(3.6.23).

2. We add any massless flux $\hat{G}_4$ which is unbounded with respect to the choice of G_4^0, following table 3.7.

3. We check whether the Stiemke's problem (3.6.17) has a non-trivial solution.

G_4^0	$\hat{G}_4$	$s^\alpha V_0$	AdS vacuum	dS vacuum
(f_4, h_0)	f_6, f_4	λ^{-2q}	No	No
$(f_2, h_1, A_{\rm loc})$	f_6, f_4	λ^0	Yes if $\alpha > 0$	No
(f_0, h_2)	f_6	λ^{2q}	No	No
(f_2, h_0)	f_6, f_4	λ^{-q}	No	No
(f_0, h_1)	f_6, f_4	λ^{q}	No	No
$(f_0, h_0, A_{\rm loc})$	f_6, f_4	λ^0	Yes if $\alpha > 0$	No

Table 3.8: All possible fluxes that have the potential to provide a minimum at parametric control.

The results are summarized in table 3.8. Interestingly, the addition of the unbounded massless fluxes allow us to find now AdS but not dS vacua. This is expected from previous results in the literature [154], since the scalar potential (3.6.20) agrees with the one in [16, 154] when taking $\alpha = 3$. Hence, we recover the no-go theorems for de Sitter [154, 187, 191] in Type IIA flux compactifications at weak coupling and large volume based on the moduli scaling of the potential, including RR, NS and metric fluxes, O6-planes and even positive curvature. We also slightly generalize it by including geometric and non-geometric fluxes yielding

the moduli dependence associated to h_1, h_2 and h_3. The requirement of keeping parametric control of the vacuum is what usually fails in previous classical de Sitter construction attempts, as also recently noticed in [186, 199].

Regarding the AdS vacua, let us recall that they only appear thanks to leaving $A_{\rm loc}$ free instead of completing a perfect square. Therefore, they are not exactly the mirror duals of the Type IIB potentials with G_3-flux, but there should be some additional contribution to $A_{\rm loc}$. In such a case, we find that there are only two possible candidates for AdS vacua at parametric control as long as $\alpha > 0$. These two possibilities indeed correspond to the pair of what would-be self-dual fluxes in IIB in the case that $A_{\rm loc}$ was not a free parameter, but they loose such an interpretation in IIA.

Let us first consider the group of flux terms $(f_0, h_0, A_{\rm loc})$ with unbounded f_4. This is precisely the combination of fluxes used in [137] to get supersymmetric AdS vacua at parametrically large volume and small coupling in massive Type IIA. Taking $A_{f_4} \sim \lambda^2$ and $\alpha = 3$, the moduli and the potential energy will scale asymptotically as

$$s \sim \lambda^{3/2} \, , u \sim \lambda^{1/2} \; : \qquad \frac{s}{u} \sim \lambda \, , \quad V \sim \frac{1}{\lambda^{9/2}} \, . \tag{3.6.24}$$

This implies that if one makes A_{f_4} large enough, $\lambda^{1/2} > \gamma \gtrsim 1$, the vacua indeed lie in the growth sector (3.5.2) and the nilpotent orbit approximation (3.3.6) is valid. Actually, one finds that for this setting one can make γ stepwise larger when increasing the flux A_{f_4}. In this limit the strict asymptotic approximation using the sl(2)-norm (3.3.27) becomes more accurate, such that the existence of the considered vacua can indeed be trusted. However, let us stress that there could be other reasons for which this vacuum cannot be lifted to a true top-down string theory construction. Here, we are only checking if the scaling of the moduli is adequate to generate a vacuum at parametric control.

The Type IIA setting has several interesting features that follow from the scaling behavior (3.6.24). Firstly, one sees that the Hubble scale $H = \sqrt{V}/M_p^2$ becomes parametrically small when sending $\lambda \to \infty$. Secondly, as stressed in [137] these Type IIA solutions also enjoy a separation of scales between the Hubble scale and the Kaluza-Klein scale. The KK scale in Type IIA Calabi-Yau compactifications is given by

$$M_{KK} = \frac{g_s M_p}{(\mathcal{V}_s^{\rm A})^{2/3}} \sim \frac{M_p}{s t^{1/2}} \sim \lambda^{-7/4} \, , \tag{3.6.25}$$

implying $H/M_{KK} \sim \lambda^{-1/2} \to 0$. This would go against the strong versions of the AdS conjectures put forward in [200, 201]. In principle, it also seems possible to

get a similar result using the unbounded massless flux f_6 instead of f_4 but this possibility should, however, be discarded when we further impose axion stabilization as discussed in section 3.7.

The other possible candidate for AdS vacuum arises from considering the group of terms $(f_2, h_1, A_{\rm loc})$ with unbounded f_4 or f_6 (as in [202]). However, in this case s and u scale the same way, implying that s/u cannot be made large and the strict asymptotic approximation fails. Hence, this vacuum cannot be trusted in our setup. Let us mention, though, for completeness, that the vacuum energy and the KK scale also scale the same way at the asymptotic limit in this example, $H \sim M_{KK} \sim \lambda^{-3/2}$, implying that there would not be scale separation unlike in the previous example.

3.6.4 No-go results for de Sitter at parametric control

The power of using the theory of limiting MHS, is that it allows us to go beyond the singularities corresponding to large volume and weak coupling and study the asymptotic vacua structure for any other type of limit in a systematic way. As explained, the type of limit will determine the moduli scaling of the flux potential by providing the values of m, n in (3.6.1) that are allowed in each case. In this section, we will generalize our previous results to other types of singularities in the Calabi-Yau four-fold as long as they can be understood as the singular limit of only two moduli becoming large. These two moduli can correspond to any two complex structure moduli of the fourfold, so either bulk complex structure, dilaton or 7-brane moduli in Type IIB. All possible singular limits of this type have been classified in table 3.4 and the potentials have been explicitly written in table 3.5. We will take the same ansatz for the fluxes as in (3.6.2), including some unbounded massless fluxes $\hat{G}_4$ in addition to fluxes with the same asymptotic scaling in G_4^0. This guarantees that the minima of the potential (if any) will occur at parametrically large field values of the moduli. We find the following no-go theorem:

No-go statement: There is no dS critical point at parametric control near any two large field limit of a Calabi-Yau fourfold in the strict asymptotic approximation if the scalar potential V vanishes at the limit $s, u \to \infty$.

Let us recall that this no-go is valid for any possible two large field limit of a Calabi-Yau fourfold. Hence, our results go beyond previous no-go theorems found at the large volume and weak string coupling limits of Type II CY compactifications [154, 185–187, 191, 199, 203]. Generically our settings, if they have a Type II interpretation at all, will yield situations in which one is not at weak string cou-

pling. The systematics to argue for the validity of our statement, though, is very similar to the one taken for previous no-go theorems in which the moduli scaling of individual terms in the potential is exploited.

Our no-go also goes beyond the famous Maldacena-Nuñez no-go theorem [141] in the context of four-dimensional $\mathcal{N} = 1$ compactifications, which is based on solving the equations of motion of the internal geometry when there are only p-form gauge fluxes. Our starting scalar potential in M-theory includes higher derivative terms, as we also include the term depending on the Euler characteristic of the Calabi-Yau fourfold (3.2.2).[9] Under M/F-duality and the application of mirror symmetry, terms are well-known to map to effects arising, for example, from O6-planes. Furthermore, a certain G_4-flux component maps under this duality chain to the Romans mass. In addition we have further generalized our discussion by allowing for independent potential terms. This can prevent cancellations and correlations between the different terms assumed in the analysis of [141].

To avoid confusion, let us clearly list the assumptions that enter in the derivation of the above de Sitter no-go theorem. We require:

- Only two fields, denoted as s and u, become large although the moduli space can be higher dimensional.
- Parametric control: the vacuum should survive in the asymptotic limit as explained around (3.6.7), i.e. for parametrically large field values of s and u.
- Strict asymptotic approximation: we only keep the leading asymptotic growth of each term of the potential, as explained below (3.3.27).
- The potential should vanish asymptotically in the limit $s, u \to \infty$.

The first three assumptions will be relaxed in future work. As for the last one, it should be understood more as a consistency constraint to keep control of the compactification. Only self-dual fluxes satisfy the equations of motion of the Calabi-Yau, but have vanishing potential. To keep the analysis as general as possible, we have allowed for any type of flux that could ever be present, which implies that we are also allowing for some breaking of the self-duality condition. However, we impose that the potential should still vanish asymptotically so this breaking is mild and can be understood as a perturbation over the warped Calabi-Yau geometry. Otherwise, it seems to us that the potential should not be trusted if it diverges at

[9] See [163–166] for a complete treatment of M-theory higher-derivative terms relevant at this order.

the large field limit. Let us recall that this is a very mild assumption and most likely not enough to guarantee consistency of the scalar potentials we study. However, since we already get a no-go theorem for de Sitter, there is no need of reducing even further the list of examples by imposing further constraints like satisfying the equations of motion of the internal geometry, which is obviously a much harder task.

We can conclude that, for the moment, our findings are compatible with a generalized Dine-Seiberg problem [135], conjectured in [62, 63], valid for any asymptotic limit of a string compactification, forbidding the presence of de Sitter vacua at parametric control.

Finally, we can also check the (asymptotic) de Sitter conjecture [62] in our setting. This conjecture, not only implies the absence of dS vacua, but goes beyond it by providing a bound on the slope of the potential that also disfavors slow roll inflation. More precisely, it was conjectured in [62, 63] that there is an order one constant γ such that

$$|\nabla V| \equiv |(\partial_{z^K} V) G^{K\bar{L}} (\partial_{\bar{z}^L} V)|^{1/2} \geq \gamma V \ . \tag{3.6.26}$$

In the remaining of this subsection we ignore the axion dependence, and write all partial derivatives with respective to saxions $\partial_i = \frac{\partial}{\partial s^i}$. Let us assume that we can establish the following bound

$$f^{-2} \geq (\kappa^i_k s^k) G_{ij} (\kappa^j_l s^l) \ , \tag{3.6.27}$$

where κ^i_k is some constant matrix which we will determine below. Then we can use Cauchy-Schwarz to show the following estimate

$$(\partial_i V G^{ij} \partial_j V)^{1/2} \geq f (\partial_i V G^{ij} \partial_j V)^{1/2} ((\kappa^i_k s^k) G_{ij} (\kappa^j_k s^k))^{1/2} \geq f \partial_j V (\kappa^j_k s^k) \tag{3.6.28}$$

Therefore, if the following inequality holds

$$f \partial_j V (\kappa^j_k s^k) \geq \gamma V \tag{3.6.29}$$

then also the conjectured de Sitter bound is satisfied.

Let us next recall the Stiemke's problem we are using to prove for the absence of dS vacua,

$$a(m_i - 4 - \alpha) + b(n_i - m_i) + c \ \geq \ 0 \ , \tag{3.6.30}$$

$$\alpha a - c \ \geq \ 0 \ . \tag{3.6.31}$$

If this system of inequalities has a solution with $c \leq 0$ ($c \geq 0$), then the potential does not have a dS (AdS) extremum. Notice that the first inequality also implies that

$$\sum_{i=1}^{\mathcal{N}} (a(m_i - 4 - \alpha) + b(n_i - m_i) + c)V_i - (c - \alpha a)V_{\mathcal{N}+1} \geq 0 \tag{3.6.32}$$

as $V_i, V_{\mathcal{N}+1} > 0$. This further implies

$$as\partial_s V + bu\partial_u V \geq -cV \tag{3.6.33}$$

which corresponds to (3.6.29) with

$$\kappa_s^s = a \ , \qquad \kappa_u^u = b \ , \qquad c = -\gamma/f \tag{3.6.34}$$

and all others vanishing. Hence, as long as (3.6.27) is satisfied, we can show that the conjecture (3.6.26) holds by using the Stiemke's inequality (3.6.30) again.

Let us then check (3.6.27). The leading behavior of the metric can be computed from the asymptotic form of the Kähler potential in (3.4.2), obtaining

$$g_{t_1\bar{t}_1} = \frac{d_1}{s^2} \ , \quad g_{t_2\bar{t}_2} = \frac{d_2 - d_1}{u^2} \tag{3.6.35}$$

where d_1, d_2 are integers characterizing the singularity type as discussed after (3.4.2). Therefore, by only using this leading term of the metric, it is trivial to check that the bound (3.6.27) gets saturated for

$$f^{-2} = ad_1 + b(d_2 - d_1) \tag{3.6.36}$$

The next to leading order terms for the metric will be further suppressed in the asymptotic regime. Combining this with (3.6.34) we get that the parameter in the de Sitter conjecture is given by

$$\gamma^2 = |c|^2/(ad_1 + b(d_2 - d_1)) \tag{3.6.37}$$

where a, b, c are constrained to satisfy (3.6.33). We have already checked that it is always possible to find some values of a, b, c such that the Stiemke's inequalities (3.6.30), and thus (3.6.33), are satisfied for all two-moduli limits of the Calabi-Yau fourfold. The remaining question is whether this solution implies $\gamma \sim \mathcal{O}(1)$. For this reason we check if the system (3.6.30) has a solution with $\gamma > 1$, which is a stronger condition. Interestingly, we find that there is always such a solution, implying that the bound (3.6.27) is always satisfied for any limit as long as $d_1 \neq 0$

and/or $d_2 - d_1 \neq 0$ and $\alpha = 0$ in (3.6.1). If $d_1 = d_2 = 0$, then the enhanced singularity is of Type I, meaning that it is at finite distance, while $\alpha = 0$ selects the potentials coming from Type IIB/F-theory flux compactifications. If $\alpha \neq 0$ the bound (3.6.29) is only satisfied if both $d_1 \neq 0$ and $d_2 - d_1 \neq 0$. However, this bound is a stronger condition than (3.6.26) so it does not imply that de Sitter conjecture is not satisfied but only that we cannot determine its fate by considering only the leading term of the field metric.

To sum up, we find that the de Sitter bound (3.6.26) is satisfied for any asymptotic limit in F-theory flux compactifications which is at infinite distance in the complex structure moduli space of a Calabi-Yau fourfold. This nicely matches with the argument in [63] that relates the de Sitter Conjecture and the Distance Conjecture, as the latter only concerns infinite distance regimes. For finite distance singularities, the bound (3.6.27) is not necessarily satisfied to leading order so the analysis becomes more difficult and we leave it for future work.

3.6.5 Candidates for AdS minima at parametric control

Let us analyze the conditions to get AdS vacua at parametric control. First of all, let us stress again that an AdS vacuum is not possible in Type IIB/F-theory Calabi-Yau compactifications as the potential is definite positive. Even if there is a negative contribution coming from localized sources, it always completes a perfect square when imposing tadpole cancellation. However, an AdS vacuum might appear when dualizing the setup to Type IIA and assuming additional contributions to the tadpole cancellation conditions that do not necessarily impose anymore the completion of the perfect square. These additional sources can correspond for example to other fluxes that do not simply map to G_3 fluxes in Type IIB. They will modify the value of the coefficients A_{mn} and usually make $A_{\rm loc}$ to also depend on the complex structure moduli, but the moduli dependence of each term on the IIA dilaton s and the IIA Kähler modulus u is expected to be the same. Since we are not specifying the value of the coefficients A_{mn} here, this possibility is automatically incorporated in our analysis. Furthermore, there is an additional overall dilaton factor appearing in the dualization process that makes the negative contribution $V_{\rm loc}$ to become moduli dependent. This moduli dependence of the negative contribution is essential to get AdS vacua, as we will see.

The main observation of this section is that, in order to get a vacuum at parametric control, it is necessary to have an unbounded massless flux $\hat{G}_4$ satisfying the properties in (3.3.39) and (3.3.40). Otherwise, in the absence of this flux, it is easy

to check that the inequalities (3.6.17) always admit a solution with $c \leq 0$ implying the absence of AdS vacua at parametric control. In this section, we identify the unbounded massless fluxes $\hat{G}_4$ that arise at the different limits of table 3.4 for a given choice of G_4^0. Recall that the background fluxes in G_4^0 are chosen to have the same asymptotic scaling in order to yield minima at parametric control. From all possible combinations of fluxes, there are only seventeen yielding a candidate for AdS vacua at parametric control as long as $\alpha > 0$, listed in table 3.9. Notice that we are only checking for extrema of the potential, so they could correspond to either minima or maxima. However, even if s and u can be made parametrically large, we need to also check that s/u is large so that we remain in a growth sector (3.5.2) and the strict asymptotic approximation is valid.

For this purpose, we need to provide the asymptotic scaling of the moduli at the large field limit. This scaling of the moduli, as well as the scaling of the vacuum energy, can be determined even without providing the explicit solution for the scalars at the minimum, as we explain in the following. Let us denote $\hat{A}_{\hat{m}\hat{n}}$ as the flux coefficient associated to $\hat{G}_4$ and $A^0_{m_i n_i}$ the ones corresponding to G_4^0. The potential reads

$$V = \frac{1}{s^\alpha}\left(\frac{\hat{A}_{\hat{m}\hat{n}}}{s^{4-\hat{m}}u^{\hat{m}-\hat{n}}} - A_{\rm loc}\right) + \frac{1}{s^\alpha}\frac{A^0_{m_i n_i}}{s^{4-m_i}u^{m_i-n_i}} \tag{3.6.38}$$

where all terms must scale the same way asymptotically in order to survive at the large field limit and yield a minimum at parametric control. Taking into account that we can scale up the flux $A_{\hat{f}} \sim \lambda^2$ and denoting the scaling of the moduli as

$$s \sim \lambda^p \ , \quad u \sim \lambda^q \tag{3.6.39}$$

with $p, q > 0$, we get that the following equalities should hold true,

$$2 + p(\hat{m} - 4) + q(\hat{n} - \hat{m}) = 0 \tag{3.6.40}$$

$$(m_i - 4)p + (n_i - m_i)q = 0 \ . \tag{3.6.41}$$

This guarantees that all terms scale the same way with λ in the limit $\lambda \to \infty$. Furthermore, if an AdS solution exists, the vacuum energy will necessarily scale as

$$|V_0| \sim \lambda^{-\alpha p} \ . \tag{3.6.42}$$

Notice that p, q are uniquely determined due to (3.6.40) and (3.6.41), so they can be determined case by case. In table 3.9 we have included two columns with the asymptotic scaling of s and u in each case. Remarkably, only one case allows

for s/u large, meaning that the other solutions cannot actually be trusted as they go away from the strict asymptotic regime. Interestingly, this single solution with s/u large corresponds to the familiar case with f_0, h_0 fluxes and unbounded f_4 or f_6 in the enhancement $\mathrm{II}_{0,1} \to \mathrm{V}_{2,2}$. This is the example already found in Type IIA flux compactifications in [137, 202], and was discussed in great detail in section 3.6.3. It is quite remarkable that there are not other AdS vacua at parametric control appearing at any of the other limits of the Calabi-Yau fourfold.

It has been recently conjectured that AdS vacua with scale separation are in the swampland [201, 204]. This means that there should be an infinite tower of states with mass of the same order than the vacuum energy. If this tower corresponds to a KK tower, it further implies that there is no scale separation between the external and internal dimensions. In Type IIA Calabi-Yau compactifications at weak coupling, the KK scale is given by

$$M_{KK} = \frac{g_s M_p}{\nu^{2/3}} \sim \frac{M_p}{s u^{1/2}} \sim \lambda^{-p-q/2} \tag{3.6.43}$$

where we have replaced the asymptotic scaling of the moduli (3.6.39) in the last step. This would imply the following ratio with respect to the vacuum energy,

$$\frac{H}{M_{KK}} \sim \lambda^{-\alpha p/2+p+q/2} \tag{3.6.44}$$

where we have defined $H \equiv \sqrt{|V_0|}/M_p$. A scale separation would then be possible if $p > q/(\alpha - 2)$. Unfortunately, we cannot determine α in general. We only know that $\alpha = 3$ at the large volume and weak coupling point, which corresponds to the enhanced singularity of our main example in section 3.6.3. In that case, scale separation occurs since $p > q$, i.e. the dilaton s grows faster than the volume u. Hence, for $\alpha = 3$ the condition of being in the strict asymptotic regime is correlated to exhibit some scale separation.

In table 3.9 we have included a column specifying the value of (3.6.44) at each of the limits yielding AdS vacua. Interestingly, none of them would exhibit scale separation except for the typical example of weak coupling and large volume of Type IIA mentioned above and discussed more carefully around eq.(3.6.24). However, it is important to remark that the use of the KK scale (3.6.43) beyond the weak coupling limit is questionable and the results of this last column should not be taken very seriously. An alternative way to define a cut-off scale valid at any infinite distance singularity, regardless whether it occurs at weak coupling or large volume, could be by means of the Swampland Distance Conjecture. At each infinite distance singularity, there will be an infinite tower of states becoming exponentially

light, and the cut-off of the effective theory is given at most by the species scale of this tower. This tower has been identified in a systematic way for every infinite distance singular limit of Calabi-Yau threefolds in [5,81,136] and we leave the analogous analysis for fourfolds for future work. It would be interesting to check if any of the examples in table 3.9 could enjoy a scale separation between the vacuum energy and this SDC cut-off.

In fact, there seems to be an even deeper relation between these AdS vacua and the Distance Conjecture. We have seen that an unbounded massless flux is required to get candidates for AdS vacua at parametric control. The presence of this type of fluxes has the same mathematical origin than the presence of an infinite massless tower of stable charged states at the large field limit. The 'masslessness' condition for which the Hodge norm $||\hat{G}_4||^2$ should asymptotically vanish is equivalent to the condition required in [5] for a charged BPS state to become massless at the singular limit in a Calabi-Yau threefold. Furthermore, the condition to be 'unbounded' resembles the condition of stability for the BPS state [5]. The infiniteness of the tower would correspond, though, to whether the flux coefficient $\hat{A}_{\hat{m}\hat{n}} = ||\rho_{\hat{m}\hat{n}}(\hat{G}_4, \phi)||_\infty$ depends on the axionic fields.

3.7 Asymptotic structure of flux vacua: axion dependence

In the previous section we have discussed the stabilization of the fields s^i, corresponding to the imaginary part of $t^i = \phi^i + is^i$, by studying the potential (3.6.1). The goal of this section is to also include the dependence on the axions ϕ^i. Firstly, we will discuss the constraints that arise upon imposing stabilization via fluxes for the candidate AdS minima discussed in section 3.6.5. Secondly, we will derive some universal backreaction effects that appear when displacing the axions at large field values and discuss their implications for axion monodromy inflationary models.

3.7.1 Axion stabilization

So far we have studied the minimization of the potential with respect to the saxions s^i and ensured that the vacua are at large values of s^i. The axions do not need to be stabilized at large field values to have a minimum at parametric control. Hence, even if we have an axionic flat direction, this could be stabilized by higher order or non-perturbative corrections to the scalar potential. This implies that, in order to derive no-go theorems for de Sitter vacua at parametric control, it is

G_4^0	$\hat{G}_4$	s	u	H/M_{KK}
$(3,4),(4,4),(5,4)$	$(3,2)$	λ^1	λ^1	λ^0
$(3,4),(4,4),(5,4)$	$(4,3)$	λ^2	λ^2	λ^0
$(3,4),(4,4),(5,4)$	$(4,2)$	λ^1	λ^1	λ^0
$(3,4),(4,4),(5,4)$	$(4,0)$	$\lambda^{1/2}$	$\lambda^{1/2}$	λ^0
$(3,4),(4,4),(5,4)$	$(3,3)$	λ^2	λ^2	λ^0
$(3,4),(4,4),(5,4)$	$(2,2)$	λ^1	λ^1	λ^0
$(3,4),(4,4),(5,4)$	$(3,0)$	$\lambda^{1/2}$	$\lambda^{1/2}$	λ^0
$(3,6),(4,4),(5,2)$	$(3,0)$	λ^1	$\lambda^{1/3}$	$\lambda^{-1/3}$
$(3,6),(4,4),(5,2)$	$(3,2)$	$\lambda^{3/2}$	$\lambda^{1/2}$	$\lambda^{-1/2}$
$(2,4),(4,4),(6,4)$	$(2,0)$	$\lambda^{1/2}$	$\lambda^{1/2}$	λ^0
$(2,4),(4,4),(6,4)$	$(4,2)$	λ^1	λ^1	λ^0
$(2,4),(4,4),(6,4)$	$(2,2)$	λ^1	λ^1	λ^0
$(1,2),(4,4),(7,6)$	$(1,0)$	$\lambda^{1/3}$	λ^1	$\lambda^{1/3}$
$(1,2),(4,4),(7,6)$	$(3,2)$	$\lambda^{1/2}$	$\lambda^{3/2}$	$\lambda^{1/2}$
$(3,4),(4,4),(5,4)$	$(1,0)$	$\lambda^{1/2}$	$\lambda^{1/2}$	λ^0
$(3,4),(4,4),(5,4)$	$(1,2)$	λ^1	λ^1	λ^0
$(3,4),(4,4),(5,4)$	$(0,0)$	$\lambda^{1/2}$	$\lambda^{1/2}$	λ^0

Table 3.9: All possible combinations of flux terms yielding an AdS extremum (assuming $\alpha > 0$). In the last column we have replaced $\alpha = 3$ to relate to Type IIA perturbative string theory. The notation has been chosen according to table 3.4 in which we provide the integers $\ell = (m,n) \in \mathcal{E}$ associated to each flux term. Only the shaded examples present s/u large, consistent with the strict asymptotic approximation.

sufficient to study stabilization of the saxions. Clearly, if we aim to find a fully-fledged minimum, it is crucial to study axion stabilization as well. For this reason it is interesting to study the fate of the AdS extrema found in section 3.6.5 upon studying axion stabilization. It turns out that minimization of the potential with respect to the axions imposes additional constraints on the values of the limiting flux norm $A_{\boldsymbol{\ell}} = \|\rho_{\boldsymbol{\ell}}(G_4,\phi)\|^2_\infty$ that can invalidate some of the AdS extrema found previously.

Let us repeat for convenience the asymptotic form of the scalar potential in the strict asymptotic approximation. In the limit of two (saxionic) fields becoming

large with $\frac{s}{u} > \gamma, u > \gamma$, the potential reads

$$V = \frac{1}{s^\alpha}\Big(\sum_{(m,n)\in\mathcal{E}} \underbrace{\|\rho_{mn}(G_4,\phi,\psi)\|^2_\infty}_{A_{mn}}\, s^{m-4}u^{n-m} - V_{\text{loc}}\Big) \tag{3.7.1}$$

where $\phi \equiv \phi^1$ and $\psi \equiv \phi^2$ are the axionic partners of s and u respectively, as in (3.5.1). The ρ_{mn} arise as in (3.5.6) from the split into the vector spaces V_{mn}. In this section we will make the replacement $N_i \to N_i^-$ in (3.5.6), as this will simplify our discussion significantly. The operator N_i^- was introduced in (3.3.10) as part of the commuting $\mathfrak{sl}(2)$-triples in section 3.3.2. We note that using N_i would induce new mixed terms that are, however, suppressed in the strict asymptotic regime. Moreover, we expect that the conclusions of section 3.7.2 are not altered under the exchange $N_i \leftrightarrow N_i^-$. Therefore, we will now consider

$$\rho^-(G_4,\phi) = e^{-\phi^i N_i^-} G_4 = \sum_{(m,n)\in\mathcal{E}} \rho^-_{mn}\,. \tag{3.7.2}$$

In order to proceed it will be convenient to use an explicit basis of V_{mn} denoted by $v^{mn}_{j_{mn}}$ as in section 3.3.4. We will show in the following how such a basis can be constructed by starting with some highest weight states, and applying the successive action of the lowering operators N_i^-.

Firstly, we recall that given an $\mathfrak{sl}(2)$-algebra with generators $\{N^-, Y, N^+\}$ as in (3.3.10), every (finite dimensional) irreducible representation is isomorphic to a vector space generated by a highest weight vector $\hat{a}^{p+4}$, defined by demanding that $(N^-)^p\hat{a}^{p+4} \neq 0$ while $(N^-)^{p+1}\hat{a}^{p+4} = 0$, and its images under N^j. In other words the irreducible representation can be written as

$$\text{span}_{\mathbb{C}}\{\hat{a}^{l+4}, N^-\hat{a}^{l+4}, \ldots, (N^-)^l\hat{a}^{l+4}\}\,. \tag{3.7.3}$$

A general representation of this $\mathfrak{sl}(2)$-algebra is then given by a direct sum of irreducible representations. Therefore it suffices to specify a set of highest weight vectors to fix a representation of the $\mathfrak{sl}(2)$-algebra.

In the case of two-moduli case introduced in section 3.3.2, we have two copies of commuting $\mathfrak{sl}(2)$-algebras acting on $H^4_{\text{p}}(Y_4,\mathbb{R})$, turning it into a representation of two $\mathfrak{sl}(2)$-algebras. In order to specify a basis for $H^4_{\text{p}}(Y_4,\mathbb{R})$, we introduce the highest weight vectors $\hat{a}^{p+4,q+p+4}_\kappa \in V_{p+4,q+p+4}$ with $p,q \geq 0$. These states are characterized by the highest powers p,q of N_1^- and N_2^- that are not annihilating $\hat{a}_\kappa \equiv \hat{a}^{p+4,q+p+4}_\kappa$ as

$$\begin{aligned} &(N_1^-)^p\hat{a}_\kappa \neq 0\,, \qquad (N_1^-)^{p+1}\hat{a}_\kappa = 0\,, \\ &(N_2^-)^q\hat{a}_\kappa \neq 0\,, \qquad (N_2^-)^{q+1}\hat{a}_\kappa = 0\,. \end{aligned} \tag{3.7.4}$$

The index κ labels how many such highest weight states exist for the considered splitting. For example, there could be multiple $\hat{a}_\kappa$ in one $V_{p+4,q+p+4}$. In mathematical terms these highest weight states capture the information about the primitive part of $V_{p+4,q+p+4}$. Let us next discuss how the highest weight vectors span the spaces $V_{m,n}$. Each vector spaces V_{mn} is defined to be the simultaneous eigenspace of Y_1 and $Y_1 + Y_2$. Using the $\mathfrak{sl}(2)$-algebra we can generate a special basis $v^{mn}_{j_{mn}}$ of $V_{m,n}$ by acting with N_1^- and N_2^- on all highest weight vectors as

$$\left\{v^{m,n}_{j_{mn}}\right\}_{j_{mn}=1}^{\dim V_{m,n}} = \left\{(N_1^-)^a (N_2^-)^b \ \hat{a}_\kappa^{m+2a,n+2a+2b}\right\} \ , \tag{3.7.5}$$

where we have to use all highest weight states and therefore also collect the possible choices for the index κ. Before using this basis in studying the axions, it is worthwhile to add two observations. Firstly, in a Calabi-Yau fourfold there is always a highest weight vector a_0 which belongs to $V_{4+d_1,4+d_2}$, where d_1, d_2 are integers characterizing the singularity type as discussed after (3.4.2). Secondly, we note that the basis given by (3.7.5) is *not* yet compatible with our normalization (3.3.33), and we would reverse some signs for some of the basis vectors to ensure compatibility. It turns out the that normalization will not be relevant in this section and it suffices to use the basis (3.7.5).

Let us now return to our discussions of the axion-couplings appearing in (3.7.1). We first expand the ρ_{mn} into the basis (3.7.5) writing

$$\rho^-_{mn} = \sum_{j_{mn}} \varrho^{j_{mn}}_{m,n}(\phi,\psi)\, v^{m,n}_{j_{mn}} \ , \qquad \text{no sum over } (m,n) \ , \tag{3.7.6}$$

where $\varrho_{mn}(\phi,\psi)$ are the axion-dependent coefficient functions. We now show by using (3.7.5) that

$$\partial_\phi \varrho^{j_{mn}}_{m,n} = -\varrho^{j_{mn}}_{m+2,n+2} \ , \qquad \partial_\psi \varrho^{j_{mn}}_{m,n} = -\varrho^{j_{mn}}_{m,n+2} \ , \tag{3.7.7}$$

which holds due to the fact that the axions ϕ, ψ appear through an exponential factor $e^{-\phi^i N_i}$ in (3.7.2). It is now straightforward to minimize the scalar potential (3.7.1) with respect to the axions (ϕ,ψ). We first rewrite it in terms of the $\varrho^{j_{mn}}_{m,n}$ as in (3.4.12). The minimization conditions then read

$$\partial_\phi V = -\frac{2}{s^\alpha} \sum_{(m,n)\in\mathcal{E}} \sum_{\substack{i_{mn}\\ j_{mn}}} Z^{mn}_{i_{mn},j_{mn}}\, \varrho^{i_{mn}}_{m,n}\, \varrho^{j_{mn}}_{m+2,n+2} = 0 \ , \tag{3.7.8}$$

$$\partial_\psi V = -\frac{2}{s^\alpha} \sum_{(m,n)\in\mathcal{E}} \sum_{\substack{i_{mn}\\ j_{mn}}} Z^{mn}_{i_{mn},j_{mn}}\, \varrho^{i_{mn}}_{m,n}\, \varrho^{j_{mn}}_{m,n+2} = 0 \ , \tag{3.7.9}$$

with the asymptotic from of $Z^{mn}_{i_{mn},j_{mn}}$ given in (3.4.13). From these conditions (3.7.8) and (3.7.9), it is eminent that the stabilization of axions by fluxes imposes additional relations between the different $\varrho^{j_{mn}}_{m,n}$-functions and, therefore, in the coefficients A_{mn}. For instance, if an axion appears only through one function $\varrho^{j_{m'n'}}_{m',n'}$, the above minimization conditions imply that this $\varrho^{j_{m'n'}}_{m',n'}$ has to vanish at the minimum. This determines the vacuum expectation value of the axion in terms of the internal fluxes, but also implies that all terms proportional $\varrho^{j_{m'n'}}_{m',n'}$ are absent when studying the stabilization with respect to the saxions. Therefore, extrema of the potential that arise from self-dual fluxes found in section 3.6.5 might disappear when imposing these further constraints as some flux terms might not be present anymore.

For concreteness, let us illustrate the implications of these constraints in our main example of section 3.6.3. Using (3.7.2) and (3.5.12) we get

$$\varrho_{30} = f_6 - f_4\psi + \frac{1}{2}f_2\psi^2 - \frac{1}{6}f_0\psi^3 - h_0\phi + h_1\phi\psi - \frac{1}{2}h_2\phi\psi^2 + \frac{1}{6}h_3\phi\psi^3, \quad (3.7.10)$$

$$\varrho_{32} = f_4 - f_2\psi + \frac{1}{2}f_0\psi^2 - h_1\phi + h_2\phi\psi - \frac{1}{2}h_3\phi\psi^2\,, \quad \varrho_{56} = h_2 - h_3\psi, \quad (3.7.11)$$

$$\varrho_{34} = f_2 - f_0\psi - h_2\phi + h_3\phi\psi\,, \quad \varrho_{54} = h_1 - h_2\psi + \frac{1}{2}h_3\psi^2, \quad (3.7.12)$$

$$\varrho_{36} = f_0 - h_3\phi\,, \quad \varrho_{52} = h_0 - h_1\psi + \frac{1}{2}h_2\psi^2 - \frac{1}{6}h_3\psi^3\,, \quad \varrho_{58} = h_3, \quad (3.7.13)$$

which matches with the ϱ-functions coupled to the three-form gauge fields obtained from dimensionally reducing Type II compactification in [173]. In section 3.6.3 we found only two possible candidates for AdS vacua at parametric control, shown in table 3.8. It can be checked that if we want to keep the unbounded flux term V_{f_6} in the last row of the table, then we also need to turn on some h_1, h_2 or h_3 flux. Otherwise, (3.7.8) implies that $\varrho_{30} = 0$ at the minimum. For V_{f_4}, there are no new restrictions appearing. The analysis for the other types of asymptotic limits should be performed analogously. However, as explained in section 3.6.5, this example was the only one leading to an AdS vacua at parametric control consistent with the growth sector, so we conclude the analysis here.

3.7.2 Backreaction in axion monodromy inflation

It is also interesting to study the implications of the form (3.7.1) of the scalar potential for axion monodromy inflation [205, 206]. In such models one axion is displaced far from its minimum and then rolls down to its true vacuum. In order that such a model can be implemented, one would like to slowly roll down the scalar

potential along an almost purely axionic direction to keep control of the potential over large field excursions. However, backreaction effects can be very important and must be properly taken into account [207]. In the context of F-term axion monodromy models [208–211] in Calabi-Yau compactifications, this constitutes a real challenge [156, 157] as the problem is linked to the difficulties of achieving significant mass hierarchies. In particular, as pointed out in [138] and further analysed in [139, 140], a large displacement of an axion ϕ can severely modify the saxion vevs which backreact on the kinetic axionic term and substantially reduce the field range. In those papers, it was found by analyzing various examples that, in typical F-term axion monodromy models in Calabi-Yau compactifications, the saxion vev behaves at large field as

$$\langle s \rangle \sim \lambda \phi \tag{3.7.14}$$

implying the following backreacted kinetic term for the axion

$$\mathcal{L} \supset \frac{1}{s^2}(\partial\phi)^2 \sim \frac{1}{\lambda^2\phi^2}(\partial\phi)^2 \tag{3.7.15}$$

and only a logarithmic growth of the proper field distance $\Delta\phi \sim \frac{1}{\lambda}\log\phi$. Furthermore, as predicted by the Swampland Distance Conjecture, large field distances are accompanied by an exponential drop-off of the quantum gravity cut-off due to an infinite tower of states becoming massless as $s \to \infty$. Due to (3.7.14), a large displacement of ϕ implies necessarily a large displacement on the saxion s, so the quantum gravity cut-off behaves as

$$\Lambda_{QG} \sim \exp\{(-\lambda\Delta\phi)\} \tag{3.7.16}$$

spoiling inflation at distances $\Delta\phi > \lambda$. It was argued [138] that λ is an order one parameter in Planck units if the axion corresponds to the closed string sector of Type II compactifications. More generally, λ might be related to the mass hierarchy between the axion and the saxion [139], allowing for some room to get large field ranges, although this mass hierarchy seems very difficult to get in fully-fledged global string compactifications and is usually incompatible with keeping the moduli masses below the Kaluza-Klein scale [140]. It is still an open question whether this mass hierarchy can truly be obtained in a well controlled string compactification.

Although promising, this analysis of the backreaction in axion monodromy is very model dependent and is missing some general understanding of the underlying reason for which the minimization of the potential should always imply (3.7.14) at large field. Interestingly, we can now revisit this issue by taking advantage of

the universal tools that the mathematical machinery of asymptotic Hodge theory provides. This will allow us to prove (3.7.14) for most of the two-parameter large field limits arising in the Calabi-Yau compactification studied in the previous sections and, more importantly, provide the underlying geometric reason for such a linear backreaction at large field.

Let us first state the observation that aim to show in the following. We consider two-parameter field limits with saxion-axion pairs (s,ϕ) and (u,ψ). Our main focus will be on the (u,ψ)-pair, since the arguments are essentially identical for the (s,ϕ)-pair. We first extract the leading potential $V^{(\psi)}$, obtained by keeping the term in each A_{mn} in (3.7.1) that is dominant for large ψ. Below we will identify the two-parameter limits in which $V^{(\psi)}$ enjoys the following homogeneity property

$$V^{(\psi)}\big(s,\zeta u;\phi,\zeta\psi\big)=\zeta^{h}\;V^{(\psi)}\big(s,u;\phi,\psi\big)\,, \tag{3.7.17}$$

for some homogeneous degree h. Let us now assume that $V^{(\psi)}$ has a extremum $\langle u\rangle>0$, i.e. one demands that

$$0=\partial_u V^{(\psi)}\big|_{u=\langle u\rangle}\,. \tag{3.7.18}$$

Then, assuming that the scalar potential $V^{(\psi)}$ is a polynomial in $u,1/u$, and ψ, we find that $\langle u\rangle$ satisfies the linear-backreaction relation

$$\langle u\rangle\sim\lambda\psi\,, \tag{3.7.19}$$

as in (3.7.14). Therefore, our target is to check the homogeneity property (3.7.17) at leading order in ψ for all possible two-parameter enhancements.

We note that the intuition for the property (3.7.17) to hold is rather simple. Notice first that the axion ψ is always accompanied with a power of N_2^-, since it only appears via $\rho^-(G_4,\phi)=e^{-\phi N_1^- -\psi N_2^-}G_4$, see (3.7.2). Now one can use the fact that $N_2^-(V_{m,n})\subset V_{m,n-2}$, which is a simple consequence of the $\mathfrak{sl}(2)$-algebra, that the image of any basis vector $v^{n,m}_{j_{mn}}$ under N_2^- will be proportional to $v^{m,n-2}_{j_{m\,n-2}}$. We then deduce that while a flux along the basis vector $v^{mn}_{j_{mn}}$ yields a term proportional to $s^{m-4}u^{n-m}$ in the scalar potential, the vector $N_2 v^{m,n}_{j_{mn}}$ will induce a term proportional to $s^{m-4}u^{n-m-2}$. In other words, the action of N_2^- reduces the power of u by 2 in the scalar potential. Since one N_2^- is accompanied by a ψ, in the scalar potential term will be proportional to ψ^2, which precisely compensates the reduced u-power. This suggests that the scalar potential indeed can admit the homogeneity behavior (3.7.17), at least if the potential is not generated by a too degenerate set of highest weight states $a^{m,n}_{j_{mn}}$ as we see in the remainder of the subsection.

Following the discussion on the $\mathfrak{sl}(2)$-representations in subsection 3.7.1, we now expand G_4 in the special basis generated from highest weight vectors as in (3.7.5),

$$G_4 = \sum_{(m,n)\in\mathcal{E}} g_{m,n} v^{m,n} \,. \tag{3.7.20}$$

In this expansion we have suppressed the sum over j_{mn} to simplify the notation. This simplification will not alter our discussion about axion backreaction. The crucial point is that the special basis (3.7.5) allows us to split G_4 into terms as

$$G_4 = \sum_{\kappa} G_4(\hat{a}_\kappa) \,, \tag{3.7.21}$$

where $\hat{a}_\kappa$ are the highest weight vectors introduced in (3.7.4) and $G_4(\hat{a}_\kappa)$ is the part of G_4 whose basis elements are only generated by $\hat{a}_\kappa$. Crucially, the decomposition (3.7.21) is orthogonal with respect to the norms $||\cdot||_\infty$ and $||\cdot||_{\mathrm{sl}(2)}$ discussed in section 3.3.3. It will therefore suffice to discuss the potential induced by the individual components $G_4(\hat{a}_\kappa)$ and then add the various terms together.

The next step is to carry out the expansion (3.7.2) of the flux $\rho^-(G_4,\phi)$ into the special basis (3.7.5). It is straightforward to compute

$$\begin{aligned}\rho^-(G_4,\phi) &= \sum_{a,b}\sum_{(m,n)\in\mathcal{E}} \frac{(-1)^{a+b}}{a!b!}\phi^a\psi^b g_{mn}(N_1^-)^a(N_2^-)^b\, v^{m,n} \\ &= \sum_{a,b}\sum_{(m',n')\in\mathcal{E}} \frac{(-1)^{a+b}}{a!b!}\phi^a\psi^b g_{m'+2a,n'+2a+2b}\, v^{m',n'} \,,\end{aligned} \tag{3.7.22}$$

where in the last equality we have shifted the sum over (m,n), so we obtain the flux component

$$\varrho_{mn} = \sum_{a,b} \frac{(-1)^{a+b}}{a!b!}\phi^a\psi^b g_{m+2a,n+2a+2b} \,, \tag{3.7.23}$$

for each $(m,n)\in\mathcal{E}$. For each ϱ_{mn} we now extract the terms that have the leading growth in ψ and then determine their contributions in the scalar potential using (3.3.27) in the strict asymptotic regime. Let us denote by b_{mn} the highest power of ψ appearing in (3.7.23) for which $g_{m+2a,n+2a+2b_{mn}} \neq 0$. This implies the leading ψ contribution in ϱ_{mn} is given by

$$\varrho_{mn} \sim \sum_{a} \frac{(-1)^{a+b_{mn}}}{a!b_{mn}!}\phi^a\psi^{b_{mn}} g_{m+2a,n+2a+2b_{mn}} \,. \tag{3.7.24}$$

In the strict asymptotic regime the leading scalar potential $V^{(\psi)}$ will then take the schematic form

$$V^{(\psi)}(u,\psi) \cong \sum_{(m,n)\in\mathcal{E}} \psi^{2b_{mn}} u^{n-m} \,, \tag{3.7.25}$$

where the factor 2 in the ψ-power arises due to the norm-squared appearing in the asymptotic growth expression (3.3.27). Note that we have omitted all factors that are not related to ψ and u. It is eminent that this $V^{(\psi)}(u,\psi)$ is not necessarily homogeneous and rather one finds

$$V^{(\psi)}(\zeta u,\zeta\psi) \cong \sum_{(m,n)\in\mathcal{E}} \zeta^{n-m+2b_{mn}}\ \psi^{2b_{mn}} u^{n-m} \,, \tag{3.7.26}$$

whether or not one can factor out ζ as an overall scaling depends on the b_{mn}.

In order to identify the situations in which $V^{(\psi)}(u,\psi)$ given in (3.7.25) is actually homogeneous, we need to further characterize the exponents $n-m+2b_{mn}$. Here the split (3.7.21) becomes important. Since the potential splits into a sum in this decomposition it will suffice to discuss one of the terms depending on one of the highest weight vectors $\hat{a} \equiv \hat{a}_{\kappa'}$. In other words, we study the potential generated by the flux $G_4(\hat{a})$ and later piece all potentials together. It will also be important to introduce the highest power $\mu \equiv \mu(G(\hat{a}))$ of N_2^- that does not annihilate $G_4(\hat{a})$ as

$$(N_2^-)^\mu G_4(\hat{a}) \neq 0, \quad (N_2^-)^{\mu+1} G_4(\hat{a}) = 0\,. \tag{3.7.27}$$

The axion ψ appears in the scalar potential generated by this flux if $\mu > 0$. Let us now note that $g_{m+2a,n+2a+2b_{mn}}$ entering the leading term in (3.7.24) is associated to the basis vector $v^{m+2a,n+2a+2b_{mn}}$. Since we are concerned with the $G_4(\hat{a})$ part of the potential, we know that this basis element can be obtained by acting on the highest weight vector $\hat{a}$ by acting with $(N_1^-)^c$, $(N_2^-)^d$ for some $c,d \geq 0$ as in (3.7.5). This implies that $\hat{a} \in V_{m+2a+2c,n+2a+2b_{mn}+2c+2d}$ such that

$$v^{m+2a,n+2a+2b_{mn}} = (N_1^-)^c (N_2^-)^d \hat{a}\ . \tag{3.7.28}$$

By using the definition (3.7.4) we know that the highest power $q \equiv q(\hat{a})$ of N_2^- that does not annihilate the highest weight vector $\hat{a}$ is given by

$$q = n - m + 2b_{mn} + 2d\ . \tag{3.7.29}$$

Since μ is defined to be the highest power of N_2^- that does not annihilate $G_4(\hat{a})$, one also has

$$(N_2^-)^\mu v^{m+2a,n+2a+2b_{mn}} \neq 0\ , \qquad (N_2^-)^{\mu+1} v^{m+2a,n+2a+2b_{mn}} = 0\ , \tag{3.7.30}$$

since otherwise its flux component will not survive in the leading order of ψ in ϱ_{mn}. Expressing the basis vector using the highest weight vector $\hat{a}$ by inserting (3.7.28) and using that (3.7.28) contains d additional powers of N_2^- we infer that (3.7.30) implies

$$\mu + d = q \ . \tag{3.7.31}$$

Inserting (3.7.29) into this expression we find the relation

$$n - m + 2b_{mn} = 2\mu(G_4(\hat{a})) - q(\hat{a}) \ . \tag{3.7.32}$$

This equation completely determines the highest power of ψ appearing in (3.7.25). Note also that the left-hand side of this expression is the scaling of the individual terms in (3.7.26), while the right-hand side depends on the highest power $q(\hat{a})$ of N_2^- that does not annihilate $\hat{a}$ and the highest power $\mu(G_4(\hat{a}))$ of N_2^- that does not annihilate $G_4(\hat{a})$. In other words, we have translated the question of homogeneity into a condition on the highest weight state $\hat{a}$ and the flux $G_4(\hat{a})$. By plugging this into (3.7.26), the flux scalar potential satisfies

$$V^{(\psi)}(\zeta u; \zeta\psi) = \sum_\kappa \zeta^{2\mu(G_4(\hat{a}))-q(\hat{a})}\ V^{(\psi)}(G_4(\hat{a}_\kappa)) \ , \tag{3.7.33}$$

where we have used that we can split the leading flux scalar potential as $V^{(\psi)}(u;\psi) = \sum_\kappa V^{(\psi)}(G_4(\hat{a}_\kappa))$ since the involved norms split orthogonally with respect to the split (3.7.21). We can now determine under what circumstances the potential becomes homogeneous at large field as in (3.7.17).

The simplest case in which the homogeneity property (3.7.17) of $V^{(\psi)}$ is realized arises when we assume that G_4 contains only flux directions generated from *a single* $\hat{a}$. This implies that the sum (3.7.21) only contains a single term. In this case the homogeneity is immediate from (3.7.32), since there is just a single $q = q(\hat{a})$ and each term in (3.7.26) has the same power $\zeta^{2\mu-q}$. Our main example discussed in section 3.5.3 displays such behavior, as all spaces V_{mn} (except for V_{44}, which is not relevant here[10]) can be spanned by basis vectors built from $\hat{a} = a_0$ and one has $q(\hat{a}) = d_2 - d_1 = 3$.[11] Clearly, our main example is very special in this respect. However, the simple homogeneity argument extends to many other fluxes also in

[10] The constant terms V_{44} and $V_{\rm loc}$ always break the homogeneity property. However, it can be shown that, as long as there is some flux with a growth proportional to a positive power of u, then these constant terms only involve a subleading correction to (3.7.25) which becomes negligible for $\psi \gg 1$.

[11] Strictly speaking one has to transform the a_0 into its sl(2)-analog denote by $\tilde{a}_0$ in [136]. With the notation defined in (3.7.4) one can also write this element as $a^{4+d_1,4+d_2}$ with $(d_1, d_2) = (1, 4)$.

other enhancements. Interestingly, cases in which there is a single highest weight state $\hat{a}_\kappa$ can be understood as arising from a superpotential in a two-dimensional moduli space. In these cases, all the flux terms arise from $\hat{a} = a_0$ and the linear backreaction is automatically satisfied.

On the other hand, the homogeneity is not automatic if (3.7.21) contains parts from different heights weight vectors $\hat{a}_\kappa$. This can occur, for instance, when there are more moduli than those sent to a limit, and whose dependence is typically hidden in the value of a_0. Assuming that the basis elements in G_4 are built from two highest weight vectors $\hat{a}_1, \hat{a}_2$, we need to check whether or not

$$2\mu(G_4(\hat{a}_1)) - q(\hat{a}_1) = 2\mu(G_4(\hat{a}_2)) - q(\hat{a}_2) \ . \tag{3.7.34}$$

In order to check if this condition can be violated we inspect Table 3.4 and read of the possible $q = y - x$ (and $p = x - 4$) of the highest weight vectors $\hat{a}_\kappa = \hat{a}_\kappa^{x,y}$ in each enhancement. The easiest way to violate (3.7.34) is to consider the cases with $\mu = 0$, in which some terms of the scalar potential are independent of ψ, and pick two appropriate highest weight vectors from Table 3.4. More involved are situations in which $\mu > 0$. In these cases, one identifies that only special fluxes in the enhancements $\mathrm{I}_{0,1} \to \mathrm{I}_{2,2}$, $\mathrm{I}_{0,1} \to \mathrm{III}_{1,1}$, $\mathrm{I}_{0,1} \to \mathrm{V}_{2,2}$ can violate (3.7.34).[12]

Let us note that violating (3.7.34) does not imply that the linear relation (3.7.14) is necessarily violated. In fact, we can proceed to order the terms $V^{(\psi)}(G_4(\hat{a}_\kappa))$ in (3.7.33) by their scaling with ζ and denote the highest weight component with maximal $2\mu - q$ by $\hat{a}_1$. Clearly, if the condition $\partial_u V^{(\psi)}(G_4(\hat{a}_1)) = 0$ allows to fix u to a vacuum $\langle u \rangle_1$ then one has a linear backreaction $\langle u \rangle_1 \sim \lambda_1 \psi$ as in (3.7.14). The additive terms appearing in the full $V^{(\psi)}$ are then only yielding sub-leading corrections that are proportional to $1/\psi^n$, $n \geq 0$. In other words, also in these more involved situations, one cannot avoid a leading term in $\langle u \rangle$ proportional to the axion at large field.

It is also important to emphasize that the leading term in the axions for each flux term has the same coefficient given by the same internal flux, so it can be factorized out and plays no role in the minimization process. This implies that λ in (3.7.14) becomes a parameter $\lambda \sim \mathcal{O}(1)$ independent of the fluxes for the case of $h^{3,1} = 2$. Hence, in this case, one cannot use the fluxes to tune the parameter to be small, and the backreaction issues found in Calabi-Yau threefolds seem to be also present in the complex structure moduli space of Calabi-Yau fourfolds. If there are more moduli than those taken to the limit, λ could also depend on these

[12] The enhancements violating the to (3.7.34) analog condition in the (s, ϕ) coordinates for $\mu > 0$ are $\mathrm{I}_{1,2} \to \mathrm{I}_{2,2}$, $\mathrm{III}_{0,1} \to \mathrm{III}_{1,1}$, and $\mathrm{V}_{1,2} \to \mathrm{V}_{2,2}$.

spectator moduli, but its precise numerical value and how much it can be tuned goes beyond the scope of this chapter. This nicely links to the results obtained in [156]. Interestingly, these properties remain to be true when replacing N_i^- by N_i, i.e. when returning to the original expression for the scalar potential, since the leading terms will keep their characteristic behavior. This further strengthens the deep link of these homogeneity properties to the underlying geometric structure and deserves more study in the future.

If the homogeneity result persists in general, it clearly has important implications for axion monodromy inflation. The fact that $\lambda \sim \mathcal{O}(1)$ implies that the backreaction cannot be delayed and that the exponential drop-off of the cut-off (3.7.16) will occur as soon as the axionic field takes transplanckian field values. In this sense, inflating along an axionic direction does not allow one to travel further than inflating along the saxion, and both types of trajectories are sensitive to the exponential drop-off of the cut-off predicted by the Swampland Distance Conjecture [57]. This is consistent with the refined Distance Conjecture [58] and the transplanckian censorship [212]. Let us recall, though, that we are only studying gradient-flow trajectories satisfying (3.7.18), while there could be other type of trajectories yielding successful inflation for a few times M_p. Hence, although highly constraining the structure of the asymptotic potentials, the phenomenological impact of our result is unclear. In any case, we find remarkable that the linear backreaction found in [138–140] is indeed tied to a deep underlying mathematical structure arising at the asymptotic limits, which allow us to check the large field behavior of gradient flow trajectories in a model independent way and test in very general terms the swampland conjectures [57, 58, 212, 213] that disfavor transplanckian field ranges.

3.8 Conclusions

Motivated by the recent swampland conjectures on de Sitter and Anti-de Sitter vacua in string theory and progress on the Swampland Distance conjecture, we initiated in this chapter the systematic study of flux compactification at asymptotic regions in field spaces. Such asymptotic flux compactifications turn out to be remarkably constrained by the arising universal structure at the boundaries of geometric moduli spaces. This structure is described by asymptotic Hodge theory and corresponds to the appearance of so-called limiting mixed Hodge structures at each limit. While generally these constructions are mathematically involved, we have exploited two of their features in this chapter that are directly useful

in flux compactifications: (1) the asymptotic expression for the Hodge norm and the asymptotic flux potential can be determined and systematically approximated, (2) the appearing regimes and asymptotic behaviors can be classified using $\mathfrak{sl}(2)^{\hat{n}}$-representation theory. Importantly, these statements are true for any Calabi-Yau fourfold and hence allow us to infer general conclusions about the validity of the swampland conjectures and common features of all effective theories arising in these asymptotic regimes.

In order to systematically study the asymptotic flux scalar potentials we have focused in this chapter on F-theory compactifications on Calabi-Yau fourfolds with G_4 and then generalized the configurations to allow for non-positive definite potentials as they occur in Type IIA flux compactifications. We classified all possible two-field limits in such settings and determined all flux induced scalar potentials that can occur in the strict asymptotic regime. It is important to stress that these potentials are rather constrained and it seems hard to infer simple rules for their construction without referring to the underlying asymptotic Hodge theory. With this set of scalar potentials at hand, we were able to show that none of them possesses de Sitter vacua, at least, when demanding parametric control and looking at scaling limits of the coordinates. This allows us to establish a new no-go theorem for de Sitter in section 3.6.4 extending the existing literature. This no-go is in accord with the recent asymptotic de Sitter conjecture [63] and we showed that the latter is indeed satisfied if one focuses on infinite distance limits in F-theory flux compactifications. We did, however, not show that the bound on the potential suggested in [62, 63, 134] is satisfied for finite distance singular limits, but rather leave this as an interesting task for future research.

It is interesting to highlight that our asymptotic approach sheds new light on flux vacua that have been investigated in the past [7, 8]. We have seen that imposing self-duality on the fluxes imposes simple conditions on the large moduli in the strict asymptotic regime, since the associated Hodge operator identifies pairwise eigenspaces of the underlying $\mathfrak{sl}(2)$-structure. Self-duality in the vacuum ensures consistency with the equations of motion of F-theory and M-theory and leads to Minkowski vacua in these settings. To violate this condition only minimally, we introduced the notion of asymptotically massless flux by imposing that its Hodge norm vanishes when taking the asymptotic limit. Such fluxes can be unbounded by the tadpole constraint and are crucial when trying to engineer chains of vacua with parametrically controlled stabilized moduli. In fact, in our generalized settings these unbounded asymptotically massless fluxes allow to identify infinite chains of candidate AdS vacua at parametric control, in analogy to the F_4 flux component

in the Type IIA vacua of [137]. It turns out that the demand for parametric control actually yields the conditions for being in the strict asymptotic regime and hence ensures self-consistency of our approximation. However, even if these candidate vacua seemingly become increasingly well controlled as one approaches large field values, more work would be required to ensure consistency of the global compactification. While we believe that our findings illuminate the underlying structure, which is also key in the Type IIA vacua of [137], our analysis does not show the existence of these vacua. In fact, we have pointed out that the geometric requirements to have infinite chains of candidate AdS vacua appear to be similar to the ones relevant for the Swampland Distance Conjecture [5, 136], which puts conditions on the validity of effective theories. We hope that this refined understanding will eventually help to elucidate the status of such chains of AdS vacua.

Last but not least, we also analyze the axion dependence on the scalar potentials and obtain universal features about the large field behavior of gradient flow trajectories. Deeply linked to the underlying mathematical structure, we get that the potential becomes to leading order a homogeneous function at large field for any asymptotic limit, implying a linear backreaction on the moduli when displacing the axions. This provides the geometric origin of the backreaction pointed out in [138] and extends it to Calabi-Yau fourfolds, so it can also potentially apply to D7-brane moduli. We also find that the parameter controlling the backreaction is flux-independent so it cannot be tuned small for $h^{3,1} = 2$, constraining the length of these trajectories to transplanckian values before the effective theory breaks down. This sheds new light to the open debate [138–140, 145, 155–157, 214] about backreaction issues in F-term axion monodromy [208–211, 215] and provides evidence for the refined Distance Conjecture [57, 58]. It would be interesting to study how much of this story can be extrapolated to other compactifications [207]. Let us remark, though, that our current asymptotic analysis does not actually establish strong constraints on inflation at the moment. Such large field inflationary models often only require axion displacements of a few orders M_p which are not necessarily excluded even if $\lambda \sim \mathcal{O}(1)$ [216], in agreement with current experimental bounds.

Our findings immediately suggest several interesting and tractable problems to address in the future. To begin with, it would be desirable to extend the analysis of two-field limits to sending more fields to be large. The classification of all possible appearing structures would then allow one to analyze all possible flux scalar potentials, at least, in the strict asymptotic regime. It is curious to see if the no-goes on de Sitter vacua and the constructions of Anti-de Sitter vacua

can be generalized, possibly by employing inductive arguments. A challenging but exciting task is to then leave the strict asymptotic approximation and show that the findings persist. This would require to include corrections containing fractions of coordinates and induce numerous mixed terms into the flux scalar potentials. Furthermore, we are not including the effect of the warping on the geometry, so it would be interesting to study how this warping factor could modify the results. Eventually it is also desirable to generalize the classification of scalar potentials by going beyond Calabi-Yau manifolds. Let us stress that the used machinery, based on asymptotic Hodge theory, is not restricted to Calabi-Yau manifolds. In fact, it is actually algebraic in nature and not even requires the existence of an underlying geometric setting.

In conclusion, the presented chapter might be viewed as only a first step towards a much bigger goal of classifying the scalar potentials that can arise in string compactifications. The universal mathematical structure that emerges in the asymptotic regimes might not only allow us to test the Swampland Conjectures, but also yield new universal patterns and constraints that any low energy effective theory should satisfy to be consistent with a UV string theory embedding. Even if we are restricted to the asymptotic limits of the moduli space, let us recall that these regions correspond to regimes in which approximate global symmetries, weakly coupled gauge theories, and an Einstein gravity description typically arise. If one could show that the realization of these properties is necessarily tied to these asymptotic regimes, the systematic analysis of these limits could have important implications for phenomenology. For the moment, this universal structure indeed hints that there should be an underlying physical reason as of why all the effective field theories arising at these limits share some common features. This could be related to the restoration of global symmetries, the notion of emergence, the ubiquitous presence of string dualities, or something still to be discovered.

Appendices

3.A Brief summary of the underlying mathematical machinery

In this section, we briefly introduce the mathematical machinery, theory of degenerating variation of Hodge structure, behind the asymptotic splitting (3.3.12) and the growth estimation (3.3.27). More information on this theory for physicists can

be found in [5, 81, 82, 136]. The original mathematical papers are [75, 76, 107] and the discussion of enhancements among singularity types can be found in [113].

While the whole machinery is very general, for the sake of concreteness, let us focus on the primitive cohomology $H^4_{\rm p}(Y_4, \mathbb{C})$ of a Calabi-Yau fourfold Y_4. When the fourfold Y_4 is smooth, the cohomology $H^4_{\rm p}(Y_4, \mathbb{C})$ enjoys a Hodge decomposition

$$H^4_{\rm p}(Y_4, \mathbb{C}) = \bigoplus_{p+q=4} H^{p,q}, \tag{3.A.1}$$

where $H^{q,p} = \overline{H^{p,q}}$ and we denote by $H^{2,2}$ the primitive part of the space of harmonic $(2,2)$-forms. The above decomposition depends on the complex structure on the fourfold Y_4. As one deforms the complex structure while keeping Y_4 smooth, one varies the Hodge decomposition (3.A.1). This is described by the theory of variation of Hodge structure on the vector space $H^4_{\rm p}(Y_4, \mathbb{C})$.

As discussed in the main text of this chapter, for interesting physics to occur, one often needs to push the complex structure moduli to certain limit in the complex structure moduli space, to the extent that one is left with a singular Calabi-Yau fourfold Y_4. When this happens, mathematicians showed that the cohomology $H^4_{\rm p}(Y_4, \mathbb{C})$ of a singular Calabi-Yau usually cannot support a Hodge decomposition like (3.A.1). Instead, another structure, called the limiting mixed Hodge structure replaces the role of the Hodge decomposition (3.A.1). This structure is commonly defined in terms of filtrations, but here we refer to a characterization of such a structure showing its similarity with the Hodge decomposition (3.A.1). A more precise description in terms of filtrations is provided in appendix 3.B.

To define a limiting mixed Hodge structure, one first fix the dimension of various subspaces $h^{4-q,q} = \dim H^{4-q,q}$ in (3.A.1). Then a limiting mixed Hodge structure on the primitive cohomology $H^4_{\rm p}(Y_4, \mathbb{C})$ is given by a decomposition (called *Deligne splitting*)

$$H^4_{\rm p}(Y_4, \mathbb{C}) = \bigoplus_{0\leq p,q\leq 4} I^{p,q}, \tag{3.A.2}$$

where a generalized conjugation property given by (3.B.9) on $I^{p,q}$ and $I^{q,p}$ holds. Moreover, certain conditions on the dimensions of the subspaces $I^{p,q}$ in (3.A.2) have to be satisfied. They are

$$\begin{aligned} \dim I^{p,q} = \dim I^{q,p}, \quad & \dim I^{p,q} = \dim I^{4-q,4-p}, \text{ for all } p, q, \\ & \dim I^{p,q} \leq \dim I^{p+1,q+1}, \text{ for } p+q \leq 2, \\ & \sum_{p=0}^{4} \dim I^{p,q} = h^{4-q,q}, \text{ for all } q. \end{aligned} \tag{3.A.3}$$

As discussed in [113] and exemplified for Calabi-Yau threefolds in [136], the conditions on the dimensions of the subspaces (3.A.3) are enough to classify all[13] possible ($\mathbb{R}$-split) limiting mixed Hodge structures (3.A.2) on the middle cohomology $H^4_{\rm p}(Y_4,\mathbb{C})$ up to some change of basis. Since the conditions are about numerical dimensions, it is handy to record these numbers on a 5×5 lattice, with the left-bottom corner representing $p=0,q=0$, and p grows to the right horizontally while q grows upwards vertically. These grids recording the dimensions of $I^{p,q}$ are called Hodge-Deligne diamonds. As an example, we show the list of Hodge-Deligne diamonds in the two-moduli example discussed in section 3.5.2. The results are given in table 3.10. Note how the diamonds reflect the conditions in (3.A.3).

The enhancement relations of the form $\mathsf{Type\ A}\to\mathsf{Type\ B}$ are then derived by decomposing the Hodge-Deligne diamond of $\mathsf{Type\ A}$ and recombining into the diamond of $\mathsf{Type\ B}$ in a way coherent with the $\mathfrak{sl}(2)$-triples (3.3.10). Precise statements of the recipe can be found in [113] and exemplified in [136]. For the two-moduli case, the enhancement network is displayed in figure 3.1. When we derive each enhancement relation, we obtain the asymptotic splitting (3.3.12) simultaneously. Explicit example of this asymptotic splitting in Calabi-Yau threefolds can be found in [82]. We can also characterize the asymptotic splitting as follows. Let $\bigoplus I^{p,q}_{\mathsf{A}}$ and $\bigoplus I^{r,s}_{\mathsf{B}}$ denote the Deligne splitting of $\mathsf{Type\ A}$ and $\mathsf{Type\ B}$, respectively. Then

$$V_{mn}\cong\left(\bigoplus_{p+q=m}I^{p,q}_{\mathsf{A}}\right)\cap\left(\bigoplus_{r+s=n}I^{r,s}_{\mathsf{B}}\right),\tag{3.A.4}$$

as complex vector spaces, where V_{mn} is understood to be the complexification. Note that in the above expression it is valid to take the intersection on the RHS as $I^{p,q}_{\mathsf{A}}$ and $I^{r,s}_{\mathsf{B}}$ are subspaces of the same vector space, $H^4_{\rm p}(Y_4,\mathbb{R})$. This finishes our brief discussion on the underlying mathematical machinery.

3.B Norms associated with some special Hodge structures

In this section, we introduce norms associated with various special Hodge structures, including the asymptotic norm $\|\cdot\|^2_\infty$, which appears in the coefficients in

[13] In fact, these conditions can fully classify the $\mathbb{R}$-split limiting mixed Hodge structures up to some change of basis on the middle cohomology of a Calabi-Yau threefold. On Calabi-Yau fourfolds, there might be complications [113]. We expect that these complications do not change much of our physical conclusions, and we will address these complications in future work.

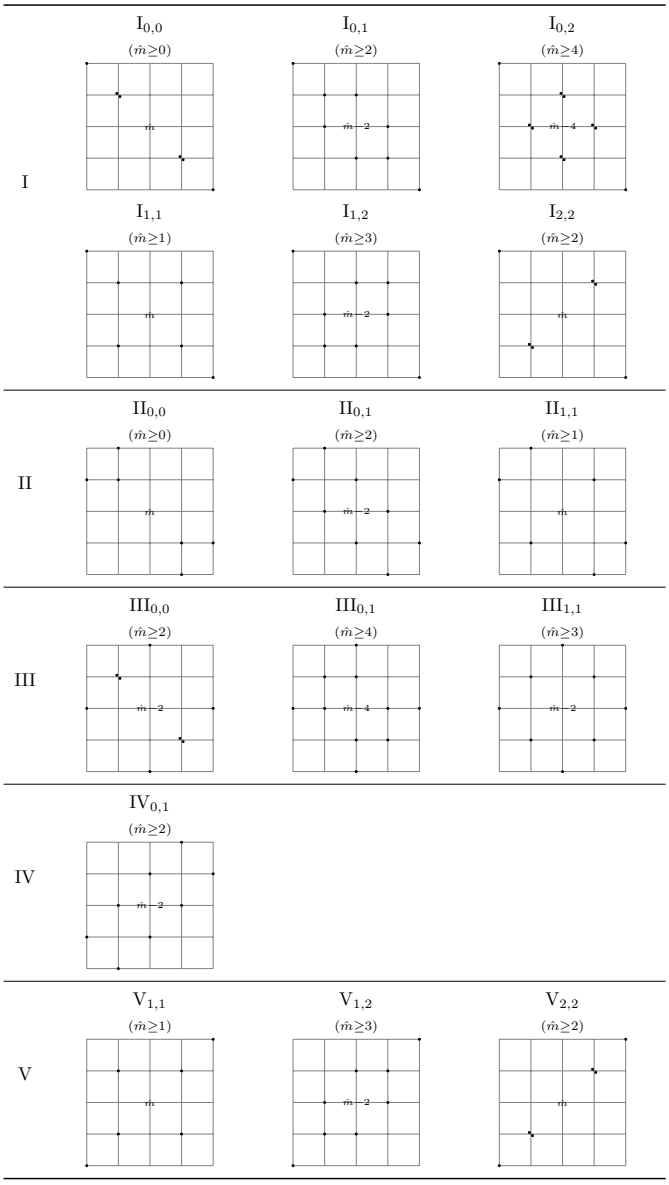

Table 3.10: Sixteen possible Hodge-Deligne diamonds with $h^{3,1} = 2$, corresponding to 16 singularity types given in table 3.3. We denote $h^{2,2} = \hat{m}$ and $i^{p,q} = \dim I^{p,q}$. Then the number of dots around the lattice point at (p, q) represents the value of $i^{p,q}$, and the label at $(2, 2)$ represents the value of $i^{2,2}$. The subscripts under a type are recording $i^{3,3}$ and $i^{3,3} + i^{3,2}$, respectively.

the asymptotic Hodge norm (3.3.27), and Weil operators $C_\infty, C_{\mathrm{sl}(2)}$ inducing these norms. We will adopt an approach different from appendix 3.A, by introducing everything in terms of filtrations so that the interested reader can compare the statements with mathematical literature [75, 76].

First we recall the definition of polarized Hodge structure on the primitive cohomology $H^4_{\mathrm{p}}(Y_4, \mathbb{C})$. To ease the notation, we denote the underlying integral cohomology $H_{\mathbb{Z}} := H^4_{\mathrm{p}}(Y_4, \mathbb{Z})$ and its complexification $H := H^4_{\mathrm{p}}(Y_4, \mathbb{C})$. A polarized Hodge structure of weight 4 on H is given by a decreasing filtration

$$0 \subset F^4 \subset F^3 \subset F^2 \subset F^1 \subset F^0 = H, \tag{3.B.1}$$

such that

$$F^p \oplus \overline{F}^{5-p} \cong H, \quad \text{for all } p. \tag{3.B.2}$$

We denote this Hodge structure on H by F when there is no danger of confusion. With such definition of a Hodge structure, one can rewrite it into the form of Hodge decomposition in (3.A.1) by setting the subspaces $H^{p,q} = F^p \cap \overline{F}^q$, where $p+q = 4$.

A Hodge structure F given by (3.B.1) also defines a Weil operator C_F, which is a linear automorphism of H such that when restricted to the subspace $H^{p,q} = F^p \cap \overline{F}^q$, it acts as a scalar multiplication by i^{p-q}: For every $v \in H^{p,q}$, define $C_F(v) = i^{p-q}v$. A polarization form of the structure (3.B.1) is given by an integer-valued bilinear form on $H_{\mathbb{Z}}$, $S : H_{\mathbb{Z}} \times H_{\mathbb{Z}} \to \mathbb{Z}$ and extended to the whole complexified space H linearly, such that $S(F^p, F^{5-p}) = 0$ for all p and $S(C_F(v), \overline{v}) > 0$ for all non-zero $v \in H$.

To compare with the existing discussion in section 3.3.3, we see that taking $F^p = \oplus_{r \geq p} H^{r,4-r}$ in the Hodge decomposition (3.A.1) gives us a Hodge filtration. Also the role of the Hodge star operator on the Calabi-Yau fourfold is played by the Weil operator, and the polarization form is given by the intersection bilinear form $\langle v, w \rangle = \int_{Y_4} v \wedge w$.

When we move into limits in the complex structure moduli space, in general the cohomology H will not support the existence of a pure Hodge structure. But we can still study the behavior of the Hodge structure in the limit. The machinery allowing such study is given by the theory of limiting mixed Hodge structures, which is developed in [75, 76]. The essential tool is a special generalization of pure Hodge structures, called limiting mixed Hodge structures. Let us briefly introduce such structures.

To define a limiting mixed Hodge structure on H, one still needs to specify a decreasing filtration

$$0 \subset F^4 \subset F^3 \subset F^2 \subset F^1 \subset F^0 = H, \tag{3.B.3}$$

but we do *not* impose conjugation property (3.B.2) on these F^p subspaces.

Furthermore, a new ingredient, weight filtration comes into the game. In the context of limiting mixed Hodge structures associated with limits of Hodge structure (3.B.1) of weight 4, the weight filtration is given by the *monodromy weight filtration* $W(N)$ depending on a given real nilpotent operator N,

$$0 \subset W_0(N) \subset W_1(N) \subset \cdots \subset W_8(N) = H_{\mathbb{R}}, \tag{3.B.4}$$

where $H_{\mathbb{R}} := H^4_{\mathrm{p}}(Y_4, \mathbb{R})$. The monodromy weight filtration is defined as the unique increasing filtration on $H_{\mathbb{R}}$ such that

$$N W_k(N) \ \subset \ W_{k-2}(N), \tag{3.B.5}$$

$$N^k : \frac{W_{4+k}(N)}{W_{3+k}(N)} \xrightarrow{\sim} \frac{W_{4-k}(N)}{W_{3-k}(N)}, \tag{3.B.6}$$

for all k. There is a compatibility condition on the filtrations F and W: On each graded quotient $\frac{W_k(N)}{W_{k-1}(N)}$, the filtration F induces a pure Hodge structure of weight k. Precise discussions on the definition of mixed Hodge structures can be found in [76]. We often denote a limiting mixed Hodge structure by $(F, W(N))$ or simply (F, N).

The filtrations F and W are related to the $I^{p,q}$ splittings discussed in appendix 3.A. In fact, the splitting $H = \bigoplus I^{p,q}$ is defined to be the unique splitting [76] such that, for all p, q, k,

$$F^p = \bigoplus_{r \geq p} I^{r,s}, \tag{3.B.7}$$

$$W_k = \bigoplus_{r+s \leq k} I^{r,s}, \tag{3.B.8}$$

$$I^{p,q} = \overline{I^{q,p}} \mod \bigoplus_{\substack{r<p \\ s<q}} I^{r,s}. \tag{3.B.9}$$

The 'big mod' in the last condition (3.B.9) looks annoying and those mixed Hodge structures without this 'big mod' deserves a special name. A mixed Hodge structure such that its $I^{p,q}$-splitting satisfies $I^{p,q} = \overline{I^{q,p}}$ for all p, q is said to be $\mathbb{R}$-split. To every mixed Hodge structure, Deligne [76,112] constructed a real operator δ such that the mixed Hodge structure $(e^{-i\delta}F, W)$ is $\mathbb{R}$-split. This operator δ is unique with certain properties, and we refer the reader to [76] for full discussion.

The limiting mixed Hodge structures and pure Hodge structures in limits are related by the nilpotent orbit theorem. Recall that locally the limit in the complex structure moduli space is given in local coordinates $t^1, \ldots, t^{\hat{n}}$ by sending

$t^1, \ldots, t^{\hat{n}} \to i\infty$. To each singular locus $t^j \to i\infty$ there is an associated nilpotent operator N_i, the logarithm of the monodromy operator. We usually record the change of the $(4,0)$-form Ω in a variation of Hodge structure on the primitive middle cohomology of a Calabi-Yau fourfold by period integrals. To describe the content of nilpotent orbit theorem, one needs to describe the dependence of the full Hodge filtration $F(t)$ on the complex structure moduli. The nilpotent orbit theorem tells us that the varying Hodge filtration $F(t)$ in the limit $t \to i\infty$ can be approximated by the so-called nilpotent orbit $F_{\rm nil}(t)$, which is a filtration given by

$$F_{\rm nil}(t) = e^{\sum_i t^i N_i} F_{\rm nil}, \tag{3.B.10}$$

where $F_{\rm nil}$ is the decreasing filtration defining a mixed Hodge structure, i.e., it does not necessarily satisfy (3.B.2). In section 3.3.1, the vector generating the subspace $F^4_{\rm nil}$ is denoted by a_0. The filtration $F_{\rm nil}$ and the monodromy weight filtration $W^{\hat{n}} := W(N_1 + \cdots + N_{\hat{n}})$ together define the limiting mixed Hodge structure $(F_{\rm nil}, W^{\hat{n}})$ associated to the degeneration of Hodge structure $F(t)$. From the discussion in the last paragraph, there is an operator δ associated to this limiting Hodge structure such that $(e^{-i\delta}F_{\rm nil}, W^{\hat{n}})$ is $\mathbb{R}$-split.

In section 3.3.2, we also discussed that when a singularity enhancement occurs, a set of commuting $\mathfrak{sl}(2)$-triples with nilnegative elements $N_1^-, \ldots, N_{\hat{n}}^-$ can be associated to such an enhancement. One conclusion of the sl(2)-orbit theorem in [76] states that, the filtration defined by

$$F_\infty = e^{i\sum_{i=1}^{\hat{n}} N_i^-} e^{-i\delta} F_{\rm nil}, \tag{3.B.11}$$

actually satisfies (3.B.2): $F^p_\infty \oplus \overline{F}^{5-p}_\infty \cong H$, for all p, and is polarized by the intersection bilinear form $\langle \cdot, \cdot \rangle$. In other words, F_∞ is a pure Hodge filtration of weight 4 polarized by $\langle \cdot, \cdot \rangle$. Let C_∞ be its Weil operator, then the asymptotic norm is defined by

$$\|v\|^2_\infty = \langle C_\infty v, \overline{v} \rangle \,. \tag{3.B.12}$$

What remains to be defined is the operator $C_{\mathrm{sl}(2)}$. This is the operator that brings the s^i/s^{i+1} scaling into the norm estimate (3.3.27). It is defined via the help of another operator

$$e(s) := \prod_{j=1}^{\hat{n}} \exp\left\{ \frac{1}{2} \log\big(s^j\big) Y_j \right\}, \tag{3.B.13}$$

where Y_i are the neutral elements in the commuting $\mathfrak{sl}(2)$-triples (3.3.10), and $e(s)$

operates on each subspace $V_{\boldsymbol{\ell}}$ as a scalar multiplication by

$$\big(\frac{s^1}{s^2}\big)^{\frac{l_1-4}{2}} \cdots \big(\frac{s^{\hat{n}-1}}{s^{\hat{n}}}\big)^{\frac{l_{\hat{n}-1}-4}{2}} (s^{\hat{n}})^{\frac{l_{\hat{n}}-4}{2}}.$$

Then the operator $C_{\mathrm{sl}(2)}$ is defined as

$$C_{\mathrm{sl}(2)} := e^{-1}(s) C_\infty e(s). \tag{3.B.14}$$

It is clear that the norm defined under $C_{\mathrm{sl}(2)}$ is given by expression (3.3.27). Note also that for any real vector v one has $\|v\|^2_{\mathrm{sl}(2)} = \big\langle C_{\mathrm{sl}(2)} v, v\big\rangle = \langle C_\infty e.v, e.v\rangle$, as e is an isometry of the polarization pairing. So our condition (3.3.31) on asymptotic self-dual fluxes G_4 with respect to $C_{\mathrm{sl}(2)}$ can also be written as a self-duality condition on $e.G_4$ with respect to F_∞.

4 Universal Axion Backreaction in Flux Compactifications

This chapter is based on: T. W. Grimm and C. Li, *Universal axion backreaction in flux compactifications*, JHEP **06** (2021), 067, [arXiv:2012.08272].

In this chapter, we study the backreaction effect of a large axion field excursion on the saxion partner residing in the same $\mathcal{N} = 1$ multiplet. Such configurations are relevant in attempts to realize axion monodromy inflation in string compactifications. We work in the complex structure moduli sector of Calabi-Yau fourfold compactifications of F-theory with four-form fluxes, which covers many of the known Type II orientifold flux compactifications. Noting that axions can only arise near the boundary of the moduli space, the powerful results of asymptotic Hodge theory provide an ideal set of tools to draw general conclusions without the need to focus on specific geometric examples. We find that the boundary structure engraves a remarkable pattern in all possible scalar potentials generated by background fluxes. By studying the Newton polygons of the extremization conditions of all allowed scalar potentials and realizing the backreaction effects as Puiseux expansions, we find that this pattern forces a universal backreaction behavior of the large axion field on its saxion partner.

4.1 Introduction and discussion

Axion monodromy inflation [171, 205–208] is an intriguing suggestion to realize large-field inflation in string theory. In such models, an axion is initially placed at a transplanckian distance away from its true vacuum and then rolls down towards the vacuum to drive inflation. The naive axion periodicity is extended in axion monodromy models by first unfolding the field range of the axion to the real line, i.e. by extending its field range to the universal covering space of the periodic axion space. An axion scalar potential is then introduced to break the approximate continuous shift symmetry of the axion. Such a potential is required to fulfil

a modified realization of a discrete axionic shift-symmetry in the sense that it is invariant under a combined transformation of the axion and some of the parameters in the potential, e.g. flux numbers. The combined transformation is called a monodromy transformation. In potentials realizing such monodromy symmetries one can then hope to implement inflation over multiple periods of the axion in a controlled fashion.

Early studies [205, 206] of axion monodromy inflation focus on its realization in non-supersymmetric Type II string compactifications with various NS-branes or D-branes. To establish such compactifications delicate control issues have to be addressed to ensure the validity of the reduction. To have from the outset more control over the stability of the setting, so-called F-term axion monodromy models were proposed in [145,207–211]. These models consider axion monodromy inflation in the context of supersymmetric flux compactifications of string theory and will serve as the main motivation for this chapter. In these settings the axion scalar potential is induced by turning on various background fluxes of higher form fields and the monodromy is realized by simultaneously shifting the axion and some flux numbers. An apparent merit of the F-term axion monodromy inflation is that various moduli of the compactified string theory share the flux-induced F-term scalar potential with the axion inflaton candidates, so that the study of the moduli stabilization and axion inflation are naturally linked.

The connection between the axion and moduli scalar potential forces one to consider the backreaction of the axion inflaton candidate on the vacuum expectation value of the moduli fixed by the F-term scalar potential. Since large field inflation requires a transplanckian displacement of the axion, it is alarming when such a large-field backreacts on the vacuum expectation value of geometric moduli of the compactification, since this requires to consider the dynamics of the combined axion-saxion system. This issue is pointed out in [138] and further analysed in [139, 140], by investigating examples in various classes of string compactifications. Their findings confirm the worry, that in these examples, a large axion excursion does indeed backreact on the geometric moduli in a linear fashion, so that the moduli is pushed towards the boundary of the moduli space at infinite distance. Invoking the Distance Conjecture [57, 58] the axion monodromy inflation program then faces more challenges as studied in the examples of [138–140]. More precisely, the Distance Conjecture states that in an effective field theory consistent with quantum gravity, a transplanckian displacement in field space is accompanied by additional light degrees of freedom, signalling a breakdown of the effective field theory. The linear backreaction of the axion onto the saxion can

thus be responsible for a breakdown of the effective theory. It remains an open debate [138–140, 145, 151, 155–157, 214] whether or not this backreaction can be avoided or sufficiently delayed to realize F-term axion monodromy models, see also the recent [87] where the authors argue that the linear backreaction is the maximum non-geodesity that would be consistent with the Distance Conjecture from a bottom-up perspective. The arising problems are also related to the difficulty of creating mass hierarchies in flux compactifications, as studied in [156, 157].

In order to study the axion backreaction problem, it is desirable to identify a general and controlled setting with a variety of axion-like fields. The complex structure moduli space of Calabi-Yau manifolds provides such a general arena. Firstly, it has long been known that the complex structure moduli descent to complex scalars in the effective theory. Secondly, it became clear in the advent of flux compactifications that these fields can obtain a scalar potential when allowing for non-trivial background fluxes [7, 8]. Within such flux compactifications, it was found in [217, 218] that fields with approximate continuous shift symmetry, i.e. axion fields, can only arise near certain boundary components of the complex structure moduli space. Near such a boundary component, the monodromy as one loops around the boundary descents to an approximate continuous shift-symmetry of the real part of the considered complex structure modulus, which is broken into a genuine discrete axionic shift-symmetry by non-perturbative effects. Moreover, by turning on background fluxes, one gets a scalar potential for the complex structure moduli which are decomposed into the axionic-like fields and the moduli controlling the geometry, and it is the very same monodromy transformation generating the shift-symmetry that is used as the monodromy transformation in the axion inflation scenario.

A concrete setting that allows us to examine complex structure axions and their flux-induced scalar potentials arises from F-theory compactifications on Calabi-Yau fourfolds. As briefly reviewed in Section 1.2.4, such compactifications lead to an $\mathcal{N} = 1$ supersymmetric effective action [41, 44] with a classical scalar potential induced by background four-form flux G_4. It is also well-known that a part of G_4 induces a non-trivial F-term potential [51] and it will be this part which will be relevant in the present chapter. The merit of studying complex structure axions in F-theory compactifications is at least two-fold. Firstly, the complex structure axions include the R-R zero-form axions of Type IIB string theory and also are dual to NS-NS two-form axions of Type IIA via duality. Moreover, one consistently incorporates certain axions that are associated to D-branes. Secondly, the scalar potential induced by the four-form flux in F-theory is particularly amenable

to be studied by asymptotic Hodge theory [75, 76] near the boundary of the complex structure moduli space as demonstrated in [13, 218]. These techniques have developed into a powerful tool to address various swampland conjectures in an example independent way [5, 13, 81, 83–86, 136, 218]. In particular, it has been observed in [218] that one can systematically analyze the axion backreaction using asymptotic Hodge theory.

In this chapter we generalize and complete the analysis of [218] and investigate, in full generality, the backreaction within a single axion-saxion pair arising near any boundary of the complex structure moduli space. Remarkably, we are now able to combine the insights from asymptotic Hodge theory and Newton polygons associated with Puiseux expansions to establish that there is universally a backreaction of the axion on its saxion partner which grows when considering large field values of the axion. To achieve this goal we first note that the asymptotic Hodge theory provides near every boundary in moduli space an approximation to the all relevant functions in the effective theory via the so-called nilpotent orbit [75]. The nilpotent orbit thus gives a near-boundary expansion that, by using the results of [75, 76], can be encoded by a set of boundary data.[1] A crucial part of this boundary data is a set of commuting $\mathfrak{sl}(2)$-algebras which decompose the middle cohomology of Calabi-Yau manifold into different $\mathfrak{sl}(2)$-representations. Also splitting a general four-form flux into such representations gives us precise control about the limiting behavior of Hodge norm and allows us to make the axion and saxion dependence in the scalar potential explicit. In fact, we find that the underlying $\mathfrak{sl}(2)$-structure ensures that the possible asymptotic scalar potentials generated by four-form fluxes form a rather constrained set. Systematically going through all allowed cases we can then study the axion backreaction generally. We do this by explicitly deriving the saxion vacuum expectation value determined by the extremization equation of the scalar potential. We evaluate this saxion vacuum value depending on the axion as a parameter and study the behavior of the solution in the limit when this parameter becomes large. The solution to this problem is given by Puiseux expansions, which present the solution as a fractional power series whose leading power is determined by a handy graphical tool called the Newton polygon. With the scalar potentials derived using asymptotic Hodge theory the Newton polygon provides visual guidance to the leading backreaction behavior of the saxion vacuum expectation value. This lets us uncover a universal backreaction behavior generalizing the result of [138–140, 218] that is present around any singularity in

[1] It was recently suggested in [13] that this is reminiscent of a holographic perspective, with an actual underlying bulk and boundary theory.

the Calabi-Yau fourfold complex structure moduli space.

Now we would like to state our results more concretely. In this chapter we focus on the backreaction of one complex structure axion field ϕ on the saxion modulus s in the same $\mathcal{N} = 1$ multiplet. We find that, when a vacuum exists, a large displacement of the axion ϕ always backreacts on the saxion vacuum expectation value $\overline{s}$ in the following fashion

$$\overline{s}(\phi) = c\phi^{\gamma} + \mathcal{O}\left(\frac{1}{\phi}\right), \tag{4.1.1}$$

where the prefactor $c > 0$ is a positive number and the exponent $0 < \gamma \leq 2$ is a rational number. There could be several different sets of c and γ corresponding to one flux configuration. We find that in almost every case, one has a solution with $\gamma = 1$, which agrees with the linear backreaction behavior found in [138–140, 218]. The cases with $\gamma > 1$ are rather restricted to the extent that only $\gamma = 2$ is allowed and they also need to satisfy a technical condition which is discussed at the end of section 4.4.3. We find only two flux configurations that generate $\gamma = 2$ backreaction and they have no $\gamma = 1$ branch. In contrast, we do not find additional restrictions on cases with $0 < \gamma < 1$ besides that the exponent γ should be rational. However, we note that for these cases there is sometimes a co-existing $\gamma = 1$ branch. Regarding the prefactor c in the backreaction, the possibility that c depends on flux numbers cannot be ruled out. Physically this implies that one cannot completely exclude a delayed backreaction. In section 4.4.3 we give a simple condition on the flux such that the delay cannot occur.

In view of our findings there are several interesting further studies that can be undertaken. Recalling the relation with the Distance Conjecture, it would be interesting to study the $\gamma \neq 1$ cases and the condition on the delay of a backreaction in the future. One first extension is to take into account subleading corrections following the strategy in [13] and check whether these extend the class of scalar potentials can arise. Furthermore, in this chapter we have only exploited the conditions for $\overline{s}$ to be at an extremum of the potential and not incorporated the additional constraints that actually is at a minimum. Hence, the relation (4.1.1) gives the necessary behavior also at minima, but it could well be that some of the cases with $\gamma \neq 1$ are not arising in an actual minimum. We would also like to point out that while for finding extrema it is sufficient to focus on one axion-saxion pair, the analysis of the conditions for having an actual minimum requires a more complete treatment of all involved moduli. We have already formulate the setting and the analysis in a general multi-variable language and we believe that it is desirable, while technically more difficult, to generalize the study of backreaction

to a multi-variable setting where the vacuum expectation values of all saxions are considered.

This chapter is structured as follows. In section 4.2, we introduce the physical setting of Calabi-Yau fourfold compactifications of F-theory, review variations of Hodge structures, and rewrite the F-theory scalar potential using Hodge theory. In section 4.3, we discuss the reason why only near the boundary of the complex structure moduli space axions can emerge, review the relevant part of asymptotic Hodge theory, and provide the asymptotic form of the F-theory scalar potential near the boundary. In section 4.4, after briefly setting up the notation for $\mathfrak{sl}(2)$-representations and reviewing the notion of Puiseux series and its associated Newton polygon, we expand the asymptotic scalar potential and solve the backreacted vacuum expectation value of the geometric moduli. There we will not only encounter the general backreaction behavior, but also collect apparent counterexamples. Those counterexamples are then ruled out at the end of that section. Finally, in appendix 4.A we provide some technical details of asymptotic Hodge theory used in the main text.

4.2 F-theory on Calabi-Yau fourfolds with G_4-flux

In this section we introduce in more detail the context in which we study axion backreaction and moduli stabilization. More precisely, we will introduce part of the low-energy supergravity theory arising when considering F-theory compactified on a family of Calabi-Yau fourfolds Y carrying G_4-flux in section 4.2.1. We will then express the induced flux scalar potential depending in terms of the Hodge decomposition in section 4.2.2 and comment on the use of the Hodge filtration. This chapter repeats certain parts of Section 3.2.1 in order to adapt the notations into the present work.

4.2.1 Scalar potential and its complex structure dependence

As reviewed in Section 1.2.4, we first compactify M-theory with G_4-flux on Calabi-Yau fourfolds Y to obtain a three-dimensional $\mathcal{N} = 2$ effective supergravity theory with a scalar potential for the complex structure moduli and Kähler structure moduli induced by the flux [167]. To connect this setting to an F-theory compactification we assume that Y admits a two-torus fibration. The three-dimensional action is then lifted to a four-dimensional $\mathcal{N} = 1$ supergravity theory by shrinking the volume of the two-torus fiber of Y. This procedure defines the reduction of

F-theory on the Calabi-Yau fourfold Y to obtain a four-dimensional effective theory [41, 44]. Crucial for our considerations is the fact that the complex structure moduli of Y reside in chiral multiplets both in the three-dimensional effective theory obtained from M-theory and the four-dimensional effective theory derived by the lift to F-theory. It was shown in [5, 217, 218] that within the complex structure moduli space, fields with approximate shift symmetry, i.e. axion fields, can only arise near the boundaries of moduli space. These boundaries will have to satisfy certain conditions, which we will recall below. It is with these axions and their partner saxions that will be the focus of this chapter.

Let us now discuss the scalar potential induced by a background flux $G_4 \in H^4(Y, \mathbb{Z}/2)$. It is well-known [167] that the three-dimensional scalar potential arising in the M-theory reduction takes the form

$$V = \frac{1}{\mathcal{V}_4^3} \left(\int_Y G_4 \wedge *G_4 - \int_Y G_4 \wedge G_4 \right) , \tag{4.2.1}$$

where $*$ is the Hodge-star operator of Y and $\mathcal{V}_4$ is the volume of the Calabi-Yau fourfold Y. Note that the scalar potential depends on complex structure and the Kähler structure deformations through the Hodge-star operator in the first integral. Furthermore, in V there is an additional Kähler structure moduli dependence through the overall volume factor. Without further inclusion of localized sources such as M2-branes filling the three-dimensional spacetime, the G_4-flux needs to satisfy the following tadpole cancellation condition [159]

$$\frac{1}{2} \int_Y G_4 \wedge G_4 = \frac{\chi(Y)}{24} . \tag{4.2.2}$$

The scalar potential (4.2.1) can be cast into a form compatible with $\mathcal{N} = 2$ supersymmetry in three dimensions. Instead of reviewing the whole construction of the characteristic $\mathcal{N} = 2$ data, we will henceforth focus only on the complex structure moduli dependence of the Hodge star in (4.2.1). This amounts to requiring that our G_4-flux lives in the *primitive* middle cohomology $H^4_{\mathrm{p}}(Y, \mathbb{Z})$ [167], which is equivalent to stating that if $J \in H^{1,1}(Y)$ is the Kähler class of the Calabi-Yau fourfold Y the fluxes under consideration satisfy the condition $J \wedge G_4 = 0$. Inserting this condition into (4.2.1), the resulting scalar potential can be shown to arise from a Kähler potential K and a superpotential W [51, 167] given by

$$K = -\log \int_Y \Omega \wedge \bar{\Omega} , \qquad W = \int_Y \Omega \wedge G_4 , \tag{4.2.3}$$

where Ω is the, up to rescaling, unique $(4,0)$-form on Y and hence represents $H^{4,0}(Y, \mathbb{C})$.

Let us note that we make a further simplification that will keep our discussion accessible. In order to not deal with integer cohomology and the many associated subtleties, we will not be careful about the quantization of the G_4 flux [219] and often write $G_4 \in H^4_{\rm p}(Y,\mathbb{R})$. While imposing the quantization conditions on G_4 is important in deriving numerical values and establishing finiteness results [13, 14] it will not be altering the conclusions about backreaction that we obtain in this chapter.

4.2.2 Scalar potential and the Hodge filtration

In order to identify the conditions for axions to arise in the complex structure moduli space and to study their backreaction effects, we need to put the above expression for the scalar potential into a Hodge-theoretic context. Let us review some of the relevant definitions in order to establish notations. For more complete information, we refer the math article [101] and the recent physics application [13, 136].

To begin with, we note that the primitive middle cohomology of a smooth Calabi-Yau fourfold Y carries a pure Hodge structure of weight four, which is described by the Hodge decomposition

$$H^4_{\rm p}(Y,\mathbb{C}) = H^{4,0} \oplus H^{3,1} \oplus H^{2,2} \oplus H^{1,3} \oplus H^{0,4}\,, \tag{4.2.4}$$

satisfying $H^{p,q} = \overline{H^{q,p}}$. Note that the $H^{2,2}$ here denotes *primitive* $(2,2)$-forms, i.e. it is a shorthand for $H^{2,2} \cap H^4_{\rm p}(Y,\mathbb{C})$, and all subspaces $H^{p,q}$ different from $H^{2,2}$ are automatically primitive in the Calabi-Yau fourfold setting. In practice it is more useful to use an equivalent description in terms of the *Hodge filtration*

$$0 \subset F^4 \subset F^3 \subset F^2 \subset F^1 \subset F^0 = H^4_{\rm p}(Y,\mathbb{C})\,, \tag{4.2.5}$$

satisfying $F^p \oplus \overline{F^{4-p+1}} \cong H^4_{\rm p}(Y,\mathbb{C})$. One can recover the Hodge decomposition by setting $H^{p,q} = F^p \cap \overline{F^q}$. On the other hand, given a Hodge decomposition, the corresponding Hodge filtration is given by

$$F^p = \bigoplus_{r\geq p} H^{4-r,r}\,. \tag{4.2.6}$$

The Hodge structure will change as one deforms the complex structure of the Calabi-Yau, and the merit of using Hodge filtration is that the filtration will change *holomorphically* with respect to the complex structure moduli t^I. The variation of Hodge structure is captured by the period map $F(t)$, which records the whole

Hodge filtration F^p, $p = 0, ..., 4$, corresponding to the complex structure moduli t^I.

Moreover, the Hodge structure is polarized by the symmetric intersection form on the Calabi-Yau fourfold

$$\langle \alpha, \beta \rangle = \int_Y \alpha \wedge \beta \,, \tag{4.2.7}$$

for $\alpha, \beta \in H^4_{\rm p}(Y, \mathbb{C})$. There is also a *Weil operator* C_F, depending on the Hodge filtration F, defined by

$$C_F(\alpha) = \mathbf{i}^{p-q}\alpha \,, \quad \text{for } \alpha \in H^{p,q} \,. \tag{4.2.8}$$

It is a standard result that on the primitive middle cohomology of a Calabi-Yau fourfold, the Weil operator coincides with the Hodge star operator. With the help of the polarization form and the Weil operator, we can define the *Hodge inner product* and its associated *Hodge norm*

$$\langle \alpha | \beta \rangle_F = \langle C_F \alpha, \overline{\beta} \rangle \,, \tag{4.2.9}$$

$$\|\alpha\|_F^2 = \langle \alpha | \alpha \rangle_F \,, \tag{4.2.10}$$

which depends on the Hodge filtration F.

For later reference, we also need to introduce the symmetry group of the variation of Hodge structures: It is the group G of linear automorphisms of $H^4_{\rm p}(Y, \mathbb{C})$ that preserves the dimension of Hodge filtration and the polarization pairing $\langle \cdot, \cdot \rangle$. There is also a real counterpart $G_{\mathbb{R}}$ of this symmetry group that consists of the automorphisms of $H^4_{\rm p}(Y, \mathbb{R})$. More concretely, in the case of Calabi-Yau fourfolds, we have

$$G = \mathrm{SO}(2 + h^{2,2}_{\rm p} + 2h^{1,3}, \mathbb{C}) \,, \quad \text{and} \quad G_{\mathbb{R}} = \mathrm{SO}(2 + h^{2,2}_{\rm p}, 2h^{1,3}) \,, \tag{4.2.11}$$

where $h^{2,2}_{\rm p} = h^{2,2} - h^{1,1}$ is the dimension of the space of primitive $(2,2)$-forms. This number follows from the Lefschetz decomposition. Namely, one has

$$H^{2,2} = H^{2,2}_{\rm p} \oplus JH^{1,1}_{\rm p} \oplus J^2 H^{0,0}_{\rm p} \,, \quad H^{1,1} = H^{1,1}_{\rm p} \oplus JH^{0,0}_{\rm p} \,, \quad H^{0,0}_{\rm p} = H^{0,0} \,, \tag{4.2.12}$$

where $JH^{p,p} = \{J \wedge \alpha | \alpha \in H^{p,p}\} \subset H^{p+1,p+1}$ contains the cup product between the Kähler class and (p,p)-classes. Since we are working with Calabi-Yau spaces, $h^{0,0} = 1$. From the last two equalities, one finds $h^{1,1}_{\rm p} = h^{1,1} - 1$. And then $h^{2,2}_{\rm p} = h^{2,2} - h^{1,1}$ follows.

We can now re-express the F-term scalar potential in the Hodge theoretical language: Note that our G_4 is real, so the scalar potential induced by G_4 can now

be written as

$$V(t) = \frac{1}{\mathcal{V}_4^3}(\|G_4\|^2_{F(t)} - \langle G_4, G_4\rangle)\,. \tag{4.2.13}$$

The first term contains the Hodge norm of G_4 evaluated at the Hodge structure $F(t)$. This is the term that we will focus on in the study of the backreaction of axions on the vacuum expectation values of stabilized saxions.

4.3 Complex structure axions and asymptotic Hodge theory

In this section we explain that in order to identify axionic directions in complex structure moduli space we have to be at its boundaries, i.e. approach a limit in which the associated Calabi-Yau fourfold degenerates. Furthermore, we will see that the considered boundary has to satisfy a set of conditions [5, 217, 218]. To formulate these conditions we have to introduce some additional facts about the moduli space and, in particular, the behavior of the Hodge decomposition (4.2.4) near its boundaries. This forces us to briefly review parts of asymptotic Hodge theory that is relevant to our study of the axion backreaction problem. In section 4.3.1 we will briefly recall why axions arise near the boundaries of the moduli space and introduce the so-called nilpotent orbit that describes the asymptotic form of the Hodge decomposition. In section 4.3.2 we then explain how one can associate to each boundary sets of commuting $\mathfrak{sl}(2)$-triples and a well-defined boundary Hodge structure. The asymptotic form of the scalar potential is then determined in section 4.3.3. We first introduce the normal form of the period mapping $F(t)$ near any boundary and use it to find the asymptotic expression of the Hodge norm. That asymptotic expression will be used in our study of the axion backreaction problem in the next section. The aim of this section is to briefly introduce the relevant results without going into mathematical details. We will supply further details in appendix 4.A. The precise mathematical statements summarized in this section are contained in the review [101] and the original papers [75], [76]. For a more physical formulation that emphasizes similar parts of asymptotic Hodge theory, see [13, 136].

4.3.1 Axions at the boundary of moduli space

In this section we identify the regions in the complex structure moduli space in which one can find fields that admit approximate continuous shift symmetries and

hence can be interpreted as axions. In order to do that we first recall that the discrete symmetries of the moduli space are encoded by the so-called monodromy group. These monodromy symmetries can then lead to an approximate continuous shift symmetry near the boundaries of moduli space.

In the following we will introduce stepwise a local description of the region near the boundaries in moduli space along which the associated Calabi-Yau manifold Y degenerates. We begin by fixing local coordinates z^I, where $I = 1, \ldots, h^{3,1}$, for a patch around a boundary locus of codimension n in the complex structure moduli space. We choose these coordinates such that the boundary is located at $z^i = 0$ for all $i = 1, \ldots, n$. It will also often be useful to implement the coordinate transformation [2]

$$t^i = \frac{1}{2\pi \mathbf{i}} \log z^i \,. \tag{4.3.1}$$

The new set of coordinates t^i take value in the upper half plane, and the singularity is now located at $t^i \to \mathbf{i}\infty$, for $i = 1, \ldots, n$. The coordinates t^i can be further decomposed into real and imaginary parts

$$t^i = \phi^i + \mathbf{i} s^i \,. \tag{4.3.2}$$

The real parts ϕ^i are the candidate axions if one is close to the boundary $s^i = \infty$ as we will see below. In fact, the ϕ^i can enjoy an approximate shift-symmetry if the monodromy transformation associated to the boundary satisfies certain conditions. In cases in which the ϕ^i are identified as axions the imaginary parts s^i is often referred to as saxion. We will sometimes use this terminology more loosely, by referring to the coordinates s^i, ϕ^i as saxion and axion without always stressing the extra condition on the associated monodromy transformation. Note that from (4.3.1) we see that t^i takes value in the upper half plane, so we have a basic constraint $s^i > 0$. The region close to the boundary is characterized by $s^i \gg 1$.

The next data one needs to record is the monodromy operators that arise when encircling the boundary locus $z^i = 0$, $i = 1, ..., n$. There are n monodromy operators and they are defined as the monodromy of the period map $F(t)$, introduced after (4.2.6), when one loops around the singular locus: When $t^i \to t^i + 1$ (equivalently $z^i \to e^{2\pi \mathbf{i}} z^i$), the period map changes $F(t^i + 1) = T_i F(t^i)$. In our geometric setting, where the variation of Hodge structure is induced from the deformation of Calabi-Yau complex structures and that there is an integral basis of the primitive middle cohomology $H^4_{\mathrm{p}}(Y, \mathbb{C})$, one can choose the coordinates in the complex

[2] The coordinates t^i are actually local coordinates on the universal cover of the near boundary patch in the moduli space.

structure moduli space such that the monodromy matrices take the form

$$T_i = e^{N_i}\,, \tag{4.3.3}$$

where N_i are nilpotent matrices. Note that the operators T_i are elements of the real symmetry group $G_{\mathbb{R}}$ given in (4.2.11), while the N_i are elements of the associated real algebra $\mathfrak{g}_{\mathbb{R}}$.

The monodromy matrices T_i, or rather the associated N_i, are essential in evaluating the Hodge decomposition (4.2.4) near the boundary. In general, the Hodge structure will degenerate exactly on the boundary $s^i = \infty$ and has to be replaced by a more sophisticated structure, a so-called 'limiting mixed Hodge structure', which we will describe in section 4.3.2. The starting point for construction of this structure is Schmid's *nilpotent orbit theorem* [75, 76]. It states that around the boundary locus $s^i = \infty$, i.e. when $s^i \gg 1$, the period map $F(t)$ is well approximated by the *nilpotent orbit* of the following form

$$F_{\rm pol}(t) = e^{t^i N_i} F_0\,, \tag{4.3.4}$$

where we sum in the exponential over $i = 1, \ldots, n$. In fact, the nilpotent orbit can be viewed as the essential part of the period map that arises by dropping certain exponential corrections $O(e^{2\pi i t^j})$, while still keeping a well-defined Hodge decomposition. Note that this implies that in many limits non-perturbative corrections are still recorded in $F_{\rm pol}(t)$ as discussed in more detail in [13,89]. Note that (4.3.4) immediately implies that in order that $\mathrm{Re}\, t^i = \phi^i$ is an axion with an approximate shift symmetry unbroken by $O(e^{2\pi i t^j})$-corrections we have to consider a boundary with N_i non-vanishing.

While we will bypass using the Kähler potential and superpotential (4.2.3), let us remark that we have given these quantities in terms of the holomorphic $(4,0)$-form Ω. In order to get the naive nilpotent orbit approximation $K_{\rm nil}$ for K we can now apply the fact that also $F^4 = H^{4,0}$ admits a representation (4.3.4). This implies that Ω, after possibly fixing an overall rescaling, can be expressed as

$$\Omega(z) = \underbrace{e^{t^i N_i} a_0}_{\Omega_{\rm nil}(t)} + \mathcal{O}(e^{2\pi i t^j})\,. \tag{4.3.5}$$

Here a_0 can still be a holomorphic function in the coordinates that are not sent to a limit. Inserting this expression we can now write

$$K_{\rm nil} = -\log\langle \Omega_{\rm nil}, \bar{\Omega}_{\rm nil}\rangle = -\log\langle e^{2is^j N_j} a_0, \bar{a}_0\rangle\,, \tag{4.3.6}$$

which is thus a logarithm of a polynomial in the s^i with a finite number of terms. This implies that $K_{\rm nil}$ is independent of the axions ϕ^i, while $K_{\rm nil}$ still depends on a considered variable s^i if $N_i a_0 \neq 0$. We therefore conclude that a sufficient condition that ϕ^i is an axion with an approximate continuous shift symmetry $\phi^i \to \phi^i + c^i$ is that $N^i a_0 \neq 0$. This latter condition is a necessary condition for the limit to be at infinite distance in the metric derived from K [126]. The appearance of the continuous shift symmetries at infinite distance singularities was discussed in [5] in the context of the Distance Conjecture. In the following, we will not restrict our attention to cases where $N_i a_0 \neq 0$, since this restriction is not necessary for our arguments to go through. While we have not checked that the Kähler metric indeed depends on the ϕ^i only through exponential corrections, we will see that in either case this does not alter our analysis. In the following we will refer to ϕ^i as axions whenever $N_i \neq 0$.

In a related matter, let us stress that, in general, the expression (4.3.6) *cannot* be used to compute the Kähler metric, since taking the nilpotent orbit approximation and taking derivatives with respect to the moduli does not commute. Nevertheless, we can use the full result (4.3.4) for the nilpotent orbit of the complete Hodge filtration to compute the Kähler metric or derivatives of the superpotential. As mentioned above, we will bypass this issue completely by working directly with the scalar potential (4.2.13) and apply the approximations to this expression. In the remainder of this section we will show how starting from the nilpotent orbit (4.3.4) we can derive an approximate scalar potential with an explicit dependence on the axions ϕ^i.

4.3.2 The boundary $\mathfrak{sl}(2)$-structures associated to a degeneration

In the last subsection we have argued that in order to have candidate axion fields ϕ^i in complex structure moduli space some of the complex structure moduli need to be close to the boundary of this moduli space. Furthermore, we have seen that the N_i associated to this boundary have to be non-vanishing. To study the dynamics of the axions we thus need to evaluate the asymptotic behavior of the scalar potential (4.2.13) near the boundary. As will become apparent below the highly non-trivial SL(2)-*orbit theorem* developed in [75] and [76] provides the necessary information about the near boundary region to attack this problem. In the following we will briefly review the ingredients of the SL(2)-orbit theorem needed in this chapter.

The main result discussed in section 4.3.1 is the fact that one can associate to

each boundary in moduli space a nilpotent orbit (4.3.4). This orbit encodes the Hodge structure (4.2.4) near the boundary at $s^i = \infty, i = 1, \ldots, n$. In summary, we have the data $(F_{\text{pol}}, N_1, \ldots, N_n)$, which is regarded as the input of the SL(2)-orbit theorem. The data constructed by the SL(2)-orbit theorem includes a collection of

$$\text{commuting } \mathfrak{sl}(2)\text{-triples:} \qquad (N_i^-, N_i^0, N_i^+)\,, \quad \text{for } i = 1, \ldots, n\,, \tag{4.3.7}$$

and a

$$\text{boundary Hodge structure:} \qquad F_\infty\,. \tag{4.3.8}$$

The commuting $\mathfrak{sl}(2)$-triples satisfy the standard relations

$$[N_i^0, N_i^\pm] = \pm 2 N_i^\pm\,, \qquad [N_i^+, N_i^-] = N_i^0\,, \tag{4.3.9}$$

and the boundary Hodge structure is again a weight-four pure Hodge structure on the primitive cohomology $H^4_{\text{p}}(Y, \mathbb{C})$ polarized by the intersection bilinear form $\langle \cdot\,, \cdot \rangle$. Unpacking the definition, this means that one is able to define its associated Hodge decomposition

$$H^4_{\text{p}}(Y, \mathbb{C}) = \bigoplus_{p+q=4} H^{p,q}_\infty\,, \quad \text{where} \quad H^{p,q}_\infty = F^p_\infty \cap \overline{F}^q_\infty\,, \quad \text{and} \quad H^{p,q}_\infty = \overline{H}^{q,p}_\infty\,, \tag{4.3.10}$$

such that the following polarization condition is satisfied

$$\langle H^{p,q}_\infty, H^{r,s}_\infty \rangle = 0\,, \quad \text{unless } (p,q) = (s,r)\,. \tag{4.3.11}$$

We can also define its associated Weil operator and Hodge norm according to equations (4.2.8) to (4.2.10)

$$\begin{aligned} C_\infty(\alpha) &= \mathbf{i}^{p-q}\alpha\,, \quad \text{for } \alpha \in H^{p,q}_\infty\,, \\ \langle \alpha, \beta \rangle_\infty &= \langle C_\infty \alpha, \overline{\beta} \rangle\,, \\ \|\alpha\|_\infty &= \langle \alpha, \alpha \rangle_\infty\,, \end{aligned} \tag{4.3.12}$$

where we abbreviate the F_∞ appearing in subscripts as ∞ to ease the notational burden.

To proceed further, it is convenient to denote the cumulated sum by braced subscripts. For example, we have

$$N^0_{(i)} = N^0_1 + \cdots + N^0_i\,. \tag{4.3.13}$$

Because the operators N^0_i commute with each other, their cumulated sums $N^0_{(i)}$ also mutually commute $[N^0_{(i)}, N^0_{(j)}] = 0$, thus they have common eigenspaces. In

other words, the operators $N^0_{(i)}$ define a multi-grading

$$H^4_{\rm p}(Y,\mathbb{R}) = \bigoplus_{\boldsymbol{\ell}=(l_1,\ldots,l_n)} V_{\boldsymbol{\ell}}\,, \tag{4.3.14}$$

where each $V_{\boldsymbol{\ell}}$ is the simultaneous eigenspace of $N^0_{(i)}$ with eigenvalue l_i [3], i.e.

$$N^0_{(i)} v_{\boldsymbol{\ell}} = l_i v_{\boldsymbol{\ell}}\,, \qquad \text{for } v_{\boldsymbol{\ell}} \in V_{\boldsymbol{\ell}} \text{ and } i = 1,\ldots,n\,. \tag{4.3.15}$$

The multi-grading (4.3.14) is defined on the real cohomology because the operators N^0_i are elements of $\mathfrak{g}_{\mathbb{R}}$. In the following, we will also work with complexified multi-grading by allowing complex linear combinations.

The multi-grading (4.3.14) and the boundary Hodge structure F_∞ are compatible with each other in the sense that the multi-grading is orthogonal with respect to the Hodge inner product $\langle\,\cdot\,|\,\cdot\,\rangle_\infty$, i.e.

$$\langle V_{\boldsymbol{\ell}} | V_{\boldsymbol{\ell}'}\rangle_\infty = 0\,, \qquad \text{unless } \boldsymbol{\ell} = \boldsymbol{\ell}'\,. \tag{4.3.16}$$

Furthermore, this Hermitian Hodge inner product becomes a symmetric positive-definite inner product after being restricted to the real cohomology $H^4_{\rm p}(Y,\mathbb{R})$, hence we can always choose a real orthonormal basis $\{e^i_{\boldsymbol{\ell}}\}$ for each $V_{\boldsymbol{\ell}}$:

$$V_{\boldsymbol{\ell}} = \mathrm{span}_{\mathbb{R}}\{e^i_{\boldsymbol{\ell}}\}\,, \quad \text{and} \quad \langle e^i_{\boldsymbol{\ell}} | e^j_{\boldsymbol{\ell}'}\rangle_\infty = \delta^{ij}\delta_{\boldsymbol{\ell}\boldsymbol{\ell}'}\,. \tag{4.3.17}$$

Such choice of orthonormal basis will be used in our analysis of the scalar potential (4.2.1) near the boundary in section 4.4.

4.3.3 Asymptotic form of periods and the scalar potential

Now we come back to the study of the asymptotic behavior of the scalar potential (4.2.13) near the boundary. Our focus will be its first term containing the Hodge metric evaluated at $F(t)$. We will first introduce a normal form of the period mapping $F(t)$, which factors $F(t)$ into nice pieces. Moreover, each factor in the normal form has a good limiting property near the boundary where $s^i = \infty$. These limits combine into each other, yielding an asymptotic form of the scalar potential that will be the object studied in section 4.4.

In order to write down the normal form, we need again the data of the nilpotent orbit $(F_{\rm pol}, N_1, \ldots, N_n)$ defined in (4.3.3) and (4.3.4). In addition, we require an extra piece of information: a holomorphic function $\Gamma(z)$ valued in the Lie algebra

[3] Note that our convention differs from the convention in [218] by a constant shift of four.

$\mathfrak{g}_{\mathbb{R}}$. This function satisfies certain properties that are reviewed in appendix 4.A. For the moment we only need to know its existence. Then the *normal form of the period map* [101] is given by

$$F(t) = e^{t^i N_i} e^{\Gamma(z)} F_0 = e^{\phi^i N_i} e^{\mathbf{i} s^i N_i} e^{\Gamma(z)} F_0 \,, \tag{4.3.18}$$

where we remind the reader that the t^j-dependence in the $\Gamma(z)$-function is introduced via $z^j = e^{2\pi \mathbf{i} t^j}$ as in (4.3.1). The normal form provides a convenient factorization of the period mapping into group elements $e^{\phi^i N_i} \in G_{\mathbb{R}}$ and $e^{\mathbf{i} s^i N_i}, e^{\Gamma(z)} \in G_{\mathbb{C}}$ acting on the filtration F_0.

We will now introduce a natural action of $G_{\mathbb{C}}$ on the Hodge norm, which will not only let us factor out the axion dependence in the scalar potential, but also turn the general study of Hodge norm in the bulk near the boundary into the study of the Hodge norm induced by F_∞ at the boundary. This action is defined as follows. For every element $g \in G_{\mathbb{C}}$ and form $\alpha, \beta \in H^4_{\mathrm{p}}(Y, \mathbb{C})$, there is a tautological relation

$$\langle \alpha | \beta \rangle_F = \langle g\alpha | g\beta \rangle_{gF} \,. \tag{4.3.19}$$

This relation then equips the following action of g on the Hodge norm of α

$$\|\alpha\|_{gF} = \|g^{-1}\alpha\|_F \,. \tag{4.3.20}$$

These properties of the Hodge norm and the normal form of the period mapping allow us to factor out the axion dependence in the scalar potential. More precisely, using the action of $G_{\mathbb{C}}$ on the Hodge norm we can write

$$\|G_4\|_{F(t)} = \left\| e^{-\phi^i N_i} G_4 \right\|_{e^{\mathbf{i} s^i N_i} e^{\Gamma(z)} F_0} \,. \tag{4.3.21}$$

In accordance with the nilpotent orbit theorem discussed in section 4.3.1 (see appendix 4.A for more details) near the boundary $s^i = \infty$, the term $e^{\Gamma(z)}$ will provide exponentially suppressed corrections. It is in this sense that near the boundary the dependence of $\|G_4\|_{F(t)}$ in the axion ϕ^i and saxion s^i are separated. Note also that the operator $e^{-\phi^i N_i}$ being an element in the group $G_{\mathbb{R}}$ by definition preserves the polarization form: $\langle e^{-\phi^i N_i} G_4, e^{-\phi^i N_i} G_4 \rangle = \langle G_4, G_4 \rangle$. These facts instruct us to define the modified G_4-flux including the axions in [218]

$$\rho(\phi, G_4) = e^{-\phi^i N_i} G_4 \,. \tag{4.3.22}$$

This redefinition has also been motivated and discussed intensively in [132,173,182]. In this chapter we find it more convenient to not use this redefinition $\rho(\phi, G_4)$, but

rather always directly display G_4. In summary, the scalar potential expressed using the split (4.3.21) takes the form

$$V(t) = \frac{1}{\mathcal{V}_4^3}\left[\left\| e^{-\phi^i N_i} G_4 \right\|^2_{e^{\mathbf{i}s^i N_i} e^{\Gamma(z)} F_0} - \langle G_4, G_4 \rangle\right]. \tag{4.3.23}$$

Let us now turn to a more in-depth study of the asymptotic form of the scalar potential (4.3.23) near the boundary. In higher-dimensional moduli spaces, the asymptotic behavior can depend on the path along which one approaches the boundary $s^i = \infty$. In order to regulate this, we need to introduce the *growth sector*

$$\mathcal{R}_{1\cdots n} = \left\{ \frac{s^1}{s^2} \geq \lambda, \ldots, \frac{s^{n-1}}{s^n} \geq \lambda, s^n > \lambda \right\}, \tag{4.3.24}$$

where we consider $\lambda \geq 1$. The definition of the growth sector binds with an ordering of the variables t^i. Setting $\lambda = 1$ one can cover the entire neighborhood of the boundary by growth sectors obtained by considering every ordering in the variables t^i. In the following we will focus on one of these sectors, namely $\mathcal{R}_{1\cdots n}$, after possibly renaming the coordinates. Gluing these sectors together can be a non-trivial task, but is not of importance in the remainder of this chapter. Note that eventually we will work in the 'strict asymptotic regime', i.e. we will assume $\lambda \gg 1$.

In order to analyze the asymptotic behavior of the Hodge norm, i.e., the first t-dependent term in (4.3.23), we will introduce an operator $e(s)$ following [101]. It is defined by

$$e(s^1, \ldots, s^n) = \exp\left\{ \frac{1}{2} (\log s^r) N_r^0 \right\}, \tag{4.3.25}$$

where r is being summed from 1 to n. One of the motivations behind the introduction of the $e(s)$-operator is the property

$$e(s) e^{\phi^j N_j} e(s)^{-1} = \exp\left\{ \sum_{j=1}^{n} \frac{\phi^j}{s^j} \left[N_j^- + \sum_{\underline{\alpha}^j > 0} \frac{N'_{j,\underline{\alpha}^j}}{\left(\frac{s^1}{s^2}\right)^{\alpha_1^j/2} \cdots \left(\frac{s^{j-1}}{s^j}\right)^{\alpha_{j-1}^j/2}} \right] \right\}, \tag{4.3.26}$$

where N_j is the log-monodromy operator introduced in (4.3.3), N_j^- is the corresponding lowering operator in the commuting $\mathfrak{sl}(2)$-triples introduced in (4.3.7). The operators $N'_{j,\underline{\alpha}^j}$ are nilpotent operators living in $\mathfrak{g}_{\mathbb{R}}$. The derivation of this expression together with the precise definition of the operators $N'_{j,\underline{\alpha}^j}$ can be found in appendix 4.A. The main point is that if one moves towards the boundary $s^i = \infty$ within the growth sector $\mathcal{R}_{1\cdots n}$, while not keeping the candidate axion ϕ^i finite,

the terms proportional to $N'_{j,\underline{\alpha}^j}$ are polynomially suppressed. This implies that in the limit of large s^i we find within $\mathcal{R}_{1\cdots n}$ the limiting behavior

$$e(s)e^{\phi^j N_j}e(s)^{-1} \to \exp\left(\sum_{j=1}^{n}\frac{\phi^j}{s^j}N_j^-\right), \tag{4.3.27}$$

$$e(s)e^{\mathbf{i}s^j N_j}e(s)^{-1} \to \exp\left(\mathbf{i}\sum_{j=1}^{n}N_j^-\right), \tag{4.3.28}$$

where the second line can be obtained from the first by formally setting $\phi^j = \mathbf{i}s^j$. If we look at the normal form of the period mapping (4.3.18), we see that some limiting expressions related to $e^{\Gamma(z)}$ and F_0 are also needed. We state the correct form of the limits here, and refer to appendix 4.A for their derivation

$$\begin{aligned} e(s)e^{\Gamma(z)}e(s)^{-1} &\to 1\,, \\ \exp\left(\mathbf{i}\sum_{j=1}^{n}N_j^-\right)e(s)F_0 &\to F_\infty\,, \end{aligned} \tag{4.3.29}$$

where F_∞ is the boundary Hodge filtration.

Combining the normal form of the period mapping (4.3.18) and equations (4.3.27) to (4.3.29) gives us the following limiting expression of the period mapping $F(t)$ near the boundary $s^i = \infty$ in the growth sector $\mathcal{R}_{1\cdots n}$

$$F(t) \to e(s)^{-1}\exp\left(\sum_{j=1}^{n}\frac{\phi^j}{s^j}N_j^-\right)F_\infty\,. \tag{4.3.30}$$

The above result can be applied immediately to the study of the scalar potential (4.3.23). Combining the action of $G_\mathbb{C}$ on the Hodge norm and the asymptotic expression of the period mapping (4.3.30), we have [4]

$$\begin{aligned} \left\|e^{-\phi^i N_i}G_4\right\|_{e^{\mathbf{i}s^i N_i}e^{\Gamma(z)}F_0} &= \left\|e(s)e^{-\phi^i N_i}G_4\right\|_{e(s)e^{\mathbf{i}s^i N_i}e^{\Gamma(z)}F_0} \\ &\sim \left\|\exp\left(\sum_{j=1}^{n}-\frac{\phi^j}{s^j}N_j^-\right)e(s)\,G_4\right\|_\infty\,. \end{aligned} \tag{4.3.31}$$

So in the strict asymptotic regime $\lambda \gg 1$ in (4.3.24), the scalar potential (4.3.23) has the following asymptotic form

$$\boxed{V(t) \sim \frac{1}{\mathcal{V}_4^3}\left[\left\|\exp\left(\sum_{j=1}^{n}-\frac{\phi^j}{s^j}N_j^-\right)e(s)G_4\right\|_\infty^2 - \langle G_4, G_4\rangle\right].} \tag{4.3.32}$$

[4] As usual, the symbol $\sim$ indicates that the quantities on both sides approximate each other increasingly well as one move towards the considered boundary.

This asymptotic form of the scalar potential is the main result from asymptotic Hodge theory that we will use in the following. The important thing to note is that all dependence in (4.3.32) on the axions ϕ^i and the saxions s^i is explicit and given in terms of the boundary structure. In particular, the norm $\|\cdot\|_\infty$ is both well-defined and independent of t^i, but can depend still on the coordinates not considered to be near the boundary. Combined with the underlying $\mathfrak{sl}(2)$-structure we can use this form of the potential to tackle the stabilization of saxions in the presence of large displacement of axions.

Let us close this section with a short comment on the apparent discrepancy between (4.3.32) and our result in section 7 of [218]. The reason of the discrepancy is that in [218] we replaced all N_i in the expression of $\rho(\phi, G_4)$, given in (4.3.22), by their commuting $\mathfrak{sl}(2)$-counterparts N_i^-. This was done to simplify the computation, but it neglected the contributions from the difference between N_i and N_i^-. Had the replacement not been done, the two approaches are equivalent because

$$\|e(s)\rho(\phi, G_4)\|_\infty \sim \left\| \exp\left(\sum_{i=1}^{n} -\frac{\phi^i}{s^i} N_i^- \right) e(s)\, G_4 \right\|_\infty , \tag{4.3.33}$$

which is the step deriving (4.3.31). The left-hand-side of the above equation is the object studied in [218] whereas the right-hand-side is the object studied in this note.

4.4 Axion backreaction on the saxion vacuum

In this section we study the backreaction of a large displacement of an axion, denoted by ϕ^k, on the saxion vacuum expectation values. This forces us to discuss moduli stabilization within the general scalar potential (4.3.32), which is a very hard problem. In particular, while we know the field dependence of (4.3.32) on the fields t^i, we have no control over its dependence on the coordinates of complex structure moduli space not considered close to the boundary. Here the power of asymptotic Hodge theory comes to the rescue, since it allows us to control at least the positivity properties and the hierarchy of certain couplings that cannot be further specified. We will then focus on one pair of axion and saxion (ϕ^k, s^k) and study the stabilization of the saxion s^k via the potential (4.3.32) to its vacuum expectation value $\overline{s}^k$. To simplify notation we use in this section the definition:

$$s \equiv s^k \ , \qquad \phi \equiv \phi^k \ . \tag{4.4.1}$$

We then find that whenever we try to fix s and assume that the associated axion ϕ is large, we find the following universal relation

$$\boxed{\overline{s}(\phi) \sim c\,\phi^{\gamma} + \mathcal{O}\left(\frac{1}{\phi}\right),} \tag{4.4.2}$$

where c is a positive number, and $0 < \gamma \leq 2$ is a rational number. While our expression is slightly more general, the relation (4.4.2) shows that one always encounters the type of backreaction that was found in [138–140]. In fact, we will argue in the end of section 4.4.3 that in most cases one indeed has $\gamma = 1$, and in general $\gamma < 1$ can appear if some special choices of parameters are allowed. The $\gamma > 1$ cases are even rarer in the sense that only two valid special cases with $\gamma = 2$ are found. In other words, the fact that one cannot displace the axion by very large values without destabilizing the saxion is a consequence of the boundary $\mathfrak{sl}(2)$-structure introduced in the last section. We stress, however, that we will not be able to make statements about the precise value of c and its dependence on the fluxes and other moduli. While c cannot be made zero, we will not exclude the possibility that it can be made small by fine-tuning leading to a somewhat delayed backreaction [139, 155–157]. A short discussion on the dependency of c and the flux numbers can also be found at the end of section 4.4.3.

Our study relies heavily on the action of the commuting $\mathfrak{sl}(2)$-triples on the cohomology $H^4_{\mathrm{p}}(Y, \mathbb{R})$, hence we will start with reviewing some elementary facts about $\mathfrak{sl}(2)$-representations in section 4.4.1. The boundary $\mathfrak{sl}(2)$-structure then allows us to bring the asymptotic scalar potential into a convenient form and can be extremized in the limit of large axion. This amounts to solving a one-parameter family of one-variable polynomial equations and study how the root depends on the parameter in certain limits. This kind of problem is exactly studied by a well-known mathematical tool called the Puiseux expansion, whose information is registered in a pictorial way in the so-called Newton diagram. We will review the notion of Puiseux expansions and their associated Newton diagrams in section 4.4.2. Having introduced these additional tools we turn in section 4.4.3 to the detailed study of the asymptotic scalar potential and its extremization condition. With the help of the boundary $\mathfrak{sl}(2)$-structure and the Newton diagram, we will show that almost all flux configurations will give an axion backreaction behavior of the form (4.4.2). We will also enumerate all possible flux configurations that can potentially generate a backreaction behavior different from (4.4.2). These flux configurations are then studied case-by-case in section 4.4.4. Interestingly, none of them actually yields a valid solution, in the sense that each case generates a saxion

vev leading term that is either negative or imaginary. We conclude this section with a list of bad cases, where some explicit examples are also provided.

Before we start, let us state again the scalar potential (4.3.32) focusing only on a single axion-saxion pair (ϕ, s), but allowing for a slight generalization with an overall factor. More precisely, we will consider in the following the scalar potential

$$\boxed{V(\phi,s) := \frac{1}{s^\alpha}\left[\left\|\exp\left(-\frac{\phi}{s}N^-\right)e(s)G_4\right\|^2_\infty - A_{\rm loc}\right],} \tag{4.4.3}$$

where we have set $N^- \equiv N_k^-$ and recall that the $e(s)$-operator is defined in (4.3.25). The localized contribution that does not depend on the complex structure moduli is collectively denoted by $A_{\rm loc}$. Following [218], we have included the overall scaling $1/s^\alpha$ with an undetermined power α. This factor can be thought of as arising from $\mathcal{V}_4$ in (4.3.32) and enables a comparison between the F-theory potential and the IIA scalar potential [16, 137]. Around the weak coupling limit of F-theory, the value of α is known to be 3 when s is related to the Type IIA dilaton as discussed in detail in [218]. In general it is not known how large α is near other singularities. However, requiring that the scalar potential (4.4.3) is finite as $s \to \infty$ restricts the possible range of α. We will find that after imposing this restriction the backreaction (4.4.2) is universal.

4.4.1 A brief review of representations of the $\mathfrak{sl}(2)$-algebra

It turns out that asymptotics of (4.4.3) with respect to $(\phi, s) \equiv (\phi^k, s^k)$ only depends on the behavior of the G_4-flux under the action of the k-th commuting $\mathfrak{sl}(2)$-triple, whose lowering and number operators are denoted by (N^-, N^0), respectively. We will abuse the notation and denote the k-th $\mathfrak{sl}(2)$-triple (N_k^-, N_k^0, N_k^+) just by (N^-, N^0). In this subsection let us recall some elementary facts of $\mathfrak{sl}(2)$-algebra representations [220]. We work over the real numbers since the $\mathfrak{sl}(2)$-triple and G_4-flux are real, nevertheless the theory holds for complex representations as well. We align with the notation in section 4.2 of [13].

For any integer $d \geq 0$, there is a $(d+1)$-dimensional irreducible representation $\mathcal{W}^d$ of the $\mathfrak{sl}(2)$-algebra (N^-, N^0). One can specify a special state $|d, d\rangle$ in $\mathcal{W}^d$ called the highest weight state of weight d. It satisfies the property

$$(N^-)^d\,|d,d\rangle \neq 0 \quad \text{and} \quad (N^-)^{d+1}\,|d,d\rangle = 0\,. \tag{4.4.4}$$

A basis of the representation $\mathcal{W}^d$ can then be constructed out of the highest weight

state $|d,d\rangle$ and the lowering operator N^- as follows

$$\mathcal{W}^d = \mathrm{span}_{\mathbb{R}}\{|d,d\rangle\,, |d,d-2\rangle\,, \ldots, |d,-d\rangle\}\,, \tag{4.4.5}$$

where

$$|d,d-2n\rangle = \frac{1}{n!}(N^-)^n\,|d,d\rangle\ , \tag{4.4.6}$$

for $n = 0,\ldots,d$. These vectors are also eigenstates of the N^0 operator, satisfying

$$N^0\,|d,l\rangle = l\,|d,l\rangle\ . \tag{4.4.7}$$

We call the eigenvalue l the weight of the state $|d,l\rangle$. This state also satisfy

$$(N^-)^{\frac{d+l}{2}}\,|d,l\rangle \neq 0 \quad \text{and} \quad (N^-)^{\frac{d+l}{2}+1}\,|d,l\rangle = 0\,. \tag{4.4.8}$$

Note that by construction, $d+l$ is always an even non-negative number.

Now we make contact with the boundary $\mathfrak{sl}(2)$-structure. In equation (4.3.7), a series of commuting $\mathfrak{sl}(2)$-triples is introduced at the boundary of the complex structure moduli space. These commuting $\mathfrak{sl}(2)$-algebras act on $H^4_{\mathrm{p}}(Y,\mathbb{R})$ and, in particular, turn $H^4_{\mathrm{p}}(Y,\mathbb{R})$ into a real representation of the k-th $\mathfrak{sl}(2)$-algebra (N^-,N^0). According to the above discussion of representations of $\mathfrak{sl}(2)$-algebras, $H^4_{\mathrm{p}}(Y,\mathbb{R})$ enjoys the following decomposition

$$H^4_{\mathrm{p}}(Y,\mathbb{R}) = \bigoplus_{d=0}^{4}\mathcal{W}[d]\,, \tag{4.4.9}$$

where

$$\mathcal{W}[d] = \mathcal{W}^d_1 \oplus \cdots \oplus \mathcal{W}^d_{\mu_d} \tag{4.4.10}$$

consists of μ_d copies of irreducible representations $\mathcal{W}^d_{i_d}$ of dimension $d+1$. Different highest weight states with the same d-label are distinguished by the index $i_d = 1,\ldots,\mu_d$: they are denoted by $|d,d;i_d\rangle \in \mathcal{W}^d_{i_d}$ and their descendants are denoted similarly by $|d,l_d;i_d\rangle$. One also sees that each basis vector in (4.4.5) has a well-defined eigenvalue under the action of N^0. Hence we relate the orthonormal basis (4.3.17) adapted to the multi-grading to the basis vectors in (4.4.5) in a one-to-one manner. We fix the basis (4.4.5) in this way, so that two basis vectors in (4.4.5) are orthogonal to each other unless they carry identical indices d, l_d and i_d.

4.4.2 A brief review of the Puiseux expansion

To determine the backreacted saxion vacuum expectation value, we need to study how the root of a one-parameter family of polynomial equations change with respect

to the parameter. This type of question can be studied expanding the solution into Puiseux series. In this subsection we briefly review the use of the Puiseux expansion and Newton diagram. We will not show any proof of the facts and the interested reader can find the proof in [221].

For simplicity, we work over the complex numbers in this subsection so that every polynomial always has roots. When we apply the Puiseux expansion to analyze the axion backreaction, we will always require the existence of a vacuum. This means that the polynomial arising from the first derivatives of the scalar potential, see (4.4.23) below, is assumed to have a real root. The method of expanding the root into a Puiseux series also applies in such circumstances.

The Puiseux expansion studies generalized polynomial equations in two variables $F(s,\hat{\phi})=0$, with the variable $\hat{\phi}$ being distinguished in the sense that the powers of $\hat{\phi}$ are allowed to be negative. The equation $F(s,\hat{\phi})=0$ can also be regarded as a one-variable polynomial equation with a parameter $\hat{\phi}$. Around $\hat{\phi}=0$, any s satisfying $F(s,\hat{\phi})=0$ can be regarded as a function of $\hat{\phi}$. The series representation of $s(\hat{\phi})$ is given by the Puiseux expansion, which is a fractional power series. More precisely, let us assume the following form of a generalized polynomial

$$F(s,\hat{\phi})=a_0(\hat{\phi})+a_1(\hat{\phi})s+\cdots+a_n(\hat{\phi})s^n\,, \tag{4.4.11}$$

where every $a_i(\hat{\phi})$ is a polynomial in $\hat{\phi}$ and $1/\hat{\phi}$ with complex coefficients

$$a_i(\hat{\phi})=\sum_j a_{ij}\hat{\phi}^j\,. \tag{4.4.12}$$

Then the Puiseux expansion states that, near $\hat{\phi}=0$, any root of the equation $F(s,\hat{\phi})=0$, regarded as a function $s=s(\hat{\phi})$, can be expanded as

$$s(\hat{\phi})=\frac{c}{\hat{\phi}^\gamma}+\sum_{i=0}^{\infty}c_i\hat{\phi}^{i/m}\,, \tag{4.4.13}$$

where c and c_i are complex numbers, γ is a rational number and m is a positive integer. Our focus is on the leading power γ. Knowing that any s-root must admit a fractional power series expansion (4.4.13), the determination of γ is standard: One inserts the expansion (4.4.13) back to the original equation (4.4.11) and solves for the γ that makes the lowest order terms cancel. This whole procedure was encoded by Newton into an intuitive gadget called the Newton polygon which we introduce next. We would like to comment that despite determining γ is straightforward once one has the Ansatz (4.4.13), the significance of the Puiseux expansion lies in the proof of convergence of the fractional series [221].

To determine γ pictorially, we need to first define the *Newton diagram* $\Delta(F)$ of $F(s,\hat{\phi})$ as follows

$$\Delta(F) = \left\{(i,j) \in \mathbb{R}^2 \mid a_{ij} \neq 0 \text{ in } F(s,\hat{\phi})\right\}, \tag{4.4.14}$$

which simply consists of the dots (i,j) on the plane such that a term $s^i\hat{\phi}^j$ with non-vanishing coefficient $a_{ij} \neq 0$ appears in the generalized polynomial $F(s,\hat{\phi})$. By our assumption on the polynomial F, its Newton diagram $\Delta(F)$ will only occupy the half plane $i \geq 0$. Then the *Newton polygon* of F is defined to be the lower convex hull of $\Delta(F)$. To illustrate the definition with an example let us consider the polynomial

$$F(s,\hat{\phi}) = \frac{a_1}{\hat{\phi}^2} + a_2 s^2 + \frac{a_3}{\hat{\phi}^2} s^3 + a_4 s^5\,, \tag{4.4.15}$$

where a_1, a_2, a_3 and a_4 are non-zero numbers. This polynomial arises in a specific 2-moduli degeneration of Calabi-Yau fourfolds.[5] The Newton diagram and Newton polygon is shown in Figure 4.1.

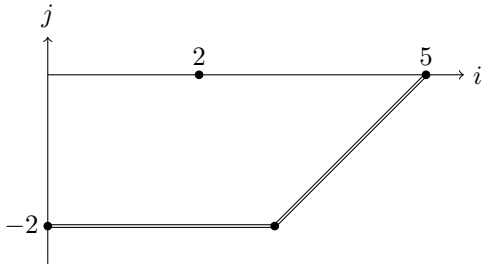

Figure 4.1: The Newton diagram $\Delta(F)$ of the polynomial (4.4.15) consists of the four solid dots shown in this figure. The corresponding Newton polygon, the lower convex hull of the Newton diagram, is labelled by double lines. The vertical axis labels the powers of $\hat{\phi}$ while the horizontal axis labels the powers of s.

The Newton polygon consists of several segments. Each segment with slope γ determines a possible leading exponent γ in the Puiseux expansion (4.4.13). In our example (4.4.15), with Newton polygon shown in Figure 4.1, the polygon consists of two segments with slopes 0 and +1. So around $\hat{\phi} = 0$, the equation has the

[5]The degeneration is classified as of type $\mathrm{I}_{01} \to \mathrm{V}_{22}$ with the G_4 flux chosen to be $G_4 = g_{42}v_{42} + g_{34}v_{34}$ in the convention of [218].

following roots represented by Puiseux expansions

$$s_1(\hat{\phi}) = \frac{c_1}{\hat{\phi}} + \sum_{i=0}^{\infty} c_{1,i}\hat{\phi}^{i/m}\,, \tag{4.4.16}$$

$$s_2(\hat{\phi}) = c_2 + \sum_{i=1}^{\infty} c_{2,i}\hat{\phi}^{i/n}\,, \tag{4.4.17}$$

where m, n are positive integers. In our application, the $\hat{\phi}$ here actually stands for the inverse of an axion field $1/\phi$ and s stands for the corresponding saxion partner s. Hence the first solution $s_1(\hat{\phi})$ represents a linear-backreacted saxion vacuum expectation value, while the second solution $s_2(\hat{\phi})$ stays finite at large ϕ.

4.4.3 Determining the backreacted saxion vacuum

We now have all the tools we need to attack the axion backreaction problem. Using the $\mathfrak{sl}(2)$-basis, we will first expand the asymptotic scalar potential (4.4.3) into a generalized polynomial in (s, ϕ). Then we will look closer at the shape of the Newton diagram to deduce the leading term in the backreacted saxion vev $\overline{s}(\phi)$.

Let us begin by decomposing the G_4-flux according to (4.4.9) as

$$G_4 = \sum_{d=0}^{4}\sum_{i_d=1}^{\mu_d}\sum_{n_d=0}^{d} g_{d,d-2n_d;i_d}\,|d, d-2n_d; i_d\rangle\ , \tag{4.4.18}$$

where $g_{d,d-2n_d;i_d}$ is the flux-component of the highest weight representation $\mathcal{W}^d$ with weight $d-2n_d$. Note that the $e(s)$-operator defined in (4.3.25) acts on a basis state $|d, l_d; i_d\rangle$ by scalar multiplication

$$e(s)\,|d, l_d; i_d\rangle = s^{\frac{l_d}{2}}\,\hat{f}_{d,l_d;i_d}\,|d, l_d; i_d\rangle\ , \tag{4.4.19}$$

where $\hat{f}_{d,l_d;i_d}$ can be a non-vanishing function[6] of all other complex structure coordinates. Then by a direct computation, the asymptotic scalar potential is found to be

$$\begin{aligned} V &= \frac{1}{s^\alpha}\left[\left\|\exp\Big(-\frac{\phi}{s}N^-\Big)e(s)G_4\right\|^2_{\infty} - A_{\rm loc}\right] \qquad (4.4.20)\\ &= \frac{1}{s^\alpha}\left[\sum_{d=0}^{4}\sum_{i_d=1}^{\mu_d}\sum_{n_d=0}^{d}\sum_{b_d=n_d}^{d}\binom{b_d}{n_d}^2 s^{d-2b_d}\phi^{2(b_d-n_d)}g^2_{d,d-2n_d;i_d}\hat{f}^2_{d,d-2n_d;i_d} - A_{\rm loc}\right]\,, \end{aligned}$$

[6]Note that in our multi-grading notation in [218], the l_d here corresponds to the $l_k - l_{k-1}$ index of $|d, l_d; i_d\rangle$ in the [218].

where in the last step we have used the orthonormal property of the basis states. We have highlighted the dependency of V only on the pair (ϕ, s) and moved the dependencies on the other complex structure moduli into the various $\hat{f}$. Note that the flux number $g_{d,d-2n_d;i_d}$ is always accompanied by the non-vanishing function $\hat{f}_{d,d-2n_d;i_d}$. We therefore introduce the redefinition $\hat{g}_{d,d-2n_d;i_d} = g_{d,d-2n_d;i_d}\hat{f}_{d,d-2n_d;i_d}$ to shorten the equations. The expanded asymptotic scalar potential now takes the form

$$V(\phi, s) = \frac{1}{s^\alpha}\left[\sum_{d=0}^{4}\sum_{i_d=1}^{\mu_d}\sum_{n_d=0}^{d}\sum_{b_d=n_d}^{d}\binom{b_d}{n_d}^2 s^{d-2b_d}\phi^{2(b_d-n_d)}\hat{g}^2_{d,d-2n_d;i_d} - A_{\text{loc}}\right]. \tag{4.4.21}$$

With the expansion of the asymptotic scalar potential, we can impose a constraint on the undetermined exponent α. We require that the potential $V(\phi, s)$ does not blow up in the limit $s \to \infty$. Physically this means that the boundary of the moduli space is viable, not obstructed by the potential. This translates to the constraint that

$$\alpha \geq \max_{g_{d,d-2n_d;i_d}\neq 0}\{d - 2n_d, 0\}, \tag{4.4.22}$$

which says that α should not be smaller than the largest weight carrying a non-zero flux component appearing in G_4.

Since we are going to study the situation where ϕ is large, it is instructive to change variable to $\hat{\phi} = 1/\phi$ so that the limit $\phi \to \infty$ corresponds to $\hat{\phi} \to 0$. In this coordinate $(s, \hat{\phi})$, we denote the derivative of V with respect to s by $F(s, \hat{\phi})$. A simple computation leads to

$$F(s, \hat{\phi}) = \frac{\partial V}{\partial s} = \frac{1}{s^\alpha}\left[\frac{\alpha A_{\text{loc}}}{s} + \sum_{d=0}^{4}\sum_{n_d=0}^{d} F_{d,n_d}(s, \hat{\phi})\right], \tag{4.4.23}$$

where we have grouped the summand according to d and n_d as

$$F_{d,n_d}(s, \hat{\phi}) = \sum_{b_d=n_d}^{d} \mathcal{C}_{d,n_d;b_d} s^{d-2b_d-1}\hat{\phi}^{-2(b_d-n_d)}, \tag{4.4.24}$$

and the coefficient is given by

$$\mathcal{C}_{d,n_d;b_d} = \sum_{i_d=1}^{\mu_d}(-\alpha + d - 2b_d)\binom{b_d}{n_d}^2 \hat{g}^2_{d,d-2n_d;i_d}. \tag{4.4.25}$$

Note that in general $\mathcal{C}_{d,n_d;b_d} \neq 0$ unless for special combinations of α, d, and b_d. For the sake of discovering the general properties of the solution that are directly

related to the boundary $\mathfrak{sl}(2)$-structure, let us temporarily assume that the value of α does not make any of the coefficients $\mathcal{C}_{d,n_d;b_d}$ vanish. We will discuss the consequence of special choices of α that kill some coefficients $\mathcal{C}_{d,n_d;b_d}$ in the end of this subsection.

Now we have the stage set up: In order to study the backreacted saxion vev, we should solve the extremization condition $F = 0$ with the polynomial F given in (4.4.23) by the Puiseux series. In order to find the Puiseux series, we should draw the Newton diagram of the polynomial F. It turns out that it is more instructive to first look at the Newton diagram of every F_{d,n_d} and then assemble them together into the Newton diagram of F.

For every d and n_d, we first note that not every power of s in F_{d,n_d} is positive. In order to apply the method of Puiseux expansions, we need to pull out sufficient power of $1/s$ so that the remaining polynomial has only positive powers on s. So we define

$$\tilde{F}_{d,n_d} = s^{d+1} F_{d,n_d} = \sum_{b_d=n_d}^{d} \mathcal{C}_{d,n_d;b_d} s^{2(d-b_d)} \hat{\phi}^{-2(b_d-n_d)} \,. \tag{4.4.26}$$

Let us check the shape of $\Delta(\tilde{F}_{d,n_d})$. Denote the powers of s by a, the powers of $\hat{\phi}$ by b, and draw the Newton diagram on the (a,b) plane. It is easy to see that it has all dots aligned along the line segment of slope $+1$ intersecting the a-axis at $(2(d-n_d),0)$ and the b-axis at $(0,-2(d-n_d))$. This immediately prompts the following important observation as we fix a d and perform the sum over n_d.

Let us fix a d, and let $\tilde{n}_d$ be the smallest n_d such that $g_{d,d-2n_d;i_d} \neq 0$. If there are multiple possible i_d for such flux components, we just arbitrarily pick one since only the values of d and n_d matter. This flux component corresponds to one of the highest weight components $g_{d,d-2\tilde{n}_d;i_d}$ of G_4 inside $\mathcal{W}[d]$. The sum over n_d with the fixed d takes the following form

$$\sum_{n_d=\tilde{n}_d}^{d} F_{d,n_d} = \frac{1}{s^{d+1}} \sum_{n_d=\tilde{n}_d}^{d} \tilde{F}_{d,n_d} \,. \tag{4.4.27}$$

The Newton diagram of each $\tilde{F}_{d,n_d}$ has been analyzed above. We notice that if we take the lower convex hull to find the Newton polygon of (4.4.27) at this stage, the polygon only depends on the lowest line in the Newton diagram, i.e. the one generated by $\tilde{F}_{d,\tilde{n}_d}$. This implies that when we further sum over d as in (4.4.23) and aiming to find the Newton polygon of the entire F, only the Newton diagram of $\tilde{F}_{d,\tilde{n}_d}$ matters for every d. This observation instructs us to just focus on the highest weight component $g_{d,d-2\tilde{n}_d;i_d}$ for every d.

With the above discussion, the derivative of V (4.4.23) becomes

$$F(s,\hat{\phi}) = \frac{\alpha A_{\rm loc}}{s^{\alpha+1}} + \sum_{d=0}^{4} \frac{\tilde{F}_{d,\tilde{n}_d}(s,\hat{\phi})}{s^{\alpha+d+1}} + \cdots , \tag{4.4.28}$$

where we put the summation that correspond to $n_d > \tilde{n}_d$ for each d into dots since, as discussed above, they will not compete for the Newton polygon hence will not alter the analysis with the Puiseux expansion.

Now we are ready to build the Newton polygon for the polynomial F. Firstly we stack all the Newton diagrams of $\tilde{F}_{d,\tilde{n}_d}$ on one (a,b)-plane. Generic pictures coming from a G_4-flux containing two different d's are shown in the left pictures in Figure 4.2 and 4.3. In order to apply the Puiseux expansion, we need to further eliminate all negative powers of s in F. Denote the highest d in G_4 by $\tilde{d}$, and note that

$$\tilde{F} = s^{\alpha+\tilde{d}+1} F = \alpha\, A_{\rm loc} s^{\tilde{d}} + \sum_{d=0}^{4} s^{\tilde{d}-d} \tilde{F}_{d,\tilde{n}_d} + \cdots \tag{4.4.29}$$

no longer has negative power of s so we can in turn study the solution of $\tilde{F}=0$ by Puiseux expansions. The extremization condition $F=0$ is equivalent to $\tilde{F}=0$ since we assume $s>0$.

The resulting Newton diagram of $\tilde{F}$ is simply a combination of the Newton diagrams of various $s^{\tilde{d}-d}\tilde{F}_{d,\tilde{n}_d}$, and each of which is itself the Newton diagram of $\tilde{F}_{d,\tilde{n}_d}$ with a shift towards the a-direction, i.e. along the horizontal axis in Figure 4.2 and 4.3, by an amount of $\tilde{d}-d$. In particular, the Newton diagram of $s^{\tilde{d}-d}\tilde{F}_{d,\tilde{n}_d}$ will have dots aligned along a line of slope $+1$ that intersects the a-axis at $(\tilde{d}+d-2\tilde{n}_d, 0)$. Moreover there will be an extra point $(\tilde{d}, 0)$ coming from the term with $A_{\rm loc}$ as coefficient, if $\alpha \neq 0$. The Newton polygon is then found by taking the lower convex hull of the Newton diagram of $\tilde{F}$. Generic pictures of the Newton diagram and Newton polygon of $\tilde{F}$ generated by a G_4-flux containing two different d's are shown in the right pictures in Figure 4.2 and 4.3.

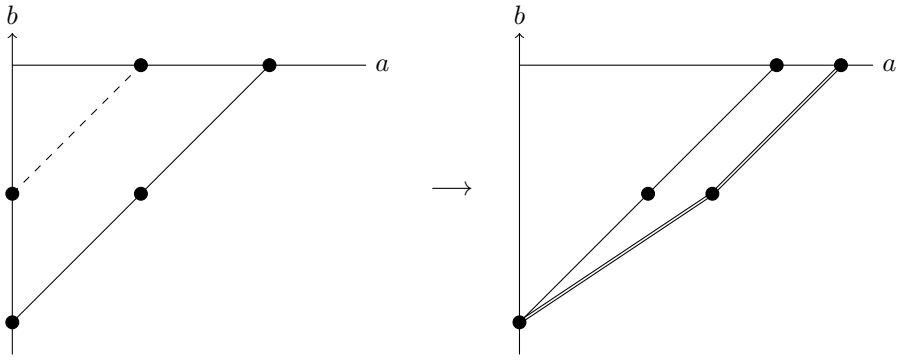

Figure 4.2: One typical configuration of the Newton diagram generated by a G_4-flux containing two different d's. In the left figure, we superpose all Newton diagrams of $\tilde{F}_{d,\tilde{n}_d}$. The solid line corresponds to $\tilde{F}_{\tilde{d},\tilde{n}_{\tilde{d}}}$ of the highest $\tilde{d}$, and the dashed line corresponds a possible lower d. On the right we show the end result. The double lines correspond to the Newton polygon of $\tilde{F}$. In the situation shown in this figure, the two segments of the Newton polygon have both positive slopes, indicating an axion backreaction behavior (4.4.30) that drives one into the regime of the Distance Conjecture.

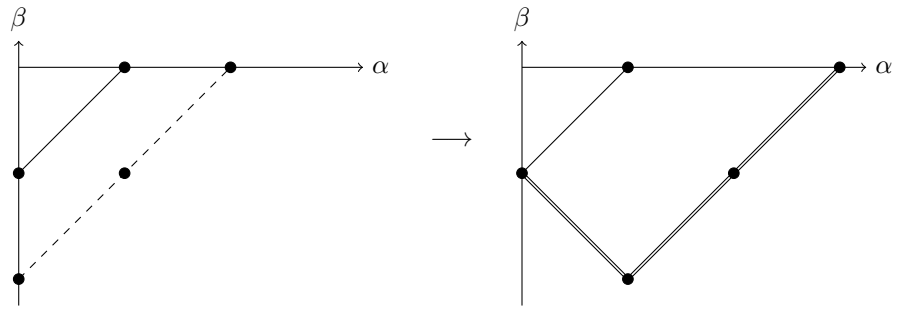

Figure 4.3: Another typical configuration of the Newton diagram generated by a G_4-flux containing two different d's. In the left figure, we superpose all Newton diagrams of $\tilde{F}_{d,\tilde{n}_d}$. The solid line corresponds to $\tilde{F}_{\tilde{d},\tilde{n}_{\tilde{d}}}$ of the highest $\tilde{d}$, and the dashed line corresponds a possible lower d. On the right we show the end result. The double lines correspond to the Newton polygon of $\tilde{F}$. In the situation shown in this figure, the segment of the Newton polygon with positive slope will generate an axion backreaction behavior similar to Figure 4.2, while the segment with negative slope will generate a backreaction (4.4.33) that drives s away from the boundary of the complex structure moduli space.

According to the general structure of the Puiseux expansion reviewed in section

4.4.2, each segment in the Newton polygon of $\tilde{F}$ with a positive slope $\gamma > 0$ corresponds to an axion backreaction behavior of the following form

$$\overline{s}(\phi) = c\phi^{\gamma} + \mathcal{O}\left(\frac{1}{\phi}\right) , \tag{4.4.30}$$

which generalizes the linear backreaction behavior found previously in the literature [138–140]. Here c is a constant that could depend on the flux numbers. We cannot formulate an general condition on the independence of c on the flux numbers, nevertheless an obvious situation is when there is only a single component $G_4 = g\,|d, l_d; i_d\rangle$, such that $l_d > 0$. In such simple cases, the flux number g will be factored out in the equation determining c, leading to a prefactor c independent from the flux-number g. Note that the analogs of such *sl(2)-elementary fluxes* play a special role in the analysis of the Weak Gravity Conjecture in [84, 86].

We also find additional constraints on the possible value of γ. Recall that our assumption on the value of α is such that it does not make any of the dots in the Newton diagram disappear. This implies that the right-most segment of the Newton polygon will be always of slope $+1$ when it is not formed by translating a single dot, i.e. it is neither from a component of the form $|d, -d\rangle$ nor from the term containing $A_{\rm loc}$. Note that the convexity condition on the Newton polygon implies that the slope of its various segments increase from left to right. We thus conclude that the backreaction of the large axion on the saxion vev always satisfy $\gamma \leq 1$. The $\gamma = 1$ cases exactly agree with the linear backreaction behavior found in [138–140]. The $0 < \gamma < 1$ cases are more subtle. One can look for these cases by the method that is used study to bad cases discussed below, and we find that the $0 < \gamma < 1$ cases appear exactly when the right-most segment in the Newton polygon is a point. The physical significance of such cases still remains unclear.

Until this point we have assumed that α takes a general value such that none of the coefficients $\mathcal{C}_{d,n_d;b_d}$ defined in (4.4.25) vanishes. Let us relax this assumption and check the consequences. Following the same arguments above, for every d that appears in the flux G_4, we need to focus on the highest weight component $|d, \tilde{n}_d; i_d\rangle$ which generates a series of terms in the polynomial $\tilde{F}_{d,\tilde{n}_d}$ that draw a segment of dots in the Newton diagram of $\tilde{F}$. Since we are interested in the lower convex hull in order to obtain the Newton polygon, only missing dots at each end of the segment will likely cause trouble. We see from (4.4.25) that for a fixed $|d, \tilde{n}_d; i_d\rangle$, if $\alpha = -d$ then the leftmost dot of the segment disappears, and if $\alpha = d - 2\tilde{n}_d$ then the rightmost dot vanishes. Let us first check what happens if a leftmost dot disappears: Taking into account the condition on the range of α in (4.4.22), we see that only the dot corresponding to the state $|0, 0\rangle$ could disappear

in such a circumstance when $\alpha = 0$. However this will extend the possible values of γ and we have also checked that it will not invalidate the discussion of the bad cases in the following subsection, either. On the other hand, when the rightmost dot disappears, new phenomena do appear. We check all possible cases with the method that is used to study bad cases discussed below and find two possible cases that generate backreaction with $\gamma = 2$. They all require $\alpha = 1$ and are given by

$$G_4^{(\mathrm{A})} = g_1 \left|3,1\right\rangle + g_2 \left|2,0\right\rangle \quad \Longrightarrow \quad \overline{s}_{\mathrm{A}}(\phi) = \frac{8g_1^2}{A_{\mathrm{loc}} - g_2^2}\phi^2 + \mathcal{O}\left(\frac{1}{\phi}\right), \tag{4.4.31}$$

$$G_4^{(\mathrm{B})} = h_1 \left|1,1\right\rangle + h_2 \left|0,0\right\rangle \quad \Longrightarrow \quad \overline{s}_{\mathrm{B}}(\phi) = \frac{2h_1^2}{A_{\mathrm{loc}} - h_2^2}\phi^2 , \tag{4.4.32}$$

where we require that $g_1, h_1 \neq 0$, while g_2, h_2 can be switched off. Note that a missing rightmost dot can surely also generate a backreaction with $0 < \gamma < 1$. It would be interesting to investigate the implication of these $\gamma = 2$ cases together with all the aforementioned $\gamma < 1$ cases.

Having finished the discussion on the cases with $\gamma > 0$, let us look at its contrary: each segment with a negative slope $-\delta < 0$ corresponds to the following solution

$$\overline{s}(\phi) = \frac{c}{\phi^\delta} + \mathcal{O}\left(\frac{1}{(\phi)^{\delta+1}}\right), \tag{4.4.33}$$

which implies that the saxion will move away from the boundary of the moduli space as the axion traverse a large field distance. A typical configuration causing such cases is shown in Figure 4.3. It remains to rule out the backreaction solution of type (4.4.33). A flux configuration potentially generating solution (4.4.33) is dubbed as a *bad case*. In the next subsection we systematically look for bad cases and show that these solutions (4.4.33) are all invalid.

4.4.4 Bad cases and their elimination

In this section, we systematically analyze bad flux configurations that can potentially generate the following backreaction behavior

$$\overline{s}(\phi) = \frac{c}{\phi^\delta} + \mathcal{O}\left(\frac{1}{\phi^{\delta+1}}\right), \tag{4.4.34}$$

where $\delta \geq 0$. The Newton polygon of F makes a systematic enumeration of these cases possible.

Let us start by noting that for a root of type (4.4.34) to appear, there must be segment of negative slope in the Newton polygon of F. Translating this condition to

the G_4 flux, one sees that there must be at least two different $\tilde{d} > d'$, whose highest weight components correspond to the basis vectors $|\tilde{d}, \tilde{d} - 2\tilde{n}_{\tilde{d}}\rangle$ and $|d', d' - 2\tilde{n}_{d'}\rangle$, such that

$$\boxed{d' - \tilde{n}_{d'} \geq \tilde{d} - \tilde{n}_{\tilde{d}}\,.} \tag{4.4.35}$$

This instructs us to enumerate the bad cases according to their number of highest weight components, and there are only three possibilities: two, three and four different d's appearing in G_4. Using the enhancement rules [136, 218], we can further reduce the possible cases by noting that $d = 4$ and $d = 3$ components cannot co-exist. The same argument also shows that bad cases with four different highest weight components cannot exist, either. Thus we are only listing two- and three-component bad cases in the following subsections.

4.4.4.1 Bad cases with two different d's

These are the fluxes of the following form

$$G_4 = g_1\,|\tilde{d}, \tilde{d} - 2\tilde{n}_{\tilde{d}}\rangle + g_2\,|d_2, d_2 - 2\tilde{n}_{d_2}\rangle\ , \tag{4.4.36}$$

where $\tilde{d} > d_2$ and $\tilde{n}_{\tilde{d}}$ and $\tilde{n}_{d_2}$ satisfy condition (4.4.35). There are 16 possible such fluxes and they are listed in Table 4.1.

We hereby present an analysis of case 13. We denote its flux configuration as

$$G_4 = g_1\,|3, -3\rangle + g_2\,|2, 0\rangle\ . \tag{4.4.37}$$

Such a flux configuration can appear, for example, in a degeneration of Calabi-Yau fourfold with $h^{3,1} = 3$. Following the notation of the singularity types in [218], the enhancement of singularity type can be $\mathrm{II}_{0,1} \to \mathrm{V}_{3,3}$.

The asymptotic scalar potential reads

$$V(s, \phi) = \frac{1}{s^\alpha}\left(\frac{\hat{g}_1^2}{s^3} + \hat{g}_2^2 + \frac{2\hat{g}_2^2\phi^2}{s^2} - A_{\mathrm{loc}}\right). \tag{4.4.38}$$

The extremization condition is given by

$$0 = \tilde{F}(s, \hat{\phi}) = \alpha(A_{\mathrm{loc}} - \hat{g}_2^2)s^3 - 4(\alpha + 2)\hat{g}_2^2\hat{\phi}^{-2}s - (\alpha + 3)\hat{g}_1^2\,. \tag{4.4.39}$$

Upon inspecting the scalar potential (4.4.38), a necessary condition for it to be not blowing up when $s \to \infty$ is $\alpha \geq 0$. Furthermore, we impose $A_{\mathrm{loc}} > 0$, otherwise there will be a runaway towards $s \to \infty$. We display the Newton polygon in Figure 4.4.

Case	g_1	g_2	δ	c	Reason
1	$\|4,0\rangle$	$\|2,2\rangle$			
2	$\|4,-2\rangle$	$\|2,0\rangle$	0		
3	$\|4,-4\rangle$	$\|2,0\rangle$		$\sqrt{-\frac{(\alpha+4)g_1^2}{(\alpha+2)g_2^2}}$	
4	$\|4,-2\rangle$	$\|2,2\rangle$	1		
5	$\|4,-4\rangle$	$\|2,2\rangle$	2		
6	$\|4,-2\rangle$	$\|1,1\rangle$	0	$\sqrt[3]{-\frac{(\alpha+4)g_1^2}{(\alpha+1)g_2^2}}$	Imaginary
7	$\|3,-1\rangle$	$\|1,1\rangle$	0	$\sqrt{-\frac{(\alpha+3)g_1^2}{(\alpha+1)g_2^2}}$	
8	$\|3,-3\rangle$	$\|1,1\rangle$	1		
9	$\|4,-4\rangle$	$\|1,1\rangle$	$\frac{2}{3}$	$\sqrt[3]{-\frac{(\alpha+4)g_1^2}{(\alpha+1)g_2^2}}(1,\omega,\omega^2)$	
10	$\|3,1\rangle$	$\|2,2\rangle$	0		
11	$\|3,-1\rangle$	$\|2,0\rangle$			
12	$\|3,-1\rangle$	$\|2,2\rangle$	2	$-\frac{(\alpha+3)g_1^2}{(\alpha+2)g_2^2}$	Negative
13	$\|3,-3\rangle$	$\|2,0\rangle$			
14	$\|3,-3\rangle$	$\|2,2\rangle$	4		
15	$\|2,0\rangle$	$\|1,1\rangle$	0	$-\frac{(\alpha+2)g_1^2}{(\alpha+1)g_2^2}$	
16	$\|2,-2\rangle$	$\|1,1\rangle$	2		

Table 4.1: Bad cases with two different d's. In the c column we have omitted non-essential normalization factors to display their shared properties. The last column points out the reason that invalidates the solution to c. Case 9 has three solutions to its prefactor c, and they differ from each other by a factor of $\omega = e^{2\pi\mathbf{i}/3}$.

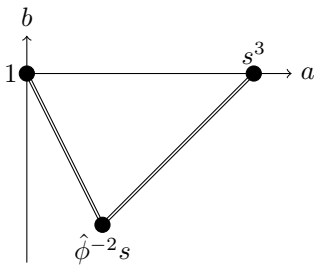

Figure 4.4: The Newton polygon of (4.4.39). It has a segment generating backreaction $\overline{s} \sim c\phi$ and another segment corresponding to $\overline{s} \sim c\phi^{-2}$.

From the Newton polygon in Figure 4.4, we read out that there are two possible solutions, one with leading term proportional to ϕ and the other with leading term proportional to $1/\phi^2$. More explicitly, they are

$$\begin{aligned}\overline{s}_{1,\pm}(\phi) &= \pm\sqrt{\frac{4(\alpha+2)\hat{g}_2^2}{\alpha(A_{\rm loc}-\hat{g}_2^2)}}\phi + \mathcal{O}\left(\frac{1}{\phi}\right),\\ \overline{s}_2(\phi) &= -\frac{(\alpha+3)\hat{g}_1^2}{4(\alpha+2)\hat{g}_2^2}\frac{1}{\phi^2} + \mathcal{O}\left(\frac{1}{\phi^3}\right).\end{aligned} \tag{4.4.40}$$

Note that among these three roots, only $\overline{s}_{1,+}$ is positive when $A_{\rm loc} > \hat{g}_2^2$. We thus conclude that for the flux (4.4.37), either there is a runaway in s, or there is a vacuum with the linear backreaction behavior

$$\overline{s}(\phi) = \sqrt{\frac{4(\alpha+2)\hat{g}_2^2}{\alpha(A_{\rm loc}-\hat{g}_2^2)}}\phi + \mathcal{O}\left(\frac{1}{\phi}\right), \tag{4.4.41}$$

when the axion ϕ is large. We would also like to point out the $\hat{g}_2$ is actually a product between g_2 and a non-vanishing function on the saxions other than s. Depending on the value of these saxions, the linearly backreacted s could even disappear. Another remark is that the leading coefficient in $\overline{s}(\phi)$ depends on the flux number g_2 and the localized contribution $A_{\rm loc}$, indicating that the backreaction effect could be delayed. A further investigation into such cases is left for future work.

4.4.4.2 Bad cases with three different d's

In this subsection, we list all *essential* flux configurations containing three different d's that are likely bad. By essential, we mean that the focus will be on the cases whose leading backreaction coefficient is determined by all three components. In the situation where this coefficient is only determined by two components, it reduces to one of the cases listed in Table 4.1. Upon inspecting possible shapes of the Newton diagram, one sees that we need to find a flux configuration

$$G_4 = g_1\,|\tilde{d}, \tilde{d}-2\tilde{n}_{\tilde{d}}\rangle + g_2\,|d_2, d_2-2\tilde{n}_{d_2}\rangle + g_3\,|d_3, d_3-2\tilde{n}_{d_3}\rangle\ , \tag{4.4.42}$$

satisfying the following conditions

$$\tilde{d} > d_2 \neq d_3\,, \tag{4.4.43}$$

$$\tilde{d}-\tilde{n}_{\tilde{d}} = d_2-\tilde{n}_{d_2} = d_3-\tilde{n}_{d_3}\,, \tag{4.4.44}$$

$$\tilde{d}-2\tilde{n}_{\tilde{d}} < d_2-2\tilde{n}_{d_2} < d_3-2\tilde{n}_{d_3}\,. \tag{4.4.45}$$

In the end there are only two bad cases and we discuss them in turn. The first one is given by

$$G_4^{(1)} = g_1\,|4,-2\rangle + g_2\,|2,0\rangle + g_3\,|1,1\rangle\ , \tag{4.4.46}$$

which induces a scalar potential of the form

$$V_1(s,\phi) = \frac{1}{s^\alpha}\left(\frac{16\hat{g}_1^2\phi^2}{s^4} + \frac{\hat{g}_1^2}{s^2} + \hat{g}_2^2 + \frac{4\hat{g}_2^2\phi^2}{s^2} + \frac{\hat{g}_3^2\phi^2}{s} + \hat{g}_3^2 s - A_{\rm loc}\right). \tag{4.4.47}$$

The condition one imposes on α is that $\alpha \geq 1$. The extremization condition $\tilde{F}_1 = 0$ is given by

$$\tilde{F}_1 = (1-\alpha)\hat{g}_3^2 s^5 + \alpha(A_{\rm loc} - \hat{g}_2^2)s^4 - (1+\alpha)\hat{g}_3^2\hat{\phi}^{-2}s^3 - (2+\alpha)(\hat{g}_1^2 + 4\hat{g}_2^2\hat{\phi}^{-2})s^2 - 16(4+\alpha)\hat{g}_1^2\hat{\phi}^{-2}\,, \tag{4.4.48}$$

whose Newton diagram is given in the left picture in Figure 4.5. From the diagram we see that there is a potential bad root with $\delta_1 = 0$. The pre-factor c_1 should satisfy the following cubic equation

$$(1+\alpha)g_3^2 c_2^3 + 4g_2^2(2+\alpha)c_2^2 + 16(4+\alpha)g_1^2 = 0\,. \tag{4.4.49}$$

Note that the coefficient in every term in the above equation is positive. In other words, there is no sign-flip in the list of coefficients in the above polynomial equation with real coefficients. The Descartes' rule of signs tells us that the number of positive root of a real polynomial equation is bounded by the number of sign-flips in its list of coefficients. Hence we conclude that even if the above quartic equation has a real root c_2, it will nevertheless be negative. This rules out the first bad case.

The last case to consider is given by

$$G_4^{(2)} = g_1\,|3,-1\rangle + g_2\,|2,0\rangle + g_3\,|1,1\rangle\ . \tag{4.4.50}$$

The corresponding scalar potential has the form

$$V_2(s,\phi) = \frac{1}{s^\alpha}\left(\frac{9\hat{g}_1^2\phi^2}{s^3} + \frac{\hat{g}_1^2}{s} + \hat{g}_2^2 + \frac{4\hat{g}_2^2\phi^2}{s^2} + \frac{\hat{g}_3^2\phi^2}{s} + \hat{g}_3^2 s - A_{\rm loc}\right). \tag{4.4.51}$$

And one has again the constraint $\alpha \geq 1$. Its extremization condition $\tilde{F}_2 = 0$ is given by

$$\tilde{F}_2 = (1-\alpha)\hat{g}_3^2 s^4 + \alpha(A_{\rm loc} - \hat{g}_2^2)s^3 - (1+\alpha)(\hat{g}_1^2 + \hat{g}_3^2\hat{\phi}^{-2})s^2 - 4(2+\alpha)\hat{g}_2^2\hat{\phi}^{-2}s^2 - 9(3+\alpha)\hat{g}_1^2\hat{\phi}^{-2}\,, \tag{4.4.52}$$

whose Newton diagram is given in the right picture in Figure 4.5. It indicates again a potential bad root with $\delta_2 = 0$, whose pre-factor c_2 satisfies the following quadratic equation

$$\hat{g}_3^2 c_2^2 + 4(2+\alpha)\hat{g}_2^2 c_2 + 9(3+\alpha)\hat{g}_1^2 = 0\,, \tag{4.4.53}$$

which has no positive real root again by Descartes' rule of sign. Hence this case is ruled out.

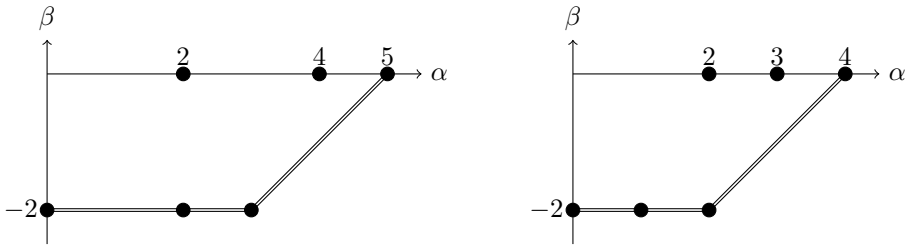

Figure 4.5: The left picture is the Newton diagram of equation (4.4.48), and the right picture corresponds to (4.4.52). Note the both diagrams show a possible linear backreaction behavior in addition to the bad constant backreaction solution.

To conclude, we have ruled out all possible bad cases which induce the backreaction behavior (4.4.34) by showing that their accompanying pre-factor c is either negative or purely imaginary. This leads to our conclusion that a large displacement of an axion ϕ can only backreacts on its saxion partner s in the way shown in equation (4.4.30) with rational exponent $0 < \gamma \leq 2$.

Appendices

4.A More detailed properties of the commuting $\mathfrak{sl}(2)$-triples

This appendix fills in some detail of the derivation of (4.3.26) and (4.3.29). We follow the proof of lemma (4.5) in [101]. In order to do this we need to take a closer look at the limiting mixed Hodge structure and the induced splittings on the infinitesimal isometry Lie algebra $\mathfrak{g}$. For definiteness we will (mostly) align with the mathematical notations in [101] in this appendix.

Recall that the Lie algebra $\mathfrak{g}_{\mathbb{R}}$ consists of the infinitesimal isometries for weight four variation of Hodge structure. Concretely, it can be identified with $\mathfrak{g}_{\mathbb{R}} = \mathfrak{so}(2 + h^{2,2}_{\mathrm{p}}, 2h^{1,3})$, where $h^{p,q}$ are the Hodge numbers of the family of Calabi-Yau fourfolds and $h^{2,2}_{\mathrm{p}}$ is the complex dimension of the space of primitive $(2,2)$-forms. The complexification of $\mathfrak{g}_{\mathbb{R}}$ is denoted by $\mathfrak{g}$ and can be identified with $\mathfrak{g} = \mathfrak{so}(2 + h^{2,2}_{\mathrm{p}} + 2h^{1,3}, \mathbb{C})$. We present these identifications merely to make the exposition more concrete but these will not be used in the following discussion.

Recall further that the log-monodromy operators $N_1, \ldots, N_n$ introduced in (4.3.3) define the *monodromy weight filtration* $W^{(n)} = W(N_1 + \cdots + N_n)[-4]$ on the primitive middle cohomology $H^4_{\mathrm{p}}(Y, \mathbb{C})$. The monodromy weight filtration together with the limiting Hodge filtration F_{pol} introduced in (4.3.4) define the *limiting mixed Hodge structure* $(F_{\mathrm{pol}}, W^{(n)})$ on $H^4_{\mathrm{p}}(Y, \mathbb{C})$. We denote the *Deligne splitting* associated to the $(F_{\mathrm{pol}}, W^{(n)})$ by

$$H^4_{\mathrm{p}}(Y, \mathbb{C}) = \bigoplus_{p,q} I^{p,q}\,, \tag{4.A.1}$$

satisfying

$$F^p_{\mathrm{pol}} = \bigoplus_{r \geq p} I^{r,s}\,, \quad W^{(n)}_k = \bigoplus_{r+s \leq k} I^{r,s}\,, \quad \text{and } I^{p,q} = \overline{I^{q,p}} \mod \bigoplus_{\substack{r<p \\ s<q}} I^{r,s}\,. \tag{4.A.2}$$

The Deligne splitting is functorial, which puts a Deligne splitting on the Lie algebra

$$\mathfrak{g} = \bigoplus_{p,q} \mathfrak{g}^{p,q}\,, \tag{4.A.3}$$

whose components can be concretely identified as

$$\mathfrak{g}^{p,q} = \left\{ X \in \mathfrak{g} \mid X(I^{r,s}) \subset I^{r+p,s+q} \right\}\,. \tag{4.A.4}$$

Recall that the SL(2)-orbit theorem constructs a set of commuting $\mathfrak{sl}(2)$-triples, whose lowering and number operators are denoted N^-_r and N^0_r, respectively in section 4.3.2. We have also defined the partial sums

$$N^0_{(r)} = N^0_1 + \cdots + N^0_r\,, \quad \text{for all } r\,. \tag{4.A.5}$$

Moreover, the SL(2)-orbit theorem constructs a series of $\mathbb{R}$-split special mixed Hodge structures from the limiting mixed Hodge structure $(F_{\mathrm{pol}}, W^{(n)})$. We denote these mixed Hodge structures by $(F_{(r)}, W^{(r)})$ and briefly state their relation to the nilpotent orbit data $(F_{\mathrm{pol}}, N_1, \ldots, N_n)$. Firstly, there is a Hodge filtration $F_{(n)}$ built

out of the data $(F_{\rm pol}, N_1, \dots, N_n)$. The $\mathbb{R}$-split mixed Hodge structure $(F_{(n)}, W^{(n)})$ is called the SL(2)-splitting of the limiting mixed Hodge structure $(F_{\rm pol}, W^{(n)})$. Then each of the remaining $(F_{(r)}, W^{(r)})$ is built recursively by taking the SL(2)-splitting of the mixed Hodge structure $(e^{\mathbf{i}N_{r+1}}, W^{(r+1)})$, where the weight filtration is give by $W^{(r)} = W(N_1 + \cdots + N_r)[-4]$. The construction of SL(2)-splitting is a bit involved and we refer to the math papers [76] and [101] for more precise information. This is also reviewed recently in a physics paper [136].

We need three important properties of the mixed Hodge structures $(F_{(r)}, W^{(r)})$. Firstly, although the filtrations $W^{(r)}$ are defined using the operators $N_1, \dots, N_r$, it turned out (by SL(2)-orbit theorem) that it agrees with the monodromy weight filtration defined by the lowering operators in the commuting $\mathfrak{sl}(2)$-triples

$$W^{(r)} = W(N_1 + \cdots + N_r)[-4] = W(N_1^- + \cdots + N_r^-)[-4]\,. \tag{4.A.6}$$

Secondly, denote the Deligne splitting of $(F_{(r)}, W^{(r)})$ by

$$H^4_{\rm p}(Y, \mathbb{C}) = \bigoplus_{p,q} I^{p,q}_{(r)}\,. \tag{4.A.7}$$

We have

$$N_{(r)}(I^{p,q}_{(r)}) \subset I^{p-1,q-1}_{(r)}\,. \tag{4.A.8}$$

Lastly, the eigenspaces of the number operators $N^0_{(r)}$ are defined in terms of $I^{p,q}_{(r)}$ as

$$N^0_{(r)} v = l v\,, \quad \text{for all } v \in \bigoplus_{r+s=l+4} I^{r,s}_{(r)}\,. \tag{4.A.9}$$

There is another splitting of the real Lie algebra $\mathfrak{g}_{\mathbb{R}}$ coming from the commuting $\mathfrak{sl}(2)$-triples. Since the number operators commute with each other, their partial sums also mutually commute

$$[N^0_{(r)}, N^0_{(s)}] = 0\,, \quad \text{for all } r, s\,. \tag{4.A.10}$$

Using the Jacobi identity, one sees that the adjoint actions $\mathrm{ad}_{N^0_{(r)}}(\,\cdot\,) = [N^0_{(r)}, \cdot\,]$ on the Lie algebra $\mathfrak{g}$ also commute with each other

$$[\mathrm{ad}_{N^0_{(r)}}, \mathrm{ad}_{N^0_{(s)}}] = 0\,, \quad \text{for all } r, s\,. \tag{4.A.11}$$

Hence these commuting adjoint actions induce a multi-grading on the Lie algebra $\mathfrak{g}$

$$\mathfrak{g} = \bigoplus_{\boldsymbol{\ell}=(l_1,\dots,l_n)} \mathfrak{g}_{\boldsymbol{\ell}}\,, \tag{4.A.12}$$

where each component is the simultaneous eigenspace of all $\mathrm{ad}_{N^0_{(r)}}$:

$$[N^0_{(r)}, X] = l_r X\,, \quad \text{for all } X \in \mathfrak{g}_{\boldsymbol{\ell}} \text{ and } r = 1, \ldots, n\,. \tag{4.A.13}$$

The eigenvalues $l_1, \ldots, l_r$ are all integers due to the general property of $\mathfrak{sl}(2)$-representations.

These two splittings (4.A.3) and (4.A.12) will be the central objects in this appendix.

4.A.1 The map $e(s)e^{\phi^i N_i}e(s)^{-1}$

Let us reproduce the definition of the $e(s)$-operator for convenience

$$e(s^1, \ldots, s^n) = \exp\left\{\frac{1}{2}(\log s^r) N^0_r\right\}\,, \tag{4.A.14}$$

where in the exponential we sum over r. It turns out that rewriting the above definition in terms of the partial sums $N^0_{(r)}$ is more suitable for our purpose in this appendix. To achieve this we formally set $s^{n+1} = 1$ and redefine variables

$$\sigma^r = \frac{s^r}{s^{r+1}}\,, \quad \text{for all } r = 1, \ldots, n\,. \tag{4.A.15}$$

With the variables σ^r one has

$$e(s^1, \ldots, s^n) = \exp\left\{\frac{1}{2}(\log \sigma^r) N^0_{(r)}\right\}\,. \tag{4.A.16}$$

We will proceed using the new form (4.A.16) of the $e(s)$-operator.

Let us spell out the expression $e(s)e^{\phi^i N_i}e(s)^{-1}$ we want to compute

$$\begin{aligned} e(s)e^{\phi^i N_i}e(s)^{-1} &= \sum_{k=1}^{\infty} \frac{(\phi^i)^k}{k!} e(s) N_i^k e(s)^{-1} \\ &= \sum_{k=1}^{\infty} \frac{(\phi^i)^k}{k!} (\mathrm{Ad}_{e(s)}(N_i))^k \\ &= e^{\phi^i\, \mathrm{Ad}_{e(s)}(N_i)}\,, \end{aligned} \tag{4.A.17}$$

where $\mathrm{Ad}_{e(s)}(N_i) = e(s)N_i e(s)^{-1}$ is the adjoint action of the group element $e(s)$ on the Lie algebra element N_i. Recall that the adjoint action of the Lie algebra on itself is defined to satisfy

$$\mathrm{Ad}_{e^X}(Y) = e^{\mathrm{ad}_X}(Y)\,, \quad \text{for all } X, Y \in \mathfrak{g}\,. \tag{4.A.18}$$

So we have reduced the quantity that we want to compute into

$$e(s)e^{\phi^i N_i}e(s)^{-1} = \exp\left\{\phi^i e^{\frac{1}{2}(\log\sigma^r)\,\mathrm{ad}_{N^0_{(r)}}}(N_i)\right\}, \tag{4.A.19}$$

where summation over i and r are assumed and we have used the new form (4.A.16) of $e(s)$-operator. From this expression we see that the important data one needs is the commutator $[N^0_{(r)}, N_i]$. This commutator depends on the relative position of r and i.

Let us first consider the case when $r \geq i$. From the property (4.A.8), we see (by contradiction) that the same property must hold for each N_i with $i \leq r$

$$N_i(I^{p,q}_{(r)}) \subset I^{p-1,q-1}_{(r)}, \quad \text{for } i = 1, \ldots, r\,. \tag{4.A.20}$$

This automatically forces the relation

$$[N^0_{(r)}, N_i] = -2N_i\,, \quad \text{for all } r \geq i\,, \tag{4.A.21}$$

by the characterization (4.A.4) of the Deligne splitting on the Lie algebra and the property (4.A.9).

Next we look at the case $r < i$. In such case we no longer have good control over the commutator $[N^0_{(r)}, N_i]$. The best result one has is simply that N_i preserves the filtration $W^{(r)}$. One way to see this is to use an explicit characterization of the monodromy weight filtration in remark (2.3) of [110] with the (-4)-shift

$$W^{(r)}_l = \sum_{j \geq \max\{-1, l-4\}} (\mathrm{Ker}\, N^{j+1}_{(r)}) \cap (\mathrm{Im}\, N^{j-l+4}_{(r)})\,, \tag{4.A.22}$$

and note that N_i commutes with $N_{(r)}$.

Using again (4.A.4), (4.A.9), and the general property of the Deligne splitting (4.A.2), we conclude that the eigen-decomposition of N_i with respect to the action of $\mathrm{ad}_{N^0_{(r)}}$ has only *non-positive* eigenvalues.

We can have more control over the eigenvalues by investigating the multi-grading (4.A.12). Remembering that $r < i$, let us diagonalize actions of all $\mathrm{ad}_{N^0_{(r)}}$ on N_i simultaneously. We split $N_i = N^-_i + N'_i$, such that $\mathrm{ad}_{N^0_{(r)}}(N^-_i) = 0$ for all $r = 1, \ldots, i-1$. And further decompose the remaining N'_i according to the multi-grading (4.A.12)

$$N'_i = \sum_{\alpha^i_1, \ldots, \alpha^i_{i-1} > 0} N'_{i, \alpha^i_1, \ldots, \alpha^i_{i-1}}, \tag{4.A.23}$$

where $\alpha^i_r > 0$ labels the eigenvalue of $\mathrm{ad}_{N^0_{(r)}}$ on N_i,

$$\left[N^0_{(r)}, N'_{i, \alpha^i_1, \ldots, \alpha^i_{i-1}}\right] = -\alpha^i_r N'_{i, \alpha^i_1, \ldots, \alpha^i_{i-1}}\,, \quad \text{for } i > r. \tag{4.A.24}$$

Moreover, it can be checked that each α_r^i is also an integer, and the components N_i^-, $N'_{i,\underline{\alpha}^i}$ are nilpotent.

To summarize, for every $i = 1, \ldots, n$, one has a decomposition

$$N_i = N_i^- + \sum_{\underline{\alpha}^i > 0} N'_{i,\underline{\alpha}^i} \,, \tag{4.A.25}$$

where $\underline{\alpha}^i = (\alpha_1^i, \ldots, \alpha_{i-1}^i)$ denotes the collection of positive integer eigenvalues, such that $[N_{(r)}^0, N_i^-] = 0$ for all $r > i$, and

$$[N_{(r)}^0, N_i] = \begin{cases} -2N_i \,, & \text{for } i \leq r \,, \\ -\sum_{\underline{\alpha}^i > 0} \alpha_r^i N'_{i,\underline{\alpha}^j} \,, & \text{for } i > r \,. \end{cases} \tag{4.A.26}$$

It is then straightforward to plug (4.A.26) into (4.A.19) and conclude

$$e(s) e^{\phi^i N_i} e(s)^{-1} = \exp\left\{ \sum_{i=1}^n \frac{\phi^i}{s^i} \left(N_i^- + \sum_{\underline{\alpha}^i > 0} \frac{N'_{i,\underline{\alpha}^i}}{(\frac{s^1}{s^2})^{\alpha_1^i/2} \cdots (\frac{s^{i-1}}{s^i})^{\alpha_{i-1}^i/2}} \right) \right\} . \tag{4.A.27}$$

This finishes the derivation of equation (4.3.26). We would like to point out that due to the nilpotent operators, this equation is actually *polynomial* in ϕ and s. This is in contrast to the quantity we want to compute in the next subsection.

4.A.2 The map $e(s)e^{\Gamma(z)}e(s)^{-1}$ in the limit

Following the procedure in the previous subsection, we have

$$e(s) e^{\Gamma(z)} e(s)^{-1} = \exp\left\{ e^{\frac{1}{2}(\log \sigma^r) \operatorname{ad}_{N_{(r)}^0}} (\Gamma(z)) \right\} = 1 + e^{\frac{1}{2}(\log \sigma^r) \operatorname{ad}_{N_{(r)}^0}} (\Gamma(z)) + \cdots \,, \tag{4.A.28}$$

where a summation over r under the exponential is assumed. In the above expression we only displayed up to the first order term in the outer exponential in hindsight as it will turn out that this first order term will be *exponentially suppressed* in the limit $\sigma^r \to \infty$, so that the expression (4.A.28) will approach 1 exponentially as shown in the first equation in (4.3.29).

The expression (4.A.28) again instructs us to look into the commutator $[N_{(r)}^0, \Gamma(z)]$. Unfortunately, we cannot work out an expression for (4.A.28) as "concrete" as (4.3.26). The best general result we have here is the limit.

Let us first state some general property of the mapping $\Gamma(z)$ following [101]. Firstly, the mapping $\Gamma(z)$ is holomorphic in z and satisfies $\Gamma(0) = 0$, which means

that it enjoys a series expansion around $z = 0$

$$\Gamma(z_1, \ldots, z_n) = \sum_{k_1,\ldots,k_n \geq 0} \Gamma^{k_1,\ldots,k_n} z_1^{k_1} \cdots z_n^{k_n} \,, \tag{4.A.29}$$

with $\Gamma^{\underline{0}} = 0$. Secondly, proposition (2.6) in [101] states that $\Gamma(z)$ satisfies

$$[N_j, \Gamma(z_1, \ldots, z_j = 0, \ldots, z_n)] = 0 \,, \quad \text{for all } j = 1, \ldots, n \,. \tag{4.A.30}$$

Combining the above identity for all $j \leq r$, we have

$$[N_{(r)}, \Gamma(0, \ldots, 0, z_{r+1}, \ldots, z_n)] = 0 \,, \quad \text{for all } r = 1, \ldots, n \,. \tag{4.A.31}$$

Let us decompose the series expansion of $\Gamma(z)$ in (4.A.29) further with respect to the multi-grading (4.A.12)

$$\Gamma^{k_1,\ldots,k_n} = \sum_{\boldsymbol{\ell}} \Gamma_{\boldsymbol{\ell}}^{k_1,\ldots,k_n} \,. \tag{4.A.32}$$

The conclusion here is that, for a fixed set of $\boldsymbol{\ell} = (l_1, \ldots, l_n)$, if a component $l_r > 0$, then

$$\Gamma^{0,\ldots,0,k_{r+1},\ldots,k_n}_{l_1,\ldots,l_r>0,\ldots,l_n} = 0 \,, \quad \text{for all } k_{r+1}, \ldots, k_n \,. \tag{4.A.33}$$

This can be seen, e.g., again by looking at the general expression of the weight filtration on the Lie algebra $\mathfrak{g}$. Note that the monodromy weight filtration on the Lie algebra $\mathfrak{g}$ no longer has the (-4)-shift, so one concludes that operators commute with $N_{(r)}$ lives below level $l_r \leq 0$.

Define

$$\Gamma_{\boldsymbol{\ell}}(z) = \sum_{k_1,\ldots,k_n} \Gamma_{\boldsymbol{\ell}}^{k_1,\ldots,k_n} \,. \tag{4.A.34}$$

Let us check the first order term in (4.A.28). For a fixed $\boldsymbol{\ell} = (l_1, \ldots, l_n)$, we have

$$e^{\frac{1}{2}(\log \sigma^r)\, \mathrm{ad}_{N^0_{(r)}}}(\Gamma_{\boldsymbol{\ell}}(z)) = (\sigma^1)^{\frac{l_1}{2}} \cdots (\sigma^n)^{\frac{l_n}{2}} \Gamma_{\boldsymbol{\ell}}(z) \,. \tag{4.A.35}$$

We would like to find the limit $e(s)e^{\Gamma(z)}e(s)^{-1}$ as $\sigma^r \to \infty$ for all r. In order to do so, we choose any norm $\|\cdot\|$ on the Lie algebra $\mathfrak{g}$ and first check $\|\Gamma_{\boldsymbol{\ell}}(z)\|$. For all possible $j = 1, \ldots, n$, there are two possibilities: If $l_j > 0$, then with (4.A.33), we have

$$\left\|\Gamma_{l_1,\ldots,l_j>0,\ldots,l_n}(z)\right\| = \left\| \sum_{k_1,\ldots,k_j>0} \Gamma^{k_1,\ldots,k_n}_{l_1,\ldots,l_n} z_1^{k_1} \cdots z_n^{k_n} \right\| \leq M \sum_{i=1}^{j} e^{-c_i s^i} \,, \tag{4.A.36}$$

for some positive constants M and c_i in the limit $\sigma^r \to \infty$ for all r. We have used the relation $z_i = e^{2\pi \mathbf{i} t^i} = e^{-2\pi s^i} e^{2\pi \mathbf{i}\phi^i}$. Plug this back into (4.A.35) and we have

$$\left\| e^{\frac{1}{2}(\log \sigma^r)\,\mathrm{ad}_{N^0_{(r)}}}(\Gamma_{\boldsymbol{\ell}}(z)) \right\| \leq M(\sigma^1)^{\frac{l_1}{2}} \cdots (\sigma^n)^{\frac{l_n}{2}} \sum_{i=1}^{j} e^{-c_i \sigma^i \cdots \sigma^n} . \tag{4.A.37}$$

Note that we have used the relation $s^j = \sigma^j \cdots \sigma^n$.

A second possibility is $l_j \leq 0$ and in such cases the estimate (4.A.37) holds trivially (recall that $\Gamma_{\boldsymbol{\ell}}(0) = 0$ for all $\boldsymbol{\ell}$).

In conclusion, the first order term in (4.A.28) satisfies the estimate (4.A.37), which means that in the limit $\sigma^r \to \infty$ it goes to 0 exponentially. We have thus conclude that $e(s)e^{\Gamma(z)}e(s)^{-1} \to 1$ with exponentially suppressed corrections in the limit $\sigma^r \to \infty$ for all r.

4.A.3 The filtration $e(s)F_0$ in the limit

We will be short in this section and mainly refer the reader to the papers [76] and [101]. The result we would like to show is that in the limit where all $\sigma^r \to \infty$, one has

$$e(s)F_0 \to F_{(n)} . \tag{4.A.38}$$

Combining with the definition that

$$F_\infty = e^{\mathbf{i}N^-_{(n)}} F_{(n)} , \tag{4.A.39}$$

this shows the second equation of (4.3.29).

Here are some facts [101] about the relation between F_0 and $F_{(n)}$. There exists an operator $\eta \in \mathfrak{g}_{\mathbb{R}}$ such that

$$F_0 = e^{\eta} F_{(n)} . \tag{4.A.40}$$

The operator η satisfies

$$\eta(I^{p,q}) \subset \bigoplus_{\substack{r<p \\ r<q}} I^{r,s} . \tag{4.A.41}$$

Moreover the operator η commutes with every (r,r)-morphism of the mixed Hodge structure $(W^{(n)}, F_{(n)})$.

Let us decompose the operator η with respect to the multi-grading (4.A.12)

$$\eta = \sum_{\boldsymbol{\ell}} \eta_{\boldsymbol{\ell}} . \tag{4.A.42}$$

Then the property (4.A.41) implies that $l_n < 0$. Furthermore, recall from (4.A.20) every N_r with $r = 1, \ldots, n-1$ is a $(-1,-1)$-morphism of the mixed Hodge structure $(W^{(n)}, F_{(n)})$, we have $[N_r, \eta] = 0$ for all $r = 1, \ldots, n-1$. According to the definition of the monodromy weight filtration, this implies that $l_r \leq 0$. So we have

$$\begin{aligned} e(s)e^{\eta}e(s)^{-1} &= \exp\left\{ e^{\frac{1}{2}(\log \sigma^r)\,\mathrm{ad}_{N^0_{(r)}}}(\eta) \right\} \\ &= \exp\left\{ \sum_{\substack{l_1,\ldots,l_{n-1}\leq 0 \\ l_n<0}} (\sigma^1)^{\frac{l_1}{2}} \cdots (\sigma^n)^{\frac{l_n}{2}} \eta_{l_1,\ldots,l_n} \right\} \to 1\,, \end{aligned} \tag{4.A.43}$$

in the limit where every $\sigma^r \to \infty$.

Summary

In this summary we give a short overview of the content of this thesis. The idea of the entire thesis is to use asymptotic Hodge theory of the internal Calabi-Yau space in string compactification to study the four-dimensional physics near various corners of the field space. This approach sets up some universal understandings of the swampland program in quantum gravity.

The first chapter is an introduction, and the remaining three chapters are based on the three publications produced by the author and collaborators during the PhD research. One ongoing research on tame geometry and swampland is only mentioned, but not included, in this thesis.

The first chapter introduces the basic concepts used in this thesis. We introduce string compactification, which connects the higher dimensional string spacetime with the lower dimensional physical spacetime. The lower dimensional physics is neatly encoded in the geometry of the compactification manifold. We also introduce the idea of swampland, which is a program aiming to distinguish consistent-looking effective field theories that are compatible with quantum gravity from those that are not. The last part of the introduction builds an intuition about asymptotic Hodge theory, and provides ample references for further study.

The second chapter uses asymptotic Hodge theory to study the swampland distance conjecture. The setting is type IIB string theory compactified on Calabi-Yau threefolds, and we examine the distance conjecture in the complex structure moduli space of the Calabi-Yau's. With the help of Hodge theory, we equip every limit in the moduli space with an algebraic structure, and classify all possible structures that can appear within a Calabi-Yau. When the Calabi-Yau admits multiple-stage degenerations, all possible transitions between the corresponding algebraic structures are also classified. Thus, an intricate network of the algebraic structures associated with infinite distance limits is discovered. Using this network of algebraic structures, we are able to find the light tower of states in the swampland distance conjecture in most infinite distance limits. The approach is exemplified in detail in two-parameter models.

The third chapter uses asymptotic Hodge theory to study the swampland de Sitter conjecture near the corners in the scalar field space. The setting is F-theory

compactified on Calabi-Yau fourfolds with four-form flux, and we work in the complex structure moduli space of the fourfolds. There are again algebraic structures associated to every asymptotic limit in the complex structure moduli space of Calabi-Yau fourfolds, and these algebraic structures can be classified. Using the classification, we further exhaust the possible forms of the scalar potentials in the asymptotic limits. We carry out this program in detail for two-parameter families of Calabi-Yau fourfolds, and study the vacuum structure of these theories near the asymptotic limit. We confirm the de Sitter conjecture near the asymptotic limits. Via dualities, these F-theoretical conclusions generalise the known results in type IIA and IIB orientifold settings. In the end, we use the same approach to write down possible asymptotic forms of the axion potentials in the axion monodromy inflation models, and we study the backreaction of axions on saxions. We discover that the previously found linear backreaction behaviour of axions on saxions in some examples are intimately related to asymptotic Hodge theory in the field space.

The fourth chapter inquires further the topic at the end of chapter three. We examine more closely the implication of asymptotic Hodge theory on the axion monodromy inflation models. We work again in the complex structure moduli space of F-theory compactified on Calabi-Yau fourfolds. The problem is approached differently than in chapter three, using no classifications of the algebraic structures associated to the limits of the field space. Thus, the asymptotic form of the axion monodromy potential is generally studied. The backreaction of axions on saxions is attacked using the Puiseux series solution of the vacuum equations, and the method is exemplified in two-parameter models. We confirm that, besides some exceptional cases, the linear backreaction of axion on saxion found previously in several examples are universal in axion monodromy models.

Samenvatting

In deze samenvatting geven we een kort overzicht van de inhoud van dit proefschrift. Het idee van het hele proefschrift is om de asymptotische Hodge-theorie van de interne Calabi-Yau-ruimte bij snaartheorie compactificaties te gebruiken om de vierdimensionale fysica nabij verschillende hoeken van de veldruimte te bestuderen. Deze benadering zorgt voor een aantal universele inzichten in het moeraslandprogramma in kwantumzwaartekracht.

Het eerste hoofdstuk is een inleiding, de overige drie hoofdstukken zijn gebaseerd op de drie publicaties die de auteur en medewerkers tijdens het promotieonderzoek hebben geproduceerd. Een lopend onderzoek naar tamme geometrie en moerasland wordt alleen genoemd, maar niet opgenomen in dit proefschrift.

Het eerste hoofdstuk introduceert de basisconcepten die in dit proefschrift worden gebruikt. We introduceren snaartheorie compactificaties, die de hoger-dimensionale ruimtetijd van snaren verbindt met de lager dimensionale fysieke ruimtetijd. De lager-dimensionale fysica is netjes gecodeerd in de geometrie van de compactificatievariëteit. We introduceren ook het idee van het moerasland, een programma dat erop gericht is om consistent-ogende effectieve veldtheorieën die compatibel zijn met kwantumzwaartekracht te onderscheiden van theorieën die dat niet zijn. Het laatste deel van de inleiding bouwt een intuïtie op over waar de asymptotische Hodge-theorie over gaat, en biedt voldoende referenties voor verder onderzoek.

In het tweede hoofdstuk wordt de asymptotische Hodge-theorie gebruikt om het moeraslandafstandsvermoeden te bestuderen. De setting is type IIB snaartheorie gecompactificeerd op Calabi-Yau drievariëteiten, en we onderzoeken het afstandsvermoeden in de complexe structuur moduliruimte van de Calabi-Yau's. Met behulp van de Hodge-theorie rusten we elke limiet in de moduliruimte uit met een algebraïsche structuur, en classificeren we alle mogelijke structuren die binnen een Calabi-Yau kunnen voorkomen. Wanneer de Calabi-Yau meertrapsdegeneraties toelaat, worden ook alle mogelijke overgangen tussen de overeenkomstige algebraïsche structuren geclassificeerd. Zo wordt een ingewikkeld netwerk van de algebraïsche structuren ontdekt die geassocieerd zijn met oneindige afstandslimieten. Met behulp van dit netwerk van algebraïsche structuren kunnen we de toren van lichte toestanden vinden in het moeraslandafstandsvermoeden in de meeste

oneindige afstandslimieten. De aanpak wordt in detail geïllustreerd in modellen met twee parameters.

Het derde hoofdstuk gebruikt de asymptotische Hodge-theorie om het De Sitter-vermoeden nabij de hoeken in de scalaire veldenruimte te bestuderen. De setting is F-theorie gecompactifieerd op Calabi-Yau viervariëten met vier-vorm flux, en we werken in de complexe structuur moduliruimte van de viervariëten. Er zijn weer algebraïsche structuren geassocieerd met elke asymptotische limiet in de complexe structuur moduliruimte van Calabi-Yau viervariëteiten, en deze algebraïsche structuren kunnen worden geclassificeerd. Met behulp van de classificatie werken we de mogelijke vormen van de scalaire potentialen in de asymptotische limieten verder uit. We voeren dit programma in detail uit voor families met twee parameters van Calabi-Yau viervariëteiten, en bestuderen de vacuümstructuur van deze theorieën nabij de asymptotische limiet. We bevestigen het vermoeden van het De Sitter-vermoeden nabij de asymptotische limieten. Via dualiteiten veralgemeniseren deze F-theoretische conclusies de bekende resultaten in de type IIA en IIB orientifold settings. Uiteindelijk gebruiken we dezelfde benadering om mogelijke asymptotische vormen van de axionpotentialen in de axion-monodromie inflatiemodellen op te schrijven, en bestuderen we de terugreactie van axions op saxions. We ontdekken dat het eerder gevonden lineaire terugreactiegedrag van axions op saxions in sommige voorbeelden nauw verband houdt met de asymptotische Hodge-theorie in de veldenruimte.

Het vierde hoofdstuk bestudeerd het onderwerp aan het einde van hoofdstuk drie verder. We onderzoeken de implicatie van asymptotische Hodge-theorie op de axion-monodromie inflatiemodellen in meer detail. We werken opnieuw in de complexe structuur moduliruimte van F-theorie gecompactificeerd op Calabi-Yau viervariëteiten. Het probleem wordt anders benaderd dan in hoofdstuk drie, waarbij geen classificaties worden gebruikt van de algebraïsche structuren die verband houden met de limieten in de veldenruimte. Zo wordt de asymptotische vorm van de axion-monodromie potentiaal algemeen bestudeerd. De terugreactie van axions op saxions wordt aangevallen met behulp van de Puiseux-reeksoplossing van de vacuümvergelijkingen, en de methode wordt geïllustreerd in modellen met twee parameters. We bevestigen dat, afgezien van enkele uitzonderlijke gevallen, de lineaire terugreactie van axions op saxions die eerder in verschillende voorbeelden werd gevonden, universeel is in axion-monodromiemodellen.

Acknowledgements

I would like to express my most sincere gratitude to my supervisor Thomas Grimm. Your trust in my mathematical capability, from the starting of my master's project to the end of my PhD, encouraged me to understand those wonderful mathematical concepts that I had never dare to read about. You also taught me how to be a thoughtful writer, and endured my procrastination on writing. I would never forget the experience of being a PhD student of you.

I would also like to thank Stefan Vandoren for being my former promoter, and for helping me arrange my promoter-shift after Thomas became a professor. Thank Umut Gürsoy for being my new co-promoter, and also for bringing me into string theory in the lectures during the spring semester in 2016.

Thank Eran Palti, Irene Valenzuela, and Stefano Lanza for being my collaborators. It is a great pleasure to collaborate with you even at the very early stage of my PhD years. I also heartedly thank Stefano for reading and providing detailed feedbacks on this thesis, for sharing your knowledge on Italian cooking, and many other things.

Thank my wife, 赵一然. My PhD study began with our marriage, with the unforgettable trip to Japan. You have provided invaluable support and encouragement during my PhD years. You have let me experience a more colourful and vivid world. I love you. Thank my parents, for constantly supporting my study in the last 29 years.

Thank 郭立业, 王乔志, 杨翘楚, 万建崧, 陈汉, 刘雪文, 赵爽怡, 阎嘉阳, 王狄, 辛猛, Natale Zinnato, Huibert het Lam and Sela Samin, for providing many useful suggestions about job hunting during the last stage of my PhD years. I would also like to thank 辛猛 for helping me acquiring some PhD thesis on Hodge theory in the UMass Amherst repository. Those documents greatly helped my understanding on this topic. Thank also my friends 郭金峰, 陈云路 and 叶隽彤 for many interesting activities we did together during these years.

Lastly, I would like to thank all my colleagues and office mates, Sebastian Greiner, Pierre Corvilain, Kilian Mayer, Damian van de Heisteeg, Jeroen Monnee, Arno Hoefnagels, Markus Dierigl, Miguel Montero, Brice Bastian, Lorenz Schlechter, Christopher Couzens, Eric Marcus, Koen Stemerdink, 念国恩, 练成, 刘

磊华, 郑建森, 廖磊, Axel Cortés Cubero, Tatjana Puškarov, Natalia Menezes, Ward Vleeshouwers, Rodrigo Arouca, Rodrigo Ozela, Lizardo Nunes, Anouar Moustaj, Robin Verstraten, Kitinan Pongsangangan, Francisco García Flórenz, and many more, for providing the great working environment at UU ITF. Particularly, I would like to thank Damian for translating both the scientific and the non-scientific summaries into Dutch, and Eric for sharing the LaTeX template.

About the author

Chongchuo Li (李翀绰) was born on 28th of Jan., 1993 in Tianjin, China.

In 2011, he entered University of Science and Technology of China to study computer science. His interest shifted towards physics in 2012, so he changed his major to theoretical physics. During the bachelor study, he was greatly impressed by a talk given by Yongbin Ruan (阮永斌) about Mirror Symmetry, and he decided to go deeper in studying the mathematical structures related to string theory. He graduated with bachelor's thesis, *Frobenius algebras and* $2D$ *topological quantum field theories* (in Chinese), under the supervision of Bailin Song (宋百林). The thesis is a reading note of the book [222] under the same title by Joachim Kock.

From 2015 to 2018, he attended the master's degree program in Theoretical Physics at Utrecht University, graduated with master's thesis, *Geometric derivations of quantum corrections for gauge coupling functions*, supervised by Thomas Grimm. The thesis is about the Seiberg-Witten solution in four-dimensional $\mathcal{N} = 2$ pure SU(2)-gauge theory, and its embedding into string theory. Upon the completion of his master's thesis, he got acquainted with the nilpotent orbit theorem, which later became the starting point of his PhD study.

From 2018 to 2022, he carried out PhD research at Utrecht University under the supervision of Thomas Grimm. The results of this period is presented in this thesis.

Bibliography

[1] Event Horizon Telescope collaboration, K. Akiyama et al., *First M87 Event Horizon Telescope Results. I. The Shadow of the Supermassive Black Hole*, *Astrophys. J. Lett.* **875** (2019) L1 [1906.11238].

[2] T. Kaluza, *Zum Unitätsproblem der Physik*, *Sitzungsber. Preuss. Akad. Wiss. Berlin (Math. Phys.)* **1921** (1921) 966 [1803.08616].

[3] O. Klein, *Quantum Theory and Five-Dimensional Theory of Relativity. (In German and English)*, *Z. Phys.* **37** (1926) 895.

[4] C. Vafa, *The String landscape and the swampland*, hep-th/0509212.

[5] T. W. Grimm, E. Palti and I. Valenzuela, *Infinite Distances in Field Space and Massless Towers of States*, *JHEP* **08** (2018) 143 [1802.08264].

[6] P. Deligne, *The Hodge conjecture*, in *The millennium prize problems*, pp. 45–53. Clay Math. Inst., Cambridge, MA, 2006.

[7] M. Grana, *Flux compactifications in string theory: A Comprehensive review*, *Phys. Rept.* **423** (2006) 91 [hep-th/0509003].

[8] M. R. Douglas and S. Kachru, *Flux compactification*, *Rev. Mod. Phys.* **79** (2007) 733 [hep-th/0610102].

[9] S. Ashok and M. R. Douglas, *Counting flux vacua*, *JHEP* **01** (2004) 060 [hep-th/0307049].

[10] F. Denef and M. R. Douglas, *Distributions of flux vacua*, *JHEP* **05** (2004) 072 [hep-th/0404116].

[11] E. Cattani, P. Deligne and A. Kaplan, *On the locus of Hodge classes*, *J. Amer. Math. Soc.* **8** (1995) 483.

[12] B. Bakker, B. Klingler and J. Tsimerman, *Tame topology of arithmetic quotients and algebraicity of Hodge loci*, *J. Amer. Math. Soc.* **33** (2020) 917.

[13] T. W. Grimm, *Moduli space holography and the finiteness of flux vacua*, *JHEP* **10** (2021) 153 [2010.15838].

[14] B. Bakker, T. W. Grimm, C. Schnell and J. Tsimerman, *Finiteness for self-dual classes in integral variations of Hodge structure*, 2112.06995.

[15] T. W. Grimm and J. Louis, *The Effective action of N = 1 Calabi-Yau orientifolds*, *Nucl. Phys. B* **699** (2004) 387 [hep-th/0403067].

[16] T. W. Grimm and J. Louis, *The Effective action of type IIA Calabi-Yau orientifolds*, *Nucl. Phys. B* **718** (2005) 153 [hep-th/0412277].

[17] L. E. Ibanez and A. M. Uranga, *String theory and particle physics: An introduction to string phenomenology*. Cambridge University Press, 2, 2012.

[18] E. Lauria and A. van Proeyen, $\mathcal{N} = 2$ *Supergravity in* $D = 4, 5, 6$ *Dimensions*, vol. 966. 3, 2020, [2004.11433].

[19] D. Z. Freedman and A. van Proeyen, *Supergravity*. Cambridge Univ. Press, Cambridge, UK, 5, 2012.

[20] L. Andrianopoli, M. Bertolini, A. Ceresole, R. D'Auria, S. Ferrara, P. Fre et al., *N=2 supergravity and N=2 super Yang-Mills theory on general scalar manifolds: Symplectic covariance, gaugings and the momentum map*, *J. Geom. Phys.* **23** (1997) 111 [hep-th/9605032].

[21] B. Craps, F. Roose, W. Troost and A. van Proeyen, *What is special Kahler geometry?*, *Nucl. Phys. B* **503** (1997) 565 [hep-th/9703082].

[22] A. Strominger, *SPECIAL GEOMETRY*, *Commun. Math. Phys.* **133** (1990) 163.

[23] D. S. Freed, *Special Kahler manifolds*, *Commun. Math. Phys.* **203** (1999) 31 [hep-th/9712042].

[24] R. Blumenhagen, D. Lüst and S. Theisen, *Basic concepts of string theory*, Theoretical and Mathematical Physics. Springer, Heidelberg, Germany, 2013.

[25] K. Becker, M. Becker and J. H. Schwarz, *String theory and M-theory: A modern introduction*. Cambridge University Press, 12, 2006.

[26] V. Bouchard, *Lectures on complex geometry, Calabi-Yau manifolds and toric geometry*, hep-th/0702063.

[27] C. Closset, *Toric geometry and local Calabi-Yau varieties: An Introduction to toric geometry (for physicists)*, 0901.3695.

[28] S. Reffert, *The Geometer's Toolkit to String Compactifications*, in *Conference on String and M Theory Approaches to Particle Physics and Cosmology*, 6, 2007, 0706.1310.

[29] P. Candelas, *Lectures on complex manifolds*, in *Superstrings and grand unification*. 1988.

[30] M. Gross, D. Huybrechts and D. Joyce, *Calabi-Yau manifolds and related geometries*, Universitext. Springer-Verlag, Berlin, 2003.

[31] D. D. Joyce, *Compact manifolds with special holonomy*, Oxford Mathematical Monographs. Oxford University Press, Oxford, 2000.

[32] D. Kotschick and S. Schreieder, *The Hodge ring of Kähler manifolds*, *Compos. Math.* **149** (2013) 637.

[33] P. Candelas and X. de la Ossa, *Moduli Space of Calabi-Yau Manifolds*, *Nucl. Phys. B* **355** (1991) 455.

[34] N. Cabo Bizet, A. Klemm and D. Vieira Lopes, *Landscaping with fluxes and the E8 Yukawa Point in F-theory*, 1404.7645.

[35] C. F. Cota, A. Klemm and T. Schimannek, *Modular Amplitudes and Flux-Superpotentials on elliptic Calabi-Yau fourfolds*, *JHEP* **01** (2018) 086 [1709.02820].

[36] A. Gerhardus and H. Jockers, *Quantum periods of Calabi–Yau fourfolds*, *Nucl. Phys. B* **913** (2016) 425 [1604.05325].

[37] H. Iritani, *Quantum cohomology and periods*, *Ann. Inst. Fourier (Grenoble)* **61** (2011) 2909.

[38] S. Bloch, M. Kerr and P. Vanhove, *Local mirror symmetry and the sunset Feynman integral*, *Adv. Theor. Math. Phys.* **21** (2017) 1373 [1601.08181].

[39] M. Graña and H. Triendl, *String theory compactifications*, in *String Theory Compactifications*, pp. 1–74. Springer, 2017.

[40] C. Vafa, *Evidence for F-theory*, *Nucl. Phys. B* **469** (1996) 403 [hep-th/9602022].

[41] F. Denef, *Les Houches Lectures on Constructing String Vacua*, *Les Houches* **87** (2008) 483 [0803.1194].

[42] T. Weigand, *Lectures on F-theory compactifications and model building*, *Class. Quant. Grav.* **27** (2010) 214004 [1009.3497].

[43] T. Weigand, *F-theory*, *PoS* **TASI2017** (2018) 016 [1806.01854].

[44] T. W. Grimm, *The N=1 effective action of F-theory compactifications*, *Nucl. Phys. B* **845** (2011) 48 [1008.4133].

[45] P. Corvilain, T. W. Grimm and D. Regalado, *Shift-symmetries and gauge coupling functions in orientifolds and F-theory*, *JHEP* **05** (2017) 059 [1607.03897].

[46] J. Wess and J. Bagger, *Supersymmetry and supergravity*. Princeton

University Press, Princeton, NJ, USA, 1992.

[47] S. Greiner and T. W. Grimm, *On Mirror Symmetry for Calabi-Yau Fourfolds with Three-Form Cohomology*, *JHEP* **09** (2016) 073 [1512.04859].

[48] S. Greiner and T. W. Grimm, *Three-form periods on Calabi-Yau fourfolds: Toric hypersurfaces and F-theory applications*, *JHEP* **05** (2017) 151 [1702.03217].

[49] A. Klemm, B. Lian, S. S. Roan and S.-T. Yau, *Calabi-Yau fourfolds for M-theory and F-theory compactifications*, *Nucl. Phys. B* **518** (1998) 515 [hep-th/9701023].

[50] B. R. Greene, D. R. Morrison and M. R. Plesser, *Mirror manifolds in higher dimension*, *Commun. Math. Phys.* **173** (1995) 559 [hep-th/9402119].

[51] S. Gukov, C. Vafa and E. Witten, *CFT's from Calabi-Yau four folds*, *Nucl. Phys. B* **584** (2000) 69 [hep-th/9906070].

[52] T. D. Brennan, F. Carta and C. Vafa, *The String Landscape, the Swampland, and the Missing Corner*, *PoS* **TASI2017** (2017) 015 [1711.00864].

[53] E. Palti, *The Swampland: Introduction and Review*, *Fortsch. Phys.* **67** (2019) 1900037 [1903.06239].

[54] M. van Beest, J. Calderón-Infante, D. Mirfendereski and I. Valenzuela, *Lectures on the Swampland Program in String Compactifications*, 2102.01111.

[55] M. Graña and A. Herráez, *The Swampland Conjectures: A Bridge from Quantum Gravity to Particle Physics*, *Universe* **7** (2021) 273 [2107.00087].

[56] D. Harlow, B. Heidenreich, M. Reece and T. Rudelius, *The Weak Gravity Conjecture: A Review*, 2201.08380.

[57] H. Ooguri and C. Vafa, *On the Geometry of the String Landscape and the Swampland*, *Nucl. Phys. B* **766** (2007) 21 [hep-th/0605264].

[58] D. Klaewer and E. Palti, *Super-Planckian Spatial Field Variations and Quantum Gravity*, *JHEP* **01** (2017) 088 [1610.00010].

[59] T. W. Grimm, S. Lanza and C. Li, *String probes, tameness, and the swampland*, *work in progress* (2022) .

[60] S.-J. Lee, W. Lerche and T. Weigand, *Emergent Strings from Infinite Distance Limits*, 1910.01135.

[61] S.-J. Lee, *On Towers of Light States at Infinite Distance*, in *Nankai*

Symposium on Mathematical Dialogues: In celebration of S.S.Chern's 110th anniversary, 12, 2021, 2112.13851.

[62] G. Obied, H. Ooguri, L. Spodyneiko and C. Vafa, *De Sitter Space and the Swampland*, 1806.08362.

[63] H. Ooguri, E. Palti, G. Shiu and C. Vafa, *Distance and de Sitter Conjectures on the Swampland*, *Phys. Lett. B* **788** (2019) 180 [1810.05506].

[64] R. Bousso, *A Covariant entropy conjecture*, *JHEP* **07** (1999) 004 [hep-th/9905177].

[65] T. W. Grimm, *Taming the Landscape of Effective Theories*, 2112.08383.

[66] R. O. Wells, Jr., *Differential analysis on complex manifolds*, vol. 65 of *Graduate Texts in Mathematics*. Springer, New York, third ed., 2008.

[67] P. Griffiths and J. Harris, *Principles of algebraic geometry*, Wiley Classics Library. John Wiley & Sons, Inc., New York, 1994.

[68] D. Huybrechts, *Complex geometry*, Universitext. Springer-Verlag, Berlin, 2005.

[69] C. Voisin, *Hodge theory and complex algebraic geometry. I*, vol. 76 of *Cambridge Studies in Advanced Mathematics*. Cambridge University Press, Cambridge, english ed., 2007.

[70] J. Bertin, J.-P. Demailly, L. Illusie and C. Peters, *Introduction to Hodge theory*, vol. 8 of *SMF/AMS Texts and Monographs*. American Mathematical Society, Providence, RI; Société Mathématique de France, Paris, 2002.

[71] E. Cattani, F. El Zein, P. A. Griffiths and L. D. Tráng, eds., *Hodge theory*, vol. 49 of *Mathematical Notes*. Princeton University Press, Princeton, NJ, 2014.

[72] A. Weil, *Introduction à l'étude des variétés kählériennes*, Publications de l'Institut de Mathématique de l'Université de Nancago, VI. Actualités Sci. Ind. no. 1267. Hermann, Paris, 1958.

[73] J. Carlson, S. Müller-Stach and C. Peters, *Period mappings and period domains*, vol. 168 of *Cambridge Studies in Advanced Mathematics*. Cambridge University Press, Cambridge, 2017.

[74] S. Hosono, A. Klemm and S. Theisen, *Lectures on mirror symmetry*, *Lect. Notes Phys.* **436** (1994) 235 [hep-th/9403096].

[75] W. Schmid, *Variation of Hodge structure: the singularities of the period mapping*, *Invent. Math.* **22** (1973) 211.

[76] E. Cattani, A. Kaplan and W. Schmid, *Degeneration of Hodge structures*, *Ann. of Math. (2)* **123** (1986) 457.

[77] C. Robles, *Degenerations of Hodge structure*, in *Surveys on recent developments in algebraic geometry*, vol. 95 of *Proc. Sympos. Pure Math.*, pp. 267–283. Amer. Math. Soc., Providence, RI, 2017.

[78] M. Green, P. Griffiths and M. Kerr, *Hodge theory, complex geometry, and representation theory*, vol. 118. American Mathematical Soc., 2013.

[79] P. A. Griffiths, *Periods of integrals on algebraic manifolds: Summary of main results and discussion of open problems*, *Bull. Amer. Math. Soc.* **76** (1970) 228.

[80] P. Griffiths and W. Schmid, *Recent developments in Hodge theory: a discussion of techniques and results*, in *Discrete subgroups of Lie groups and applicatons to moduli (Internat. Colloq., Bombay, 1973)*, pp. 31–127. 1975.

[81] P. Corvilain, T. W. Grimm and I. Valenzuela, *The Swampland Distance Conjecture for Kähler moduli*, *JHEP* **08** (2019) 075 [1812.07548].

[82] T. W. Grimm and D. van de Heisteeg, *Infinite Distances and the Axion Weak Gravity Conjecture*, *JHEP* **03** (2020) 020 [1905.00901].

[83] T. W. Grimm, F. Ruehle and D. van de Heisteeg, *Classifying Calabi–Yau Threefolds Using Infinite Distance Limits*, *Commun. Math. Phys.* **382** (2021) 239 [1910.02963].

[84] N. Gendler and I. Valenzuela, *Merging the weak gravity and distance conjectures using BPS extremal black holes*, *JHEP* **01** (2021) 176 [2004.10768].

[85] S. Lanza, F. Marchesano, L. Martucci and I. Valenzuela, *Swampland Conjectures for Strings and Membranes*, *JHEP* **02** (2021) 006 [2006.15154].

[86] B. Bastian, T. W. Grimm and D. van de Heisteeg, *Weak gravity bounds in asymptotic string compactifications*, *JHEP* **06** (2021) 162 [2011.08854].

[87] J. Calderón-Infante, A. M. Uranga and I. Valenzuela, *The Convex Hull Swampland Distance Conjecture and Bounds on Non-geodesics*, *JHEP* **03** (2021) 299 [2012.00034].

[88] T. W. Grimm, J. Monnee and D. van de Heisteeg, *Bulk Reconstruction in Moduli Space Holography*, 2103.12746.

[89] B. Bastian, T. W. Grimm and D. van de Heisteeg, *Modeling General Asymptotic Calabi-Yau Periods*, 2105.02232.

[90] E. Palti, *Stability of BPS states and weak coupling limits*, *JHEP* **08** (2021) 091 [2107.01539].

[91] B. Bastian, T. W. Grimm and D. van de Heisteeg, *Engineering Small Flux Superpotentials and Mass Hierarchies*, 2108.11962.

[92] T. W. Grimm, E. Plauschinn and D. van de Heisteeg, *Moduli Stabilization in Asymptotic Flux Compactifications*, 2110.05511.

[93] T. W. Grimm and J. Monnee, *Deformed WZW Models and Hodge Theory - Part I -*, 2112.00031.

[94] S. S. Chern, W. H. Chen and K. S. Lam, *Lectures on differential geometry*, vol. 1 of *Series on University Mathematics*. World Scientific Publishing Co., Inc., River Edge, NJ, 1999.

[95] T. Eguchi, P. B. Gilkey and A. J. Hanson, *Gravitation, Gauge Theories and Differential Geometry*, *Phys. Rept.* **66** (1980) 213.

[96] Y. Thiry, *Les équations de la théorie unitaire de Kaluza*, *C. R. Acad. Sci. Paris* **226** (1948) 216.

[97] A. Lichnerowicz, *Théories relativistes de la gravitation et de l'électromagnétisme. Relativité générale et théories unitaires*. Masson et Cie, Paris, 1955.

[98] S. A. Filippini, H. Ruddat and A. Thompson, *An introduction to Hodge structures*, in *Calabi-Yau varieties: arithmetic, geometry and physics*, vol. 34 of *Fields Inst. Monogr.*, pp. 83–130. Fields Inst. Res. Math. Sci., Toronto, ON, 2015.

[99] A. H. Durfee, *A naive guide to mixed Hodge theory*, in *Singularities, Part 1 (Arcata, Calif., 1981)*, vol. 40 of *Proc. Sympos. Pure Math.*, pp. 313–320. Amer. Math. Soc., Providence, RI, 1983.

[100] E. Cattani and A. Kaplan, *Algebraicity of Hodge loci for variations of Hodge structure*, in *Hodge theory, complex geometry, and representation theory*, vol. 608 of *Contemp. Math.*, pp. 59–83. Amer. Math. Soc., Providence, RI, 2014.

[101] E. Cattani and A. Kaplan, *Degenerating variations of hodge structure*, *Astérisque* (1989) .

[102] V. S. Kulikov and P. F. Kurchanov, *Complex algebraic varieties: periods of integrals and Hodge structures [MR1060327 (91k:14010)]*, in *Algebraic geometry, III*, vol. 36 of *Encyclopaedia Math. Sci.*, pp. 1–217, 263–270.

Springer, Berlin, 1998.

[103] J.-L. Brylinski and S. Zucker, *An overview of recent advances in Hodge theory*, in *Several complex variables, VI*, vol. 69 of *Encyclopaedia Math. Sci.*, pp. 39–142. Springer, Berlin, 1990.

[104] S. Usui, *Period maps and their extensions (algebraic geometry and hodge theory)*, *数理解析研究所講究録* **803** (1992) 26.

[105] C. A. M. Peters and J. H. M. Steenbrink, *Mixed Hodge structures*, vol. 52 of *Ergebnisse der Mathematik und ihrer Grenzgebiete. 3. Folge. A Series of Modern Surveys in Mathematics [Results in Mathematics and Related Areas. 3rd Series. A Series of Modern Surveys in Mathematics]*. Springer-Verlag, Berlin, 2008.

[106] P. Deligne, *Théorie de Hodge. II*, *Inst. Hautes Études Sci. Publ. Math.* (1971) 5.

[107] M. Kashiwara, *The asymptotic behavior of a variation of polarized Hodge structure*, *Publ. Res. Inst. Math. Sci.* **21** (1985) 853.

[108] M. Kashiwara, *A study of variation of mixed Hodge structure*, *Publ. Res. Inst. Math. Sci.* **22** (1986) 991.

[109] M. Kashiwara and T. Kawai, *The Poincaré lemma for variations of polarized Hodge structure*, *Publ. Res. Inst. Math. Sci.* **23** (1987) 345.

[110] J. Steenbrink and S. Zucker, *Variation of mixed Hodge structure. I*, *Invent. Math.* **80** (1985) 489.

[111] P. Deligne, *Théorie de Hodge. III*, *Inst. Hautes Études Sci. Publ. Math.* (1974) 5.

[112] P. Deligne, *Structures de Hodge mixtes réelles*, in *Motives (Seattle, WA, 1991)*, vol. 55 of *Proc. Sympos. Pure Math.*, pp. 509–514. Amer. Math. Soc., Providence, RI, 1994.

[113] M. Kerr, G. J. Pearlstein and C. Robles, *Polarized relations on horizontal* SL(2)*'s*, *Doc. Math.* **24** (2019) 1295.

[114] C. Robles, *Classification of horizontal* SL(2)*s*, *Compos. Math.* **152** (2016) 918.

[115] E. Cattani and A. Kaplan, *Polarized mixed Hodge structures and the local monodromy of a variation of Hodge structure*, *Invent. Math.* **67** (1982) 101.

[116] S.-J. Lee, W. Lerche and T. Weigand, *Tensionless Strings and the Weak Gravity Conjecture*, *JHEP* **10** (2018) 164 [1808.05958].

[117] S.-J. Lee, W. Lerche and T. Weigand, *A Stringy Test of the Scalar Weak Gravity Conjecture*, *Nucl. Phys. B* **938** (2019) 321 [1810.05169].

[118] P. Candelas, X. de La Ossa, A. Font, S. H. Katz and D. R. Morrison, *Mirror symmetry for two parameter models. 1.*, *Nucl. Phys. B* **416** (1994) 481 [hep-th/9308083].

[119] P. Candelas, A. Font, S. H. Katz and D. R. Morrison, *Mirror symmetry for two parameter models. 2.*, *Nucl. Phys. B* **429** (1994) 626 [hep-th/9403187].

[120] M. Alim, *Lectures on Mirror Symmetry and Topological String Theory*, 1207.0496.

[121] E. Viehweg, *Quasi-projective moduli for polarized manifolds*, vol. 30 of *Ergebnisse der Mathematik und ihrer Grenzgebiete (3) [Results in Mathematics and Related Areas (3)]*. Springer-Verlag, Berlin, 1995.

[122] H. Hironaka, *Resolution of singularities of an algebraic variety over a field of characteristic zero. I, II*, *Ann. of Math. (2)* ***79*** *(1964), 109–203; ibid. (2)* **79** (1964) 205.

[123] A. Landman, *On the Picard-Lefschetz transformation for algebraic manifolds acquiring general singularities*, *Trans. Amer. Math. Soc.* **181** (1973) 89.

[124] D. Ž. Djoković, *Closures of conjugacy classes in classical real linear Lie groups. II*, *Trans. Amer. Math. Soc.* **270** (1982) 217.

[125] D. H. Collingwood and W. M. McGovern, *Nilpotent orbits in semisimple Lie algebras*, Van Nostrand Reinhold Mathematics Series. Van Nostrand Reinhold Co., New York, 1993.

[126] C.-L. Wang, *On the incompleteness of the Weil-Petersson metric along degenerations of Calabi-Yau manifolds*, *Math. Res. Lett.* **4** (1997) 157.

[127] C.-L. Wang, *Aspects on Calabi-Yau moduli*, in *Uniformization, Riemann-Hilbert correspondence, Calabi-Yau manifolds & Picard-Fuchs equations*, vol. 42 of *Adv. Lect. Math. (ALM)*, pp. 527–550. Int. Press, Somerville, MA, 2018.

[128] D. R. Morrison, *Compactifications of moduli spaces inspired by mirror symmetry*, *Astérisque* **218** (1993) .

[129] P. Candelas, X. C. de La Ossa, P. S. Green and L. Parkes, *A Pair of Calabi-Yau manifolds as an exactly soluble superconformal theory*, *Nucl. Phys. B* **359** (1991) 21.

[130] L. Katzarkov, M. Kontsevich and T. Pantev, *Hodge theoretic aspects of mirror symmetry*, *Proc. Symp. Pure Math.* **78** (2008) 87 [0806.0107].

[131] C. T. C. Wall, *Classification problems in differential topology. V. On certain* 6*-manifolds*, *Invent. Math.* **1** (1966) 355.

[132] A. Herraez, L. E. Ibanez, F. Marchesano and G. Zoccarato, *The Type IIA Flux Potential, 4-forms and Freed-Witten anomalies*, *JHEP* **09** (2018) 018 [1802.05771].

[133] K. Kato, C. Nakayama and S. Usui, SL(2)*-orbit theorem for degeneration of mixed Hodge structure*, *J. Algebraic Geom.* **17** (2008) 401.

[134] S. K. Garg and C. Krishnan, *Bounds on Slow Roll and the de Sitter Swampland*, *JHEP* **11** (2019) 075 [1807.05193].

[135] M. Dine and N. Seiberg, *Is the Superstring Weakly Coupled?*, *Phys. Lett. B* **162** (1985) 299.

[136] T. W. Grimm, C. Li and E. Palti, *Infinite Distance Networks in Field Space and Charge Orbits*, *JHEP* **03** (2019) 016 [1811.02571].

[137] O. DeWolfe, A. Giryavets, S. Kachru and W. Taylor, *Type IIA moduli stabilization*, *JHEP* **07** (2005) 066 [hep-th/0505160].

[138] F. Baume and E. Palti, *Backreacted Axion Field Ranges in String Theory*, *JHEP* **08** (2016) 043 [1602.06517].

[139] I. Valenzuela, *Backreaction Issues in Axion Monodromy and Minkowski 4-forms*, *JHEP* **06** (2017) 098 [1611.00394].

[140] R. Blumenhagen, I. Valenzuela and F. Wolf, *The Swampland Conjecture and F-term Axion Monodromy Inflation*, *JHEP* **07** (2017) 145 [1703.05776].

[141] J. M. Maldacena and C. Nunez, *Supergravity description of field theories on curved manifolds and a no go theorem*, *Int. J. Mod. Phys. A* **16** (2001) 822 [hep-th/0007018].

[142] N. Arkani-Hamed, L. Motl, A. Nicolis and C. Vafa, *The String landscape, black holes and gravity as the weakest force*, *JHEP* **06** (2007) 060 [hep-th/0601001].

[143] A. Font, A. Herráez and L. E. Ibáñez, *The Swampland Distance Conjecture and Towers of Tensionless Branes*, *JHEP* **08** (2019) 044 [1904.05379].

[144] E. Palti, *On Natural Inflation and Moduli Stabilisation in String Theory*, *JHEP* **10** (2015) 188 [1508.00009].

[145] S. Bielleman, L. E. Ibanez, F. G. Pedro, I. Valenzuela and C. Wieck,

Higgs-otic Inflation and Moduli Stabilization, *JHEP* **02** (2017) 073 [1611.07084].

[146] E. Palti, *The Weak Gravity Conjecture and Scalar Fields*, *JHEP* **08** (2017) 034 [1705.04328].

[147] A. Hebecker, P. Henkenjohann and L. T. Witkowski, *Flat Monodromies and a Moduli Space Size Conjecture*, *JHEP* **12** (2017) 033 [1708.06761].

[148] M. Cicoli, D. Ciupke, C. Mayrhofer and P. Shukla, *A Geometrical Upper Bound on the Inflaton Range*, *JHEP* **05** (2018) 001 [1801.05434].

[149] R. Blumenhagen, D. Kläwer, L. Schlechter and F. Wolf, *The Refined Swampland Distance Conjecture in Calabi-Yau Moduli Spaces*, *JHEP* **06** (2018) 052 [1803.04989].

[150] E. Gonzalo, L. E. Ibáñez and A. M. Uranga, *Modular symmetries and the swampland conjectures*, *JHEP* **05** (2019) 105 [1812.06520].

[151] G. Buratti, J. Calderón and A. M. Uranga, *Transplanckian axion monodromy!?*, *JHEP* **05** (2019) 176 [1812.05016].

[152] F. Marchesano and M. Wiesner, *Instantons and infinite distances*, *JHEP* **08** (2019) 088 [1904.04848].

[153] S.-J. Lee, W. Lerche and T. Weigand, *Emergent Strings, Duality and Weak Coupling Limits for Two-Form Fields*, 1904.06344.

[154] M. P. Hertzberg, S. Kachru, W. Taylor and M. Tegmark, *Inflationary Constraints on Type IIA String Theory*, *JHEP* **12** (2007) 095 [0711.2512].

[155] A. Landete, F. Marchesano, G. Shiu and G. Zoccarato, *Flux Flattening in Axion Monodromy Inflation*, *JHEP* **06** (2017) 071 [1703.09729].

[156] A. Hebecker, P. Mangat, F. Rompineve and L. T. Witkowski, *Tuning and Backreaction in F-term Axion Monodromy Inflation*, *Nucl. Phys. B* **894** (2015) 456 [1411.2032].

[157] R. Blumenhagen, D. Herschmann and E. Plauschinn, *The Challenge of Realizing F-term Axion Monodromy Inflation in String Theory*, *JHEP* **01** (2015) 007 [1409.7075].

[158] M. J. Duff, J. T. Liu and R. Minasian, *Eleven-dimensional origin of string-string duality: A One loop test*, *Nucl. Phys. B* **452** (1995) 261 [hep-th/9506126].

[159] S. Sethi, C. Vafa and E. Witten, *Constraints on low dimensional string compactifications*, *Nucl. Phys. B* **480** (1996) 213 [hep-th/9606122].

[160] M. Berg, M. Haack and H. Samtleben, *Calabi-Yau fourfolds with flux and supersymmetry breaking*, *JHEP* **04** (2003) 046 [hep-th/0212255].

[161] K. Becker and M. Becker, *M-theory on eight-manifolds*, *Nucl. Phys. B* **477** (1996) 155 [hep-th/9605053].

[162] K. Dasgupta, G. Rajesh and S. Sethi, *M theory, orientifolds and G - flux*, *JHEP* **08** (1999) 023 [hep-th/9908088].

[163] T. W. Grimm, T. G. Pugh and M. Weissenbacher, *On M-theory fourfold vacua with higher curvature terms*, *Phys. Lett. B* **743** (2015) 284 [1408.5136].

[164] T. W. Grimm, T. G. Pugh and M. Weissenbacher, *The effective action of warped M-theory reductions with higher derivative terms — part I*, *JHEP* **01** (2016) 142 [1412.5073].

[165] T. W. Grimm, T. G. Pugh and M. Weissenbacher, *The effective action of warped M-theory reductions with higher-derivative terms - Part II*, *JHEP* **12** (2015) 117 [1507.00343].

[166] T. W. Grimm, K. Mayer and M. Weissenbacher, *One-modulus Calabi-Yau fourfold reductions with higher-derivative terms*, *JHEP* **04** (2018) 021 [1712.07074].

[167] M. Haack and J. Louis, *M-theory compactified on Calabi-Yau fourfolds with background flux*, *Phys. Lett. B* **507** (2001) 296 [hep-th/0103068].

[168] A. Sen, *F-theory and orientifolds*, *Nucl. Phys. B* **475** (1996) 562 [hep-th/9605150].

[169] T. W. Grimm, *The Effective action of type II Calabi-Yau orientifolds*, *Fortsch. Phys.* **53** (2005) 1179 [hep-th/0507153].

[170] G. Dvali, *Three-form gauging of axion symmetries and gravity*, hep-th/0507215.

[171] N. Kaloper and L. Sorbo, *A Natural Framework for Chaotic Inflation*, *Phys. Rev. Lett.* **102** (2009) 121301 [0811.1989].

[172] N. Kaloper, A. Lawrence and L. Sorbo, *An Ignoble Approach to Large Field Inflation*, *JCAP* **03** (2011) 023 [1101.0026].

[173] S. Bielleman, L. E. Ibanez and I. Valenzuela, *Minkowski 3-forms, Flux String Vacua, Axion Stability and Naturalness*, *JHEP* **12** (2015) 119 [1507.06793].

[174] F. Carta, F. Marchesano, W. Staessens and G. Zoccarato, *Open string*

multi-branched and Kähler potentials, *JHEP* **09** (2016) 062 [1606.00508].

[175] T. W. Grimm, T.-W. Ha, A. Klemm and D. Klevers, *The D5-brane effective action and superpotential in N=1 compactifications*, *Nucl. Phys. B* **816** (2009) 139 [0811.2996].

[176] T. W. Grimm and D. Vieira Lopes, *The N=1 effective actions of D-branes in Type IIA and IIB orientifolds*, *Nucl. Phys. B* **855** (2012) 639 [1104.2328].

[177] M. Kerstan and T. Weigand, *The Effective action of D6-branes in N=1 type IIA orientifolds*, *JHEP* **06** (2011) 105 [1104.2329].

[178] F. Farakos, S. Lanza, L. Martucci and D. Sorokin, *Three-forms, Supersymmetry and String Compactifications*, *Phys. Part. Nucl.* **49** (2018) 823 [1712.09366].

[179] I. Bandos, F. Farakos, S. Lanza, L. Martucci and D. Sorokin, *Three-forms, dualities and membranes in four-dimensional supergravity*, *JHEP* **07** (2018) 028 [1803.01405].

[180] D. Escobar, F. Marchesano and W. Staessens, *Type IIA flux vacua and α'-corrections*, *JHEP* **06** (2019) 129 [1812.08735].

[181] S. Lanza, F. Marchesano, L. Martucci and D. Sorokin, *How many fluxes fit in an EFT?*, *JHEP* **10** (2019) 110 [1907.11256].

[182] F. Marchesano and J. Quirant, *A Landscape of AdS Flux Vacua*, *JHEP* **12** (2019) 110 [1908.11386].

[183] E. García-Valdecasas and A. Uranga, *On the 3-form formulation of axion potentials from D-brane instantons*, *JHEP* **02** (2017) 087 [1605.08092].

[184] R. Donagi, S. Katz and M. Wijnholt, *Weak Coupling, Degeneration and Log Calabi-Yau Spaces*, *Pure Appl. Math. Quart.* **09** (2013) 665 [1212.0553].

[185] C. Roupec and T. Wrase, *de Sitter Extrema and the Swampland*, *Fortsch. Phys.* **67** (2019) 1800082 [1807.09538].

[186] D. Junghans, *Weakly Coupled de Sitter Vacua with Fluxes and the Swampland*, *JHEP* **03** (2019) 150 [1811.06990].

[187] R. Flauger, S. Paban, D. Robbins and T. Wrase, *Searching for slow-roll moduli inflation in massive type IIA supergravity with metric fluxes*, *Phys. Rev. D* **79** (2009) 086011 [0812.3886].

[188] A. Clingher, R. Donagi and M. Wijnholt, *The Sen Limit*, *Adv. Theor. Math. Phys.* **18** (2014) 613 [1212.4505].

[189] S. S. Haque, G. Shiu, B. Underwood and T. van Riet, *Minimal simple de*

Sitter solutions, *Phys. Rev. D* **79** (2009) 086005 [0810.5328].

[190] B. de Carlos, A. Guarino and J. M. Moreno, *Flux moduli stabilisation, Supergravity algebras and no-go theorems*, *JHEP* **01** (2010) 012 [0907.5580].

[191] T. Wrase and M. Zagermann, *On Classical de Sitter Vacua in String Theory*, *Fortsch. Phys.* **58** (2010) 906 [1003.0029].

[192] U. Danielsson and G. Dibitetto, *On the distribution of stable de Sitter vacua*, *JHEP* **03** (2013) 018 [1212.4984].

[193] J. Blåbäck, U. Danielsson and G. Dibitetto, *Fully stable dS vacua from generalised fluxes*, *JHEP* **08** (2013) 054 [1301.7073].

[194] D. Andriot and J. Blåbäck, *Refining the boundaries of the classical de Sitter landscape*, *JHEP* **03** (2017) 102 [1609.00385].

[195] D. Andriot, *On classical de Sitter and Minkowski solutions with intersecting branes*, *JHEP* **03** (2018) 054 [1710.08886].

[196] D. Andriot, *New constraints on classical de Sitter: flirting with the swampland*, *Fortsch. Phys.* **67** (2019) 1800103 [1807.09698].

[197] J. Blåbäck, U. Danielsson and G. Dibitetto, *A new light on the darkest corner of the landscape*, 1810.11365.

[198] P. Shukla, *T-dualizing de Sitter no-go scenarios*, *Phys. Rev. D* **102** (2020) 026014 [1909.08630].

[199] A. Banlaki, A. Chowdhury, C. Roupec and T. Wrase, *Scaling limits of dS vacua and the swampland*, *JHEP* **03** (2019) 065 [1811.07880].

[200] L. F. Alday and E. Perlmutter, *Growing Extra Dimensions in AdS/CFT*, *JHEP* **08** (2019) 084 [1906.01477].

[201] D. Lüst, E. Palti and C. Vafa, *AdS and the Swampland*, *Phys. Lett. B* **797** (2019) 134867 [1906.05225].

[202] P. G. Camara, A. Font and L. E. Ibanez, *Fluxes, moduli fixing and MSSM-like vacua in a simple IIA orientifold*, *JHEP* **09** (2005) 013 [hep-th/0506066].

[203] D. Andriot, *Open problems on classical de Sitter solutions*, *Fortsch. Phys.* **67** (2019) 1900026 [1902.10093].

[204] F. F. Gautason, M. Schillo, T. van Riet and M. Williams, *Remarks on scale separation in flux vacua*, *JHEP* **03** (2016) 061 [1512.00457].

[205] E. Silverstein and A. Westphal, *Monodromy in the CMB: Gravity Waves and String Inflation*, *Phys. Rev. D* **78** (2008) 106003 [0803.3085].

[206] L. McAllister, E. Silverstein and A. Westphal, *Gravity Waves and Linear Inflation from Axion Monodromy*, *Phys. Rev. D* **82** (2010) 046003 [0808.0706].

[207] L. McAllister, E. Silverstein, A. Westphal and T. Wrase, *The Powers of Monodromy*, *JHEP* **09** (2014) 123 [1405.3652].

[208] F. Marchesano, G. Shiu and A. M. Uranga, *F-term Axion Monodromy Inflation*, *JHEP* **09** (2014) 184 [1404.3040].

[209] A. Hebecker, S. C. Kraus and L. T. Witkowski, *D7-Brane Chaotic Inflation*, *Phys. Lett. B* **737** (2014) 16 [1404.3711].

[210] R. Blumenhagen and E. Plauschinn, *Towards Universal Axion Inflation and Reheating in String Theory*, *Phys. Lett. B* **736** (2014) 482 [1404.3542].

[211] L. E. Ibáñez and I. Valenzuela, *The inflaton as an MSSM Higgs and open string modulus monodromy inflation*, *Phys. Lett. B* **736** (2014) 226 [1404.5235].

[212] A. Bedroya and C. Vafa, *Trans-Planckian Censorship and the Swampland*, *JHEP* **09** (2020) 123 [1909.11063].

[213] P. Draper and S. Farkas, *Transplanckian Censorship and the Local Swampland Distance Conjecture*, *JHEP* **01** (2020) 133 [1910.04804].

[214] M. Kim and L. McAllister, *Monodromy Charge in D7-brane Inflation*, *JHEP* **10** (2020) 060 [1812.03532].

[215] L. E. Ibanez, F. Marchesano and I. Valenzuela, *Higgs-otic Inflation and String Theory*, *JHEP* **01** (2015) 128 [1411.5380].

[216] M. Scalisi and I. Valenzuela, *Swampland distance conjecture, inflation and α-attractors*, *JHEP* **08** (2019) 160 [1812.07558].

[217] I. García-Etxebarria, T. W. Grimm and I. Valenzuela, *Special Points of Inflation in Flux Compactifications*, *Nucl. Phys. B* **899** (2015) 414 [1412.5537].

[218] T. W. Grimm, C. Li and I. Valenzuela, *Asymptotic Flux Compactifications and the Swampland*, *JHEP* **06** (2020) 009 [1910.09549].

[219] E. Witten, *On flux quantization in M-theory and the effective action*, *J. Geom. Phys.* **22** (1997) 1 [hep-th/9609122].

[220] J.-P. Serre, *Complex semisimple Lie algebras*, Springer Monographs in Mathematics. Springer-Verlag, Berlin, 2001.

[221] R. J. Walker, *Algebraic Curves*, Princeton Mathematical Series, vol. 13.

Princeton University Press, Princeton, N. J., 1950.

[222] J. Kock, *Frobenius algebras and 2D topological quantum field theories*, vol. 59 of *London Mathematical Society Student Texts*. Cambridge University Press, Cambridge, 2004.

Asymptotic Hodge Theory and String Theory

Chongchuo Li

Asymptotic Hodge Theory and String Theory

An application to the swampland program

Chongchuo Li

INVITATION

It is my great pleasure to invite you to attend the public defense of my PhD thesis entitled

Asymptotic Hodge Theory and String Theory

An application to the swampland program

which will be held on Friday 17th of June at 10:15 in the Academiegebouw of Utrecht

Chongchuo Li